A THEORY FOR THE HUGONIOT OF CONDENSED MEDIA

Thesis by

Paul Klenett Salzman

In Partial Fulfillment of the Requirements

for the Degree of

Doctor of Philosophy

California Institute of Technology

Pasadena, California

1971

(Submitted May 28, 1971)

© 1971

PAUL KLENETT SALZMAN

ALL RIGHTS RESERVED

ACKNOWLEDGMENT

First of all, I want to express my deep appreciation to my research advisor, Professor C. J. Pings, for his support and encouragement during the long course of this work. I would also like to acknowledge the valuable discussions with Dr. A. F. Collings and S. Y. Wu.

Special thanks go to June Gray and Ruth Stratton for preparation of the figures and text respectively and to C. H. McBride, C. S. Pierce and, especially, G. A. Spraker, for their extra-curricular typing efforts.

I am indebted to General Dynamics Corporation for the financial support given me in the latter years of my graduate study and to Aerojet-General Corporation for their aid in the earlier years. The encouragement and support of H. Dershin, C. L. McMillan, T. H. Tennant and Dr. L. F. Buchanan of General Dynamics is hereby also gratefully acknowledged.

I would like to thank Dr. R. H. Wright for valuable and enlightening discussions which were of great help in completing this work.

Finally, I would like to thank my wife, Helene, for her patience, understanding and fortitude through the years of my research and production of this thesis.

ABSTRACT

A shock model is developed that leads to an analytical expression for the Hugoniot of condensed media. In the analysis the final state is selected to coincide with the end of the shock transition so that the total energy change across the shock front is evaluated from changes in configurational energy only using an n-6 pair potential (shown to be valid for all $n > 0$) and a given lattice structure. Thermal energy changes are ignored because the dwell time of the molecules in the shock transition region is less than the thermal relaxation time. The total energy change is equated to the Hugoniot energy change in the Rankine-Hugoniot conservation relations. This together with the assumption of linear compression across the shock transition gives the desired expression for the Hugoniot.

In the "weak form" (WF) solution the Hugoniot depends on molecular (atomic) weight M and initial density ρ_o as well as the collision diameter σ, depth of the potential well ε and repulsive exponent n of the pair potential. Extrapolation of this solution, under certain conditions, yields an expression for the sound velocity U_o dependent on M, ε and n. In the "strong form" (SF) solution the Hugoniot depends only on U_o and n.

The shock data for 13 liquids and 23 metals are compiled and a selection process used to eliminate poor data and data affected by phase transitions. Using σ from the literature and ε from a melting point correlation, the WF solution Hugoniot is applied to the

liquids and the "best" values of n determined using numerical fitting techniques. Excellent fits are obtained with values of n from 6.2 to 11.7. A common value of 9.2 is found to fit the shock data for argon at four different initial states. Failure of the theory is noted only for (di-)ethyl ether and water. The results are generally concluded to support the validity of the shock model. Values of n for argon, mercury and nitrogen compare favorably with values reported in the literature. The WF solution does not yield accurate values of U_o.

The SF solution is expanded in a Taylor series to eliminate singularities and applied to the shock data for 10 fcc and 13 bcc metals and the "best" values of n determined. For the fcc metals excellent fits are found for values of n from 4.0 to 6.3. Based on the "pseudo-atom" concept, it is concluded that metals have "softer" potentials than liquids. The results for the fcc metals are concluded to generally support the validity of the shock model. For the bcc metals excellent fits are found for $n = 0.1$ to 4.6 and it is concluded that bcc metals are "softer" than fcc metals. Since σ is "not defined" for all $n < 3$ it is speculated that the Hugoniot might not be "well defined" in these cases. The theory is found to be not applicable to Cs and Ba. The values of n found for Cu, Al and Pb agree well with values in the literature. The n for metals are found to roughly correlate with the Grüneisen coefficient γ.

The major assumption of the theory, that the transition region is "sufficiently thin," is analyzed and found to be reasonable. The

mean number of molecular layers in the transition region is ~ 7 and the mean residence time $\sim 2 \times 10^{-12}$ sec. In addition the n-6 potential is judged to be adequate for the present study.

The SF solution Hugoniot is shown to be compatible with the classic linear U-μ relation ($U = A + Bu$) when $x-1 \ll 1$. Values of the slope B from experimental data are found to agree closely with the derived relation $B \simeq (n + 5)/6$ for the corresponding metals. Recommendations for further studies with liquids, fcc and bcc metals are made, including an evaluation of an explicit expression generally relating the pair potential to the shock data.

In several subsidiary studies a new method of computing temperatures along the Hugoniot is found, two statistical approaches to the definition of "nearest neighbor distance" and its use as a measure of liquid structure are developed and the effect of phase transitions on the shock model is determined.

TABLE OF CONTENTS

PART	TITLE	PAGE NO.
	TITLE PAGE	i
	ACKNOWLEDGMENT	ii
	ABSTRACT	iii
	TABLE OF CONTENTS	vi
	LIST OF FIGURES	x
	LIST OF TABLES	xiii
	LIST OF APPENDICES	xv
	NOMENCLATURE	xvii
I.	INTRODUCTION	1
II.	THEORY	3
	A. CONSERVATION RELATIONS	3
	1. Definition of Shock Properties	3
	2. Conservation Equations--Per Unit Area/Unit Time	5
	a. Conservation of mass flux	5
	b. Conservation of momentum flux	5
	c. Conservation of energy flux	5
	3. Conservation Relations	7
	4. Specific Objective	9
	5. U vs. μ Linearity and Mass Conservation	11
	6. Extrapolation to U_o	13
	B. DEVELOPMENT OF SHOCK MODEL	15
	1. "Receding" Shock	15
	2. Transformation Equivalence Conditions	19

3. Energy Partitioning--Relaxation Effects 20

4. Energy Equation 23

5. Integration of Pair Potential 31

C. PAIR POTENTIAL FUNCTIONS 33

1. List of Suggested Potential Functions 37

2. Choice for Work 41

3. Special Properties of the n-6 Potential 45

a. The 6-6 potential 45

b. The $n < 6$ potential 45

4. Integration for Use in Model 49

D. STRUCTURE 51

1. Liquids 51

2. Solids 54

3. Generalization of Structure 55

E. SHOCK HUGONIOT 58

1. Linear Compression 58

2. General Expression 60

F. PROPERTIES OF THE DEVELOPED FUNCTION (EQUATION (95)) 62

1. Extrapolation to Sound Velocity 62

2. U vs. μ Linearity 66

3. Effects as $n \rightarrow 6$ 68

III. APPLICATION OF THEORY 70

A. AVAILABLE EXPERIMENTAL DATA 70

1. Shock Experiments 70

2. Compilation of Data 82

3. Selection Process 101

B. LIQUIDS 107

1. Development of Parameters 108

2. Treatment of Data 118

3. Results 129

C. METALS 151

1. Method of Approach 152

2. Treatment of Data 165

3. Results 173

IV. DISCUSSION AND CONCLUSIONS 185

A. THEORY 185

1. Evaluation of Assumptions 185

a. Shock front thickness 185
b. Pair potential 193
c. Structure 196
d. Extrapolation to sound velocity 196
e. U vs. μ linearity 197

2. Adequacy of Theory 204

3. Recommendations 210

B. APPLICATION OF THEORY 219

1. Data 219

2. Liquids 228

a. Preliminary conclusions 228
b. Argon 230
c. Other liquids 233
d. General conclusion 240
e. Recommendations 242

3. Metals 246

a. Preliminary conclusions 246
b. Taylor expansion of SF solution 247
c. fcc metals 248
d. bcc metals 253
e. General conclusion 261
f. Recommendations 266

REFERENCES 271

APPENDICES (see page xv for LIST OF APPENDICES) 280

PROPOSITION 1. OPTIMIZATION OF CHEMICAL REACTIONS 489

PROPOSITION 2. DETERMINATION OF THE MAXIMUM TRANSMITTED SHOCK AT THE INTERFACE BETWEEN TWO CONDENSED MEDIA 512

PROPOSITION 3. THE THEORY OF CRITICAL GEOMETRY 515

LIST OF FIGURES

NO.	TITLE	PAGE NO.
1	One-Dimensional Shock Propagating Into a Stationary Medium	4
2	Coordinate System	6
3	Receding Shock Wave--Skiers	16
4	Receding Shock--Model	17
5	Potentials for Shaded Molecule	24
6	Interactions for Shaded Molecule	29
7	LRO Behavior	36
8	n-6 Potential	43
9	Pair Potential Function for Various Values of n	48
10	Structure	56
11	Shock Wave Production	72
12	Hugoniot "Reflection" Method	75
13	"Impact" Method	77
14	Elements Included in Study Superimposed on Period Table	86
15	U vs. μ Data--A, Hg	88
16	U vs. μ Data--N_2, H_2, CS_2	89
17	U vs. μ Data--CCl_4, CH_3OH,	90
18	U vs. μ Data--$(C_2H_5)_2O$, C_6H_{14}	91
19	U vs. μ Data--C_6H_6, $C_6H_5CH_3$	92
20	U vs. μ Data--H_2O	93
21	U vs. μ Data--Cu, Ag, Au	94
22	U vs. μ Data--Co, Ni, Pd, Pt	95
23	U vs. μ Data--Al, Ca, Pb	96

NO.	TITLE	PAGE NO.
24	U vs. μ Data--Li, Na, K, Rb, Cs	97
25	U vs. μ Data--V, Nb, Ta	98
26	U vs. μ Data--Cr, Mo, W	99
27	U vs. μ Data--Zr, Ba	100
28	Roots of μ^2 vs. x	124
29	μ vs. x Fit of Theory for Common Value of n for Argon	145
30	U vs. μ Fit of Theory for Common Value of n for Argon	146
31	U vs. μ Fit of Theory--Hg, N_2, H_2, CS_2	147
32	U vs. μ Fit of Theory--CCl_4, CH_3OH, C_2H_5OH	148
33	U vs. μ Fit of Theory--$(C_2H_5)_2O$, C_6H_{14}, C_6H_6, $C_6H_5CH_3$	149
34	U vs. μ Fit of Theory--H_2O	150
35	U vs. μ Fit of Theory--Cu, Ag, Au	178
36	U vs. μ Fit of Theory--Co, Ni, Pd, Pt	179
37	U vs. μ Fit of Theory--Al, Ca, Pb	180
38	U vs. μ Fit of Theory--Li, Na, K, Rb, Cs	181
39	U vs. μ Fit of Theory--V, Nb, Ta	182
40	U vs. μ Fit of Theory--Cr, Mo, W	183
41	U vs. μ Fit of Theory--Zr, Ba	184
E1	Potentials for Shaded Molecule	295
H1	$\phi_o(r)$ vs. r	311
J1	Interactions of the Shaded Molecule in the (p',z') Plane	323
K1	Definition of a_o and z_o	328

NO.	TITLE	PAGE NO.
L1	Nearest Neighbor	333
L2	Pair Distribution Function	335
L3	Spherical Shell	337
L4	Intermediate Structures	348
M1	Three-Body Interaction	352
T1	First- and Second-Order Phase Transitions	426
T2	U-μ Behavior Corresponding to FO and SO Transitions	428
T3	Pressure Distributions in Split Waves and in Phase 2 Region	430

LIST OF TABLES

NO.	TITLE	PAGE NO.
1	PAIR POTENTIAL FUNCTIONAL FORMS	38
2	TIME-OF-ARRIVAL AND CONTINUOUS-DISTANCE TIME DETERMINATIONS	80
3	PRESSURE AND DENSITY DETERMINATIONS	81
4	SUBSTANCES INCLUDED IN STUDY	84
5	REPORTED ERROR IN DATA	102
6	REPORTED PHASE TRANSITIONS	103
7	AVAILABLE σ, ε , C_{ab} DATA--LIQUIDS	111
8	PRELIMINARY COMPUTATIONS--$f(n) = C_{ab}/\sigma\varepsilon^6$	113
9	ε/k vs. T_M CORRELATION--LIQUIDS	117
10	FITTING OF DATA--LIQUIDS	121
11	RESULTS--PRELIMINARY CALCULATIONS	130
12	PUFI APPLIED TO ARGON	132
13	VALUE IN USING PUSC	136
14	PUFI APPLIED TO LIQUIDS	140
15	COMMON VALUE OF n FOR ARGON	144
16	AVAILABLE σ , r_o, ε , C_{ab} DATA--METALS	153
17	PRELIMINARY COMPUTATIONS--METALS	156
18	ε/k vs. T_M CORRELATION--METALS	161
19	PUFF APPLIED TO METALS	163
20	FIFO APPLIED TO METALS	174
21	AVAILABLE SHOCK FRONT THICKNESS AND RELAXATION TIME DATA	190
22	COMPARISON OF VALUES OF B FROM THEORY AND EXPERIMENT	202

NO.	TITLE	PAGE NO.
23	SUMMARY OF DATA SELECTION	220
D1	VALIDITY OF EQUATION (19)	290
D2	VALIDITY OF EQUATION (19) USING EQUATION (D10)	293
L1	STRUCTURE FOR VARIOUS CRYSTAL LATTICES	347
U1	FITTING OF DATA USING σ AND C_{ab}--LIQUIDS	437
Y1	DETERMINATION OF $\sigma(2^s\rho_o N/M)^{1/3}$ FOR LIQUIDS	465

LIST OF APPENDICES

NO.	TITLE	PAGE NO.
A	Derivation of Equations (4) - (7)	281
B	Derivation of Equation (8)	284
C	Derivation of Equation (18)	287
D	Validity of Equation (19)	288
E	New Way to Compute Temperatures Along the Hugoniot	294
F	Derivation of Equations (69) and (70)	300
G	Derivation of Equation (73)	303
H	Derivation of Equation (75)	308
I	Proof of Monotonicity of $\phi(r)$	312
J	Derivation of Equations (78) - (80)	322
K	Nearest Neighbor Distance; Distance Between Molecular Layers	327
L	"Snapshot" and "Probability" Approach--Nearest Neighbor Distance	332
M	Relation of r^* to r_o	350
N	Derivation of Equation (94)	354
O	Derivation of Equation (103)	356
P	Derivation of Equation (108)	359
Q	Derivation of Equation (114)	361
R	Derivation of Equations (115) - (122)	364
S	Compilation of Raw and Adjusted U-μ Data	367
T	Phase Transitions and the Shock Model	425
U	Fit of Theory Using σ and C_{ab}	435
V	Effect of Added Attraction	439

NO.	TITLE	PAGE NO.
W	ε/k vs. $T_{M.}$--Linear Least Squares	445
X	Derivation of 1, 2 and 3 Parameter Fit Equations	448
Y	Demonstration of Additional Root of Equation (135)	458
Z	Derivation of Equation (147)	471
AA	Removal of Singularities	474

NOMENCLATURE

A	intercept of linear U-μ relation
a_o	nearest neighbor distance
a,b,c,d,e	molecular parameters
B	slope of linear U-μ relation
b	constant
bcc	body-centered-cubic
C	constant, correlated
C_B	sound speed from P. W. Bridgman data
C_o	sound velocity
C_1, C_2, C_3	constants
C_V	heat capacity
$C_{ab}, C'_{ab}, C''_{ab}$	dispersion constants
D	detonation velocity
E	internal energy
e	base of natural logarithms--2.71828
FIFO	computer program
FO	first-order
FOMP	computer program
f	figure of merit
fcc	face-centered-cubic
g(r)	pair (or radial) distribution function
hcp	hexagonal-close-packed
I_o	integral
i	index

k	Boltzmann's constant--1.38045×10^{-16} erg/^{o}K-molecule
k_f	radius of Fermi sphere
L	$\sum_i R_i^2$, literature
L_o	molecular layer far removed from shock front
L_1	first molecular layer in compressed zone
L_e	molecular layer in final equilibrium state
LRO	long range oscillatory
ℓ	thickness of sample
ℓ_o	mean-free-path length
M	molecular (atomic) weight
$\mathcal{M}$	Mach number
m	molecular parameter, number of data points, constant
m_i	number of space sectors
N	Avogadro's number--6.023×10^{23} molecules/mole
N_h	number of molecules in half-space in Figure 5
N_1	first coordination number
n	repulsive exponent, number of molecules
n_L	number of molecular layers in transition region
n_1	particular value of repulsive exponent n
P	pressure
$P(r)$	polynomial in r
PDF	pair distribution function
PF	parameter fit
PUFF	computer program
PUFI	computer program
PUMP	computer program

PUSC	computer program
p	small integer
p',θ',z'	cylindrical coordinate system for a molecule
q	dummy variable, heat
R	remainder
R,R'	distances in Figure 5, ratios
R,R',R''	distances in Figure E1
R_i	residual for data set i
RDF	radial distribution function
RE	residual
Rem	remainder
r	intermolecular distance
r_o	position of the potential well
r*	position of the potential well in presence of other molecules
r_1, r_2	molecular parameters
S	entropy
SF	strong form
SO	second-order
S_{μ^2}	standard error of estimate
s	structure constant
sc	simple cubic
T	temperature
T_M	melting temperature
t	time
t_r	residence time in transition region

t.o.a.	time-of-arrival
U	shock velocity
U_o	$\lim_{\mu \to 0} U$
UNFI	computer program
u	dummy variable
V	specific volume
v_1, v_2	velocities of slug and disturbance in Figure 4
WF	weak form
w(r)	effect of three-body and higher interactions
X_R	root of μ^2 vs. x
x	ρ/ρ_o
x',y',z'	Cartesian coordinate system for a molecule
y	arbitrary fraction, dummy variable
Z	chemical valence, atomic number
z	characteristic spacing between molecular layers
z_f	shock front thickness

Greek

α, β, γ	molecular parameters
α, β	constants
α', β'	constants
$\Gamma(\ )$	gamma function--$\Gamma(m) = \int_0^\infty e^{-y}\, y^{m-1}\, dy$
γ	ratio of specific heats, Grüneisen's coefficient
δ	constant

ε	depth of the potential well
ε'	error of the fit
θ'	see p',θ',z'
μ	particle velocity
ν	vibrational frequency
π	pi -- 3.14159
ρ	density
σ	collision diameter, standard deviation
τ	relaxation time
ϕ	intermolecular potential function
Φ	total configurational energy
ψ	configurational energy of a single molecule, dummy variable
ω	work, dummy variable

Subscripts

e	equilibrium
f	flight
fs	free-surface
i	index
M	melting
max	maximum
min	minimum
o	initial state
r	rarefaction, reference
rev	reversible
1,2,3,4	index

Superscripts

L_o	layer L_o
L_1	layer L_1
L_e	layer L_e
(1)	changes from L_o to L_1
(2)	changes from L_1 to L_e
'	prime
-	average

Operators

cos	cosine
$\frac{d}{d}$	derivative
d	differential
Δ	difference
f( )	function
g( )	function
$\frac{\partial}{\partial}$	partial derivative
lim	limit
ℓn	natural logarithm
P{ }	probability
| |	absolute value
$\sum$	summation
$\int$	integral

I. INTRODUCTION

One of the fundamental properties of interest in the study of shock wave phenomena is the shock Hugoniot, i.e., the locus of states attainable by propagation of a shock wave through the medium of interest. If an explicit thermodynamic equation-of-state is available for the given material, the Hugoniot can be determined by simultaneous solution of this equation with the Rankine-Hugoniot relations which express conservation of mass, momentum and energy across the shock front.

Since there is no completely satisfactory quantitative equation-of-state for condensed media, these materials are generally treated empirically, semi-empirically or numerically (i.e., statistically); explicit functional equations for the Hugoniot are not generally found.

The primary objective of this study is to derive a relation which circumvents the problem of choosing a macroscopic equation-of-state and leads to an analytical expression for the Hugoniot. This is done by developing a model of the shock transition process and evaluating the energy change across the (finite) shock front from configurational and structural considerations, without recourse to the final equilibrium state.

The secondary objective of the study is to apply the derived Hugoniot to available experimental data for several liquids and metals to help determine the validity of the theory. This is done

using standard (numerical) fitting techniques.

An additional objective is to determine if the "classic" linear shock/particle velocity relationship can be derived from the developed theory.

This study differs from the large body of work on shock waves in that the thermodynamics of the shock transition is not required in the development and an analytical expression for the Hugoniot is sought. This somewhat different view of the nature of shock waves in condensed media is, in effect, evaluated in the course of the study.

II. THEORY

A. CONSERVATION RELATIONS

1. Definition of Shock Properties

Consider a one-dimensional shock wave propagating at velocity U through a stationary medium of density ρ_o as pictured in Figure 1. Behind the disturbance, which for present purposes may be considered "infinitely thin", the material is accelerated to velocity μ (the "particle" velocity) and compressed to density ρ. The other state parameters are the temperature, shock pressure and internal energy which rise from the initial state T_o, P_o, E_o^* to T, P and E^*.

In defining these properties it has been assumed that a state of equilibrium exists both before and after passage of the "discontinuity". In this case, the variables ρ, P, T and E represent true thermodynamic properties and should be found on the general equation-of-state surface of the medium in question.

The particle velocity μ represents the gross (bulk) motion of the medium necessary for producing a shock. On the other hand, U, the shock propagational velocity, describes the motion of a geometrical "line" (the discontinuity) in space and does not imply the motion of a mass. Neither U or μ can be considered "thermodynamic" variables although both, through the conservation relations, are intimately involved with all the others.

---

*E_o and E have the units of energy per unit mass.

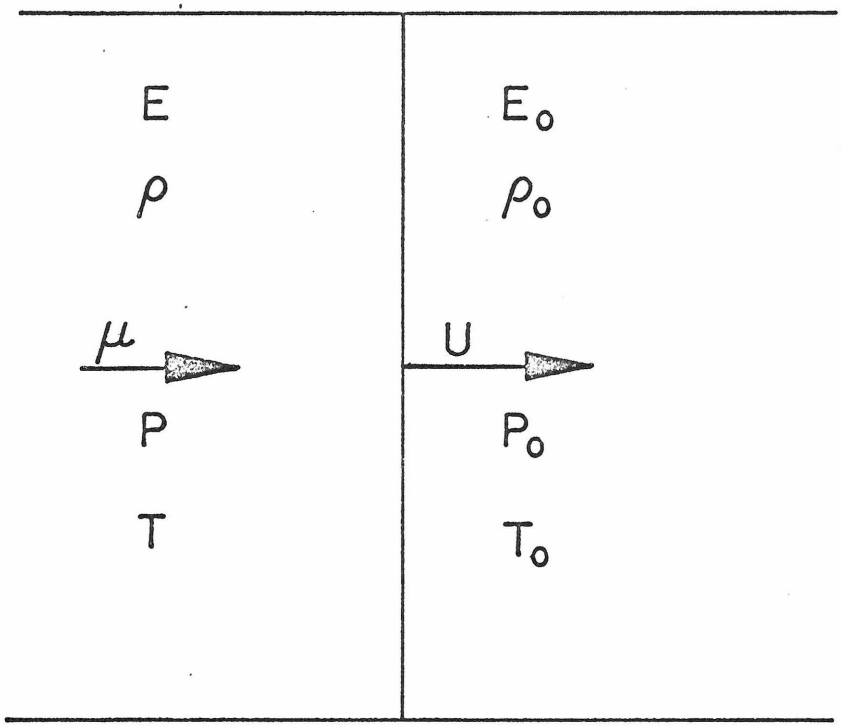

U = SHOCK VELOCITY
μ = PARTICLE VELOCITY
P = PRESSURE
T = TEMPERATURE
ρ = DENSITY
E = INTERNAL ENERGY
SUBSCRIPT o = "INITIAL" STATE

Figure 1. One-Dimensional Shock Propagating into a Stationary Medium

2. Conservation Equations-Per Unit Area/Unit Time

Consider a unit square in the plane of the shock in Figure 1 travelling with the wave at velocity U as pictured in Figure 2. If we choose this as our coordinate system, the relations for conservation of mass, momentum and energy flux may be easily deduced* from the fact that mass is flowing towards the unit area at velocity U and density ρ_o and leaving at velocity $(U-\mu)$ at density ρ.

a. Conservation of mass flux:

$$\rho_o U = \rho(U-\mu) \tag{1}$$

b. Conservation of momentum flux:

$$(\rho_o U)U + P_o = [\rho(U-\mu)](U-\mu) + P \tag{2}$$

c. Conservation of energy flux:

$$\frac{1}{2}(\rho_o U)U^2 + UP_o + U\rho_o E_o = \frac{1}{2}[\rho(U-\mu)](U-\mu)^2 + (U-\mu)P + (U-\mu)\rho E \tag{3}$$

*Laboratory coordinates, where the unit area is fixed in space, may also be used to derive the conservation relations.

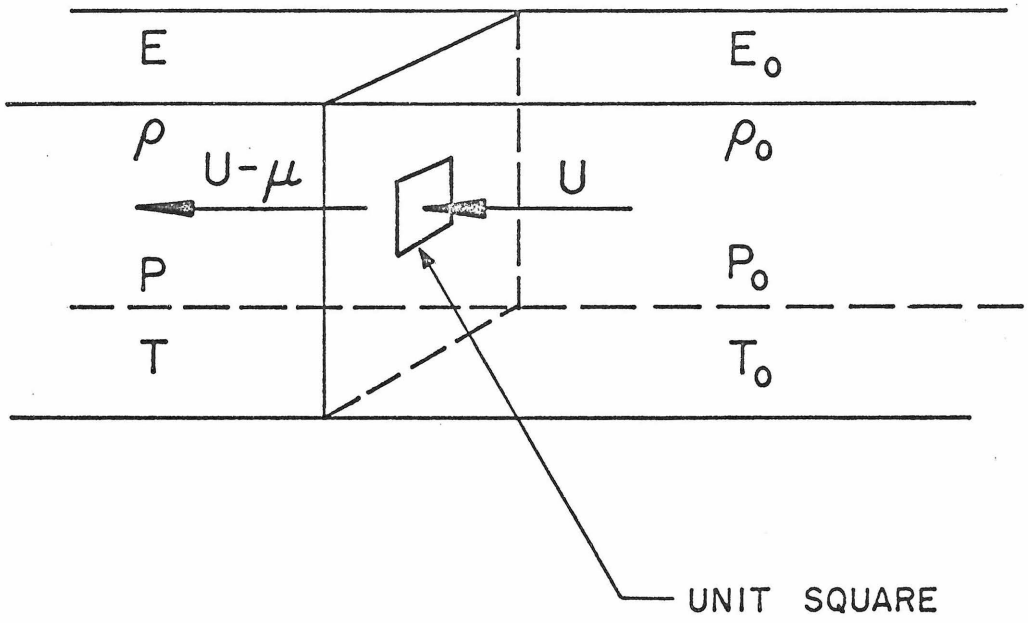

Figure. 2. Coordinate System

3. Conservation Relations

Equations (1) - (3) may be combined and rearranged (Appendix A) to give the more familiar expressions:

$$U = \frac{\mu}{1 - \rho_o/\rho} \qquad \text{(Mass)} \qquad (4)$$

$$P - P_o = \rho_o U \mu \qquad \text{(Mass + Momentum)} \qquad (5)$$

$$\Delta E = \frac{1}{2}(P_o + P)\left(\frac{1}{\rho_o} - \frac{1}{\rho}\right) \qquad \text{(Mass + Momentum + Energy)} \qquad (6)$$

or:

$$\Delta E = P_o\left(\frac{1}{\rho_o} - \frac{1}{\rho}\right) + \frac{1}{2}\mu^2 \qquad \text{(Mass + Momentum + Energy)} \qquad (7)$$

Equations (4) - (6) are known as the Rankine-Hugoniot (R-H) relations, the first two of which were first derived in 1870 by Rankine[1]. The correct form of the energy equation was first derived by Hugoniot[2] in 1889. Equation (7) is an alternate form of Equation (6) and is used in the following development.

It may be noted that the temperature T does not appear explicitly in any of Equations (1) - (7). The changes in thermal energy across the shock wave are accounted for in the internal energy change ΔE . From the basic laws governing thermodynamic systems it can be shown that (Appendix B):

$$dE = T\left(\frac{\partial P}{\partial T}\right)_V dV - PdV + C_V dT \qquad (8)$$

where $V = 1/\rho$.

Division by $C_V dV$ and rearrangement gives:

$$\frac{dT}{dV} + \left[\frac{(\partial P/\partial T)_V}{C_V}\right] T = \left[\frac{dE}{dV} + P\right] \tag{9}$$

If the coefficient of T is nearly constant[3] and the right-hand-side is a function of V only, this is an ordinary differential equation in T the solution of which is:

$$T = T_o\, e^{b(V_o - V)} + e^{-bV} \int_{V_o}^{V} e^{bV} \left[\frac{dE}{dV} + P\right] dV \tag{10}$$

where T_o is the initial temperature and $b = \left[\frac{(\partial P/\partial T)_V}{C_V}\right]$.

4. Specific Objective

Equations (4), (5) and (7) contain the 5 unknowns U, μ, ρ, P and ΔE. Assigning a thermodynamic equation-of-state for the material under consideration:

$$E = f(P,\rho) \tag{11}$$

provides a fourth relation in the same variables. Elimination of any three variables among these equations leads to a unique relation among the remaining pair. When this is in the form:

$$P = f(\rho) \tag{12}$$

it is called the "Hugoniot curve"[4] or "Hugoniot". However, since any pair of variables (excluding T) can be transformed to any other pair from the conservation relations, we shall use the term "Hugoniot" to refer to any of such pairs developed.

Unfortunately, for condensed media (dense gases, liquids and solids), the Hugoniot cannot be found directly because there is no satisfactory quantitative equation of state available for these substances. They are, generally, treated empirically, although a number of attempts have been made to solve the problem theoretically[5-9].

Since the Hugoniot represents a "cut" on the equation-of-state surface of the medium, it is clear that in the derivation of Equations (1) - (12) thermodynamic equilibrium prevails. This is further emphasized by the assumption that (a) either the shock front is a "discontinuity" and therefore infinitely thin, or (b) the measurements of P, ρ, T and E are made sufficiently far from the front that such

an equilibrium state obtains.

The specific objective of this study is to use a simple model to derive a relation which circumvents the need for a macroscopic equation-of-state, and leads to an analytical expression for the Hugoniot. This is done without recourse to the equilibrium state and the applicability of Equations (1) - (7) must be shown under these circumstances.

5. U vs. μ Linearity and Mass Conservation

An empirical solution to the determination of the Hugoniot is expressed experimentally in the well established relation between U and μ in the form:

$$U = A + B\mu \tag{13}$$

Here A represents the limiting shock velocity (U_o) in the medium when the shock wave is infinitely weak (i.e., when $\mu = 0$). Although Equation (13) seems to be generally valid*, it was noted by Duvall and Fowles[10] and Alder[11] that no satisfactory theoretical explanation of this relation has been given.

Part of the objective of this investigation is to determine if the proposed theory can explain the form of Equation (13). However, before doing this it is instructive to examine Equation (4), the conservation of mass flux, more closely:

$$U = \frac{\mu}{1 - \rho_o/\rho} = \frac{\mu}{1 - [1/(\rho/\rho_o)]} = \frac{\mu}{1 - \frac{1}{x}} \tag{14}$$

where $x \equiv \rho/\rho_o$. It is seen immediately that U and μ should be linearly related when μ is sufficiently high. That is, as μ increases, U increases and thus P increases (see Equation (5)). This leads to an increase in x. Therefore as μ increases, the denominator

*A number of exceptions to Equation (13) exist. In some cases a quadratic fit (i.e., $U = A + B\mu + C\mu^2$) has been found to better express the experimental U-μ data. In others, a generalized power series or other equations are used to fit the data.

of Equation (14) eventually approaches a limiting value where further changes in μ yield only very small changes in x and $1 - 1/x \simeq$ constant. The linearity of U and μ in these circumstances is apparent. This behavior is in accordance with Equation (13) only when $B\mu >> A$.

If radiation effects are neglected Zel'dovich and Raizer suggest the maximum compression ratio x (for $P \rightarrow \infty$) is $\simeq 4$ [12]. In this case $x_{max} \simeq 4$, $1 - 1/x_{max} \simeq 3/4$ and:

$$U \simeq 1.33\mu \tag{15}$$

Correspondence with Equation (13) (when $B\mu >> A$) implies that*:

$$B \simeq 1.33 \tag{16}$$

which is reasonably close to values reported for a number of substances[10].

It appears that there is some theoretical justification for the form of Equation (13) based solely on conservation of mass flux considerations, at least in the limit of very high pressures. It is interesting that this justification does not allow for higher order (quadratic and above) terms in μ .

---

* This result was pointed out by Alder[11].

6. Extrapolation to U_o

A further requirement of Equation (13) is that A ($\tilde{=} U_o$) should be equal to the sound velocity C_o of the medium*. From fits of many materials using this relation it has been shown that this approximation is valid to within $\sim 1.5\%$ (at least for metals[13]), although systematic discrepancies have been found[14].

Another objective of this study is to determine if the proposed theory can adequately describe the Hugoniot in the neighborhood of C_o.

Again some insight can be gained by further examination of Equation (14). Since $x \to 1$ (since $\rho \to \rho_o$) as $\mu \to 0$, it is clear that:

$$U_o \equiv \lim_{\mu \to 0} U = \lim_{\mu \to 0} \frac{\mu}{1 - \frac{1}{x}} \Longrightarrow \frac{0}{0} \tag{17}$$

a clearly indeterminate form. Application of L'Hôspital's rule[15] gives (Appendix C):

$$U_o = \lim_{x \to 1} \frac{d\mu}{dx} \tag{18}$$

Therefore it is clear that, if the quantity $d\mu/dx$ is finite at $x = 1$, the behavior of Equations (13) and (14) are in accordance with each other.

---

*Since an infinitely weak shock wave is a sound wave[4] $U_o = C_o$ and the two notations can be used interchangeably. However, in this study U_o is used to represent the extrapolated value of U (i.e., $\lim_{\mu \to 0} U$) in the theory while C_o is used for sound velocity data.

Part of the U-μ behavior in Equation (13) can be explained simply by examination of mass flux conservation. However, Equation (13) cannot be considered a true analytical representation of U vs. μ but only a convenient empirical form, since Equation (14) is clearly nonlinear between $\mu = 0$ and the sufficiently large value of μ that makes it linear.

In order to derive theoretically the form of the U-μ relation for comparison with Equation (13), it is necessary to develop a model for a shock wave.

B. DEVELOPMENT OF SHOCK MODEL

From Equation (7) the energy change across the shock front is given by:

$$\Delta E = P_o\left(\frac{1}{\rho_o} - \frac{1}{\rho}\right) + \frac{1}{2}\mu^2 \tag{7}$$

Since the only states considered in this study are those which consider relatively strong shocks and/or sonic conditions, it may be assumed that (Appendix D):

$$\frac{1}{2}\mu^2 >> P_o\left(\frac{1}{\rho_o} - \frac{1}{\rho}\right) \tag{19}$$

so that Equation (7) becomes:

$$\Delta E \doteq \frac{1}{2}\mu^2 \tag{20}$$

In combination with Equations (14) and (20) an independent expression for the internal energy change as a function of x would yield the Hugoniot.

1. "Receding" Shock

The model for a shock wave used in this study was inspired by the classic drawing shown in the first printing of Reference 4 and is reproduced in Figure 3. This "receding" shock may be visualized as depicted in Figure 4*. Here a microscopic view of the following process is depicted. A long slug of material of density ρ_o and characteristic spacing z_o has impacted a perfectly rigid wall at

*The current edition[4] discusses models of this type on pp. 129-130.

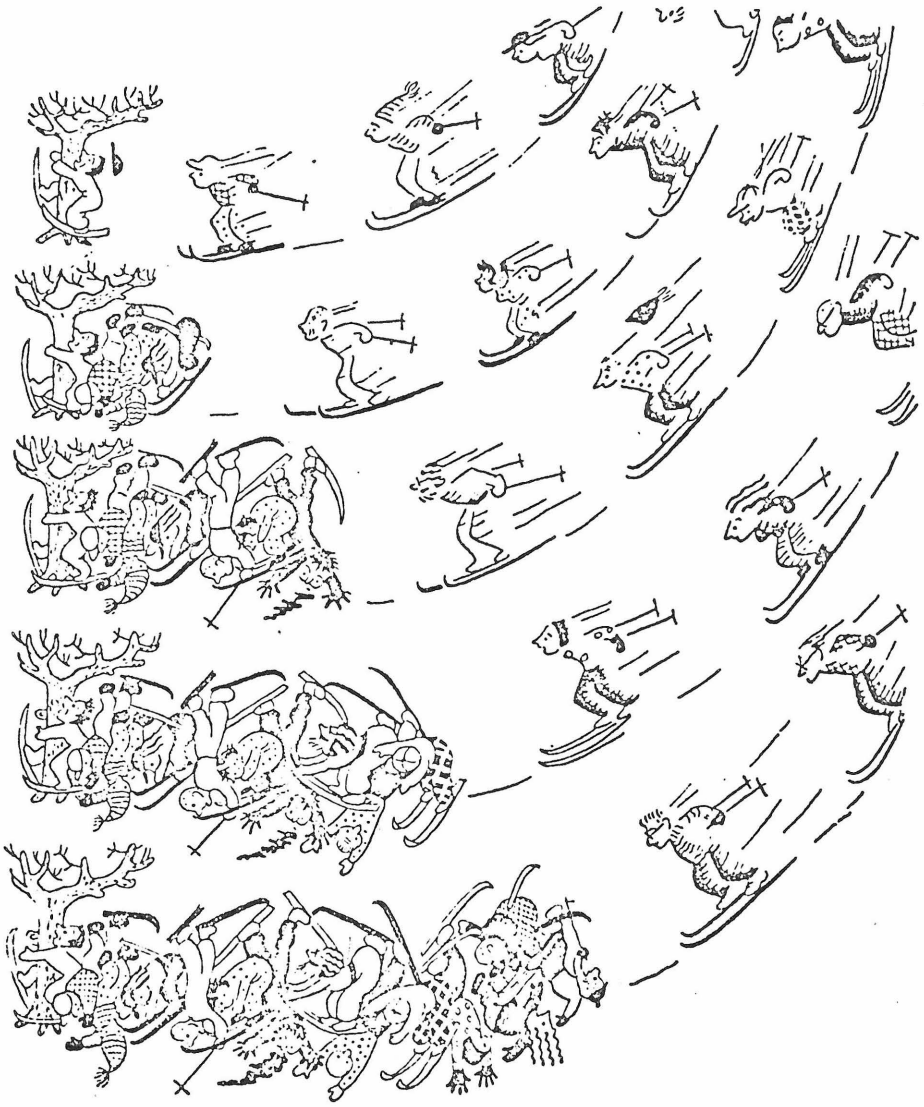

Figure 3. Receding Shock Wave--Skiers

[Reproduced with permission from Courant and Friedrichs, 1948.]

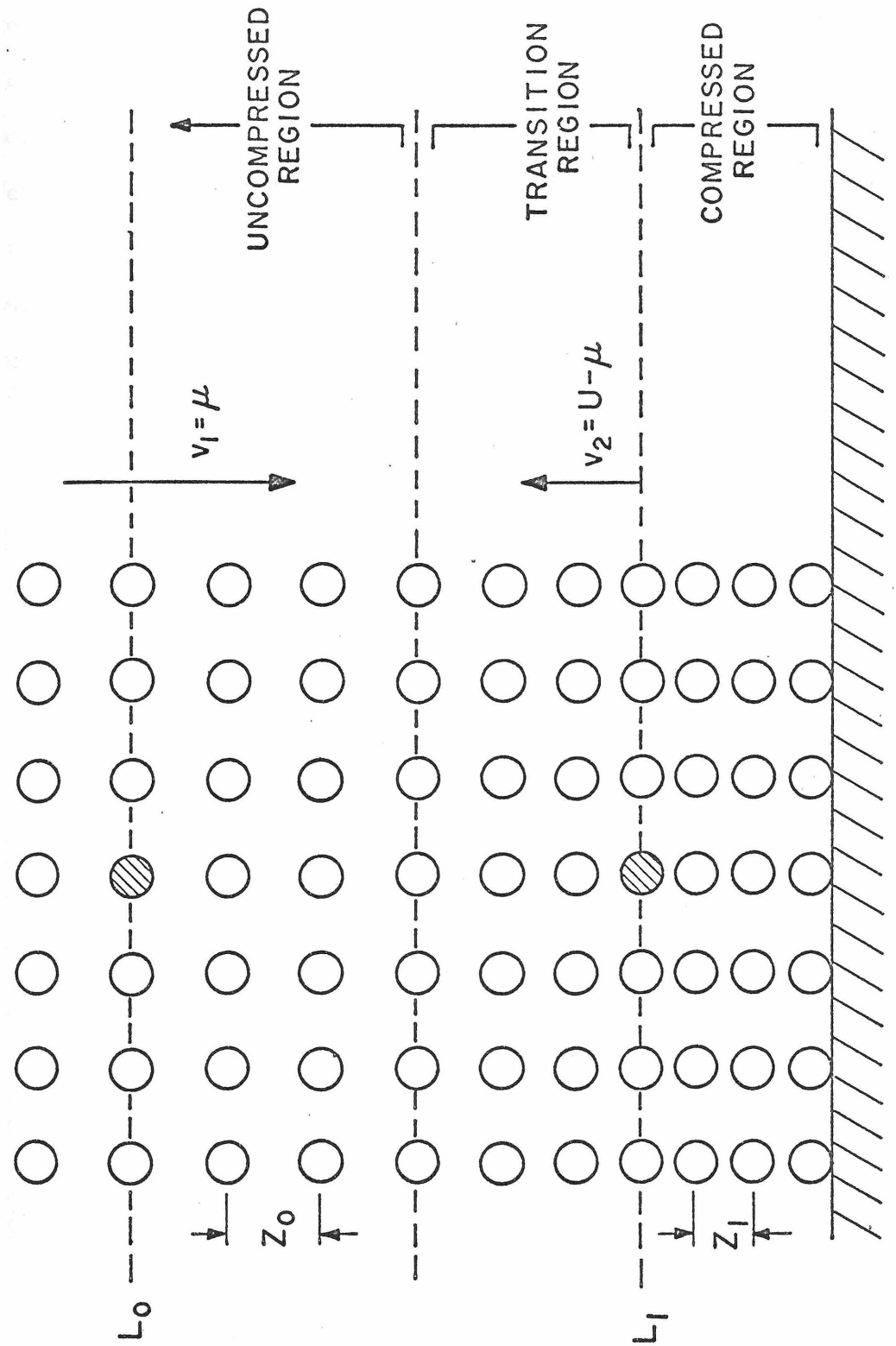

Figure 4. Receding Shock--Model

velocity v_1 . The material compresses to density ρ and characteristic spacing $z(z < z_o)$ and a disturbance, measured at the last fully compacted layer, proceeds upward at velocity v_2 (in laboratory coordinates). The molecules decelerate in the "thin" shock transition region indicated in Figure 4 and come to rest in the compressed region. It is noteworthy that, in this picture, it is assumed that the molecules compress <u>linearly</u> in the direction of motion (i.e., no transverse motion) at least throughout the transition region.

2. Transformation Equivalence Conditions

The model in Figure 4 can be made identical to the shock propagating in Figure 1 by making the physical conditions the same. For the conditions in Figure 1 the material ahead of the shock is not in motion. This is duplicated in Figure 4 if an observer is considered moving along with the original slug at v_1. In this case the velocity at which the disturbance propagates towards this observer should be the shock velocity U. From Figure 4 this is given by:

$$U = v_1 + v_2 \tag{21}$$

For this same observer the velocity of the particles behind the front in Figure 1 is μ and from Figure 4:

$$\mu = v_1 \tag{22}$$

Simultaneous solution of this with Equation (21) gives:

$$U - \mu = v_2 \tag{23}$$

Equations (22) and (23) are the transformation relations between the shocks depicted in Figures 1 and 4. It is clear that if the initial slug velocity v_1 is chosen equal to μ the two shocks are equivalent in all respects and are thus completely interchangeable. As a consequence the change in internal energy across the shock transition is still given by Equation (20).

Subsequent analyses may now be made in terms of the model in Figure 4 (with $v_1 = \mu$, $v_2 = U-\mu$) without loss of generality.

3. Energy Partitioning-Relaxation Effects

In developing the model, we wish to consider the change in internal energy of a molecule initially in layer L_o (a state far removed from the shock front) in Figure 4 (shaded circle) as it passes to the final state chosen as the first layer in the compressed zone and denoted by L_1 (see Figure 4). It remains to be shown that if such a change is determined, (a) it is related to the ΔE in Equation (20), and (b) it and the other R-H relations (Equations (4) - (7)) are valid for changes between layers L_o and L_1.

It is assumed that the transition region is sufficiently thin that the molecules at L_1 have not yet had time to relax to thermal equilibrium, and thus have had no net motion other than in the direction of the (one-dimensional) shock (i.e., linear compression). Under this assumption all of the energy change associated with the shock transition is accounted for by consideration of the difference in the configurational energy only, in the two states. This means that, at least for the change being considered, there is no temperature change across the shock front because the dwell time of the molecules in the transition zone is less than the thermal relaxation time (the pressure rise precedes the temperature rise!).

Since all of the internal energy change is accounted for between L_o and L_1, it is clear that the proposed change is identical to ΔE (per molecule) in Equation (20). Further, if mass, momentum and energy flux conservation is computed between layers L_o and L_1 it is found that Equations (1) - (3) are (necessarily) reproduced. Thus it is claimed that the particular method proposed for

evaluation of the energy change across a shock front is generally in accord with the R-H relations, Equations (4) - (7) (although not with Equations (8) - (10) which assume thermal equilibrium). That the change is only configurational depends on the validity of the assumption of a sufficiently thin transition region.

We are not concerned here with relaxation phenomena beyond L_1 and with how ΔE is partitioned into thermal and potential energy in the eventual equilibrium state. The choice of the positions of L_o and L_1 and the assumption of "thinness" of the transition zone allows a state (albeit a transient, non-equilibrium one) from which a sufficient evaluation of ΔE can be made.

This argument, fundamental to the proposed model, may be seen more clearly by considering the change ΔE as the sum of all changes taking place from L_o (the initial equilibrium state far removed from the shock front) to L_1 and from L_1 to the equilibrium state.

$$\Delta E = \Delta E^{(1)} + \Delta E^{(2)} \tag{24}$$

Each of these has a thermal and configurational part, and:

$$\Delta E^{(1)} = \Delta E^{(1)}_{\text{thermal}} + \Delta E^{(1)}_{\text{configurational}} \tag{25}$$

$$\Delta E^{(2)} = \Delta E^{(2)}_{\text{thermal}} + \Delta E^{(2)}_{\text{configurational}} \tag{26}$$

Because the transition zone is assumed "thin":

$$\Delta E^{(1)}_{\text{thermal}} = 0 \tag{27}$$

and Equation (25) becomes:

$$\Delta E^{(1)} = \Delta E^{(1)}_{\text{configurational}} \tag{28}$$

Also, since there are no pressure/density changes taking place between L_1 and the equilibrium state and the process is adiabatic (i.e., no radiative, magnetic, etc. processes occurring):

$$\Delta E^{(2)} = 0 \tag{29}$$

which implies that:

$$\Delta E^{(2)}_{\text{thermal}} = - \Delta E^{(2)}_{\text{configurational}} \tag{30}$$

The observed temperature rise in the equilibrium state is due solely to a decrease in the abnormally high configurational energy existing at L_1 as the "fluid" compressed in one dimension redistributes itself (i.e., relaxes) in three dimensions. The partition of energy between the thermal and configurational portions in the equilibrium state depends on the structure of the relaxed fluid. This reasoning, together with Equation (30) and the subsequent developments, is suggestive of a new way to compute temperatures along the Hugoniot (Appendix E).

Substitution of Equations (28) and (29) into Equation (24) leads to:

$$\Delta E = \Delta E^{(1)}_{\text{configurational}} \tag{31}$$

which will now be considered.

4. Energy Equation

The configurational energy difference required in Equation (31) may be computed by again considering the shaded molecule in Figure 4. The molecule in each of the states L_o and L_1 interacts with each of the other molecules of the system according to some, as yet unspecified, intermolecular potential function ϕ at the time the particular state exists. When these effects are integrated over all space, the total configurational energy for that state is obtained. Denoting this total energy by Φ Equation (31) becomes:

$$\Delta E = \Delta E^{(1)}_{\text{configurational}} = \frac{N}{M} \left[\Phi^{L_1} - \Phi^{L_o} \right] \tag{32}$$

where the superscripts refer to layers in Figure 4 and the coefficient (N is Avogadro's number and M is the molecular weight) reflects the fact that ΔE is in the units of energy/mass, while Φ will be considered in units of energy/molecule. Each of the potentials in Equation (32) may be further broken down into component parts by consideration of Figures 5a and 5b where the separate effect of each of the several regions in Figure 4 on Φ^{L_o} and Φ^{L_1} is shown.

In Figure 5a $\Phi_1^{L_o}$, $\Phi_2^{L_o}$, $\Phi_3^{L_o}$ and $\Phi_4^{L_o}$ represent, respectively, the separate contributions of configurational energy to Φ^{L_o} of material above L_o, material below L_o but above the transition region, material in the transition region and material below L_1. Similar definitions apply to $\Phi_1^{L_1}$, $\Phi_2^{L_1}$, $\Phi_3^{L_1}$ and $\Phi_4^{L_1}$ in Figure 5b. The distances R and R' reflect the fact that certain of the regions

Figure 5a

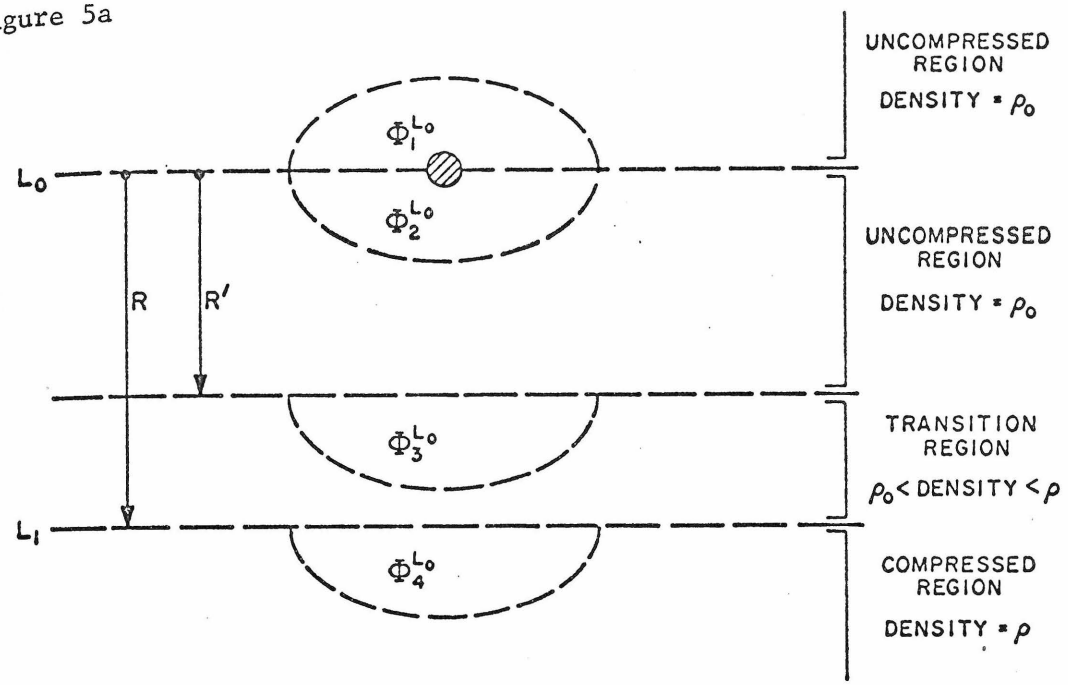

Figure 5b

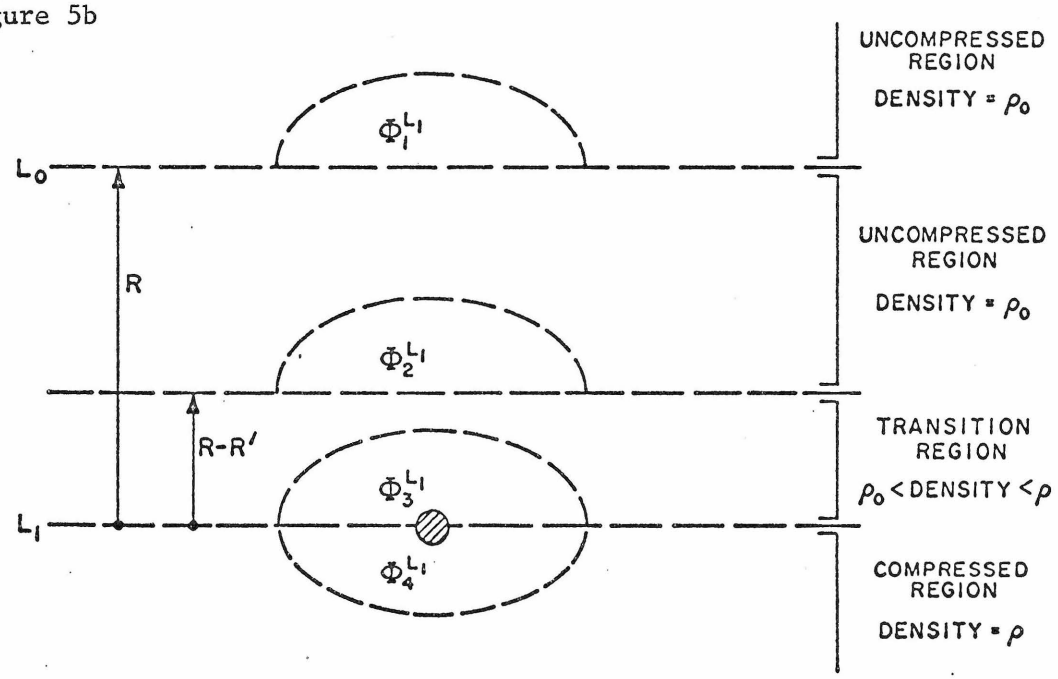

Figure 5. Potentials for Shaded Molecule

are not adjacent to the molecule under consideration. Of course R and R' are the same in Figures 5a and 5b, which are "snapshots" in the progress of the shaded molecule taken at different times. Clearly then, by the principle of superposition:

$$\Phi^{L_o} = \Phi_1^{L_o} + \Phi_2^{L_o} + \Phi_3^{L_o}(R') + \Phi_4^{L_o}(R) \tag{33}$$

$$\Phi^{L_1} = \Phi_1^{L_1}(R) + \Phi_2^{L_1}(R-R') + \Phi_3^{L_1} + \Phi_4^{L_1} \tag{34}$$

Considering Figure 5a, if R' (and R) are large (i.e., L_o is far removed from the shock front as previously assumed) then it is clear that:

$$\Phi_4^{L_o}(R) \simeq 0 \tag{35}$$

$$\Phi_3^{L_o}(R') \simeq 0 \tag{36}$$

and:

$$\Phi_1^{L_o} \simeq \Phi_2^{L_o} \tag{37}$$

leading to:

$$\Phi^{L_o} \simeq 2\Phi_2^{L_o} \tag{38}$$

By the same token, in Figure 5b:

$$\Phi_1^{L_1}(R) \simeq 0 \tag{39}$$

and:

$$\Phi^{L_1} \simeq \Phi_2^{L_1}(R-R') + \Phi_3^{L_1} + \Phi_4^{L_1} \tag{40}$$

If it is now assumed that (R-R') is very small (on the order of a few molecular spacings) and/or that the effects of $\Phi_3^{L_1}$ on the molecule at L_1 are not substantially different from those that would obtain if all the material in the transition region were at density ρ_o, then:

$$\Phi_3^{L_1} + \Phi_2^{L_1}(R-R') \simeq \Phi_1^{L_o} \tag{41}$$

That is, given the above assumption(s), the material above the molecule in L_1 is identical to that above the molecule in L_o; the net configurational contribution will be the same in both cases. Substitution of Equation (41) into Equation (40) gives:

$$\Phi^{L_1} \simeq \Phi_1^{L_o} + \Phi_4^{L_1} \tag{42}$$

Noting Equation (37) this may be written:

$$\Phi^{L_1} \simeq \Phi_2^{L_o} + \Phi_4^{L_1} \tag{43}$$

Substitution of Equations (43) and (38) into Equation (32) gives:

$$\Delta E = \frac{N}{M}\left[\Phi_4^{L_1} - \Phi_2^{L_o}\right] \tag{44}$$

The chain of reasoning leading to Equation (44) may be summarized by reference to Figure 4, noting that[16] "the molecule in L_o 'sees' above it a medium of density ρ_o and characteristic spacing Z_o; this is also true of the molecule in L_1, except for the material in the shock transition region. However, if this region is sufficiently thin, its effect on the configurational energy may be

ignored. In this case, the contributions to the configurational integral for material above L_o and L_1 are the same, and will cancel in the difference. The determination of ΔE, therefore, requires only an evaluation of the configurational energy of all material below the molecule at L_1 minus that below the molecule at L_o. Since again, L_o is far removed from the shock front, we may take this difference as" in Equation (44).

Because of the way in which the states L_o and L_1 are picked, the errors in Equations (35), (36), and (39) can be made as small as desired by choosing R as large as needed, and the error in Equation (44) depends solely on the error in the assumptions leading to Equation (41).

The terms in Equation (44) are more usefully defined by:

$$\Phi_4^{L_1} = \psi(\rho,z) + \psi^{L_1}(z_o) \tag{45}$$

$$\Phi_2^{L_o} = \psi(\rho_o,z_o) + \psi^{L_o}(z_o) \tag{46}$$

where $\psi(\rho,z)$ is the configurational energy of a single isolated molecule positioned a distance z from a semi-infinite medium of density ρ, and $\psi^{L_1}(z_o)$, $\psi^{L_o}(z_o)$ are the configurational energy contributions of the <u>other</u> molecules in layers L_1 and L_o, respectively. Since these molecules remain at spacing z_o throughout the transition (see Figure 4, noting the earlier assumption of linear compression):

$$\psi^{L_o}(z_o) = \psi^{L_1}(z_o) \tag{47}$$

and the terms will cancel in Equation (44), which now becomes:

$$\Delta E = \frac{N}{M} [\psi(\rho,z) - \psi(\rho_o,z_o)] \tag{48}$$

Based on the definitions of ${}^{L_1}\Phi$ and ${}^{L_o}\Phi$ and the subsequent development, it should be clear that the $\psi(\rho,R)$ are computed by summation of the interactions between the shaded molecule and each of the molecules in the half-space indicated in Figure 6.

When this interaction is described by an intermolecular potential function ϕ, and this potential is assumed to be dependent only on the distance separating molecules r_i (i.e., ϕ is a pair potential*) $\phi = \phi(r_i)$ and:[17,18]

$$\psi(\rho,z) = \sum_{i=1}^{N_h} \phi(r_i) , \quad r_i \geq z \tag{49}$$

where N_h is the number of molecules in the half-space and i is the index for counting each of the N_h interactions; on a per unit volume basis it is clear that $N_h \sim \rho$.

Evaluation of Equation (49) is made difficult by the fact that values for the r_i are generally unknown since the structure depicted in Figure 6 is unrealistic (other than for perfect crystals). Furthermore, even if the r_i were known at any instant of time, they would be changing continuously because of molecular fluctuations**.

---

* We ignore three-body (and higher) interactions.

** Even for solids with a reasonably rigid lattice structure, vibrational motion around the fixed position would result in variations in the r_i. For liquids, of course, molecular mobility is great and large variations in the r_i are expected.

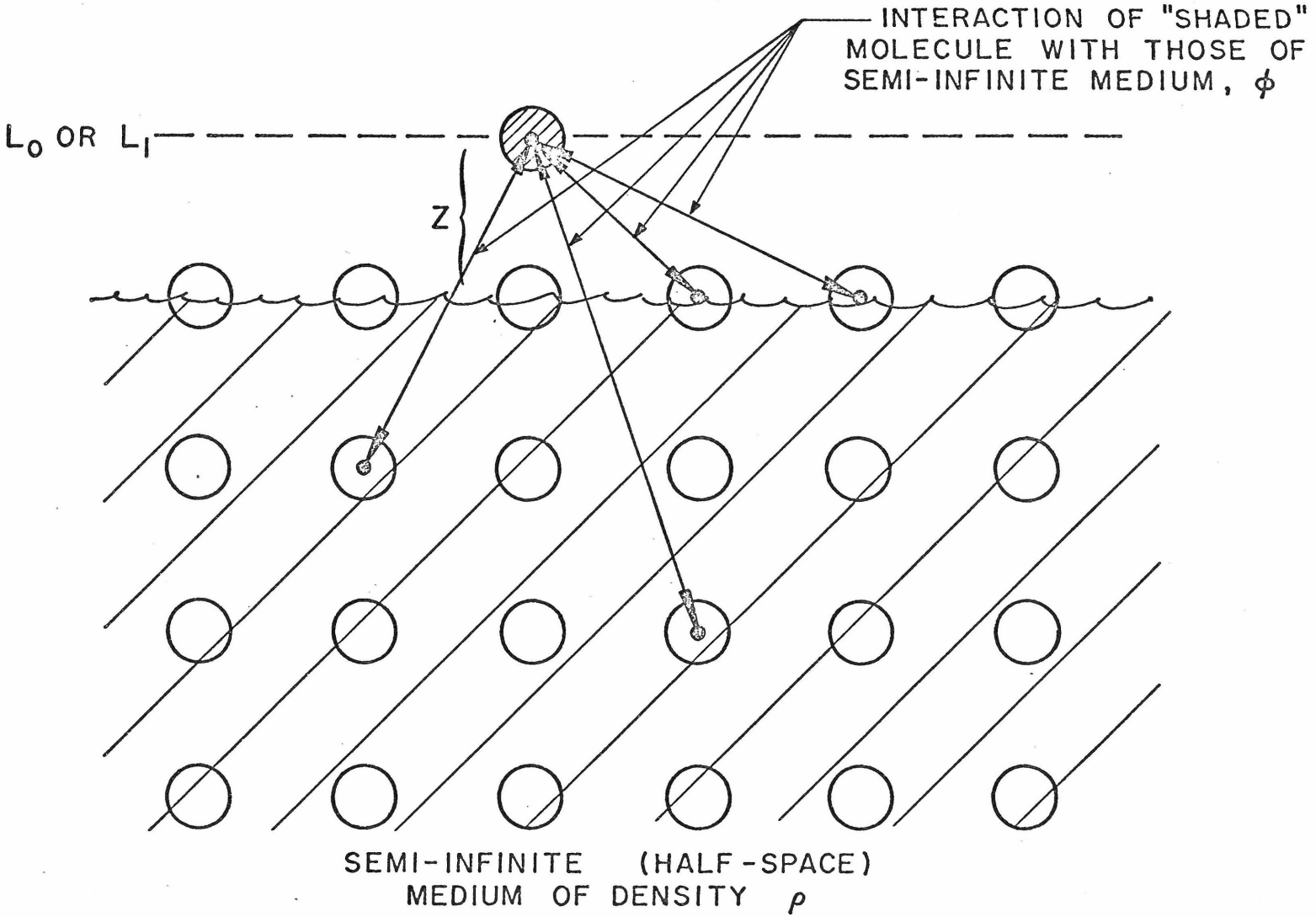

Figure 6. Interactions for Shaded Molecule

Variations in molecular positions imply that $r_i = r_i(t)$ and that $\psi = \psi(t)$. To avoid this difficulty N_h is usually chosen large enough (on the order of 10^{23}; a mole) so that the sum of the variations will be essentially constant in time. However, this still leaves the difficulty of assigning a set of positions to the molecules for evaluation of the summation and adds the further difficulty of requiring a very large number of calculations. Equation (49) is, instead, evaluated from statistical mechanics.

5. Integration of Pair Potential

Consider a cartesian coordinate system (x',y',z') centered at the shaded molecule in Figure 6. The average number of molecules at a distance between x',y',z' and x'+ dx', y'+ dy', z'+ dz' from that molecule (in the half-space) is $(\rho N/M)\, g(r)\, dx'dy'dz'$ where $g(r)$ is the "pair distribution function" (PDF)[17] or "radial distribution function" (RDF)[19,20] defined as the probability of finding a molecule at r (i.e., in the volume element dx'dy'dz') if there is a molecule at the origin ($g(r)$ is normalized to unity at large r) and r is generally a function of x', y' and z'*. The average potential energy of interaction with the molecules in the volume element is $(\rho N/M)\, g(r)\, \phi(r)\, dx'dy'dz'$ and integration over the half-space gives the total configurational energy (i.e., $\psi(\rho,z)$ in Equation (49)):

$$\psi(\rho,z) = \int_{z'=z}^{\infty} \int_{y'=0}^{\infty} \int_{x'=0}^{\infty} (\rho N/M)\, g(r)\, \phi(r)\, dx'dy'dz' \qquad (50)$$

For convenience the z' axis has been chosen colinear with z, "downward" being positive (see Figure 6). Since ρ (and ρ_o) are, by definition, independent of x', y' and z' (they are the mean continuum densities for the media) the terms of Equation (48) become:

$$\psi(\rho,z) = (\rho N/M) \int_{z'=z}^{\infty} \int_{y'=0}^{\infty} \int_{x'=0}^{\infty} g(r,\rho,T)\, \phi(r)\, dx'dy'dz' \qquad (51)$$

$$\psi(\rho_o,z_o) = (\rho_o N/M) \int_{z'=z_o}^{\infty} \int_{y'=0}^{\infty} \int_{x'=0}^{\infty} g(r,\rho_o,T_o)\, \phi(r)\, dx'dy'dz' \qquad (52)$$

*Note that the PDF is state-dependent, i.e., $g(r,\rho,T)$.

It is assumed that the effect of $g(r)$ on the two integrals is small and/or approximately the same (numerically) and will therefore be unimportant and/or cancel in the difference in Equation (48). The above become:

$$\psi(\rho,z) = (\rho N/M) \int_{z'=z}^{\infty} \int_{y'=0}^{\infty} \int_{x'=0}^{\infty} \phi(r)\, dx'dy'dz' \tag{53}$$

$$\psi(\rho_o,z_o) = (\rho_o N/M) \int_{z'=z_o}^{\infty} \int_{y'=0}^{\infty} \int_{x'=0}^{\infty} \phi(r)\, dx'dy'dz' \tag{54}$$

Integration of Equations (53) and (54) and further development of Equation (48) require the specification of the pair-potential function $\phi(r)$.

C. PAIR POTENTIAL FUNCTIONS

That there are attractive (cohesive) forces between molecules is demonstrated by the fact that all molecules tend to aggregate at low temperatures[21,22]. There must also be repulsive forces between molecules (at least at short distances) or matter could not exist in the first place[21,22]. These facts suggest formation of an intermolecular function of the form:

$$\phi = \phi_{repulsion} - \phi_{attraction} \tag{55}$$

although an equation of this type appears to be somewhat arbitrary[21,5].

The forces leading to $\phi_{repulsion}$ are called <u>short-range</u> forces because they dominate at short distances. They are also known as <u>valence forces</u> or <u>chemical forces</u>[5] because they "arise when molecules come close enough together for their electron clouds to overlap"[5]. This description is the source of the additional name for $\phi_{repulsion}$, viz., overlap energy[21].

The forces leading to $\phi_{attraction}$ are called <u>long-range</u>[5] forces because they predominate at long distances (compared to the short-range forces; at very long ranges, of course, $\phi_{repulsion} = 0 = \phi_{attraction}$). They are also called <u>van der Waals forces</u>[21,23].

Rigorous treatments of repulsive forces are apparently very difficult to generalize and in most cases only particular pairs of molecules are studied[5]. However, it is known that this overlap energy can asymptotically be represented by an equation of the form:

$$\phi_{repulsion} \simeq P(r)\, e^{-\alpha r} \tag{56}$$

where α is a molecular parameter and $P(r)$ is a polynomial in both positive and negative powers of r [5,17,21-23]. Unfortunately, it turns out that when Equation (56) is reasonably accurate r is so large that $\phi_{attraction} >> \phi_{repulsion}$ and little use can be made of the results. Because of this, empirical functional forms have been used for the repulsive energy. The two most widely used are:

$$\phi_{repulsion} = ar^{-n} \tag{57}$$

$$\phi_{repulsion} = ae^{-\alpha r} \tag{58}$$

where a, n, α are molecular parameters. Forms of this type are chosen for purposes of simplifying calculations and it appears that "there is no compelling theoretical reason to prefer any (other) simple form(s)...." [21].

The long-range attractive forces are amenable to fairly rigorous quantum mechanical treatment and are of four types; electrostatic, induction, dispersion and resonance. These contributions all vary inversely as powers of intermolecular separation r [5]. A full discussion of each of these four types of attractive forces may be found in Reference (5). Generally the attractive energy is written in the form:

$$\phi_{attraction} = br^{-6} + cr^{-8} + dr^{-10} + \cdots \tag{59}$$

where b, c and d are molecular parameters. In the simplest cases $c = d = \cdots = 0$ leaving the most common form, br^{-6}.

It has been shown [24-26,17,27-31] that for metals the long-range energy has a decreasing oscillatory form and that regions of .

repulsion and attraction both exist. This is substantively different from Equation (59), which is typically applied to non-metals (insulators), in that only attractive forces are involved in that case. This difference will be seen more clearly in the following paragraphs. Egelstaff[17] has suggested that for metals the "attractive" energy might have the form:

$$\phi_{attraction} = br^{-3} e^{-\beta r} \cos \gamma r \tag{60}$$

where b, β and γ are molecular parameters.

Equations (57) - (60) may be combined in Equation (55) in four ways to give "general" expressions for the pair-potential function. In each case the dependent variable is the center-to-center molecular separation r and, clearly, $\phi = \phi(r)$ only. Thus Equation (55) becomes:

$$(r) = ar^{-n} - (br^{-6} + cr^{-8} + dr^{-10}) \tag{61}$$

$$(r) = ae^{-\alpha r} - (br^{-6} + cr^{-8} + dr^{-10}) \tag{62}$$

$$\phi(r) = ar^{-n} - br^{-3} e^{-\beta r} \cos \gamma r \tag{63}$$

$$\phi(r) = ae^{-\alpha r} - br^{-3} e^{-\beta r} \cos \gamma r \tag{64}$$

Many of the more commonly used potential functions may be derived from these equations by appropriate choice of the parameters a, b, n, α, β, γ . The functional difference between those with (Equations (63) and (64)), and without (Equations (61) and (62)) long-range oscillatory (LRO) behavior is shown in Figure 7.

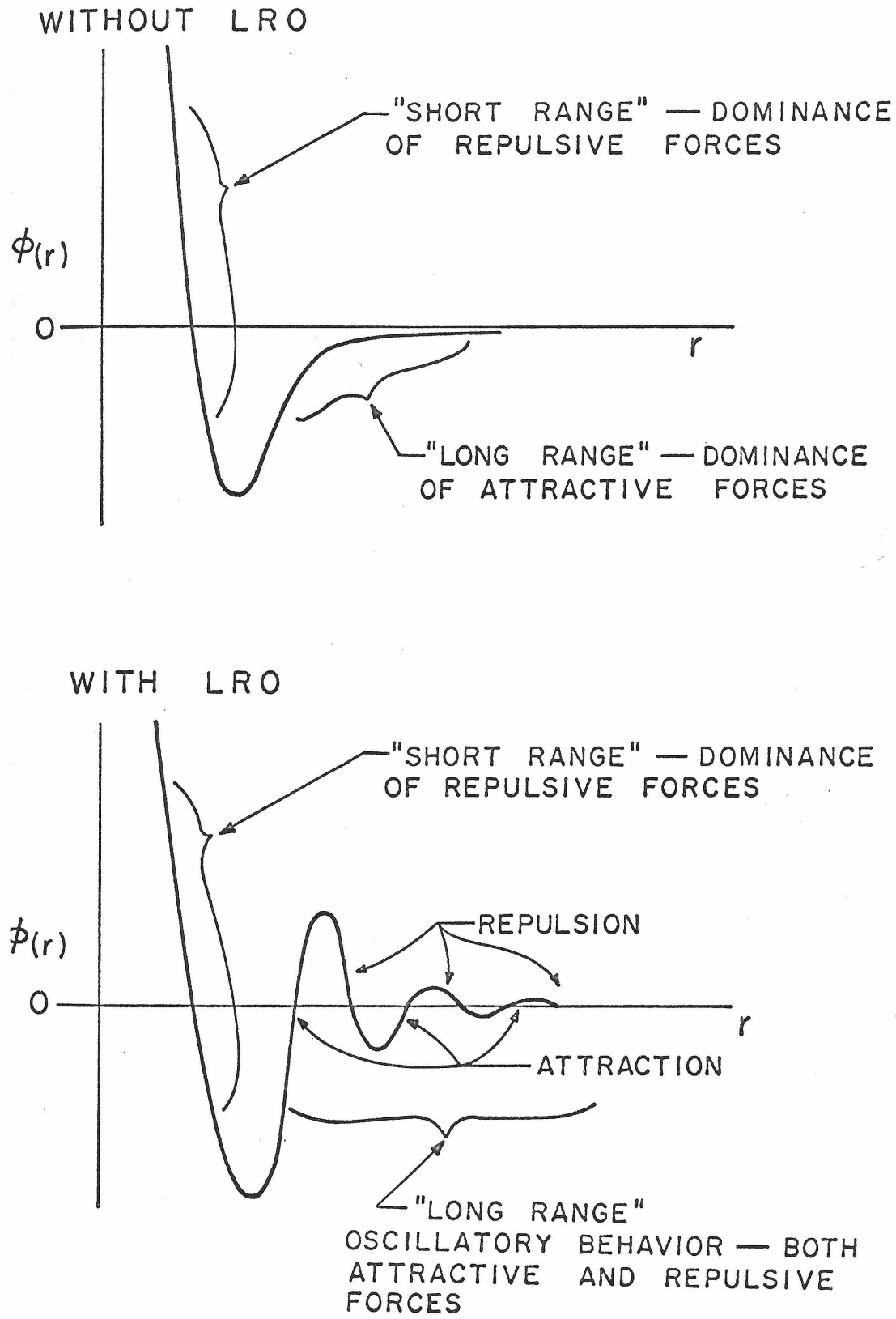

Figure 7. LRO Behavior

1. List of Suggested Potential Functions

Table 1 is a partial list of the many pair-potential functions suggested over the past 40 years*. Some of these can be derived from Equations (61) - (64) with appropriate choice of the parameters. Number 23, the numerical potential, has no analytical form but consists of a data set of potential energy vs. distance which purports to best represent the actual pair-interaction.

---

*Angle-dependent pair potential functions have been excluded, but for working purposes they are usually averaged over all orientations to yield an angle-independent form similar to those in Table 1.

Table 1

PAIR POTENTIAL FUNCTION FORMS

$\phi(r) = f(r)$

No.	Name	f(r)	Parameters	References
1	Hard Sphere	$\begin{cases} \infty, & r < a \\ 0, & r > a \end{cases}$	a	5, 32, 17, 33
2	Square Well	$\begin{cases} \infty, & r < a \\ -b, & a < r < c \\ 0, & r > c \end{cases}$	a,b,c	5, 32, 34, 35
3	Bireciprocal or n-m or Mie-Lennard-Jones	$ar^{-n} - br^{-m}$	a,b,n,m	21,36,23,5,37,22,38 32,39,14,35,40,41
4	n-6	$ar^{-n} - br^{-6}$	a,b,n	21,42-45,16
5	12-6 or Lennard-Jones	$ar^{-12} - br^{-6}$	a,b	36,23,46,5,22,47,38 48-50,32,51-54,17,33, 55
6	Kihara	$\begin{cases} \infty, & r < c \\ a(r-6)^{-12} - b(r-c)^{-6}, & r \geq c \end{cases}$	a,b,c	34,56,57,35,45,33,55
7	Extended n-6	$ar^{-n} - (br^{-6} + cr^{-8} + dr^{-10})$	a,b,c,d	36
8		$ar^{-12} - (br^{-6} + cr^{-3} + dr^{-4})$	a,b,c,d	58

Table 1 (continued)

No.	Name	f(r)	Parameters	References
9	Repulsive	ar^{-n}	a,n	5,59,49,60
10	Polynomial	$a+br+cr^2+dr^3+er^4$	a,b,c,d,e	41
11	Guggenheim-McGlashan	$\begin{cases} \infty & , r < r_1 \\ a+b(r-c)^2+d(r-c)^3(2c-r) & r \le r \le r_2 \\ ar^{-6} & , r > r_2 \end{cases}$	a,b,c,d,r_1,r_2,r_3	56,50,55
12	Morse	$ae^{-\alpha r} - be^{-\beta r}$	a,b,α,β	37,49,61,45,62,41,55
13	Exponential-6, or Modified Buckingham	$\begin{cases} \infty & , r \le r_1 \\ ae^{-\alpha r} - br^{-6}, & r > r_1 \end{cases}$	a,b,α,r_1	21,36,59,5,37,49,34,63,64,35,17,45,53,65,66,41,67-69,55
14	Lauger	$ae^{-\alpha r} - (br^{-6} + cr^{-9})$	a,b,c,α	54
15	Yntema-Schneider or Buckingham	$ae^{-\alpha r} - (br^{-6}+ cr^{-8})$	a,b,c,α	5,62
16	Buckingham-Corner	$\begin{cases} ae^{-\alpha r}- (br^{-6}+ cr^{-8})e^{-4(r_1/r-1)^3}, & r \le r_1 \\ ae^{-\alpha r}- (br^{-6}+ cr^{-8}), & r \ge r_1 \end{cases}$	a,b,c,α,r_1	5

Table 1 (continued)

No.	Name	f(r)	Parameters	References
17	Phillipson-Morse-Dalgarno	$\begin{cases} ae^{-\alpha r} - be^{-\beta r}, & r \leq r_1 \\ cr^{-6}, & r > r_1 \end{cases}$	a,b,α,β,r_1	62
18	Exponential or Sutherland	$\begin{cases} \infty, & r < r_1 \\ ae^{-\alpha r}, & r > r_1 \end{cases}$	a,α,r_1	62
19	Munn-Smith	$\frac{1}{r}[a + e^{-\alpha r^2}(b + cr^2 + dr^4 + er^6)]$	a,b,c,d,e,α	41,55
20		$ar^{-3}e^{-\alpha r}\cos \beta r$	a,α,β	25
21		$ae^{-\alpha r} + br^{-3}\cos(\beta r + \gamma)$	a,b,α,β,γ	26
22		$ar^{-n} + br^{-3}e^{-\alpha r}\cos \beta r$	a,b,α,β,n	17
23	Numerical	No functional form		70,71,27,72, 30,33,73,74
24	Quantum-Mechanical	$P(r)e^{-\alpha r} + \sum_{i=0}^{\infty} a_i r^{-i}$	P ≡ polynomial	21,23,22,55

2. Choice for Work

In this study the only forms of interest were numbers 4 and 7 in Table 1 which are immediately derivable from Equation (61) (in the former case $c = 0 = d$).

This choice was made on the basis of simplicity, since no a priori judgments could be made on the success or failure of the shock model. It was felt that more "realistic" potential functions could not be justified until the reasonableness of the model itself was demonstrated.

It was (and is) recognized that a single exponent n could not completely describe repulsion over a wide region[64,53] and that, at least for metals, the attractive term might be very unrealistic[75]. However, since most of the data being dealt with in this study are concerned with strong shock waves, pressures are generally high, $\sim$10 - 100 Kbar, and we should be operating far "up" in the repulsive region in Figure 7. Examination of all equations with an exponential repulsive term (Equations (62) and (64) and numbers 12-18 in Table 1) show that a (spurious) maximum must be reached with these functions at small r (since $e^{-\alpha r} \Rightarrow 1$ as $r \Rightarrow 0$). In order to assure that sufficient repulsion exists (under shock compression) in these equations a and α would have to be adjusted arbitrarily to avoid this maximum. On the other hand the repulsive form chosen has the desirable property that $r^{-n} \Rightarrow \infty$ as $r \Rightarrow 0$ for any value of n (called the "repulsive exponent").

Furthermore, it was felt that the attractive form was reasonably justified because: (a) at the pressures mentioned, repulsion is

expected to dominate (i.e., $\phi_{repulsion} >> \phi_{attraction}$) and (b) the LRO behavior of metals is not found in every determination of the potential function for these materials[76] and should not therefore be considered as firmly established; in other instances the computed potentials show only slight LRO behavior[30].

The potential chosen for most of the calculations in this study is the n-6 potential (Number 4 in Table 1):

$$\phi(r) = ar^{-n} - br^{-6} \tag{65}$$

The parameters a and b may be specified in terms of molecular quantities by consideration of Figure 8. Here σ is the so-called[23, 5, 22] "collision diameter" determined from the condition:

$$\phi(\sigma) = 0 \tag{66}$$

The "depth of the potential well"[5] ε is determined noting that:

$$\phi(r_o) = -\varepsilon \tag{67}$$

is the minimum value of $\phi(r)$. From elementary calculus:

$$\left[\frac{d\phi(r)}{dr}\right]_{r=r_o} = 0 \tag{68}$$

at this point. Use of Equations (66) - (68) with Equation (65) leads to the usual form of the n-6 potential (see Appendix F).

$$\phi(r) = \varepsilon \frac{(n/6)^{n/n-6}}{n/6 - 1} \left[\left(\frac{\sigma}{r}\right)^n - \left(\frac{\sigma}{r}\right)^6\right] \tag{69}$$

and:

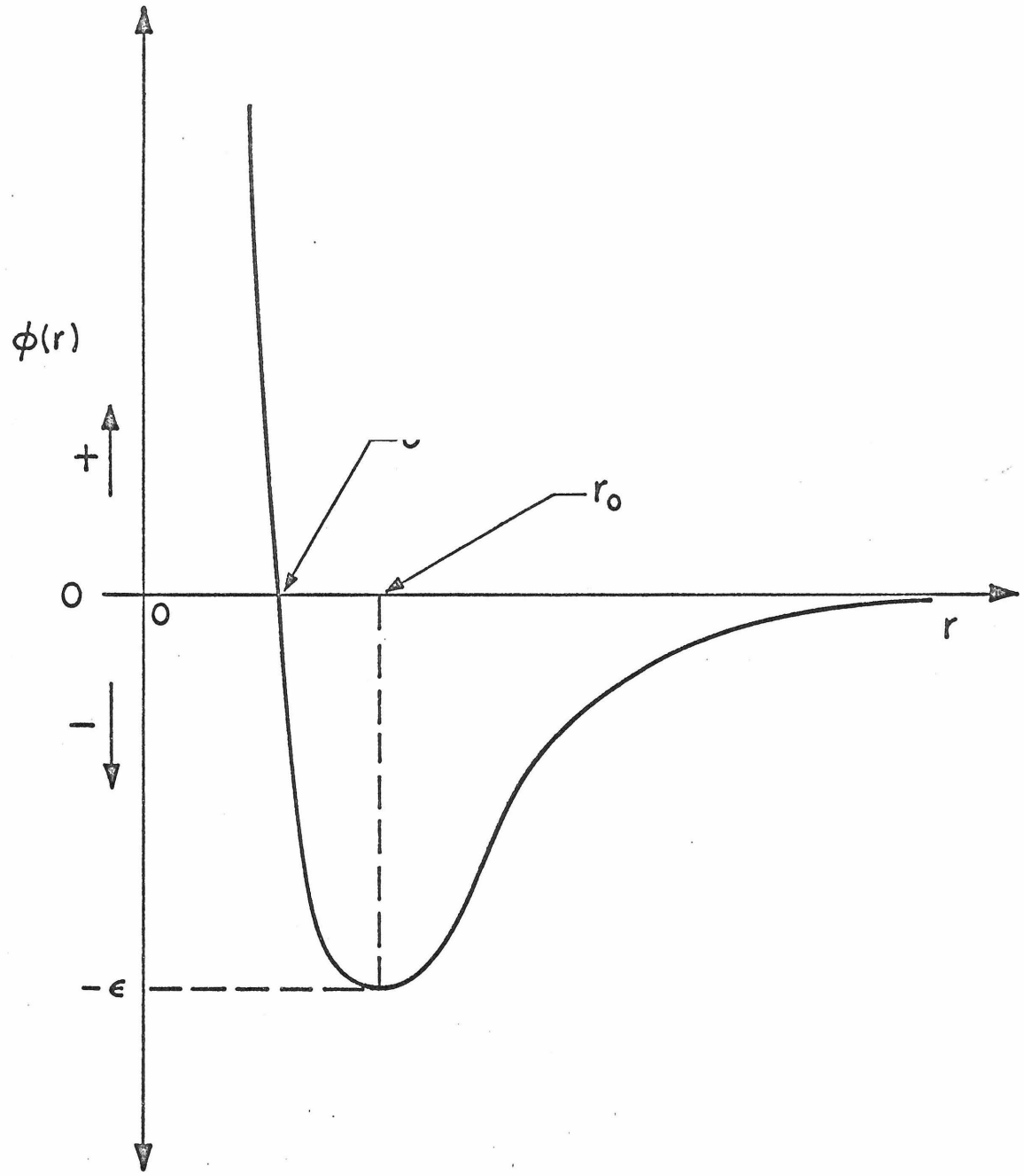

Figure 8. n-6 Potential

$$r_o = (n/6)^{\frac{1}{n-6}} \sigma \tag{70}$$

Letting :

$$f(n) = \frac{(n/6)^{\frac{n}{n-6}}}{n/6 - 1} \tag{71}$$

Equation (69) can be written:

$$\phi(r) = \varepsilon f(n) \left[\left(\frac{\sigma}{r}\right)^n - \left(\frac{\sigma}{r}\right)^6 \right] \tag{72}$$

Equation (72) is the pair potential function to be used in Equations (53) and (54) for determination of the configurational energy of the shaded molecule in Figure 6.

3. Special Properties of the n-6 Potential

a. The 6-6 potential. At first glance it would appear that Equation (69) is valid only for $n > 6$; $\phi(r)$ should be zero for $n = 6$. That this is not so may be demonstrated by carrying out the limiting process, as in Appendix G. The resulting equation is:

$$\phi_6(r) = 6\varepsilon\, e\left(\frac{\sigma}{r}\right)^6 \ell n\left(\frac{\sigma}{r}\right) \tag{73}$$

where $e = 2.71728...$ the base of natural logarithms and the subscript 6 indicates $n \equiv 6$. Equation (73) reproduces all of the features of Equation (69) as expressed by Equations (66) - (68); i.e., $\phi_6(\sigma) = 0$, $\phi_6(r_o) = -\varepsilon$, and $\left(\frac{d\phi_6}{dr}\right)_{r=r_o} = 0$ (see Appendix G). The significance of Equation (73) will be discussed in later sections, but it is important to recognize such a potential exists and that it is compatible with the more familiar form in Equation (69).

b. The n < 6 potential. Consideration of $n \equiv 6$ leads directly to the question; can n be < 6 ? Again, at first glance it would seem that for small r in Equation (69):

$$\left|(\sigma/r)^n\right| < \left|(\sigma/r)^6\right| \tag{74}$$

for $n < 6$ and the potential would be negative (i.e., attractive!). However, this sign change is corrected for by the coefficient $(1/(n/6 - 1))$ in Equation (69) such that $\phi(r) > 0$ for every value of $n > 0$ when $r < \sigma$ *. Therefore it appears that Equation (69) is also

---

*If $n < 0$ the leading term of Equation (69) would have an r^{+n} dependence and $\phi(r)$ would increase at very large values of r.

valid for all values of n from 0 to 6. In fact, at $n = 0$ it has the form (Appendix H):

$$\phi_o(r) = \varepsilon \left[\left(\frac{\sigma}{r}\right)^6 - 1\right] \tag{75}$$

which also is compatible with Equations (66)-(68) although in a "degenerate" form (Appendix H).

As the repulsive exponent n decreases, the potential is said to become "softer" in that the repulsive part of the potential curve (see Figure 7) is not as steep as with larger values of n.

A key question in the application of Equation (69) for $n < 6$ is: Is the $n < 6$ potential <u>monotonically</u> softer for all values of n between 6 and 0? Stated another way the question may be phrased as: Is Equation (69) monotonically "harder" for all values of n from $n = 0$ to $n = \infty$?

These questions are important, since careful examination of Equation (69) shows that for $n < 6$ it would more properly be written:

$$\phi(r) = \varepsilon \frac{(n/6)^{n/n-6}}{1 - n/6} \left[\left(\frac{\sigma}{r}\right)^6 - \left(\frac{\sigma}{r}\right)^n\right] \tag{76}$$

The roles of the repulsive and attractive terms in Equations (55) and (65) have been reversed; the attractive term now depends on the exponent n. This is unrealistic* and Equation (76) is considered not as the sum of attractive and repulsive terms, but simply as an overall expression describing $\phi(r)$ vs. r. This viewpoint is not unreasonable considering the somewhat arbitrary assumption of superposition of attractive and repulsive terms in Equation (55) to begin with. Since

*In particular the attractive term no longer has the r^{-6} dependence of insulators.

It is no longer obvious that as n decreases the repulsive term gets softer (because the repulsive term cannot be identified); it will suffice to show that as n decreases, $\phi(r)$ decreases in the repulsive region (i.e., where $r < \sigma$). This question is examined in Appendix I, where it is proven that Equation (69) (or Equation (76)) is monotonically increasing with n ("harder") for all values of n from 0 to ∞ for $(\sigma/r) > 1$.

Based on this discussion it is clear that the n-6 potential exists for all values of $n \geq 0$ and that Equation (69) may be used in all cases except when $n \equiv 6$ in which case Equation (73) applies.

To compare these functions over a range of values of n , Figure 9 has been prepared in the form:

$$\frac{\phi(r)}{\varepsilon} = f(\sigma/r) \tag{77}$$

for each of several values of n . It is notable that the variation in the (appearance of the) potential with n , over the whole range of n, is not extraordinary!

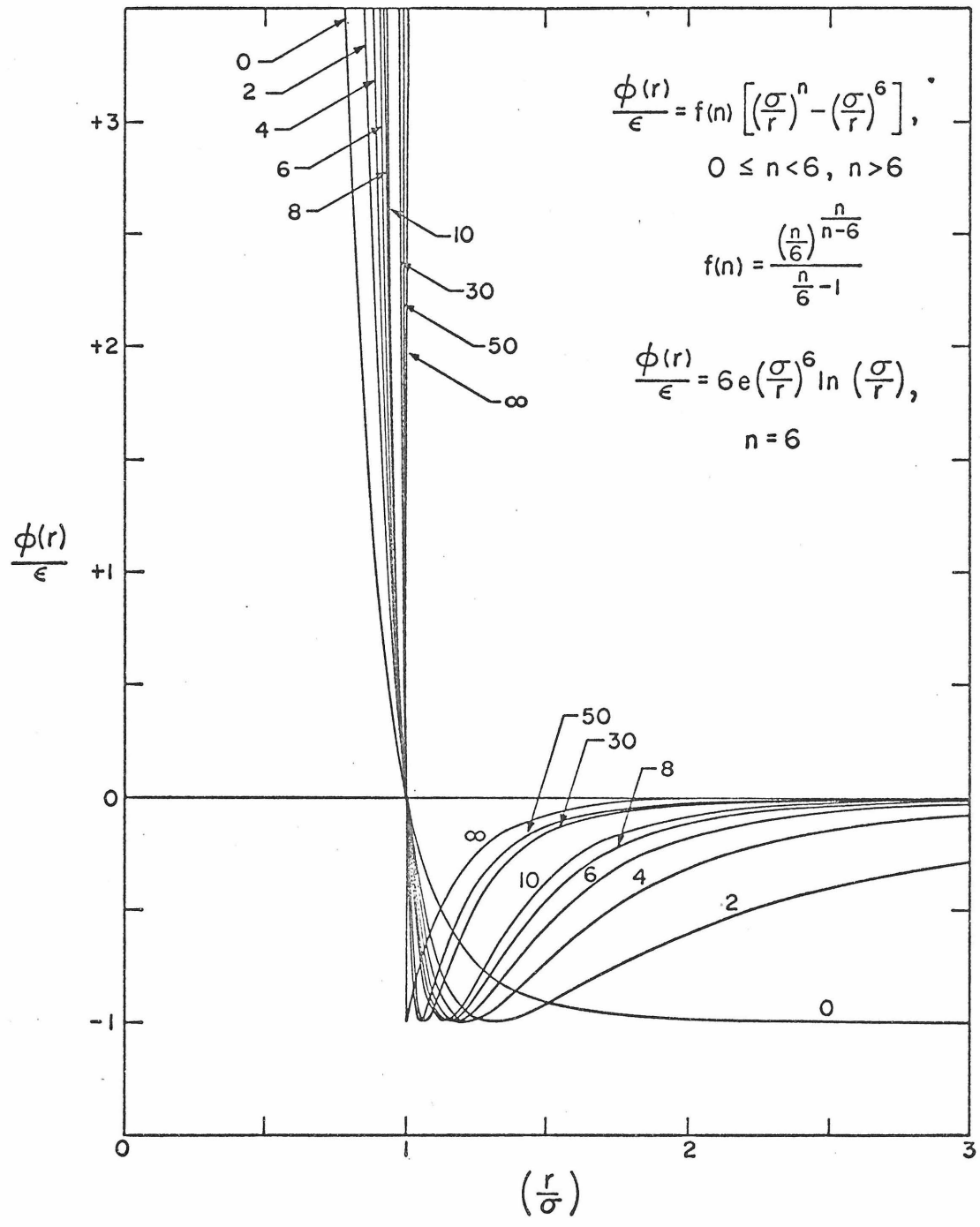

Figure 9. Pair Potential Function for Various Values of n

4. Integration for Use in Model

When Equation (72) is substituted into Equations (53) and (54) and the integrations carried out (Appendix J), the result is*:

$$\psi(\rho,z) = 2\pi\varepsilon(\rho N/M)\ f(n)\left[\frac{\sigma^n}{(n-2)(n-3)}\frac{1}{z^{n-3}} - \frac{\sigma^6}{12z^3}\right] \tag{78}$$

$$\psi(\rho_o,z_o) = 2\pi\varepsilon(\rho_o N/M)\ f(n)\left[\frac{\sigma^n}{(n-2)(n-3)}\frac{1}{z_o^{n-3}} - \frac{\sigma^6}{12z_o^3}\right] \tag{79}$$

The type of problem leading to these results appear as a problem in a textbook by Hill[19] where the Lennard-Jones (LJ) 12-6 potential was considered. This result exactly matches that of Equation (78) when $n \equiv 12$ and $\sigma = 2^{-1/6} r_o$ ($r_o = r^*$ in Reference (19)) as in Equation (70).

Substitution of Equations (78) and (79) into Equation (48) and rearrangement (Appendix J) gives:

$$\Delta E = 2\pi\varepsilon\left(\frac{N}{M}\right)^2 f(n)\left[\frac{\sigma^n}{(n-2)(n-3)}\left(\frac{\rho}{z^{n-3}} - \frac{\rho_o}{z_o^{n-3}}\right) - \frac{\sigma^6}{12}\left(\frac{\rho}{z^3} - \frac{\rho_o}{z_o^3}\right)\right] \tag{80}$$

The goal of an independent expression for ΔE as a function of $x\ (\equiv \rho/\rho_o)$ is almost realized. It is only necessary to determine the relation between z_o and ρ_o for the medium under consideration, and to specify the function z vs. ρ. The former is a function of the

---

*Since the integrals in Equations (53) and (54) are independent of n, the form of the result for $n \equiv 6$ may be found either from substitution of Equation (73) into this pair or by finding the limits as $n \Rightarrow 6$ of Equations (78) and (79). This will be considered in a later section.

"structure" of the substance, while the latter is related to the way in which compression takes place.

D. STRUCTURE

Since this study deals with condensed media, only liquids and solids will be considered.

1. Liquids

The structure of liquids has a vast literature[21,5,18,37,22,19,77,17,78,79] and, although it is recognized as a gross oversimplification, it is assumed that the molecules in the uncompressed state are arranged in the form of a face-centered-cubic (fcc) lattice[5,p.286]. Such an assumption is useful in providing a simple "average" relationship between z_o and ρ_o that can be used in the general development of Equation (80).

Although it is known that such a lattice is inaccurate (unrealistic) in detail (i.e., at the molecular level) it is not clear, a priori, that it is inaccurate on a macroscopic ("on the average") scale.

Assuming an fcc structure, the nearest neighbor distance is fixed geometrically and depends only on density:

$$a_o = 2^{1/6}(M/\rho_o N)^{1/3} \tag{81}$$

(Appendix K). Two ways to view this assumption in the context of a more "realistic" physical situation are discussed in detail in Appendix L. The first, called the "snapshot" approach, is similar to a geometric theory of liquid structure suggested by Bernal[80]. The second, called the "probability" approach, considers the pair distribution function (PDF) previously mentioned and uses elementary probability theory. In both cases, a way of computing a_o is

presented* for comparison with Equation (81). Agreement would tend to support the macroscopic "accuracy" of the fcc assumption.

Without numerical determinations of a_o from either the "snapshot" or "probability" approaches, it is of interest to know the greater of a_o and r_o (or r*) .

Examination of Figure 8 indicates that near the minimum, the probability of a molecule being $< r_o$ or $> r_o$ is approximately the same but as distances further removed from r_o are considered, the situation changes. The repulsive forces remain steep $<< r_o$ but the attractive forces slacken off $>> r_o$. This means that nearest neighbors at large r are possible (if comparatively unlikely) while nearest neighbors at small r are essentially impossible**. Therefore in determining the mean nearest neighbor distance (over all r) the curve will be weighted to larger values of r (i.e., skewed to the right) and it is expected that a_o is greater than r_o .

Since r_o is greater than r* (Appendix M), we may write:

$$a_o > r_o > r^* \tag{82}$$

Equation (82) may be used as a bound check of the assumption of an fcc lattice. That is, a_o from Equation (81) should be larger than r_o for the substance of interest in order that Equation (82) not be violated. It is, of course, recognized that just because Equation

---

*Calculations of the type suggested are extensive and are beyond the scope of this study.

**The same reasoning and result obtains when Figure L-2 and r* are considered.

(82) is satisfied does not imply that the fcc lattice assumption is verified.

For some liquids a number of investigators[58,37,81-83,54] have proposed a tetrahedral or "diamond"-like rather than an fcc lattice. In this instance it can be shown (Appendix K) that the nearest neighbor distance is given by:

$$a_o = \frac{3^{1/2}}{2} (M/\rho_o N)^{1/3} \tag{83}$$

rather than by Equation (81). In such instances the arguments previously developed for determination of a_o would be the same except that comparison would now be made with Equation (83).

If the assumed structure for liquids is judged "macroscopically accurate", and the expression for a_o is accepted (Equations (81) or (83)), the desired relation between z_o and ρ_o can be simply determined since z_o and a_o are geometrically related. This is shown in Appendix K with the results:

$$z_o = (M/2\ \rho_o N)^{1/3} \quad , \text{ fcc lattice} \tag{84}$$

$$z_o = (M/8\ \rho_o N)^{1/3} \quad , \text{ diamond lattice} \tag{85}$$

2. Solids

The structure of solids, compared to liquids, is accurately assessed on the basis of equilibrium lattice positions for each atom. Although there is vibrational motion about these lattice points, a macroscopic nearest neighbor distance is easily visualized and considered physically accurate. In this study fcc and body-centered cubic (bcc) solids only were considered and in all cases they were metals.

As shown in Appendix K for a bcc lattice:

$$a_o = 3^{1/2}\ 4^{-1/3}(M/\rho_o N)^{1/3} \tag{86}$$

$$z_o = (M/4\ \rho_o N)^{1/3} \tag{87}$$

The equivalent equations for an fcc metal lattice are given by Equations (81) and (84).

3. Generalization of Structure

The results in Appendix K are compiled in Figure 10 for the three structures of interest; fcc, bcc and "diamond" lattices. Both a_o and z_o decrease with the structure sequence fcc → bcc → diamond for equal density conditions. It is interesting that the coefficients for the relationship of interest (z_o vs. ρ_o) can be correlated by the equation:

$$z_o = \left(\frac{M}{2^s \rho_o N}\right)^{1/3} \tag{88}$$

where s is defined as a "structure" factor. For Figure 13*:

$s = 1$ corresponds to an fcc lattice (89)

$s = 2$ corresponds to a bcc lattice (90)

$s = 3$ corresponds to a "diamond" lattice (91)

Equation (88) is the "simple" relation sought for use in the general development of Equation (80). It applies to both liquids and solids although in the former case it is considered an "average" relationship that is only macroscopically accurate.

With regard to liquids, Equation (88) implies a generalization of structure not discussed previously. That is, for solids, discrete values of s (i.e., 0, 1, 2, etc.) are expected on physical grounds, since the proposed structures apparently exist at the molecular (atomic) level. However, for liquids, there is really no (a priori) physical/theoretical reason to pick a discrete value of s and specify an

* $s = 0$ corresponds to a simple cubic lattice.

a_0 = NEAREST NEIGHBOR DISTANCE
Z_0 = DISTANCE BETWEEN LAYERS

NAME	SKETCH	SHADED PLANE PROJECTION	a_0	Z_0	$a_0(\rho_0 N/M)^{\frac{1}{3}}$	$Z_0(\rho_0 N/M)^{\frac{1}{3}}$
fcc	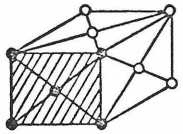	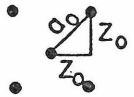	$2^{1/6}\left(\frac{M}{\rho_0 N}\right)^{1/3}$	$\left(\frac{M}{2\rho_0 N}\right)^{1/3}$	1.1225	0.7937
bcc	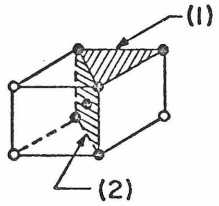	(1) 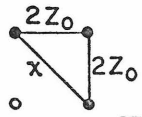 (2) 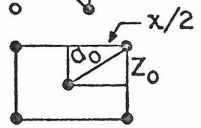	$\frac{3^{1/2}}{4^{1/3}}\left(\frac{M}{\rho_0 N}\right)^{1/3}$	$\left(\frac{M}{4\rho_0 N}\right)^{1/3}$	1.0911	0.6300
DIAMOND	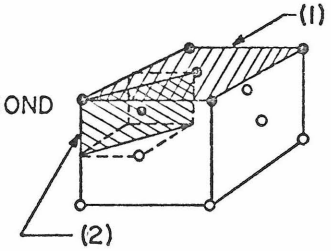	(1) 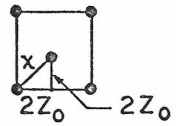 (2) 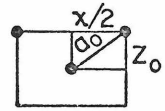	$\frac{3^{1/2}}{2}\left(\frac{M}{\rho_0 N}\right)^{1/3}$	$\left(\frac{M}{8\rho_0 N}\right)^{1/3}$	0.8660	0.5000

Figure 10. Structure

fcc, bcc or other lattice. Although this was done in the numerical part of this study, it is conceivable that s should be considered a continuous variable. This might further be consistent with results of the determination of a_o by molecular dynamic and/or statistical schemes in that the resultant values might (probably?) not match one of the coefficients in Figure 10 exactly.

With s a continuous variable, a range of structures are available that may or may not make sense*. Therefore limits and restrictions on s would have to be established and the meaning of the structures elucidated. This will not be done in the current work, but the concept might be of interest.

---

* (a) What is halfway between fcc and bcc, i.e., s = 1.5 ?

(b) What is the meaning of s > 3 ?

(c) Can s be < 0 ? , etc.

E. SHOCK HUGONIOT

To complete the development of Equation (80) only the relation between z and ρ is needed.

1. Linear Compression

In the shock model being developed we are considering a one-dimensional shock wave* and the molecules are assumed to compress linearly in the direction of motion as in Figure 4. If it is again assumed that the shock transition region is sufficiently thin, no transverse motion will occur (in the transition region) and the molecules in the compressed region will (at least initially) be a "squashed-only-in-the-direction-of-motion" version of that in the uncompressed region as pictured in Figure 4.

It is clear that, independent of structure, the density increase across the transition results from a simple sandwiching of the molecular layers. Therefore:

$$z/z_o = \rho_o/\rho \tag{92}$$

Upon relaxation of the structure after the shock transition, the molecules will redistribute themselves to yield a new equilibrium state. The characteristic spacing between layers would concurrently change from the value given by Equation (92) to some equilibrium value z_e. Since ρ_o and z_o are constants and ρ is assumed not to change between L_1 and the equilibrium state, it is clear that

*Indeed, the Rankine-Hugoniot equations are derived only for motion in one dimension[4,84,5,85,86,10,87,88,16].

Equation (92) can be valid only before relaxation has taken place. For the previous assumption of a sufficiently thin transition region, the relation will be valid (at least) at L_1 . This is all that is required, since z in Equation (80) is (in effect) defined as the characteristic spacing for molecules at L_1 .

Therefore Equation (92) is the desired relation between z and ρ except for the elimination of z_o . This is done using Equation (88) with the result:

$$z = (M/2^s \rho_o N)^{1/3} \rho_o/\rho \qquad (93)$$

2. General Expression

The appropriate relationships have been developed in Equations (88) and (93) and they may each be substituted into Equation (80) for the final step in finding an independent expression for ΔE as a function of $x(\equiv \rho/\rho_o)$. Carrying out the associated manipulations (Appendix N) yields:

$$\Delta E = \frac{2}{2^s}\left(\frac{N\pi\varepsilon}{M}\right) f(n)\left[\frac{\sigma^n}{(n-2)(n-3)}\left(\frac{2^s\rho_o N}{M}\right)^{n/3}(x^{n-2}-1) - \frac{\sigma^6}{12}\left(\frac{2^s\rho_o N}{M}\right)^2(x^4-1)\right] \tag{94}$$

Equation (94) is a unique relation between the internal energy change across a shock and the compression ratio x. It contains a single thermodynamic parameter (ρ_o), three molecular parameters (σ, ε and n) one structural parameter (s), and one atomic property (M).

Combining Equation (94) with Equation (20) yields a general expression for the Hugoniot:

$$\mu^2 = \frac{4}{2^s}\left(\frac{N\pi\varepsilon}{M}\right) f(n)\left[\frac{\sigma^n}{(n-2)(n-3)}\left(\frac{2^s\rho_o N}{M}\right)^{n/3}(x^{n-2}-1) - \frac{\sigma^6}{12}\left(\frac{2^s\rho_o N}{M}\right)^2(x^4-1)\right] \tag{95}$$

Using Equation (95) the Hugoniot may be expressed by any pair of shock parameters noting*:

---

*It is interesting that the classical form of the Hugoniot (i.e., Equation (12)) can be found from Equations (5), (14) and (95) in analytical form. The result is (assuming $P >> P_o$):

$$P = \frac{4\rho_o}{2^s}\left(\frac{N\pi\varepsilon}{M}\right) f(n)\left(\frac{x}{x-1}\right)\left[\frac{\sigma^n}{(n-2)(n-3)}\left(\frac{2^s\rho_o N}{M}\right)^{n/3}(x^{n-2}-1) - \frac{\sigma^6}{12}\left(\frac{2^s\rho_o N}{M}\right)^2 \times (x^4-1)\right]$$

$$f(n) = (n/6)^{n/n-6} \Big/ (n/6 - 1) \tag{71}$$

$$U = \mu / (1 - 1/x) \tag{14}$$

and:

$$P - P_o = \rho_o U \mu \tag{5}$$

Equation (95), whose properties are examined in the next section, is the sought-after analytical expression for the Hugoniot. It was developed without recourse to a post-shock equilibrium state.

F. PROPERTIES OF THE DEVELOPED FUNCTION (EQUATION (95))

Having obtained the Hugoniot in general-analytical form, it is desirable to examine the resulting function for certain properties of interest.

1. Extrapolation to Sound Velocity

From Equation (95) the Hugoniot may be written in functional form as:

$$\mu^2 = \alpha(x^{n-2} - 1) - \beta(x^4 - 1) \tag{96}$$

where:

$$\alpha = \frac{4}{2^s}\left(\frac{N\pi\varepsilon}{M}\right) f(n) \frac{\sigma^n}{(n-2)(n-3)} \left(\frac{2^s \rho_o N}{M}\right)^{n/3} \tag{97}$$

$$\beta = \frac{4}{2^s}\left(\frac{N\pi\varepsilon}{M}\right) f(n) \frac{\sigma^6}{12} \left(\frac{2^s \rho_o N}{M}\right)^2 \tag{98}$$

The limiting process towards sound velocity is described by Equation (18):

$$U_o = \lim_{x \to 1} \frac{d\mu}{dx} \tag{18}$$

and for Equation (95):

$$\frac{d\mu}{dx} = \frac{1}{2} \frac{[(n-2)\alpha x^{n-3} - 4\beta x^3]}{\mu} \tag{99}$$

Substitution in Equation (18) leads to*:

---

*Examination of Eq. (95) shows that, as expected:

$$\lim_{x \to 1} \mu = 0$$

$$U_o = \frac{1}{2} \lim_{x \to 1} \frac{[(n-2)\alpha x^{n-3} - 4\beta x^3]}{\mu} \Rightarrow \frac{(n-2)\alpha - 4\beta}{0} \Rightarrow \pm\infty \qquad (100)$$

which diverges! * The limit can exist if and only if:

$$(n-2)\alpha - 4\beta \equiv 0 \qquad (101)$$

In this case Equation (100) becomes:

$$U_o = \frac{1}{2} \lim_{x \to 1} \frac{[(n-2)\alpha\, x^{n-3} - 4\beta x^3]}{\mu} \Rightarrow \frac{0}{0} \qquad (102)$$

which implies another application of L'Hôspital's rule. This can be shown to result in the relation (Appendix 0):

$$U_o^2 = \frac{1}{2}[(n-2)(n-3)\alpha - 12\beta] \qquad (103)$$

Clearly, Equation (103) must be considered in light of the condition expressed in Equation (101). However, we may first consider Equation (103) alone. Substitution for α and β gives, after manipulation:

$$U_o^2 = \frac{2}{2^s}\left(\frac{N\pi\epsilon}{M}\right) f(n) \left[\sigma^n \left(\frac{2^s \rho_o N}{M}\right)^{n/3} - \sigma^6 \left(\frac{2^s \rho_o N}{M}\right)^2\right] \qquad (104)$$

which is an expression for U_o dependent only on the molecular parameters σ, ϵ and n.

The "condition", Equation (101), can be written, after substitution for α and β and rearrangement:

---

*For certain values of α and β, $\mu = 0$ at $x = X_R$ $(X_R > 1)$. In this case the limiting process in Equation (17) is not valid and Equation (18) does not obtain. In fact, in this case $U_o = 0$. This is discussed in a later section.

$$\sigma^{n-6}\left(\frac{2^s N\rho_o}{M}\right)^{\frac{n-6}{3}} = \left(\frac{n-3}{3}\right) \tag{105}$$

For given values of σ and n the magnitude of the difference between the sides of Equation (105) describes the accuracy with which the required "condition" for Equation (104) is met. Equations (104) and (105) are treated in this manner in the "weak" form (WF) solution discussed in a later section. On the other hand, a rearrangement of Equation (105) shows that:

$$\sigma = \left(\frac{n-3}{3}\right)^{\frac{1}{n-6}} \left(\frac{M}{2^s \rho_o N}\right)^{1/3} \tag{106}$$

The "condition" therefore requires that σ be fixed in terms of n only. Substitution of this into Equation (104) yields:

$$U_o^2 = \frac{2}{3 \cdot 2^s}\left(\frac{N\pi\varepsilon}{M}\right)(n-6)\, f(n)\left(\frac{n-3}{3}\right)^{\frac{6}{n-6}} \tag{107}$$

which is an expression for U_o dependent only on ε and n.

For a given value of n, σ may be computed from Equation (106) (and compared to values from the literature). For this n and a given value of ε, U_o^2 may be computed from Equation (107). This approach called the "medium" form (MF) solution is discussed further in a later section.

Although it is ordinarily not considered so, the sound velocity C_o of a medium is certainly a valid data point in the set of shock data available[14]. Since $C_o (= U_o)$ is usually known with considerable accuracy compared to the other shock data, it seems reasonable to "force" the theory through this point. This suggests using Equation

(107) to eliminate ε in Equation (95). When Equation (106) is used to eliminate σ also in Equation (95), the condition for Equation (107) is exactly satisfied, and the Hugoniot becomes (Appendix P):

$$\mu^2 = U_o^2\left(\frac{2}{n-6}\right)\left[\frac{x^{n-2}-1}{n-2} - \frac{x^4-1}{4}\right] \tag{108}$$

This is an expression for the Hugoniot which depends on only <u>one</u> thermodynamic (macroscopic) parameter (U_o) and only <u>one</u> molecular (microscopic) parameter (n) . It is significant that not only were σ and ε eliminated in the substitution, but ρ_o, M and s were also. Clearly, all this information is contained in U_o .

Use of Equation (108) only, instead of Equations (95), (104) and (105), represents the "strong" form (SF) solution discussed in a later section.

2. U vs. μ Linearity

To determine if Equation (13) has any theoretical basis, it is necessary to cast the Hugoniot (Equations (95), (96) or (108)) in the form of U vs. μ . From Equation (14):

$$x = \frac{U}{U - \mu} \tag{109}$$

and Equation (108) becomes*:

$$\mu^2 = U_o^2\left(\frac{2}{n-6}\right)\left[\frac{\left(\frac{U}{U-\mu}\right)^{n-2} - 1}{n-2} - \frac{\left(\frac{U}{U-\mu}\right)^{4} - 1}{4}\right] \tag{110}$$

There is no obvious way in which Equation (110) can be made to match the form of Equation (13) except (perhaps) by Taylor series expansion.**

Another simple way to compare Equations (108) and (13) is to reverse the procedure and put the latter into the form of μ vs. x . From Equation (13):

$$B\mu = U - A \tilde{=} U - U_o \tag{111}$$

and by using Equation (14):

$$B\mu \tilde{=} \frac{\mu}{1 - 1/x} - U_o \tag{112}$$

which leads to:

$$\mu \tilde{=} \frac{U_o}{\frac{1}{1 - \frac{1}{x}} - B} = U_o\left[\frac{x-1}{x - B(x-1)}\right] \tag{113}$$

---

*This form was chosen for convenience, since U_o appears in the equation.

**It is not apparent how even this should be done.

Comparing this to Equation (108) shows that, for the forms to be compatible $[\frac{x-1}{x - B(x-1)}]$ must be identified with $(2/(n-6))^{1/2}$ $\times [\frac{x^{n-2} - 1}{n-2} - \frac{x^4 - 1}{4}]^{1/2}$. That this is so is not readily apparent, although later analyses show that, indeed, this is the case*. In this case it appears that the theory, as developed, does provide a satisfactory theoretical explanation of Equation (13). Of course, the latter must be considered only a first approximation to a function (U vs. μ) which has "gentle" or little curvature**. That Equations (96) (or Equation (108)) and (14) reproduce this property and give a better approximation to the function is shown in later sections.

---

*See Part IV, DISCUSSION AND CONCLUSIONS

**As confirmed by plotting experimental U vs. μ data.

3. Effects as $n \to 6$

In a prior section it was shown that the n-6 potential has a finite limit as $n \to 6$, Equation (73). The same limiting process can be applied to Equation (95) resulting in* (Appendix Q):

$$\mu^2 = \frac{2e}{2^s}\left(\frac{N\pi\varepsilon}{M}\right)\sigma^6\left(\frac{2^s\rho_o N}{M}\right)^2\left[x^4 \ell n x + \left(\ell n\, \sigma\left(\frac{2^s\rho_o N}{M}\right)^{1/3} - \frac{7}{12}\right)(x^4 - 1)\right] \tag{114}$$

Paralleling the development in Equations (96) to (113), the following results are obtained (Appendix R):

$$\mu^2 = \alpha' x^4 \ell n\, x + \beta'(x^4 - 1) \tag{115}$$

where:

$$\alpha' = \frac{2e}{2^s}\left(\frac{N\pi\varepsilon}{M}\right)\sigma^6\left(\frac{2^s\rho_o N}{M}\right)^2 \tag{116}$$

$$\beta' = \frac{2e}{2^s}\left(\frac{N\pi\varepsilon}{M}\right)\sigma^6\left(\frac{2^s\rho_o N}{M}\right)^2\left(\ell n\, \sigma\left(\frac{2^s\rho_o N}{M}\right)^{1/3} - \frac{7}{12}\right) \tag{117}$$

The WF solution is given by:

$$U_o^2 = \frac{4e}{2^s}\left(\frac{N\pi\varepsilon}{M}\right)\sigma^6\left(\frac{2^s\rho_o N}{M}\right)^2 \tag{118}$$

and the "condition" by:

---

*Of course, this result could be obtained directly by using Equation (73) instead of Equation (72) in the general development of Equation (95).

$$\sigma^3 \left(\frac{2^s \rho_o N}{M}\right) = e \tag{119}$$

The MF solution is given by:

$$\sigma = e^{1/3} \left(M/2^s \rho_o N\right)^{1/3} \tag{120}$$

and:

$$U_o^2 = \frac{4e^3}{2^s} \left(\frac{N\pi\varepsilon}{M}\right) \tag{121}$$

The SF solution is given by:

$$\mu^2 = \frac{1}{2} U_o^2 [x^4 \ln x - \frac{1}{4} (x^4 - 1)] \tag{122}$$

To determine if Equations (114), (115) or (122) provide a basis for the form of Equation (13), it can easily be shown that $[\frac{x-1}{x - B(x-1)}]$ must be identified with $2^{-1/2}[x^4 \ln x - \frac{x^{4-1}}{4}]^{1/2}$. As before, the correspondence can be demonstrated* and the Hugoniot with $n = 6$ supports the prior conclusion.

*See Part IV. DISCUSSION AND CONCLUSIONS

III. APPLICATION OF THEORY

A. AVAILABLE EXPERIMENTAL DATA

As previously discussed, measurement or knowledge of any two shock parameters allows determination of all the others by use of Equations (4) - (6) and (10). In the majority of cases the two variables measured are U and μ. Although there are techniques for measuring P and μ also, they are indirect and the experiments are usually difficult to perform.

1. Shock Experiments

The two sources of energy for the production of "strong" shock waves are high explosives and "guns".

When a high explosive is properly initiated, a steady-state detonation wave is propagated throughout the mass of the material at a characteristic velocity D. The wave consists of a leading shock wave (shock "front") followed by a zone of chemical reaction which releases large quantities of heat, light and gaseous reaction products. Further, energy transfer from the reaction zone back to the shock front supports the continued propagation of the wave at velocity D (thus a steady-state phenomenon). The detonation wave is a "strong" shock and is capable of transferring strong shocks into other (inert) materials. Further, the overall detonation process can be used to accelerate sample (inert) materials to high velocity.

Guns are used to accelerate selected projectiles to high speed using the gases from the deflagration* of propellants. No extreme

*As opposed to detonation.

shocks are involved. Strong shocks are produced when the projectile impacts another object.

The most common methods of carrying out the experiments to measure shock-wave parameters are sketched in Figure 11. Methods 1, 2 and 3a use high explosives, while the last, 3b, uses a gun.

In the first method (called the "free-surface", "break-away" or "split-off" method)[12] a block of high explosive is detonated in direct contact with the sample. Upon reaching the interface between the two, the detonation wave (at velocity D) is transformed into two shock waves; one passes back into the explosion products, while the other propagates through the sample at some characteristic (shock) velocity U*. When this wave reaches the free-surface (at the right of the sample in Figure 11) it is reflected back into the sample as a rarefaction wave, satisfying the boundary conditions of continuity of pressure and particle velocity[85,90,86,91,92,89,10,11,87,93,64,94,12]. As a consequence, the surface of the sample is accelerated to μ_{fs}, the free surface velocity. In general:

$$\mu_{fs} = \mu + \mu_r \tag{123}$$

where μ and μ_r are the particle velocity behind the shock wave and rarefaction wave respectively. To an excellent approximation over a

---

*Since the detonation is compressive (i.e., not a rarefaction wave), it it can be shown[89] that the wave in the sample is also compressive irrespective of the nature of the wave passing back into the detonation products.

It is assumed that the distance ℓ is small enough so that the shock velocity does not vary (attenuate) in the sample; $\frac{dU}{d\ell} \simeq 0$.

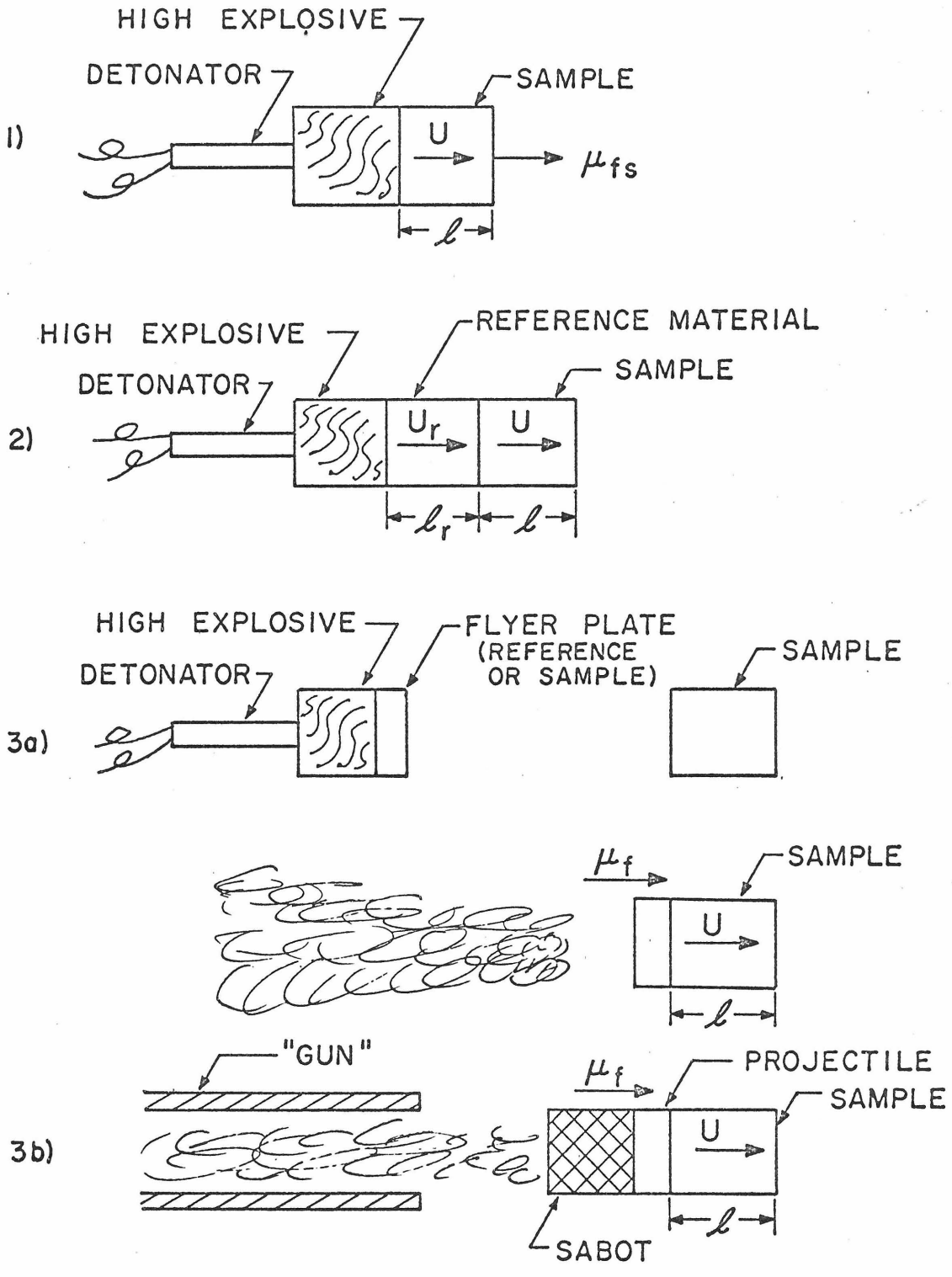

Figure 11. Shock Wave Production

wide range of conditions and materials[3,85,90,91,86,13,89,10,87,64,95,96,12]:

$$\mu_r \tilde{=} \mu \tag{124}$$

and from the above:

$$\mu \tilde{=} \mu_{fs}/2 \tag{125}$$

Measurement of U and μ_{fs} for a single experiment and use of Equation (125) gives one set of U-μ data.

In the second method (called the "impedance-match"[10], calibrated "reflection"[12] or Hugoniot "reflection" method[97]) the high explosive charge is in contact with a reference material whose Hugoniot has been previously established. The sample is placed in contact with the reference material.

The shock wave from the detonation propagates through the reference with a velocity U_r and is incident upon the interface with the sample. Two waves are produced: one reflects back into the reference, while the other propagates through the sample at velocity U^*. The relative strengths of the waves are governed by the requirement of continuity of pressure and particle velocity across the interface and the Hugoniot of the reference and sample. This is used in the Hugoniot "reflection" method from which the particle velocity (and/or pressure) in the sample μ, can be found. The method considers the Hugoniot of

---

*As before, if the shock in the reference material is compressive, so is the wave in the sample irrespective of the reflected wave, which can be a compression or rarefaction wave, depending on conditions.

the reference material in the P-μ plane as shown in Figure 12. Identification of P_r and μ_r can be made by knowing U_r and ρ_{o_r} (the initial density) for the reference material considering Equation (5), the conservation of mass plus momentum flux. For strong shocks ($P >> P_o$) this may be written:

$$P_r = (\rho_{o_r} U_r)\ \mu_r \tag{126}$$

The intersection of the (straight) line through the origin with slope $\rho_{o_r} U_r$ will intersect the reference Hugoniot at the P_r-μ_r condition corresponding to U_r. This is the solid straight line in Figure 12.

It can be shown[4,86,10] that the reflected wave in the reference material must lie on the curve formed by a 180^o reflection of the original Hugoniot about a vertical line passing through the point P_r-μ_r. This is also shown in Figure 12. Because of the requirement of continuity of pressure and particle velocity at the interface, a point on this "reflected" Hugoniot also represents conditions behind the shock wave in the sample. This point is located by applying Equation (5) in the form:

$$P = (\rho_o U)\,\mu \tag{127}$$

The intersection of the line through the origin with slope $\rho_o U$ * will intersect the reference Hugoniot at the P-μ condition corresponding to U. This is shown as the dashed line in Figure 12. Although $P < P_r$ for the illustration in Figure 12, it is clear that

---

*It is assumed that the initial density of the sample ρ_o is known or measured.

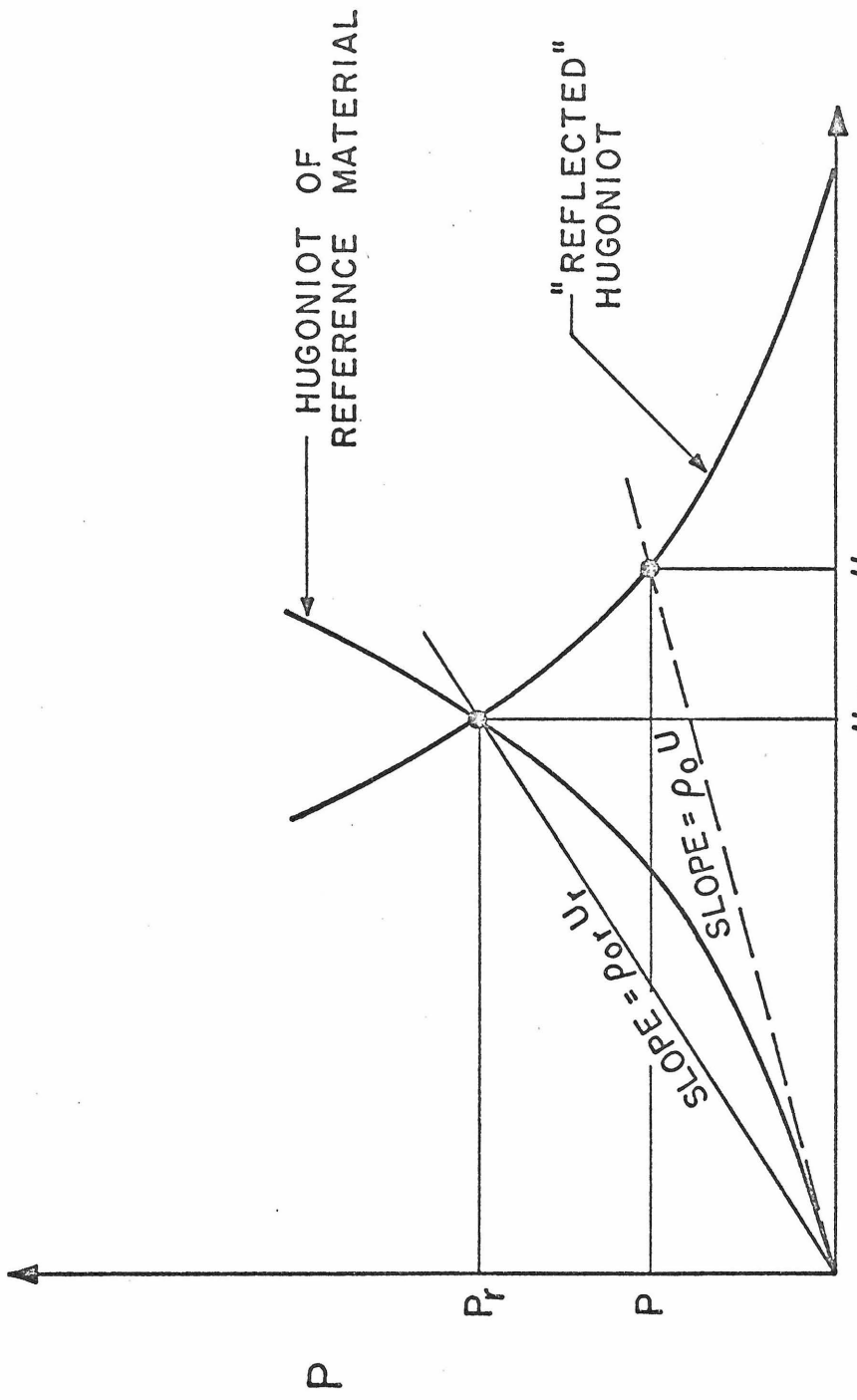

Figure 12. Hugoniot "Reflection" Method

if $\rho_o U > \rho_{o_r} U_r$ (i.e., if the "impedance" of the sample was higher than the "impedance" of the reference) then P would be greater than P_r. In general, both cases occur*. Clearly, measurement of U and U_r for a single experiment and application of the Hugoniot "reflection" method (which assumes knowledge of the Hugoniot of the reference material) yields one set of U-μ data.

In the third method (called variously, the "collision", "impact", "braking" or "momentum transfer" method[10,12]) the detonation of a high explosive (3a in Figure 11) or firing of a gun (3b in Figure 11) accelerates a flyer plate (or projectile) to flight velocity μ_f. Upon impact with the sample two shocks are produced. One propagates to the right in the sample at velocity U, while the other moves to the left back into the flyer plate**. If the projectile and sample are composed of the same material, the shocks produced at impact are identical and it is easy to show that[12]:

$$\mu = \mu_f/2 \tag{128}$$

If the projectile is a reference material*** (known Hugoniot) the particle velocity can be computed by a variation of the Hugoniot "reflection" method. This is shown in the P-μ plot in Figure 13.

---

*In the former case ($P < P_r$) the reflected wave is a rarefaction. When $P > P_r$, the reflected wave is compressive[86,89,10,12].

**Since it is the impact of the flyer plate on the sample that causes the desired shock, there is no difference in the analysis of cases 3a and 3b, i.e., the method of acceleration of the projectile to μ_f is irrelevant to the subsequent events.

***This would be done because higher shock pressures can be produced with selected reference materials at the same value of μ_f.

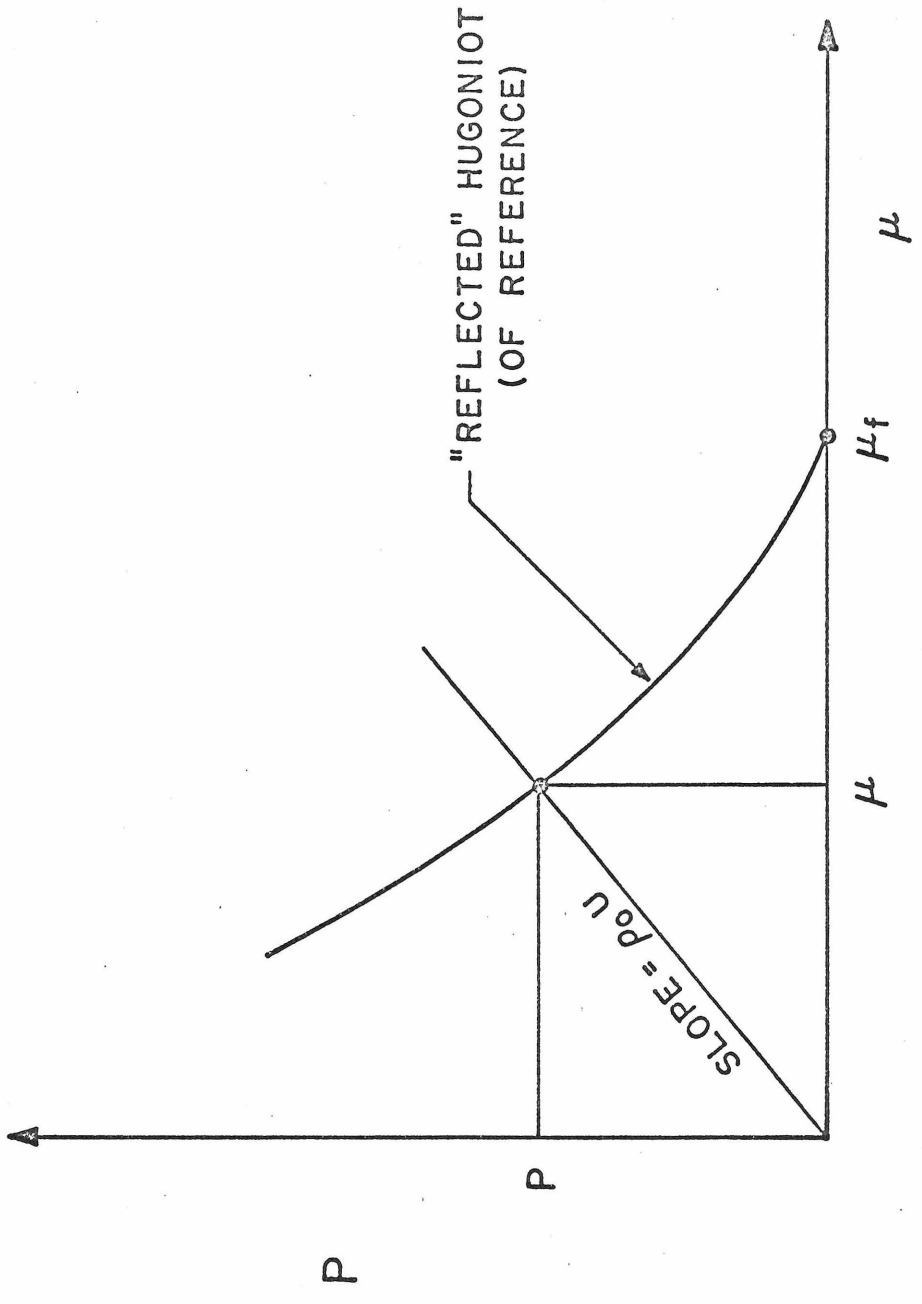

Figure 13. "Impact" Method

Consideration of the requirement of continuity of pressure and particle velocity at the interface shows that some point on the "reflected" Hugoniot of the reference material "centered" at the flight velocity μ_f * represents conditions in both the flyer plate and sample. As before, this point is located by the intersection of Equation (5):

$$P = (\rho_o U)\ \mu \tag{129}$$

with the "reflected" Hugoniot as shown in Figure 13.

Therefore measurement of U and μ_f for an experiment, along with Equation (128) or the procedure in Figure 13, leads to one set of U-μ data.

In each of the three methods in Figure 11 only velocity measurements are required; shock velocity in the sample or reference, free-surface velocity of the sample and flight velocity of the projectile (flyer plate). Generally these are accomplished by time-of-arrival (t.o.a.) techniques, although continuous distance-time measurements are also used.

In the former case U and U_r are computed from:

$$U = \frac{\ell}{\Delta t} \quad , \quad U_r = \frac{\ell_r}{\Delta t_r} \tag{130}$$

where it is assumed that the reference and sample are both thin enough to preclude significant attenuation. Both Δt and Δt_r are determined from "t.o.a." data. In the latter case of continuous distance-time

---

*For the sample the initial condition is $P = 0 = \mu$ but for the projectile the initial condition is $P = 0$, $\mu = \mu_f$.

measurements U and U_r are computed by numerical differentiation of the data. Free surface and projectile velocities (μ_{fs} and μ_f) are similarly determined.

Techniques for determining the required "t.o.a." or distance-time measurements are briefly summarized in Table 2. While not being exhaustive or fully descriptive*, the table does indicate the range of methods available and major features of each. Because of the short time associated with the events being considered, all electrical methods use a rasteroscillograph system to record the data, while all of the optical methods use a (high-speed: $\sim$10 mm/μsec writing rate) streak camera.

Although almost all measurements of shock parameters involve U and μ, direct measurements of P and ρ have been made[10,96], usually with the set-up in Method 1 of Figure 11. The techniques used are summarized in Table 3, where again only the major features are indicated. At present these methods are not as accurate as those for U-μ measurements.

---

*An excellent description of these methods is given in Reference 10. Other sources are References 96 and 86. In each case the original references are quoted.

Table 2

TIME-OF-ARRIVAL AND CONTINUOUS-DISTANCE TIME DETERMINATIONS

No.	Classification of Technique	Sensing Phenomenon	Key Measurement Element	Recording Instrumentation	Continuous or Time-of-Arrival	Used for U, μ_{fs}, or μ_f	Limitations/ Assumptions	Description
1	Electrical-Pin Probe	Switch closure	Mechanical pin probe	Raster-oscillograph and circuitry	t.o.a.	U, μ_{fs}, μ_f		Probe contains both leads; shorted by crush of shock
2	Electrical-Pin Probe	Switch closure	Bare wire	Raster-oscillograph and circuitry	t.o.a.	U, μ_{fs}	Sample must be conducting	One lead is surface of sample (if conducting); shock closes
3	Electrical-Resistance Wire	Resistance vs. time	Pair of resistance wires	Raster-oscillograph and circuitry	continuous	μ_{fs}	Need constant resistance/ length	Wires are angled to surface so that motion shorts them progressively
4	Electrical-Capacitance	Capacitance vs. time	Parallel plate condenser	Raster-oscillograph and circuitry	continuous	μ_{fs}	Sample must be conducting	Surface of sample is one plate of condenser which closes with motion.
5	Electrical-Piezoelectric	Voltage Pulse	Piezoelectric crystal	Raster-oscillograph and circuitry	t.o.a.	U, μ_{fs}		Shock or free surface causes compression and electrical pulse
6	Optical-Flash	Light Flash	Luminous gas	Streak Camera	t.o.a.	U, μ_{fs}	Planarity of shock	Shock compresses and illuminates gas in prepared gaps in sample
7	Optical-Mirror	Loss of Reflectivity	Mirror	Streak Camera	t.o.a. continuous	U, μ_{fs}		External illumination reflected into camera is cut-off on shock arrival
8	Optical-Lever	Shift in Reflection	Polished surface	Streak Camera	continuous	μ_{fs}	Sensitive to variations in μ_{fs}	Polished surface of sample shifts reflection position when shock arrives obliquely
9	Optical-Image	Image Movement	Polished surface and wire	Streak Camera	continuous	μ_{fs}		Image of wire on polished sample surface moves with free surface motion
10	Optical-Direct	Shadow of Wave	Photographic Film	Streak Camera	continuous	U	Sample must be transparent	Shock wave causes shadow on backlighted sample
11	Optical-Direct	Shadow of Free-Surface	Photographic Film	Streak Camera	continuous	μ_{fs}		Watch free-surface motion (from side) block out backlighting
12	Optical-Direct	Shadow of Projectile	Photographic Film	Streak or Framing Camera	continuous	μ_f		Watch shadow motion with respect to backlighting or bulk motion frame-to-frame.

Table 3

PRESSURE AND DENSITY DETERMINATIONS

No.	Classification of Technique	Sensing Phenomenon	Key Measurement Element	Recording Instrumentation	Used to Measure	Limitations/Assumptions	Description
1	Electrical-Conductivity	Change in Conductivity	Sulfur Wafer	Raster-oscillograph and circuitry	P	Need Hugoniot of sample to properly adjust data	Large change in resistivity of sulfur under shock compression
2	Electrical-Piezoelectric	Voltage Pulse	Quartz Transducer	Raster-oscillograph and circuitry	P	Current flow related to P by weak theory	Shock causes compression and electrical pulse
3	Radiographic	Absorption of X-rays	Photographic Film	Film Plate	ρ	Data reduction difficult	X-rays through shock show film density gradients proportional to actual ones

2. Compilation of Data

Using the methods outlined in the previous section, a large body of shock wave (Hugoniot) data has been accumulated since the first investigations in 1945[86]. The major portion of the work has been done in the United States, but significant contributions have been made in the U.S.S.R., France and England.

Almost all this data, through 1966, is included in an excellent compendium[96,98] edited by Van Thiel. This compilation*, plus the more recent work, was extensively used in forming the data set used in this study.

The substances considered in the current work are shown in Table 4 which is divided into two parts, liquids** and solids.

For the liquids, the choice of materials to be studied was limited to those for which both shock data and reasonable values of the molecular parameters σ and ε were available. A preliminary study[16] of the shock model considered six of these liquids: A, Hg, N_2, H_2, CCl_4 and C_6H_6 (benzene). This group was chosen because these molecules are simple and offered the best chance of obeying the (spherically symmetric; non-angle-dependent) n-6 potential considered***, within "reasonable" bounds. The results of that study

---

*Whenever possible the original papers were consulted for details of the experiments, accuracy of results, etc.

**A, N_2 and H_2 which are "normally" gases at standard conditions were all studied in the liquid state under appropriate T_o, P_o conditions.

***Equation (8) of Reference 16 which is equivalent to Equation (72) in this study.

appeared to justify an attempt to apply the ideas to more complex molecules. This was done by considering the seven additional liquids shown in Table 4 where polar molecules (methanol, ethanol, ether and water), longer linear molecules (carbon disulphide and hexane) and a perturbed ring structure (toluene) are included. In each case both shock and molecular parameter data are available. The "original" six liquids were reinvestigated also because additional shock and/or molecular parameter data were found*, theoretical refinements had occurred, and new methods of treating the data were developed.

As previously mentioned, the only solids considered in this study were metals with an fcc or bcc lattice. Ten of the former and thirteen of the latter, for which shock data are available, are shown in Table 4. Since very little (if any) reliable data on σ and ε for metals are available this was not considered limiting in choosing solids. For each lattice structure the metals are listed with respect to their positions in the periodic table. Several well-known "groups" are included. This is seen in Figure 14 which shows these and all the elements considered in the study superimposed on a periodic chart. At least one element from each group (except Group VII) and period was studied.

The raw U-μ data for the 13 liquids and 23 solids are compiled in Appendix S** where the (mean) initial conditions and sound

---

*For argon, shock data for two additional initial states were found.

**Also included are the (several) adjusted data sets discussed in the following paragraphs.

Table 4

SUBSTANCES INCLUDED IN STUDY

LIQUIDS

Code**	Substance	Structure	Comments
L1	Argon	A	Monatomic; spherically symmetric *
L2	Mercury	Hg	Monatomic; spherically symmetric
L3	Nitrogen	$N \equiv N$	Diatomic
L4	Hydrogen	$H - H$	Diatomic
L5	Carbon Disulphide	$S \equiv C \equiv S$	Triatomic
L6	Carbon Tetrachloride	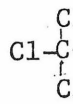	Tetrahedral; 1 carbon atom; symmetric
L7	Methanol		Polar; 1 carbon atom; some symmetry
L8	Ethanol	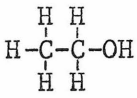	Polar; 2 carbon atoms
L9	Ethyl Ether	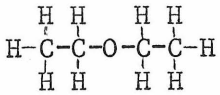	Polar; 4 carbon atoms
L10	Hexane	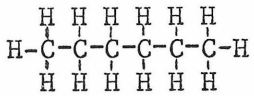	Long-Chain; 6 carbon atoms
L11	Benzene	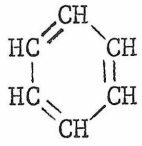	Ring structure
L12	Toluene	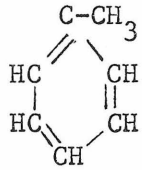	Ring structure
L13	Water	H-O-H	Polar

*Data available at four different initial states

**L = Liquid

Table 4

SUBSTANCES INCLUDED IN STUDY

SOLIDS

fcc lattice

Code***	Substance	Symbol	Position in Periodic Table Group/Period	Comments
F1	Copper	Cu	IB/4	Noble Metals
F2	Silver	Ag	IB/5	
F3	Gold	Au	IB/6	
F4	Cobalt	Co	VIII/4	Ferromagnetic Metals
F5	Nickel	Ni	VIII/4	
F6	Palladium	Pd	VIII/5	Transition Metals
F7	Platinum	Pt	VIII/6	
F8	Aluminum	Al	IIIA/3	
F9	Calcium	Ca	IIA/4	Alkaline Earth Metal
F10	Lead	Pb	IVA/6	

bcc lattice

B1	Lithium	Li	IA/2	Alkali Metals
B2	Sodium	Na	IA/3	
B3	Potassium	K	IA/4	
B4	Rubidium	Rb	IA/5	
B5	Cesium	Cs	IA/6	
B6	Vanadium	V	VB/4	Transition Metals
B7	Niobium	Nb	VB/5	
B8	Tantalum	Ta	VB/6	
B9	Chromium	Cr	VIB/4	
B10	Molybdenum	Mo	VIB/5	
B11	Tungsten	W	VIB/6	
B12	Zirconium	Zr	IVB/5	
B13	Barium	Ba	IIA/6	Alkaline Earth Metal

*** F = fcc metal, B = bcc metal

Table 4

SUBSTANCES INCLUDED IN STUDY

SOLIDS

fcc lattice

Code***	Substance	Symbol	Position in Periodic Table Group/Period	Comments
F1	Copper	Cu	IB/4	Noble Metals
F2	Silver	Ag	IB/5	
F3	Gold	Au	IB/6	
F4	Cobalt	Co	VIII/4	Ferromagnetic Metals
F5	Nickel	Ni	VIII/4	
F6	Palladium	Pd	VIII/5	Transition Metals
F7	Platinum	Pt	VIII/6	
F8	Aluminum	Al	IIIA/3	
F9	Calcium	Ca	IIA/4	Alkaline Earth Metal
F10	Lead	Pb	IVA/6	

bcc lattice

B1	Lithium	Li	IA/2	Alkali Metals
B2	Sodium	Na	IA/3	
B3	Potassium	K	IA/4	
B4	Rubidium	Rb	IA/5	
B5	Cesium	Cs	IA/6	
B6	Vanadium	V	VB/4	Transition Metals
B7	Niobium	Nb	VB/5	
B8	Tantalum	Ta	VB/6	
B9	Chromium	Cr	VIB/4	
B10	Molybdenum	Mo	VIB/5	
B11	Tungsten	W	VIB/6	
B12	Zirconium	Zr	IVB/5	
B13	Barium	Ba	IIA/6	Alkaline Earth Metal

*** F = fcc metal, B = bcc metal

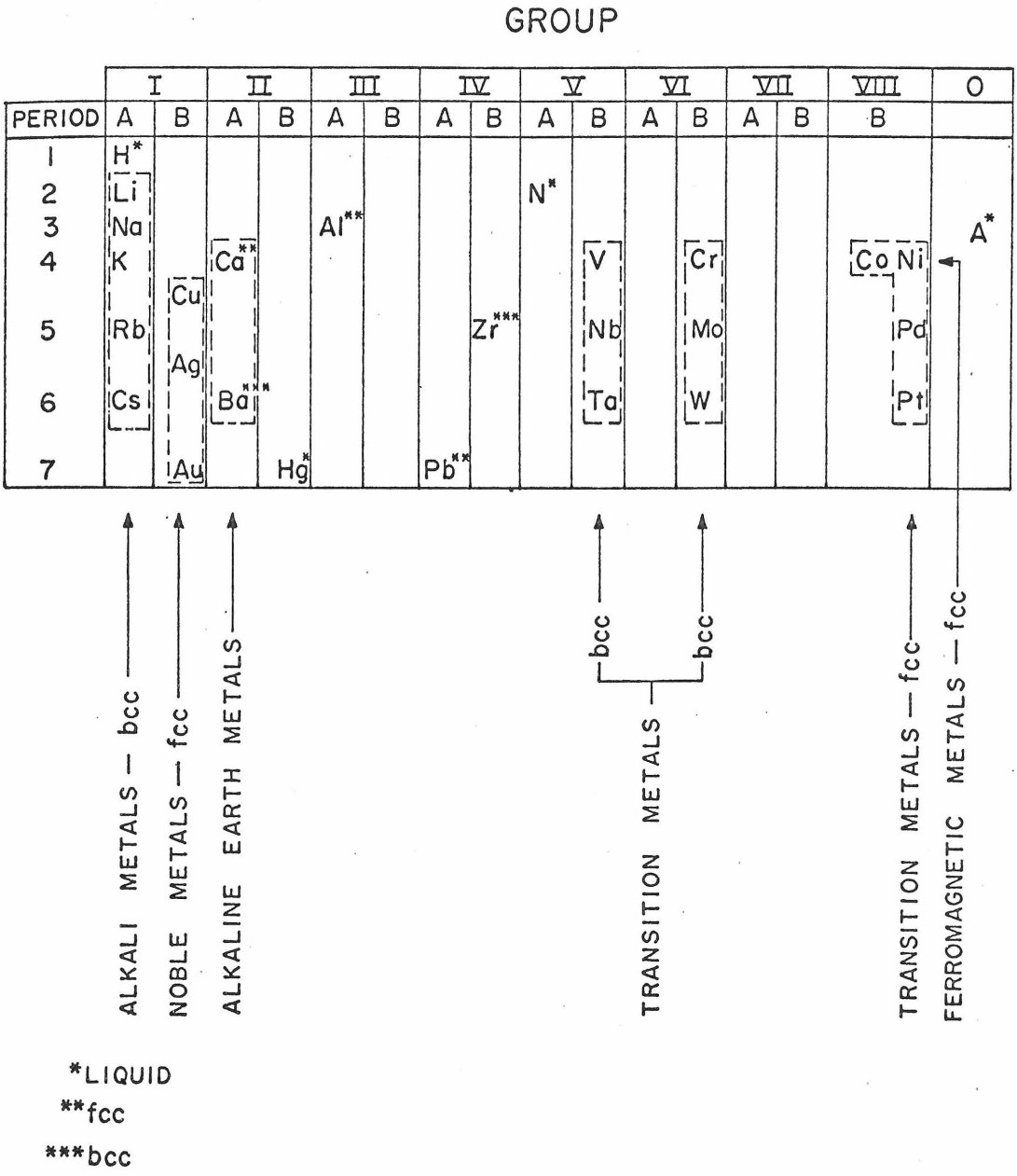

Figure 14. Elements Included in Study Superimposed on Periodic Table

velocity C_o for each substance are given[64,96,90,42,60,99,101,94, 100,98,102,85,92,103,104,13,105,95,106,93,107,108]. These data are plotted in Figures 15-27, where liquids of similar structure and solids of the same periodic group have been, as far as possible, placed together.

With no attempt at interpretation or significance, a smooth curve originating at C_o, was "faired" through the data for each material, to help in the selection process discussed in the next section. The general objective was to determine if a smooth (i.e., all derivatives continuous) continuous curve could be drawn through the combined data. It is notable that in some instances this could not be done and a "break" in the plotted data was indicated.

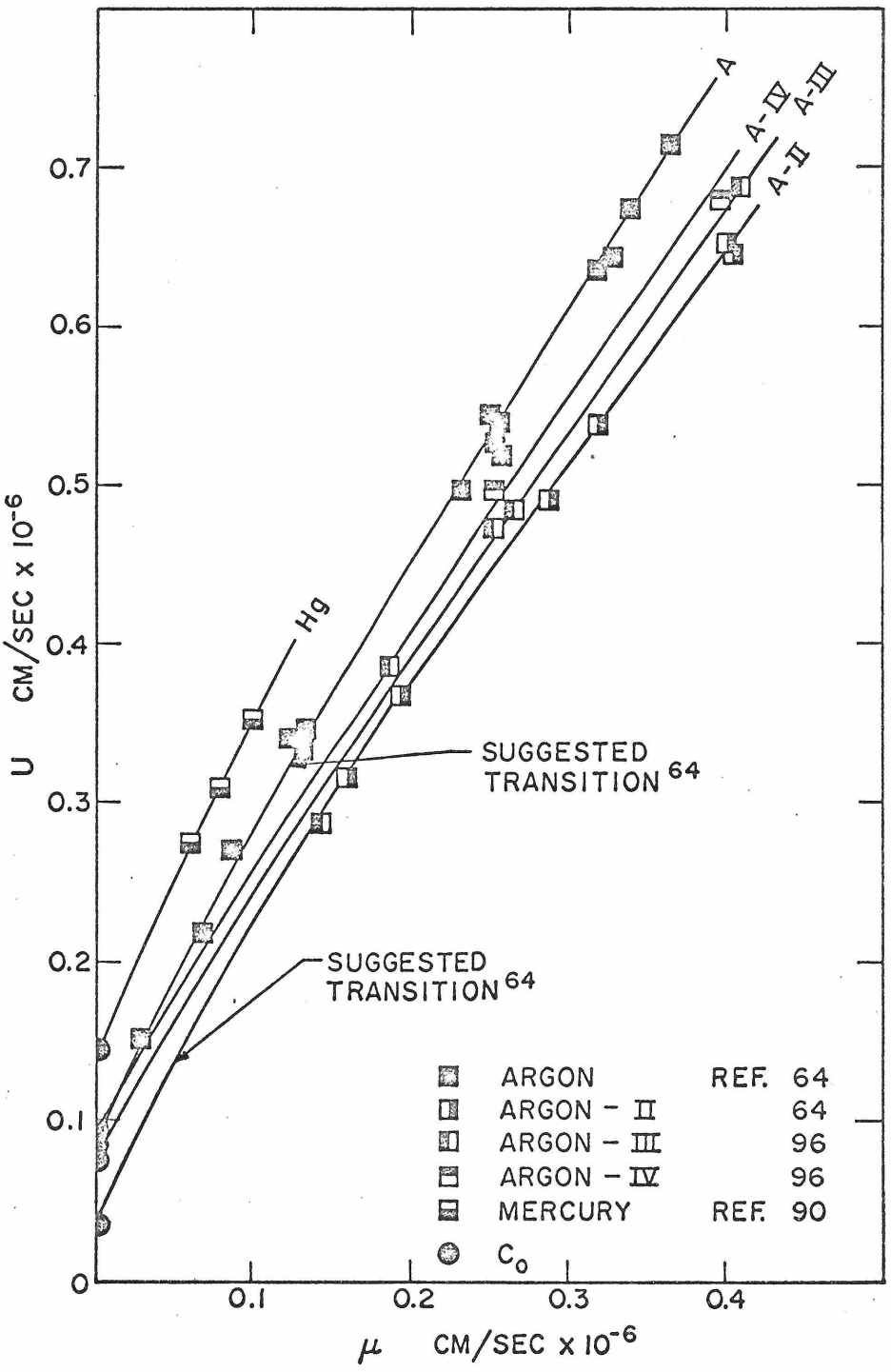

Figure 15. U vs. μ Data--A, Hg

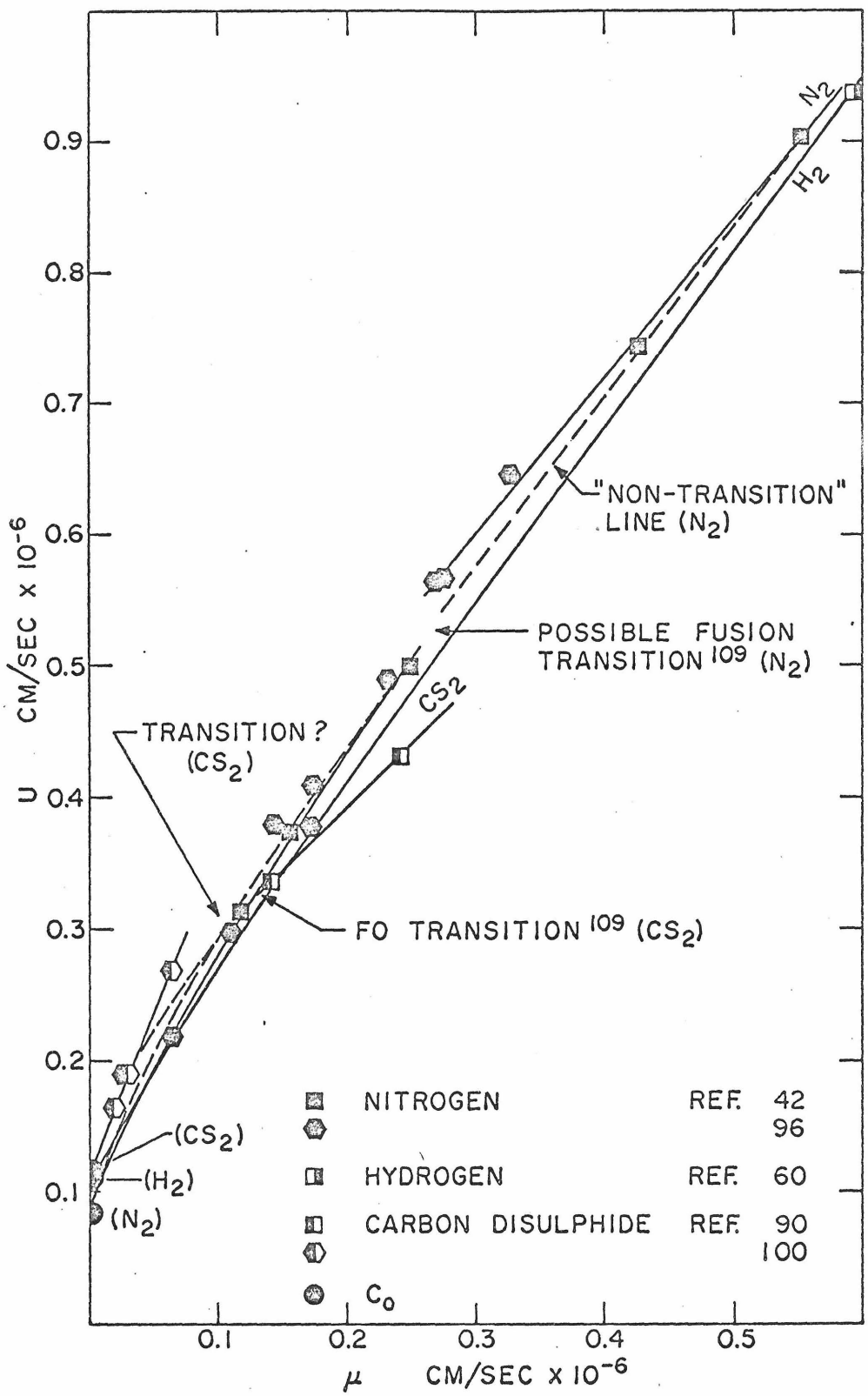

Figure 16. U vs. μ Data--N_2, H_2, CS_2

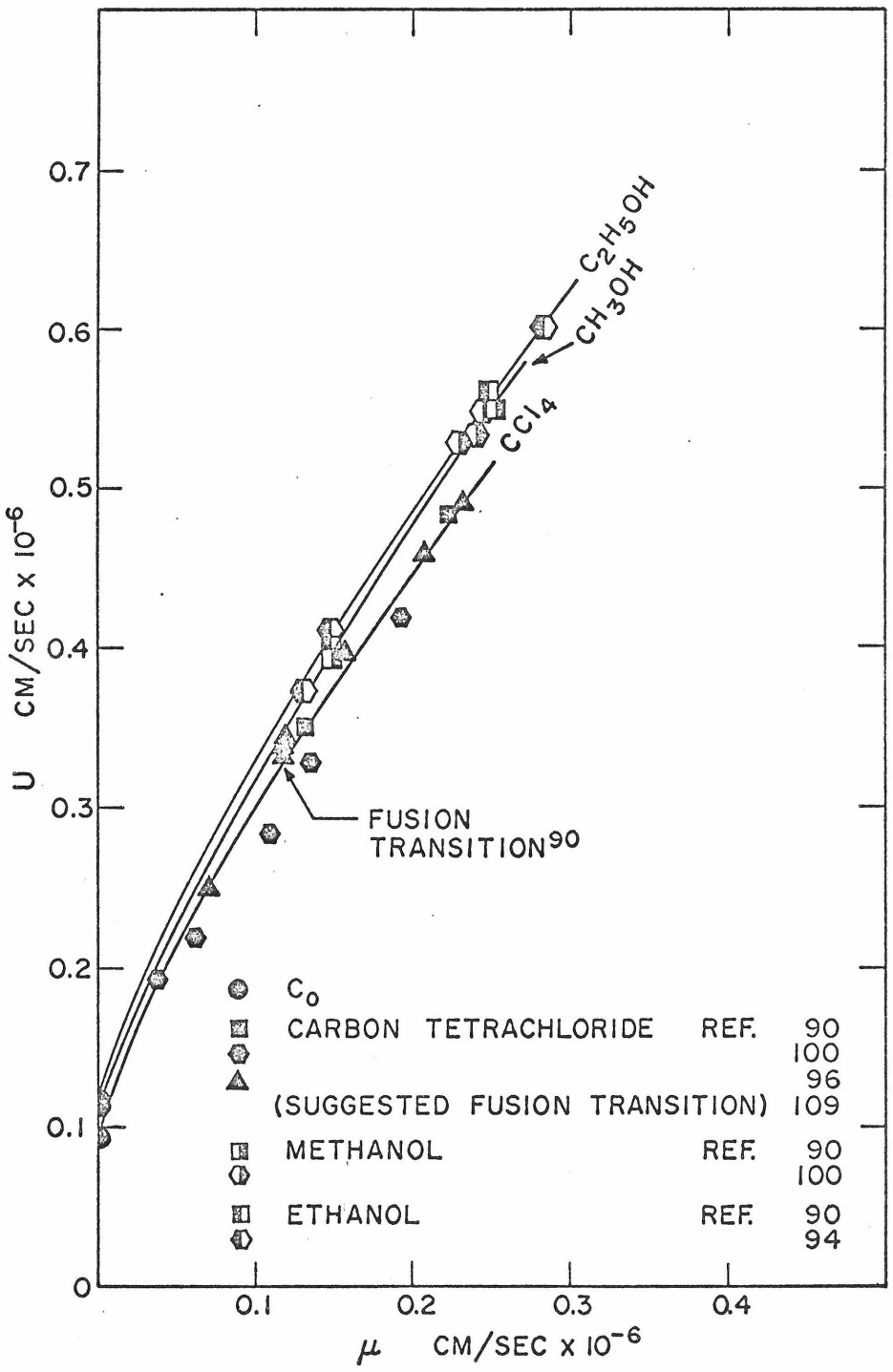

Figure 17. U vs. μ Data--CCl_4, CH_3OH, C_2H_5OH

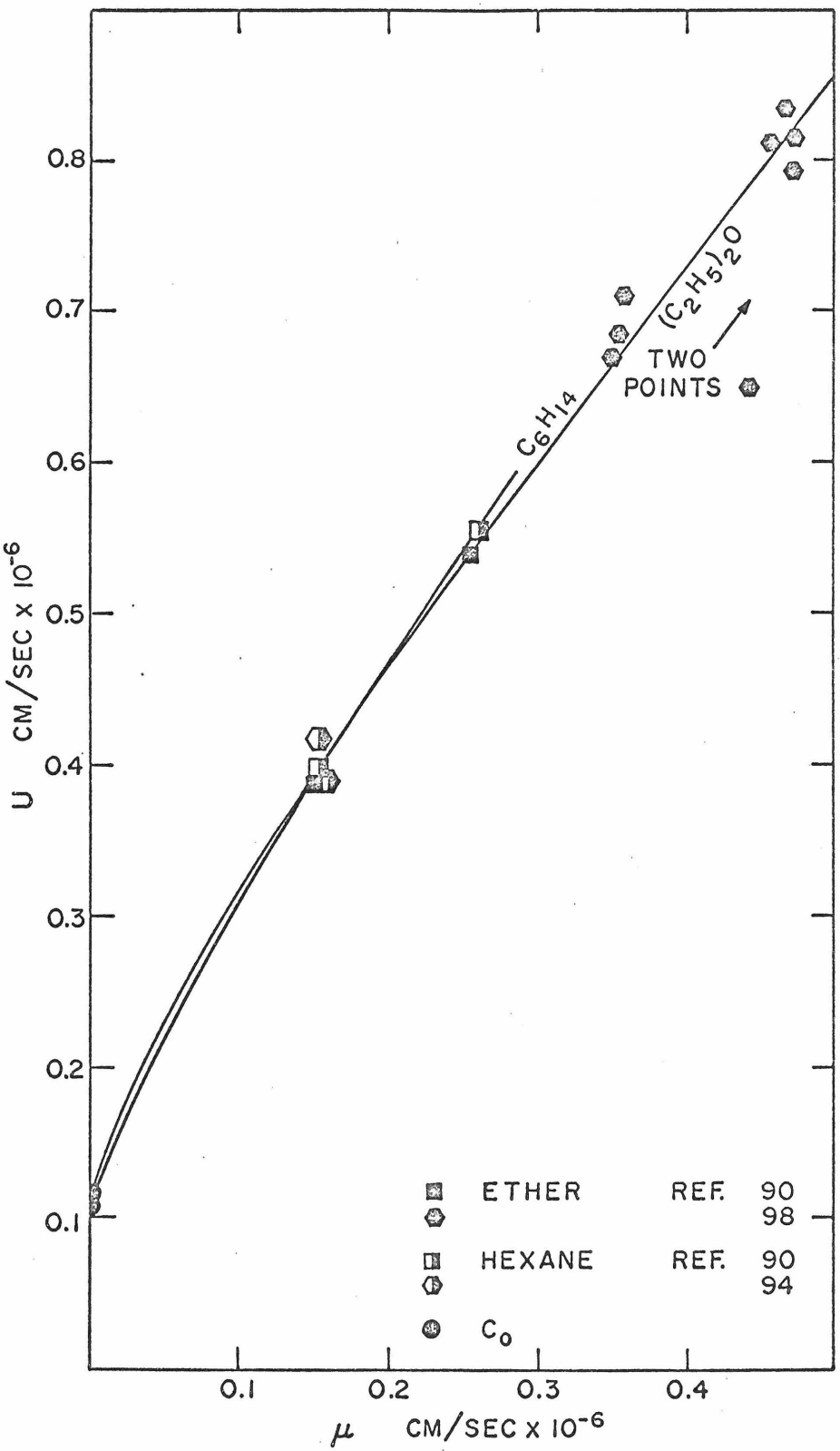

Figure 18. U vs. μ Data--$(C_2H_5)_2O$, C_6H_{14}

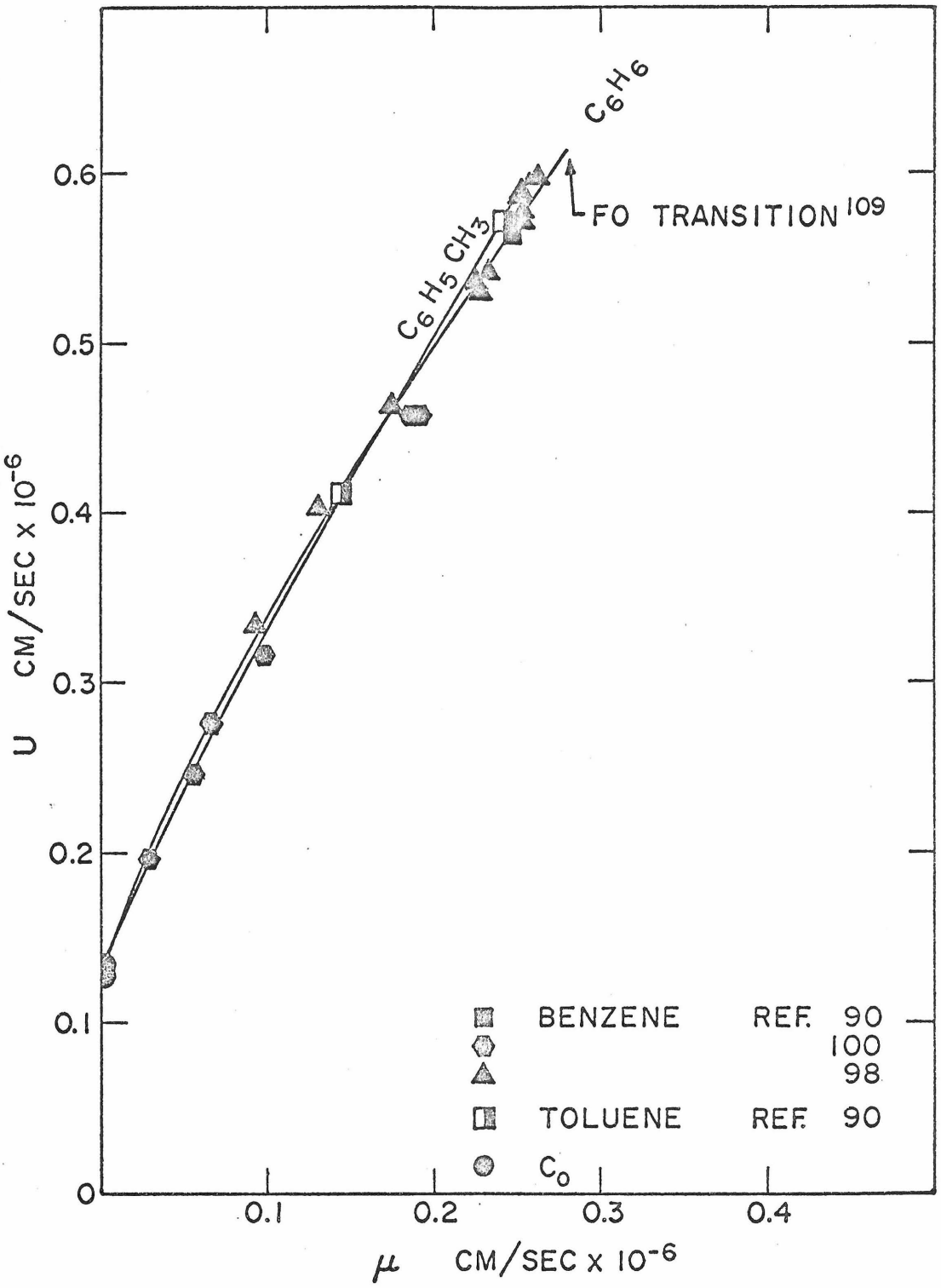

Figure 19. U vs. μ Data--C_6H_6, $C_6H_5CH_3$

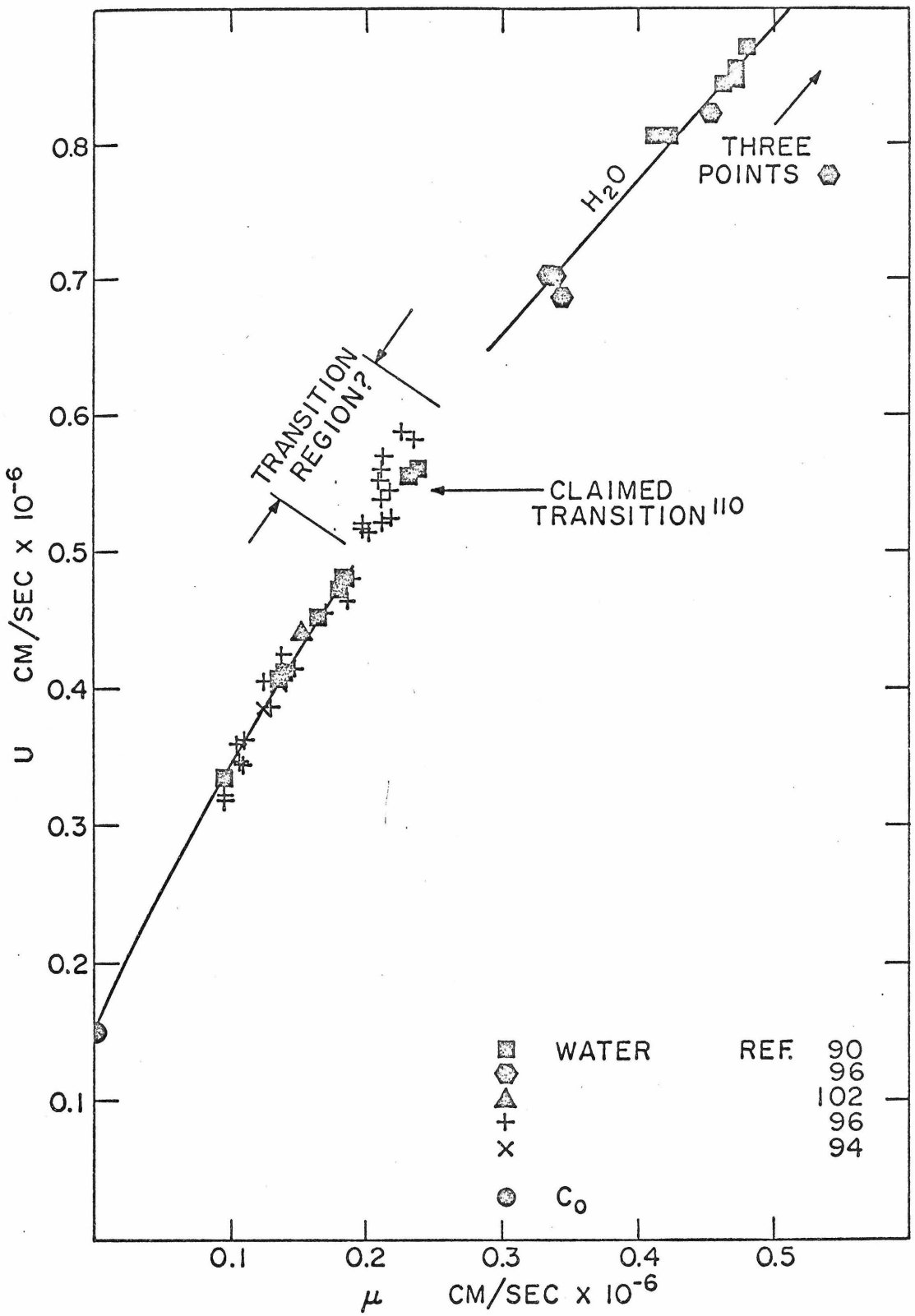

Figure 20. U vs. μ Data--H_2O

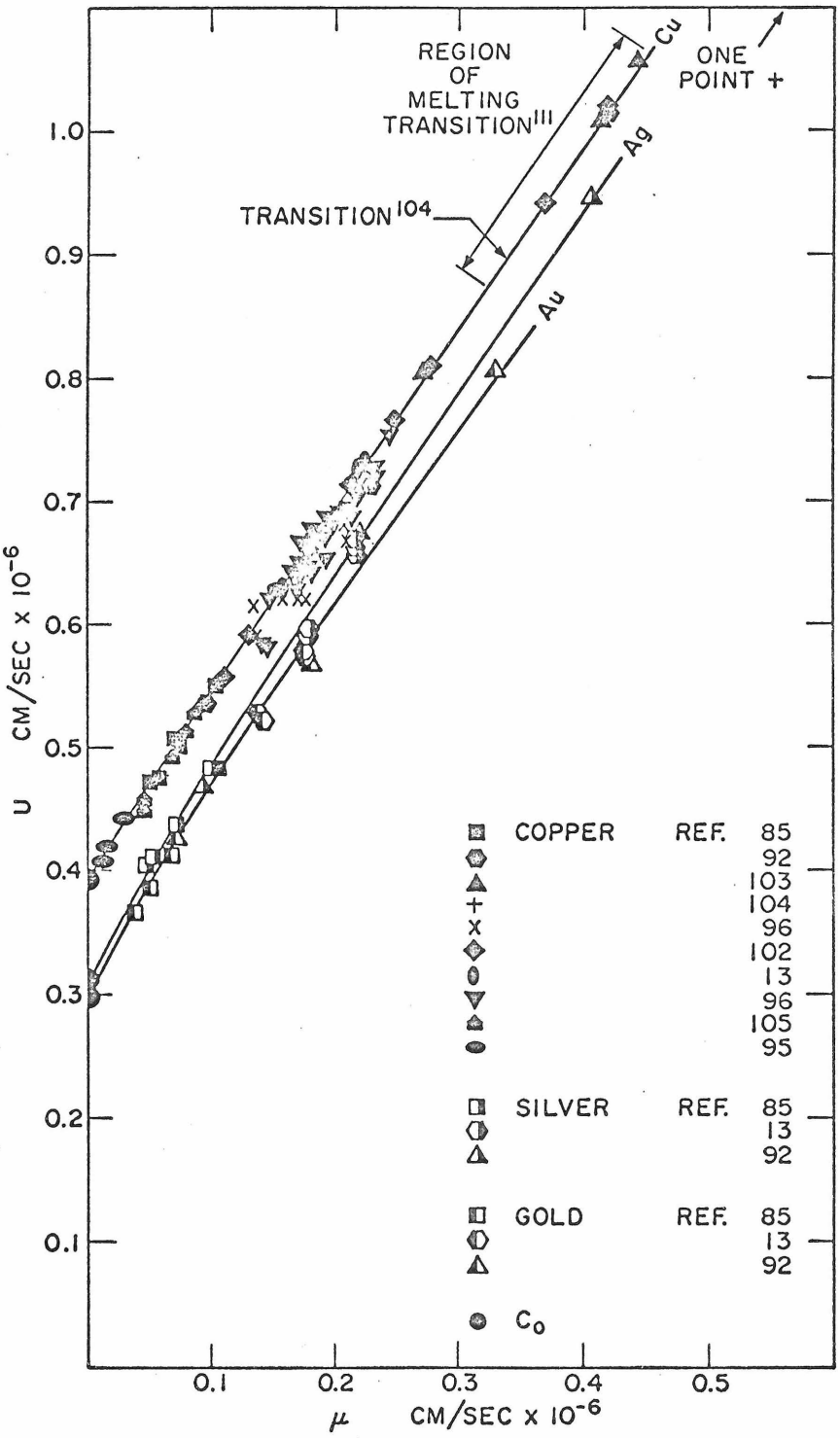

Figure 21. U vs. μ Data--Cu, Ag, Au

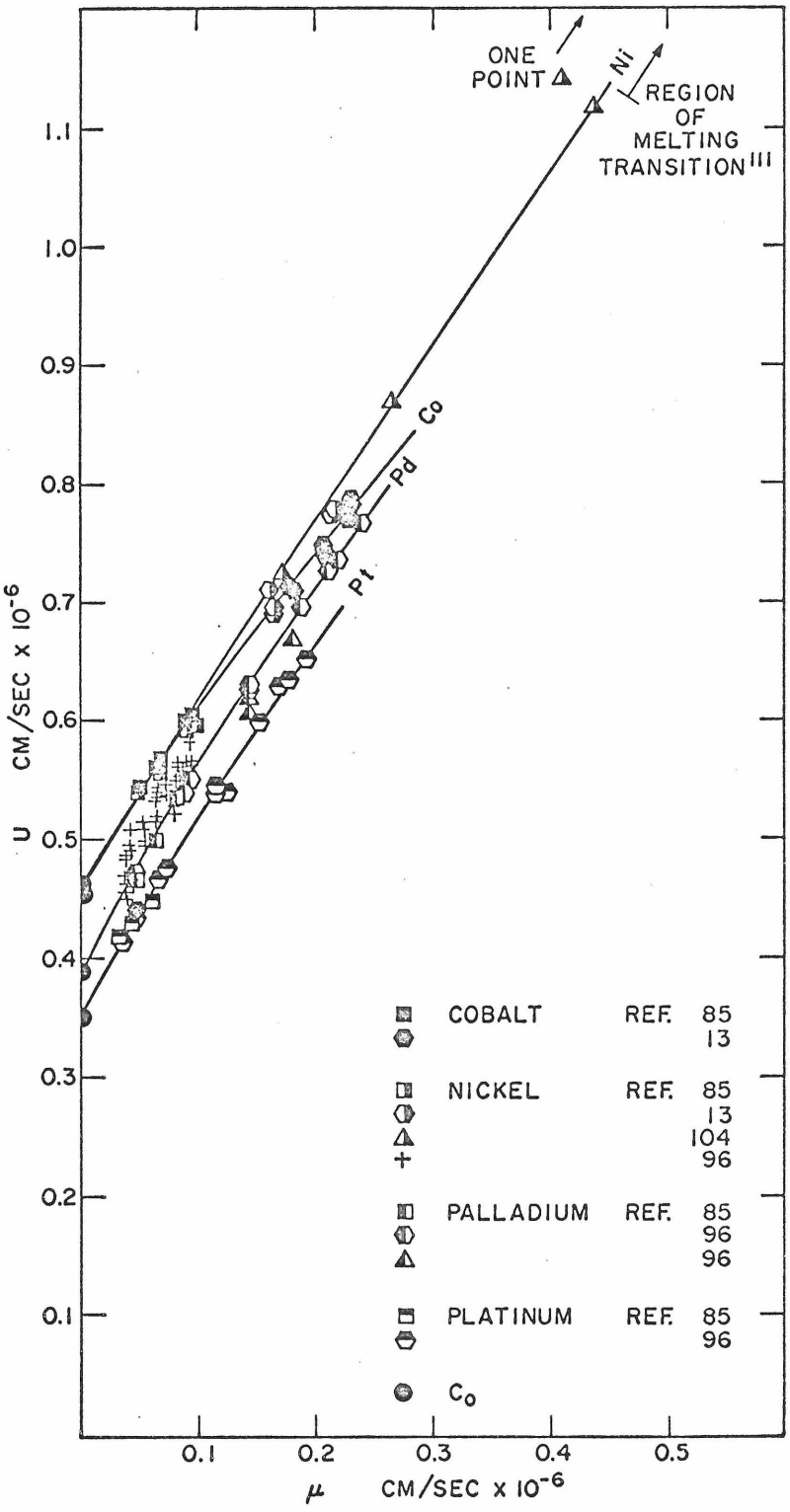

Figure 22. U vs. μ Data--Co, Ni, Pd, Pt

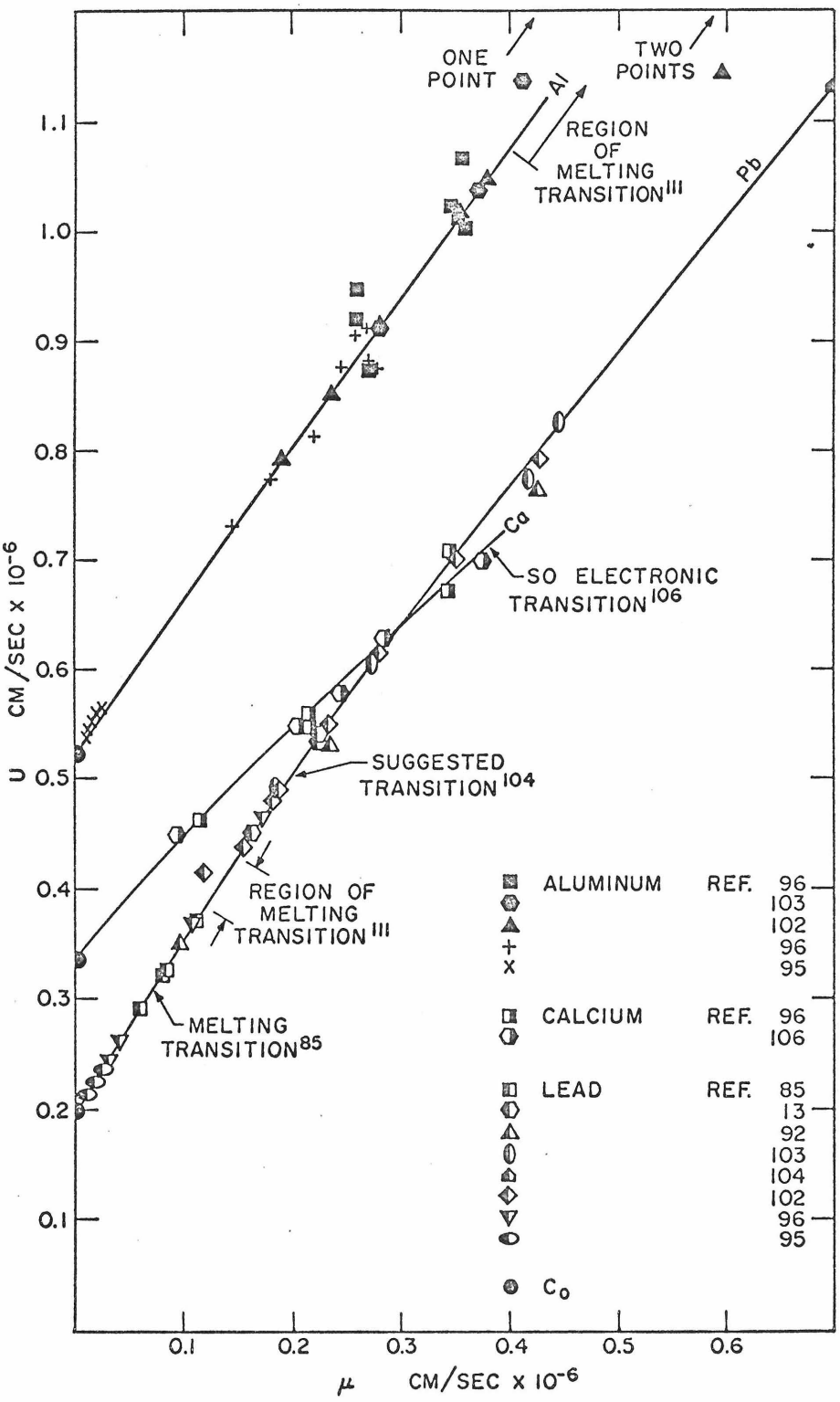

Figure 23. U vs. μ Data--Al, Ca, Pb

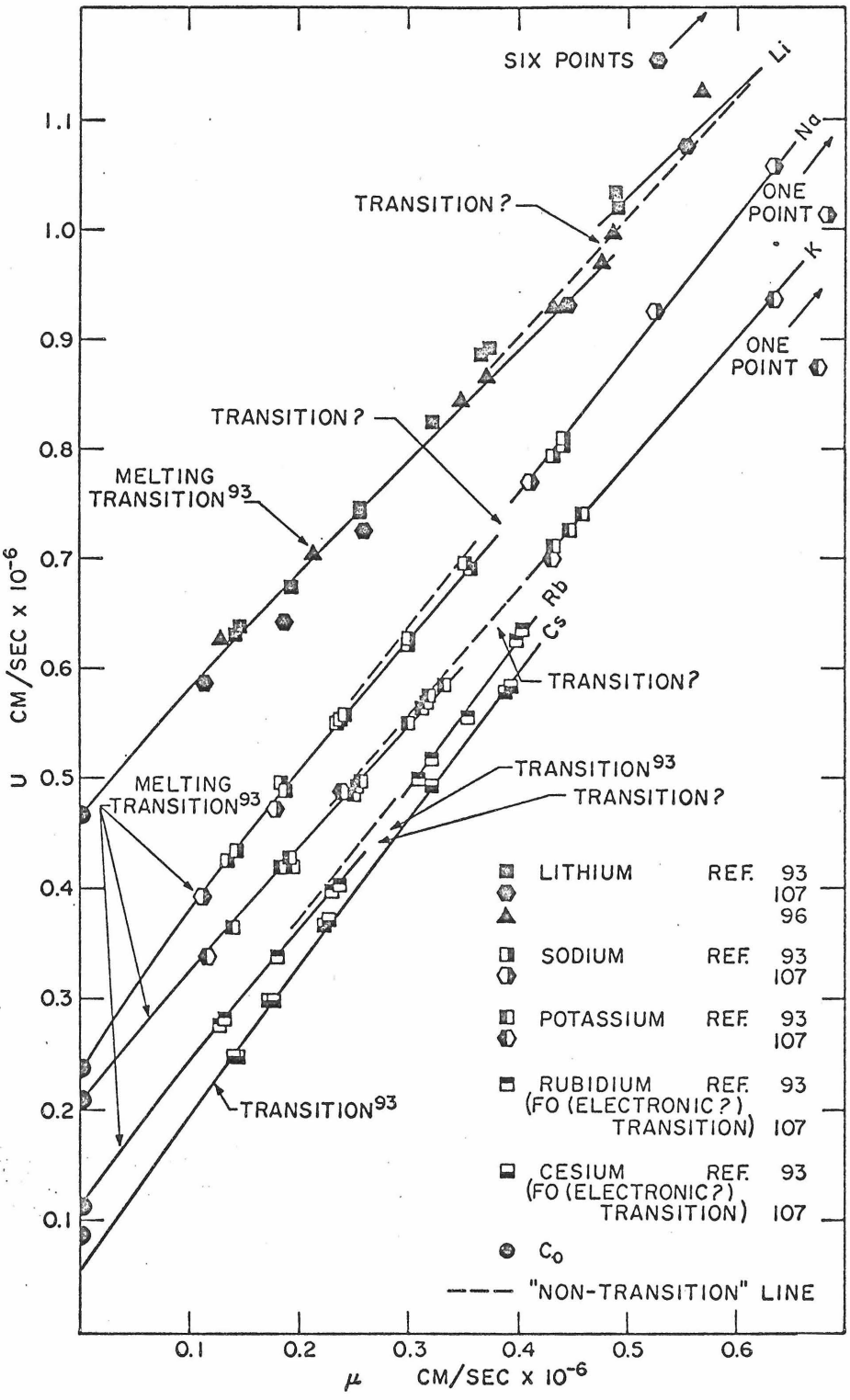

Figure 24. U vs. μ Data--Li, Na, K, Rb, Cs

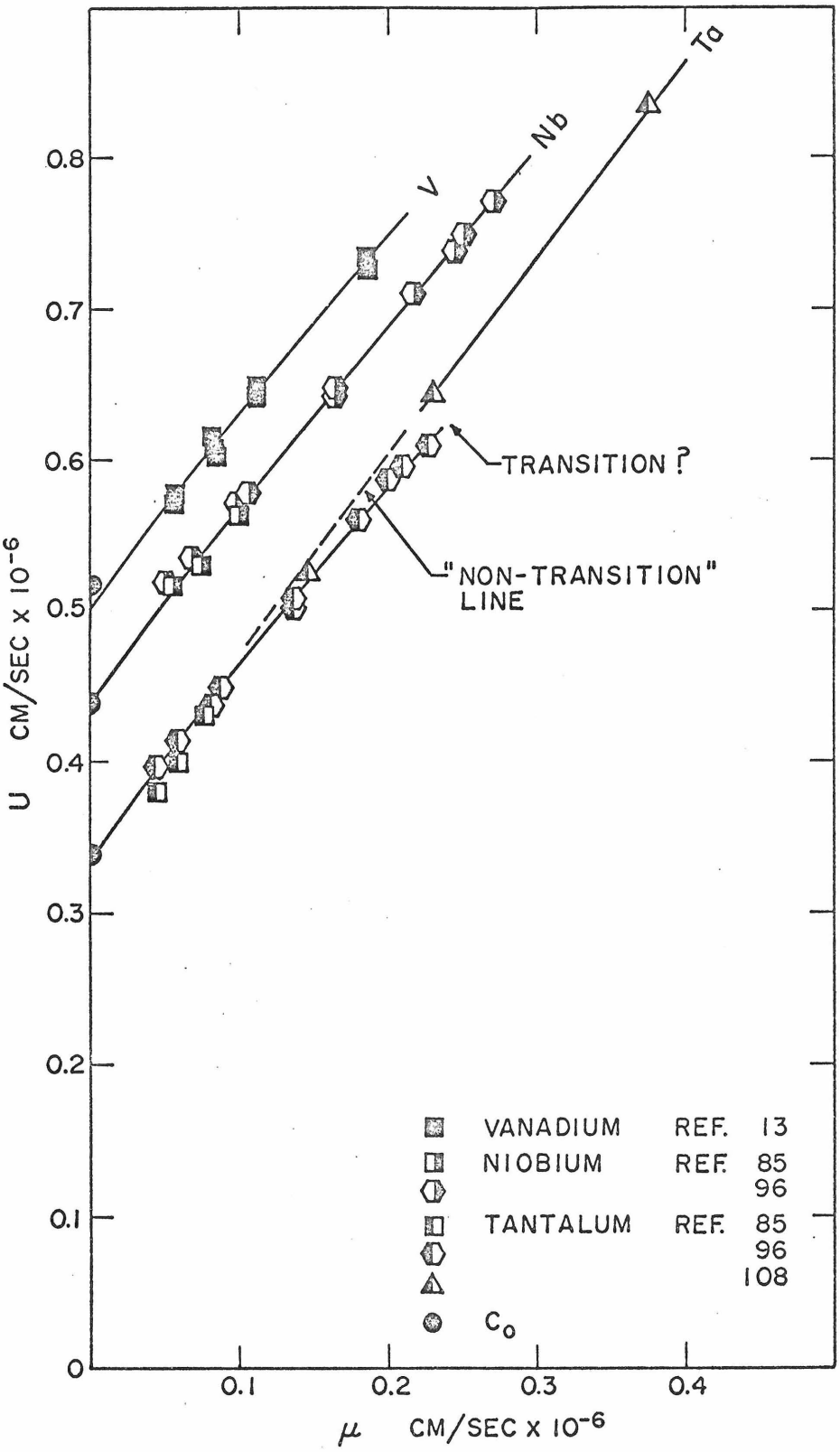

Figure 25. U vs. μ Data--V, Nb, Ta

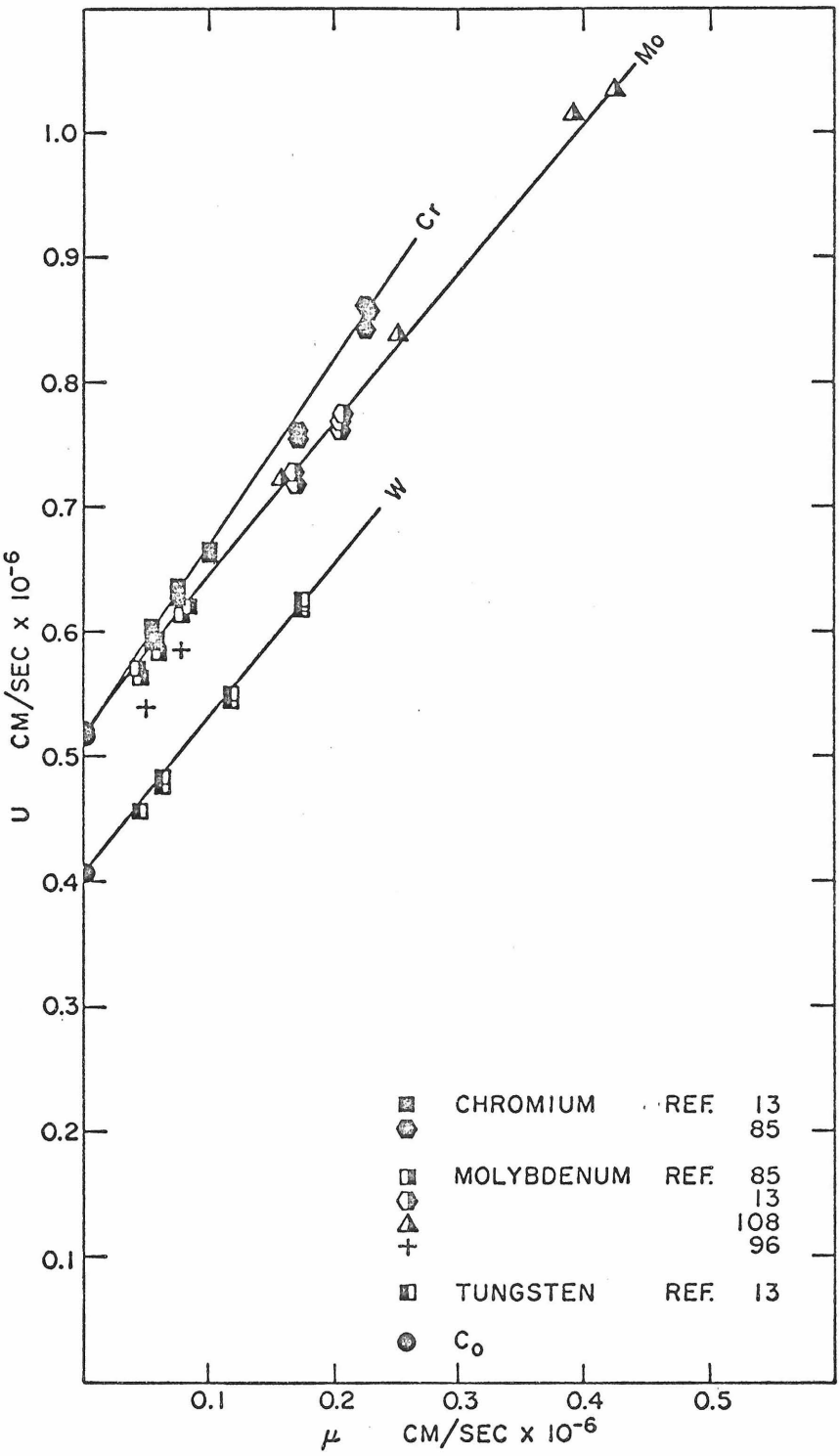

Figure 26. U vs. μ Data--Cr, Mo, W

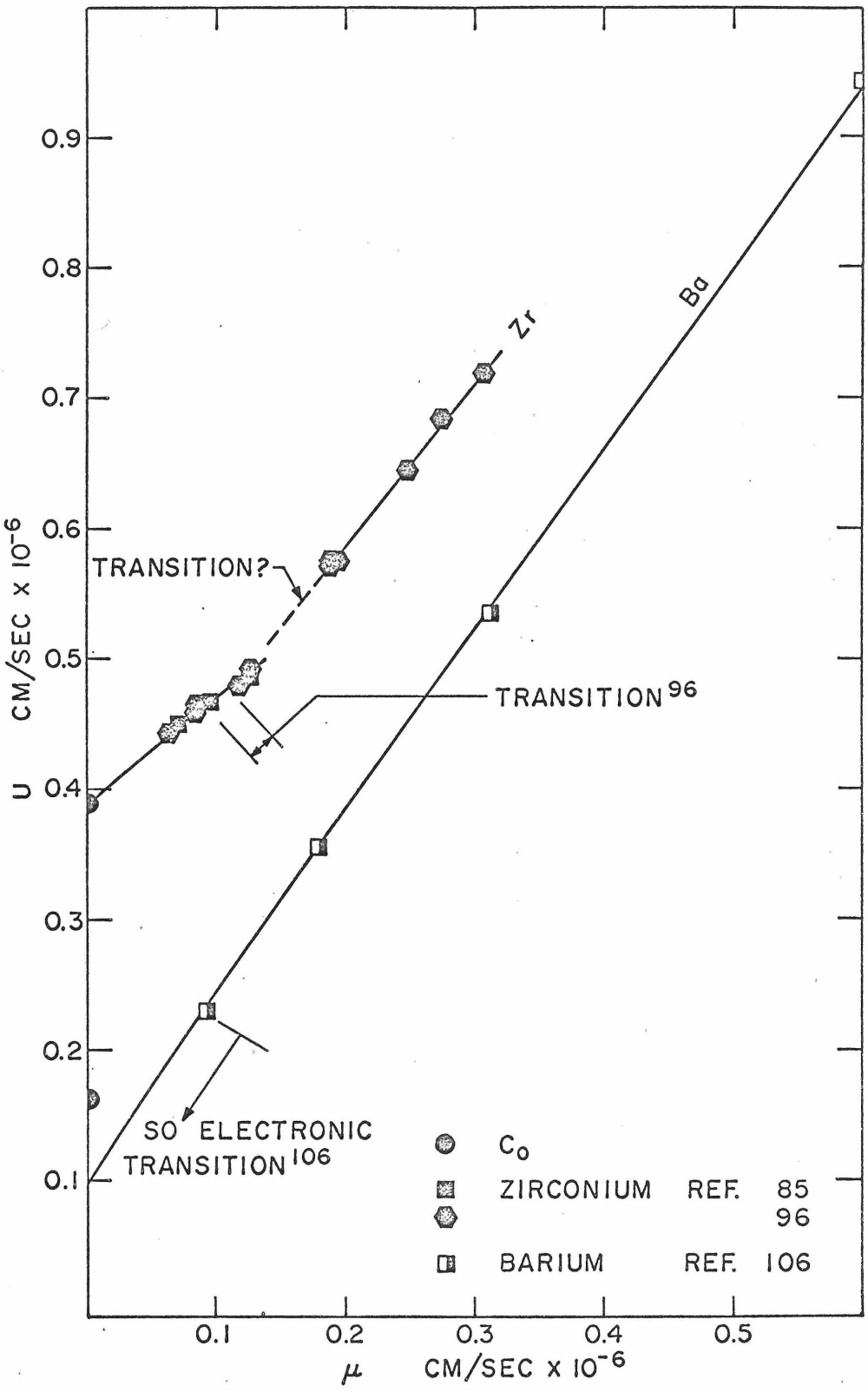

Figure 27. U vs. μ Data--Zr, Ba

3. Selection Process

A careful examination of Figures 15-27 shows that the data are not all of the same quality; in some cases considerable variations exist from investigator to investigator, even though most error estimates for velocity determinations are claimed to be $\leq$ 3% (see Table 5). Furthermore, a number of phase transitions have been reported for various materials under shock loading (see Table 6) which in some instances could affect the smoothness of the U-μ curve*. Lastly, the "fairing" process discussed previously shows clear "breaks" in the U-μ data indicating a change in behavior of the material.

For these reasons, all data used in this study were put through a selection process designed to minimize problems due to "questionable" data. The guidelines were:

(a) When data from a single source differed substantially from a number of other investigators, these data were eliminated.

(b) When phase transitions were suspected because of a "break" in the U-μ data**, higher data were eliminated.

(c) When first-order (FO) or second-order (SO) phase transitions were theoretically predicted, the data were carefully examined to see if any effects were evident on the U-μ data. If not, the prediction was ignored.

---

*A discussion of phase transitions and their effect on the theory developed in this work is included in Appendix T.

**It is assumed that the U-μ curve is a smooth, well-behaved, continuous function with continuous derivatives.

Table 5

REPORTED ERROR IN DATA

Reference	Substances	% Error in U	% Error in μ
64	A,A-II	< 2	< 2
96	A-III,A-IV	1.5	1.5
42	N_2	1 - 2	1 - 2
96	N_2	3	3
90	Hg,CCl_4,C_6H_6,Toluene,CS_2,Ethanol, Methanol,Ether,Hexane,Water	0.5	-
60	H_2	1	0.5
100	CCl_4,C_6H_6,Toluene,Methanol	-	-
96	CCl_4		
98	C_6H_6	-	-
94	Ethanol,Hexane,Water	1.5	-
98	Ether	-	-
96	Water,Al	-	-
102	Water,Cu,Al,Pb	-	-
96	Water,Cu,Ni	-	-
85	Cu,Pb,Cr,Co,Au,Mo,Ni,Ag,Nb, Pd,Pt,Ta,Zr	0.7	-
92	Cu,Ag,Au,Pb	-	-
103	Cu,Al,Pb	< 1	< 1
105	Cu	0.5	0.5
104	Cu,Pb,Ni	1.5	-
96	Cu	3	3
13	Pb,Ag,Au,Co,Cu,Mg,Ni,V,W,Cr	0.5	-
96	Pb,Ca,Mo,Li	-	-
96	Pt,Pd,Nb,Zr,Ta	-	-
96	Pd	-	-
96	Al	-	-
95	Cu,Pb,Al	-	-
93	Li,Na,K,Rb,Cs	-	-
107	Li,Na,K	1.0 - 1.5	1.0 - 1.5
108	Mo,Ta	-	-
106	Ca,Ba	-	-

Table 6

REPORTED PHASE TRANSITIONS

Substance	Type	Shock Pressure--Kbar	Reference	Comments
A*	?	58	64	Suggested by two-line fit
A-II**	?	< 6	64	Suggested by curvature of U vs.μ
N_2	Fusion	-	109	Suggested by two-line fit
	?	103 - 116	This study	Apparent "break" in plotted data
CS_2	First Order	55	109	Two wave structure
	?	28 - 47	This study	Apparent "break" in plotted data
CCl_4	Fusion	> 60	90	Opacity measurement
	Fusion	-	109	Suggested by two-line fit
C_6H_6	First Order	155	109	Two wave structure
H_2O	?	115	110	Optical and U vs. μ support
	?	93 - 190	This study	Apparent "break" in plotted data
Cu	?	2650	104	Suggested by two-line fit
	Melting	2540 - 4300	111	Theoretical computation
Ni	Melting	7400	111	Theoretical computation
Al	Melting	1150 - 2350	111	Theoretical calculation
Ca	Second Order	405	106	Two-line fit; Electronic transition
Pb	?	1240	104	Suggested by two-line fit
	Melting	> 245	85	Calculation
	Melting	500-730	111	Theoretical computation
Li	Melting	70	93	Calculation
	?	255	This study	Apparent "break" in plotted data

Table 6 (continued)

Substance	Type	Shock Pressure--Kbar	Reference	Comments
Na	Melting	40	93	Calculation
	?	275	This study	Apparent "break" in plotted data
K	Melting	15	93	Calculation
	?	225	This study	Apparent "break" in plotted data
Rb	?	193	93	Static test results
	Melting	10	93	Calculation
	First Order	?	107	No data; electronic transition
	?	180	This study	Apparent "break" in plotted data
Cs	?	45	93	Static test results
	First Order	?	107	No data; electronic transition
Ta	?	2390	This study	Apparent "break" in plotted data
Zr	?	258 - 365	96	
	?	560	This study	Apparent "break" in plotted data
Ba	Second Order	< 76	106	Inferred electronic transition

* A = Argon with initial state $T_o = 86^oK$, $P_o = 1.97$ atm.

** A-II = Argon with initial state $T_o = 148.2^oK$, $P_o = 69.2$ atm.

(d) When FO or SO transitions were suggested by a "two-line" fit*, an examination of the combined data was used to determine if the assumption of a transition was justified. If so, higher data were eliminated. However, in several instances[104,11,64,109,112] it appears that whenever the U-μ data did not conform to a straight line (Equation (13)) a "two-line" fit was made and a transition at the intersection assumed! Since this procedure has no a priori justification (except to preserve the (unnecessary) notion of U-μ linearity), it was simply assumed that, in these cases, the U-μ relation was curved. There is a wealth of support for a curved U-μ relation[105,113,92,86,104,93,14,95,60,114,106]. If the data could be fitted by a smooth curve the assumed "transitions" were ignored.

(e) In a number of instances a decision could not be made on the basis of (a) to (d) above, and the data set with and without the "questionable" data was carried through the first calculations. This was usually sufficient to distinguish between the two sets and eliminate "questionable" data.

It is recognized that this process was not carried out on any absolute basis and that the decisions to eliminate data were, ultimately, discretionary in nature. However, this is done without apology since more formal guidelines are at present unknown to the author.

---

*Examination of Figure T-2 in Appendix T shows that FO and SO phase transitions can be characterized by "two-line" fits, especially if the mixed phase region for FO transitions is small. In many cases there are not sufficient data to characterize the mixed region and "two-lines" suffice to fit all the data.

The items considered in the selection process are generally detailed in Figures 15-27 where the effects of each of the reported phase transitions (Table 6) on the data are seen. The selection resulted in an adjusted data set for N_2, CS_2 and H_2O among the liquids; Ni and Al among the fcc metals; and Li, Na, K, Rb, Ta and Zr among the bcc metals.*

*The adjusted data are listed in Appendix S on the page following the raw data for each of the substances indicated.

B. LIQUIDS

Values of σ and ε for a number of substances have been determined from viscosity[5], second virial coefficient[5], thermal conductivity[74] and thermal diffusivity data[74]. Most of the available values are compiled in Reference 5. Because these data are considered to represent physically meaningful quantities, it is assumed that they can be used to reasonably accurately describe the "true" pair-potential function. Because σ,ε data are available for all the liquids considered in this study, advantage was taken of this fact by using the solutions to the Hugoniot in WF (Equations (105)-(107), (113), (114), (124)-(128)) or MF (Equations (105)-(107), (115), (116), (124)-(126), (129), (130)). This allows full use of the σ,ε data available and establishes a more "realistic" base for any conclusions drawn from the analysis*.

*Because advantage was taken of the σ,ε data available does not mean that the values presented in the literature were accepted prima facie. In fact, a correlation of ε with melting points eventually proved to give "better" results than the raw values.

1. Development of Parameters

From Equations (105)-(107) it would appear that the best test of the theory would be to pick σ and ε (from available data) and compare the predicted Hugoniot with the available data for various values of n. However, a reconsideration of Equation (72) shows that this comparison can be done in more than one way. Equation (72) is:

$$\phi(r) = \varepsilon f(n) \left[\left(\frac{\sigma}{r}\right)^n - \left(\frac{\sigma}{r}\right)^6\right] \tag{72}$$

where $f(n)$ is given by Equation (71). The quantities ε and σ have physical meaning in that they are considered real measures of the pair interaction (see Figure 8) even if Equation (72) does not truly represent that interaction over the whole range of r. Thus σ is considered the true minimum interaction energy and is the distance at which the interaction energy is actually zero. The first suggested method of testing the theory is clearly logical.

An examination of Equation (70) and Figure 8 shows that an equally logical pair of parameters to fix would be r_o and ε. That is, r_o is also a physical quantity (the position of the minimum) that could be picked along with ε to describe the interaction*. In this case the various values of n used to make the comparison would determine σ through Equation (70). Although this alternate mode of comparison is theoretically possible it was not pursued because r_o data for liquids are not generally available in the literature.

Another method of comparison may be seen by expansion of Equation (72) in the following form:

$$\phi(r) = \frac{\varepsilon\, f(n)\, \sigma^n}{r^n} - \frac{\varepsilon\, f(n)\, \sigma^6}{r^6} \tag{131}$$

As previously mentioned, the second term, representing attractive forces, is amenable to fairly rigorous treatment (at least for insulators) and the coefficient of the r^{-6} term has been calculated by a number of authors[21,36,23,115,58,5,116-121, 56,81,55,122]. This coefficient is called the "dispersion" constant** and is usually denoted C_{ab}. Therefore:

$$C_{ab} = \varepsilon\, f(n)\, \sigma^6 \tag{132}$$

may also be considered a "real" quantity that describes the attractive

---

*The fact that Equation (72) is written in terms of ε and σ instead of ε and r_o is not inherently significant. Clearly, substitution of Equation (70), solved for σ, into Equation (72) would yield $\phi(r)$ as a function of ε and r_o. This same substitution for σ would be made in Equations (96)-(98), etc.

**For molecules without a dipole moment.

behavior of the molecules; the portion of the curve to the right of the minimum in Figure 8. Since C_{ab} contains both ε and σ (as well as n) the pair of parameters to describe the interaction could be C_{ab} and ε or C_{ab} and σ. In general the latter pair was considered, since the available σ data are believed to be more accurate than the available ε data. In that instance $\varepsilon = C_{ab}/f(n)\sigma^6$ and Equation (131) becomes (after substitution and rearrangement):

$$\phi(r) = \frac{C_{ab}}{\sigma^6}\left[\left(\frac{\sigma}{r}\right)^n - \left(\frac{\sigma}{r}\right)^6\right] \qquad (133)$$

To help determine the preferred parameter pair (σ and ε or σ and C_{ab}) for making comparison of the theory with experiment, a number of preliminary computations were made using some of the available σ,ε and C_{ab} data which are compiled in Table 7.

Equation (132) shows that if C_{ab}, ε and σ are known for a given material $f(n)$ and therefore n (see Equation (71)) is fixed, at least for the pair potential chosen, Equation (72). Using the data in Table 7 such computations were made for A, Hg, N_2 and H_2 for various combinations of the parameters*. The results, shown in Table 8, indicate the values of n that satisfy the particular set of "real" parameters σ, ε and C_{ab}. That is, for these values of n, Equation (72) goes through the given values of σ and ε and exhibits the correct long-range attractive behavior. The question remains: Are these values consistent with the shock data which are in the strongly

*The C_{ab} data are determined independently of the σ,ε pairs and can therefore be combined with any of them.

Table 7

AVAILABLE σ, ε, C_{ab} DATA -- LIQUIDS

Substance	σ-Å	ε/k-°K*	Reference	Date	C_{ab}-. erg-cm^6 $\times 10^{60}$	Reference	Date
A	3.405	124	5	1942 1949	52	36	1937
	3.30	152	25	1964	55.4	5	1938
	3.44	110	25	1964	55.9	118	1961
	-	147.7	55	1967	65.16	119	1961
	3.38	134	71	1967	68.1	120	1963
	3.28	[138.2]	74	1969	61	56	1964
					63.85	121	1964
					61.3	55	1967
					65.9	122	1968
Hg	2.898	851	5	1954	255	5	1930
	2.88	654	25	1964			
	2.86	195	25	1964			
N_2	3.71	95.9	5	1925	57.2	5	1938
	3.72	96.7	23	1944	62	23	1944
	3.73	[91.5]	42	1962	57.5	118	1961
					65.7	118***	--
H_2	2.87	29.2	5	1941	11.4	5	1938
	2.92	31.0	23	1944	11.3	23	1944
	2.968	33.3	123	1950	11.4	118	1961
					13.0	118***	--
					12.7	120	1963
CS_2	4.438	488	5	1933			
CCl_4	5.881	327	5	--			
	5.77	[378]	54	1967			
CH_3OH	3.666	452	5**	1961			

Table 7 - (continued)

Substance	σ-Å	ε/k-°K*	Reference	Date	C_{ab}-erg-cm^6×10^{60}	Reference	Date
C_2H_5OH	4.370	415	5**	1961			
$(C_2H_5)_2O$	5.539	351	5**	1961			
C_6H_{14}	5.916	423	5**	1962			
C_6H_6	5.270	440	5	--			
$C_6H_5CH_3$	12.0	185	5**	1958			
	5.932	377	5**	1962			
H_2O	2.648	382.4	58	1951	57.0	58	1951
	2.725	355.8	124	1969	247	5	1952
					52.2	81	1965
					86.0	81	1965

*k = Boltzmann's constant = 1.38045 erg/°K

**Reference 5, corrected, with notes added, 1964.

***A comparison of References 118 and 121 for the rare gases indicates a (possible) systematic error in the former. This factor (1.142) was applied to C_{ab} for all of the reported values in Reference 118.

Table 8

PRELIMINARY COMPUTATIONS

$$f(n) = C_{ab}/\varepsilon\sigma^6$$

Substance	σ-Å	ε/k-°K	C_{ab}-erg-cm$^6\times10^{60}$	f(n)*	n
A	3.28	138.2	65.9	2.774	16.7
Hg	2.898	851	255	3.664	12.8
	2.88	654	255	4.950	10.5
	2.86	195	255	17.31	7.0
N_2	3.71	95.9	57.5	1.666	> 30
	3.73	91.5	62.0	1.823	> 30
	3.71	95.9	62.0	1.796	> 30
	3.73	91.5	57.5	1.690	> 30
H_2	2.87	29.2	11.4	5.061	10.3
	2.968	33.3	12.7	4.041	11.9
	2.87	29.2	12.7	5.638	9.8
	2.968	33.3	11.4	3.628	12.9

* $f(n) = (n/6)^{n/n-6} \big/ (n/6-1)$; $\lim_{n \to 6} f(n) \Rightarrow \infty$, $\lim_{n \to \infty} f(n) = 1$

repulsive region?

For the σ , C_{ab} parameter combination this was tested by fitting the associated theory (see Appendix U) to argon (σ = 3.28Å, $C_{ab} = 65.9 \times 10^{-60}$ erg-cm^6) and nitrogen (σ = 3.71Å, $C_{ab} = 57.5 \times 10^{-60}$ erg-cm^6). The resultant best fit values of n were 10.4 and 9.2 respectively, which differ considerably from the values in Table 8. Resubstitution of these values into Equation (132) along with the σ and C_{ab} values used, yields values of ε of 77°K and 25°K respectively for argon and nitrogen; $\sim$ 1/2 and $\sim$ 1/4 of the "actual" values in Table 8.

These results indicate that for the n-6 potential, a single value of n will not satisfy strong repulsion, σ , ε and long-range attraction (C_{ab}) simultaneously*. Further, it appears that satisfaction of strong repulsion, σ and C_{ab} leads to well depths ε that are too small**.

Because of this, the σ,ε parameter pair was chosen for the comparison of the shock data and theory***. It is understood that C_{ab} (the attraction region) will not be satisfied in this instance but

---

* This has been pointed out previously[125,64,53].

** An attempt was made to reduce the values of n in Table 8 by accounting for additional attraction implied by Equation (59). The results, shown in Appendix V, do not materially affect the conclusions made.

*** This intuitively makes more sense because the shock data are in the strongly repulsive region and it is sufficient to satisfy σ and ε (see Figure 8) which define all the compressive (repulsive) states. No advantage is gained by "jumping over" ε to satisfy the attractive forces.

this is accepted as a limitation of the potential chosen. Of course, in many of the compressive states defined by the shock data, the attractive forces will be, by comparison, negligible and the error involved in this procedure will be small.

Chapman[126] in a recent paper showed that the viscosity of several liquid metals could be correlated with atomic (molecular) parameters such as ε and σ over a considerable temperature range. To establish a more fundamental footing for this correlation he showed that the energy parameter is independently correlatable with melting points*. He would have made this correlation with respect to critical temperatures, but found them unavailable for the materials being considered.

Although Chapman considered only liquid metals, the ideas developed should apply generally and correlations should be possible for critical temperatures, boiling points as well as melting temperatures**[23,5]. The latter parameter was chosen for the correlation for this study, since it represented the only one for which values

---

*Chapman used values of ε for Na and K taken incorrectly from a paper by Ling[76], to generate ε values for the other metals. Although his resulting correlation is numerically incorrect, his evidence for such a correlation remains valid.

**Reference 5 gives as approximate relations $\varepsilon/k = 0.77\ T_c = 1.15\ T_b = 1.92\ T_M$. Correspondingly, Reference 23 gives $\varepsilon/k = 0.75\ T_c = 1.25\ T_b$ which are not much different. When Chapman's correlation for liquid metals $\varepsilon/k = 5.20\ T_M$ is corrected for the erroneous data read from Ling[76] (a factor of ~ 3.3), it becomes $\varepsilon/k = 1.57\ T_M$ which is in fair agreement with Reference 5. Considering that the former deals with liquid metals and the latter with spherical nonpolar molecules, the agreement is notable.

were available for all of the substances included in the study (see Table 4).

The most reliable values of ε/k for the liquids in Table 7 are those in brackets for argon, nitrogen and CCl_4. The respective melting temperatures are 83.9°K, 63.2°K and 250.1°K. Based on this data set, a least-squares best-fit line was computed with the result (see Appendix W):

$$\varepsilon/k = 1.5\ T_M + 4\ ^oK \tag{134}$$

Using Equation (134) a new set of ε values was computed for all of the liquids studied based on available T_M data[101]. The results are shown in Table 9 and compared to the similar data in Table 7. It is notable that this procedure leads to a large reduction in ε/k for CS_2, CH_3OH, C_2H_5OH, $(C_2H_5)_2O$, C_6H_{14} and $C_6H_5CH_3$ but reasonable agreement for H_2, C_6H_6 and H_2O. Although these reductions in ε/k are not as substantial as those produced by using the σ, C_{ab} parameter pair, they are significant changes and the matter of choosing between the "original" data (Table 7) or "correlated" data (Table 9) must be decided by the relative success of each when fitting the shock data. This is discussed in the following sections.

Table 9

ε/k vs. T_M CORRELATION--LIQUIDS

$\varepsilon/k = 1.5\ T_M + 4$

Substance	T_M - °C	T_M - °K	ε/k - °K	From Table 7 ε/k - °K
A	-189.2	83.9	129.9	138.2
Hg	- 38.87	234.2	355.3	195-851
N_2	-209.86	63.2	98.8	91.5
H_2	-252.8	20.3	34.5	29.2-33.3
CS_2	-108.6	164.5	250.8	488
CCl_4	- 23.0	250.1	379.2	378
CH_3OH	- 97.8	175.3	267.0	452
C_2H_5OH	-117.3	155.8	237.7	415
$(C_2H_5)_2O$	-116.3	156.8	239.2	351
C_6H_{14}	- 94.3	178.8	272.2	423
C_6H_6	5.51	278.6	421.9	440
$C_6H_5CH_3$	- 95.	178.1	271.2	377
H_2O	0.0	273.1	413.7	355.8-382.4

2. Treatment of Data

Equations (96)-(98) with specified values of σ and ε (and s, ρ_o and M) are to be used to find the "best" value of n, the repulsive exponent, from the various sets of shock data. When this is done, the resultant value of n can, for the WF solution, be used in Equation (104) to determine U_o and in Equation (105) to determine if the "condition" previously described is met. The equivalent MF solution uses Equations (106) and (107) respectively*.

Substitution of Equations (97) and (98) in Equation (96) gives (back) Equation (95) which, noting Equation (71), may be written:

$$\mu^2 = \frac{4}{2^s}\left(\frac{N\pi\varepsilon}{M}\right)\frac{(n/6)^{n/n-6}}{(n/6-1)}\left[\frac{\sigma^n}{(n-2)(n-3)}\left(\frac{2^s\rho_o N}{M}\right)^{n/3}(x^{n-2}-1)\right.$$

$$\left.-\frac{\sigma^6}{12}\left(\frac{2^s\rho_o N}{M}\right)^2(x^4-1)\right] \qquad (135)$$

Letting:

---

* Equations (115)-(121) apply only when $n \to 6$. Since it was shown that $n > 6$ for all the liquids considered, these equations were not of interest.

$$\left.\begin{aligned} C_1 &= \frac{4}{2^s}\,\frac{N\pi}{M} \\ C_2 &= \left(\frac{2^s \rho_o N}{M}\right)^{1/3} \\ C_3 &= \frac{1}{12}\left(\frac{2^s \rho_o N}{M}\right)^2 \end{aligned}\right\} \qquad (136)$$

this becomes after rearrangement:

$$\mu^2 = C_1 \varepsilon \sigma^6 \frac{(n/6)^{n/n-6}}{n/6 - 1}\left[\frac{\sigma^{n-6}\, C_2^n}{(n-2)(n-3)}\,(x^{n-2} - 1) - C_3(x^4 - 1)\right] \qquad (137)$$

In Equation (137) the system molecular parameters σ, ε and n have been separated out; C_1, C_2 and C_3 are reliably fixed constants. For the data set $U_i - \mu_i$, Equation (4) may be used to produce the set $\mu_i - x_i$ and least-squares techniques may then be used to fix n for given values of σ and ε ("one-parameter fit" = 1PF). By the same token, these same methods can be used to (a) fix n and σ for a given value of ε ("two-parameter fit" = 2PF); (b) fix n and ε for a given value of σ (2PF); or (c) fix n, σ and ε, none being given

("three-parameter fit" = 3PF). It is clear that such a progression is equivalent to "increasing the number of adjustable parameters" in the theory. Confidence in the physical reality of the model is proportionally decreased.

However this may be, the 2PF's were carried out in every instance to provide cross-confirmation of the 1PF*, while the 3PF was computed to provide a measure of the best fit possible for the functional form being considered, i.e., Equation (137). As confirmed in almost all cases, the 3PF was found to be essentially insensitive to n ; a large range of values of n fit the data equally well with different sets of σ and ε . The general approach is summarized in Table 10.

For a given data set $\mu_i - x_i$ the residuals R_i for Equation (137) may be expressed:

$$R_i = \mu_i^2 - C_1\varepsilon\sigma^6 \frac{(n/6)^{\frac{n}{n-6}}}{(n/6 - 1)} \left[\frac{\sigma^{n-6}\, C_2^n}{(n-2)(n-3)} (x_i^{n-2} - 1) - C_3(x_i^4 - 1)\right] \tag{138}$$

Of interest are the equations:

$$\frac{\partial \sum_i R_i^2}{\partial n} = 0 \tag{139}$$

$$\frac{\partial \sum_i R_i^2}{\partial \sigma} = 0 \tag{140}$$

---

*That is, if the 2PF's reproduced the assumed values of σ and ε, and gave the minima at the same n as the 1PF, the latter would be additionally confirmed.

Table 10

FITTING OF DATA--LIQUIDS

Parameter Fit	Fix	Seeking
1	σ,ε	n
2	ε	σ,n
2	σ	ε,n
3	-	σ,ε,n

$$\frac{\partial \sum_i R_i^2}{\partial \varepsilon} = 0 \qquad (141)$$

which suffice to determine the values of σ, ε and n which minimize the sum of the squares of the residuals according to the principle of least-squares[15]. The derivations and resultant relations for the 1PF, 2PF's and 3PF are shown in Appendix X.

Because an equation as complex as the implicit relation defining the desired value of n (Appendix X, Equation (X7)) might have many roots, the one of interest (i.e., the one that minimizes residuals) might be difficult to locate. For this reason it was decided to index through the entire range of n desired, incrementing by 0.1 at each step. For each value of n the corresponding values of σ and ε for each of the 1PF, 2PF's and 3PF can easily be found (Appendix X). Also, for each value of n the sum-of-the-squares of the residuals:

$$L = \sum_i R_i^2 = \sum_i \left\{ \mu_i^2 - C_1 \varepsilon \sigma^6 \frac{(n/6)^{\frac{n}{n-6}}}{(n/6 - 1)} \left[\frac{\sigma^{n-6} C_2^n}{(n-2)(n-3)} (x_i^{n-2} - 1) - C_3 (x_i^4 - 1) \right] \right\}^2 \qquad (142)$$

was found. Of course, the value of n sought is that which gives the minimum in L.

In order to assess the quality of the "fit" for any substance and to compare the relative quality from one material to another, two parameters were computed. The first is related to the "standard error of estimate"[127] S_{μ^2}, defined as the root-mean-square of the residuals (deviations) in μ^2, or:

$$S_{\mu^2} \equiv \sqrt{\sum_i R_i^2/m} = \sqrt{L/m} \tag{143}$$

where $i = 1,2,\cdots,m$; m is the number of data points. This accounts for variations in the amount of data for the different substances but does not account for the fact that the range of μ_i might be numerically higher for some substances than for others*. This was accounted for by finding the mean-square of μ :

$$\overline{\mu^2} \equiv \sum_i \mu_i^2/m \tag{144}$$

and dividing this into S_{μ^2}. The resultant parameter, called the "error of the fit" ε', is then:

$$\varepsilon' \equiv S_{\mu^2} / \overline{\mu^2} \tag{145}$$

Clearly ε' is a quantity that can be used to compare the results of one substance to another and gives an overall measure of the quality of the fit for the particular set of data. It fails, however, to account for the fact that ε' might be large in a given instance because of a large spread in the <u>data</u>. To account for this effect, a second parameter, called the "figure of merit" f was defined by:

$$f \equiv \frac{\varepsilon'_{min}}{\varepsilon'} = \frac{S_{\mu^2 min} / \overline{\mu^2}}{S_{\mu^2} / \overline{\mu^2}} = \frac{\sqrt{L_{min}/m}}{\sqrt{L/m}} = \sqrt{\frac{L_{min}}{L}} \tag{146}$$

where the subscript "min" refers to the "best" fit possible with the given function, Equation (137). As previously mentioned, this (L_{min}) is taken from the results of the 3PF. The parameter f gives an indication of how well the given solution compares to the "best" the

*For argon μ_i varies from 0.8 to 3.6×10^5 cm/sec, while for Hg the range is from 0.6 to 1.0×10^5 cm/sec.

theory can do considering the particular set of data. The main difficulty in the use of f is that it is independent of m (see Equation (146)). Consequently, for substances for which m is small (say 2 or 3), $L_{min} \ll L$ and $f \simeq 0$, although L is certainly small enough to be considered reasonable. This occurs when the 3PF almost exactly goes through the 2 or 3 points for a given substance, while the 1PF comes reasonably close to the points*. In these cases the value of f is ignored.

An examination of Equation (135) shows that as $x \to 1$, $\mu \to 0$ since the two terms in square brackets each $\to 0$. However, it is also clear that, if the $(x^4 - 1)$ term is ever greater than the respective $(x^{n-2} - 1)$ term, another root must exist for some value of $x > 1$. In this instance $\mu^2 < 0$ for values of x between 1 and X_R (the value at the root**) and μ is imaginary (and therefore meaningless) in this region (see Figure 28)***. The function should

---

*In general a "good" value of $L \simeq 10^{18}$ to $10^{20} cm^4/sec^4$. If $L_{min} \simeq 10^{12}$ to $10^{15} cm^4/sec^4$, because the 3PF is almost exact, it is clear that $f \simeq 10^{-3}$ to 10^{-8}.

**At $x = X_R$, $\mu = 0$ and from Equation (17):

$$U_o \equiv \lim_{\mu \to 0} U = \lim_{\mu \to 0} \frac{\mu}{1 - \frac{1}{x}} = \frac{0}{1 - \frac{1}{X_R}} = 0$$

This is the case mentioned earlier, i.e., the limit expressed in Equation (17) and thus Equation (100) does not occur. Clearly the theory does not extrapolate to a realistic U_o in this case. It should be noted that even if $X_R = 1$, the extrapolation may not yield a finite value of U_o. In fact, generally, $U_o \to \pm\infty$.

***It is interesting to note that for $0 \leq n < 3$, $\mu^2 > 0$ for all $x > 1$ and therefore that there is no second root (i.e., $X_R = 1$). Equation (135) (or Equation (95)) thus "exists" for all $n \geq 0$ except for $n = 3$ where there is a singularity and for all $x < X_R$ ($X_R > 1$) when $n > 3$.

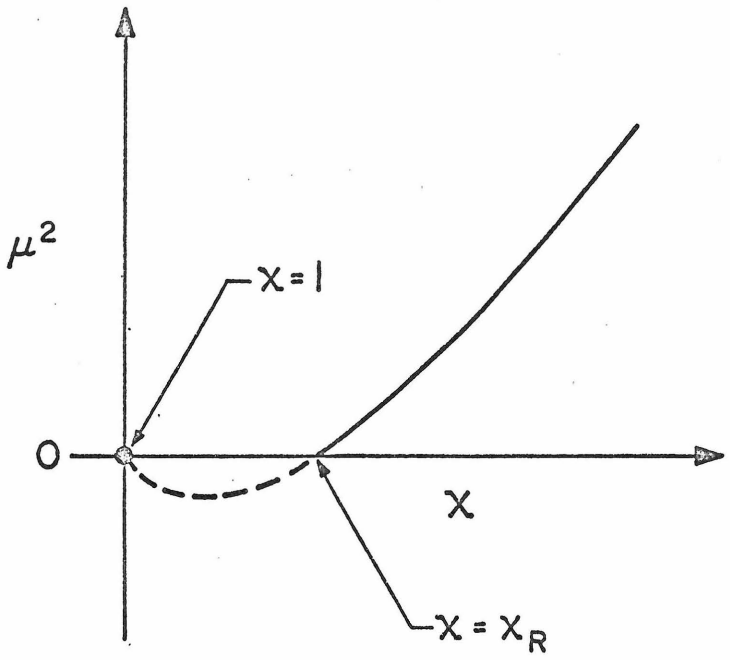

Figure 28. Roots of μ^2 vs. x

be "cut-off" for $x \leq \sim X_R$.

An analysis of the coefficients in Equation (135) (see Appendix Y) shows that, for all but three conditions for two of the liquids considered, such an additional root exists, although in some instances it lies close to $x = 1$. The root was determined for each value of n , for each of the fits, using a Newton-Raphson iterative scheme. The resultant recursion relation developed is (Appendix Z):

$$X_{R_{i+1}} = X_{R_i} - \frac{X_{R_i}^{n-2} - (\frac{\beta}{\alpha}) X_{R_i}^4 + (\frac{\beta}{\alpha} - 1)}{(n-2)X_{R_i}^{n-3} - 4(\frac{\beta}{\alpha})X_{R_i}^3} \tag{147}$$

where α and β are given by Equations (97) and (98). These give, after rearrangement:

$$\beta/\alpha = \frac{12}{(n-2)(n-3)} \left[\left(\frac{M}{2^s \rho_o N} \right)^{1/3} \Big/ \sigma \right]^{n-6} \tag{148}$$

To facilitate the computational procedures all of the pertinent equations were programmed for use on an IBM 360/75 digital computer using FORTRAN IV language. For liquids the main program was called PUFI* in which the input data were m, M, ρ_o, σ, ε, s and the shock data U_i-μ_i . Using Equation (4), a preliminary calculation established the data set μ_i-x_i . Following this, the following set of computations were performed for each value of n from 6.1 to 15.1 in increments of 0.1 . For each of the 1PF, 2PF's and 3PF, Equations (147) and (148) were used to determine X_R . For the 2PF's and the 3PF the appropriate values of σ and ε were computed from

*A listing is available from the author on request.

Equations (X17), (X20), (X34) and (X36) in Appendix X. The input σ and ε and these values were used in Equation (X7), Appendix X (to help determine the roots of this implicit relation for n^*) and in Equation (142) to determine L for all the fits. To help visualize the minimum of L a line plot of L vs. n was found in each case.

After this, n was again incremented in the same way and a set of values of r_o were calculated (Equation (70)) for each value of σ for each fit. This was followed by (a) the WF calculation of the difference in the two sides of Equation (105) and the value of U_o from Equation (104) and (b) the MF calculation of U_o from Equation (107). This set was repeated for each of the 1PF, 2PF's and 3PF . The last calculation was the computation of the MF value of σ given by Equation (106)**.

Because the choice of the increment in n (0.1) was arbitrary, another program called PUSC*** was prepared which was identical to PUFI in all respects except that n was incremented in steps of 0.01****. The range of n was left variable but the number of increments (i.e., 90 as in PUFI) was held the same.

After evaluating the results of PUFI for each substance (which includes determination of ε' and f which were <u>not</u> included in PUFI)

---

*A root in the relation is indicated when, for successive values of n, the sign of the computed value of Equation (X7), Appendix X, changes from + to - or from - to + .

**This computation depends only on n and is the same for the 1PF, 2PF's and 3PF.

***Available from the author on request.

****In a later section it is shown that the need for PUSC is limited at best, $\partial\varepsilon'/\partial n$ is shown to be small for such small increments in n .

the best values of n, σ and ϵ for each fit were found. Using these values, a set of x, μ and U data was tabulated, using Equation (135) and Equation (4). From this tabulation, line plots of U vs. μ and μ vs. x were superimposed on the corresponding U-μ and μ-x data to "see" how well the theory fits the data. To visualize the potential, $\phi(r)$ vs. r was tabulated and plotted for each fit from Equation (69) using a program called PUMP*.

*Available from the author on request.

3. Results

In order to check the computer program PUFI, a series of preliminary calculations were performed on the same group of substances and same set of data* previously published[90,42,100,64,60]. A tabulation of the results is shown in Table 11 in which only the 1PF was included. The values of n that give the best fit in each case are (essentially) the same as those reported[16]. In the current study a separate computation was made for each of the two initial states for argon. The two values of n compare favorably (within 4%) with each other and the single value that would fit both data sets well would be $n \tilde{=} 8.5$. This agrees with the single value of n used for argon in Reference 16.

Generally speaking, the values of ε' and f in Table 11 indicate excellent fits. This was borne out by using the results in Table 11 in the PUMP program to produce U-μ and μ-x plots for each material. These essentially reproduced the results in Reference 16 (Figures 6-16) where excellent fitting of the data was obtained.

After completion of the preliminary computations PUFI was applied to all of the liquids shown in Table 4. Because there are four fits for each run and a number of runs for each material (since there are various parameter sets for each; see Tables 7 and 9), a large set of computed results was obtained. Instead of detailing all these results in this document the major features of the computations

---

*Additional data for N_2, CCl_4 and C_6H_6 were used in the current study.

Table 11

RESULTS--PRELIMINARY CALCULATIONS

Substance	σ-Å	ε/k-°K	Fit	n	X_R	L	ε'	f	Comments
A	3.405	124.0	1	8.6	1.132	1.63E21	0.184	$\leq$ 0.975	
A-II	3.405	124.0	1	8.3	1.406	5.08E20	0.097	0.822	
Hg	2.898	851.0	1	8.5	1.030	7.66E16	0.025	-	m=3
N_2	3.71	95.9	1	7.0	1.187	8.57E19	0.035	0.565	
H_2	2.87	29.2	1	6.9	1.560	3.18E19	0.016	-	m=1
CCl_4	5.881	327.0	1	6.4	1.009	5.90E17	0.016	-	m=2
C_6H_6	5.270	440.0	1	6.8	1.135	9.98E19	0.165	$\leq$ 0.891	

will be described for a single substance and the remaining materials appropriately summarized. Argon was chosen as the "test" material. It is the substance of most interest because (a) there are shock data available at four different initial states (if the theory is valid it should give the same value of n for any initial state for the same substance), (b) it is monatomic and is therefore spherically symmetric (which is, in effect, assumed throughout the development of the model; see Figures 4-9), and (c) the pair potential has been investigated extensively and is probably better known than for any other material (the σ,ε sets used are probably close to the "true" physical values).

The 5 σ,ε pairs for argon in Table 7, along with the appropriate input data (Appendix S), were used in PUFI to determine the "best" fit of the theory to the data in each case. The results are shown in Table 12.

For each σ,ε pair in Table 12, comparing results for the 1PF, 2PF's and 3PF, it is clear that ε' and f should correspondingly decrease and increase for this progression because the number of adjustable parameters increases (see Table 10)*. This general condition serves as a self-consistency check on the fitting equations

*The two 2PF's both have two adjustable parameters and either might give a better "fit". The particular order seen in Table 12 is not significant.

Table 12

PUFI APPLIED TO ARGON (A)

Input Data (Appendix S):

$m = 19$, $M = 39.944$ g/g-mole, $\rho_o = 1.405$ g/cc, $T_o = 86^oK$, $P_o = 1.97$ atm, $C_o = 0.0848 \times 10^6$ cm/sec, $s = 1$ (fcc), $^{\circ}a_o = 4.057\text{Å}$, $\overline{\mu^2} = 0.504 \times 10^{11}\text{cm}^2/\text{sec}^2$

Table 7 σ-Å	ε/k-^oK	Fit	Eq.(X7) n	Eq.(147) X_R	Eq.(X17) σ-Å	Eq.(70) r_o-Å	Eq.(X20) ε/k-^oK	Eq.(105) RE	Eq.(104) U_o-cm/sec $\times 10^{-6}$	Eq.(106) σ-Å	Eq.(107) U_o-cm/sec $\times 10^{-6}$	Eq.(142) L-cm^4/sec^4	Eq.(145) ε'	Eq.(146) f
3.405	124	1	8.6	1.132	-	3.911	-	-0.305	0.0984	3.647	0.1501	1.63E21**	0.184	$\leq$ 0.975
		2	9.4	1.167	3.281	3.744	-	-0.554	0.0802	3.584	0.1462	1.57E21	0.180	$\leq$ 0.993
		3	9.8	1.085	-	3.874	69.5	-0.348	0.0808	3.558	0.1446	1.57E21	0.180	$\leq$ 0.993
		4*										$\leq$ 1.55E21	$\leq$ 0.179	-
3.30	152	1	8.8	1.181	-	3.784	-	-0.0453	0.0890	3.630	0.1649	1.60E21	0.182	$\leq$ 0.984
		2	9.2	1.194	3.246	3.709	--	-0.0582	0.0805	3.599	0.1628	1.58E21	0.181	$\leq$ 0.990
		3	9.5	1.153	-	3.763	111.5	-0.533	0.0800	3.578	0.1614	1.57E21	0.180	$\leq$ 0.993
		4*										$\leq$ 1.55E21	$\leq$ 0.179	-
3.94	110	1	8.6	1.113	-	3.951	-	-0.263	0.0991	3.647	0.1414	1.64E21	0.184	$\leq$ 0.972
		2	9.4	1.146	3.319	3.788	-	-0.491	0.0823	3.584	0.1377	1.57E21	0.180	$\leq$ 0.993
		3	9.8	1.065	-	3.914	62.4	-0.272	0.1206	3.558	0.1362	1.56E21	0.180	$\leq$ 0.997
		4*										$\leq$ 1.55E21	$\leq$ 0.179	-
3.38	134	1	8.6	1.145	-	3.882	-	-0.334	0.0974	3.647	0.1560	1.63E21	0.184	$\leq$ 0.975
		2	9.3	1.176	3.271	3.736	-	-0.557	0.0809	3.592	0.1524	1.57E21	0.180	$\leq$ 0.993
		3	9.7	1.102	-	3.849	78.8	-0.398	0.0811	3.564	0.1507	1.57E21	0.180	$\leq$ 0.993
		4*										$\leq$ 1.55E21	$\leq$ 0.179	-
3.28	138.2	1	9.2	1.175	-	3.749	-	-0.531	0.0833	3.599	0.1552	1.59E21	0.182	$\leq$ 0.987
		2	9.3	1.182	3.261	3.725	-	-0.572	0.0803	3.592	0.1548	1.58E21	0.181	$\leq$ 0.990
		3	9.5	1.164	-	3.740	118.8	-0.568	0.0788	3.578	0.1539	1.57E21	0.180	$\leq$ 0.993
		4*										$\leq$ 1.55E21	$\leq$ 0.179	-

*The minimum in L for the 3PF occurs outside the range $6.1 \leq n \leq 15.1$. Since the 3PF does not depend on either σ or ε, it will be the same for all cases in the table.

** Written in computer language, e.g., 1.63E20 $\equiv 1.63 \times 10^{20}$.

(Appendix X). The condition is met for the results in Table 12, although the magnitude of the changes in ε' and f are small*.

The relative usefulness of the 1PF, 2PF's and 3PF was investigated by examination of the L vs. n plots. The results were typical of almost all substances studied; the 1PF curve was very steep in the region of the minimum, the 2PF curves both had distinct minima but were much less steep than the 1PF, and the 3PF curve was nearly flat**,***. This means that, for 1PF's a distinct value of n can be considered as the "best" value without ambiguity. For 2PF's this must be modified in that any of a range of values of n will give equally "good" fits. For 3PF's almost <u>any</u> value of n (within the "flat" range) will give an equally "good" fit. For the 1PF, L changed significantly as n passed through the "best" fit (e.g., at $n = 9.2$ for the set $\varepsilon = 3.28\text{Å}$, $\varepsilon/k = 138.2^{\circ}\text{K}$). For the 2PF's, L remained

---

*Argon is an exception in this case. Significantly larger differences occur for other substances.

**A sudden rise in L for $n \gtrsim 10.5$ was a computer derived numerical artifact. Actually this portion of the curve does not exist because σ in Equation (X34) in Appendix X depends on the root of a negative number, for these values of n. The computer simply converts the negative quantity to a positive one and continues the computation. This sudden rise in L for the 3PF is typical and occurs for nearly all substances.

***For some materials the portion before the sudden rise in L is "very" flat; l varying $< 1/2\%$ in this region.

the same (within 1/2%) for the ranges $n = 9.0$ to 9.6 and $n = 9.3$ to 9.7 respectively and varied very slowly even outside this range. For the 3PF, L changed very little over the whole range of n, although for this particular example, not less than the second 2PF. Because of this behavior it was concluded that a critical test of the theory would be accomplished only if 1PF values were considered. The 2PF's and 3PF simply have too much latitude in the choice of n.

In some instances the 2PF's gave results very close to the 1PF. This was considered significant in that it strongly supports the value of n found in the 1PF; the data are "uniquely" satisfied by the theory with the given parameter set σ, ε and n. The 2PF's were considered useful in this context only; when agreement did occur this was noted in the 1PF results.

An excellent example of the agreement of the 2PF's with the 1PF is shown in Table 12 for the set $\sigma = 3.28\text{Å}$, $\varepsilon/k = 138.2^{\circ}\text{K}$. The best values of n were 9.2, 9.3 and 9.5 for the 1PF and 2PF's respectively. Further, the best values of σ and ε/k for the 2PF's, 3.26Å and 118.8°K, agree closely with the particular 1PF input values above. This kind of agreement for argon is notable. It does not occur for most substances. In fact, examination of Table 12 shows that this agreement is not nearly as good even for argon with other parameter sets.

The 3PF was used only to determine L_{min} for the computation of f for the 1PF.

An examination of Table 12 shows that in all cases the prediction of $C_o (= U_o)$ in the WF solution is much superior to that in the

MF solution*. The value of σ determined from the "condition", Equation (106), is in all cases higher than the σ values from Table 7. This "unrealistically" high value makes U_o too high in Equation (107). On the other hand, if the (lower) values of σ in Table 7 are used directly in Equation (104), reasonably good values of U_o result. In this instance the error in not satisfying the "condition" is measured by the residual (RE in Table 12) defined by Equation (105). The failure to meet this condition with mathematical exactness is accepted as a limitation of the model and/or potential in the low pressure region**.

Because the MF solution "forces" values of σ that are too high, only the WF solution was considered for the remainder of the study.

The steepness of the L vs. n for the lPF led to a determination of the value in using PUSC where n is incremented in values of 0.01 (instead of 0.1 as in PUFI)***. From the PUFI output, the change in ε' and f with n for values near the minimum in L can be estimated. This is done in Table 13. The effect of the uncertainty in the $\mu_i - x_i$ data (1-5%) plus that in σ (1-3%) and ε (5-20%) is expected to lead to an uncertainty in L of up to 20%, since $L \sim \mu_i^4$ (see Equation (142)). However, since $\varepsilon' \sim L^{1/2}$ (Equations

---

*This conclusion applies to all of the liquids studied.

**Of course, a number of assumptions of the model (e.g., a "thin" transition region) may not hold as $U \to U_o$.

***Since this curve is as steep for argon as any of the other liquids the conclusions drawn here are considered conservative.

Table 13

VALUE IN USING PUSC

Data from Appendix S

Substance: Argon

ρ_o: 1.405 g/cc

σ: 3.28Å

ε/k: 138.2°K

μ^2: 0.504×10^{11} cm^2/sec^2

L_{min}: $\leq$ 1.55E21 cm^4/sec^4

n	L cm^4/sec^4	ε'	f	Δn	$\Delta\varepsilon'$	Δf
9.1	1.65E21	0.185	$\leq$0.969	+ 0.1	-0.003	+0.028
9.2	1.59E21	0.182	$\leq$0.987	+ 0.1	+0.015	-0.077
9.3	1.87E21	0.197	$\leq$0.910			

(143)-(145)) and $f \sim L^{-1/2}$ (Equation (146)) the propagated uncertainty should be $\sim 10\%$. For values of $\varepsilon' \simeq 0.2$ and $f \simeq 1.0$ the uncertainties $\Delta\varepsilon'$ and Δf would be ~ 0.02 and ~ 0.1 respectively. These are sufficiently larger than the corresponding values in Table 13 to lead to the conclusion that PUSC is not necessary. The effect of a change in n of 0.1 on ε' and f is less than the inherent variability in the computation of ε' and f.

A careful examination of the U-μ plots (and of Figures 7, 8, 11, 12 and 14 of Reference 16) showed in most cases that, as $\mu \to 0$, U drops very rapidly. In fact, in these cases $U \to 0$. This is consistent with the existence of the spurious root of Equation (135) at $X_R > 1$ *. For those cases in which $X_R = 1$ (i.e., no spurious root) $U \to +\infty$ ** as $\mu \to 0$. This is required by Equation (100) when the "condition", Equation (101), is not exactly met. This difficulty is further aggravated by the following consideration. After computation of μ for a given x from Equation (137), U is computed from Equation (4):

$$U = \frac{\mu}{1 - \frac{1}{x}} \tag{4}$$

As $x \to 1$ and therefore $\mu \to 0$, Equation (4) becomes <u>numerically</u> unstable in that either the numerator or denominator approaches the

---

*It was shown previously that, in this instance, $U_o = 0$.

**When there is no spurious root and $n > 6$ (see Table 14), it can be shown from Equation (100) that only the + sign obtains.

limit faster. In the former case $U \to 0$, in the latter $U \to +\infty$ *. When $U \to +\infty$ the U-μ curve exhibits a minimum at some small value of μ; an example of this type of behavior has been previously observed[128].

The instability in the use of Equation (100) is accentuated** by the fact that, unless the value of σ specified in the MF solution is used (Equation (106)), μ and x do not approach 0 and 1 respectively in Equation (137) at the rate necessary for $U \to U_o$ in Equation (4). That is to say, the numerical instability in the extrapolation aggravates the theoretical instability in the WF solution.

For argon or for any other liquid, no solutions near $n = 6$ were found. Equations (115)-(121) were, consequently, not used.

For some liquids the data selection process discussed previously was decided by comparison of the ε' and f values with and without the "questionable" data. This was usually sufficient to make a decision.

Examination of the 1PF's in Table 12 shows that the last parameter set $\sigma = 3.28$A, $\varepsilon/k = 138.2^{o}$K gives the best results*** (minimum ε' and maximum f) although just barely. In fact all the 1PF's are so close it is difficult to distinguish between them; in light of the previously estimated 10% uncertainty in ε' and f, the maximum

---

*Note that this behavior is a numerical artifact. Even if the theory extrapolated to U_o exactly (i.e., the condition in Equation (101) was met), small errors in the values of μ and x would eventually cause the same result.

**In some instances the effects tend to counteract each other.

***It is notable that these are the latest (Table 7) and "best"[74] values of σ and ε.

variations in ε' and f ($\sim$ 0.1% and $\sim$ 1% respectively) are very small. However, because there is no reason not to take the best fit, the indicated parameter pair was chosen. The significance of this choice shows up in the WF determination of U_o. For the chosen pair this value is within 2% of C_o, while for the others the error varies from 5 - 17% *. These changes in ε', f and U_o occur for changes of 5% and 38% in σ and ε/k respectively. Clearly, ε' and f are weak functions of σ and (especially) ε/k while U_o is a strong function of (especially) σ and ε/k.

Based on this analysis of argon in Table 12, only the 1PF, WF solutions for PUFI need be considered for the other liquids. Accordingly, PUFI was run for all the materials in Table 7 and where a choice existed the "best" parameter pair was chosen. Because of the T_M correlation previously discussed (see Equation (134)), another set of independently determined ε/k values exists (Table 9). The σ values of the "best" pairs in Table 7 were combined with these values** and PUFI was run for these values. The overall results appear in Table 14.

The values of ε' and f show that all the fits are excellent with the exception of ethyl ether and perhaps water. The theory fits the available data closely for adjustments in only one parameter, n.

---

*Argon is exceptional here in that U_o is generally not as close to C_o for most other liquids (see Table 14).

**Except for A-II and Hg.

Table 14

PUFI APPLIED TO LIQUIDS

Substance	L/C*	σ-Å	ε/k-°K	n	X_R	r_o-Å	RE	U_o-cm/sec × 10^{-6}	C_o-cm/sec × 10^{-6}	L-cm^4/sec^4	ε'	f	Comments
A	L	3.28	138.2	9.2	1.175	3.749	-0.531	0.0833	0.0848	1.59E21	0.182	≤ 0.987	Close 2PF agreement
	C	3.28	129.9	9.3	1.171	3.746	-0.543	0.0813	0.0848	1.57E21	0.180	≤ 0.993	Close 2PF agreement
A-II	L	3.405	124	8.3	1.406	3.921	-0.695	0.024	0.035	5.08E20	0.097	0.822	
	C	3.28	129.9	8.9	1.443	3.758	-0.988	-	0.035	6.80E20	0.112	0.710	
A-III	L	3.28	138.2	9.3	1.385	3.746	-1.050	0.017	0.077	3.34E20	0.114	0.819	
	C	3.28	129.9	9.4	1.381	3.743	-1.082	0.017	0.077	3.42E20	0.116	≤ 0.809	
A-IV	L	3.28	138.2	8.6	1.311	3.767	-0.687	0.042	0.091	5.03E20	0.143	-	
	C	3.28	129.9	8.8	1.302	3.761	-0.739	0.041	0.091	5.28E20	0.146	-	
Hg	L	2.88	654.0	9.5	1.000	3.284	+0.001	0.1494	0.1451	5.15E16	0.020	-	
	C	2.86	355.3	11.7	1.000	3.216	+0.488	0.1285	0.1451	7.30E15	0.008	-	Close 2PF agreement
N_2	L	3.73	91.5	7.2	1.163	4.342	-0.134	0.1049	0.0854	2.52E20	0.190	≤ 0.835	
	C	3.73	98.8	7.0	1.177	4.352	-0.116	0.1071	0.0854	2.50E20	0.189	≤ 0.829	
H_2	L	2.87	29.2	6.9	1.560	3.352	-0.300	-	0.1119	3.18E19	0.016	-	
	C	2.87	34.5	6.5	1.599	3.368	-0.166	-	0.1119	1.03E19	0.009	-	
CS_2	L	4.438	488.0	8.7	1.104	5.093	-0.258	0.154	0.115	1.07E17	0.109	≤ 0.116	
	C	4.438	250.8	10.6	1.036	5.022	-0.205	0.129	0.115	4.04E15	0.021	≤ 0.653	
CCl_4	L	5.77	378.0	6.2	1.063	6.798	-0.007	0.1348	0.0941	2.07E20	0.174	≤ 0.983	
	C	5.77	379.2	6.2	1.063	6.798	-0.007	0.1351	0.0941	2.07E20	0.174	≤ 0.983	
CH_3OH	L	3.666	452.0	6.7	1.331	4.292	-0.140	0.1349	0.1125	9.06E19	0.083	≤ 0.692	
	C	3.666	267.0	8.0	1.242	4.233	-0.376	0.1135	0.1125	9.17E19	0.083	≤ 0.646	
C_2H_5OH	L	4.370	415.0	6.7	1.233	5.116	-0.100	0.1505	0.1152	5.49E19	0.081	≤ 0.569	
	C	4.370	237.7	8.0	1.147	5.046	-0.236	0.1270	0.1152	6.62E19	0.089	≤ 0.431	
$(C_2H_5)_2O$	L	5.539	351.0	6.8	1.139	6.477	-0.070	0.1423	0.1155	1.37E23	0.443	≤ 0.978	
	C	5.539	239.2	7.5	1.091	6.427	-0.101	0.1254	0.1155	1.34E23	0.436	≤ 0.989	
C_6H_{14}	L	5.916	423.0	6.7	1.150	6.926	-0.065	0.1421	0.1083	4.98E19	0.103	≤ 0.789	
	C	5.916	272.2	7.8	1.076	6.844	-0.108	0.1267	0.1083	5.56E19	0.108	≤ 0.747	
C_6H_6	L	5.270	440.0	7.0	1.115	6.148	-0.076	0.162	0.129	4.41E20	0.129	≤ 0.978	
	C	5.270	421.9	7.1	1.108	6.141	-0.081	0.160	0.129	4.41E20	0.129	≤ 0.978	

Table 14 (continued)

Substance	L/C*	σ-Å	ε/k-°K	n	X_R	r_o-Å	RE	U_o-cm/sec $\times 10^{-6}$	C_o-cm/sec $\times 10^{-6}$	L-cm^4/sec^4	ε'	f	Comments
$C_6H_5CH_3$	L	5.932	377.0	6.7	1.017	6.945	-0.007	0.1850	0.1328	1.19E19	0.062	-	
	C	5.932	271.2	7.5	1.000	6.883	+0.048	0.1723	0.1328	1.02E19	0.057	-	
H_2O	L	2.725	355.8	8.0	1.293	3.147	-0.444	0.1529	0.1483	3.17E20	0.180	$\leq$0.421	
	C	2.725	413.7	7.6	1.316	3.159	-0.359	0.1377	0.1483	3.72E20	0.195	$\leq$0.381	

*L = Literature values of ε

C = Correlated values of ε

Based on ε' and f a choice between ε/k determined from the literature (L) or from the melting point correlation (C) is difficult. Except for mercury and water the change from L to C results in changes in ε' and f that are within the estimated 10% uncertainty in the determination of ε' and f. Furthermore, no trends are apparent (i.e., the change from L to C does not always raise or lower ε' or f). That the large changes in ε/k do not greatly affect ε' and f supports the previous conclusion that the latter are weak functions of the former.

An examination of the sound velocity predictions (U_o) in Table 14 shows that the correlated values of ε/k tend to yield U_o values closer to C_o giving a preference to this set. However, it should be noted that both L and C consistently give $U_o > C_o$, except for argon, mercury and water. For L, U_o is, on the average, 30% greater than C_o; for C the figure is 20%. This occurs even though σ is lower than the value required by the MF solution (Equation (106) and the fact that $RE < 0$, Equation (105)) and ε' is (generally) lowered by the ε/k correlation*; both of these effects tend to lower U_o (see Equation (104)). It is clear that U_o is not lowered sufficiently. It is interesting to note that since $U_o \propto \sigma^3$ (Equation (104)), a 20% reduction in U_o would be effected by only a 6% reduction in σ. However, no (physical) justification for such a reduction is apparent.

---

*Note that in going from L to C, n generally increases. This should lead to a decrease in σ for the MF solution which, in turn, leads to an increased negative value of RE. This effect is seen in Table 14.

Using the results for the correlated values, it is desirable to choose a single ("common") value of n for argon and determine how well that value fits all the argon states. To do this, the results in Table 14 for argon were weighted by the number of points in each state as shown in Table 15. From the resultant "common" value (9.2) the fits for A, A-II, A-III and A-IV were re-evaluated. The resultant values of ε' and f, also shown in Table 15, do not indicate as good a fit as the corresponding data in Table 14*. However, the fits are reasonable as demonstrated by Figures 29 and 30, where the theory with the common value of n is compared to the data for all four argon states.

To generally demonstrate the excellent fits in Table 14 for all the other liquids, the theory with the listed values of n (for the C results) is compared to the data, in Figures 31-34.

---

*As indeed they should not, since the set in Table 14 represents the "best" fits.

Table 15

COMMON VALUE OF n FOR ARGON

Substance	m*	n**	
A	19	9.3	Σ m = 32
A-II	6	8.9	
A-III	5	9.4	Σ mn = 294.7
A-IV	2	8.8	

$$\bar{n} = \frac{\Sigma\ mn}{\Sigma\ m} = 9.209$$

For $\dot{n} = 9.2$, $\sigma = 3.28\text{Å}$, $\varepsilon/k = 129.9^{\circ}K$:

Substance	X_R	r_o-Å	RE	U_o-cm/sec $\times 10^{-6}$	C_o-cm/sec $\times 10^{-6}$	L-cm^4/sec^4	ε'	f
A	1.175	3.749	- 0.531	0.0808	0.0848	1.75E21	0.190	$\leq$0.941
A-II	1.429	3.749	- 1.090	-	0.035	2.42E21	0.211	0.377
A-III	1.390	3.749	- 1.019	0.0169	0.077	6.62E20	0.161	$\leq$0.581
A-IV	1.302	3.749	- 0.841	0.0424	0.091	2.40E21	0.311	-

*m = number of data points

**From C calculation in Table 14.

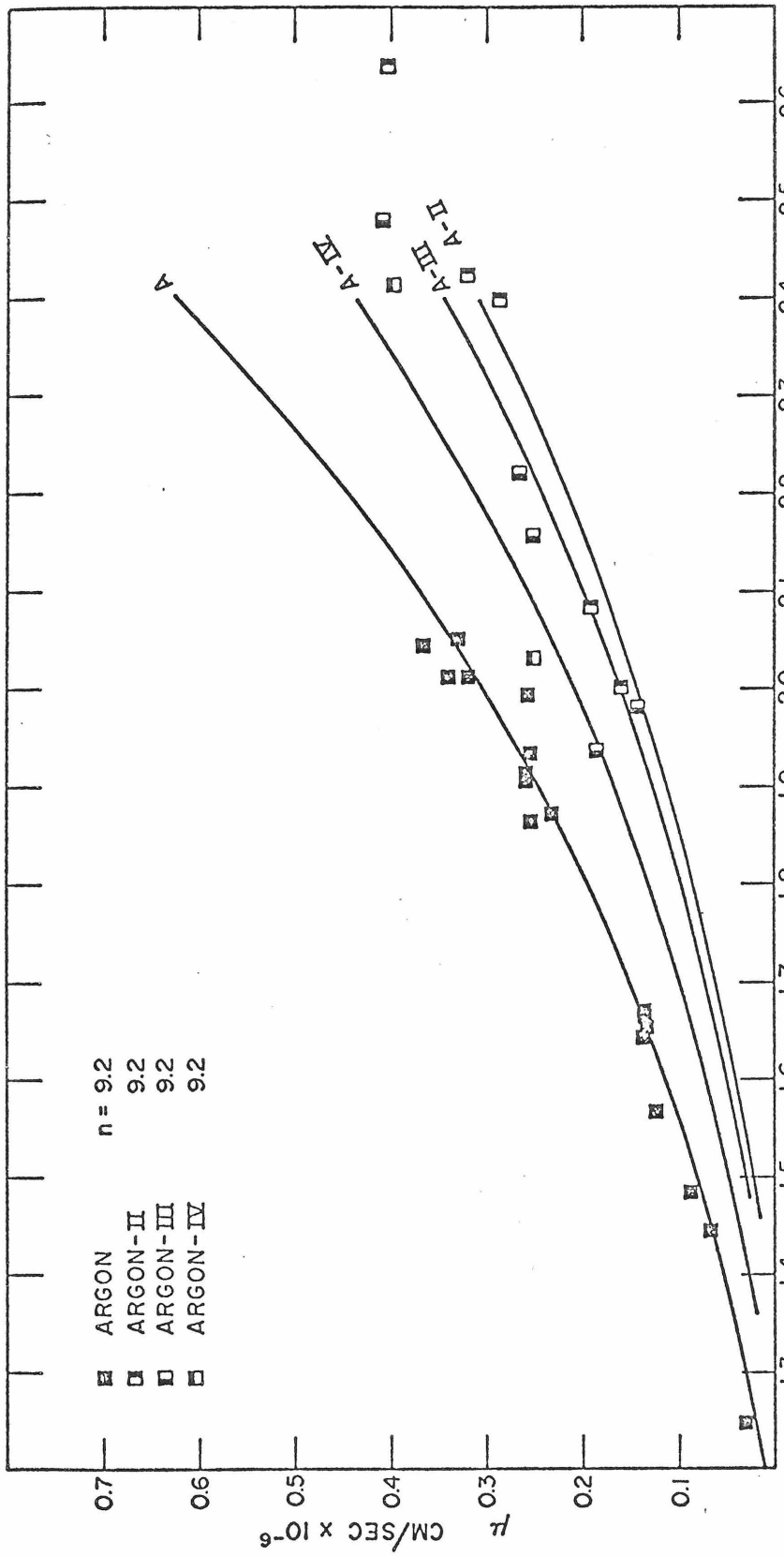

Figure 29. μ vs. x Fit of Theory for Common Value of n for Argon

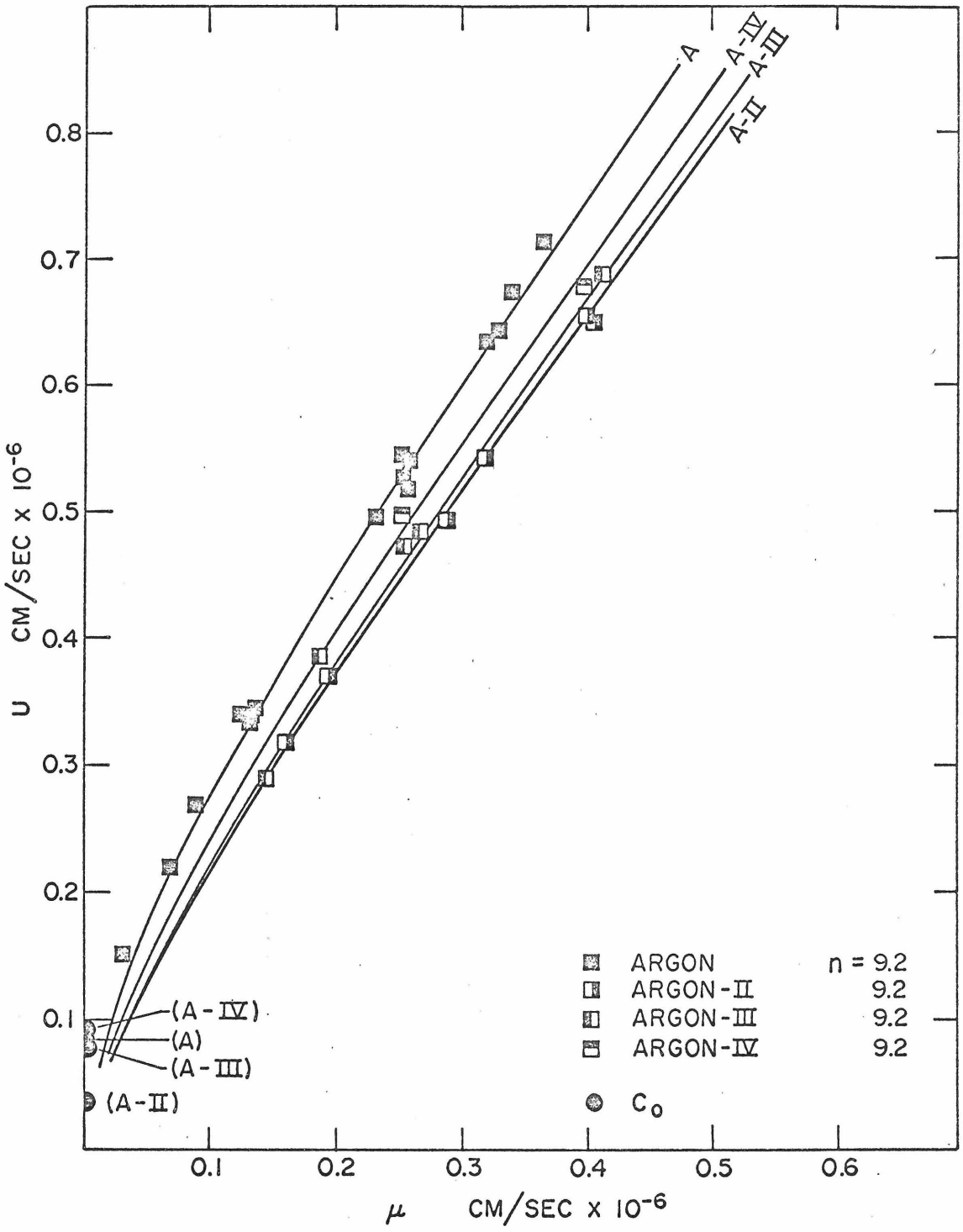

Figure 30. U vs. μ Fit of Theory for Common Value of n for Argon

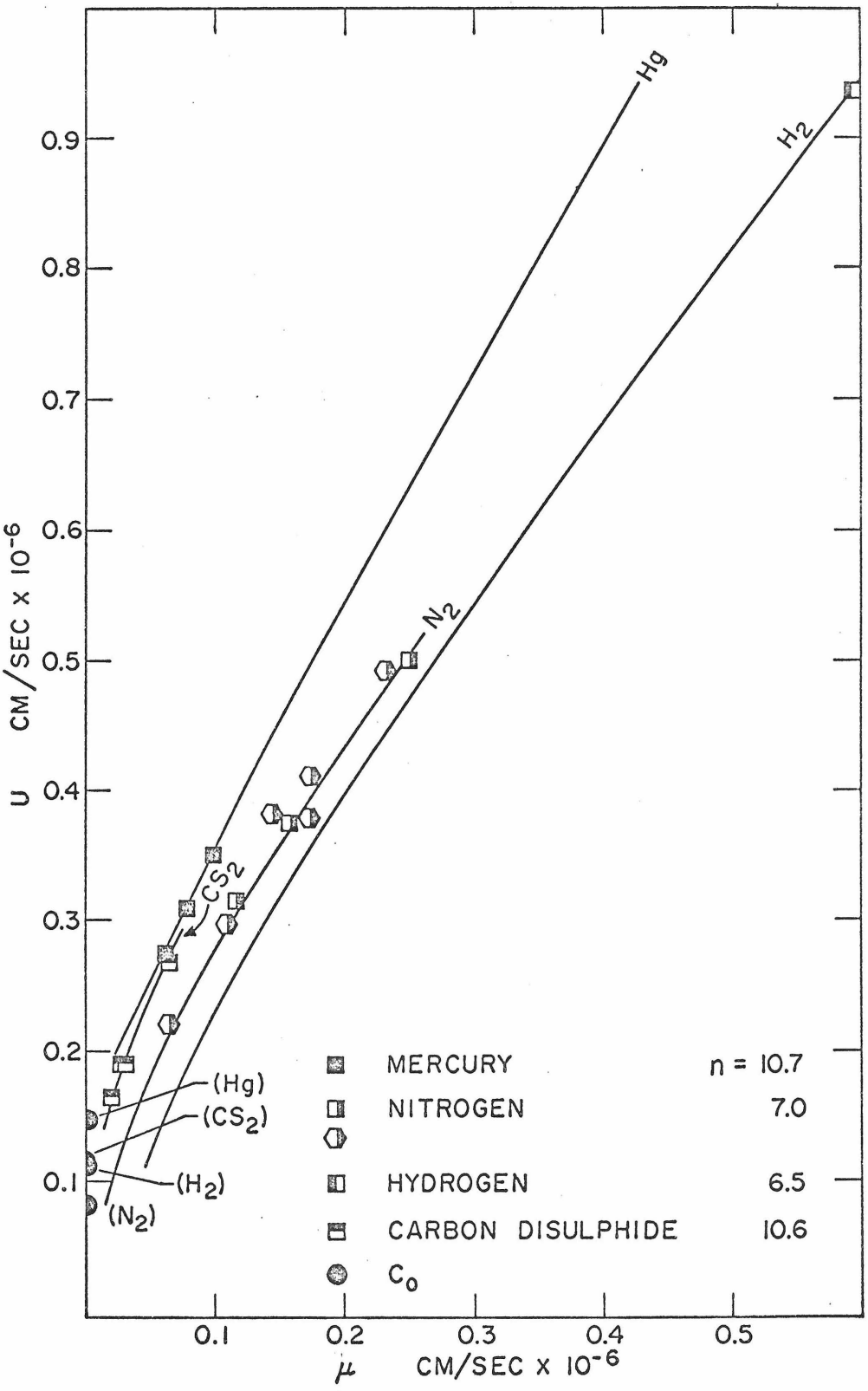

Figure 31. U vs. μ Fit of Theory--Hg, N_2, H_2, CS_2

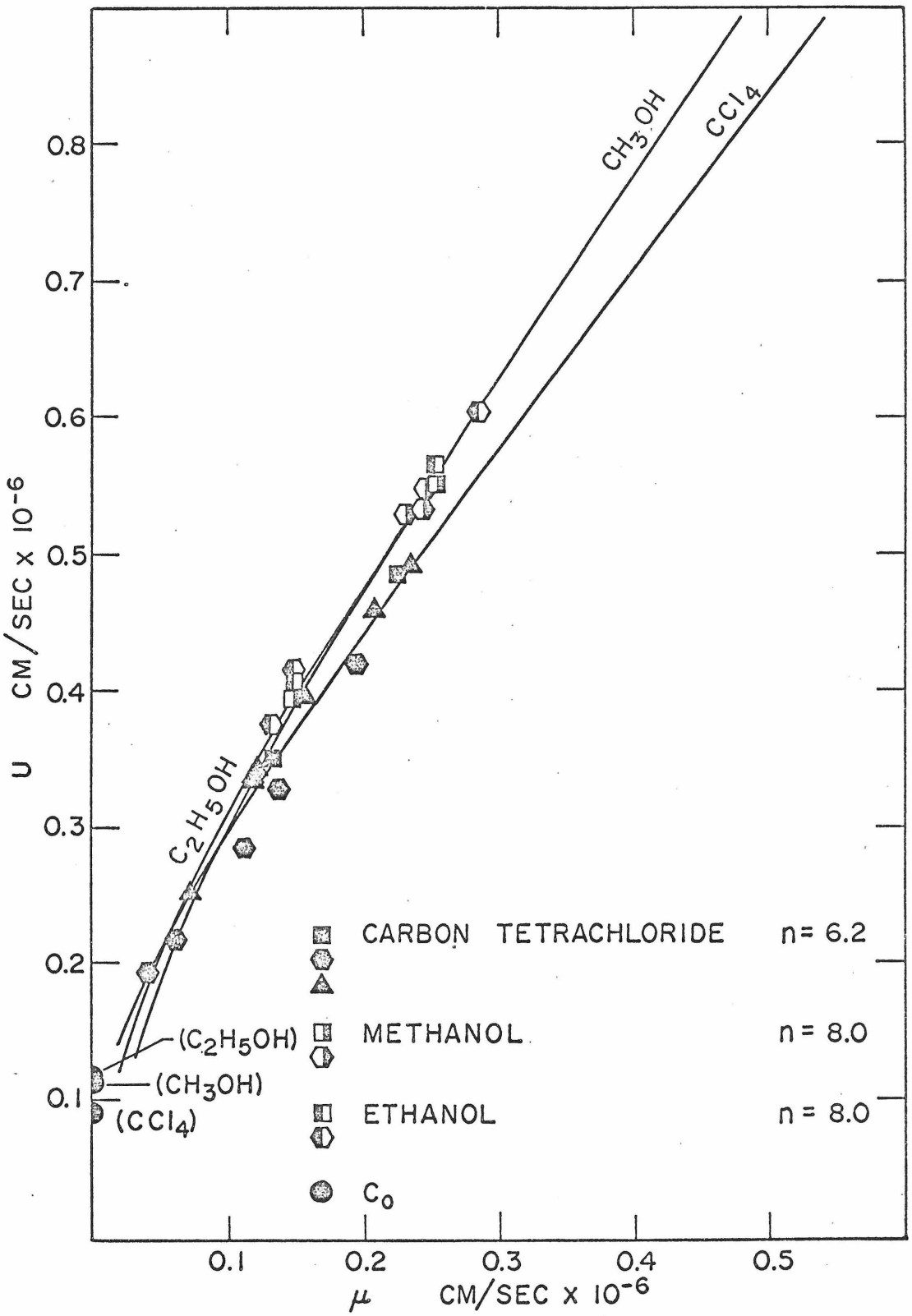

Figure 32. U vs. μ Fit of Theory--CCl_4, CH_3OH, C_2H_5OH

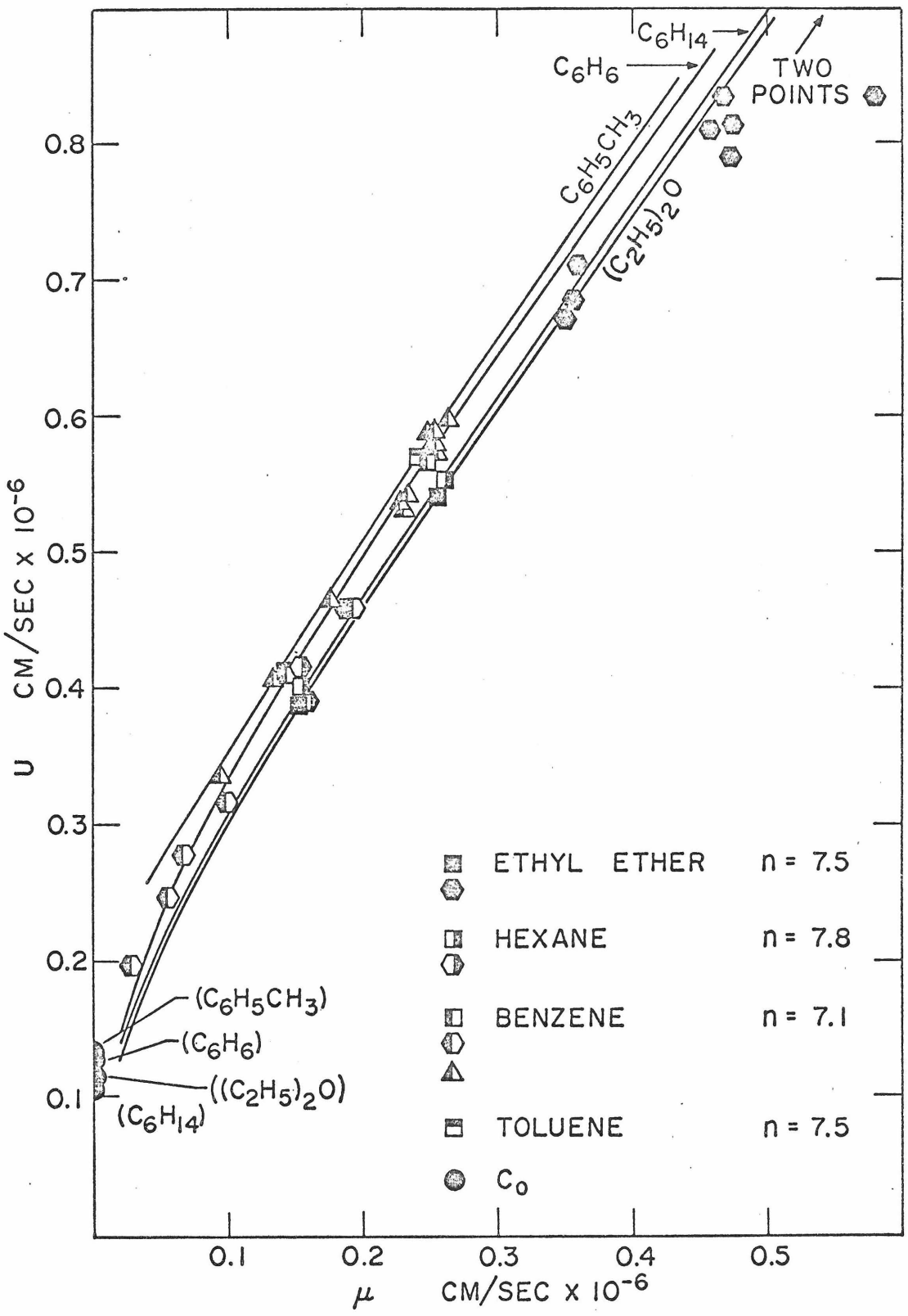

Figure 33. U vs. μ Fit of Theory--$(C_2H_5)_2O$, C_6H_{14}, C_6H_6, $C_6H_5CH_3$

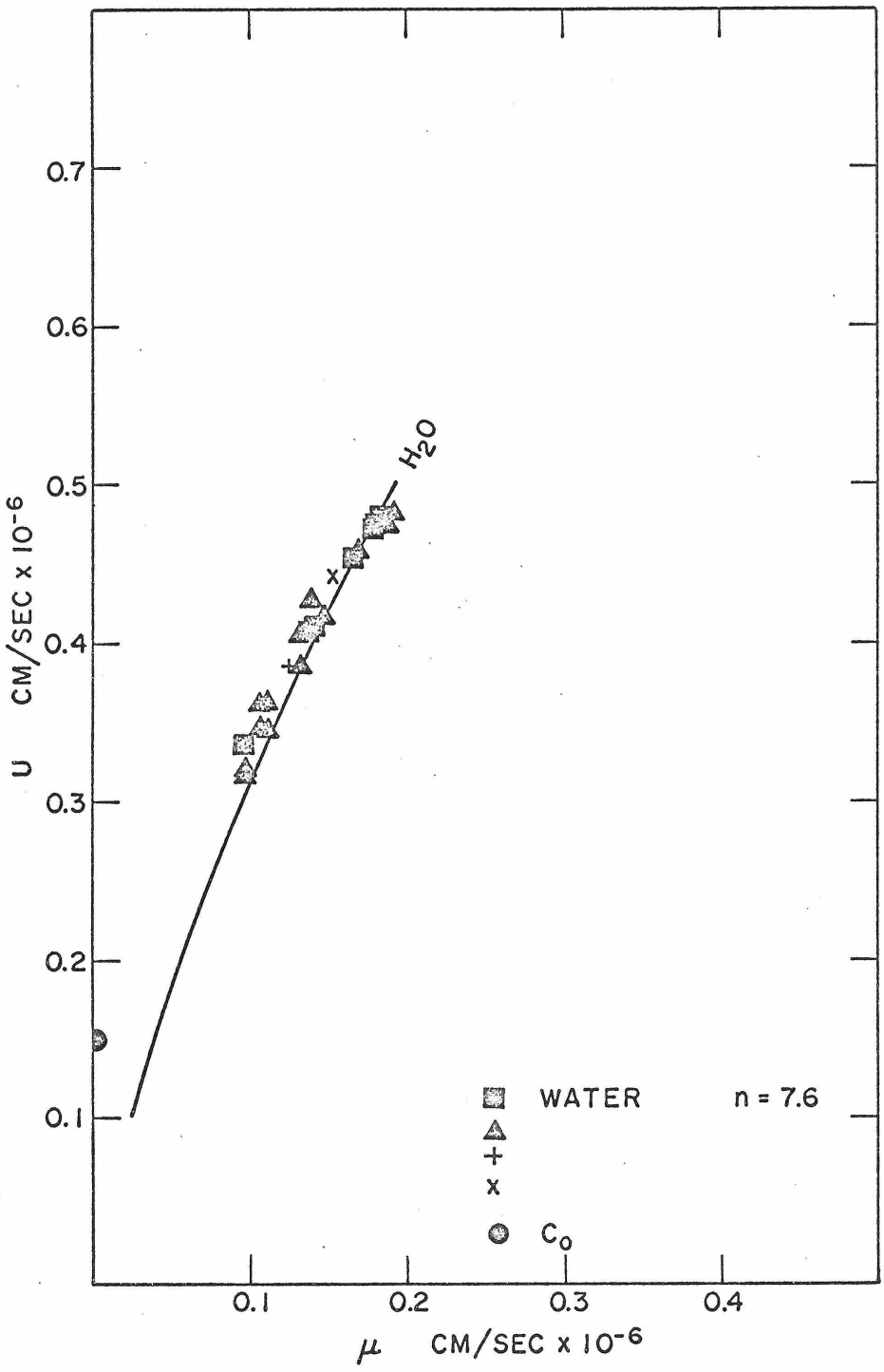

Figure 34. U vs. μ Fit of Theory--H_2O

C. METALS

Inasmuch as metals have been described as "ions in a bath of electrons"[37,17,29,129], it would be expected that the net intermolecular forces would differ from those of insulators such as were considered in the last section. This is evidenced by the long-range oscillatory (LRO) behavior of metals predicted theoretically[130,24,17,27,30,73] and deduced from experiment[25]. Nevertheless, a number of treatments either do not consider LRO behavior[131,76,118] or find the oscillations to be of much lower amplitude[27,30] and/or at much larger distances[30] than is generally implied[25,26,28,75,73,31,129]. Furthermore, the differences between the potentials with and without LRO behavior need not be large[75], especially in the repulsive region which is, of course, where most of the shock data considered in this study lie.

On this basis the n-6 potential, Equation (65) or Equation (69) without LRO behavior was used in applying the theory to metals. This is done without apology* although it is recognized that this choice, at best, only represents an effective (ion-ion) potential that is a reasonable approximation to the true state of affairs.

Use of the same potential function as in the case of liquids leads to consideration of the WF or MF solutions as before. Further, this approach leads to concern over the parameter pair preferred among (σ,ε), (σ,r_o), (σ,C_{ab}), etc. for describing the potential.

---

*It is not clear that any other potential function would give better results, although an investigation of Equations (63) and (64) in this role are recommended in a later section.

1. Method of Approach

Values of σ, r_o and ε for a number of metals have been deduced from an analysis of X-ray measurements[76,25] as well as from several analytical methods including molecular dynamics techniques[26, 31], model pseudo-potential calculations[24,27,132,73], and lattice dynamic calculations[30]. In addition, Fontana[118] predicted values of C_{ab} for the alkali metals using the theory of angular momentum. The available data of interest are compiled in Table 16. Note that data only exist for 7 of the 23 metals considered in this study.

The data in Table 16 show variations in σ of from* 0-14% (average $\simeq$ 7%) and in ε/k of from* 21-48% (average $\simeq$ 37%)! Since the theory is approximately proportional to σ^6 and ε (see Equation (95)) the propagated error in μ^2 could be $\sim (1.07)^6 (1.37) \simeq 2.0$. The associated error in μ would be $\sim$ 40%.

The implication is that, unless one or the other of the sets of data is shown to be superior**, the choice of a preferred parameter pair may be academic. There is no way to pick the best numerical values.

---

*This did not include Reference 27 which "appears" to give somewhat unusual values of σ and ε. Inclusion of this data would amplify the conclusions reached.

**No such preference is immediately obvious from an examination of the methods used in developing the data in Table 16.

Table 16

AVAILABLE σ, r_o, ε, C_{ab} DATA--METALS

Substance	fcc/bcc	σ-Å	r_o-Å	ε/k-°K	Reference**	Date	C_{ab}-erg/cm$^6 \times 10^{60}$	Reference	Date
Al	fcc	2.72	3.00	733.3	25	1964			
		2.68	3.04	872.6	25	1964			
		2.56	-	1198.0	31	1969			
Pb	fcc	3.04	3.38	1188.2	25	1964			
		3.04	3.36	877.2	25	1964			
Li	bcc	3.00	3.46	505.9	25	1964	500	118	1961
		3.04	3.32	431.7	25	1964	571	118*	1961
		2.58	3.03	2052.0	27	1967			
		2.94	3.41	392.7	30	1968			
Na	bcc	3.27	3.83	563.6	76	1956	817	118	1961
		2.96	3.68	587.1	25	1964	933	118*	1961
		3.12	3.78	466.5	25	1964			
		-	3.72	313.3	26	1966			
		-	3.72	557.0	26	1966			
		3.38	3.87	271.6	27	1967			
		3.43	4.07	499.2	27	1967			
		3.46	4.07	385.0	30	1968			
		3.24	-	599.0	31	1969			

Table 16 (continued)

Substance	fcc/bcc	σ-Å	r_o-Å	ε/k-°K	Reference**	Date	C_{ab}-erg/cm^6 $\times 10^{60}$	Reference	Date
K	bcc	3.97	4.65	517.2	76	1956	1630	118	1961
		4.22	4.74	580.2	25	1964	1861	118*	1961
		4.04	4.80	362.0	25	1964			
		4.58	5.35	320.0	27	1967			
		4.27	5.00	373.4	30	1968			
Rb	bcc	4.42	5.04	408.4	25	1964	1590	118	1961
		4.74	5.18	348.1	25	1964	1816	118*	1961
		5.55	6.52	241.7	27	1967			
		4.56	5.32	323.4	30	1968			
Cs	bcc	4.46	5.16	707.8	25	1964	2200	118	1961
		4.60	5.34	236.7	25	1964	2512	118*	1961
		5.16	6.07	256.5	27	1967			
		5.17	6.00	261.8	30	1968			

*See Footnote(***) in Table 7.

**The parameters were deduced in conjunction with the following methods: Reference (25) Analysis of X-Ray Measurements; (31) Monte Carlo and Molecular Dynamics Techniques; (27) Model Pseudo-Potential Calculations; (30) Lattice-Dynamic Calculations; (76) Analysis of X-Ray Measurements--L-J 6-12 Potential assumed; (26) Molecular Dynamics Calculations; (5) Viscosity Measurements; (118) Theory of Angular Momentum.

In Table 16 it may be noted that, as opposed to the case of liquids (Table 7), r_o data are available. Examination of Equation (70) shows that these values along with σ fix n for the potential being considered. The results of preliminary computations of this type are shown in Table 17. The values of n in column 5 satisfy the set of parameters σ and r_o. That is, for the given values of n, Equation (72) goes through σ and has a minimum at r_o*. This minimum is not necessarily of depth ε. From Equation (132) it is clear that for this set (n, σ and r_o) the long-range attractive behavior C_{ab} and well-depth ε are directly proportional to each other, neither being fixed.

In line with the wide range of values of σ and r_o, a wide range of values of n results**. As before, the question is: Are any of the values consistent with the shock data? This was tested by applying PUFI using the available σ,ε data (Table 16 and columns 2 and 6 of Table 17). The results, shown in column 7, indicated that in all but two cases $n \leq 6.1$ and that there is no general agreement with the values in column 5. Potential agreement only occurs for those instances for Na and K where $n < 6$ (in column 5). However, in every case*** the fits were from poor to very poor (i.e., ε' large, f small) for $n = 6.1$, implying that the minima are not near $n = 6$.

---

* In opposition to satisfying σ and C_{ab} (as was the case for liquids) this pair is more desirable in that both σ and r_o are more nearly on the "repulsive" side of the potential.

** It is notable that for Na and K some of the parameter pairs lead to $n < 6$. This is discussed in a later section.

*** Even for Pb where minima in L are found, the resultant fits are generally poor.

Table 17

PRELIMINARY COMPUTATIONS--METALS

$g(n) = r_o/\sigma$ $\qquad$ $f(n) = C_{ab}/\varepsilon\sigma^6$

Column No.	1	2	3	4	5	6	7	8	9	10	11	12	13	14	15	16	17
							PUFI 1PF	UNFI 0PF	C_{ab}-erg-cm^6			C_{ab}-erg-cm^6			C_{ab} fixed** 2PF FIFI		
Substance		σ-Å	r_o-Å	g(n)*	n	ε/k-°K	n	n ≡ 6	× 10^{60}**	f(n)	n	× 10^{60}***	f(n)	n	n	σ-Å	ε/k-°K
Al		2.72	3.00	1.103	16.0	733.3	≤ 6.1	Poor fit									
		2.68	3.04	1.134	10.3	872.6	≤ 6.1	Poor fit									
Pb		3.04	3.38	1.112	13.9	1188.2	6.6	Fair fit									
		3.04	3.36	1.105	15.5	877.2	7.1	Fair fit									
Li		3.00	3.46	1.153	8.1	505.9	≤ 6.1		500	9.82	7.9	571	11.21	7.6			
		3.04	3.32	1.092	19.2	431.7	≤ 6.1		↓	10.63	7.7	↓	12.14	7.5			
		2.58	3.03	1.174	6.5	2052.0				5.99	9.5		6.84	8.9			
		2.94	3.41	1.160	7.5	392.7	≤ 6.1		↓	14.28	7.3	↓	16.31	7.1			
Na		3.27	3.83	1.171	6.7	563.6			817	8.59	8.2	933	9.81	7.9	6.2	3.52	35.5
		2.96	3.68	1.243	3.4	587.1	≤ 6.1	Poor fit	↓	14.99	7.2	↓	17.12	7.0	↓	↓	↓
		3.12	3.78	1.212	4.5	466.5	≤ 6.1	Poor fit	↓	13.75	7.3	↓	15.70	7.1	↓	↓	↓
		3.38	3.87	1.145	9.0	271.6			↓	14.61	7.2	↓	16.68	7.1	↓	↓	↓
		3.43	4.07	1.187	5.7	499.2			↓	7.28	8.7	↓	8.31	8.3	↓	↓	↓
		3.46	4.07	1.176	6.3	385.0	≤ 6.1	Poor fit	↓	8.96	8.1	↓	10.23	7.8	↓	↓	↓
		3.24	-	-	-	599.0			↓	8.54	8.3	↓	9.75	7.9	↓	↓	↓
K		3.97	4.65	1.171	6.7	517.2			1630	5.83	9.6	1861	6.66	9.0	6.1	10.44	0.06
		4.22	4.74	1.123	11.9	580.2	≤ 6.1		↓	3.60	13.0	↓	4.11	11.8	↓	↓	↓
		4.04	4.80	1.188	5.6	362.0	≤ 6.1		↓	7.50	8.6	↓	8.56	8.2	↓	↓	↓
		4.58	5.35	1.168	6.9	320.0			↓	4.00	12.0	↓	4.57	11.0	↓	↓	↓
		4.27	5.00	1.171	6.7	373.4	≤ 6.1	Poor fit	↓	5.22	10.2	↓	5.96	9.5	↓	↓	↓
Rb		4.42	5.04	1.140	9.5	408.4	≤ 6.1		1590	3.78	12.5	1816	4.32	11.4	6.6	3.25	349.9
		4.74	5.18	1.093	18.9	348.1	≤ 6.1		↓	2.92	15.8	↓	3.34	13.9	↓	↓	↓
		5.55	6.52	1.175	6.4	241.7			↓	1.63	>30.0	↓	1.86	>30.0	↓	↓	↓
		4.56	5.32	1.167	7.0	323.4	≤ 6.1	Poor fit	↓	3.96	12.1	↓	4.52	11.0	↓	↓	↓

Table 17 (continued)

1	2	3	4	5	6	7	8	9	10	11	12	13	14	15	16	17
						PUFI 1PF	UNFI 0 PF	C_{ab}-erg-cm^6			C_{ab}-erg-cm^6			C_{ab} fixed** 2PF FIFI		
Substance	σ-Å	r_o-Å	g(n)*	n	ε/k-°K	n	n ≡ 6	× 10^{60}**	f(n)	n	× 10^{60}***	f(n)	n	n	σ-Å	ε/k-°K
Cs	4.46	5.16	1.157	7.8	707.8	≤ 6.1		2200	2.86	16.1	2512	3.27	14.1	7.0	2.87	1549.2
	4.60	5.34	1.161	7.4	236.7	≤ 6.1		↓	7.11	8.8	↓	8.12	8.4	↓	↓	↓
	5.16	6.07	1.176	6.3	256.5			↓	3.29	14.0	↓	3.76	12.6	↓	↓	↓
	5.17	6.00	1.161	7.4	261.8	≤ 6.1	Poor fit	↓	3.19	14.5	↓	3.64	12.9	↓	↓	↓

*$g(n) = (n/6)^{1/n-6}$; $\lim_{n \to 0} g(n) \Rightarrow \infty$, $\lim_{n \to 6} g(n) = e^{1/6} \approx 1.1814$, $\lim_{n \to \infty} g(n) = 1$

**Reference 118

***See Footnote (***) in Table 7

To test this, the WF solution for $n = 6$ (Equations (115)-(119)) was used in another computer program (called UNFI*) which parallels PUFI in essentially all respects except that there are one zero parameter fit (OPF), two 1PF's and one 2PF in this case**. Application of UNFI to selected cases gave poor fits in all cases except for Pb*** for the OPF (column 8, Table 17)****. This confirmed the notion that the minima of PUFI were considerably < 6 .

As in the case of liquids, values of C_{ab}, σ and ε fix n through Equation (132). Using the data in Table 16, n was computed for the alkali metals. The results, shown in columns 11 and 14 of Table 17, satisfy the particular C_{ab}, σ, ε parameter set indicated. Although the variation in n for each substance is reduced considerably***** the results must ultimately be compared to the shock data. This was done in a less restricted way than previously by using the 2PF with C_{ab} fixed (see Appendix U ; the program was called FIFI******), and finding both n and σ . The results are shown in columns 15 and

---

*Available from the author on request.

**The recursion relation (equivalent to Equation (147)) for the spurious root of Equation (115) at $x = X_R$ is shown in Note 1 of Appendix Z. The condition for existence of the root was indicated in Appendix Y.

***The fits in this case were fair as would be expected from the values of n determined by PUFI (column 7, Table 17).

****The OPF in UNFI corresponds to the 1PF in PUFI.

*****The adjusted values of C_{ab} (column 14) do not greatly affect n .

******Available from the author on request.

16 of Table 17. Except for some of the values for Na, the differences in n (compared to column 14) and σ (compared to column 2) are large. Substitution of these values into Equation (132) along with the values of C_{ab} from column 9 gives the values of ε/k shown in column 17. Comparison within the "actual" values (column 6) shows that, except for Rb, large differences exist.

From these results it is clear that, as in the case of liquids, satisfaction of C_{ab}, σ and ε is not consistent with the shock data even when the value of σ in the latter case is not restricted. Because of this, attempts to satisfy long-range attractive behavior (i.e., C_{ab}) were abandoned and the error in doing so was accepted as an inherent limitation of the n-6 potential. As before, for strong compressive states, the effect of this will be small since the attractive forces will by comparison be small.

The preliminary calculations show that (a) the σ , r_o data are internally inconsistent and give values of n not consistent with the σ,ε set and the shock data, (b) consideration should be given to $n < 6$, (c) satisfying long-range attractive behavior (C_{ab}), σ and ε simultaneously improves internal consistency but does not improve the agreement with the shock data and (d) ignoring long-range attractive behavior may not introduce large errors. Considering these and noting that, in any case σ,ε data are available for only 7 metals* (of 23 being considered), it was concluded that although σ,ε is probably the

---

*C_{ab} data are only available for 4 metals.

preferred pair the best numerical values to use are unknown.

For liquids, a simple correlation of ε/k with melting points was found following Chapman[126] (see Equation (134)). Since the original paper[126] dealt with liquid metals, it would appear that such a correlation should also hold for present purposes, thus giving a reasonably consistent physical basis for (at least) one molecular parameter for each material*. As there is no reason why the correlation previously established in Equation (134) is not as accurate as any other, it was used to generate the data set in Table 18. For Al, Pb and the alkali metals, these are compared to the corresponding values from Table 16. It is notable that the correlated values fall generally within the range of the "reported" values**.

This correlation was tested using a modification of the PUFI program described earlier. This program, called PUFF***, differed only in that the index n ran from 3.1 to 12.1 instead of from 6.1 to 15.1****. This was done to investigate values of $n < 6$ ***** as previously

---

* As previously indicated σ,ε data are available only for 7 metals.

** For Na and K the correlated values 559.9°K and 507.1°K fall very close to those reported by Ling[76], 563.6°K and 517.2°K.

*** Available from the author on request.

**** Equation (147) was again used to determine the spurious root of Equation (135). The condition for the existence of the root for $3 < n < 6$ was indicated in Appendix Y.

***** Although the potential function exists for all $n > 0$, examination of Equation (97) and Equation (96) shows a singularity at $n = 3$. Furthermore, Equation (105) for the WF solution and Equations (106) and (107) for the MF solution all have roots of negative numbers for $n < 3$. For these reasons only values of $n > 3$ were considered in PUFF. (Actually, as previously noted, Equation (96) (or Equation (95)) "exists" for $0 \leq n < 3$ and values in this region could have been considered. Although this proved to be unnecessary for the WF and MF solutions (see Table 19) this was not the case for the SF solution discussed in the following sections.)

Table 18

ε/k vs. T_M CORRELATION--METALS

Substance	Structure	T_M-°C	T_M-°K	ε/k-°K	From Table 16 ε/k-°K
Cu	fcc	1083.0	1356.1	2038.0	
Ag		960.8	1233.9	1855.0	
Au		1063.0	1336.1	2008.0	
Co		1495.0	1768.1	2656.0	
Ni		1455.0	1728.1	2596.0	
Pd		1549.4	1822.5	2738.0	
Pt		1773.5	2046.6	3074.0	
Al		659.7	9932.8	1403.0	733.3-1198.0
Ca		842.0	1115.1	1678.0	
Pb		327.4	600.5	904.8	877.2-1188.2
Li	bcc	186.0	459.1	692.7	392.7-2052.0
Na		97.5	370.6	559.9	271.6-599.0
K		62.3	335.4	507.1	320.0-580.2
Rb		38.5	311.6	471.4	241.7-408.4
Cs		28.5	301.6	456.4	236.7-707.8
V		1710.0	1983.1	2979.0	
Nb		2500.0	2773.1	4164.0	
Ta		2996.0	3269.1	4908.0	
Cr		1890.0	2163.1	3249.0	
Mo		2620.0	2893.1	4344.0	
W		3370.0	3643.1	5469.0	
Zr		1857.0	2130.1	3199.0	
Ba		725.0	998.1	1501.0	

suggested. Because an independent evaluation of σ was not available, only the 2PF (with ε fixed) was considered with PUFF (see Table 10). The results are shown in Table 19.

As indicated by the preliminary calculations, solutions do exist for $n < 6$ (see column 3). Comparison of the corresponding values of ε' and f (columns 13 and 14) with those determined in Table 14 shows that the fits are generally adequate, although not excellent; the low values of f indicate that the solutions are not equal to the "best" the theory can do.

For fcc metals the values of σ from the 2PF (column 5, Table 19) appear to be reasonable; for Al and Pb they generally agree with the available data in Table 16. The corresponding WF solution gives values of U_o in good agreement with C_o in all but one case (calcium). The differences range from 0.2% (copper) to 13.4% (cobalt), the average being 6.3%. These are clearly superior to the MF solutions which consistently give values of U_o that are too high.

On the other hand, for bcc metals, the values of σ given by the 2PF are low at least for the alkali metals (see Table 16), and the WF solution gives low values of U_o. Although the MF solution gives high values of U_o for the alkali metals, it gives values in very good agreement with C_o for the remaining materials excepting barium. The differences range from 0.8% (chromium) to 10.1% (tungsten) with an average of 3.6%.

These results are generally encouraging in that they indicate that the melting point correlation for ε may well be physically reasonable. However, such a conclusion would be premature in light of

Table 19

PUFF APPLIED TO METALS

Column No. 1	2	3	4	5	6	7	8	9	10	11	12	13	14
						WF Solution		MF Solution					
Substance	Table 18 ε/k-°K	Eq.(X7) n	Eq.(147) X_R	Eq.(X17) σ-Å	Eq.(70) r_o-Å	Eq.(105) RE	Eq.(104) U_o-cm/sec × 10^{-6}	Eq.(106) σ-Å	Eq.(107) U_o-cm/sec × 10^{-6}	C_o-cm/sec × 10^{-6}	Eq.(142) L-cm^4/sec^4	Eq. (145) ε'	Eq. (146) f
Cu	2038.0	5.5	1.203	2.349	2.795	+0.044	0.3931	2.603	0.6237	0.394	8.74E21	0.225	0.291
Ag	1855.0	5.5	1.127	2.760	3.285	+0.027	0.3448	2.943	0.4567	0.313	9.02E19	0.071	0.470
Au	2008.0	5.4	1.061	2.869	3.420	+0.015	0.3137	2.959	0.3578	0.298	1.41E19	0.042	0.803
Co	2656.0	7.3	1.149	2.162	2.514	-0.137	0.4008	2.335	0.6107	0.463	2.81E20	0.129	0.141
Ni	2596.0	5.6	1.234	2.241	2.663	+0.042	0.4177	2.524	0.7207	0.456	7.01E21	0.319	≤0.145
Pd	2738.0	6.8	1.086	2.504	2.928	-0.044	0.3831	2.616	0.4782	0.390	7.99E19	0.010	0.105
Pt	3074.0	6.7	1.043	2.593	3.035	-0.018	0.3404	2.649	0.3778	0.351	1.88E19	0.091	0.297
Al	1403.0	5.6	1.219	2.587	3.074	+0.039	0.4709	2.891	0.7814	0.524	8.38E21	0.249	0.159
Ca	1678.0	6.7	1.576	2.802	3.280	-0.232	0.0191	3.775	0.6161	0.335	1.30E22	0.534	≤0.031
Pb	904.8	5.3	1.110	3.424	4.088	+0.030	0.1886	3.618	0.2385	0.198	3.23E21	0.173	≤0.859
Li	692.7	6.6	1.364	1.971	2.311	-0.129	0.2295	2.831	0.6786	0.469	2.00E22	0.414	≤0.041
Na	559.9	5.4	1.327	2.633	3.139	+0.084	0.1812	3.108	0.3910	0.233	2.03E21	0.194	0.114
K	507.1	5.1	1.409	3.222	3.860	+0.142	0.1187	3.957	0.3028	0.206	1.42E21	0.149	0.260
Rb	471.4	5.2	1.426	3.391	4.056	+0.137	0.0708	4.202	0.1934	0.113	1.21E20	0.139	≤0.058
Cs	456.4	7.8	1.473	3.145	3.639	-0.582	0.0094	4.044	0.1157	0.087	6.91E19	0.041	0.662
V	2979.0	6.8	1.084	1.948	2.278	-0.043	0.4111	2.034	0.5104	0.518	2.95E20	0.200	≤0.119
Nb	4164.0	6.6	1.107	2.117	2.482	-0.038	0.3478	2.236	0.4548	0.439	3.24E20	0.182	≤0.070
Ta	4908.0	6.6	1.123	2.105	2.468	-0.044	0.2589	2.241	0.3538	0.339	2.08E20	0.129	≤0.171
Cr	3249.0	7.0	1.040	1.892	2.207	-0.027	0.4675	1.931	0.5193	0.515	3.87E19	0.087	0.475
Mo	4344.0	5.4	1.104	2.168	2.584	+0.025	0.4262	2.284	0.5332	0.519	1.33E21	0.231	≤0.266
W	5469.0	6.8	1.038	2.089	2.443	-0.019	0.3312	2.130	0.3640	0.405	1.38E19	0.086	0.022
Zr	3199.0	7.4	1.056	2.299	2.671	-0.057	0.3258	2.365	0.3785	0.388	2.88E18	0.117	≤0.020
Ba	1501.0	10.1	1.539	2.290	2.600	-1.673	-	3.090	0.1906	0.161	2.39E20	0.062	≤0.813

the previously discussed objection to the 2PF; i.e., it is not discriminating enough in choosing a distinct "best" value of n. Examination of the L vs. n plots for the PUFF solutions in Table 19 shows that indeed in every instance, a range of values of n will give equally "good" fits.

Even with the (limited) success of the melting point correlation, it was concluded that the preferred σ,ε pair for metals is generally unknown. Further, since the objective with metals is limited to finding an "effective" potential only, it is not clear that <u>real</u> values of σ and ε are best. This difficulty is avoided by use of the SF solution discussed previously. In this instance, the sound velocity $C_o(= U_o)$ is considered as a valid data point in the set of shock data available and the theory is "forced" through this point by elimination of σ and ε between Equations (96)-(98), (106) and (107). The resulting expression, Equation (108), only depends on one molecular parameter, n. Because of this only 1PF's are now possible* and, hopefully, an unambiguous distinct choice of n will result. This will, of course, be determined by the success of Equation (108) in fitting the shock data. This is discussed in the following sections.

---

*Because of the mathematical development, Equation (108) intrinsically depends on only one molecular parameter (n) and one thermodynamic parameter (U_o); 2PF's and a 3PF are not possible.

2. Treatment of Data

Equation (108) with a specified value of U_o is to be used to find the "best" value of n from the shock wave data. Since it is anticipated that values of n both greater and less than 6 will be examined, the SF solution for $n = 6$, Equation (122), will also be considered in the following developments.

Equations (108) and (122) are both in the functional form previously considered for liquids, i.e., μ vs. x. However, both contain U_o which suggests (temporary) consideration of the Hugoniot in the form U vs. x. This can be done by eliminating μ using Equation (4). Equations (108) and (122) become:

$$U^2 = U_o^2 \left(\frac{2}{n-6}\right)\left(\frac{x}{x-1}\right)^2 \left[\frac{x^{n-2} - 1}{n-2} - \frac{x^4 - 1}{4}\right] \tag{149}$$

$$U^2 = U_o^2 \left(\frac{1}{2}\right)\left(\frac{x}{x-1}\right)^2 \left[x^4 \ln x - \frac{x^4 - 1}{4}\right] \tag{150}$$

Because of the SF development it is necessary that $U \to$ (exactly) U_o as $x \to 1$ in Equations (149) and (150). Therefore no theoretical instability occurs in the computation as $x \to 1$ *. However, since there are two singularities at $x = 1$ (one for each $(x-1)$ factor in the denominator)**, it is clear that the numerical instabilities previously discussed with liquids, still exist.

---

*Taking the limit of Equations (149) and (150) as $x \to 1$ yields $U = U_o$ in both cases.

**There is also a singularity at $n = 6$ in Equation (149). Of course Equation (150) is just the result of removing that singularity by finding the limit of Equation (149) as $n \to 6$. See Appendix R.

To assure computational accuracy to as low a value of x as desired, Equations (149) and (150) were expanded in a Taylor series in the interval $1 \leq x < 2$ (see Appendix AA). The number of terms in the expansion was chosen to give accuracy to at least 5 decimal places. The resulting expressions for $n \neq 6$ are:

$$U^2 = U_o^2 \, f(x,n) \quad , \qquad 1 \leq x < 2 \tag{151}$$

where*:

$$f(x,n) = x^2\Big[1 + \left(\frac{n-1}{3}\right)(x-1) + \left(\frac{n^2 - 6n + 11}{12}\right)(x-1)^2 + \left(\frac{n-3}{3}\right)\left(\frac{n-4}{4}\right)\left(\frac{n-5}{5}\right)(x-1)^3 \left\{1 + \left(\frac{n-7}{6}\right)(x-1)\left(1 + \left(\frac{n-8}{7}\right)(x-1) \cdots \left(1 + \left(\frac{n-16}{15}\right)(x-1)\right)\right)\right\}\Big] \tag{152}$$

and:

$$U^2 = U_o^2\left(\frac{2}{n-6}\right)\left(\frac{x}{x-1}\right)^2 \left[\frac{x^{n-2} - 1}{n-2} - \frac{x^4 - 1}{4}\right] \quad , \qquad x > 2 \tag{153}$$

For $n = 6$ the equivalent expressions are:

$$U^2 = U_o^2 \, g(x) \quad , \qquad 1 \leq x < 2 \tag{154}$$

---

*It may be noted that the singularity at $n = 6$ has also been (fortuitously) removed in the development of Equation (152). This implies that $f(x,6)$ should be equal to $g(x)$ in Equation (155), a limiting process not being necessary.

$$g(x) = x^2 \left[1 + \frac{5}{3}(x-1) + \frac{11}{12}(x-1)^2 + \frac{1}{10}(x-1)^3 \right.$$

$$\times \left\{1 + (x-1)(-\frac{1}{6} + (x-1)(\frac{1}{21} + (x-1)(-\frac{1}{56} + (x-1)(\frac{1}{126} + (x-1)(-\frac{1}{152}\right.$$

$$+ (x-1)(\frac{1}{462} + (x-1)(-\frac{1}{792} + (x-1)(\frac{1}{1287} + (x-1)(-\frac{1}{2002}$$

$$+ (x-1)(\frac{1}{3003} + (x-1)(-\frac{1}{4368} + (x-1)(\frac{1}{6188} + (x-1)(\frac{-1}{8568}$$

$$+ (x-1)(\frac{1}{11628} + (x-1)(\frac{-1}{15504} + (x-1)(\frac{1}{20349} + (x-1)(\frac{-1}{26334}$$

$$+ (x-1)(\frac{1}{33649} + (x-1)(\frac{-1}{42504} + (x-1)(\frac{1}{53130} + (x-1)(\frac{-1}{65780})$$

$$\left.\left.))))))))))))))))))\right\}\right] \qquad (155)$$

and:

$$U^2 = U_o^2(\frac{1}{2})(\frac{x}{x-1})^2 \left[x^4 \ln x - \frac{x^4 - 1}{4}\right] , \qquad x \geq 2 \qquad (156)$$

Examination of Equations (152) and (155) shows that the singularities have been removed and the computations should be stable near $x = 1$.

In order to be consistent with prior fits, Equation (4) was used in Equations (151), (153), (154) and (156) to recast the Hugoniot in the μ vs. x functional form. This resulted* in, for $n \neq 6$:

---

*Note that this step introduces no singularities since the denominator of Equations (157) and (159) cannot vanish (i.e., $x \geq 0$).

$$\mu^2 = U_o^2\left(\frac{x-1}{x}\right)^2 f(x,n) \quad , \qquad 1 \leq x < 2 \tag{157}$$

$$\mu^2 = U_o^2\left(\frac{2}{n-6}\right)\left[\frac{x^{n-2}-1}{n-2} - \frac{x^4-1}{4}\right] \quad , \quad x \geq 2 \tag{158}$$

and for $n = 6$:

$$\mu^2 = U_o^2\left(\frac{x-1}{x}\right)^2 g(x) \quad , \qquad 1 \leq x < 2 \tag{159}$$

$$\mu^2 = U_o^2\left(\frac{1}{2}\right)\left[x^4 \ln x - \frac{x^4-1}{4}\right] \quad , \quad x \geq 2 \tag{160}$$

Using least-squares fitting techniques Equations (157)-(160) can be used to find the "best" value of n from the $U_i - \mu_i$ data converted to $\mu_i - x_i$ using Equation (4). For this data set the residuals R_i are for $n \neq 6$:

$$R_i = \mu_i^2 - U_o^2\left(\frac{x_i-1}{x_i}\right)^2 f(x_i,n) \quad , \quad 1 \leq x_i < 2 \tag{161}$$

$$R_i = \mu_i^2 - U_o^2\left(\frac{2}{n-6}\right)\left[\frac{x_i^{n-2}-1}{n-2} - \frac{x_i^4-1}{4}\right] \quad , \quad x_i \geq 2 \tag{162}$$

and for $n = 6$:

$$R_i = \mu_i^2 - U_o^2\left(\frac{x_i-1}{x_i}\right)^2 g(x_i) \quad , \qquad 1 \leq x_i \leq 2 \tag{163}$$

$$R_i = \mu_i^2 - U_o^2\left(\frac{1}{2}\right)\left[x_i^4 \ln x_i - \frac{x_i^4-1}{4}\right] \quad , \quad x_i \geq 2 \tag{164}$$

The equation of interest is:

$$\frac{\partial \sum_i R_i^2}{\partial n} = 0 \tag{165}$$

in which the appropriate equation for R_i is to be used. Equation (165) should fix the value of n which will minimize the sum of the squares of the residuals[15].

Formalization of this procedure with Equations (161)-(164) will lead to complex, implicit functions for n having many roots. The one of interest might be difficult to find. Therefore, as was done previously for 1PF's, n was indexed from 0 to 15 * in increments of 0.1 and the sum-of-the-squares of the residuals found from:

$$L = \sum_i R_i^2 = \sum_i \{\mu_i^2 - U_o^2(\frac{x_i - 1}{x_i})^2 f(x_i,n)\}^2 \quad , \quad 1 \leq x_i < 2 \qquad (166)$$

$$L = \sum_i R_i^2 = \sum_i \{\mu_i^2 - U_o^2(\frac{2}{n-6})[\frac{x_i^{n-2} - 1}{n-2} - \frac{x_i^4 - 1}{4}]\}^2 \quad , \quad x \geq 2 \qquad (167)$$

for $n \neq 6$ and:

$$L = \sum_i R_i^2 = \sum_i \{\mu_i^2 - U_o^2(\frac{x_i - 1}{x_i})^2 g(x_i)\}^2 \quad , \quad 1 \leq x_i < 2 \qquad (168)$$

$$L = \sum_i R_i^2 = \sum_i \{\mu_i^2 - U_o^2(\frac{1}{2})[x_i^4 \ln x_i - \frac{x_i^4 - 1}{4}]\}^2 , \quad x_i \geq 2 \qquad (169)$$

for $n = 6$. The desired value of n is clearly that which gives the lowest value of L , the appropriate equation being used.

Following exactly the approach used in the assessment of liquids, the same two measures ε' and f were used to measure the quality of the "fit". By definition (Equations (143)-(146)):

---

*The possibility of solutions with $n < 3$ was anticipated.

$$\varepsilon' = \sqrt{L/m} \; / \; \overline{\mu^2} \tag{170}$$

and:

$$f = \sqrt{L_{min}/L} \tag{171}$$

Although the first parameter can be determined directly from the computations, the second cannot, since L_{min} is unknown. In the WF or MF solutions L_{min} is taken from the 3PF (the "best" the theory can do) but for the SF solution there is no counterpart 3PF. Therefore L_{min} was (somewhat arbitrarily) taken as the minimum of the 3PF found previously with PUFF. This should give a direct comparison (at least with regard to f) with the results in Table 19.

The limitations and difficulties in the use of ε' and f discussed previously apply in this case also and care in interpreting results is required.

In the case of liquids it was possible to show that a spurious root could exist in the μ^2 vs. x relation (Equation (135)) for all the materials of interest, and the function was "cut-off" at the value of the root X_R. Examination of the SF solution equations in the present case (Equations (108) and (122)) indicates that the same behavior might occur near $x = 1$. However, it was shown (Note 1 of Appendix Y) that no second (spurious) root of these equations can exist for all $x > 1$, $n \geq 0$ *. No computations of X_R were

---

*It is also shown that there are no singularities in the SF solution and therefore that it "exists" for all $x > 1$, $n \geq 0$.

considered in this case*.

As in the case of liquids, a computer program was written to carry out the computations. For metals the main program was called FIFO** in which the input data were m, M, ρ_o, s, U_o and the shock data U_i-μ_i. Preliminary calculations consisted of a computation of x_i (using Equation (4)) and U_i/U_o for each U_i-μ_i pair. The following computations were then made for each value of n from 0.1 to 15.1 (in increments of 0.1). For $n \neq 6$, σ was calculated from Equation (106), r_o from Equation (70), and ε from a rearrangement of Equation (107) using the input value of U_o. For $n = 6$ the values of σ, r_o and ε were determined, respectively, from Equation (120), the limit of Equation (70)*** and a rearrangement of

---

*It may be noted that the Taylor series expansions, Equations (157) and (159), and not Equations (158) and (160) (the counterparts of Equations (108) and (122)) are used for computations for $1 \leq x < 2$. Although these equations are numerically (and theoretically) stable (the expansions can be shown to be convergent for all $n \geq 0$), and the associated pair for U must extrapolate to U_o (see Equations (151) and (154)), the fact that no spurious root exists in Equations (108) or (122) helps assure that Equations (157) and (159) have no anomalies (i.e., they are "well-behaved") in the neighborhood of $x = 1$.

**A listing is available from the author on request.

***
$$\lim_{n \to 6} r_o = \lim_{n \to 6} (n/6)^{1/n-6} \sigma = e^{1/6}\sigma \simeq 1.1814\sigma$$

Equation (121). For general comparison a residual computation modeled on Equations (166)-(169) was made for U, using Equations (151)-(156). The appropriate equation was dependent on n and the particular value of x_i. This was followed by a determination of the (more significant) residuals from Equations (166)-(169), the equation being used according as $n \neq 6$ or $n = 6$ and $x_i \leq 2$ or $x_i > 2$. The last two computations made were the standard error or estimate S_{μ^2} (see Equation (143)) and the "error of the fit" ε' from Equation (170).

To help visualize the minimum of the summed residuals squared a line plot of L vs. n was determined for each substance*.

Based on the results obtained with liquids and the general "sharpness" of the L vs. n plots for the current materials, an increment finer than 0.1 in n was not considered.

After evaluating the results of FIFO for each material (including f which was not included in the program) the best value of n and the corresponding values of σ and ε were found. Using the former in Equations (151)-(153) along with Equation (4), a set of x, U and μ data were tabulated. From this, line plots of U vs. μ and μ vs. x were superimposed on the corresponding raw data to visualize the fit. Using the σ and ε values, $\phi(r)$ vs. r values were tabulated using Equation (69) and subsequently plotted using a program called FOMP**.

---

*For comparison, the residuals in U were also plotted on the same sheet.

**Available from the author on request.

3. Results

FIFO was applied to all of the metals shown in Table 4 and the summarized results are listed in Table 20.

The values of ε' and f obtained show that, except for Ca, Cs and Ba, all of the fits are excellent and some are truly outstanding. The SF theory fits the available data closely for adjustments in only one parameter, n.

A comparison of these results with those in Table 19 for PUFF shows that FIFO generally gives a much better fit; f is considerably increased for all but two cases (Cs and Ba) and ε' is decreased for all but these two cases and for Pd. Since FIFO uses a 1PF the difficulty in choosing a distinct value of n encountered with the 2PF in PUFF should not occur. Examination of the L vs. n plots for the solutions in Table 20 showed that this was the case; the "best" values of n were sharply defined.

For fcc metals the values of n are close to those found with PUFF (Table 19). That solutions exist for $n < 6$ is clearly reiterated. The values of σ found (column 3) appear reasonable, although they are generally higher than those found in Table 19. For Al and Pb the σ are notably higher than the "reported" values (Table 16). On the other hand the ε/k values in Table 20 are consistently and considerably below both those in Tables 18 and 16. They do not appear to be low by any single factor. The singular result for Ca is considered in the following discussion.

For bcc metals the values of n are much less than the corresponding values found with PUFF (Table 19). They are also generally

Table 20

FIFO APPLIED TO METALS

Substance	n	σ-Å	r_o-Å	ε/k-°K	L-cm^4/sec^4	ε'	f*	Comments
Cu	5.3	2.642	3.155	756.9	2.55E21	0.122	0.539	
Ag	6.3	2.808	3.304	1079.4	2.51E19	0.037	0.891	
Au	5.8	2.881	3.413	1581.3	1.28E19	0.039	0.843	
Co	3.7	3.333	4.113	249.5	6.08E18	0.019	0.958	
Ni	5.0	2.648	3.177	824.2	3.48E20	0.071	$\leq$0.652	
Pd	5.6	2.785	3.309	1382.2	1.06E19	0.038	0.916	
Pt	5.6	2.808	3.336	2048.5	2.74E18	0.035	0.778	
Al	4.0	3.502	4.289	233.4	3.18E20	0.048	0.817	
Ca	0.5	-	-	-	4.32E21	0.307	$\leq$0.305	$n \leq 2$; σ,ε/k "not defined"
Pb	5.2	3.648	4.362	599.1	2.89E21	0.162	$\leq$0.915	
Li	0.7	-	-	-	4.09E20	0.059	$\leq$1.41	$n \leq 2$; σ, ε/k "not defined"
Na	3.6	4.190	5.184	39.7	4.67E19	0.030	0.753	
K	1.2	-	-	-	1.39E20	0.047	0.832	$n \leq 2$; σ, ε/k "not defined"
Rb	3.0	-	-	-	8.73E18	0.037	$\leq$0.900	$2 < n \leq 3$; σ,ε/k "not defined"
Cs	4.3	5.094	6.196	86.7	1.88E21	0.213	0.126	
V	1.9	-	-	-	5.20E18	0.027	$\leq$0.896	$n \leq 2$; σ, ε/k "not defined"
Nb	2.5	-	-	-	1.70E18	0.013	$\leq$0.970	$2 < n \leq 3$; σ,ε/k "not defined"
Ta	2.3	-	-	-	6.08E18	0.036	$\leq$1.00	$2 < n \leq 3$; σ,ε/k "not defined"

Table 20 (continued)

Substance	n	σ-Å	r_o-Å	ε/k-°K	L-cm^4/sec^4	ε'	f*	Comments
Cr	4.6	2.269	2.743	1521.0	1.16E19	0.047	0.870	
Mo	2.5	-	-	-	8.66E19	0.059	$\leq$ 1.04	$2 < n \leq 3$; $\sigma, \varepsilon/k$ "not defined"
W	2.5	-	-	-	4.53E17	0.016	0.815	$2 < n \leq 3$; $\sigma, \varepsilon/k$ "not defined"
Zr	$\leq$ 0.1	-	-	-	$\leq$ 2.95E17	$\leq$ 0.037	$\leq$ 0.444	$n \leq 2$; $\sigma, \varepsilon/k$ "not defined"
Ba	4.4	4.03	4.895	333.3	7.06E21	0.338	$\leq$ 0.148	

*See Equation (171); L_{min} is taken from the 3PF's of the corresponding PUFF solutions shown in Table 19.

below the values just found for the fcc metals*. It was previously shown (Appendix I) that the potential chosen for this study (Equation (69)) exists and is monotonically "harder" for all n from $n = 0$ to $n = \infty$**. This should also be the case for the Hugoniot equation for the SF solution (Equation (108)) which, despite the apparent singularity at $n = 2$***, was shown to "exist" for all $n \geq 0$. However, the condition for extrapolation to U_o (Equation (101)) leads to Equation (106) for σ which has roots of negative numbers for $n < 3$ (as previously pointed out in the discussion of PUFF)****. Since this equation is used to eliminate σ in the SF solution development, it may be speculated that Equation (108) is not "well defined" under these conditions*****. Although this point is moot, it is clear that σ is "not defined" for all $n < 3$ and values were not listed in

---

*The bcc metals have much "softer" potentials than the fcc metals.

**The only mathematical difficulty would appear to occur at $n = 6$. This was taken care of in the development of Equation (73).

***As shown in Appendix Y (Equations (Y49)-(Y53)) when $n = 2$ Equation (108) becomes :

$$\mu^2 = \frac{1}{2} U_o^2 \left[\frac{x^4-1}{4} - \ell n\, x\right] \qquad (Y53)$$

****It can be shown that the n-6 potential (strictly) exists for all $n \geq 0$ only when σ and ε are independently specified. If σ is fixed by Equation (106) the potential is unrealistic when σ is unrealistic, i.e., when $0 < n \leq 3$.

*****Examination of Figures 37-39 and 41 shows that the U-μ Hugoniot curve has a <u>decreasing</u> slope as $x \to 1$ ($\mu \to 0$), when $n \leq 2$. As this contrasts with all prior results (which indicate an increasing or (at least) constant slope as $x \to 1$) anomalous behavior might be indicated for $n \leq 2$. This occurred for Ca (for fcc metals) and Li, K, V and Zr (for bcc metals) as noted in Table 20.

Table 20*. Since ε depends directly on σ (Equation (104)) it was "not defined" in these cases either. This affected Rb, Nb, Ta, Mo and W as indicated in Table 20.

For the remaining metals (Na, Cs, Cr and Ba) the values of σ found are reasonable, although they are generally higher than those found in Table 19. For Na, σ is somewhat higher than the "reported" values in Table 16, although the corresponding figures for Cs are fairly close. As was the case for the fcc metals, the ε/k values for Na, Cs, Cr and Ba are well below the corresponding values in Tables 18 and 16. Again they do not appear to be low by a common factor.

To illustrate the excellent fits for the FIFO results in Table 20, the SF theory with the listed values of n is compared to the U-μ data in Figures 35-41.

---

*Although the solution for Rb ($n = 3.0$ exactly) is on the borderline (i.e., the minimum might actually be at $n > 3$ or $n < 3$), the value of σ (nominally $\to \infty$, see Equation (106)) was not listed in this case either.

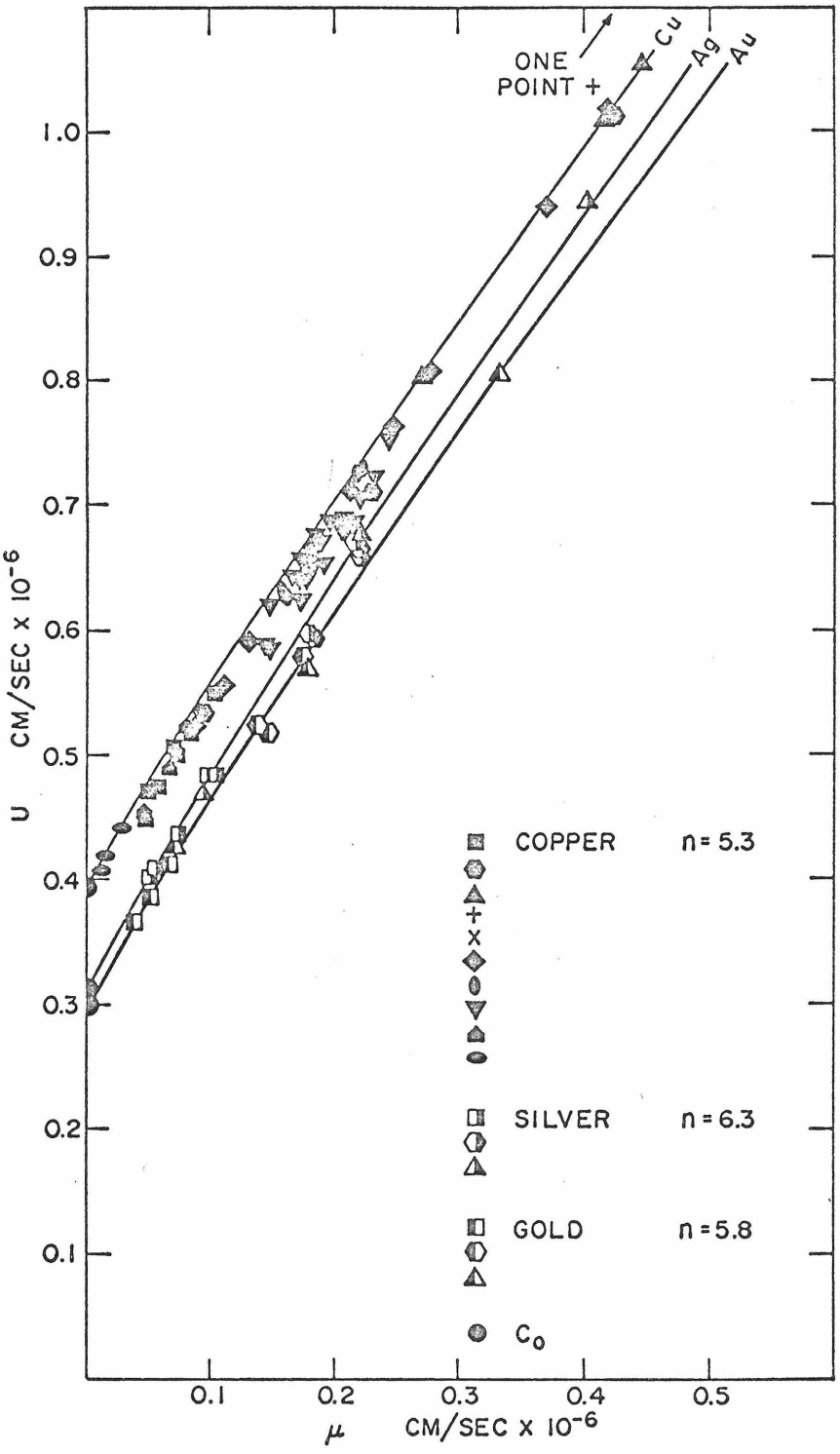

Figure 35. U vs. μ Fit of Theory--Cu, Ag, Au

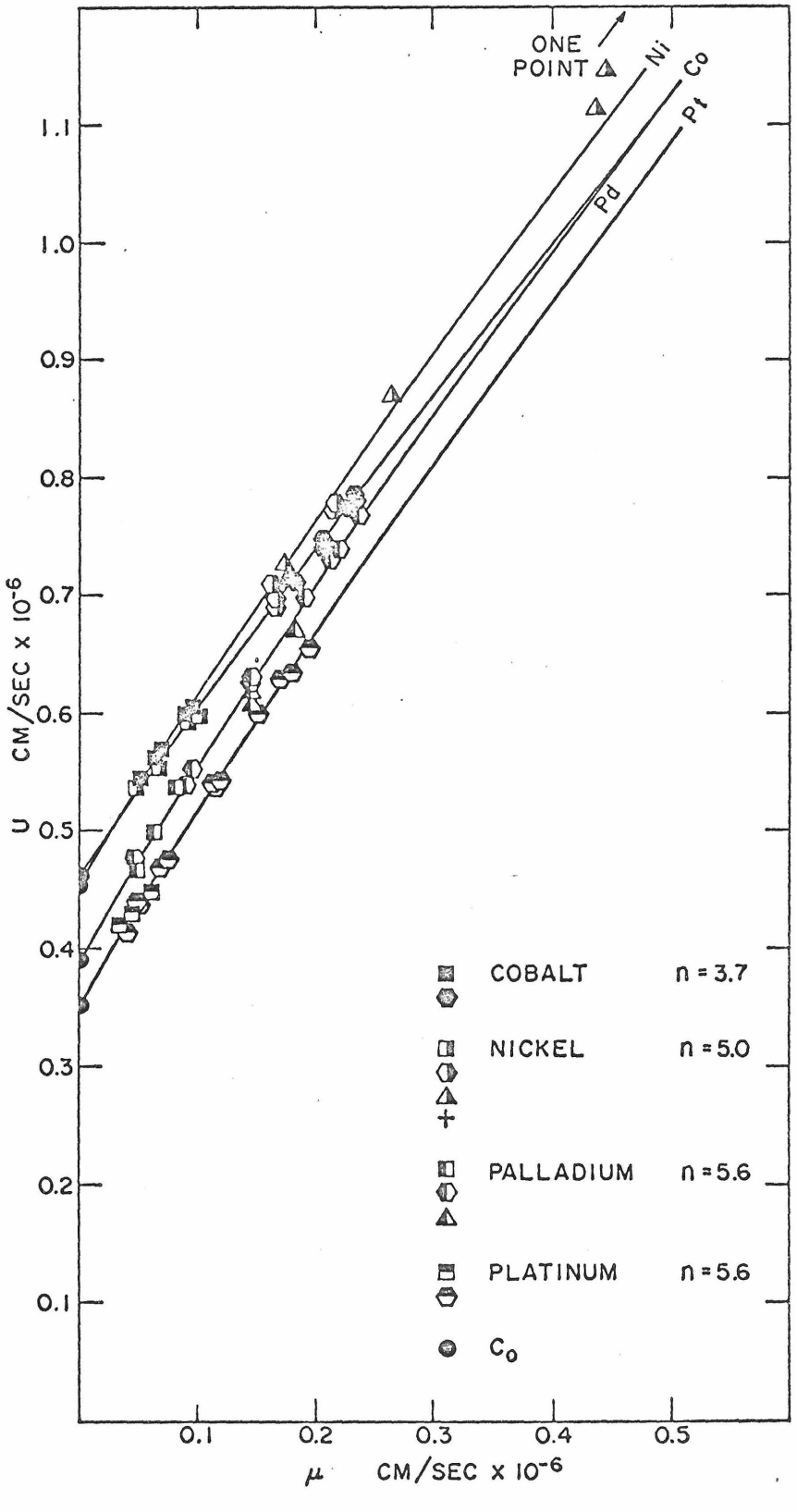

Figure 36. U vs. μ Fit of Theory--Co, Ni, Pd, Pt

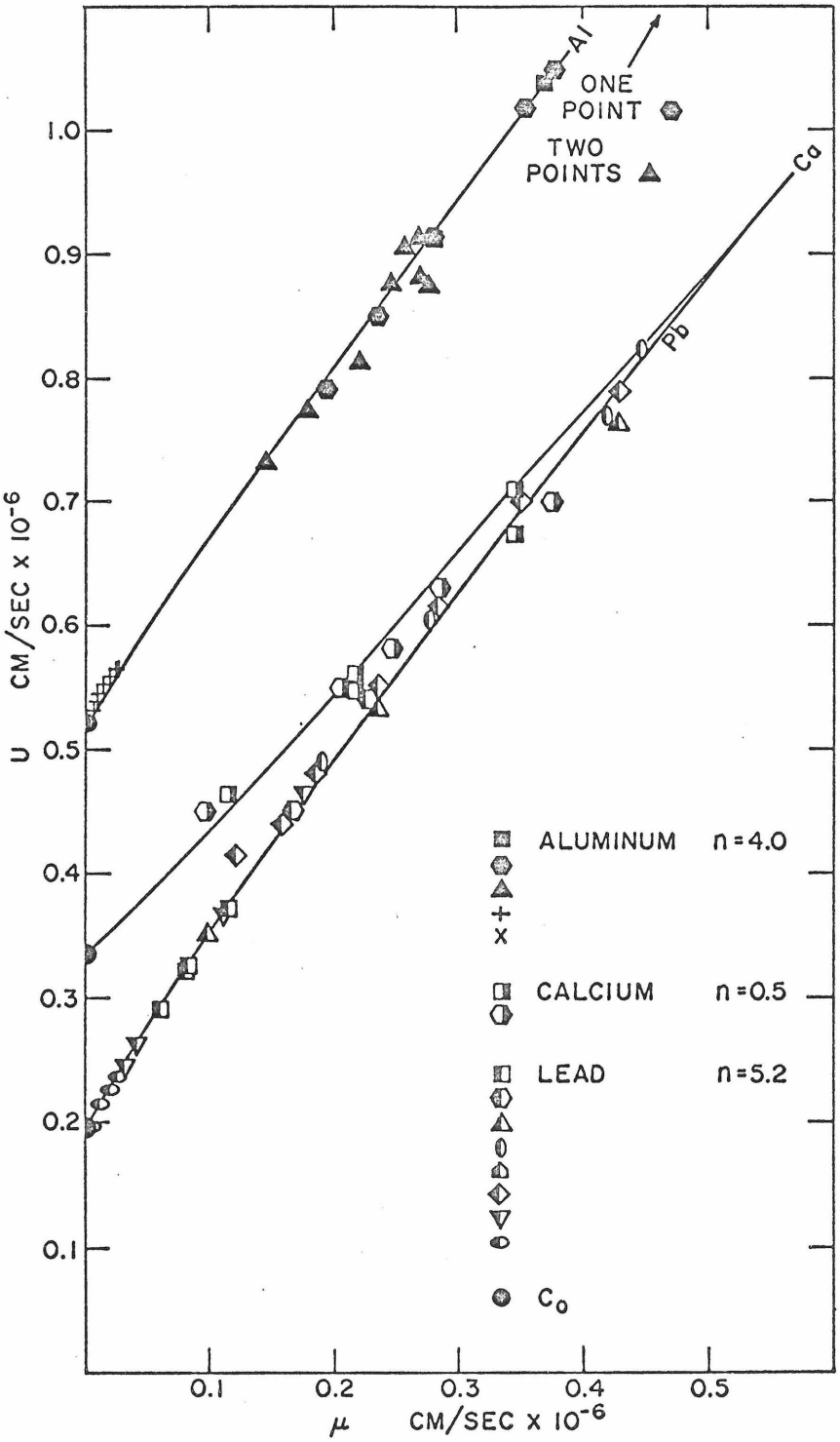

Figure 37. U vs. μ Fit of Theory--Al, Ca, Pb

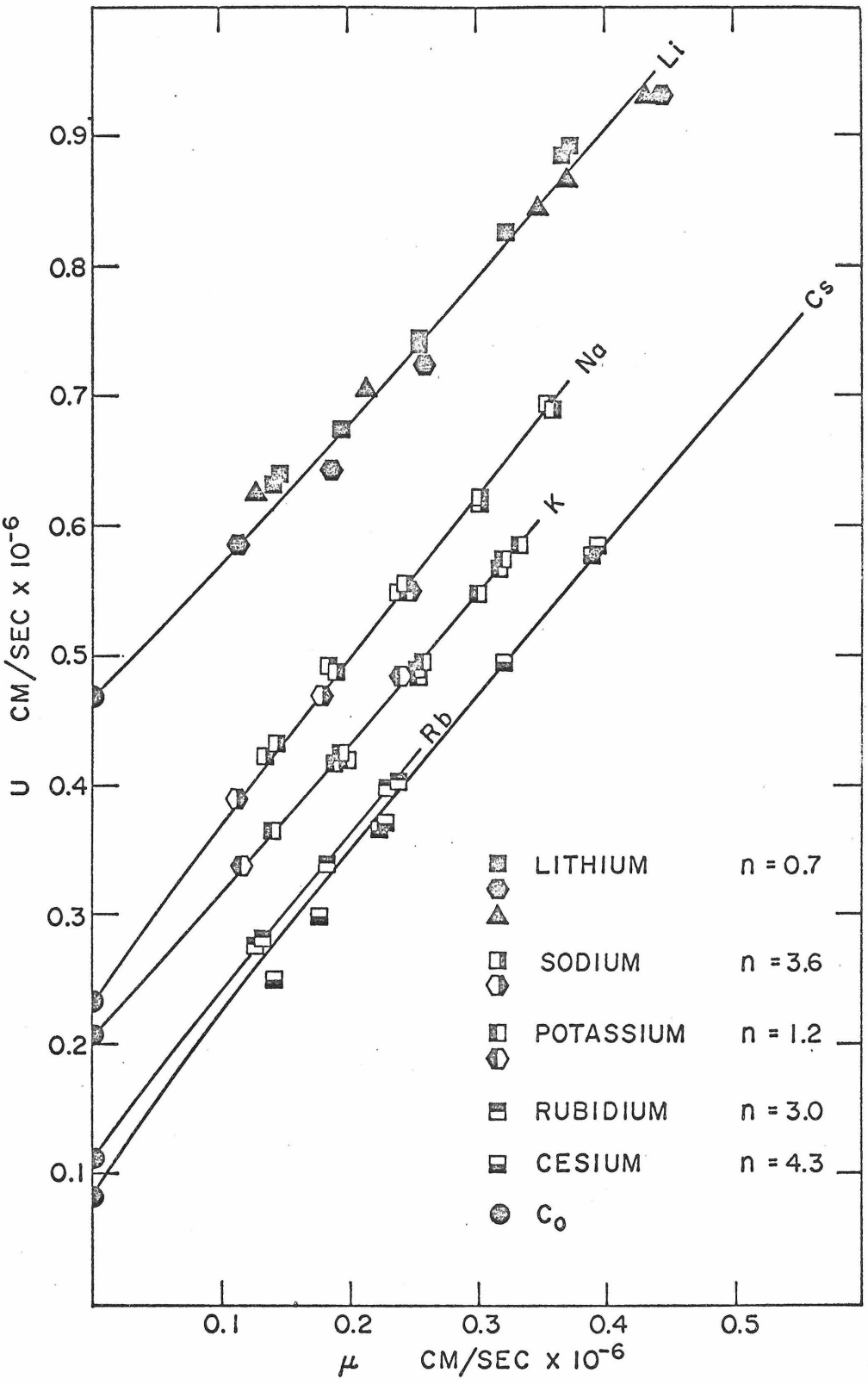

Figure 38. U vs. μ Fit of Theory--Li, Na, K, Rb, Cs

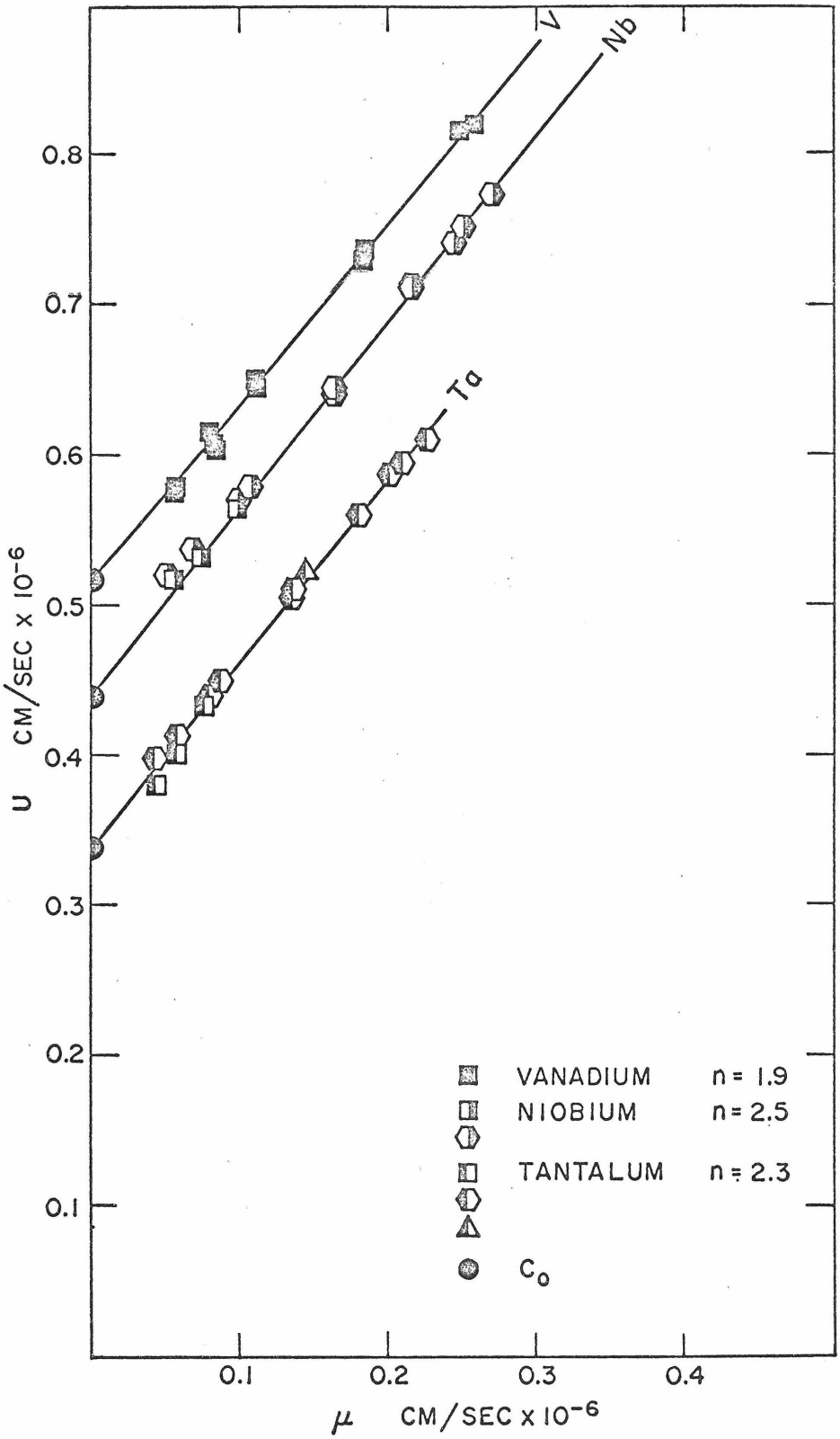

Figure 39. U vs. μ Fit of Theory--V, Nb, Ta

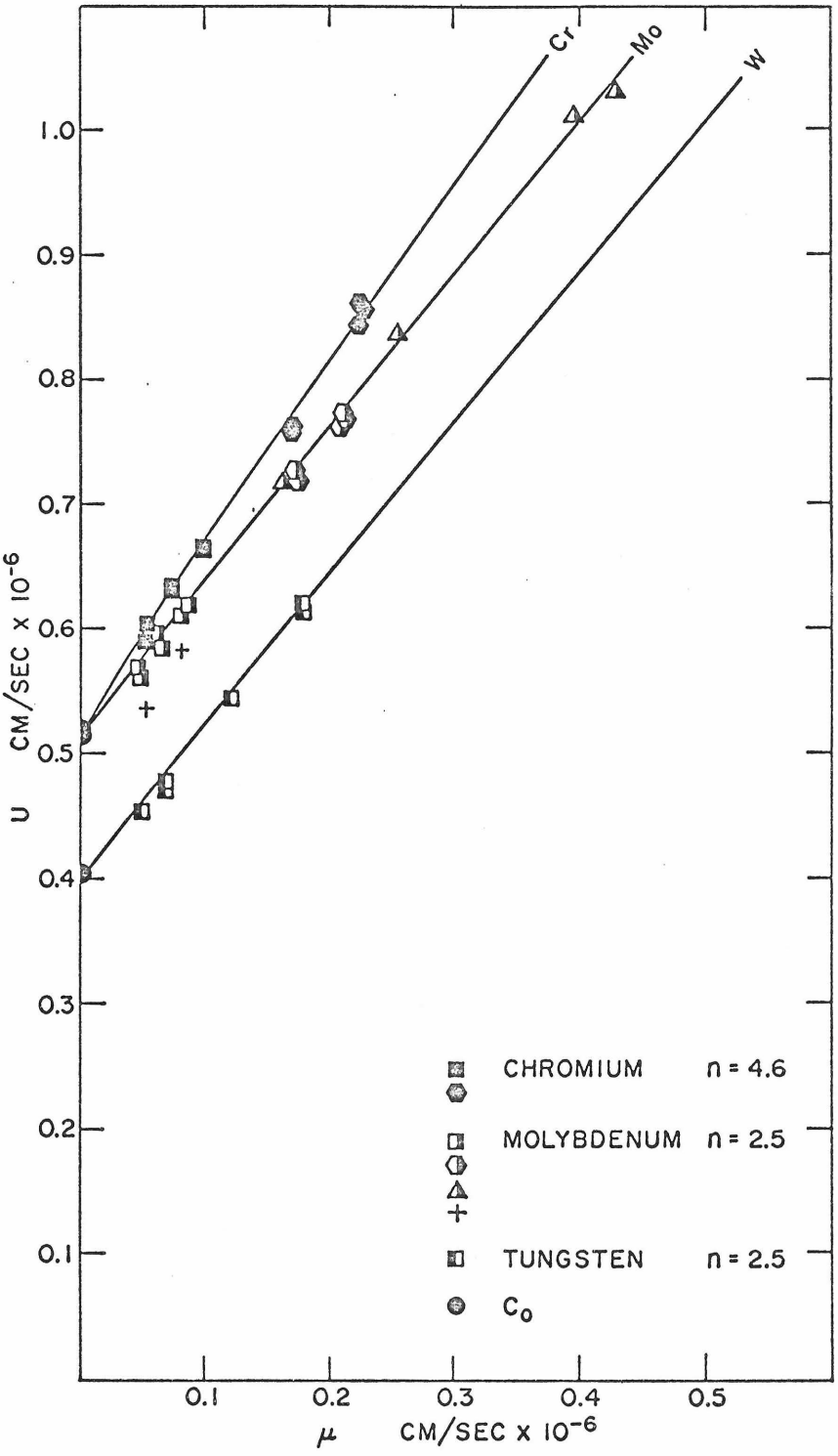

Figure 40. U vs. μ Fit of Theory--Cr, Mo, W

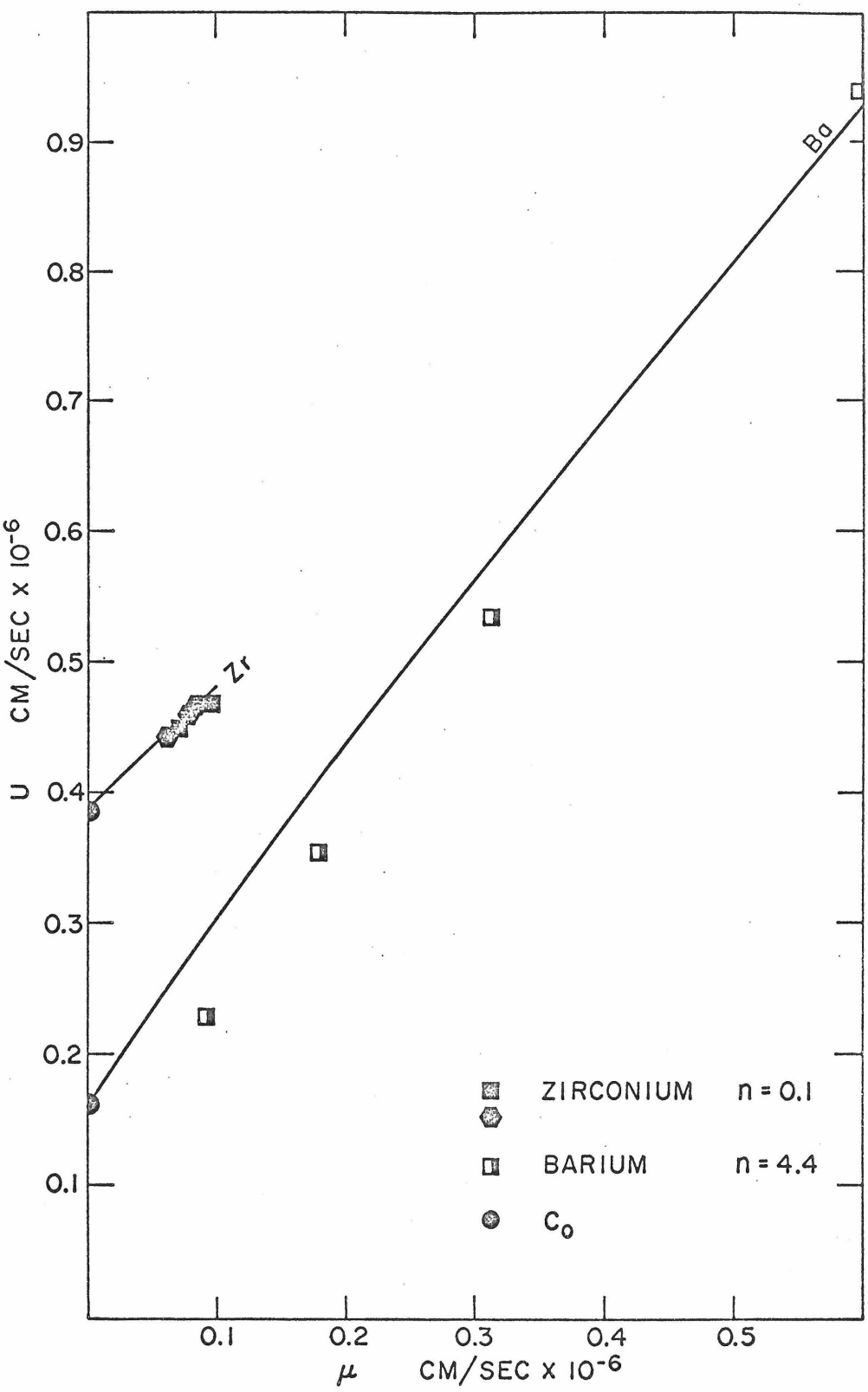

Figure 41. U vs. μ Fit of Theory--Zr, Ba

IV. DISCUSSION AND CONCLUSIONS

A. THEORY

1. Evaluation of Assumptions

a. Shock front thickness. The most critical assumption made in the development of the theory concerns the thickness of the shock front or "transition region" between the two density zones shown in Figures 4 and 5. Only if the front is "sufficiently thin" will the interval of time in which the molecules are in the transition region (the dwell time) be less than the thermal relaxation time. It is only under these circumstances that (a) the energy change across the transition region may be evaluated by consideration of the configurational energy change only (Equation (27) is valid; there is no temperature rise across the shock front), (b) the molecules respond solely in the direction of the shock (no (net) transverse motion) and compress linearly (Equation (92) is valid), and (c) the configurational energy of adjacent molecules before and after the transition region remains constant (Equation (47) is valid). The rise in temperature and resumption of a more normal structure (relieving the abnormally high potential energy associated with linear compression) takes place in the high density state after the layer of molecules of interest has reached the end of the transition region. Further, only if the front is sufficiently thin will Equation (41) be valid; i.e., will the contributions to the configurational integral for material above the layer of molecules of interest be the same both before and after the transition.

Consider the shaded molecule (in layer L_o) in Figure 5a. The total configurational energy (for this molecule) in this state is

given by Equation (33):

$$\Phi^{L_o} = \Phi_1^{L_o} + \Phi_2^{L_o} + \Phi_3^{L_o}(R') + \Phi_4^{L_o}(R) \tag{33}$$

If R (and R') are large the first two terms are approximately equal (Equation (37)) while the latter two are (comparatively) negligible (Equations (35) and (36)). Therefore (see Equations (35)-(37)):

$$\Phi_2^{L_o} + \Phi_3^{L_o}(R') + \Phi_4^{L_o}(R) \tilde{=} \Phi_1^{L_o} \tag{172}$$

The preservation of this relation (i.e., that the total configurational energy above and below the shaded molecule are the same and identical to that at L_o) may be used to define the shock front thickness z_f ($\equiv R - R'$) as follows. Consider the molecule (in layer L) as it approaches the compressed region; Φ_2^L decreases (since there is less mass below the molecule in the uncompressed region) while $\Phi_3^L(R')$ increases (since R' is decreasing). When $R' = 0$, $\Phi_2^L = 0$ and Equation (172) becomes* ($R = z_f$):

$$\Phi_3^L(0) + \Phi_4^L(z_f) \tilde{=} \Phi_1^{L_o} \tag{173}$$

Since $\rho > \rho_o$ a value of z_f can always be found such that:

$$\Phi_3^L(0) \tilde{=} \Phi_1^{L_o} \tag{174}$$

and Equation (173) will be valid (meeting the required condition) if:

---

* Note that $\Phi_1^L = \Phi_1^{L_o}$ always.

$$\Phi_4^L(z_f) \tilde{=} 0 \tag{175}$$

The terms in Equations (173)-(175) may be more usefully defined by (see Equations (45) and (46)):

$$\Phi_1^{L_o} = \psi(\rho_o,z_o) + \psi^{L_o}(z_o) \tag{176}$$

$$\Phi_3^L(0) = \psi(\rho',z') + \psi^L(z_o) \tag{177}$$

$$\Phi_4^L(z_f) = \psi(\rho,z_f) \tag{178}$$

Here ρ' and z' are some density and spacing intermediate between ρ_o and ρ and z_o and z respectively; $\psi(\rho,z)$ is the configurational energy of an isolated molecule a distance z from a medium of density ρ; and $\psi^{L_o}(z_o)$ and $\psi^L(z_o)$ are the configurational energy contributions of the other molecules in L_o and L respectively*. Since these others remain at spacing z_o (see Equation (47)):

$$\psi^{L_o}(z_o) = \psi^L(z_o) \tag{179}$$

Substitution of Equations (176)-(179) into Equations (173)-(175) gives:

$$\psi(\rho',z') + \psi(\rho,z_f) \tilde{=} \psi(\rho_o,z_o) \tag{180}$$

$$\psi(\rho',z') \tilde{=} \psi(\rho_o,z_o) \tag{181}$$

---

*There are no "other" molecules for $\Phi_4^L(z_f)$ since we are here only considering the shaded molecule at L and not at L_1.

and:

$$\psi(\rho, z_f) \overset{\sim}{=} 0 \tag{182}$$

the last of which serves to define z_f .

The approximation in Equation (182) may be expressed in Equation (180) by setting:

$$\psi(\rho, z_f) = y\psi(\rho_o, z_o) \tag{183}$$

where y is some (arbitrarily) small fraction. Substituting directly from Equations (78) and (79) (with $z = z_f$) gives, after rearrangement:

$$z_f^{n-6} + z_f^{n-3} \frac{y}{x} \left[\frac{12}{(n-2)(n-3)} \frac{\sigma^{n-6}}{z_o^{n-3}} - \frac{1}{z_o^3}\right] - \frac{12}{(n-2)(n-3)} \sigma^{n-6} = 0 \tag{184}$$

From Equation (88):

$$z_o = (M/2^s \rho_o N)^{1/3} \tag{88}$$

and Equation (184) becomes:

$$z_f^{n-6} + z_f^{n-3} \frac{y}{x} \left[\frac{12}{(n-2)(n-3)} \frac{\sigma^{n-6}}{(M/2^s \rho_o N)^{\frac{n-3}{3}}} - \left(\frac{2^s \rho_o N}{M}\right)\right] - \frac{12}{(n-2)(n-3)} \sigma^{n-6} = 0 \tag{185}$$

which is a transcendental equation in z_f depending functionally only on x and parametrically only on σ and n and the arbitrary fraction y . For a given substance (σ, n, ρ_o, M) this can be solved for z_f using an iterative technique (such as Newton-Raphson) for a chosen value of y . This was done for several liquids with $y = 0.05$ for a range of values of x from 1.2 to 2.0. With little variation, the

mean value of z_f was $\sim 25\text{Å}$ at the lower compression ratios* increasing only $\sim 4\text{Å}$ over the whole compression range**. These values may be compared with predictions for several liquids shown in Table 21. Considering (a) the general lack of agreement between the tabulated values (b) the need for extrapolating two of the results[134,133] from 17 and 700 atm to 5 Kbar ($\tilde{=}$5000 atm), and (c) the fact that the pressure variation of z_f is opposite to that of the current theory (see second footnote below), the values of z_f predicted above would seem to be reasonable although perhaps conservatively large.

---

*For $x \tilde{=} 1.2$, $P \tilde{=} 5$ Kbar for most of the liquids which is generally well below the lowest value for the data used in this study (see Appendix S).

**The definition of z_f used here (Equation (175) leading to Equation (183)) requires that z_f increase with x (or P) since as ρ increases, $\psi(\rho,z_f)$ will be the same fraction of $\psi(\rho_o,z_o)$ at lower values of z_f (see Equations (78) and (79)), i.e., the dense region will have an equal effect on the shaded molecule at greater distances, as ρ increases. This increase (of z_f with P) may be contrasted to a general decrease predicted by Becker[135], Eyring, et al[84], Flook and Hornig[134] and Eisenmenger[133]. It is believed that this difference is caused by a difference in (effective) definition; the developments in Equations (172)-(185) are intended only to yield a gross estimate of z_f (i.e., its order of magnitude as predicted by the theory) rather than as a definitive prediction of z_f and its functionality. The referenced studies had as their objective the determination of z_f.

Table 21

AVAILABLE SHOCK FRONT THICKNESS AND RELAXATION TIME DATA

Substance(s)	P-Kbar	z_f - Å	Reference	Date	Comments
CCl_4	5	47.8	133	1964	Extrapolated to 5 Kbar from 700 atm
CH_3OH	5	3.5	133	1964	Extrapolated to 5 Kbar from 700 atm
C_2H_5OH	5	4.0	134	1955	Extrapolated to 5 Kbar from 17 atm
	5	5.7	133	1964	Extrapolated to 5 Kbar from 700 atm
$(C_2H_5)_2O$	0.1	520	84	1949	Quotes Becker[135]
	1.0	53			
	10	6.5			
	100	1.4			
	5	0.3	134	1955	Extrapolated to 5 Kbar from 17 atm
$C_6H_5CH_3$	5	14.8	133	1964	Extrapolated to 5 Kbar from 700 atm
H_2O	5	4.7	134	1955	Extrapolated to 5 Kbar from 17 atm
H_2O	5	14.4	133	1964	Extrapolated to 5 Kbar from 700 atm
Liquids	-	100-1000	87.	1948	

Table 21 (continued)

Substance(s)	$\tau \times 10^{12}$ sec	Reference	Date	Comments
A	5.0	129	1970	Structural relaxation time
Hg	~ 1.0	136	1965	Bulk viscosity relaxation time
CS_2	2830	137	1959	Average thermal relaxation time
CCl_4	126	137	1959	Average thermal relaxation time
CH_3OH	13.0	137	1959	Average thermal relaxation time
	0.2	136	1965	Bulk viscosity relaxation time
C_6H_{14}	15.2	137	1959	Average thermal relaxation time
	~ 3.0	136	1965	Bulk viscosity relaxation time
C_6H_6	270	137	1959	Average thermal relaxation time
	60	136	1965	Bulk viscosity relaxation time
$C_6H_5CH_3$	4.4	136	1965	Bulk viscosity relaxation time
H_2O	0.7 - 3.5	137	1959	Average thermal relaxation time
	1.0	77	1965	
	~ 0.1	82	1966	Structural relaxation time
Liquids	~10	36	1937	Viscosity relaxation time
	~10	129	1970	Structural relaxation time
Condensed matter	> 0.1-0.01	77	1965	

Using Equation (84), the data in Appendix S and the results for z_f, values of n_L, the number of molecular layers in the transition region, were found from:

$$n_L = z_f/z_o \tag{186}$$

Again, little variation was found from substance to substance; the resultant mean value ($\bar{n}_L$) was ~ 7 layers in the low pressure region*. Although this figure is somewhat larger than previously speculated[16], it is believed that the actual (effective) thickness is < 7 layers (since the z_f estimate is probably conservative; Table 21) and that, nevertheless, this figure satisfies the requirement of a "sufficiently thin" shock front.

The residence (dwell) time of the molecules in the shock wave is given approximately by**:

$$t_r = \frac{z_f}{U - \frac{1}{2}\mu} \tag{187}$$

From Equation (14) this becomes:

$$t_r = 2\frac{z_f}{\mu}\left(\frac{x-1}{x+1}\right) \tag{188}$$

Computations (at $x \cong 1.2$) for several liquids (again) showed only small variations; the mean value of t_r was $\sim 2 \times 10^{-12}$sec***. Comparison of this value with (several types of) relaxation times

---

*Because z_f increases $\sim 4\text{Å}$, $\bar{n}_L \cong 8$ layers at the higher pressures.

**Since μ (in laboratory coordinates) goes from zero (initially) to its full final value (at the end of the transition region) the <u>average</u> velocity in the front is $\sim \mu/2$.

***Since t_r decreases with x (as opposed to z_f) this value is conservative, i.e., $\bar{t}_r < 2 \times 10^{-12}$sec.

reported in the literature, shows that $\bar{t}_r < \tau$ in most instances and that generally* $\bar{t}_r << \tau$ when thermal relaxation times are considered (see Table 21).

It is concluded that, at least for liquids** the assumption of a "sufficiently thin" shock front width is a reasonable approximation.

b. Pair potential. In the development of the energy equation it is necessary to evaluate the interaction of a given molecule with those in a half-space such as in Figure 6. The expression used (Equation (49)) implies a basic assumption: "The potential energy is equal to the sum of the potentials developed between pairs of molecules"(17)***. As this is identical to the assumption nearly always made in basic statistical mechanical developments(17,18,20,etc.) it is made here without further discussion or justification except to quote Egelstaff(17): "In any event this term (i.e., the pair potential) is likely to be the major term in the potential energy."

In the integration of the pair potential (Equations (51) and (52)) it is assumed that the effect of $g(r)$ is small and/or will cancel in Equation (48). In their study of liquid argon Mikolaj and

---

*A notable exception is H_2O.

**A similar analysis for solids (metals) was not performed. However, because of the excellent agreement of the theory with the data (see Figures 35-41), a similar conclusion would be anticipated.

***That is, the potential between a pair of molecules is unaffected by the presence or absence of other molecules.

Pings[138] determined $g(r)$ for several thermodynamic states. An examination of their data shows that $g(r) \tilde{=} 1$ for all $r > 5\text{Å}$. From Equation (84) and Appendix S, $z_o \tilde{=} 2.9\text{Å}$ and it is clear that at least for the integration in Equation (52), which starts at $z' = z_o$, $g(r)$ will only have an effect between the first and second layers (see Figure 6). Since the contributions of material up to $\sim 25\text{Å}$ distant is expected to have an effect (see computations on shock wave thickness), the ultimate effect of $g(r)$ on the integral should be small. Since $x_{max} \tilde{=} 2$, $z_{min} \tilde{=} z_o/2$ (see Equation (92)) and for the integration in Equation (51), which starts at $z' = z$, $g(r)$ should only have an effect between the first and third layers. Again the ultimate effect is expected to be small. In any case, any residual effects of $g(r)$ on either integral will tend to cancel when the difference of Equations (53) and (54) is found in Equation (48).

This general conclusion is expected to hold for all the liquids studied. On the other hand, for metals, the LRO behavior in the pair potential might imply a pair distribution function for which $g(r) \tilde{\neq} 1$ for r greater than some (small) value. In this case the residual terms of the integrals may not be small, although they may still cancel in Equation (48). The adequacy of the assumption is, in this case, generally unknown.

The choice of the n-6 potential on physical grounds is indefensible since it is known to be inaccurate for nonconducting materials and unrealistic for metals (which exhibit LRO behavior). On the other hand, since we are only interested in the strongly repulsive region in this study (dealing with strong <u>compression</u> waves >10 Kbar), this

potential might well be adequate in this region. Of the many ways to "fit" the theory to the experimental data, use of the parameters on the "repulsive side" of the potential (i.e., σ and ε) were eventually shown to be best. Advantages in the use of the n-6 potential include: (a) mathematical simplicity; all results are in simple explicit form*, and (b) monotonicity; $\phi(r)$ exists and is monotonically "harder" for all n from $n = 0$ to $n = \infty$ ($r < \sigma$), as well as the fact that (c) the resulting Hugoniot can be extrapolated to sound velocity, and (d) U vs. μ linearity can be demonstrated from the theory (see later discussion). Disadvantages are: (a) inaccuracy and/or unrealism in the attractive region**, (b) theoretical*** and numerical instability in the developed Hugoniot as $U \to U_o$, and (c) the lack of definition of σ and ε for the SF solution when $n < 3$ (Equations (106) and (107)) leading to a (possibly) not "well defined" Hugoniot in this region.

It is concluded that, for the present study, the n-6 potential is probably adequate, although other potential functions may ultimately prove to be more accurate/realistic.

---

*Also no spurious maxima occur at small values of r .

**Also, additional attractive terms are ignored (see Appendix V).

***Extrapolation is possible only if Equation (105) holds "exactly".

c. Structure. The use of a lattice-like structure in relating the distance between molecular layers z_o to density ρ_o (Equations (84), (85) and (87)) and even the subsequent generalization of structure (Equation (88)) is a simple extension* of several well-known cell models of liquids[5,19]. As previously discussed, Equation (88) is considered microscopically accurate for solids (for discrete values of s) and macroscopically accurate for liquids** (for, perhaps, a continuous range of values of s).

d. Extrapolation to sound velocity. One of the strongest points of the theory is that it can be extrapolated to sound velocity. However, to do this (exactly) a subsidiary condition (Equation (106)) is developed that fixes σ in terms of n (only). Although no assumptions are required for this development it is clear that the "condition" reduces the number of independent parameters of the system from 3 to 2 (i.e., from σ, ε and n to ε and n). It is assumed that this reduction is compatible with known values of σ (at least for liquids) where n is fixed by the shock data. Generally this is only roughly true (see discussion below) but as previously discussed this is considered a limitation of the particular potential used and not (necessarily) of the theory itself***. It is concluded that

---

*This may not be the case for the "snapshot" and "probability" approaches to the determination of a_o, the nearest neighbor distance, and the use of a_o as a measure of liquid structure.

**In a previous study[16] a ±10% variation in z_o from (the equivalent of) Equation (84) was shown not to materially affect the Hugoniot prediction for argon at two initial states.

***For example, if a four parameter potential were used, extrapolation to U_o could be used to relate one of the parameters to the other 3.

extrapolation to sound velocity is a desirable feature of the theory but is too restrictive in that it leads to a (possibly) unrealistic relation among system parameters. Of course, for metals, where σ and ε are poorly defined and the SF solution is used, extrapolation to sound velocity is highly significant in that it leads to a unique and (dramatically) simplified expression for the Hugoniot in terms of a single microscopic parameter (Equation (108)).

e. U vs. μ linearity. One of the original motivations in developing the current theory was a desire to explain the form of Equation (13), the linear U-μ relation. In Equations (109)-(113) it was shown that, to do this, two diverse functions must be identified with each other. As the correspondence between the functions is not obvious, consider the following. The SF solution of the Hugoniot is given by Equation (108):

$$\mu^2 = U_o^2\left(\frac{2}{n-6}\right)\left[\frac{x^{n-2}-1}{n-2} - \frac{x^4-1}{4}\right] \tag{108}$$

Expansion in a Taylor series gives:

$$\mu^2 = U_o^2\left(\frac{x-1}{x}\right)^2 f(x,n) \quad , \quad 1 \leq x < 2 \tag{157}$$

where $f(x,n)$ is given by Equation (152). For $x-1 \ll 1$ $(x \ll 2)$, $f(x,n)$ becomes, to a good approximation:

$$f(x,n) \tilde{=} x^2\left[1 + \left(\frac{n-1}{3}\right)(x-1)\right] \quad , \quad x \ll 2 \tag{189}$$

and substitution into Equation (157) gives:

$$\mu^2 = U_o^2(x-1)^2\left[1 + \left(\frac{n-1}{3}\right)(x-1)\right] \quad , \quad x \ll 2 \tag{190}$$

Now let:

$$[1 + (\frac{n-1}{3})(x-1)] = (\frac{1}{1-q})^2 \tag{191}$$

where[127]:

$$(\frac{1}{1-q})^2 = 1 + 2q + 3q^2 + 4q^3 + \cdots , \quad q^2 < 1 \tag{192}$$

If $q << 1$, Equation (192) reduces to:

$$(\frac{1}{1-q})^2 \simeq 1 + 2q \tag{193}$$

and combination with Equation (191) yields:

$$[1 + (\frac{n-1}{3})(x-1)] = 1 + 2q \tag{194}$$

In this case:

$$q = (\frac{n-1}{6})(x-1) \tag{195}$$

Since $x - 1 << 1$ (and $\frac{n-1}{6} < 2$ generally), $q << 1$ and Equation (193) is justified. Substituting Equation (195) in Equation (191) gives:

$$[1 + (\frac{n-1}{3})(x-1)] = \left(\frac{1}{1 - (\frac{n-1}{6})(x-1)}\right)^2 \tag{196}$$

Substitution into Equation (190) gives:

$$\mu^2 = U_o^2(x-1)^2 \left(\frac{1}{1 - (\frac{n-1}{6})(x-1)}\right)^2 , \quad x << 2 \tag{197}$$

Taking roots and rearranging gives:

$$\mu[(\frac{1}{x-1}) - (\frac{n-1}{6})] = U_o , \qquad x << 2 \tag{198}$$

From Equation (14):

$$\left(\frac{1}{x-1}\right) = \frac{U-\mu}{\mu} \tag{199}$$

and Equation (198) becomes, with rearrangement:

$$U = U_o + \left(\frac{n+5}{6}\right)\mu \quad , \qquad x << 2 \tag{200}$$

which is the desired relation; it may be compared directly to Equation (13) from which it is noted that:

$$B = \frac{n+5}{6} \tag{201}$$

Thus it is clear that, indeed, the linear U-μ relation is derivable from the developed theory*. The development elucidates the conditions under which the derivation is valid, i.e., that $x << 2$. This implies that the linear relation should only be valid near sound velocity (i.e., at small values of x) and that, generally, higher order terms in μ should be required as x increases to 2 and beyond. This, of course, explains the great success of the linear form for metals. In these cases (see Reference 13 for example) x is generally somewhat less than 2.

If the linear relation is valid near sound velocity then, from Equation (13):

$$\lim_{\mu \to 0} \frac{dU}{d\mu} = B \tag{202}$$

---

*The correspondence of the "diverse" relations following Equation (113) can be shown in a manner similar to the development in Equations (189)-(201). In fact, the form in Equation (191) was actually chosen on the basis of the square of Equation (113) rather than on an arbitrary basis.

even if there are other terms in the expression. If the development leading to Equation (201) is valid, the same result should be produced when the condition expressed by Equation (202) is applied to the theory. This can be done by direct differentiation of Equation (108) (without Taylor series expansion) as follows:

$$\frac{dU}{d\mu} = \frac{dU}{dx} \cdot \frac{dx}{d\mu} = \frac{dU/dx}{d\mu/dx} = \frac{2UdU/dx}{2Ud\mu/dx} \tag{203}$$

and noting Equation (14):

$$\frac{dU}{d\mu} = \frac{2UdU/dx}{\left(\frac{x}{x-1}\right) 2\mu d\mu/dx} = \left(\frac{x-1}{x}\right) \frac{dU^2/dx}{d\mu^2/dx} \tag{204}$$

The numerator and denominator may be determined directly from Equations (149) and (108) yielding:

$$\frac{dU}{d\mu} = \frac{x(x-1) - 2\left(\frac{\frac{x^{n-2}-1}{n-2} - \frac{x^4-1}{4}}{x^{n-3} - x^3}\right)}{(x-1)^2} \tag{205}$$

Taking the limit of Equation (205) as $x \to 1$ (i.e., as $\mu \to 0$) gives, after repeated application of L'Hospital's rule:

$$\lim_{x \to 1} \frac{dU}{d\mu} = \lim_{\mu \to 0} \frac{dU}{d\mu} = \left(\frac{n+5}{6}\right) \tag{206}$$

which, noting Equation (202), is the same as Equation (201). It is concluded that the proposed theory explains the form of Equation (13) and furthermore, relates the slope B to the repulsive exponent n.

The accuracy of Equation (201) may be assessed by comparing the predicted values of B, based on the values of n in Tables 14 (for the C solution) and 20, with values found by fitting available data

to Equation (13). This is done in Table 22. The results are as generally expected: For liquids the value of B from the theory (Equation (201)) is high because the range of x in the experimental data is large (the condition in Equation (200) is not fulfilled) and the U-μ slope should decrease as μ increases (i.e., the linear fit would tend to reduce $\overline{B}$); for solids the value of B from the theory is much closer to the fitted values (within $\sim$10%) although it is still on the high side. It is concluded that when $x << 2$, Equation (201) is a reasonable estimate of the slope of the linear U-μ relation, i.e., of B*.

---

*The estimate of B in Equation (16), when used in Equation (201), leads to $n = 3$. It is interesting that this value is close to those determined for many of the bcc metals which have "soft" potentials.

Table 22

COMPARISON OF VALUES OF B FROM THEORY AND EXPERIMENT

Theory: $B = (n+5)/6$

Data: Best Fit of $U=A+B\mu$ to Experimental Data*

Liquids				fcc Metals				bcc Metals			
Substance	n	B=(n+5)/6	$\overline{B}$**	Substance	n	B=(n+5)/6	$\overline{B}$**	Substance	n	B=(n+5)/6	$\overline{B}$**
A	9.2	2.4	2.1	Cu	5.3	1.7	1.5	Li	0.7	1.0	1.1
A-II	9.2	2.4	1.4	Ag	6.3	1.9	1.6	Na	3.6	1.4	1.3
A-III	9.2	2.4	1.4	Au	5.8	1.8	1.6	K	1.2	1.0	1.2
A-IV	9.2	2.4	1.4	Co	3.7	1.5	1.4	Rb	3.0	1.3	1.2
Hg	11.7	2.8	2.4	Ni	5.0	1.7	1.5	Cs	4.3	1.6	1.6
N_2	7.0	2.0	1.5	Pd	5.6	1.8	1.8	V	1.9	1.2	1.2
H_2	6.5	1.9	1.8	Pt	5.6	1.8	1.4	Nb	2.5	1.4	1.2
CS_2	10.6	2.6	0.9	Al	4.0	1.5	1.4	Ta	2.3	1.4	1.3
CCl_4	6.2	1.9	1.5	Cg	0.5	0.8	1.1	Cr	4.6	1.6	1.5
CH_3OH	8.0	2.2	1.5	Pb	5.2	1.7	1.5	Mo	2.5	1.4	1.2
C_2H_5OH	8.0	2.2	1.6					W	2.5	1.4	1.3
$(C_2H_5)_2O$	7.5	2.1	1.5					Zr	0.1	0.9	0.9
C_6H_{14}	7.8	2.1	1.4					Ba	4.4	1.6	1.4
C_6H_6	7.1	2.0	1.6								

Table 22 (continued)

Liquids			
Substance	n	B=(n+5)/6	$\overline{B}$**
$C_6H_5CH_3$	7.5	2.1	1.6
H_2O	7.6	2.1	1.6

*From References 85, 86, 92, 13, 103, 104, 108, 10, 107, 93, 64, 96, 60, 98, 95, 106

** $\overline{B}$ is average value of B from several references.

2. Adequacy of Theory

Equation (95), the sought-after expression for the Hugoniot, embodies all the essential features of the theory; most of the other relationships of interest (e.g., Equations (104), (106), (108), etc.) can be derived directly from it. This expression was derived by combining a model of the shock transition process with a (particular) intermolecular potential function and a lattice-like structure. It provides a generalized functionality of two macroscopic properties (μ and x) in terms of three microscopic (molecular/atomic) properties (σ, ε, and n) for a given substance (M) in a given initial state (ρ_o). By thus connecting observed experimental results with properties of matter at the molecular level, the theory fulfills one of the objectives of statistical mechanics[19] as well as its (the author's) intended "mission". In this sense (at least) the (formalism of the) theory may be considered adequate.

The degree to which the theory is self-consistent and in accord with the generally known properties of shock waves is another measure of its adequacy. The following features may be enumerated: (a) the theory will extrapolate to U_o although the process is theoretically unstable and requires a subsidiary condition that reduces the number of independent parameters of the system, (b) all theoretical and numerical instabilities of the theory can be removed by expanding the SF solution in a Taylor series of arbitrary number of terms, (c) the theory is applicable to all $n > 0$ except $n = 3$ where Equation (95)

has a singularity* and for all $x > X_R$ ($X_R > 1$) when $n > 3$, (d) the linear U-μ relation can be derived from the theory when it is extrapolated to U_o and expanded in a Taylor series, and (e) the slope of the U-μ Hugoniot near U_o can be derived and evaluated from the theory in terms of a single molecular parameter.

Besides the accuracy of the assumptions of the shock model itself, the adequacy of the theory depends on the applicability of the potential function (Equation (72)) and structure equation (Equation (88)) to the shock phenomena under consideration. Since, as previously discussed, the potential used might be unrealistic (if convenient), its use is considered a (possibly very significant) weakness of the theory. The structure equation, although adequate for metals, may or may not be theoretically sound for liquids. Whether this represents a significant weakness in the theory is therefore dependent on the success in justifying this relation by methods such as those presented in Appendix L.

When dealing with gases the dwell time of the molecules in the transition region may be evaluated as follows: Zel'dovich and Raizer[12] give the approximate expression:

$$z_f \cong \ell_o \frac{m}{m^2-1} \tag{207}$$

*Although Equation (108) exists for $n = 3$, $\sigma \to \infty$, $\varepsilon = 0$ from Equations (106) and (107). Further, when $0 \leq n < 3$ the latter equations contain roots of negative numbers.

where ℓ_o is the mean-free path length at initial conditions and:

$$\mathcal{M} \equiv U/C_o = \text{Mach number} \tag{208}$$

The appropriate velocity differential can be shown to be*:

$$U - \frac{1}{2}\mu \tilde{=} \frac{1}{2}U = \frac{1}{2}\mathcal{M}C_o \tag{209}$$

and from Equation (187):

$$t_r = \frac{\ell_o}{C_o}\left(\frac{2}{\mathcal{M}^2-1}\right) \tag{210}$$

For moderate to strong shocks ($\mathcal{M}$ = 2 to 10) in gases originally at

---

*Generally:

$$U - \frac{1}{2}\mu = \frac{1}{2}(2U-\mu) = \frac{1}{2}(U+U-\mu)$$

For gases[88]:

$$U-\mu = U\left(\frac{\gamma-1}{\gamma+1}\right), \quad \gamma = \text{ratio of specific heats}$$

and therefore:

$$U - \frac{1}{2}\mu = U\left(\frac{\gamma}{\gamma+1}\right)$$

For γ = 1.1 to 1.6, $\gamma/\gamma+1$ = 0.52 to 0.62 or:

$$U - \frac{1}{2}\mu \tilde{=} \frac{1}{2}U$$

(approximately) standard conditions* ($\ell_o \tilde{=} 10^{-5}$cm (5), $C_o \tilde{=} 0.3 \times 10^5$ cm/sec), this gives:

$$t_r = 6 \times 10^{-10} \text{ to } 6 \times 10^{-12} \text{sec} \tag{211}$$

Comparison of these dwell times with typical relaxation times τ for gases and vapors given by Herzfeld and Litovitz[137] (which range from 10^{-7} to 10^{-9}sec) shows that generally $t_r \ll \tau$. It appears then that, even for gases (at approximately standard conditions), the pressure rise runs in advance of the temperature rise for moderate to strong shocks**. Although the shock front widths for gases are $\sim 10^2$-10^3 larger than for liquids, the corresponding relaxation times are $\sim 10^2$-10^3 longer. The net effect is that, in both cases the relaxation times exceed the residence times. This result does not (in itself) imply that the theory can be applied to gases. It does show, however, that one of the major assumptions of the theory (apparently) applies as well to gases as to condensed media.

To further demonstrate the applicability of the theory to gases would require justification of the structure relation, Equation (88).

---

*Since $\ell_o \propto 1/\rho_o$ (5) and $C_o \propto P_o^{1/2} \rho_o^{-1/2}$, the ratio $\ell_o/C_o \propto (P_o\rho_o)^{-1/2}$. Thus even if $P_o\rho_o$ decreases by a factor of 100, ℓ_o/C_o only increases by a factor of 10.

**It is assumed that in the Mach number range of interest there are no radiation effects.

There is no obvious way to do this* and the question remains moot. On the other hand, it is instructive to assume that Equation (88) is valid and determine n_L, the number of layers in the transition region. Since $\rho_{o_{liquid}}/\rho_{o_{gas}} \tilde{=} 350$ (137), $z_{o_{gas}} \tilde{=} 7\, z_{o_{liquid}}$ from Equation (88). Noting Equations (186) and (207):

$$n_L = \frac{\ell_o}{7 z_{o_{liquid}}} \left(\frac{m}{m^2-1}\right) \tag{212}$$

From the data in Appendix S (for z_o) and the prior value of ℓ_o:

$$n_L = 40\left(\frac{m}{m^2-1}\right) \tag{213}$$

For $m = 2$ to 10, n_L goes from 25 to 4. Therefore, depending on Mach number, the number of molecular layers in the transition region for gases is from 1/2 to 5 times that for liquids. The criterion of "sufficient thinness" would, in some cases, apparently be satisfied! The flaw in the argument is that the absolute distances involved are much larger for gases than for liquids. Since, generally $z_{o_{liquid}} \tilde{=} 3.6\text{Å}$ (Appendix S) $z_{o_{gas}} \tilde{=} 7\, z_{o_{liquid}} \tilde{=} 25\text{Å}$; the average distance between layers for gases is equal to the entire front width in liquids**. At

---

*Except, perhaps, by the methods described in Appendix L where an interesting structure relation for perfect gases is derived.

**That is, the distance between layers in a gas is as large as the maximum range of the integrated effect of the entire compressed region on a given molecule, in liquids.

these ranges the potential $\phi(r)$, which functionally depends only on r, will be relatively weak* and it would be expected that effective interactions for any given layer would only take place with immediately adjacent layers. In this case a key approximation (Equation (41)) in the development of the energy equation (Equation (48)) fails and the remaining developments are invalid. It is for this reason (and the applicability of the structure equation) that the model is not applicable to gases**.

From the above discussions it is concluded that the theory is probably adequate for condensed media only, but that even so, a final judgment in the matter should await the results of further investigations of the accuracy of key assumptions (e.g., shock front thickness) and relationships (e.g., pair-potential and structure equation) used in the theoretical development.

---

*For N_2 with $\varepsilon/k = 98.8^{\circ}K$, $|\phi(25\text{Å})/k| \tilde{=} 0.02^{\circ}K$. For C_6H_6 with $\varepsilon/k = 421.9^{\circ}K$, $|\phi(25\text{Å})/k| = 0.63^{\circ}K$.

**It is of course possible that the approach to structure in Appendix L will provide the appropriate $z_o - \rho_o$ relation and that the error in Equation (41) can be accounted for. In this case the theory might be applied to gases also.

3. Recommendations

Based on all prior developments, the following are recommended (generally without comment) for further study and investigation of the theory. The significance of each has been previously discussed.

(a) If the shock model is accurate it should be possible to work "backward" through the theory and predict the pair potential from a set of (accurate) shock data for a given material. To assure that no other assumptions/approximations of the theory would affect the accuracy of this test the substance chosen should (ideally) be condensed, preferably solid (of known structure*), monatomic (for radial symmetry of the molecule (atom) and applicability of the central force assumption**) and have a known or calculable radial distribution function.

Such a test of the model has recently become possible with the publication of reasonably accurate shock data for solid argon[139]. As all of the above requirements are met for this substance (i.e., $s = 1$, radial symmetry, etc.) the test would be particularly meaningful.

Working "backward" in the theory might be accomplished as follows. Consider Equation (48) (the energy equation) and eliminate ΔE using Equation (20) and the configurational energy terms using Equations (51) and (52). This gives:

---

*This would eliminate any errors in Equation (88), the generalized structure relation.

**That is, forces between molecules act from the geometric center of the molecules. This has been implicitly assumed in all prior developments, but there is evidence[54] that for some (fairly complicated) molecules it may not be valid.

$$\mu^2 = 2\left(\frac{N}{M}\right)^2\left[\rho\int_{z'=z}^{\infty}\int_{y'=0}^{\infty}\int_{x'=0}^{\infty} g(r,\rho,T)\phi(r)dx'dy'dz' - \rho_o\int_{z'=z_o}^{\infty}\int_{y'=0}^{\infty}\int_{x'=0}^{\infty} g(r,\rho_o,T_o)\phi(r)dx'dy'dz'\right] \quad (214)$$

From Equations (J9) and (J10) in Appendix J these integrals may be partially evaluated and the result substituted into Equation (214) to give:

$$\mu^2 = 4\pi\left(\frac{N}{M}\right)^2\left\{\rho\int_{z'=z}^{\infty}\left[\int_{r=z'}^{\infty} g(r,\rho,T)\phi(r)rdr\right]dz' - \rho_o\int_{z'=z_o}^{\infty}\left[\int_{r=z'}^{\infty} g(r,\rho_o,T_o)\phi(r)rdr\right]dz'\right\} \quad (215)$$

Noting that the second term is a definite integral (there are no functional terms) and thus a constant, Equation (215) may be written:

$$\frac{\mu^2}{\rho} = 4\pi\left(\frac{N}{M}\right)^2\left\{\int_{z'=z}^{\infty}\left[\int_{r=z'}^{\infty} g(r,\rho,T)\phi(r)rdr\right]dz' - \frac{\rho_o}{\rho} I_o\right\} \quad (216)$$

where:

$$I_o = \int_{z'=z_o}^{\infty}\left[\int_{r=z'}^{\infty} g(r,\rho_o,T_o)\phi(r)rdr\right]dz' \quad (217)$$

From the linear compression assumption, Equation (92) ($z/z_o = \rho_o/\rho$), this becomes:

$$\frac{\mu^2}{\rho} = 4\pi\left(\frac{N}{M}\right)^2\left\{\int_{z'=z}^{\infty}\left[\int_{r=z'}^{\infty} g(r,\rho,T)\phi(r)rdr\right]dz' - z\frac{I_o}{z_o}\right\} \quad (218)$$

and differentiation with respect to z gives:

$$\frac{d(\frac{\mu^2}{\rho})}{dz} = 4\pi(\frac{N}{M})^2\left\{\frac{d}{dz}\int_{z'=z}^{\infty}\left[\int_{r=z'}^{\infty} g(r,\rho,T)\phi(r)rdr\right]dz' - \frac{I_o}{z_o}\right\} \tag{219}$$

From the general equation for differentiating improper integrals[15]:

$$\frac{d}{dz}\int_{z'=z}^{\infty}\left[\int_{r=z'}^{\infty} g(r,\rho,T)\phi(r)rdr\right]dz' = -\int_{r=z}^{\infty} g(r,\rho,T)\phi(r)rdr \tag{220}$$

and Equation (219) becomes:

$$\frac{d(\frac{\mu^2}{\rho})}{dz} = 4\pi(\frac{N}{M})^2\left\{-\int_{r=z}^{\infty} g(r,\rho,T)\phi(r)rdr - \frac{I_o}{z_o}\right\} \tag{221}$$

Differentiating again gives:

$$\frac{d^2(\frac{\mu^2}{\rho})}{dz^2} = 4\pi(\frac{N}{M})^2\, g(z,\rho,T)\phi(z)z \tag{222}$$

which may be written:

$$\phi(z) = (\frac{M}{N})^2 \frac{1}{4\pi\, zg(z,\rho,T)} \frac{d^2(\frac{\mu^2}{\rho})}{dz^2} \tag{223}$$

Since: $$z = z_o\rho_o/\rho \tag{92}$$

and: $$z_o = (M/2^s\, \rho_o N)^{1/3} \tag{88}$$

it is possible to generate $\phi(z)$ vs. z points from the shock data (U-μ converted to μ-ρ using Equation (14)) if $g(z,\rho,T)$ is known or calculable*. Of course, since the distance at which the potential (or radial distribution function) is evaluated is z it may be replaced with r. Whether the raw data are sufficiently accurate to give an accurate value of the second derivative in Equation (223) remains to be determined.

*As is the case for solid argon, since it is known to have an fcc lattice.

Since shock data generally represent strongly compressive states, the resultant $\phi(r)$ vs. r points may be restricted to the strongly repulsive region far from the potential well. An estimate of σ and ε from the data might then not be possible. The only means of testing the theory would be to compare the results obtained to measurements of $\phi(r)$ from an independent source (e.g., molecular beam experiments, etc.).

(b) Continue the investigation of shock wave thickness.

Use the results in Table 14 for σ, ε and n and obtain more exact values of z_f for liquids.

Substitute Equations (106) and (107) (used in the SF solution) into Equation (185) and obtain values of z_f for metals.

Reconsider the definition of z_f implicit in Equations (182) and (183) and try to determine each of $\psi(\rho_o,z_o)$, $\psi(\rho',z')$* and $\psi(\rho,z_f)$ as the (shaded) molecule approaches the compressed region. Use the failure of Equation (180) (which implies failure of Equations (173) and (172) and thus of Equation (38)) to define z_f.

(c) Consider other pair potential functions in the development of the theory in place of the n-6 potential (Equation (72)) used in this study.

For liquids use the "Quantum-Mechanical" potential (No. 24 in Table 1):

---

*In this case the integrations in Appendix J would be carried out over finite limits (z_o to z_f) and ρ' would be approximated by (say) $(\rho_o+\rho)/2$.

$$\phi(r) = P(r)\ e^{-\alpha r} + \sum_{i=0}^{\infty} a_i r^{-i} \qquad (224)$$

where $P(r)$ = polynomial in positive and negative powers of r . Consider initially*:

$$P(r) = a/r^n \qquad (225)$$

$$a_6 = -b\ , \quad a_i = 0 \quad \text{for all} \quad i \neq 6 \qquad (226)$$

to give:

$$\phi(r) = a\frac{e^{-\alpha r}}{r^n} - \frac{b}{r^6} \qquad (227)$$

which is a four-parameter potential (a, b, n, α). Since this is one more than in the n-6 potential used in the current study, extrapolation of the (resultant) Hugoniot to U_o might, in this case, be used to relate the parameter of least physical significance to (one or more of) the other three. This would eliminate the difficulty of the subsidiary "condition" previously discussed that (perhaps unrealistically) relates system parameters.

For metals use No. 22 in Table 1:

$$\phi(r) = ar^{-n} + br^{-3}\ e^{-\alpha r} \cos \beta r \qquad (228)$$

---

*The simpler case of $P(r) = a$, which leads to the "Exponential-6" or "Modified Buckingham" potential, is considered undesirable because of the spurious maximum at $r = r_1$ (see No. 13 in Table 1). The form chosen (Equation (225)) should eliminate this difficulty.

and determine if the attempt to account for LRO behavior in the second term has a significant effect on the resultant values of n. Although this is a five parameter potential (a, b, n, α, β), the U_o extrapolation should eliminate one of them, and another, β, is known from[17]:

$$\beta = 2k_f = 2(3\pi^2 Z \rho_o N/M)^{1/3} \tag{229}$$

where k_f is the radius of the "Fermi sphere" and Z is chemical valence.

(d) In order to utilize Equation (88) for liquids, it is necessary to determine s, the structure factor. In the current study this was done for liquids by simply assuming $s = 1$ (an fcc lattice). Such an assumption is generally unsatisfactory, since there is no a priori reason why liquids should (macroscopically) be structured exactly as an fcc lattice or why, furthermore, this would be true for all liquids.

The essential features of the structural properties of liquids are contained in the PDF. It would be useful if s could be correlated with this empirically determined function. In Appendix L, in the probability approach to nearest neighbor distance, it was shown that $\bar{r}$ in Equation (L9) depends solely on $g(r)$ (the PDF) and that it might be approximately equal to a_o, the nearest neighbor distance. Also in Note 5 of Appendix L, the use of a_o as a measure of liquid structure was developed in terms of a correlation of $a_o(\rho_o N/M)^{1/3}$ with first coordination numbers N_1. The correlation was developed from and is consistent with the known values of

$a_o(\rho_o\ N/M)^{1/3}$ and N_1 for fcc, bcc, sc (simple cubic) and diamond lattices. The next step in the determination of s (from the PDF) would be to correlate z_o with N_1, or a_o directly, for various lattices. This would give the desired correlation in either of the alternate forms:

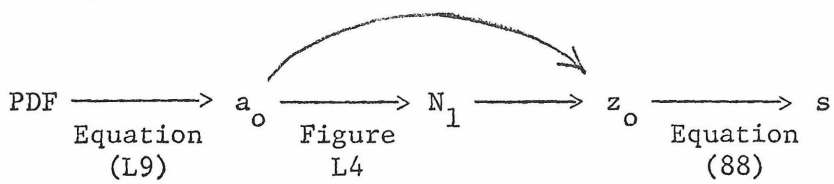

(230)

It is recommended that the possibility of developing these correlations be investigated. One known pitfall should be considered in doing this. Examination of Figure 10 indicates that $a_o(\rho_o\ N/M)^{1/3}$ and $z_o(\rho_o\ N/M)^{1/3}$ are both decreasing with the indicated sequence of lattice types. In addition N_1 decreases for the same sequence (see Table L1). The results for sc lattices appear to contradict the correlation. In this case $a_o(\rho_o\ N/M)^{1/3} = 1.0$, $N_1 = 6$ and sc should fall between bcc and diamond; on the other hand it appears that $z_o(\rho_o\ N/M)^{1/3}$ is not in the corresponding interval 0.500 to 0.630 (see Figure 10)*. Of course, monotonicity of this kind is not necessary to establish a correlation but an explanation of this deviation and an examination of other structure types would be required to justify the correlation.

(e) In conjunction with the above, continue the investigation of the "snapshot" and "probability" approaches to the nearest neighbor

---

*The definition of z_o for sc lattices is open to some interpretation; values of $z_o(\rho_o\ N/M)^{1/3}$ of from (at least) 0.707 to 1.000 are possible. The range of results is, however, still not in the desired interval.

distance concept.

In the former case consider a computerized routine for determination of:

$$\overline{(\overline{a_o})} = \frac{1}{k}\sum_{i=1}^{k}(\overline{a_o})_{t_i} = \frac{1}{k}\sum_{i=1}^{k}\sum_{j=1}^{m_i} a_{ji}/m_i \qquad (231)$$

where m_i is the number of space sectors required to make $(\overline{a_o})_{t_i}$ essentially constant and k is the number of repetitions of the process (i.e., time intervals) necessary to make $\overline{(\overline{a_o})}$ essentially constant. Two-dimensional data might be generated by photographing spheres in a shallow, "jiggling" box or by purely mathematical (e.g., random walk) techniques. Three-dimensional data might be generated by (physical) models such as those used by Bernal[80] or by mathematical methods.

For the "probability" approach a direct application of theory is possible using the PDF data of Mikolaj and Pings[138] for argon. For each thermodynamic state, ρ_o and $g(r)$ can be used in Equation (L9) to determine $\overline{r}$. The result might be compared to the equivalent value of a_o computed from Equation (81), which assumes an fcc lattice. Similar calculations can be made for any substance for which $g(r)$ is available.

It is also recommended that the adequacy and development of the "probability" approach itself be further investigated for potential value in developing a quantitative measure of liquid structure.

(f) The assumption that the effect of $g(r)$ on the integrations in Equations (51) and (52) is small and/or will cancel in

Equation (48) can be checked using the (same) $g(r)$ data of Mikolaj and Pings[138] for argon. It is recommended that this be done using the n-6 potential to determine if Equations (78) and (79) and/or Equation (80) are justified.

It is further recommended that the same determination be made for one or more metals for which LRO behavior is known to occur and for which $g(r)$ is available.

(g) Complete the method for computing temperatures along the Hugoniot in Appendix E by developing the required two-dimensional counterparts of Equation (50) for evaluation of $\psi^{L_e}(z_e)$ and $\psi^{L_o}(z_o)$. Compute and compare temperatures using this method to calculations using current methods[105,85] for several substances.

B. APPLICATION OF THEORY

1. Data

The (raw) shock data considered for use in this study are compiled in Appendix S, plotted in Figures 15-27 and summarized in Table 23 which outlines the motivation and results of the (previously mentioned) selection process.

Considering the wide range of substances and initial conditions* and the number of different sources of data (20)**, the quality of the data, as judged by the scatter*** (column 5 in Table 23), is considered typical of shock experiments. The overall average scatter is $\sim$ 3.8%.

It may be noted that this figure does not compare with the relatively low error reported for individual velocity measurements (0.5-3%, see Table 5). This indicates that the observed data variations are caused by inaccuracies in the test set-up, sample (state) variations, etc., rather than by imprecision in the measurements. This would imply that, in order to judge data quality in each case, an analysis of the source and magnitude of these types of error in each of the referenced studies (based on the details of the particular

---

*13 liquids, 10 fcc metals, 13 bcc metals (columns 1 and 2 in Table 23); M from 2(H_2) to 207 (Pb) g/mole, ρ_o from 0.07 (H_2) to 21 (Pt) g/cc, T_o from 20 (H_2) to 306 (CS_2) ^oK, C_o from 0.04 (A-III) to 0.52 (Al) $\times 10^6$cm/sec.

**Including the compendium, References 96 and 98.

***Mean maximum variation in U for a given value of μ <u>not</u> including regions where a transition is indicated.

Table 23

SUMMARY OF DATA SELECTION

Column No.	1	2	3	4	5	6	7	8	9	10	11	12	13
	Code*	Substance	Number of Points	Number of Sources	Scatter %	Comments	Transition	Comments	C_o data	Altered Data	Number of Points	Scatter %	Remarks
	L1	A	19	1	5.9	-	No	-	O.K.	None	-	-	
	L2	A-II	6	1	0.5	-	No	-	O.K.	None	-	-	
	L3	A-III	5	1	6.7	-	No	-	O.K.	None	-	-	
	L4	A-IV	2	1	-	-	No	-	O.K.	None	-	-	
	L5	Hg	3	1	-	-	No	-	O.K.	None	-	-	
	L6	N_2	14	2	8.2	-	Yes	"break" in data	O.K.	Eliminated data $U > 0.5\times10^6$	9	8.2	
	L7	H_2	1	1	-	-	-	-	O.K.	None	-	-	
	L8	CS_2	6	2	0.0	-	Yes	"break" in data, two-wave structure(109)	O.K.	Eliminated data $U > 0.3\times10^6$	4	0.0	
	L9	CCl_4	14	3	6.4	"Poor"data(100)	No	-	O.K.	None	-	-	**
	L10	CH_3OH	5	2	2.9	-	No	-	O.K.	None	-	-	
	L11	C_2H_5OH	5	2	2.3	-	No	-	O.K.	None	-	-	
	L12	$(C_2H_5)_2O$	11	2	5.5	-	No	-	O.K.	None	-	-	
	L13	C_6H_{14}	4	2	5.5	-	No	-	O.K.	None	-	-	
	L14	C_6H_6	19	3	5.7	-	Yes	Two-wave structure (109)	O.K.	None	-	-	Transition above data
	L15	$C_6H_5CH_3$	2	1	-	-	No	-	O.K.	None	-	-	
	L16	H_2O	52	5	9.1	"Poor"data(96)	Yes	"break"in data	O.K.	Eliminated data $U > 0.5\times10^6$	23	4.7	
	F1	Cu	98	10	7.2	"Poor"data(96)	No	-	O.K.	None	-	-	**,***
	F2	Ag	14	3	1.9	-	No	-	O.K.	None	-	-	
	F3	Au	12	3	1.6	-	No	-	O.K.	None	-	-	
	F4	Co	16	2	1.6	-	No	-	O.K.	None	-	-	
	F5	Ni	63	4	12.6	"Poor"data(96)	No	-	O.K.	Eliminated Ref.96 data	16	2.2	
	F6	Pd	17	3	3.5	-	No	-	O.K.	None	-	-	

Table 23 (continued)

Column No.	1	2	3	4	5	6	7	8	9	10	11	12	13
	Code*	Substance	Number of Points	Number of Sources	Scatter %	Comments	Transition	Comments	C_o data	Altered Data	Number of Points	Scatter %	Remarks
	F7	Pt	15	2	2.2	-	No	-	O.K.	None	-	-	
	F8	Al	40	5	8.3	"Poor" data (96)	No	-	O.K.	Eliminated Ref.96 data	29	4.1	
	F9	Ca	10	2	5.5	-	No	-	O.K.	None	-	-	
	F10	Pb	37	8	3.6	-	No	-	O.K.	None	-	-	
	B1	Li	29	3	4.8	-	Yes	"break" in data	O.K.	Eliminated data $U>0.95\times10^6$	17	4.8	
	B2	Na	25	2	0.6	-	Yes	"break" in data	O.K.	Eliminated data $U > 0.7\times10^6$	18	0.6	
	B3	K	23	2	1.9	-	Yes	"break" in data	O.K.	Eliminated data $U > 0.6\times10^6$	17	1.9	
	B4	Rb	10	1	0.0	-	Yes	"break" in data	O.K.	Eliminated data $U > 0.5\times10^6$	5	0.0	
	B5	Cs	9	1	0.8	-	No	-	C_o high?	None	-	-	Low U transition?
	B6	V	14	1	1.5	-	No	-	C_o high?	None	-	-	Low U transition?
	B7	Nb	14	2	1.1	-	No	-	O.K.	None	-	-	
	B8	Ta	16	3	4.9	-	Yes	"break" in data	O.K.	Eliminated $U>0.63\times10^6$	14	4.9	
	B9	Cr	13	2	2.2	-	No	-	O.K.	None	-	-	
	B10	Mo	18	4	5.7	"Poor" data (96)	No	-	O.K.	None	-	-	**,***
	B11	W	9	1	1.3	-	No	-	O.K.	None	-	-	
	B12	Zr	14	2	0.7	-	Yes	"break" in data	O.K.	Eliminated $U > 0.5\times10^6$	5	0.7	
	B13	Ba	4	1	0.0	-	No	-	C_o high?	None	-	-	Low U transition?

*L = liquid , F = fcc metal , B = bcc metal

**Alterations not justified based on comparative numerical results with and without questionable data.

***Further investigation warranted.

methods employed) would have to be performed. This was considered impractical* well beyond the scope of the current study. Instead it was concluded that the data should be considered "as is" and that statistical self-consistency and agreement with other investigators would be sufficient measures of raw data quality.

An examination of individual substances in Table 23 shows that a considerable range in scatter** (i.e., data quality) exists***; from essentially nil**** to > 7%*****. In the latter cases (N_2, H_2O, Cu, Ni and Al) alteration of the data was considered.

The large value of scatter for N_2 (Figure 16) was due to a single data point and, since overall consistency and agreement between sources was generally maintained, no alterations (due to scatter) were made in this case. For each of H_2O, Cu, Ni and Al (Figures 20-23) a

---

*Does the author describe his technique and procedures in detail?, etc.

**Between and (sometimes) within, data sources.

***The observation that the average scatter for liquids (∿ 4.9%) is siderably greater than that for metals (∿ 3.2%) is not considered significant. This is expected because of the greater handling difficulties in carrying out the shock experiments and the higher precision required to maintain constant initial conditions from test to test.

****∿ 0.1%; CS_2, Rb and Ba.

*****In some cases (A-IV, Hg, N_2, $C_6H_5CH_3$) no judgment was made because of a paucity of data (1-3 points).

set of "poor" data was identified*. However, only for the latter two were the data in question eliminated (see Columns 6 and 10 in Table 23). For Cu this was found not be be numerically justified; for H_2O the questionable data were too close to a presumed transition to consider the effects separately.

For both CCl_4 and Mo (Figures 17 and 26), "poor" data were identified even though the scatter in these cases was "reasonable (6.4 and 5.7% respectively). In both cases it was shown that alterations to the data were not numerically justified (see Table 23).

It was concluded that, based on scatter alone, only alterations in the Ni and Al data were justified but that in these cases a considerable improvement resulted (see columns 11 and 12 in Table 23).

In Appendix T it was shown that if a phase transition occurs at a certain shock state the model will, in general, only be valid for weaker shock states. Because of this and the large number of reported transitions (Table 6) the data were carefully scrutinized for evidence of this type of behavior. On the other hand, recognizing that the only actual (experimental) evidence of a transition is the formation of a two-wave structure** (see Appendix T), and that this was reported only for C_6H_6 and CS_2[109] (Table 6), the reported transitions were not accepted without further evidence. In this study, "further evidence" was a clear "break" in the plotted U-μ data.

---

*Although all are from Reference 96 (the compendium) two separate sources are involved.

**Opacity measurements (observations)[90,110] have also been cited[110] as evidence of (fusion) transitions but there is some doubt[90] about the interpretation of the phenomenon.

Following Table 6 the transitions suggested[64] for A and A-II based on a two-line fit and curvature of the U-μ relation were considered unwarranted based on the plotted data (Figure 15). For N_2 (Figure 16) the data show a break at essentially the point suggested by a two-line fit[109]. A transition was assumed in this case and data $U > 0.5 \times 10^6$ cm/sec were eliminated (columns 7, 8 and 10 in Table 23). Similar results were obtained with CS_2 [109] (Figure 16) while for CCl_4 the reported transition[109] is above all the data (Figure 19) and no alterations were made.

A careful examination of all the H_2O data (Figure 20), in light of the "poor" data previously identified, indicates that the transition reported[110] might well exist. This was assumed to be the case in the current study and data $U > 0.5 \times 10^6$ cm/sec were eliminated.

Despite the transitions suggested[104,111,106,104,85] for Cu, Ni, Al, Ca and Pb (Table 6) no evidence for these, or any of the fcc metals (Figures 21-23) was found in the plotted data. None of the data were altered in these cases.

For the alkali metals melting transitions at low pressure are predicted for Li, Na, K and Rb [93], while electronic transitions[107] and perhaps another (unknown*) type[93] are suggested for each of Rb and Cs (Table 6). Breaks in the data do occur (for all but Cs; Figure 24) but generally at pressures considerably above those calculated for the melting transitions. Because of this the latter were ignored in altering the data (Table 23). On the other hand it is interesting that

---

*Based on static test results. Of course these may be the electronic transitions in Reference 107.

for Rb the "other" transition (whether electronic or otherwise) appears to occur at the "break". Similar behavior for Cs suggests that the transition indicated below the data (Figure 24) might be real. Such an instance would generally preclude application of the theory although no (real, experimental) knowledge of the transition existed. This could unwittingly lead to serious errors in judging the validity of the shock model. However, if a transition does not exist, the plotted data should extrapolate, in a smooth way, to (or near) C_o, the sound velocity. As this is not the case for Cs, the existence of the transition is inferred*. This tentative conclusion and one of the alternatives are indicated in columns 13 and 9 of Table 23. The observation generally suggests a means of avoiding the inherent difficulty with low pressure transitions; if the data extrapolate to C_o the transition does not exist, but if not the transition might occur. Although such an inferred conclusion would be weak, at best, the observation would at least suggest caution in applying the theory to the particular set of data. For Cs the results obtained were viewed in this regard.

For V (Figure 25) behavior similar to Cs is observed, although no transitions are reported in the literature. It is suspected that

---

*Two alternative interpretations suggest themselves. The C_o value is too high and/or the Hugoniot curve has a decreasing slope as $\mu \to 0$ and a "smooth" curve should be drawn "the other way". The first case is unjustified[93,96], while the second is generally not true although there may be some exceptions[14].

in this case the value of C_o is simply too high* (see columns 9 and 13 of Table 23). The data for Nb do not suggest a transition and none is reported. However, for Ta a "break" in the data is observed (Figure 25) and the data were appropriately altered (column 10, Table 23). For Cr, Mo and W no transitions are reported (Table 6) or suggested by the data (Figure 26).

For Zr a definite "break" is seen in the data (Figure 27) close to a reported transition[96]. It was assumed that the transition exists in this case and the data were altered as in Table 23.

The case for Ba is similar to that for Cs; the data do not extrapolate to C_o** (Figure 27) and a transition below the data is reported (Table 6). With the same reservations (i.e., the U-μ curve has a decreasing slope as $\mu \to 0$) the same conclusion was drawn (i.e., a transition is inferred and the application of the theory is viewed with caution).

Column 10 of Table 23 describes, in each case, the action taken*** in altering the data as a result of the selection process. For the substances involved, the remaining number of points (i.e., the

---

*For some materials (including V) C_o was determined solely from Bridgman's static data[14,96] which appears to give values that are (generally) $\sim$5% higher than other sources. A downward correction of approximately this amount would correct the noted discrepancy (Figure 25).

**For Ba, C_o was <u>not</u> determined from Bridgman's data and the 5% reduction (as for V) would not apply. Further the extrapolated value is considerably less than 0.95 C_o (see Figure 27).

***Overall, 135 of 688 data points were eliminated; $\sim$20% of the original set.

adjusted data) and associated scatter* are shown in columns 11 and 12. For these and the unadjusted data, the overall average scatter dropped to 3.2%.

The adjusted data sets and associated initial parameters are listed in Appendix S on the page following the original data for each substance affected. All subsequent analyses and plots (i.e., Figures 29-41) used these adjusted data.

---

*Since regions with (suspected) transitions were not originally included in the scatter, these values only change when "poor" data were eliminated (see column 12).

2. Liquids

In applying the theory to liquids only the WF and MF forms of the Hugoniot were considered. This was done to take advantage of the "realistic" σ,ε data available.

a. Preliminary conclusions. Several alternate schemes for determining the applicability of the theory to (the available shock data for) liquids were considered. To decide among them, various calculations were performed (see Part III. APPLICATION OF THEORY) and from the results the following set of preliminary conclusions were reached.

A single value of n will not simultaneously satisfy strong repulsion (i.e., the shock data), σ,ε and long-range attraction (i.e., C_{ab}).

The σ,ε parameter pair is preferred over the others because such data are available and the prior limitation will be minimized*.

The above conclusions are not affected if additional attractive terms are considered in the potential (Appendix V).

---

* The shock data are all compressive and thus in the repulsive region of the potential. The parameters σ and ε are on the repulsive "side" of the potential.

Chapman's correlation of ε with T_M, although numerically incorrect, was concluded to be sufficiently founded (physically) to warrant application* to all the liquids. The (simple) correlation developed was:

$$\varepsilon/k = 1.5\ T_M + 4\ ,\ ^oK \qquad (134)$$

A spurious root in the μ^2 vs. x relation (Equation (135)) near the ($\mu = 0$, $x = 1$) origin, was shown to exist for all liquids except Hg and $C_6H_5CH_3$** (Appendix Y). When $x = X_R$ (the value at the root) $\mu^2 = 0$, $\mu = 0$, and $U_o = 0$. For $1 \leq x < X_R$, $\mu^2 < 0$ and μ is imaginary (not defined). It was concluded that the μ^2 vs. x (and U vs. μ) relation should be "cut-off" for $x \leq \sim X_R$.

The computer programs developed in this study were concluded to be adequate since the results in Reference 16 were (essentially) reproduced when common values of σ and ε were used (Table 11).

Only the 1PF will provide a critical test of the theory; the 2PF's and 3PF have too many adjustable parameters and a single "best" value of n cannot be identified. The 2PF's were occasionally useful in supporting 1PF results. The 3PF was used only to determine f for the 1PF.

---

*The uncorrelated values were also considered.

**For Hg this occurred for both the original and correlated values of ε while for $C_6H_5CH_3$ the spurious root is absent only for the correlated value of ε.

The WF solution is preferred to the MF solution because the prediction of C_o is better in this instance (Table 12). It was concluded that the error in not satisfying the associated "condition" (Equation (105)) is a limitation of the model and/or potential.

An analysis of the effect of the uncertainty in the μ_i-x_i data, σ and ε on ε' and f (the measures of the fit) showed that increments < 0.1 in n were not meaningful.

The U-μ plots showed that as $\mu \to 0$, either $U \to 0$ (when $X_R > 1$) or $U \to +\infty$ (when there is no spurious root). This behavior was concluded to be a consequence of the theoretical instability of the WF solution and, in the latter case, the numerical instability in the computation of U.

b. Argon. The results of application of the theory to argon is of especial interest because many of the (implicit and/or explicit) assumptions of the model are satisfied (e.g., it is monatomic and thus spherically symmetric, etc.) and the pair potential (i.e., σ and ε) is presumably well known. Therefore, if the theory is valid it should give meaningful results for argon*.

Argon is of further interest because there are shock data at four different initial states** (Appendix S) and, as stated previously, if the theory is valid it should give the same value of n for any

---

*This may be restated in the negative as: If the theory doesn't work for argon, it probably is not valid.

**Argon is the only material for which shock data at various initial states were available.

initial state for the same material*. The Hugoniot in Equation (135) clearly accounts for state variations through the single thermodynamic parameter ρ_o. The theory can thus be meaningfully tested by determining if, for a given set σ, ε and n, Equation (135) reproduces the Hugoniot for various initial states (i.e., values of ρ_o) or, alternatively, by determining if the values of n that "best" fit given shock (Hugoniot) data for several initial states are (essentially) the same.

This was, in effect, done when the WF solution was applied to all the liquids; the (1PF) results for A, A-II, A-III and A-IV appear as the first four entries in Table 14. For the C (correlated) results** the values of n that "best" fit the data are, respectively, 9.3, 8.9, 9.4 and 8.8***.

Considering the scatter in the data and the paucity of points for A-IV (see Table 23) the agreement between values**** is striking; the maximum percent difference is $\sim$ 7%! From this result (alone) it was concluded that the shock model might well be fundamentally sound and that perhaps the theory is limited mainly by the accuracy of the potential function and the structure relation.

---

*Since the "true" pair potential is state independent[71], the molecular parameters σ, ε and n (ideally) depend only on molecular constitution; they are fixed constants for a given substance.

**Later shown to be preferable to the L (literature, i.e., uncorrelated) results.

***The first two values are somewhat higher than the corresponding ones found in the prior study[16] (see Table 11) primarily because of the smaller value of σ used in the current work.

****Of course, each determination was independent of the others.

Assuming the differences in n to be statistical, a common value of n is desired*. This was found by weighting the above values by the number of points in each state (Table 15). The resultant value was 9.2.

Comparison of the values of ε' and f in Tables 14 and 15 indicate that, except for A a nontrivial reduction in the quality of the fit has resulted. However, examination of Figures 29 and 30 shows that they are, nevertheless, quite reasonable. It was concluded that the best (single) value of n for argon is 9.2 and that the theory adequately fits all the data**.

Except for A the prediction of C_o in both Tables 14 and 15 is poor. Correspondingly the values of X_R and RE in these cases are relatively high although for RE this is also true for A. Although the possibility exists that these results can be accounted for by a low pressure transition and/or poor C_o data it was felt that this was not the case. Instead it was concluded that the WF solution does not always adequately predict (i.e., Equation (104)) C_o whether the associated "condition" (i.e., Equation (105)) is satisfied closely or not. The excellent agreement of U_o and C_o for A (within 5%) must be considered somewhat fortuitous.

---

*The resultant values of ε' and f can be compared to the "best" values in Table 14 to see if the common value materially affects the quality of the fit.

**The recently published shock data for solid argon[139] (ρ_o=1.75g/cc) suggest a test of the common value of n determined in this study. Preliminary calculations show that, with $n = 9.2$, $\sigma = 3.28$Å, $\varepsilon/k = 129.9^oK$ (see Table 15), the theory very closely fits the data!

c. Other liquids. The results of application of the 1PF, WF solution to all the liquids included in this study (see Table 4) is shown in Table 14 for both the (L) uncorrelated (i.e., literature) and (C) correlated (i.e., Equation (134)) values of ε. Because the U_o predictions for the C results were generally closer to C_o, they were preferred over the L results. However, considering the prior discussion of the adequacy of the WF solution in predicting C_o and the fact that the U_o for the C results were generally 20% higher than C_o, this choice is considered a convenience only. There is no substantial (e.g., physical) justification for considering one set "superior" to the other*.

The values of ε' and f in Table 14 indicate generally excellent fits as seen in Figures 31-34 and discussed in the following paragraphs.

Monatomics - Hg Because there are only three data points for mercury (the other monatomic liquid besides argon), and there is essentially no scatter in them, the values of L (cm^4/sec^4) and thus ε' in Table 14 (for the C results) are very small. The corresponding fit for n = 11.7 in Figure 31 is excellent. Because L is so small there are several values of n that will also give excellent fits and acceptable (although larger) values of ε'. Therefore the "best"

---

*Although the quality of the fits, as measured by ε' and f, is about the same for the L and C results, a slight (average) improvement is noted for the latter set; $\overline{\varepsilon}'$ decreases from 0.13 to 0.12, f increases from 0.71 to 0.74 and $\overline{X}_R$ decreases from 1.18 to 1.15 for the liquids (excluding argon) in Table 14.

value ($n = 11.7$*) may be somewhat ambiguous. Because of this and the fact that small errors in any of the three data points will have a relatively large effect on the choice of n, it was concluded that more shock data are needed before n for Hg can be fixed with certainty.

It is noted (without comment) that for Hg, U_o and C_o in Table 14 agree within $\sim$ 13% for the given value of n.

Diatomics - N_2, H_2. The fit for nitrogen shown in Figure 31 is quite reasonable considering the scatter in the data**. For $n = 7.0$*** the values of ε' and f in Table 14 are comparable to the results for A. In this case U_o and C_o agree within $\sim$ 14%.

Because there is only one data point for H_2, the resultant fit (with $n = 6.5$)**** in Figure 31 is excellent but no conclusions are drawn. It is noteworthy that in this case X_R is large ($\sim$ 1.6)

---

*This value is larger than the one previously found for the same data[16] (see Table 11) mainly because of the much smaller value of ε/k used in the current work.

**A comparison of r_o (Table 14) and a_o (Appendix S) shows that, strictly speaking, nitrogen does not conform to Equation (82), i.e., $a_o \neq r_o$. However, because the values are within < 1% of each other no physical significance was attached to this observation. The differences are easily within the error in determining a_o and especially r_o.

***This agrees with the value previously determined[16] (Table 11) for N_2 although in the current study more data were utilized.

****This is smaller than the previous value[16] (Table 11) because of the larger value of ε/k used in this study.

and the U_o determination was not meaningful.

Triatomics - CS_2. The results for carbon disulphide are very similar to those for Hg; few data points and an excellent fit (Table 14 and Figure 31). For the same reasons, it was concluded that the "best" value of n (10.6) might be somewhat ambiguous. More shock data in this region (i.e., below the presumed transition; see Table 23) are needed. For CS_2, U_o and C_o agree within $\sim$ 12%.

Tetrahedral - CCl_4. Because of its symmetry, carbon tetrachloride would appear to conform to most of the assumptions of the model and reasonable results were expected. Considering the scatter in the data, the fit in Figure 32 is quite good. For $n = 6.2$*, the values of ε' and f in Table 14 are comparable to those for A and N_2. In this case, however, $U_o > C_o$ by $\sim$ 43%.

A comparison of r_o (Table 14) and a_o (Appendix S) shows that, contrary to Equation (82), $r_o > a_o$. Since the difference is not ascribable to errors in the determination of these parameters, the assumption of an fcc lattice must be called into question for CCl_4 and the above result considered potentially unrealistic**.

Polar - CH_3OH, C_2H_5OH, $(C_2H_5)_2O$. The results for the two alcohols are notably similar, as seen in Figure 32 and Table 14. In both cases $n = 8.0$; ε' and f are comparable and indicate very

---

*This value of n is close to that determined previously[16] (Table 11). The small decrease is due to the increased value of ε/k used in this study.

**Narten, Danford and Levy[54] conclude that the structure of CCl_4 is not of the simple fcc type (interactions between Cl atoms being significant) and that, further, the assumption of central force interactions may not be valid.

good fits. For methyl and ethyl alcohol U_o and C_o agree within ∿1% and ∿10% respectively.

The results for (di-)ethyl ether given in Table 14 and Figure 33 indicate a much poorer fit than for the other liquids; $\varepsilon \tilde{=} 0.44$ (>2 times any other value in Table 14). Because the scatter in the data is not exceptional (see Table 23) it was (tentatively) concluded that the theory fails for this substance*,**. Interestingly, U_o and C_o in this instance agree within ∿ 9%.

Long Chain - C_6H_{14}. The results for hexane are shown in Table 14 and Figure 33. Although there are few data and little variation in them (three of the four points are closely bunched) it appears that the fit for $n = 7.8$ is quite good**. In this case U_o exceeds C_o by ∿ 17%.

Ring Structure - C_6H_6, $C_6H_5CH_3$. Benzene was one of the liquids considered in the previous study[16] and because of its (reasonable) symmetry it should conform to most of the assumptions of

---

*A reconsideration of the data for $(C_2H_5)_2O$ in Figure 18 (and the fit in Figure 33) suggests the possibility of a transition in the region $U > 0.75 \times 10^6$ cm/sec. This could explain the large value of ε found.

**Although $r_o > a_o$ for this substance (Table 14 and Appendix S) this was not considered significant (as in case for N_2), since the difference between these values (<4%) is within the error of their determination.

the model. Indeed, as seen in Figure 33, the fit for $n = 7.1$* is very good. The corresponding values of ε' and f in Table 14 are superior to those for argon, nitrogen and carbon tetrachloride. For benzene U_o is $\sim$ 24% greater than C_o.

Because there are only two data points for toluene, results similar to those for mercury and carbon disulphide were expected; i.e., very small values of L (cm^4/sec^4) and ε' and a correspondingly excellent fit. However, the results in Table 14 and Figure 33 (although indicating a very good fit) clearly do not support this expectation**; the plotted result misses one of the points completely, indicating that the theory does not conform to the data. It was (tentatively) concluded that either the theory fails for this substance, or at least one of the data points represents an extremum in the "normal" variation of shock data. Further examination of Table 14 and Appendix S shows that for $C_6H_5CH_3$, $r_o > a_o$ by a significant amount. This implies failure of the assumption of an fcc lattice and further indicates the (possible) inapplicability of the theory to this substance. On the other hand, these conclusions must be considered preliminary because there are only two data points and the results could (alternatively) stem from the (relatively) high value of σ (compared to C_6H_6) given in Table 7. Pending additional data, the applicability of the theory is considered moot. For toluene U_o exceeds C_o by $\sim$ 30%.

---

*This value is slightly higher than that determined previously(16) because of a small decrease in the value of ε/k used.

**It was also noted that the "best" fit value of n for toluene was unambiguously defined by the data. This was not the case for Hg and CS_2.

Water - H_2O. Because of its unique properties, water was considered separately from the other liquids. The results of application of the theory in Table 14 show that the "error of the fit" ε' is comparable to that for A but that the "figure of merit" f is quite poor (< 1/2 that of A). This is reflected in Figure 34; the fit is poor compared to some of the other substances for which a substantial amount of data was available*. Further, the values of X_R and RE in Table 14 are generally higher than most of the other liquids**. It was concluded that the theory fails for water because it does not satisfactorily fit the "form" of the shock data***.

Although the pair potential for water is sometimes used in a (simple) form similar to Equation (72)[81], orientation dependent terms representing electrostatic contributions are generally added[58, 5,124] for this and most polar substances. In fact, both pairs of values of σ and ε/k given in Table 7 for water were derived from angle-dependent potentials[58,5,124]. Since in the current study no such terms were added to the potential, the use of the given parameters in Equation (72) must be considered generally inconsistent. Under these circumstances difficulties would be expected in applying the theory to water****.

---

*e.g., H, N_2, CCl_4, C_6H_6.

**On the other hand, in this case $a_o > r_o$ in conformance to Equation (82).

***The shock data for water are not dissimilar to most liquids[90].

****Although the results for the (polar) alcohols are reasonable, it is noteworthy that in both cases f is generally lower than for the other liquids.

Although Barker and Watts used a cubic lattice for water[124], a tetrahedral (diamond) structure (due to hydrogen bonds) is generally assumed[58,81,82,83,140,141]. In fact Orentlicher[82] states that analyses of the dielectric, thermodynamic, spectroscopic and transport properties of water support this hypothesis. Since an fcc lattice was assumed in this study (s = 1; see Equations (88)-(91)), additional difficulties with water would be anticipated*.

Considering that both the potential and structure used for water are inadequate, the poor fit in Figure 34 (for the potential parameters considered; see Table 14) is not surprising. In fact this result might be considered (weak) indirect support for the model; it fails when it should fail**.

For water U_o and C_o agree within 8%.

---

*An attempt was made to consider a diamond lattice (s = 3) by comparing the results (using the first parameter pair in Table 7) with an fcc lattice (s = 1). A considerable decrease in the quality of the fit resulted. Of course, in this comparison, the potential was not corrected for electrostatic contributions.

**It is interesting that application of the SF solution to water (with s = 1) gives an excellent fit ($\varepsilon' = 0.087$). For this solution $n = 8.5$, $\sigma = 3.141$A and $\varepsilon/k = 54.2^{\circ}$K which may be compared to the results in Table 14. Although the latter value is much lower than the "realistic" value (as was the case for most of the liquids fitted with the SF solution) the result shows that the Hugoniot can be reproduced with an "effective" pair potential of the type considered.

d. General conclusion. From the results in Table 14 and Figures 29-34 it was generally concluded that the WF solution adequately reproduces the Hugoniot of the liquids studied. Excellent fits were obtained for (four states of) argon, nitrogen, benzene, mercury and carbon disulphide, although in the latter two cases sufficient shock data were not available to unambiguously fix n. Very good fits were found for methyl and ethyl alcohol and hexane. For hydrogen and toluene too few data were available to adequately judge the applicability of the theory. The fit for carbon tetrachloride was generally excellent but the assumption of an fcc structure for this material appears questionable. Failure of the theory was noted for (di-)ethyl ether and water. In the former case a previously unsuspected transition in the data could explain the result. For water the potential and structure used were known, a priori, to be inadequate and the result was anticipated. Considering the range in the properties and structures of the liquids studied (see Table 4) these results tend to support the general validity of the shock model.

From the results in Table 14 it was concluded that the WF solution does not give an accurate estimate of C_o although several exceptions exist. Generally U_o exceeds C_o by $\simeq 20\%$.

It may be noted that for all liquids $6 < n < 12$. This was considered significant because there is no restriction on n in the theoretical development. It was concluded that, in the region of the shock data, liquids have potentials that are "softer" than the traditional 12-6 Lennard-Jones pair potential (Table 1, No. 5; $n \equiv 12$) but "harder" than the potentials for metals (considered in the following

sections).

Van Thiel and Alder[64] and Jordan et al[142] calculated values of n for argon of 5.6-13 and 8.46 respectively. Based on molecular beam measurements Amdur and Mason[59] obtained a corresponding value of 8.33. These are all in reasonable agreement with the (common) value found in the current study ($n = 9.2$, Table 15).

Using (in effect) the bireciprocal (or Mie-Lennard-Jones or n-m) potential function (see Table 1, No. 3) Moelwyn-Hughes[37] computes (from compressibility data) $mn \simeq 54.3$ and $m+n \simeq 15.5$ for mercury. Since $m \equiv 6$ in the current study these give values of n of 9.1 and 9.5 respectively. These compare favorably with the value of $n = 11.7$ found in the current work, considering the possible ambiguity in this figure.

For nitrogen Zubarev and Telegin[42] calculate a value of n of 9 while Herzfeld and Litovitz[49] (quoting Amdur and Pearlman)[143-145] give a value of 7.48. More recently Jordan et al[142] give $n = 7.4$ (taken from the measurements of Belyaev and Leonas) while Dick[147] shows that values of 7, 9 and 12 have been used in various calculations. These results compare favorably with the value determined in the current study (Table 14), $n = 7.0$.

For hydrogen we find that $n = 6.5$ (Table 14) which is somewhat below the value calculated by Van Thiel and Alder[60] (8.5).

Kamb[81] gives values of n for water of from 8.9 to 10.2 for a repulsive potential similar in form to that used in this study*.

*The repulsion is treated as spherically symmetric.

Although these values are reasonably close to that shown in Table 14 ($n = 7.6$), this was not considered significant because of the poor fit obtaining for water. The comparison might be more meaningful if electrostatic contributions were included in the potential used to determine n.

To determine if the n found in Table 14 were related to the type or structure of the molecules being considered, they were plotted against the number of atoms per molecule and molecular (atomic) weights of the corresponding substances. In both cases no correlation was found. It was concluded that the speculation suggested in the prior study[16] (i.e., that n is related to structure) is not justified by the current results*.

e. Recommendations. Based on the prior results and conclusions the following are recommended for the liquids studied.

---

*It is interesting that a plot of n vs. $\sigma\,(2^s\rho_o\,N/M)^{1/3}$ shows a crude inverse correlation when Hg, H_2 and CS_2 are neglected. However, an examination of Equation (106) shows that this is expected; the function $\left(\frac{n-3}{3}\right)^{\frac{1}{n-6}}$ (or any multiple of it) decreases with increasing n. Therefore if the "condition" in Equation (105) is reasonably accurately met (or deviated from by approximately the same amount for each substance) Equation (105) would be met also, and the (inverse) correlation would follow (see column 8 of Table 14).

Using the common value of $n = 9.2$ for argon, compute the Hugoniot (Equation (135)) of the solid*,** at an initial density $\rho_o = 1.65$ g/cc, using $\sigma = 3.28\text{Å}$ and $\varepsilon/k = 129.9^{\circ}\text{K}$ (Table 14). Assess the quality of the prediction by comparing the result to the recently published[139] shock data for the solid at the same initial condition. Because the prediction is "absolute" (i.e., a "zero-parameter fit") the comparison represents an excellent test of the theory.

For those liquids well-characterized by existing data (N_2, CH_3OH, C_2H_5OH, C_6H_6 and perhaps C_6H_{14}) shock experiments should be performed at (several) other initial states (as in the case of argon) and the theory tested on the same ("absolute") basis as above. Assuming the crystal structure of the corresponding solids is known, shock data under these conditions would also be desirable.

Several liquids are poorly characterized by the existing data (Hg, H_2, CS_2, $C_6H_5CH_3$ and perhaps C_6H_{14}). It is clearly desirable that additional shock data be obtained at the same initial conditions (see Appendix S); for Hg and CS_2 this might eliminate the ambiguities in the determination of n. For the remaining substances this would lead to a more meaningful evaluation of the theory.

---

*The theory (Equation (135)) makes no distinction between solids and liquids except in terms of structure. For liquids Equation (88) is assumed to hold "on-the-average" while for solids it is assumed to be "accurate" (and therefore appropriate for solid argon). In either case the same equation is used and the same Hugoniot function results, i.e., Equation (135).

**The solid is known to have an fcc structure[148,149,139].

For the difficulties experienced with CCl_4, $(C_2H_5)_2O$ and H_2O (and perhaps the alcohols) it is recommended that an angle-dependent potential* (e.g., Stockmayer[5], Rowlinson[58], etc.) be considered in the derivation of the Hugoniot to account for electrostatic contributions. A (successful) refit of the shock data using this function (consideration being given to various possible structures; $1 < s < 3$) would provide additional support for the validity of the shock model.

As pointed out earlier in this study, the Hugoniot of condensed media are difficult to determine because a satisfactory quantitative equation-of-state is not generally available for these substances. On the other hand, numerous calculations of this type have been made with varying degrees of success. Generally, the Lennard-Jones and Devonshire (LJD) cell model equation-of-state[123] is used with either the Lennard-Jones (12-6) or exponential-6 intermolecular potential (see Table 1, Nos. 5 and 13)**. In this way Fickett and Wood[47], David and Hamann[150], Van Thiel and Alder[64], Ross and Alder[51], Hamann[151], and Dick et al[139] computed the Hugoniot for liquid and, in the last two instances, solid argon. Using the same equation-of-state, Zubarev and Telegin[42] and Dick[147] computed the Hugoniot for (liquid) nitrogen***. In some of the above instances[47,64,53] for argon, calculations were also made with the Monte Carlo (statistical) equation-of-state. In more recent studies Ross and Alder[65] and

---

*Or at least one containing an additional term (e.g., Kamb[81]).

**In some cases the Morse potential (No. 12, Table 1) is considered.

***In the latter case it is interesting to note that the author assumes an fcc lattice (i.e., 12 nearest neighbors) for the calculations.

Ross[68] used the Thomas-Fermi-Dirac model for calculations with argon and xenon. On the other hand, Cook and Rogers[100] used the Tait and Murnaghan[8] equation-of-state in an investigation of the Hugoniots of CH_3OH, C_6H_6, CS_2 and CCl_4.

Because the goal of each of these computations is essentially the same as the main objective of the current study, it is recommended that a comprehensive comparison between methods be made and their relative merits determined.

3. Metals

In applying the theory to metals only the SF solution for the Hugoniot was found to be useful because meaningful σ,ε data were not generally available.

a. Preliminary conclusions. To decide again among several possible alternative methods of applying the theory to the data for metals, a set of preliminary calculations were performed. From these results the following conclusions were reached.

The σ,ε parameter pair is probably preferred over the others but the best numerical values are unknown because of the variability in values from source to source.

Neither the n satisfying the (few) available σ,r_o parameter pairs nor those satisfying long-range attraction (C_{ab}) and the σ,ε parameter pairs are consistent with the shock data.

The shock data imply values of $n < 6$.

A 2PF with ε determined from the melting point correlation (Equation (134)) gives reasonably good fits to the shock data. Solutions exist for $n < 6$, and the WF solution (at least for fcc metals) yields reasonable values of σ and U_o predictions in very

good agreement with C_o . However, the validity of this approach is questionable since the values of f found are generally low and the inherent lack of discrimination of the 2PF did not allow a distinct "best" value of n to be determined.

The SF solution, which depends only on n and (the measured value of) U_o *, should be used to apply the theory to metals, since the preferred σ,ε pair is generally unknown**.

b. Taylor expansion of SF solution. In applying the SF solution the given functional relation (μ vs. x) was first cast in the form of U vs. x and then expanded in a Taylor series*** in the interval $1 \leq x < 2$ ****. This led to the removal of all numerical instabilities***** in the Hugoniot equation and it was concluded that computations could be made as accurately as desired to as low

---

*"Real" values of σ and ε are not needed, the U_o prediction is eliminated and $X_R \equiv 0$ since the theory is "forced" through U_o .

**And perhaps of little value if it was known. Since the n-6 potential (without LRO) is used as an effective ion-ion potential in the strongly repulsive (shock) region, "real" values of σ and ε may not give the best results.

***The effect of expanding the WF (and MF) solutions in a Taylor series was not investigated in this study.

****The resulting equation when truncated after two terms was previously used to show that the "classic" linear U-μ relation is derivable from the theory.

*****The SF solution has no theoretical instability as $x \to 1$ since $U \to U_o$ (and $\mu \to 0$) exactly.

a value of x as desired*.

The (expanded) Hugoniot was then recast in the μ vs. x functional form and the "best" value of n found from the shock data in much the same manner as for liquids. The only differences were that in the determination of f, L_{min}** was taken from the 3PF of the prior WF solution (the SF solution has no counterpart 3PF) and the "cut-off" at the spurious root was ignored since it was shown that such a root does not exist in the SF solution. To test the "reasonableness" of the fit the "effective" potential parameters σ and ε were found from Equations (106) and (107), using the "best" value of n.

c. fcc metals. The results of application of the SF solution to the fcc metals included in this study (Table 4) are shown in Table 20. The values of ε' and f indicate excellent fits (in all but one case) as confirmed in Figures 35-37. Comparing these results to those (for ε' and f) in Table 19, shows that the SF solution gives a much superior fit to (even) the 2PF of the WF solution. Since an examination of the L vs. n plots in the current instance also showed that the "best" values of n were sharply defined, it was concluded that the SF solution was (at least functionally) adequate for fcc metals.

It is notable in Table 20 that in all but one instance, $n < 6$. This is in line with prior trends (in the preliminary calculations) and

---

*The (apparent) singularity at $n = 6$ in the SF solution was also (fortuitously) removed.

**See Equation (171).

speculations and is fully acceptable from the mathematical development of both the potential and Hugoniot function. The question remains: Are values of $n < 6$ (physically) reasonable?

By assuming that the n-6 (pair) potential represents an effective ion-ion potential in metals we have, in effect, introduced the concept of the neutral "pseudo-atom" described by Egelstaff[17]: "The conduction electrons distribute themselves around each ion to form screening clouds and a 'pseudo-atom' is the ion plus its screening charge."* Since pseudo-atoms interact weakly[129] (compared to "finite" ions[152]) the repulsive exponent would be expected to be small and values of $n < 6$ are considered legitimate[153].

The pseudo-atom concept also explains why the repulsive exponents for solids are less** than those for liquids (see Table 14); the liquids are generally insulators and therefore have no "electron bath" and associated screening effect.

---

*Although this viewpoint is generally discussed in the context of liquid metals, we apply it to solid metals as well, since all condensed media appear to behave similarly under strong shock loading. March[152] also suggests that the concept might apply to both solids and liquids. Moelwyn-Hughes[37] applies the n-m potential directly to solid metals although he concludes that it is probably inadequate in this instance.

**To show that the values of $n < 6$ found with metals were not fortuitously imposed by the form of the SF solution, all the prior liquids were fit with the SF solution. Contrary to the current case it was found that in every case $n > 6$. The values generally matched those in Table 14 (i.e., the WF solution) within $\sim \pm 15\%$.

It was concluded that for the SF solution the repulsive potential for metals should be generally "softer" than for liquids and that values of $n < 6$ are acceptable.

The potential parameters predicted for the fcc metals (Table 20) differ considerably from both the reported (Table 16) and correlated (ε only; see Table 18) values; the σ are high and the ε/k low. The predicted σ exceed not only the reported values of both σ and r_o (Table 16) but generally match (and often exceed) the values of a_o in Appendix S; in every case (except one) the r_o in Table 20 exceed the corresponding a_o*. Although this clearly violates Equation (82) this is overlooked because we are concerned only with an effective potential. Further, large σ are (reasonably) consistent with the pseudo-atom concept which is presumed to lead to large, "fluffy" atoms.

The predicted ε/k are not only less than the reported and correlated values, but are also generally below the corresponding melting points (Table 18)**,***. Because of the inverse dependency on σ (see Equation (104)) this would also be explained in terms of the pseudo-atom concept.

---

*This suggests overlapping "electron clouds" but in light of the subsequent discussion this is not (necessarily) considered to be physically meaningful.

**In only one case (Au) $\varepsilon/k > T_M$. In two others (Pt and Pb) ε/k agrees with T_M within $\sim 0.1 - 0.3\%$! The significance of this (notable) agreement is unknown.

***Although $\varepsilon/k < T_M$ is unexpected, most of the existing correlations[5,26] of this type are empirically derived and no theoretical objections to this result are apparent.

It was concluded that the potential parameters predicted in the SF solution are probably reasonable but not necessarily physically significant.

The individual fits seen in Figures 35-37 are discussed in the following paragraphs.

Noble Metals (Group IB) - Cu, Ag, Au. The fit for copper in Figure 35 is reasonable, but not as good as might have been expected (compare ε' and f in Table 20 with the other fcc metals). It is clear that the predicted Hugoniot ($n = 5.3$) falls above much of the data although the functional form (shape of the curve) appears to be correct. Since the theory is "forced" through C_o one explanation considered was that the sound velocity used (Appendix S) was too high. A recheck of the literature[92,85,103,13,14,96,95] showed that this was not the case. Considering the scatter in the data previously noted (Table 23) and the fact that one particular source was considered poor*, bias in the data (see Figure 35) could (at least partially) account for the observed results. Since it is also possible that the result represents a failure in the theory, it was concluded that a further investigation of copper is required before the adequacy of the theory and the appropriate value of n can be determined with certainty.

---

*Although these data were not previously eliminated on numerical grounds, the possibility of doing so for other reasons cannot be discounted. A further investigation was recommended in Table 23.

The results for silver and gold are also shown in Figure 35 and Table 20. For $n = 6.3$ and 5.8 respectively, the values of ε' and f and the plots indicate outstanding fits.

Ferromagnetic Metals (Group VIII) - Co, Ni. Although the values of ε' and f in Table 20 would indicate a better fit for cobalt than for silver or gold, this does not appear to be the case in Figure 36; the curve falls (slightly) below one group of points*. Nevertheless the fit, for $n = 3.7$, is considered very good.

The fit for nickel in Figure 36 is quite good considering the scatter in the data. For $n = 5.0$ the values of ε' and f in Table 20 are reasonable.

Transition Metals (Group VIII) - Ni, Pd, Pt. Ni was considered in the previous paragraph**.

The results for palladium and platinum are similar to each other and to the noble metals silver and gold. For $n = 5.6$ in both cases, the values of ε' and f indicate excellent to outstanding fits. This is borne out by the plots in Figure 36.

---

*If the value of C_o used (Appendix S) were (arbitrarily) raised by $\sim$ 5% the fit would be considerably improved. Unfortunately no (known) justification exists for doing this.

**See Table 4 and Figure 14. Nickel is both a ferromagnetic and transition metal.

Group IIIA - Al. Aluminum was considered separately because it is the only metal from Group III (see Table 4 and Figure 14) considered in this study. Notwithstanding the scatter in (even) the altered data* the fit for $n = 4.0$ in Figure 37 is quite good. The values of ε' and f in Table 20 are comparable to most of the other metals with excellent fits.

Alkaline Earth Metals (Group IIA) - Ca. The results for calcium are unique among the fcc metals; see Table 20 and Figure 37. Because the exhibited behavior is similar to some of the bcc metals and the counterpart alkaline earth metal (Ba) is a bcc metal, it was considered in a later section.

Group IVA - Pb. Since lead was the only fcc metal from Group IV studied, it was considered separately. The values for ε' and f in Table 20 indicate a very good fit for $n = 5.2$. This is supported by the plot in Figure 37.

d. bcc metals. The results of application of the SF solution to the bcc metals considered in this study (Table 4) are shown in Table 20. The values of ε' and f imply excellent fits (in all but two cases) as evidenced by the plots in Figures 38-41. Comparison with the results in Table 19 shows that the SF solution is much superior to the 2PF of the WF solution in all but two cases: Cs and Ba. Since the L vs. n plots again sharply defined "best" values of n it was concluded that the SF solution, at least from this point of view, was

*See Table 23.

adequate for bcc metals.

It is noted in Table 20 that the values of n are generally much less than for fcc metals. This is consistent with the known "softness" of the bcc metals as evidenced by the shock wave data itself (Figures 21-27), the slope B of the linear U-μ relation (Table 22), and the greater compressibility of the bcc metals[154], especially sodium[67] and the other alkali metals[107,31].

The low values of n in Table 20 for bcc metals are interpreted in terms of the weakly interacting "pseudo-atoms" described earlier and from this point of view the "softness" of the potentials is considered acceptable.

It is noted that in all but four cases $n < 3$ and in several $n < 2$. In the former case ($2 < n \leq 3$) the resultant fits (Rb in Figure 36; Nb and Ta in Figure 39; Mo and W in Figure 40) appear to be reasonable, but since the Hugoniot can be considered not "well defined"*, the legitimacy of the result is considered moot. In the latter case ($0 < n < 2$) the fits** (Ca (fcc metal) in Figure 37; Li and K in Figure 38; V in Figure 39; Zr in Figure 41) appear to decrease in slope as $x \to 1$! This is unusual (possibly anomalous) behavior, although there appears to be no theoretical reason why it is not possible. Pastine and Piacesi[14] indicate this is the case for

---

*The associated potential parameters σ and ε are clearly "not defined" in this instance (see Equations (106) and (107)) and the resultant pair potential is unrealistic.

**Of course, in these cases also, the Hugoniot is possibly not "well defined" and σ and ε are "not defined".

sodium although this is not confirmed in the current calculations (Table 20 and Figure 38). Since the SF theory is "forced" through C_o the very low values of n and (consequent) decreasing slope as $x \to 1$ might result from an erroneously high value of C_o. As indicated in the discussion of Table 23, this might explain the result for V (only). A third explanation of these very "soft" potentials is the occurrence of a low pressure transition to a less compressive state. Although this is not indicated in Table 23 for the metals of interest, recent information indicates it might be the case for Ca[154]. Of course, the fourth "explanation" of the results for $0 < n < 2$ is failure of the theory because the Hugoniot is not "well defined" in this region.

It was concluded that for the bcc metals the low values of n for the SF solution should be treated with caution and investigated in greater depth before being accepted.

Since there are only four solutions with $n > 3$ in Table 20 (Na, Ca, Cr and Ba) it is only in these cases that finite values of the potential parameters are predicted. In every case (except for σ for Cs) these values differ considerably from both the reported (Table 16, Na and Cs only) and correlated (ε only, Table 18) values; the σ are (generally) high and the ε/k low*. The predicted σ for Na not only exceeds the reported values of σ and r_o but also the value of a_o in Appendix S. For Cs the predicted σ lies in the range of reported values given in Table 16 but the corresponding

*As was the case for the fcc metals.

r_o (Table 20) exceeds a_o in Appendix S. As discussed previously for fcc metals these "violations" of Equation (82) are accepted because we are considering effective (not necessarily "real") potentials based on the pseudo-atom concept.

As expected, the predicted ε/k for the four solutions with $n > 3$ in Table 20 are below the corresponding melting points given in Table 18. Because ε is inversely proportional to σ (see Equation (104)) these values are also explained on the basis of the pseudo-atom concept.

It was concluded that insufficient data are available to assess the reasonableness or physical significance of the predicted potential parameters for the bcc metals.

The individual fits seen in Figures 38-41 and Figure 37 (calcium) are discussed in the following paragraphs.

Alkali Metals (Group (IA) - Li, Na, K, Rb, Cs. Although the properties of the alkali metals are generally found to be monotonic in the sequence Li-Cs* this is certainly not the case for the results in Table 20.

Considering the scatter in the (altered) data (Table 23) the fit for Li ($n = 0.7$) is reasonably good as seen in Figure 38 and the values of ε' and f in Table 20. However, since $n < 2$, the possible difficulties enumerated in the prior paragraphs should be investigated before a definitive conclusion is made.

---

*For example, the cohesive energy[155], the Hugoniot data[93], and the (calculated) pair potentials[30].

The results for sodium are shown in Figure 38 and in Table 20. For $n = 3.6$ the values of ε' and f indicate a very good fit although it is noted on the plot that several points lie (just) above the curve.

The results for potassium are similar to those for lithium, $n < 2$, decreasing slope as $x \to 1$, etc. The values of ε' and f in Table 20 and the plot in Figure 38 for $n = 1.2$ indicate an excellent fit. Again, the previously discussed difficulties with $n < 2$ should be investigated before a firm conclusion is reached.

Because the altered data for rubidium contain only five points with essentially no scatter in them (Table 23) the value of L in Table 20 is the lowest among the alkalis. The corresponding ε' and f indicate an excellent fit* as confirmed by the results in Figure 38 for $n = 3.0$. For this borderline condition (i.e., to the range $2 < n \leq 3$) the possibility that the Hugoniot is not "well defined" must be considered before a definitive conclusion can be made.

The results for cesium are shown in Table 20 where the given values of ε' and f indicate a poor fit. This is confirmed in Figure 38 where much of the data is seen to fall (considerably) below the curve. However, it was noted in a previous section that the data for cesium do not smoothly extrapolate to C_o and a low pressure transition was inferred (Table 23)**. On this basis it was concluded that

---

*Note that the ε' and f for rubidium are <u>not</u>, respectively, the lowest and highest among the alkalis.

**Such a transition is independently suggested in the literature (see Table 6).

the transition is (probably) real and that the theory is not applicable to the given data set. In this case the values of n, σ, r_o, etc. given in Table 20 are not considered meaningful.

It is noteworthy that for all the alkalis except cesium a low pressure melting transition is predicted below or nearly below (for lithium) the given data set[93]. Since such a transition should not affect the Hugoniot greatly it would not be obvious from the shock data even though the effect on n was significant. On the other hand, for Cs an electronic transition is indicated[107] which should have a relatively large effect on the Hugoniot and thus be quite apparent from the plotted data*. Since both hypotheses are consistent with observation (see Figure 38) they might explain both the non-monotonicity in the results for the sequence Li-Rb and the disparate result for Cs. Of course this reasoning is considered speculative at best. Accurate shock data in the low pressure region are needed before any definitive conclusions can be made.

Transition Metals (Group VB) - V, Nb, Ta. The results for vanadium are shown in Table 30 and Figure 39. For $n = 1.9$ the values of ε' and f and the plot indicate a very good fit although the difficulties previously discussed for $n < 2$ place the legitimacy of the result in question. However, it was previously noted that the value of C_o might be erroneously high for vanadium, and if so this

*The observed "break" in the plotted data for Li-Rb (Table 23) might represent the electronic transitions corresponding to that suggested for Cs.

would be expected to increase n^*. It was concluded that an accurate value of C_o is needed before the "correct" value of n can be determined with certainty.

The results for niobium and tantalum are also shown in Figure 39 and in Table 20. For $n = 2.5$ and 2.3 respectively, the values of ε' and f and the plots indicate excellent to outstanding fits. Of course, since $2 < n < 3$ the possibility that the Hugoniot is not "well defined" mitigates the certainty of this conclusion.

Transition Metals (Group VIB) - Cr, Mo, W. The results for chromium are somewhat unusual in that they more closely resemble those for the fcc rather than bcc metals. As seen in Table 20, $n > 3$, σ is comparatively small and ε/k is comparatively large. The corresponding values of ε' and f and the plot in Figure 40 show that the fit for $n = 4.6$ is very good and since transitions (of any kind) are neither indicated (Table 23) nor reported (Table 6), the result is considered valid. The observed behavior (similarity to fcc results) might be related to the electronic configuration of chromium which leads to the smallest molar volume among the bcc metals considered (7.33 cc/mole). This low value approaches those of the closest 4th period neighbors (Figure 14) cobalt (6.66 cc/mole) and nickel (6.57 cc/mole), which are both fcc metals, and might account for the relatively high value of n found. It was concluded that chromium is an exception to the general rule of the "softness" of bcc metals (at least when compared to the fcc metals).

---

*Probably to a value close to those found for Nb and Ta discussed in the following paragraphs.

The results for molybdenum and tungsten are similar to each other and to the Group VB transition metals niobium and tantalum. For $n = 2.5$ in both cases the values of ε' and f indicate excellent fits*. This is confirmed by the plots in Figure 40. Of course, the difficulties with $2 < n < 3$ previously noted apply in these cases also.

Group IVB - Zr. Zirconium was considered separately because it is the only metal from Group IV considered in this study (see Table 4 and Figure 14). Although the values of ε' and f in Table 20 indicate a fair fit as evidenced by the plot in Figure 41, the value of n obtained (≤ 0.1) must be considered extraordinary (although not necessarily anomalous). Because of the previously discussed difficulties when $n < 2$, the possible effects of the paucity of data (5 points below the "break" in the raw data; see Table 23) and/or a (possibly) high value of C_o, a further investigation should be made before a definite conclusion is reached.

Alkaline Earth Metals (Group IIA) - Ca, Ba. Although the fit for calcium in Figure 37 ($n = 0.5$) appears to be similar to that for lithium in Figure 38 ($n = 0.7$) the values of ε' and f in Table 20 indicate a substantial difference. In fact, as previously noted, the very "soft" potential in this case may be due to a low pressure transition[154]. Considering the scatter in the data and the difficulties with $n < 2$ no definite conclusion was reached.

---

*The potentially "poor" data for Mo noted in Table 23, which cause the (fairly large) scatter indicated, appear to have not greatly affected the results.

Calcium appears to be to the fcc metals what chromium was to the bcc metals; a substance whose "softness" is opposite to that of the respective group. The observed behavior (i.e., $n < 2$) might therefore again be related to the molar volume which for calcium is the largest (by far) among the fcc metals (26.33 cc/mole) and reasonably close to its Group IIA neighbor Ba (37.77 cc/mole), a bcc metal. It was concluded that barium is probably an exception to the general rule of the relative "hardness" of the fcc metals.

The results for barium shown in Table 20 and Figure 41 are similar to those for cesium (Figure 38); the values of ε' and f and the plots indicate a poor fit. Since, as with cesium, the data also do not extrapolate to C_o a low pressure transition was (previously) inferred (Table 23). This is independently suggested in literature (Table 6). On this basis the transition is considered "real" and the theory thus inapplicable to the data. The values of n, σ, r_o, etc. in Table 20 are not considered valid.

e. General conclusion. From the results in Table 20 and Figures 35-37 it was generally concluded that the SF solution with $n < 6$ quite adequately describes the Hugoniot of the fcc metals (with one possible exception). The associated potential parameters are considered reasonable although not necessarily physically meaningful. Excellent or outstanding fits were obtained for silver, gold, palladium and platinum. Very good fits were found for cobalt, nickel, aluminum and lead. The fit for copper was reasonably good, but a further investigation of "questionable" data is required before the applicability of the theory can be judged.

From the results in Table 20 and Figures 38-41 it was concluded that the SF solution adequately describes the Hugoniot of (most of) the bcc metals although it may not be "well defined" when $n < 3$. The associated potential parameters are "not defined" when $n < 3$. Excellent or outstanding fits were found for potassium, rubidium, niobium, tantalum, molybdenum and tungsten. Very good fits were found for sodium, vanadium and chromium. Fair to reasonably good fits were found for zirconium and lithium. The theory was considered inapplicable to cesium and barium because of a (inferred) low pressure electronic transition. No definite conclusion was reached for the fit for calcium. Several pertinent observations possibly affecting these conclusions were, that the results for the first four alkalis (Li, Na, K, Rb) may be influenced by a possible low pressure melting transition, the C_o for V may be too high, and the value of n for Cr (Ca) is higher (lower) than expected for bcc (fcc) metals.

Considering the number of metals studied and the wide range of properties involved (Table 4) the results for the fcc metals are believed to generally support the validity of the shock model. Whether this is also true for the bcc metals requires further investigation.

It may be noted that for all but one metal $n < 6$ and that, generally, the values for bcc metals are less than those for fcc metals. These results are considered significant in that n is not restricted in the theoretical development. It was concluded that metals have potentials "softer" than those for liquids (see Table

14)* and that fcc metals are softer than bcc metals**. The first conclusion is considered reasonable based on the "pseudo-atom" concept, while the second one might be explained by arguments similar to those given by Mott and Jones(3).

Using the Mie-Lennard-Jones (or m-n or bireciprocal) potential function (Table 1, No. 3) Al'tshuler et al(103) computed values of n of 4.3, 3.5 and 5.0 for copper, aluminum and lead respectively***. These are in notable agreement with the results in Table 20 which indicate values of 5.3, 4.0 and 5.2 respectively for the three metals.

Also using the bireciprocal potential, Moelywn-Hughes(37) computes (from compressibility data****) mn ≃ 24.2, 19.5 and 29.3 and m+n ≃ 10.0, 17.4 and 10.2 respectively for copper, silver and aluminum. Setting $m \equiv 6$ as in the current study, these lead to values of n of 4.0 for copper, 4.9 - 11.4 for silver and 4.2 - 4.9 for

---

*Although the WF solution was used with liquids it was previously noted that application of the SF solution resulted in very similar results (i.e., $n > 6$).

**The restrictions and limitations associated with $n < 3$ for the bcc metals (e.g., the potential parameters are "not defined") limits the surety of this conclusion.

***In Reference 103 the nomenclature for m and n are the reverse of that used in this study. Also it should be noted that for Pb (the "attractive" exponent) $m = 7.0$, not 6.0, as is the case for Al and Cu (and all cases) in the current study.

****Actually from values of Grüneisen's number. This is discussed in a following paragraph.

aluminum. These compare favorably with the respective values in Table 20 or 5.3, 6.3 and 4.0.

To determine if the n found in Table 20 were related to an independently measured property of the metals being considered, several correlations were attempted as described in the following paragraphs.

Al'tshuler et al[56] (referring to several fcc metals) and Bakanova et al[107] (referring to the alkali (bcc) metals) indicate that the elements with the largest (initial) atomic volume are compressed the most. This was tested by plotting n (from Table 20) against atomic volumes (from Appendix S) for all the metals considered in this study. Although several fcc metals (Ni, Co, Pd, Au and perhaps Ag) appear to fall on a single line* the points are generally widely scattered and it was concluded that the current results do not justify a correlation between n and atomic volume.

To determine if n was related to an energy parameter of the metals it was plotted against the cohesive energy[131,155] (per mole) for the available data[155]. As in the prior case no correlation was found and it was concluded that these parameters were not functionally related.

In discussing cohesive forces Mott and Jones[131] suggest that Grüneisen's coefficient (γ)** might be a useful measure of the

---

*The slope of this line has the opposite slope to that expected; n increases (rather than decreases) with an increase in atomic volume.

**Defined by[56]:

$$\gamma \equiv \frac{d \ln \nu}{d \ln V}$$

where ν is the vibrational frequency of the atoms and V is volume.

repulsive "exchange" forces between ions. Accordingly n was plotted against γ* for several of the metals studied[85,13,93]. For the fcc metals ($\gamma \simeq 2.0 - 3.0$) two (crude but distinct) linear relations** of equal slope were identified; one correlated Cu, Ag, Ni and Pd, while the other passes through Au, Co, Pt, Al, and Pb. For the bcc metals ($\gamma \simeq 0.8 - 1.6$) a line was found to pass through Li, Na and Rb while another of different slope passed through Nb, Ta, Mo, Zr and perhaps V and W. Only K and Cr deviate considerably from any of the lines. From this it was concluded that a (real) correlation probably exists between n and γ*** but that more data and a more extensive analysis are needed before a realistic assessment can be made.

---

*To be sure that the values of γ did not depend on the shock data (as does n) and thus that they represented a (truly) "independently measured property" of the metal, the correlation was made with γ_o, defined as the value of γ when $P = 0$, determined from static pressure measurements.

**The slope of the line has the appropriate sign; n increases with an increase in γ.

***Actually the form of the relation between n and γ is well known and was (in reality) used by Moelwyn-Hughes[37] in the prior determination of values of n for Cu, Ag and Al. The general form is:

$$\gamma = \frac{1}{6}(n + m + a)$$

where m is the attractive exponent ($\equiv 6$ in this study) and a is either 1 or 3 [103]. This certainly confirms the linear relation observed but does not explain the four fits found (implying four intercepts) with at least two different slopes.

To determine if the n found in Table 20 was related to the type of metal being considered they were "plotted" on the periodic table (Figure 14) in the appropriate position. Except for some similarity in the n for the 3 fcc transition metals, the 5 bcc transition metals (not including Cr) and (perhaps) the 3 noble metals, no substantial correlation was found. It was concluded that, at least within the accuracy of the determination of n, a relation between n and the position of the metal in the periodic table is not justified by the current results.

f. Recommendations. Based on the prior results and conclusions the following are recommended for the metals studied.

Expand the WF (and MF) solutions in a Taylor series and determine the applicability of the resultant equations to metals assuming that adequate values of σ and ε/k can be defined.

Refit the copper data using the SF solution without the data from Reference 96 to determine if an improved fit can be obtained.

Several bcc metals are poorly or (perhaps) insufficiently characterized by the existing data (Li, Na, K, Rb, Cs, V, Zr, Ba and Ca (fcc)). Additional shock data in selective regions of the U-μ curve would be highly desirable; for the alkali metals this might help determine the existence and effect of the "predicted" low pressure melting transition (Li-Rb) and the inferred "electronic" transition for Cs. For V an accurate value of C_o and additional low pressure shock data would help determine a more meaningful value of n. Additional low pressure data would also be useful for Zr (to assess the very low value of n found), Ba (to evaluate the inferred

"electronic" transition) and Ca (to reduce the scatter and determine the reality of a transition). In each case the additional data would lead to a more meaningful assessment of the theory.

The correlation of n with Grüneisen's coefficient γ should be investigated empirically to determine if an accurate, independent (a priori) determination is possible from static pressure measurements. This should be done in conjunction with redetermination of the analytical relationship between n and γ using the current theory (i.e., Equations (95) or (108)) and Slater's relation[156] or the modification proposed by Dugdale and MacDonald[86].

Although the n-6 potential appears to be adequate for the fcc metals the (generally mathematical*) difficulties with the low values of n for the bcc metals casts doubt on the applicability of the theory for these materials. Further, there appear to be physical reasons why a potential of this type would not yield good results for the bcc structure**. This point should be investigated and a determination made if a separate potential function for bcc metals is necessary.

To determine the effect of accounting for LRO behavior on both the values of n and on the difficulties experienced with the bcc metals, it is recommended that the theory developed using the previously recommended potential function (Equation (228)) be applied to all the metals. A successful refit would provide additional support for the

---

*For $n < 3$ the Hugoniot is not "well defined" and the potential parameters are "not defined". For $n < 2$ the slope of the U-μ curve decreases as $x \to 1$.

**Fowler[21] reports that the n-6 potential will lead to an fcc structure in preference to a bcc structure. March[152] also indicates that the form of the "force law" (i.e., potential) leads to a particular stable structure.

validity of the shock model.

Although the pair potential approximation may be justified for metals[75,152] it is not clear that two terms (as used in the current study and by Egelstaff[17], etc.) can sufficiently describe the interaction even if LRO behavior is taken into account. This "deficiency" could be handled most conveniently* by considering the n-6 potential with an added term (to account for electrostatic interactions) in the form[21,115,37]:

$$\phi(r) = ar^{-n} + br^{-6} + cr^{-p} \qquad (232)$$

where c is a constant and p is a small integer $(1 < p < 3)$. It is recommended that Equation (232) be considered in the development of the theory and the resultant Hugoniot applied to all the metals. It may be noted that (at least) one additional potential parameter (c) has been added and that it must be fixed independently or by the shock data.

As previously discussed with liquids it would be interesting to work "backward" through the theory and use the shock data to predict the (effective) intermolecular pair potential**. Noting the derivation of Equation (223) this can be accomplished directly from the data if

---

*In pseudopotential theory the total interaction is usually given as the sum of several (> 2) terms[130,24,27,157,132] but not in an analytical form suitable for use with the current theory.

**It is notable that Tsai and Beckett[114] also suggest this in their study of shock wave propagation in cubic lattices.

g(r) is known. However, for metals g(r) can be (roughly) computed from simple geometrical considerations (g(r) may be defined as the ratio of local to bulk density[19]) given the particular lattice structure (fcc, bcc, etc.). It is recommended that calculations of this type be performed to determine if meaningful (effective) potential functions can be obtained for metals.

As pointed out earlier in this study and discussed with liquids a satisfactory equation-of-state is generally needed before the Hugoniot of condensed media can be determined. For metals, numerous calculations of this type have been made that (almost exclusively) start with the Mie-Grüneisen equation-of-state[86,10]. Using this and a Morse potential, Pastine[61] determined the Hugoniots for Al, Cu, Ag, Zr and Mg with mixed results. In a similar manner, using a Born-Mayer lattice potential, Huang[9] computed the Hugoniots for Ag, Cu, and Pb and determined a "general" equation-of-state for metals. In later studies Pastine[14,67] used an n-m potential (Table 1, No. 3) to compute several (hypothetical) Hugoniots and a detailed evaluation of the cohesive energy to determine the Hugoniot of Na. Ruoff[158] used a previously derived P-x relationship to determine the Hugoniot for KBr, CsI and Na and, using an n-m potential, Xe. In several cases[85,91,102,13] the Mie-Grüneisen equation-of-state has been used with experimental data and/or analytical fits of that data, to compute thermodynamic properties of several metals, including γ and T etc., instead of the Hugoniot itself. Munson and Barker[95] obtained the isentropic and isothermal hydrostats of Cu, Al and Pb in a similar manner. Al'tshuler et al[103,104] supplemented the

Mie-Grüneisen equation-of-state with terms that take into account the electronic components of the energy and pressure and used the shock data to determine T, γ, etc. for several metals. In a later study Krupnikov et al[108] performed similar calculations for Ti, Mo, Ta and Fe. A single exception to the use of the Mie-Grüneisen equation-of-state for metals is the study by Tsai and Beckett[114] in which lattice dynamics was applied to wave propagation in cubic lattices using several "interaction" potential functions. Numerical solutions to the equations of motion yielded the Hugoniot for several lattice-type, potential-function combinations*.

Because the general goal of each of these computations is (essentially) the same as the objectives of the current study, it is recommended that, as in the case with liquids, a comprehensive comparison between the several methods be made to determine the relationship(s) between them and their relative merits.

In a recent pair of papers Barker[40] and Broadhurst and Mopsik[159] computed the Grüneisen numbers for polymeric solids and linear polymers using a "bundle-of-chains" model. It is recommended that the applicability of the current shock model to materials of this type be investigated.

---

*It is notable that Tsai and Beckett's approach is the only one (other than the current study) in which the Hugoniot calculations do not depend on the thermodynamics of the shock transition.

REFERENCES

1. W. J. M. Rankine, Phil. Trans. 160, 277 (1870).

2. H. Hugoniot, J. de l'Ecole Polytechnique 58, 1 (1889).

3. J. M. Walsh and R. H. Christian, Phys. Rev. 97, 1544 (1955).

4. R. Courant and K. O. Friedrichs, Supersonic Flow and Shock Waves (Interscience Publishers, Inc., New York, 1948).

5. J. O. Hirschfelder, C. F. Curtiss and R. B. Bird, Molecular Theory of Gases and Liquids (John Wiley and Sons, Inc., New York, 1954).

6. E. Gruneisen, Handbuch der Physik 10, 22 (1926).

7. J. E. Lennard-Jones and A. F. Devonshire, Proc. Roy. Soc. (London) A163, 53 (1937).

8. F. D. Murnaghan, Finite Deformation of an Elastic Solid (John Wiley and Sons, Inc., New York, 1951).

9. Y. K. Huang, J. Chem. Phys. 45, 1979 (1966).

10. G. E. Duvall and G. R. Fowles, High Pressure Physics and Chemistry, Vol. 2, R. S. Bradley, Ed. (Academic Press, London, 1963).

11. B. J. Alder, Solids Under Pressure, W. Paul and D. W. Warschauer, Eds. (McGraw-Hill Book Company, New York, 1963).

12. Y. B. Zel'dovich and Y. P. Raizer, Physics of Shock Waves and High-Temperature Hydrodynamic Phenomena, Vol. II (Academic Press, New York, 1967).

13. R. G. McQueen and S. P. Marsh, J. App. Phys. 31, 1253 (1960).

14. D. J. Pastine and D. Piacesi, "The Existence and Implications of Curvature in the Relation Between Shock and Particle Velocities for Metals", NOLTR 65-233 (Naval Ordnance Laboratory, White Oak, Maryland, 1966).

15. Fundamental Formulas of Physics, Vol. One, D. H. Menzel, Ed. (Dover Publications, Inc., New York, 1960).

16. P. K. Salzman, A. F. Collings and C. J. Pings, J. Chem. Phys. 50, 935 (1969).

17. P. A. Egelstaff, An Introduction to the Liquid State (Academic Press, Inc., London, 1967).

18. T. L. Hill, Statistical Mechanics (McGraw-Hill Book Company, Inc., New York, 1956).

19. T. L. Hill, An Introduction to Statistical Thermodynamics (Addison-Wesley Publishing Company, Reading, Mass., 1960).

20. C. J. Pings, Physics of Simple Liquids, H. N. V. Temperley, J. S. Rowlinson and G. S. Rushbrooke, Eds. (North Holland Publishing Co., Amsterdam, 1968), p. 386.

21. R. H. Fowler, Statistical Mechanics (Cambridge at the University Press, London, 1936).

22. J. S. Rowlinson, Liquids and Liquid Mixtures (Butterworth's, London, 1959).

23. S. Glasstone, Theoretical Chemistry (D. Van Nostrand Company, Inc., New York, 1944).

24. W. A. Harrison, Phys. Rev. 129, 2512 (1963).

25. M. D. Johnson, P. Hutchinson and N. H. March, Proc. Roy. Soc. 282A, 283 (1964).

26. A. Paskin and A. Rahman, Phys. Rev. Letters 16, 300 (1966).

27. W. M. Shyu and G. D. Gaspari, Phys. Rev. 163, 667 (1967).

28. A. Paskin, Adv. Phys. 16, 223 (1967).

29. The Properties of Liquid Metals, P. D. Adams, H. A. Davies and S. G. Epstein, Eds. (Taylor and Francis, Ltd., London, 1967).

30. P. S. Ho, Phys. Rev. 169, 523 (1968).

31. D. Schiff, Phys. Rev. 186, 151 (1969).

32. E. McLaughlin, Chem. Rev. 64, 389 (1964).

33. D. A. Copeland and N. R. Kestner, J. Chem. Phys. 49, 5214 (1968).

34. A. E. Sherwood and J. M. Prausnitz, J. Chem. Phys. 41, 429 (1964).

35. M. Klein, J. Res. National Bur. Standards 70A, 259 (1966).

36. J. A. V. Butler, Ann. Rep. Chem. Soc. (London) 34, 75 (1937).

37. E. A. Moelwyn-Hughes, Physical Chemistry (Pergamon Press, New York, 1957).

38. S. D. Hamann, Austral. J. Chem. 13, 325 (1960).

39. E. Hundhausen and H. Pauly, Z. Physik 187, 305 (1965).

40. R. E. Barker, J. App. Phys. 38, 4234 (1967).

41. G. K. Horton, Am. J. Phys. 36, 93 (1968).

42. V. N. Zubarev and G. S. Telegin, Sov. Phys.-Dokl. 7, 34 (1962).

43. W. J. Moore, Physical Chemistry, Third Ed. (Prentice-Hall, Inc., New Jersey, 1962).

44. B. Kamb, J. Chem. Phys. 43, 3917 (1965).

45. H. J. M. Hanley and M. Klein, "On the Selection of the Intermolecular Potential Function: Application of Statistical Mechanical Theory to Experiment", NBS Tech. Note 360 (National Bur. Standards, Washington, D.C., 1967).

46. R. H. Wentorf, R. J. Buehler, J. O. Hirschfelder and C. F. Curtiss, J. Chem. Phys. 18, 1484 (1950).

47. W. Fickett and W. W. Wood, Phys. Fl. 3, 204 (1960).

48. H. G. David and S. D. Hamann, Austral. J. Chem. 14, 1 (1961).

49. K. F. Herzfeld, Dispersion and Absorption of Sound by Molecular Processes, S. Sette, Ed. (Academic Press, Inc., New York, 1963).

50. A. A. Khan, Phys. Rev. 134, A367 (1964).

51. L. S. Tee, S. Gotoh and W. Stewart, I & EC Fund. 5, 356 (1966).

52. J. S. Rowlinson, Ind. Eng. Chem. 59, 28 (1967).

53. M. Ross and B. Alder, J. Chem. Phys. 46, 4203 (1967).

54. A. H. Narten, M. D. Danford and H. A. Levy, J. Chem. Phys. 46, 4875 (1967).

55. J. A. Barker and A. Pompe, Austral. J. Chem. 21, 1683 (1968).

56. J. A. Barker, W. Fock and F. Smith, Phys. Fl. 7, 897 (1964).

57. L. S. Tee, S. Gotoh and W. Stewart, I & EC Fund. 5, 363 (1966).

58. J. S. Rowlinson, Trans. Fara. Soc. 47, 120 (1951).

59. I. Amdur and E. A. Mason, J. Chem. Phys. 22, 670 (1954).

60. M. Van Thiel and B. J. Alder, Mol. Phys. 10, 427 (1966).

61. D. J. Pastine, J. App. Phys. 35, 3407 (1964).

62. L. W. Bruch, Phys. Fl. 10, 2531 (1967).

63. R. W. Keeler, M. Van Thiel and B. J. Alder, Physica 31, 1437 (1965).

64. M. Van Thiel and B. J. Alder, J. Chem. Phys. 44, 1056 (1966).

65. M. Ross and B. J. Alder, J. Chem. Phys. 47, 4129 (1967).

66. D. E. Williams, J. Chem. Phys. 47, 4680 (1967).

67. D. J. Pastine, Phys. Rev. 166, 703 (1968).

68. M. Ross, Phys. Rev. 171, 777 (1968).

69. B. K. Annis, H. E. Humphreys and E. A. Mason, Phys. Fl. 11, 2122 (1968).

70. P. G. Mikolaj and C. J. Pings, Phys. Rev. Letters 16, 4 (1966).

71. P. G. Mikolaj and C. J. Pings, J. Chem. Phys. 46, 1412 (1967).

72. J. D. Robinson and J. R. Ferron,"Direct Determination of Intermolecular Potentials from Transport Data", Reprint 33A, Symposium on Transport Properties (AIChE, Los Angeles, 1968).

73. F. Sommer and K. Werber, Phys. Letters 27A, 425 (1968).

74. J. H. Dymond and B. J. Alder, J. Chem. Phys. 51, 309 (1969).

75. J. E. Enderby and N. H. March, The Properties of Liquid Metals, P. D. Adams, H. A. Davies and S. G. Epstein, Eds. (Taylor and Francis, Ltd., London, 1967), p. 691.

76. R. C. Ling, J. Chem. Phys. 25, 609 (1956).

77. H. Pavlevsky, Liquids: Structure, Properties, Solid Interactions, T. J. Hughel, Ed. (Elsevier, New York, 1965).

78. Physics of Simple Liquids, H. N. V. Temperley, J. S. Rowlinson and G. S. Rushbrooke, Eds. (North Holland Publishing Co., Amsterdam, 1968).

79. H. S. Green, The Molecular Theory of Fluids (Dover Publications, Inc., New York, 1969).

80. J. D. Bernal, Liquids: Structure, Properties, Solid Interactions, T. J. Hughel, Ed. (Elsevier, New York, 1965), p. 25.

81. B. Kamb, J. Chem. Phys. 43, 3917 (1965).

82. M. Orentlicher and P. O. Vogelhut, J. Chem. Phys. 45, 4719 (1966).

83. A. H. Narten, M. D. Danford and H. A. Levy, Trans. Fara. Soc. 43 (1967).

84. H. Eyring, R. E. Powell, A. H. Duffey and R. B. Parlin, Chem. Rev. 45, 69 (1949).

85. J. M. Walsh, M. H. Rice, R. G. McQueen and F. L. Yarger, Phys. Rev. 108, 196 (1957).

86. M. H. Rice, R. G. McQueen and J. M. Walsh, Solid State Physics Vol. 6, Advances in Research and Applications, Compression of Solids by Strong Shock Waves, F. Seitz, and D. Turnbull, Eds. (Academic Press, Inc., New York, 1958).

87. R. H. Cole, Underwater Explosions (Dover Publications, Inc., New York, 1965).

88. Y. B. Zel'dovich and Y. P. Raizer, Physics of Shock Waves and High-Temperature Hydrodynamic Phenomena, Vol. I (Academic Press, New York, 1967).

89. J. S. Rinehart, Quart. Colo. School of Mines 55, 1 (1960).

90. J. M. Walsh and M. H. Rice, J. Chem. Phys. 26, 815 (1957).

91. L. V. Al'tshuler, K. K. Krupnikov, B. N. Ledenev, V. I. Zhuchikhin and M. I. Brazhnik, Sov. Phys. JETP 34, 606 (1958).

92. L. V. Al'tshuler, K. K. Krupnikov and M. I. Brazhnik, Sov. Phys. JETP 34, 614 (1958).

93. M. H. Rice, J. Phys. Chem. Solids 26, 483 (1965).

94. T. J. Ahrens and M. H. Ruderman, J. App. Phys. 37, 4758 (1966).

95. D. E. Munson and L. M. Barker, J. App. Phys. 37, 1652 (1966).

96. M. Van Thiel, Compendium of Shock Wave Data, UCRL-50108, Vol. 1 (Lawrence Radiation Laboratory, University of California, Livermore, California, 1966).

97. P. K. Salzman, AIAA J. 2, 359 (1964).

98. M. Van Thiel, Compendium of Shock Wave Data, UCRL-50108, Vol. 2 (Lawrence Radiation Laboratory, University of California, Livermore, California, 1966).

99. A. Van Itterbeek, W. Van Dael and A. Cops, Physica 27, 111 (1961).

100. M. A. Cook and L. A. Rogers, J. App. Phys. 34, 2330 (1963).

101. Handbook of Chemistry and Physics, 42nd Edition, C. D. Hodgman, Ed. (The Chemical Rubber Publishing Company, Ohio, 1960).

102. L. V. Al'tshuler, S. B. Kormer, M. I. Brazhnik, L. A. Vladimirov, M. P. Speranskaya and A. I. Funtikov, Sov. Phys. JETP 11, 766 (1960).

103. L. V. Al'tshuler, S. B. Kormer, A. A. Bakanova and R. F. Trunin, Sov. Phys. JETP 11, 573 (1960).

104. L. V. Al'tshuler, A. A. Bakanova and R. F. Trunin, Sov. Phys. JETP 15, 65 (1962).

105. J. M. Walsh and R. H. Christian, Phys. Rev. 97, 1544 (1955).

106. A. A. Bakanova and I. P. Dudoladov, JETP Letters 5, 265 (1967).

107. A. A. Bakanova, I. P. Dudoladov and R. F. Trunin, Sov. Phys.--Solid State 7, 1307 (1965).

108. K. K. Krupnikov, A. A. Bakanova, M. I. Brazhnik and R. F. Trunin, Sov. Phys.--Doklady 8, 205 (1963).

109. R. D. Dick, Bull. Am. Phys. Soc. 13, 579 (1968).

110. L. V. Al'tshuler, A. A. Bakanova and R. F. Trunin, Sov. Phys.--Doklady 3, 761 (1958).

111. V. D. Urlin, A. A. Ivanov, Sov. Phys.--Doklady 8, 380 (1963).

112. J. Skalyo, R. D. Dick and R. H. Warnes, Bull. Am. Phys. Soc. 13, 579 (1968).

113. M. H. Rice and J. M. Walsh, J. Chem. Phys. 26, 824 (1957).

114. D. S. Tsai and C. W. Beckett, J. Geophys. Res. 71, 2601 (1966).

115. S. Glasstone, Textbook of Physical Chemistry, 2nd Ed. (D. Van Nostrand Company, Inc., Princeton, New Jersey, 1946).

116. A. Dalgarno and A. E. Kingston, Proc. Phys. Soc. (London) 73, 455 (1959).

117. L. Salem, Mol. Phys. 3, 441 (1960).

118. P. R. Fontana, Phys. Rev. 123, 1865 (1961).

119. A. Dalgarno and A. E. Kingston, Proc. Phys. Soc. 78, 607 (1961).

120. A. Dalgarno, Rev. Mod. Phys. 35, 522 (1963).

121. J. A. Barker and P. J. Leonard, Phys. Letters 13, 127 (1964).

122. R. G. Gordon, J. Chem. Phys. 48, 3929 (1968).

123. R. H. Wentorf, R. J. Buehler, J. O. Hirschfelder and C. F. Curtiss, J. Chem. Phys. 18, 1484 (1950).

124. J. A. Barker and R. O. Watts, Chem. Phys. Letters 3, 144 (1969).

125. T. L. Cottrell, Disc. Fara. Soc. 22, 10 (1956).

126. T. W. Chapman, AIChE J. 12, 395 (1966).

127. Handbook of Mathematical Tables, 2nd Ed., Supplement to Handbook of Chemistry and Physics (The Chemical Rubber Company, Ohio, 1964).

128. A. F. Collings (private communication, 1968).

129. S. H. Chen,"Structure of Liquids", Preprint No. 1064, Department of Nuclear Engineering (Massachusetts Institute of Technology, 1970).

130. W. A. Harrison, Phys. Rev. 129, 2503 (1963).

131. N. F. Mott and H. Jones, The Theory of the Properties of Metals and Alloys (Clarendon Press, Oxford, England, 1936).

132. A. Meyer, C. W. Nestor and W. H. Young, The Properties of Liquid Metals, P. D. Adams, H. A. Davies and S. G. Epstein, Eds. (Taylor and Francis, Ltd., London, England, 1967), p. 581.

133. W. Eisenmenger, Acoustica 14, 187 (1964).

134. W. M. Flook and D. F. Hornig, J. Chem. Phys. 23, 816 (1955).

135. R. Becker, Z. Physik 8, 321 (1921).

136. V. F. Nozdrev, The Use of Ultrasonics in Molecular Physics (The Macmillan Company, New York, 1965).

137. R. F. Herzfield and T. A. Litovitz, Absorption and Dispersion of Ultrasonic Waves (Academic Press Inc., New York, 1959).

138. P. G. Mikolaj and C. J. Pings, J. Chem. Phys. 46, 1401 (1967).

139. R. D. Dick, R. H. Warnes and J. Skaylo, J. Chem. Phys. 53, 1648 (1970).

140. M. C. R. Symons, M. J. Blandamer and M. F. Fox, New Scientist 34, 345 (1967).

141. A. Ben-Naim, J. Chem. Phys. 52, 5531 (1970).

142. J. E. Jordan, S. O. Colgate, I. Amdur and E. A. Mason, J. Chem. Phys. 52, 1143 (1970).

143. I. Amdur and H. Pearlman, J. Chem. Phys. 8, (1940).

144. I. Amdur and H. Pearlman, J. Chem. Phys. 8, 998 (1940).

145. I. Amdur and H. Pearlman, J. Chem. Phys. 9, 503 (1941).

146. Yu. N. Belyaev and V. B. Leonas, Sov. Phys.--Doklady 11, 866 (1967).

147. R. D. Dick, J. Chem. Phys. 52, 6021 (1970).

148. C. S. Barret and T. B. Massalski, Structure of Metals, 3rd Ed. (McGraw-Hill Book Company, New York, 1966).

149. C. J. Smithells, Metals Reference Book, 4th Ed., Vol. 1 (Butterworth's, London, 1967).

150. H. G. David and S. D. Hamman, Austral. J. Chem. 14, 372 (1961).

151. S. D. Hamman, Austral. J. Chem. 22, 637 (1969).

152. N. H. March, Physics of Simple Liquids, H. N. V. Temperley, J. S. Rowlinson and G. S. Rushbrooke, Eds. (North Holland Publishing Company, Amsterdam, 1968), p. 645.

153. J. E. Enderby (private communication, March 1969).

154. C. J. M. Rooymans, Advances in High Pressure Research, Vol. 2 R. S. Bradley, Ed. (Academic Press, New York, 1969), p. 1.

155. E. P. Wigner and F. Seitz, Solid State Physics, Vol. 1, Advances in Research and Applications, Qualitative Analysis of the Cohesion of Metals, F. Seitz and D. Turnbull, Eds. (Academic Press, New York, 1955).

156. J. C. Slater, Introduction to Chemical Physics (Dover Publications, New York, 1970).

157. T. Schneider and E. Stoll, The Properties of Liquid Metals, P. D. Adams, H. A. Davies and S. G. Epstein, Eds. (Taylor and Francis, Ltd., London, England, 1967), p. 581.

158. A. L. Ruoff, J. App. Phys. 38, 4976 (1967).

159. M. G. Broadhurst and F. I. Mopsik, J. Chem. Phys. 52, 3634 (1970).

160. H. Margenau and G. M. Murphy, The Mathematics of Physics and Chemistry (D. Van Nostrand Company, Inc., New York, 1956).

161. A. E. Taylor, Advanced Calculus (Ginn and Company, New York, 1955).

162. S. A. Rice, Liquids: Structure, Properties, Solid Interactions, T. J. Hughel, Ed. (Elsevier, New York, 1965), p. 51.

163. W. Feller, An Introduction to Probability Theory and Applications, Vol. I (John Wiley and Sons, New York, 1950).

164. E. Parzen, Modern Probability Theory and Its Applications (John Wiley and Sons, New York, 1960).

165. K. Huang, Statistical Mechanics (John Wiley and Sons, New York, 1963).

166. K. S. Kunz, Numerical Analysis (McGraw-Hill Book Company, Inc., New York, 1957).

APPENDICES

Appendix A

Derivation of Equations (4) - (7)

Equations (1), (2) and (3) are:

$$\rho_o U = \rho(U - \mu) \tag{1}$$

$$(\rho_o U)U + P_o = [\rho(U - \mu)](U - \mu) + P \tag{2}$$

$$\frac{1}{2}(\rho_o U)U^2 + UP_o + U\rho_o E_o = \frac{1}{2}[\rho(U - \mu)](U - \mu)^2 + (U - \mu)P + (U - \mu)\rho E \tag{3}$$

Equation (1) may be directly solved for U to give:

$$U = \frac{\mu}{1 - \frac{\rho_o}{\rho}} \tag{4}$$

which is Equation (4).

Rearrangement of Equation (2) gives:

$$P - P_o = \rho_o U^2 - \rho(U - \mu)^2 \tag{A1}$$

Substitution of $\rho(U - \mu)$ from Equation (1) gives:

$$P - P_o = \rho_o U^2 - \rho_o U(U - \mu) = \cancel{\rho_o U^2} - \cancel{\rho_o U^2} + \rho_o U\mu \tag{A2}$$

$$P - P_o = \rho_o U\mu \tag{5}$$

which is Equation (5).

From Equation (1):

$$U - \mu = \frac{\rho_o}{\rho} U \tag{A3}$$

Substitution into Equation (3) and rearranging gives:

$$\rho_o \cancel{U} E - \rho_o \cancel{U} E_o = \frac{1}{2}(\rho_o \cancel{U})U^2 - \frac{1}{2}(\rho_o \cancel{U})\left(\frac{\rho_o}{\rho} U\right)^2 + \cancel{U} P_o - \frac{\rho_o}{\rho} \cancel{U} P \tag{A4}$$

or:

$$\Delta E \equiv E - E_o = \frac{1}{2} U^2[1 - (\rho_o/\rho)^2] + \frac{P_o}{\rho_o} - \frac{P}{\rho} \tag{A5}$$

$$\Delta E = \frac{1}{2} U^2(1 - \rho_o/\rho)(1 + \rho_o/\rho) + \frac{P_o}{\rho_o} - \frac{P}{\rho} \tag{A6}$$

Substitution of μ in Equation (4) into Equation (5) gives:

$$P - P_o = \rho_o U^2(1 - \rho_o/\rho) \tag{A7}$$

or:

$$U^2 = \frac{P_o - P_o}{\rho_o(1-\rho_o/\rho)} \tag{A8}$$

Substitution above gives:

$$\Delta E = \frac{1}{2}(1 - \rho_o/\rho)(1 + \rho_o/\rho) \frac{(P - P_o)}{\rho_o(1-\rho_o/\rho)} + \frac{P_o}{\rho_o} - \frac{P}{\rho} \tag{A9}$$

$$\Delta E = \frac{1}{2}\frac{P}{\rho_o} + \frac{1}{2}\frac{P}{\rho} - \frac{1}{2}\frac{P_o}{\rho_o} - \frac{1}{2}\frac{P_o}{\rho} + \frac{P_o}{\rho_o} - \frac{P}{\rho} \tag{A10}$$

$$\Delta E = \frac{1}{2}\frac{P}{\rho_o} + \frac{1}{2}\frac{P_o}{\rho_o} - \frac{1}{2}\frac{P}{\rho} - \frac{1}{2}\frac{P_o}{\rho} = \frac{1}{2}\frac{(P + P_o)}{\rho_o} - \frac{1}{2}\frac{(P + P_o)}{\rho} \tag{A11}$$

$$\Delta E = \frac{1}{2}(P + P_o)\left(\frac{1}{\rho_o} - \frac{1}{\rho}\right) \tag{6}$$

which is Equation (6).

Substituting Equation (4) into Equation (5) gives:

$$P - P_o = \rho_o\mu^2/(1 - \rho_o/\rho) \quad , \quad P = P_o + \rho_o\mu^2/(1 - \rho_o/\rho) \tag{A12}$$

Substituting this into Equation (6) gives:

$$\Delta E = \frac{1}{2}\left(2P_o + \frac{\rho_o\mu^2}{(1-\rho_o/\rho)}\right)\left(\frac{1}{\rho_o} - \frac{1}{\rho}\right) \tag{A13}$$

or:

$$\Delta E = P_o\left(\frac{1}{\rho_o} - \frac{1}{\rho}\right) + \frac{1}{2}\,\frac{\rho_o\mu^2}{(1-\rho_o/\rho)}\,\frac{(1-\rho_o/\rho)}{\rho_o} \qquad \text{(A14)}$$

$$\Delta E = P_o\left(\frac{1}{\rho_o} - \frac{1}{\rho}\right) + \frac{1}{2}\,\mu^2 \qquad (7)$$

which is Equation (7).

Appendix B

Derivation of Equation (8)

The equation of state of any material can be written in the form:

$$E = f(V,T) \tag{B1}$$

Since dE is an exact differential[160] (based on the first law of thermodynamics) it may be written:

$$dE = \left(\frac{\partial E}{\partial V}\right)_T dV + \left(\frac{\partial E}{\partial T}\right)_V dT \tag{B2}$$

Now:

$$C_V \equiv \left(\frac{\partial E}{\partial T}\right)_V \tag{B3}$$

and the above becomes:

$$dE = \left(\frac{\partial E}{\partial V}\right)_T dV + C_V dT \tag{B4}$$

The first law of thermodynamics may be written:

$$dE = q - \omega \tag{B5}$$

For a reversible change:

$$q_{rev} = T\, dS \tag{B6}$$

$$\omega_{rev} = Pd\, V \tag{B7}$$

and:

$$dE = T\, dS - Pd\, V \text{ ; reversible change} \tag{B8}$$

Since each of these quantities is a function of state only, the equation is general and may be written:

$$dE = T\,dS - P\,dV \tag{B9}$$

Dividing through by dV gives:

$$\frac{dE}{dV} = T\frac{dS}{dV} - P \tag{B10}$$

For constant temperature processes this becomes:

$$\left(\frac{\partial E}{\partial V}\right)_T = T\left(\frac{\partial S}{\partial V}\right)_T - P \tag{B11}$$

Dividing Equation (B9) through by dT gives:

$$\frac{dE}{dT} = T\frac{dS}{dT} - P\frac{dV}{dT} \tag{B12}$$

and for constant volume processes this gives:

$$\left(\frac{\partial E}{\partial T}\right)_V = T\left(\frac{\partial S}{\partial T}\right)_V \tag{B13}$$

Taking the partial derivative of Equation (B11) with respect to V and Equation (B13) with respect to T gives:

$$\frac{\partial^2 E}{\partial V \partial T} = T\frac{\partial^2 S}{\partial V \partial T} + \left(\frac{\partial S}{\partial V}\right)_T - \left(\frac{\partial P}{\partial T}\right)_V \tag{B14}$$

$$\frac{\partial^2 E}{\partial T \partial V} = T\frac{\partial^2 S}{\partial T \partial V} \tag{B15}$$

Since E and S are continuous functions the mixed derivatives are equal in the above and subtraction yields:

$$\left(\frac{\partial S}{\partial V}\right)_T = \left(\frac{\partial P}{\partial T}\right)_V \tag{B16}$$

Substituting Equation (B16) into Equation (B11) gives:

$$\left(\frac{\partial E}{\partial V}\right)_T = T\left(\frac{\partial P}{\partial T}\right)_V - P \qquad (B17)$$

Substitution into Equation (B4) gives:

$$dE = T\left(\frac{\partial P}{\partial T}\right)_V dV - PdV + C_V dT \qquad (8)$$

which is Equation (8).

Appendix C

Derivation of Equation (18)

Equation (17) is:

$$U_o \equiv \lim_{\mu \to 0} U = \lim_{\mu \to 0} \frac{\mu}{1 - \frac{1}{x}} \Longrightarrow \frac{0}{0} \tag{17}$$

Applying L'Hôspital's rule[15] by differentiating numerator and denominator with respect to μ gives:

$$U_o = \lim_{\mu \to 0} \frac{1}{-(-\frac{1}{x^2}) \frac{dx}{d\mu}} \tag{C1}$$

or:

$$U_o = \lim_{\mu \to 0} x^2 \frac{d\mu}{dx} \tag{C2}$$

Since $x \to 1$ as $\mu \to 0$ this may be written:

$$U_o = \lim_{x \to 1} x^2 \frac{d\mu}{dx} \tag{C3}$$

or:

$$U_o = \lim_{x \to 1} \frac{d\mu}{dx} \tag{18}$$

which is Equation (18).

Appendix D

Validity of Equation (19)

Equation (19) is:

$$\frac{1}{2}\mu^2 >> P_o\left(\frac{1}{\rho_o} - \frac{1}{\rho}\right) \tag{19}$$

Since

$$x \equiv \rho/\rho_o \tag{D1}$$

this becomes:

$$\frac{1}{2}\mu^2 >> \frac{P_o}{\rho_o}\left(1 - \frac{1}{x}\right) \tag{D2}$$

which is to be shown. Clearly, the maximum value of the right-hand-side (rhs) of Equation (D2) will occur when $x \to \infty$, $\left(1 - \frac{1}{x}\right) \to 1$. Thus Equation (19) will be satisfied if:

$$\frac{1}{2}\mu^2 >> \frac{P_o}{\rho_o} \tag{D3}$$

The minimum value of the left-hand-side (lhs) of Equation (D3) will occur when $\mu = \mu_{min}$ which may be found for each substance from the compiled raw data (Appendix S). Equation (19) will be satisfied if:

$$\frac{1}{2}\mu_{min}^2 >> \frac{P_o}{\rho_o} \tag{D4}$$

or if:

$$R \equiv \frac{\frac{1}{2}\mu_{min}^2}{P_o/\rho_o} >> 1 \tag{D5}$$

From the data in Appendix S, rough calculations of R were made for all the substances considered in this study. The results are shown in Table D1.

Table D1

VALIDITY OF EQUATION (19)

Substance	$\sim\rho_o$-g/cc	$\sim P_o$-atm.	$\sim\mu_{min}$-cm/sec $\times 10^{-6}$	$\sim P_o/\rho_o$-cm^2/sec^2 $\times 10^{-6}$	$\sim \mu^2_{min}$/2-cm^2/sec^2 $\times 10^{-6}$	R
A	1.4	2	0.03	1.4	450	321
A-II	0.9	69	0.15	76.7	11250	147
A-III	1.0	1050	0.14	1070	9800	9.2
A-IV	1.1	1600	0.25	1455	31250	21
Hg	13.5	1	0.06	0.07	1800	25714
N_2	0.8	1	0.06	1.3	1800	1385
H_2	0.07	2	0.60	28.8	180000	6250
CS_2	1.3	1	0.02	0.77	200	260
CCl_4	1.6	1	0.04	0.63	800	1270
CH_3OH	0.79	1	0.15	1.27	11250	8860
C_2H_5OH	0.78	1	0.13	1.28	8450	6600
$(C_2H_5)_2O$	0.71	1	0.15	1.41	11250	7979
C_6H_{14}	0.67	1	0.15	1.49	11250	7550
C_6H_6	0.88	1	0.03	1.14	450	395
$C_6H_5CH_3$	0.88	1	0.14	1.14	9800	8596
H_2O	1.0	1	0.095	1.0	4513	4513
Cu	8.9	1	0.01	0.112	50	446
Ag	10.5	1	0.05	0.095	1250	13150
Au	19.3	1	0.04	0.052	800	15380
Co	8.8	1	0.05	0.113	1250	11060
Ni	8.9	1	0.03	0.112	450	4020
Pd	12.0	1	0.045	0.083	1013	12200
Pt	21.4	1	0.03	0.047	450	9570
Al	2.7	1	0.0004	0.37	0.08	0.22
Ca	1.5	1	0.10	0.67	5000	7460
Pb	11.3	1	0.002	0.088	2	22.7
Li	0.53	1	0.11	1.9	6050	3184
Na	1.0	1	0.13	1.0	8450	8450

Table D1 (continued)

Substance	$\sim\rho_o$-g/cc	$\sim P_o$-atm.	$\sim\mu_{min}$-cm/sec $\times 10^{-6}$	$\sim P_o/\rho_o$-cm^2/sec^2 $\times 10^{-6}$	$\sim\mu_{min}^2/2$-cm^2/sec^2 $\times 10^{-6}$	R
K	0.86	1	0.12	1.16	7200	6207
Rb	1.5	1	0.13	0.67	8450	12600
Cs	1.8	1	0.14	0.56	9800	17500
V	6.1	1	0.06	0.16	1800	11250
Nb	8.6	1	0.05	0.12	1250	10400
Ta	16.6	1	0.04	0.06	800	13333
Cr	7.1	1	0.05	0.14	1250	8930
Mo	10.2	1	0.04	0.10	800	8000
W	19.2	1	0.045	0.05	1013	20260
Zr	6.5	1	0.07	0.15	2450	16300
Ba	3.6	1	0.09	0.28	4050	14460

In all but four cases (A-III, A-IV, Al and Pb) R > 100 and Equation (D5) (and thus Equation (19)) is satisfied to at least 1% *.

For the four exceptions it may be noted that in using Equation (D5) the most stringent conditions were assumed, i.e., in Equation (D2) the lhs was a minimum while the rhs was a maximum. A less severe but equally satisfactory condition may be developed as follows. From Equation (14):

$$1 - \frac{1}{x} = \frac{\mu}{U} \tag{D6}$$

and substituting into Equation (D2) gives:

$$\frac{1}{2}\mu^2 >> \frac{P_o}{\rho_o}\frac{\mu}{U} \tag{D7}$$

or:

$$\frac{1}{2}\mu U >> \frac{P_o}{\rho_o} \tag{D8}$$

Equation (19) will clearly be satisfied if:

$$\frac{1}{2}(\mu U)_{min} >> \frac{P_o}{\rho_o} \tag{D9}$$

or if**:

$$R' \equiv \frac{\frac{1}{2}(\mu U)_{min}}{P_o/\rho_o} >> 1 \tag{D10}$$

---

*In most cases R >> 100; Equation (19) is thereby an excellent assumption.

**Since U > μ, generally, Equation (D9) is clearly less stringent than Equation (D5) in satisfying Equation (19).

Using Equation (D10) calculations of R' were made for A-III, A-IV, Al and Pb. The results appear in Table D2.

Since $R' > 100$ for Al and Pb, Equation (19) is satisfied to 1% in these two cases. The values of R' for A-III and A-IV in Table D2 indicate that Equation (19) is considerably less well satisfied for these substances than for any of the others. However, even in these cases the assumption is valid within $\sim$ 5% and $\sim$2%, respectively.

Table D2

VALIDITY OF EQUATION (19) USING EQUATION (D10)

Substance	$\sim P_o/\rho_o$ - $cm^2/sec^2 \times 10^{-6}$	$\sim 1/2(U\mu)_{min}$ - $cm^2/sec^2 \times 10^{-6}$	R'
A-III	1070	20400	19
A-IV	1455	62600	43
Al	0.37	98	265
Pb	0.088	183	2080

Appendix E

New Way to Compute Temperatures along the Hugoniot

Consider the shaded molecule in Figure 4 in the final equilibrium state at L_e, a layer far removed from the shock front. The structure has relaxed from the (abnormal) state at L_1 and the molecules have redistributed themselves to new equilibrium positions with characteristic spacing z_e.

From Equation (30):

$$\Delta E^{(2)}_{\text{thermal}} = - \Delta E^{(2)}_{\text{configurational}} \tag{30}$$

and following the development of Equation (32):

$$\Delta E^{(2)}_{\text{configurational}} = \frac{N}{M} [\Phi^{L_e} - \Phi^{L_1}] \tag{E1}$$

Each of the potentials in Equation (E1) may be further broken down by consideration of Figures E1a and E1b (see Figures 5a and 5b) where the effect of each of the several regions is shown. From superposition:

$$\Phi^{L_1} = \Phi_1^{L_1}(R) + \Phi_2^{L_1}(R-R') + \Phi_3^{L_1} + \Phi_4^{L_1} + \Phi_5^{L_1}(R'') \tag{E2}$$

$$\Phi^{L_e} = \Phi_1^{L_e}(R''+R) + \Phi_2^{L_e}(R''+R-R') + \Phi_3^{L_e}(R'') + \Phi_4^{L_e} + \Phi_5^{L_e} \tag{E3}$$

Since R'' is large (i.e., L_e is far removed from the shock front) it is clear that:

$$\Phi_5^{L_1}(R'') \cong 0 \tag{E4}$$

and from Equations (39) - (43):

Figure E1a

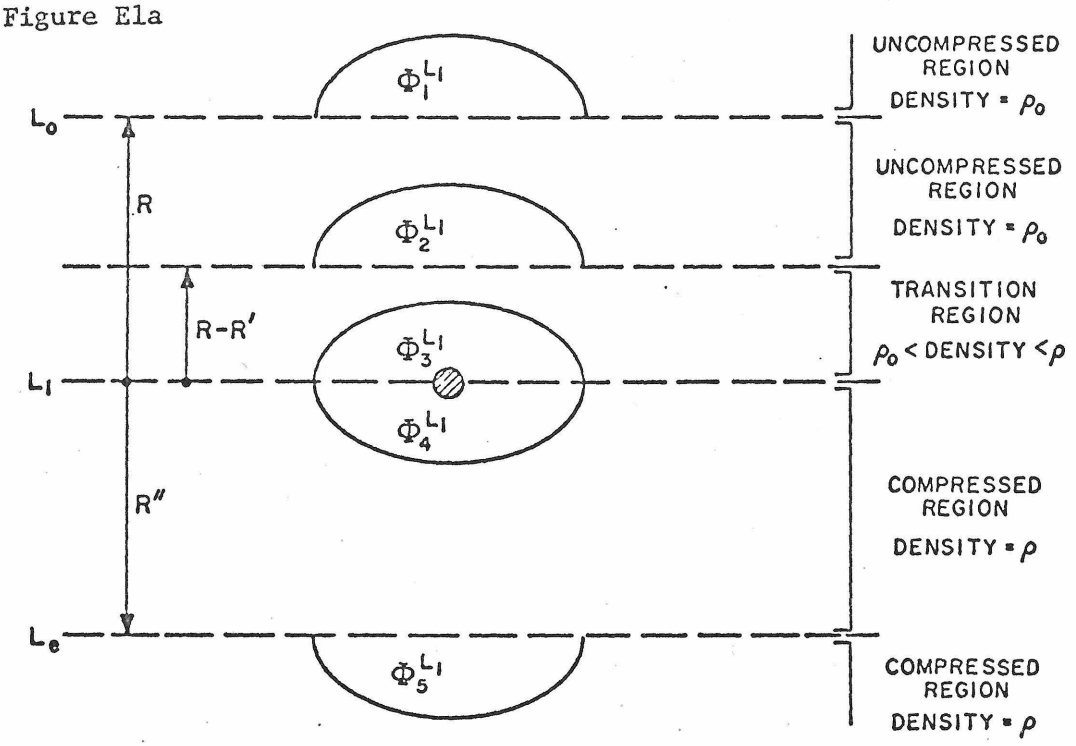

Figure E1b

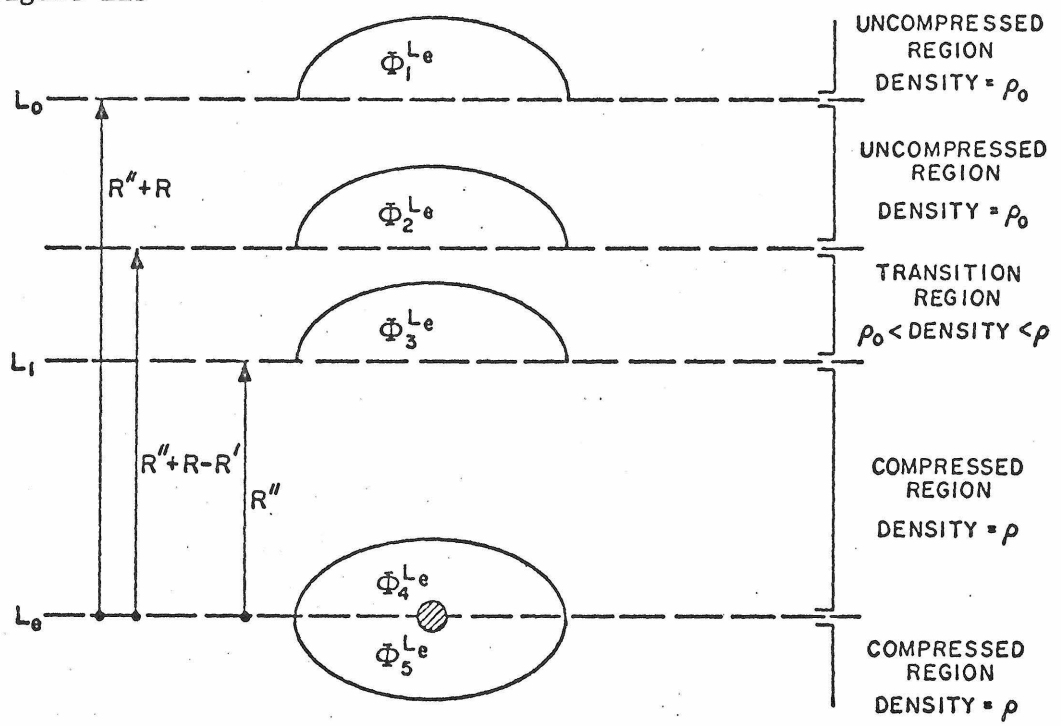

Figure E1. Potentials for Shaded Molecule

$$\Phi^{L_1} \simeq \Phi_2^{L_o} + \Phi_4^{L_1} \tag{E5}$$

By the same reasoning in Figure E1b:

$$\Phi_1^{L_e}(R''+R) \simeq \Phi_2^{L_e}(R''+R-R') \simeq \Phi_3^{L_e}(R'') \simeq 0 \tag{E6}$$

and:

$$\Phi_4^{L_e} \simeq \Phi_5^{L_e} \tag{E7}$$

leading to:

$$\Phi^{L_e} \simeq 2\Phi_5^{L_e} \tag{E8}$$

Substituting Equations (E5) and (E8) into Equation (E1) gives:

$$\Delta E^{(2)}_{\text{configurational}} = \frac{N}{M}\left[2\Phi_5^{L_e} - \Phi_2^{L_o} - \Phi_4^{L_1}\right] \tag{E9}$$

The reasoning leading to Equation (E9) may be summarized as follows. The molecule at L_1 "sees" above it a medium of density ρ_o (except for the transition region which is assumed small) at a distance z_o. Below it is a medium of density ρ at a distance z. The molecule in L_e "sees" above and below it a medium of density ρ but at a distance z_e (instead of z)*.

---

* Thus $\Phi_5^{L_1} (= \Phi_4^{L_e}) \neq \Phi_4^{L_1}$.

Following Equations (45) and (46):

$$\Phi_4^{L_1} = \psi(\rho,z) + \psi^{L_1}(z_o) \tag{45}$$

$$\Phi_2^{L_o} = \psi(\rho_o,z_o) + \psi^{L_o}(z_o) \tag{46}$$

$$\Phi_5^{L_e} = \psi(\rho,z_e) + \psi^{L_e}(z_e) \tag{E10}$$

where $\psi(\rho,z)$ is the configurational energy of a single isolated molecule positioned a distance z from a semi-infinite medium of density ρ, and $\psi^{L_1}(z_o), \psi^{L_o}(z_o)$ and $\psi^{L_e}(z_e)$ are the configurational energy contributions of the <u>other</u> molecules in layers L_1, L_o and L_e respectively*. Noting Equation (47) substitution of Equations (45), (46) and (E10) into Equation (E9) gives:

$$\Delta E^{(2)}_{\text{configurational}} = \frac{N}{M}[\, 2\psi(\rho,z_e) - \psi(\rho,z) - \psi(\rho_o,z_o) + 2\psi^{L_e}(z_e) - 2\psi^{L_o}(z_o)\,] \tag{E11}$$

The second and third terms of Equation (E11) are given directly by Equations (78) and (79) for the pair potential in Equation (72). The first term of Equation (E11) is given by Equation (78) with $z' = z_e$. The last two terms of Equation (E11) may be evaluated from the two-dimensional counterpart of Equation (50) and the assumed pair

---

*Note that in L_1 the adjacent molecules remain at z_o throughout the transition. This is not true in L_e where relaxation has taken place. In this case the adjacent molecules are at z_e.

potential, Equation (72).

In order to completely define the right-hand-side of Equation (E11) the relations z_o vs. ρ_o, z vs. ρ and z_e vs. ρ must be specified. The first two relationships are given by Equations (88) and (92) respectively and are:

$$z_o = (M/2^s \rho_o N)^{1/3} \tag{88}$$

$$z/z_o = \rho_o/\rho \tag{92}$$

If it is assumed that the structure factor s is a constant (i.e., that the structure in the equilibrium state is the same as in the uncompressed state) then z_e is given directly by the counterpart of Equation (88)*:

$$z_e = (M/2^s \rho N)^{1/3} \tag{E12}$$

Therefore for a given shock state (i.e., for given values of ρ) all the terms in Equation (E11) may be evaluated and $\Delta E^{(2)}_{\text{configurational}}$ determined. From Equation (30) this determines $\Delta E^{(2)}_{\text{thermal}}$.

From Appendix B :

$$dE = \left(\frac{\partial E}{\partial V}\right)_T dV + C_V dT \tag{B4}$$

where $V = 1/\rho$. Since there are no pressure/density changes taking place between L_1 and L_e, $dV = 0$ and Equation (B4)

---

*Of course, since Equation (E12) is generally applicable it may be used even if s changes, if the new value is known.

becomes*:

$$dE = C_V dT \tag{E13}$$

and integration gives**:

$$\Delta E = \int_{T_o}^{T} C_V dT \tag{E14}$$

Equating ΔE with $\Delta E^{(2)}_{\text{thermal}}$ gives:

$$\int_{T_o}^{T} C_V dT = \Delta E^{(2)}_{\text{thermal}} = - \Delta E^{(2)}_{\text{configurational}} \tag{E15}$$

which, along with Equations (E11), (78), (79), (88), (92), (E12) and the two-dimensional counterpart of Equation (50), uniquely defines the temperature T for a given value of ρ.

---

*Considering the non-equilibrium state at L_1 the applicability of Equation (84) (derived from basic thermodynamics) to changes taking place from L_1 to L_e is not assured.

**Since there is no temperature change across the shock front, $T = T_o$ at L_1.

Appendix F

Derivation of Equations (69) and (70)

Equations (65) - (68) are:

$$\phi(r) = ar^{-n} - br^{-6} \tag{65}$$

$$\phi(\sigma) = 0 \tag{66}$$

$$\phi(r_o) = -\varepsilon \tag{67}$$

$$\left[\frac{d\phi(r)}{dr}\right]_{r=r_o} = 0 \tag{68}$$

Use of Equation (66) in Equation (65) gives:

$$\phi(\sigma) = 0 = a\sigma^{-n} - b\sigma^{-6} \tag{F1}$$

or:

$$\frac{a}{b} = \sigma^{n-6} \tag{F2}$$

Differentiating Equation (65) gives:

$$\frac{d\phi(r)}{dr} = -nar^{-n-1} + 6br^{-7} \tag{F3}$$

and applying Equation (68) gives:

$$0 = -nar_o^{-n-1} + 6br_o^{-7} \tag{F4}$$

or:

$$r_o^{n-6} = \left(\frac{n}{6}\right)\left(\frac{a}{b}\right) \tag{F5}$$

$$r_o = \left(\frac{n}{6}\right)^{\frac{1}{n-6}} \left(\frac{a}{b}\right)^{\frac{1}{n-6}} \tag{F6}$$

Using Equation (F2) gives:

$$r_o = \left(\frac{n}{6}\right)^{\frac{1}{n-6}} \sigma \tag{70}$$

which is Equation (70).

Use of Equation (67) in Equation (65) gives:

$$-\varepsilon = a r_o^{-n} - b r_o^{-6} \tag{F7}$$

Substituting for a from Equation (F2) and for r_o from Equation (70) gives:

$$-\varepsilon = b\sigma^{n-6}\left(\frac{n}{6}\right)^{-\frac{n}{n-6}} \sigma^{-n} - b\left(\frac{n}{6}\right)^{-\frac{6}{n-6}} \sigma^{-6} \tag{F8}$$

$$-\varepsilon = b\sigma^{-6}\left[\left(\frac{n}{6}\right)^{-\frac{n}{n-6}} - \left(\frac{n}{6}\right)^{-\frac{6}{n-6}}\right] \tag{F9}$$

Now:

$$\left(\frac{n}{6}\right)^{-\frac{n}{n-6}} - \left(\frac{n}{6}\right)^{-\frac{6}{n-6}} = \left(\frac{n}{6}\right)^{-\frac{n}{n-6}}\left[1 - \left(\frac{n}{6}\right)^{-\frac{6}{n-6}}\left(\frac{n}{6}\right)^{\frac{n}{n-6}}\right] \tag{F10}$$

or:

$$\left(\frac{n}{6}\right)^{-\frac{n}{n-6}} - \left(\frac{n}{6}\right)^{-\frac{6}{n-6}} = \left(\frac{n}{6}\right)^{-\frac{n}{n-6}}\left[1 - \frac{n}{6}\right] \tag{F11}$$

and Equation (F9) becomes:

$$-\varepsilon = b\sigma^{-6}\left(\frac{n}{6}\right)^{-\frac{n}{n-6}}\left[1 - \frac{n}{6}\right] \tag{F12}$$

so that:

$$b = \frac{\varepsilon \left(\frac{n}{6}\right)^{\frac{n}{n-6}} \sigma^6}{\left(\frac{n}{6} - 1\right)} \tag{F13}$$

From Equation (F2):

$$a = b\sigma^{n-6} = \frac{\varepsilon \left(\frac{n}{6}\right)^{\frac{n}{n-6}} \sigma^n}{\left(\frac{n}{6} - 1\right)} \tag{F14}$$

Substituting Equations (F13) and (F14) into Equation (65) gives:

$$\phi(r) = \frac{\varepsilon \left(\frac{n}{6}\right)^{\frac{n}{n-6}} \sigma^n r^{-n}}{\left(\frac{n}{6} - 1\right)} - \frac{\varepsilon \left(\frac{n}{6}\right)^{\frac{n}{n-6}} \sigma^6 r^{-6}}{\left(\frac{n}{6} - 1\right)} \tag{F15}$$

or:

$$\phi(r) = \frac{\varepsilon \left(\frac{n}{6}\right)^{\frac{n}{n-6}}}{\left(\frac{n}{6} - 1\right)} \left[\left(\frac{\sigma}{r}\right)^n - \left(\frac{\sigma}{r}\right)^6\right] \tag{69}$$

which is Equation (69).

Appendix G

Derivation of Equation (73)

Equation (69) is:

$$\phi(r) = \varepsilon \frac{(\frac{n}{6})^{\frac{n}{n-6}}}{(\frac{n}{6}-1)} \left[(\frac{\sigma}{r})^n - (\frac{\sigma}{r})^6\right] \tag{69}$$

which may be written in the form:

$$\phi(r) = \varepsilon (\frac{n}{6})^{\frac{n}{n-6}} \left[\frac{(\frac{\sigma}{r})^n - (\frac{\sigma}{r})^6}{\frac{n}{6} - 1}\right] \tag{G1}$$

Taking the limit as $n \to 6$ gives:

$$\phi_6(r) = \lim_{n \to 6} \phi(r) = \lim_{n \to 6} \varepsilon(\frac{n}{6})^{\frac{n}{n-6}} \left[\frac{(\frac{\sigma}{r})^n - (\frac{\sigma}{r})^6}{\frac{n}{6} - 1}\right] \tag{G2}$$

Since the limit of a product is the product of the limits[161] this may be written:

$$\phi_6(r) = \varepsilon \lim_{n \to 6} (\frac{n}{6})^{\frac{n}{n-6}} \lim_{n \to 6} \left[\frac{(\frac{\sigma}{r})^n - (\frac{\sigma}{r})^6}{\frac{n}{6} - 1}\right] \tag{G3}$$

Therefore:

$$\phi_6(r) \implies \varepsilon \lim_{n \to 6} (\frac{n}{6})^{\frac{n}{n-6}} \frac{0}{0} \tag{G4}$$

which is an indeterminate form. The first limit may be evaluated as follows:

$$\lim (\frac{n}{6})^{\frac{n}{n-6}} \implies 1^{\infty} \tag{G5}$$

Let:

$$\left(\frac{n}{6}\right)^{\frac{n}{n-6}} = e^{\ln\left(\frac{n}{6}\right)^{\frac{n}{n-6}}} = e^{\left(\frac{n}{n-6}\right)\ln\left(\frac{n}{6}\right)} \tag{G6}$$

Then:

$$\lim_{n \to 6} f_1(n) = \lim_{n \to 6} \left(\frac{n}{6}\right)^{\frac{n}{n-6}} = \lim_{n \to 6} e^{\left(\frac{n}{n-6}\right)\ln\left(\frac{n}{6}\right)} = e^{\lim\limits_{n \to 6}\left(\frac{n}{n-6}\right)\ln\left(\frac{n}{6}\right)} \tag{G7}$$

or:

$$\lim_{n \to 6} f_1(n) = e^{\lim\limits_{n \to 6} \frac{n\left(\frac{n}{6}\right)}{\left(\frac{n-6}{n}\right)}} \Longrightarrow e^{\frac{0}{0}} \tag{G8}$$

which is an indeterminate form for which L'Hôspital's rule[15] applies.

Differentiating numerator and denominator with respect to n gives:

$$\lim_{n \to 6} f_1(n) = e^{\lim\limits_{n \to 6} \frac{1/n}{6/n^2}} = e^{\lim\limits_{n \to 6} \frac{n}{6}} = e \tag{G9}$$

Clearly the first limit exists and Equation (G4) becomes:

$$\phi_6(r) \Longrightarrow \varepsilon\, e^{\frac{0}{0}} \tag{G10}$$

Therefore from Equation (G3) and L'Hôspital's rule:

$$\phi_6(r) = \varepsilon\, e^{\lim\limits_{n \to 6} \frac{\left(\frac{\sigma}{r}\right)^n \ln\left(\frac{\sigma}{r}\right)}{1/6}} \tag{G11}$$

or:

$$\phi_6(r) = 6\varepsilon\, e^{\left(\frac{\sigma}{r}\right)^6 \ln\left(\frac{\sigma}{r}\right)} \tag{73}$$

which is Equation (73).

Equation (70) is:

$$r_o = \left(\frac{n}{6}\right)^{\frac{1}{n-6}} \sigma \tag{70}$$

As $n \to 6$ this becomes:

$$r_o = \lim_{r \to 6} \left(\frac{n}{6}\right)^{\frac{1}{n-6}} \sigma \tag{G12}$$

or:

$$r_o/\sigma \implies 1^{\infty} \tag{G13}$$

Let:

$$\left(\frac{n}{6}\right)^{\frac{1}{n-6}} = e^{\ell n\left(\frac{n}{6}\right)^{\frac{1}{n-6}}} = e^{\left(\frac{1}{n-6}\right) \ell n\left(\frac{n}{6}\right)} = e^{\frac{\ell n\left(\frac{n}{6}\right)}{n-6}} \tag{G14}$$

Therefore:

$$\lim_{n \to 6} \left(\frac{n}{6}\right)^{\frac{1}{n-6}} = \lim_{n \to 6} e^{\frac{\ell n\left(\frac{n}{6}\right)}{n-6}} = e^{\lim_{n \to 6} \frac{\ell n\left(\frac{n}{6}\right)}{n-6}} \implies e^{\frac{0}{0}} \tag{G15}$$

Applying L'Hôspital's rule gives:

$$\lim_{n \to 6} \left(\frac{n}{6}\right)^{\frac{1}{n-6}} = e^{\lim_{n \to 6} \frac{1/n}{1}} = e^{1/6} \tag{G16}$$

Equation (G12) becomes:

$$r_o = e^{1/6} \sigma \quad , \quad \sigma/r_o = e^{-1/6} \tag{G17}$$

Therefore from Equation (73):

$$\phi_6(r_o) = 6\varepsilon \, e\left(\frac{\sigma}{r_o}\right)^6 \ell n\left(\frac{\sigma}{r_o}\right) \tag{G18}$$

or using Equation (G17):

$$\phi_6(r_o) = 6\varepsilon e(e^{-1/6})^6 \ln(e^{-1/6}) = \cancel{6}\cancel{\varepsilon}\cancel{e}(\frac{1}{\cancel{e}})(-\frac{1}{\cancel{6}}\ln e) \qquad (G19)$$

or:

$$\phi_6(r_o) = -\varepsilon$$

which was to be shown. Also from Equation (73):

$$\frac{d\phi_6(r)}{dr} = 6\varepsilon e \left[(\frac{\sigma}{r})^6 (\frac{r}{\sigma})(-\frac{\sigma}{r^2}) + 6(\frac{\sigma}{r})^5 (-\frac{\sigma}{r^2}) \ln(\frac{\sigma}{r})\right] \qquad (G20)$$

or:

$$\frac{d\phi_6(r)}{dr} = -6\varepsilon e(\frac{\sigma}{r})^6 (\frac{1}{r}) [1 + 6 \ln(\frac{\sigma}{r})] \qquad (G21)$$

Therefore:

$$\left[\frac{d\phi_6(r)}{dr}\right]_{r=r_o} = -6\varepsilon e(\frac{\sigma}{r_o})^6 (\frac{1}{r_o}) [1 + 6 \ln(\frac{\sigma}{r_o})] \qquad (G22)$$

From Equation (G17) this becomes:

$$\left[\frac{d\phi_6(r)}{dr}\right]_{r=r_o} = -6\varepsilon e(e^{-1/6})^6 (\frac{1}{e^{1/6}\sigma})[1 + 6 \ln(e^{-1/6})] \qquad (G23)$$

$$\left[\frac{d\phi_6(r)}{dr}\right]_{r=r_o} = -\frac{6\varepsilon}{e^{1/6}\sigma}[1 - 1] = 0$$

which was to be shown. Also from Equation (73):

$$\phi_6(\sigma) = 6\varepsilon e(\frac{\sigma}{\sigma})^6 \ln(\frac{\sigma}{\sigma}) = 0$$

which was to be shown.

The long range behavior of Equation (73) may be determined from:

$$\phi_6(\infty) = \lim_{r \to \infty} \phi_6(r) = \lim_{r \to \infty} 6\varepsilon e\left(\frac{\sigma}{r}\right)^6 \ell n\left(\frac{\sigma}{r}\right) \tag{G24}$$

or:

$$\phi_6(\infty) = -6\varepsilon e\sigma^6 \lim_{r \to \infty} \frac{\ell n\left(\frac{r}{\sigma}\right)}{r^6} \Longrightarrow \frac{\infty}{\infty} \tag{G25}$$

Applying L'Hôspital's rule gives:

$$\phi_6(\infty) = -6\varepsilon e\sigma^6 \lim_{r \to \infty} \frac{1/r}{6r^5} = -\varepsilon e\sigma^6 \lim_{r \to \infty} \frac{1}{r^6} \tag{G26}$$

or:

$$\phi_6(\infty) = -0 \tag{G27}$$

which matches the behavior of Equation (69) (see Figure 8).

Appendix H

Derivation of Equation (75)

Equation (69) is:

$$\phi(r) = \varepsilon \frac{(\frac{n}{6})^{\frac{n}{n-6}}}{(\frac{n}{6} - 1)} [(\frac{\sigma}{r})^n - (\frac{\sigma}{r})^6] \tag{69}$$

Taking the limit as $n \to 0$ gives:

$$\phi_o(r) = \lim_{n \to 0} \phi(r) = \lim_{n \to 0} \varepsilon \frac{(\frac{n}{6})^{\frac{n}{n-6}}}{(\frac{n}{6} - 1)} [(\frac{\sigma}{r})^n - (\frac{\sigma}{r})^6] \tag{H1}$$

Since the limit of a product is the product of the limits[161] this becomes:

$$\phi_o(r) = \varepsilon \lim_{n \to 0} (\frac{n}{6})^{\frac{n}{n-6}} \lim_{n \to 0} \frac{[(\frac{\sigma}{r})^n - (\frac{\sigma}{r})^6]}{(\frac{n}{6} - 1)} \tag{H2}$$

or:

$$\phi_o(r) = \varepsilon[(\frac{\sigma}{r})^6 - 1] \lim_{n \to 0} (\frac{n}{6})^{\frac{n}{n-6}} \tag{H3}$$

The remaining limit may be evaluated as follows.

$$\lim_{n \to 0} (\frac{n}{6})^{\frac{n}{n-6}} \Longrightarrow 0^o \tag{H4}$$

Let:

$$(\frac{n}{6})^{\frac{n}{n-6}} = e^{\ln(\frac{n}{6})^{\frac{n}{n-6}}} = e^{(\frac{n}{n-6}) \ln(\frac{n}{6})} \tag{H5}$$

Therefore:

$$\lim_{n \to 0} (\frac{n}{6})^{\frac{n}{n-6}} = \lim_{n \to 0} e^{(\frac{n}{n-6}) \ln(\frac{n}{6})} = e^{\lim_{n \to 0} (\frac{n}{n-6}) \ln(\frac{n}{6})} \tag{H6}$$

or:

$$\lim_{n \to 0} \left(\frac{n}{6}\right)^{\frac{n}{n-6}} = e^{\lim_{n \to 0} \frac{\ell n(\frac{6}{n})}{(\frac{6-n}{n})}} \Longrightarrow e^{\frac{\infty}{\infty}} \tag{H7}$$

Applying L'Hôspital's rule gives:

$$\lim_{n \to 0} \left(\frac{n}{6}\right)^{\frac{n}{n-6}} = e^{\lim_{n \to 0} \frac{-1/n}{-6/n^2}} = e^{\lim_{n \to 0} \frac{n}{6}} = e^{o} = 1 \tag{H8}$$

Substituting Equation (H8) into Equation (H3) gives:

$$\phi_o(r) = \varepsilon \left[\left(\frac{\sigma}{r}\right)^6 - 1\right] \tag{75}$$

which is Equation (75).

Equation (70) is:

$$r_o = \left(\frac{n}{6}\right)^{\frac{n}{n-6}} \sigma \tag{70}$$

As $n \to 0$ this becomes:

$$r_o = \lim_{n \to 0} \left(\frac{n}{6}\right)^{\frac{n}{n-6}} \sigma = (0)^{\frac{1}{0-6}} \sigma = (0)^{-1/6} \sigma \tag{H9}$$

or:

$$r_o = \left(\frac{1}{0}\right)^{1/6} \sigma \Longrightarrow \infty \tag{H10}$$

This implies that $\phi_o(r)$ has no minimum and is thus "degenerate" in form. However, from Equation (75):

$$\phi_o(r_o) = \phi_o(\infty) = \varepsilon[0 - 1] = -\varepsilon \tag{H11}$$

which is compatible with Equation (67). Also from Equation (75):

$$\frac{d\phi_o(r)}{dr} = \varepsilon\sigma^6(-6)\ r^{-7} = -\frac{6\varepsilon\sigma^6}{r^7} \tag{H12}$$

and:

$$\left[\frac{d\phi_o(r)}{dr}\right]_{r=r_o} = \left[\frac{d\phi_o(r)}{dr}\right]_{r=\infty} = 0 \tag{H13}$$

which is compatible with Equation (68). Also from Equation (75):

$$\phi_o(\sigma) = \varepsilon[(\frac{\sigma}{\sigma})^6 - 1] = 0 \tag{H14}$$

which is compatible with Equation (66). The long range behavior of Equation (75) may be determined from:

$$\phi_o(\infty) = \varepsilon[0 - 1] = -\varepsilon \tag{H15}$$

which confirms that $\phi_o(r)$ has no minimum (i.e., $r_o \Rightarrow \infty$) . A plot of $\phi_o(r)$ is shown in Figure H1.

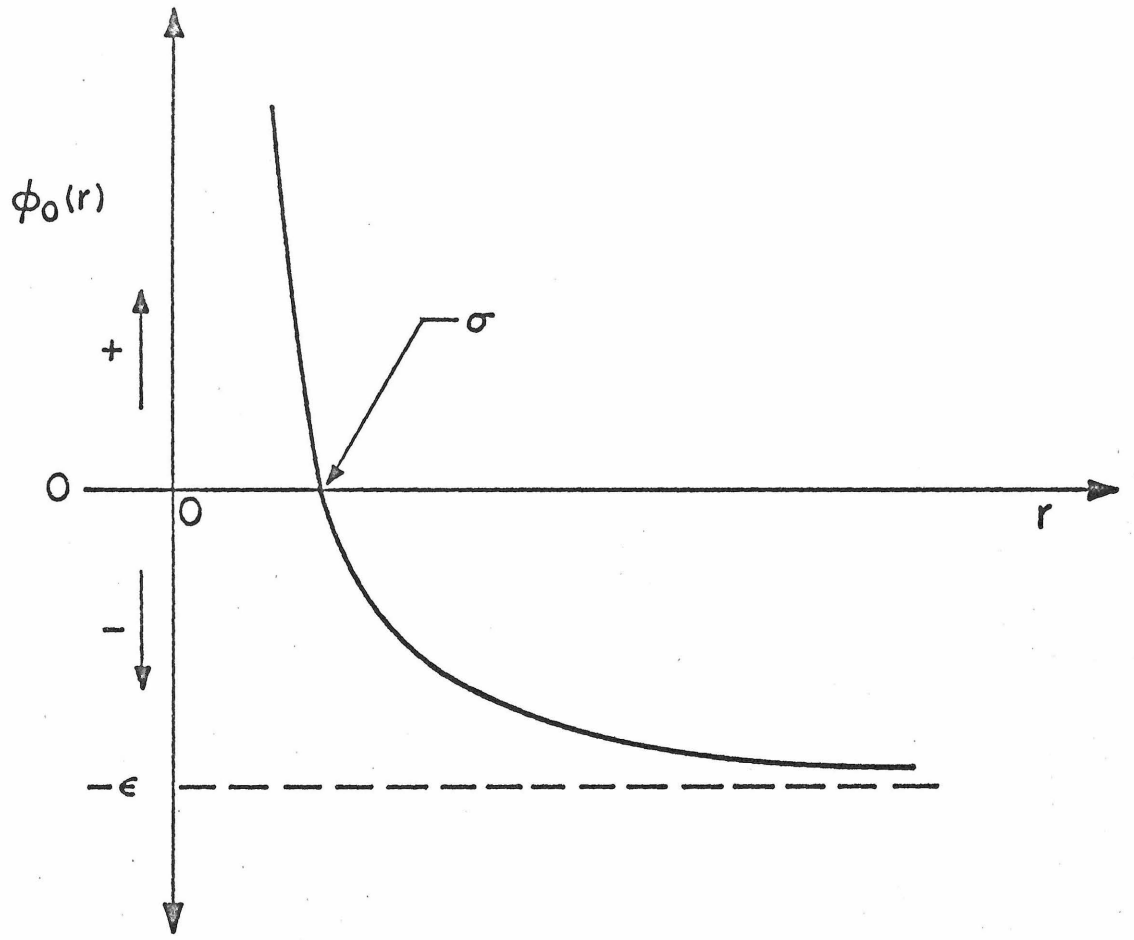

Figure H1. $\phi_o(r)$ vs. r

Appendix I

Proof of Monotonicity of $\phi(r)$

Equation (69) is:

$$\phi(r) = \frac{(\frac{n}{6})^{\frac{n}{n-6}}}{(\frac{n}{6} - 1)} [(\frac{\sigma}{r})^n - (\frac{\sigma}{r})^6] \tag{69}$$

Let:

$$\omega = \sigma/r \tag{I1}$$

and note that since we are considering the repulsive region:

$$\omega > 1 \tag{I2}$$

Noting Equation (I1) and dividing through by ε gives:

$$\frac{\phi(r)}{\varepsilon} = \frac{(\frac{n}{6})^{\frac{n}{n-6}}}{(\frac{n}{6} - 1)} (\omega^n - \omega^6) \tag{I3}$$

Clearly if $\phi(r)/\varepsilon$ is monotonically increasing with n, $\phi(r)$ is also, and we may define:

$$\psi(\omega) = \psi = \frac{\phi(r)}{\varepsilon} \tag{I4}$$

Equation (I4) becomes:

$$\psi = \frac{(\frac{n}{6})^{\frac{n}{n-6}}}{(\frac{n}{6} - 1)} (\omega^n - \omega^6) \tag{I5}$$

Consider first the question: Is ψ monotonically increasing in the interval from $n = 0$ to $n = 6$?

Noting that, in this case, $(n/6 - 1) \leq 0$ and $(\omega^n - \omega^6) \leq 0$ (since $\omega > 1$), Equation (I5) may be rearranged to:

$$\psi = \frac{(\frac{n}{6})^{\frac{n}{n-6}}}{(1 - \frac{n}{6})} (\omega^6 - \omega^n) = 6 \frac{(\frac{6}{n})^{\frac{n}{6-n}}}{(6 - n)} (\omega^6 - \omega^n) \tag{I6}$$

or:

$$\psi = 6 \left[(\frac{6}{n})^{\frac{n}{6-n}} \right] \left[\frac{\omega^6 - \omega^n}{6 - n}\right] \tag{I7}$$

If both factors of Equation (I7) are monotonically increasing with n from 0 to 6, then ψ is also. This can be examined by finding a lower limit of each factor at $n = 0$ and an upper limit at $n = 6$ and then proving monotonicity between these limits.

Consider the first factor $(\frac{6}{n})^{n/6-n}$. The lower limit is given by:

$$\lim_{n \to 0} (\frac{6}{n})^{\frac{n}{6-n}} = \lim_{n \to 0} (\frac{n}{6})^{\frac{n}{n-6}} \tag{I8}$$

and from Equation (H8):

$$\lim_{n \to 0} (\frac{6}{n})^{\frac{n}{6-n}} = 1 \tag{I9}$$

The upper limit is given by:

$$\lim_{n \to 6} (\frac{6}{n})^{\frac{n}{6-n}} = \lim_{n \to 6} (\frac{n}{6})^{\frac{n}{n-6}} \tag{I10}$$

and from Equations (G6) - (G9):

$$\lim_{n \to 6} \left(\frac{6}{n}\right)^{\frac{n}{6-n}} = e \qquad \text{(I11)}$$

If the factor is monotonic $\partial/\partial n$ is always > 0 in the interval.

$$\frac{\partial \left(\frac{6}{n}\right)^{\frac{n}{6-n}}}{\partial n} = \left(\frac{n}{6-n}\right)\left(\frac{6}{n}\right)^{\frac{n}{6-n}-1}\left(\frac{-6}{n^2}\right) + \left(\frac{6}{n}\right)^{\frac{n}{6-n}} \ln\left(\frac{6}{n}\right) \frac{(6-n) - n(-1)}{(6-n)^2} \qquad \text{(I12)}$$

or:

$$\frac{\partial \left(\frac{6}{n}\right)^{\frac{n}{6-n}}}{\partial n} = \left(\frac{6}{n}\right)^{\frac{n}{6-n}} \left[- \left(\frac{\cancel{n}}{6-n}\right)\left(\frac{\cancel{n}}{\cancel{6}}\right)\left(\frac{\cancel{6}}{\cancel{n}^2}\right) + \ln\left(\frac{6}{n}\right) \frac{6}{(6-n)^2}\right] \qquad \text{(I13)}$$

$$\frac{\partial \left(\frac{6}{n}\right)^{\frac{n}{6-n}}}{\partial n} = \left(\frac{1}{6-n}\right)\left(\frac{6}{n}\right)^{\frac{n}{6-n}} \left[\left(\frac{6}{6-n}\right) \ln\left(\frac{6}{n}\right) - 1\right] \qquad \text{(I14)}$$

Since (for $n < 6$) the first two factors must be > 0 it is only necessary to show that:

$$\left(\frac{6}{6-n}\right) \ln\left(\frac{6}{n}\right) > 1 \qquad \text{(I15)}$$

to meet the requirement (i.e., that $\partial/\partial n > 0$) *.

---

*For $n=6$ Equation (I14) becomes:

$$\frac{\partial \left(\frac{6}{n}\right)^{\frac{n}{n-6}}}{\partial n} = \lim_{n \to 6} \left(\frac{1}{6-n}\right)\left(\frac{6}{n}\right)^{\frac{n}{6-n}} \left[\left(\frac{6}{6-n}\right) \ln\left(\frac{6}{n}\right) - 1\right]$$

$$= \lim_{n \to 6} \left(\frac{6}{n}\right)^{\frac{n}{6-n}} \lim_{n \to 6} \left[\frac{\ln\left(\frac{6}{n}\right)^{\frac{n}{6-n}} - 1}{6 - n}\right]$$

$$= \lim_{n \to 6} \left(\frac{6}{n}\right)^{\frac{n}{6-n}} \lim_{n \to 6} \left[\frac{6 \ln\left(\frac{6}{n}\right) - (6-n)}{(6-n)^2}\right] \Rightarrow [1^{\infty}] \cdot \left[\frac{0}{0}\right] \qquad \text{(continued)}$$

Equation (I15) may be written:

$$\ell n(\frac{6}{n}) > \frac{6-n}{6} \tag{I16}$$

From a Taylor series expansion[127] of $\ell n\, u$:

$$\ell n\, u = \frac{u-1}{u} + \frac{1}{2}(\frac{u-1}{u})^2 + \frac{1}{3}(\frac{u-1}{u})^3 + \cdots , \quad u > \frac{1}{2} \tag{I17}$$

If u is set equal to $6/n$ then the condition on Equation (I17) is met over the whole range of n since $u = \frac{6}{n} > 1$. Further, since $u > 1$ each of the terms of Equation (I17) is > 0 and the expansion may be written:

$$\ell n\, u = \frac{u-1}{u} + R \quad , \qquad R > 0 \tag{I18}$$

Since $u = 6/n$ this becomes:

$$\ell n(\frac{6}{n}) = \frac{\frac{6}{n} - 1}{\frac{6}{n}} + R \tag{I19}$$

or:

$$\ell n(\frac{6}{n}) = \frac{6-n}{6} + R \tag{I20}$$

---

*(continued)

From Equation (I11) and L'Hôspital's rule:

$$= e \cdot \lim_{n \to 6} \frac{-6/n + 1}{2(6-n)(-1)} \Rightarrow e \cdot [\frac{0}{0}]$$

$$= e \cdot \lim_{n \to 6} \frac{6/n^2}{-2(-1)} = e/12 > 0$$

which meets the requirement.

Substituting Equation (I20) into Equation (I16) gives:

$$\frac{6-n}{6} + R > \frac{6-n}{6} \tag{I21}$$

and the requirement is clearly met. Therefore the first factor, $(\frac{6}{n})^{\frac{n}{6-n}}$ is monotonically increasing with n.

Consider the second factor $(\frac{\omega^6 - \omega^n}{6 - n})$. The lower and upper limits are given by:

$$\lim_{n \to 0} (\frac{\omega^6 - \omega^n}{6 - n}) = \frac{\omega^6 - 1}{6} \tag{I22}$$

and:

$$\lim_{n \to 6} (\frac{\omega^6 - \omega^n}{6 - n}) \Rightarrow \frac{0}{0} = \lim_{n \to 6} -\frac{\omega^n \ln \omega}{-1} = \omega^6 \ln \omega \tag{I23}$$

It is first necessary to show that:

$$\omega^6 \ln \omega > \frac{\omega^6 - 1}{6} \tag{I24}$$

Rearrangement gives:

$$\ln \omega^6 > \frac{\omega^6 - 1}{\omega^6} \tag{I25}$$

From Equation (I17) we may set $u = \omega^6$ and, noting that $\omega > 1$, write:

$$\ln \omega^6 = \frac{\omega^6 - 1}{\omega^6} + R \quad , \quad R > 0 \tag{I26}$$

Substituting this into Equation (I25) gives:

$$\frac{\omega^6 - 1}{\omega^6} + R > \frac{\omega^6 - 1}{\omega^6} \tag{I27}$$

which demonstrates the validity of Equation (I24) (i.e., the upper

limit exceeds the lower limit). If the (second) factor is monotonic, $\partial/\partial n$ is always > 0 in the interval.

$$\frac{\partial\left(\frac{\omega^6 - \omega^n}{6-n}\right)}{\partial n} = \frac{(6-n)(-1)\omega^n \ell n\omega - (\omega^6 - \omega^n)(-1)}{(6-n)^2} \tag{I28}$$

or:

$$\frac{\partial\left(\frac{\omega^6 - \omega^n}{6-n}\right)}{\partial n} = \frac{(\omega^6 - \omega^n) - (6-n)\,\omega^n \ell n\omega}{(6-n)^2} \tag{I29}$$

In this case (for $n < 6$) it is necessary to show that*:

$$\omega^6 - \omega^n > (6-n)\,\omega^n \ell n\omega \tag{I30}$$

or:

$$\omega^{6-n} - 1 > \ell n\, \omega^{6-n} \tag{I31}$$

---

*For $n = 6$ Equation (I29) becomes:

$$\frac{\partial\left(\frac{\omega^6 - \omega^n}{6-n}\right)}{\partial n} = \lim_{n \to 6} \frac{(\omega^6 - \omega^n) - (6-n)\,\omega^n \ell n\omega}{(6-n)^2} \Rightarrow \frac{0}{0}$$

From L'Hôspital's rule:

$$\frac{\partial\left(\frac{\omega^6 - \omega^n}{6-n}\right)}{\partial n} = \lim_{n \to 6} -\frac{\omega^n \ell n\,\omega - (6-n)\omega^n (\ell n\,\omega)^2 - (-1)\omega^n \ell n\omega}{2(6-n)(-1)}$$

$$= \lim_{n \to 6} \frac{1}{2}\omega^n (\ell n\,\omega)^2 = \frac{1}{2}\omega^6 (\ell n\,\omega)^2 > 0$$

which meets the requirement.

Exponentiating both sides gives:

$$e^{\omega^{6-n}-1} > \omega^{6-n} \tag{I32}$$

The Taylor series expansion of e^u is[127]:

$$e^u = 1+u+\frac{u^2}{2!}+\frac{u^3}{3!}+\cdots \tag{I33}$$

Letting:

$$u = \omega^{6-n} - 1 \tag{I34}$$

this becomes:

$$e^{\omega^{6-n}-1} = 1 + \omega^{6-n} - 1 + R = \omega^{6-n} + R \tag{I35}$$

where $R > 0$ since $\omega > 1$ and thus $u > 0$. Substituting Equation (I35) into Equation (I32) gives:

$$\omega^{6-n} + R > \omega^{6-n} \tag{I36}$$

and the requirement is met for the second factor.

Since both the first and second factors of Equation (I7) are monotonically increasing, ψ and therefore $\phi(r)$ are monotonically increasing with n from $n = 0$ to $n = 6$.

The second question to address is: Is ψ monotonically increasing when $n > 6$ (i.e., to $n \to \infty$)?

In this case consider Equation (I5) in the form given. Rearrangement gives:

$$\psi = 6[(\frac{n}{6})^{\frac{n}{n-6}}][\frac{\omega^n - \omega^6}{n-6}] \tag{I37}$$

For the first factor the limits are:

$$\lim_{n \to 6} \left(\frac{n}{6}\right)^{\frac{n}{n-6}} = e \tag{I38}$$

from Equations (G6) - (G9) and:

$$\lim_{n \to \infty} \left(\frac{n}{6}\right)^{\frac{n}{n-6}} = \lim_{n \to \infty} \left(\frac{n}{6}\right)^{\frac{1}{1-\frac{6}{n}}} \Longrightarrow \infty \tag{I39}$$

As before, if the factor is monotonic, $\partial/\partial n > 0$.

$$\frac{\partial \left(\frac{n}{6}\right)^{\frac{n}{n-6}}}{\partial n} = \frac{n}{n-6}\left(\frac{n}{6}\right)^{\frac{n}{n-6}-1}\left(\frac{1}{6}\right) + \left(\frac{n}{6}\right)^{\frac{n}{n-6}} \ln\left(\frac{n}{6}\right) \frac{(n-6) - n}{(n-6)^2} \tag{I40}$$

or:

$$\frac{\partial \left(\frac{n}{6}\right)^{\frac{n}{n-6}}}{\partial n} = \left(\frac{n}{6}\right)^{\frac{n}{n-6}} \left[\left(\frac{\cancel{n}}{n-6}\right)\left(\frac{\cancel{6}}{\cancel{n}}\right)\left(\frac{1}{\cancel{6}}\right) - \frac{6}{(n-6)^2} \ln\left(\frac{n}{6}\right)\right] \tag{I41}$$

$$\frac{\partial \left(\frac{n}{6}\right)^{\frac{n}{n-6}}}{\partial n} = \left(\frac{1}{n-6}\right)\left(\frac{n}{6}\right)^{\frac{n}{n-6}} \left[1 - \left(\frac{6}{n-6}\right) \ln\left(\frac{n}{6}\right)\right] \tag{I42}$$

Since (for $n > 6$) the first two factors must be > 0 it remains to show that:

$$1 > \frac{6}{n-6} \ln\left(\frac{n}{6}\right) \tag{I43}$$

or:

$$\frac{n}{6} - 1 > \ln\left(\frac{n}{6}\right)$$

Exponentiating both sides:

$$e^{\frac{n}{6} - 1} > \frac{n}{6} \tag{I44}$$

From Equation (I33) this becomes:

$$1 + \frac{n}{6} - 1 + R > \frac{n}{6} \tag{I45}$$

where $R > 0$ (since $(\frac{n}{6} - 1) > 0$) . Therefore:

$$\frac{n}{6} + R > \frac{n}{6} \tag{I46}$$

and the requirement is met for the first factor.

For the second factor the limits are:

$$\lim_{n \to 6} \left(\frac{\omega^n - \omega^6}{n-6}\right) \Rightarrow \frac{0}{0} = \lim_{n \to 6} \omega^n \ell n\omega = \omega^6 \ell n\omega \tag{I47}$$

and:

$$\lim_{n \to \infty} \left(\frac{\omega^n - \omega^6}{n-6}\right) \Rightarrow \frac{\infty}{\infty} = \lim_{n \to \infty} \omega^n \ell n\omega \Rightarrow \infty \tag{I48}$$

If the factor is monotonic, $\partial/\partial n > 0$.

$$\frac{\partial\left(\frac{\omega^n - \omega^6}{n-6}\right)}{\partial n} = \frac{(n-6)\omega^n \ell n\, \omega - (\omega^n - \omega^6)}{(n-6)^2} \tag{I49}$$

In this case (for $n > 6$) it is necessary to show that:

$$(n-6)\omega^n \ell n\omega > \omega^n - \omega^6 \tag{I50}$$

or:

$$\ell n\, \omega^{n-6} > 1 - \omega^{6-n} \tag{I51}$$

Since $n > 6$ and $\omega > 1$, $\omega^{n-6} > 1$ and from Equation (I17):

$$\ell n\ \omega^{n-6} = \frac{\omega^{n-6} - 1}{\omega^{n-6}} + R \quad , \quad R > 0 \tag{I52}$$

Substituting into Equation (I51) gives:

$$1 - \omega^{6-n} + R > 1 - \omega^{6-n} \tag{I53}$$

which meets the requirement.

Since both the first and second factors of Equation (I37) are monotonically increasing, ψ and therefore $\phi(r)$ are monotonically increasing with n for all $n > 6$.

From this and the prior conclusion it is clear that $\phi(r)$ is monotonically increasing for all values of n from 0 to ∞ for $(\sigma/r) > 1$.

Appendix J

Derivation of Equations (78) - (80)

Equations (53), (54) and (72) are:

$$\psi(\rho,z) = (\rho N/M) \int_{z'=z}^{\infty} \int_{y'=0}^{\infty} \int_{x'=0}^{\infty} \phi(r)\, dx'dy'dz' \tag{53}$$

$$\psi(\rho_o,z_o) = (\rho_o N/M) \int_{z'=z_o}^{\infty} \int_{y'=0}^{\infty} \int_{x'=0}^{\infty} \phi(r)\, dx'dy'dz' \tag{54}$$

$$\phi(r) = \epsilon\, f(n)\, [(\frac{\sigma}{r})^n - (\frac{\sigma}{r})^6] \tag{72}$$

Transforming the Cartesian coordinate system (x',y',z') into a cylindrical coordinate system (p',θ',z') (still centered at the shaded molecule in Figure 6) gives for Equations (53) and (54):[167]

$$\psi(\rho,z) = (\rho N/M) \int_{z'=z}^{\infty} \int_{p'=0}^{\infty} \int_{\theta'=0}^{\infty} \phi(r)\, p'd\theta'dp'dz' \tag{J1}$$

$$\psi(\rho_o,z_o) = (\rho_o N/M) \int_{z'=z_o}^{\infty} \int_{p'=0}^{\infty} \int_{\theta'=0}^{\infty} \phi(r)\, p'd\theta'dp'dz' \tag{J2}$$

The interaction of the shaded molecule with the (cylindrical) volume element $p'd\theta'dp'dz'$ is pictured in Figure J1 in the (p',z') plane. Since $\phi(r)$ is generally independent of θ'* Equations (J1) and (J2)

---

*By definition (and notational form) $\phi(r)$ depends only on r, the distance between molecules, and not on spatial orientation. Therefore at a given value of r in Figure J1, $\phi(r)$ would be a constant for all values of θ'.

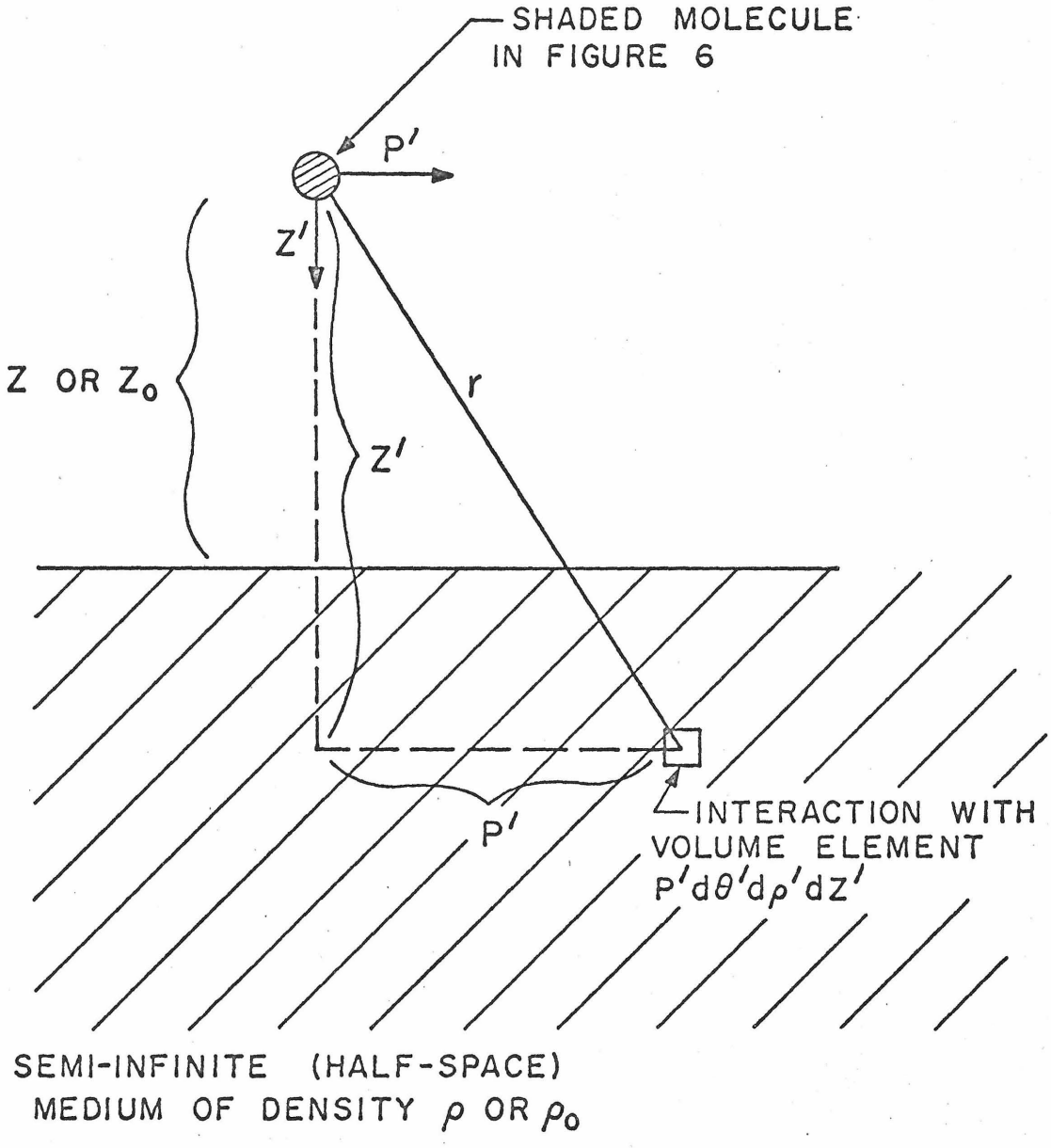

Figure J1. Interactions of the Shaded Molecule in the (p',z') Plane

may be integrated directly to give:

$$\psi(\rho,z) = 2\pi(\rho N/M) \int_{z'=z}^{\infty} \int_{p'=0}^{\infty} \phi(r)\ p'dp'dz' \tag{J3}$$

$$\psi(\rho_o,z_o) = 2\pi(\rho_o N/M) \int_{z'=z_o}^{\infty} \int_{p'=0}^{\infty} \phi(r)\ p'dp'dz' \tag{J4}$$

From Figure J1:

$$r^2 = p'^2 + z'^2 \tag{J5}$$

or:

$$p'^2 = r^2 - z'^2 \tag{J6}$$

Therefore, holding z' (temporarily) constant:

$$2p'dp' = 2rdr \tag{J7}$$

or:

$$p'dp' = rdr \tag{J8}$$

From Equation (J5) it is clear that when $p' = 0$, $r = z'$ and when $p' = \infty$, $r = \infty$. Noting these limits and Equation (J8), Equations (J3) and (J4) become:

$$\psi(\rho,z) = 2\pi(\rho N/M) \int_{z'=z}^{\infty} \left[\int_{r=z'}^{\infty} \phi(r)\ rdr \right] dz' \tag{J9}$$

$$\psi(\rho_o,z_o) = 2\pi(\rho_o N/M) \int_{z'=z_o}^{\infty} \left[\int_{r=z'}^{\infty} \phi(r)\ rdr \right] dz' \tag{J10}$$

Considering Equation (72) the bracketed term in both equations becomes:

$$\left[\int_{r=z'}^{\infty} \phi(r)\ r dr\right] = \int_{r=z'}^{\infty} \varepsilon\ f(n)\ [(\frac{\sigma}{r})^n - (\frac{\sigma}{r})^6]\ r\,dr \qquad \text{(J11)}$$

or:

$$\left[\int_{r=z'}^{\infty} \phi(r)\ r dr\right] = \varepsilon\ f(n)\left[\sigma^n \int_{r=z'}^{\infty} r^{-n+1} dr - \sigma^6 \int_{r=z'}^{\infty} r^{-5}\ dr\right] \qquad \text{(J12)}$$

$$\left[\int_{r=z'}^{\infty} \phi(r) r dr\right] = \varepsilon\ f(n)\left[\sigma^n \frac{r^{-n+2}}{-n+2}\Big|_{r=z'}^{\infty} - \sigma^6 \frac{r^{-4}}{-4}\Big|_{r=z'}^{\infty}\right] \qquad \text{(J13)}$$

$$\left[\int_{r=z'}^{\infty} \phi(r)\ r dr\right] = \varepsilon\ f(n)\left[\frac{\sigma^n}{(n-2)}\ z'^{-n+2} - \frac{\sigma^6}{4}\ z'^{-4}\right] \qquad \text{(J14)}$$

Substitution in Equations (J9) and (J10) gives:

$$\psi(\rho,z) = 2\pi(\rho N/M) \int_{z'=z}^{\infty} \varepsilon\ f(n)\ [\frac{\sigma^n}{(n-2)}\ z'^{-n+2} - \frac{\sigma^6}{4}\ z'^{-4}]dz' \qquad \text{(J15)}$$

$$\psi(\rho_o,z_o) = 2\pi(\rho_o N/M) \int_{z'=z_o}^{\infty} \varepsilon\ f(n)[\frac{\sigma^n}{(n-2)}\ z'^{-n+2} - \frac{\sigma^6}{4}\ z'^{-4}]dz' \qquad \text{(J16)}$$

or:

$$\psi(\rho,z) = 2\pi\varepsilon(\rho N/M)\ f(n)\left[\frac{\sigma^n}{(n-2)}\ \frac{z'^{-n+3}}{-n+3}\Big|_{z'=z}^{\infty} - \frac{\sigma^6}{4}\ \frac{z'^{-3}}{-3}\Big|_{z'=z}^{\infty}\right] \qquad \text{(J17)}$$

$$\psi(\rho_o,z_o) = 2\pi\varepsilon(\rho_o N/M)\ f(n)\left[\frac{\sigma^n}{(n-2)}\ \frac{z'^{-n+3}}{-n+3}\Big|_{z'=z_o}^{\infty} - \frac{\sigma^6}{4}\ \frac{z'^{-3}}{-3}\Big|_{z'=z_o}^{\infty}\right] \qquad \text{(J18)}$$

or:

$$\psi(\rho,z) = 2\pi\epsilon(\rho N/M)\ f(n)\ [\frac{\sigma^n}{(n-2)(n-3)}\frac{1}{z^{n-3}} - \frac{\sigma^6}{12}\frac{1}{z^3}] \tag{78}$$

$$\psi(\rho_o,z_o) = 2\pi\epsilon(\rho_o N/M)\ f(n)\ [\frac{\sigma^n}{(n-2)(n-3)}\frac{1}{z_o^{n-3}} - \frac{\sigma^6}{12}\frac{1}{z_o^3}] \tag{79}$$

which are Equations (78) and (79). Equation (48) is:

$$\Delta E = \frac{N}{M}\ [\psi(\rho,z) - \psi(\rho_o,z_o)] \tag{48}$$

and substitution from Equations (78) and (79) gives:

$$\Delta E = \frac{N}{m}\Big\{ 2\pi\epsilon(\rho N/M)\ f(n)\ [\frac{\sigma^n}{(n-2)(n-3)}\frac{1}{z^{n-3}} - \frac{\sigma^6}{12}\frac{1}{z^3}]$$
$$- 2\pi\epsilon(\rho_o N/M)\ f(n)\ [\frac{\sigma^n}{(n-2)(n-3)}\frac{1}{z_o^{n-3}} - \frac{\sigma^6}{12}\frac{1}{z_o^3}]\Big\} \tag{J19}$$

or:

$$\Delta E = 2\pi\epsilon(\frac{N}{M})^2\ f(n)\Big[\frac{\sigma^n}{(n-2)(n-3)}\frac{\rho}{z^{n-3}} - \frac{\sigma^6}{12}\frac{\rho}{z^3}$$
$$- \frac{\sigma^n}{(n-2)(n-3)}\frac{\rho_o}{z_o^{n-3}} + \frac{\sigma^6}{12}\frac{\rho_o}{z_o^3}\Big] \tag{J20}$$

which becomes:

$$\Delta E = 2\pi\epsilon(\frac{N}{M})^2\ f(n)\ [\frac{\sigma^n}{(n-2)(n-3)}\ (\frac{\rho}{z^{n-3}} - \frac{\rho_o}{z_o^{n-3}}) - \frac{\sigma^6}{12}\ (\frac{\rho}{z^3} - \frac{\rho_o}{z_o^3})] \tag{80}$$

which is Equation (80).

Appendix K

Nearest Neighbor Distance; Distance between Molecular Layers

Sketches showing the definitions for the nearest neighbor distance a_o and the distance between layers z_o are shown in Figure K1 for fcc, bcc and diamond lattices.

fcc lattice

$$\frac{\rho_o N}{M} = \frac{\text{number of molecules}}{\text{unit volume}} = \frac{(6)(\frac{1}{2}) + (8)(\frac{1}{8})}{(2z_o)^3} = \frac{4}{8z_o^3} \tag{K1}$$

or:

$$z_o^3 = \frac{M}{2\rho_o N} \tag{K2}$$

$$z_o = (\frac{M}{2\rho_o N})^{1/3} \tag{84}$$

which is Equation (84).

This may be written:

$$z_o(\rho_o N/M)^{1/3} = 2^{-1/3} = 0.7937 \tag{K3}$$

From the shaded plane in Figure K1:

$$a_o^2 = z_o^2 + z_o^2 = 2z_o^2 \tag{K4}$$

$$a_o = 2^{1/2}\, z_o \tag{K5}$$

and from Equation (84) :

$$a_o = 2^{1/2}\, 2^{-1/3}\, (M/\rho_o N)^{1/3} \tag{K6}$$

a_o = NEAREST NEIGHBOR DISTANCE

Z_o = DISTANCE BETWEEN LAYERS

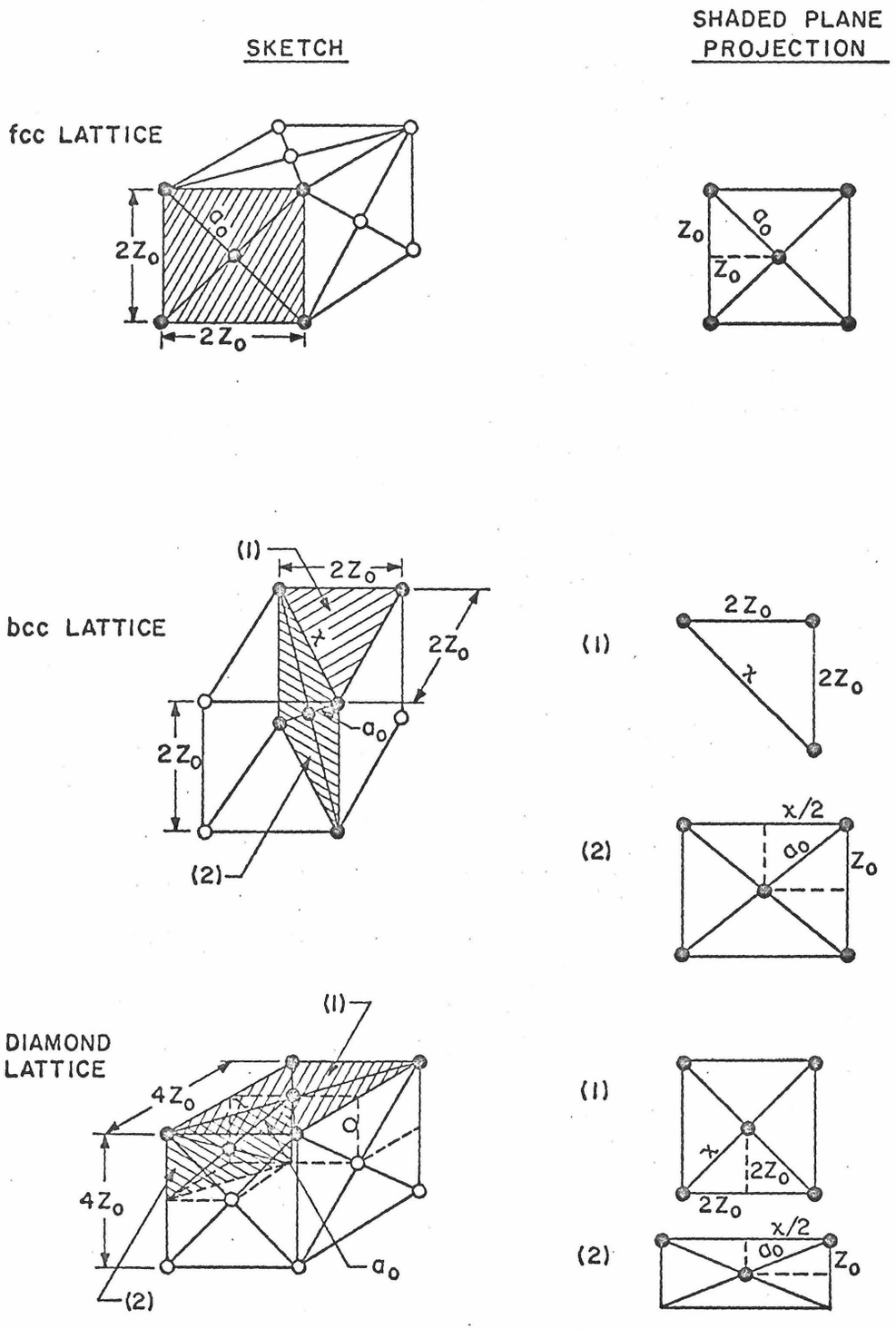

Figure K1. Definition of a_o and z_o

or:

$$a_o = 2^{1/6}(M/\rho_o N)^{1/3} \tag{81}$$

which is Equation (81).

This may be written:

$$a_o(\rho_o N/M)^{1/3} = 2^{1/6} = 1.1225 \tag{K7}$$

bcc lattice

$$\frac{\rho_o N}{M} = \frac{\text{number of molecules}}{\text{unit volume}} = \frac{1 + (8)(\frac{1}{8})}{(2z_o)^3} = \frac{2}{8z_o^3} \tag{K8}$$

or:

$$z_o = (\frac{M}{4\rho_o N})^{1/3} \tag{87}$$

which is Equation (87).

This may be written:

$$z_o(\rho_o N/M)^{1/3} = 4^{-1/3} = 0.6300 \tag{K9}$$

From the shaded planes in Figure K1:

$$x^2 = (2z_o)^2 + (2z_o)^2 = 8z_o^2 \tag{K10}$$

$$a_o^2 = z_o^2 + (x/2)^2 = z_o^2 + \frac{x^2}{4} \tag{K11}$$

Substituting Equation (K10) into Equation (K11) gives:

$$a_o^2 = z_o^2 + (\frac{1}{4})\ 8z_o^2 = 3z_o^2 \tag{K12}$$

or:

$$a_o = 3^{1/2} z_o \tag{K13}$$

and from Equation (87):

$$a_o = 3^{1/2} 4^{-1/3} (M/\rho_o N)^{1/3} \tag{86}$$

which is Equation (86). This may be written:

$$a_o (\rho_o N/M)^{1/3} = 3^{1/2} 4^{-1/3} = 1.0911 \tag{K14}$$

diamond lattice

$$\frac{\rho_o N}{M} = \frac{\text{number of molecules}}{\text{unit volume}} = \frac{4 + (6)(\frac{1}{2}) + (8)(\frac{1}{8})}{(4z_o)^3} = \frac{8}{64 z_o^3} \tag{K15}$$

or:

$$z_o = \left(\frac{M}{8\rho_o N}\right)^{1/3} \tag{85}$$

which is Equation (85). This may be written:

$$z_o (\rho_o N/M)^{1/3} = 8^{-1/3} = 0.5000 \tag{K16}$$

From the shaded planes in Figure K1:

$$x^2 = (2z_o)^2 + (2z_o^2) = 8z_o^2 \tag{K17}$$

$$a_o^2 = z_o^2 + (x/2)^2 = z_o^2 + x^2/4 \tag{K18}$$

Substituting Equation (K17) into Equation (K18) gives:

$$a_o^2 = z_o^2 + (\tfrac{1}{4})\, 8z_o^2 = 3z_o^2 \tag{K19}$$

or:

$$a_o = 3^{1/2} z_o \tag{K20}$$

and from Equation (85):

$$a_o = 3^{1/2}\ 8^{-1/3}(M/\rho_o N)^{1/3} \tag{K21}$$

$$a_o = \frac{3^{1/2}}{2}\ (M/\rho_o N)^{1/3} \tag{83}$$

which is Equation (83). This may be written:

$$a_o(\rho_o N/M)^{1/3} = \frac{3^{1/2}}{2} = 0.8660 \tag{K22}$$

Equations (84), (K3), (81), (K7), (87), (K9), (86), (K14), (85), (K16), (83) and (K22) appear in Figure 10.

Appendix L

"Snapshot" and "Probability" Approach--Nearest Neighbor Distance

"Snapshot" Approach

Consider the reasonably realistic (chaotic) molecular view in Figure L1a, which is assumed to be a "snapshot" of a liquid at some time t_1. Picking one molecule at random (say the dark one) we may arbitrarily divide the space around it into m_1 sectors of equal angle* (in Figure L1a, $m_1 = 8$ the angle being 45^o). For each sector a "nearest" neighbor can be identified** and the distance a_i from it to the dark molecule recorded. The mean value of these measurements ($\overline{(a_o)}_{t_1} = \sum_{i=1}^{m_1} a_i/m_1$; Figure L1a) would be the mean nearest neighbor distance at time t_1 of the snapshot***. The value of m_1 is fixed by the minimum number of sectors that produces no significant change in $\overline{(a_o)}_{t_1}$ with an increase in m_1.

Figure L1b represents a snapshot of the same liquid at some (reasonably large) time later**** t_2. We repeat the above process for a new, randomly chosen, molecule (with m_2 sections) and obtain another mean value of the nearest neighbor distance $\overline{(a_o)}_{t_2}$. This is then repeated a sufficient number of times k such that the mean

---

* In the "real" case this would be done in three dimensions; radial sectors.

** Molecules that fall in two sectors can be arbitrarily assigned to the one in which most of its volume lies.

*** This evaluation could certainly be carried out for more than one of the molecules in Figure L1a and an overall average found. This would eliminate the effects of "clustering"

**** Of course, all thermodynamic properties (i.e., P, T, etc.) remain the same in Figures L1a and L1b.

Figure L1a

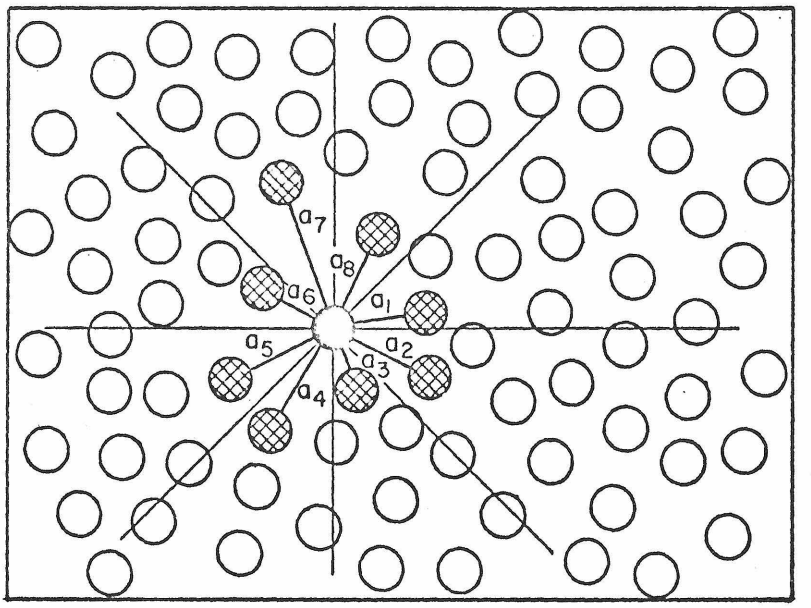

$$(\overline{a_0})_{t_1} = \frac{\sum_{i=1}^{m_1} a_i}{m_1} = \frac{a_1+a_2+a_3+a_4+a_5+a_6+a_7+a_8}{8}$$

Figure L1b

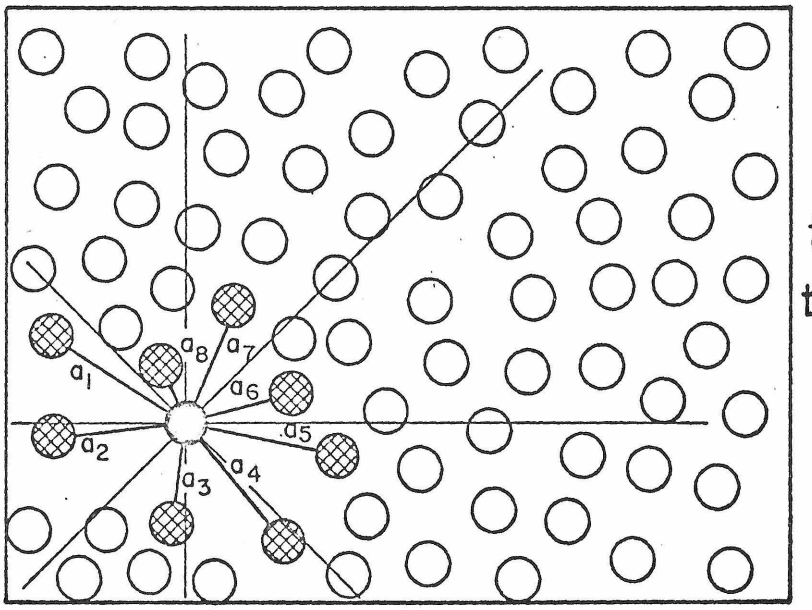

$$(\overline{a_0})_{t_2} = \frac{\sum_{i=1}^{m_2} a_i}{m_2} = \frac{a_1+a_2+a_3+a_4+a_5+a_6+a_7+a_8}{8}$$

Figure L1. Nearest Neighbor

value of each of the individual means $(\overline{a_o})_{t_i}$ does not change significantly with additional measurements and:

$$\overline{(\overline{a_o})} = \sum_{i=1}^{k} (\overline{a_o})_{t_i} / k \qquad \text{(L1)}$$

By taking $m_1, m_2, \cdots m_k$ and k large enough, space and time variations in the "nearest" neighbor distance are (arbitrarily) minimized. Equation (L1) identifies a mean quantity which may be compared to a_o in Equation (81). If the two values are reasonably close the use of Equation (81) appears justified, i.e., the assumption of an fcc structure leads to an "accurate" macroscopic relationship.

Although such an approach must necessarily be considered a "thought" experiment, it does elucidate the nature of the assumption of a lattice structure for a liquid, at least with regard to its use in the theory being developed. On the other hand, since several molecular dynamic approaches to the problem of the structure of liquids[31,129] consider molecular models of the type pictured in Figure L1 (using computer techniques to handle the many possible configurations) a calculation of the type indicated in Equation (L1) might be possible.

Probability Approach

Another way to view the assumption of an fcc lattice (i.e., Equation (81)) is to consider the pair (or radial) distribution function (PDF) $g(r)$ mentioned earlier. This is sketched in Figure L2 for liquid argon[138]. At low values of r, $g(r) \simeq 0$ because of the strong repulsive forces in this region. As r increases $g(r)$ increases rapidly to a first peak representing the shell of nearest neighbors.

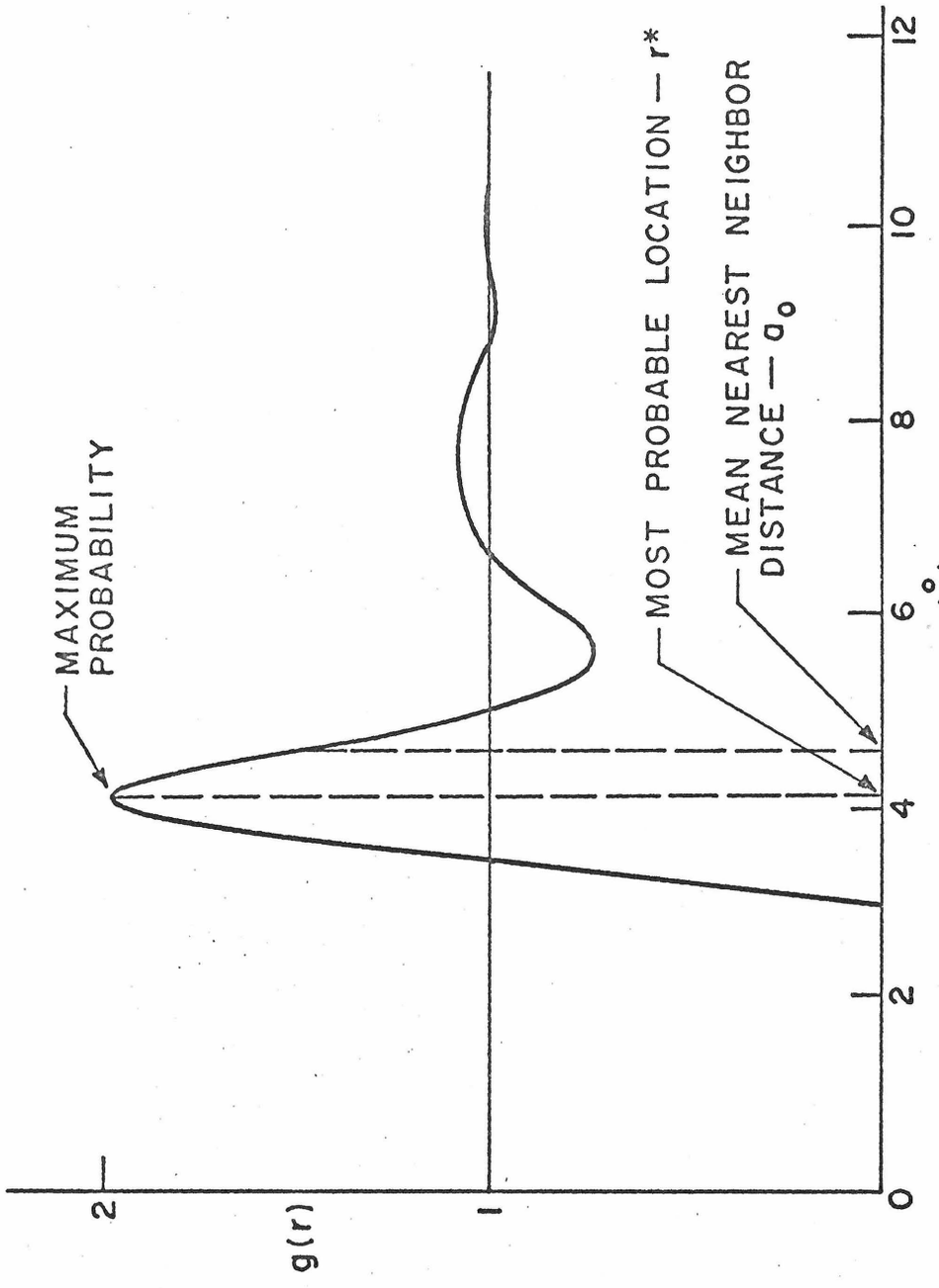

Figure L2. Pair Distribution Function
[From Mikolaj and Pings[138]]

This occurs at a value of r (denoted r^*) close to r_o in Figure 8, i.e., at the position corresponding to the "depth of the potential well" in the pair potential[19,17]. In general r^* is slightly less than r_o (Appendix M). At higher values of r the subsequent peaks represent more distant neighbors*.

From Equation (L1) it is clear that a_o in Equation (81) does not correspond to the most probable location (the one of highest probability) but rather to the mean location and is therefore not equal to r_o or r^*. This is clear since r_o for the true pair potential function is state independent[71] while a_o depends on density. Consideration of the data of Mikolaj and Pings[138] shows that the variation with ρ of r^* is essentially nil.

For a fluid described by the $g(r)$ in Figure L2 consider a differential spherical shell located a distance r from the central molecule as shown in Figure L3. Assuming the particles are distributed in accordance with a Poisson distribution[163] the probability of finding exactly n molecules in the sphere of radius r is[163]:

$$P\{n;V\} = e^{-\int_0^V \rho'(r)dV} \frac{\left[\int_0^V \rho'(r)dV\right]^n}{n!} \qquad \text{(L2)}$$

*It is because of these peaks (of descending probability) that the liquid is considered to have "short-range" order compared to the "long-range" order of a solid whose $g(r)$ is periodic[19,162].

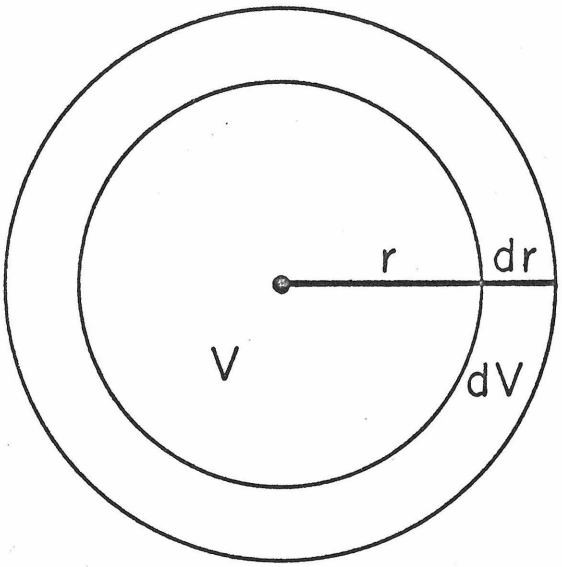

Figure L3. Spherical Shell

where V is the sphere volume ($V = \frac{4}{3}\pi r^3$, $dV = 4\pi r^2 dr$) and $\rho'(r)$ is the average number of particles per unit volume at r and the integral is necessary to establish an "average" particle density in the sphere*. Differentiating Equation (L2) with respect to V gives (see Note 1 at the end of this appendix):

$$P\{n;dV\} = P\{n;V\} \left[\frac{n}{\int_0^V \rho'(r)dV} - 1 \right] \rho'(r)dV \qquad \text{(L3)}$$

From these it is possible to show that (Note 2 at end of this appendix):

$$P\{0;V\} = e^{-\int_0^V \rho'(r)dV} \qquad \text{(L4)}$$

$$P\{\geq 1;dV\} = e^{-\int_0^V \rho'(r)dV} \rho'(r)dV \qquad \text{(L5)}$$

where $P\{0;V\}$ is the probability of <u>not</u> having a molecule in the volume V and $P\{\geq 1;dV\}$ is the probability of having one or more molecules in the element dV. The joint probability of Equations (L4) and (L5) exactly expresses the condition necessary for a nearest neighbor in Figure L3.

Therefore:

---

*It is assumed that the Poisson distribution is valid even though there is a gradient in $\rho'(r)$. The equation is exact when $\rho'(r) = \rho' =$ constant (i.e., perfect gases) in which case[163]:

$$P\{n;V\} = e^{-\rho'V} \frac{[\rho'V]^n}{n!}$$

$$P_{joint}dV = P\{0;V\} \cdot P\{\geq 1;dV\} = e^{-2\int_0^V \rho'(r)dV} \rho'(r)dV \qquad (L6)$$

The mean value of the nearest neighbor is defined by*:

$$\bar{r} \equiv 2\int_{-\infty}^{+\infty} r\, P_{joint}\, dV \qquad (L7)$$

and, using Equation (L6):

$$\bar{r} = 2\int_{-\infty}^{+\infty} e^{-2\int_0^V \rho'(r)dV} \rho'(r)dV \qquad (L8)$$

Since generally $V = \frac{4}{3}\pi r^3$ and, by definition $\rho'(r) = \rho'_o\, g(r)$, Equation (L8) may be written (noting that r goes from 0 to ∞ and that $\rho'_o = \frac{\rho_o N}{M}$):

$$\bar{r} = 8\pi\left(\frac{\rho_o N}{M}\right)\int_0^{\infty} e^{-8\pi\left(\frac{\rho_o N}{M}\right)\int_0^r g(r)r^2dr} g(r)r^3dr \qquad (L9)$$

The integrations may be carried out when the $g(r)$ is known**:

It is not clear from this development that $\bar{r}$ is, in fact, identical to $\overline{(a_o)}$ in Equation (L1) but it certainly is a similar quantity and the general approach to the actual numerical determination of a_o is indicated. That $\bar{r}$ (or a_o) is intimately connected

---

*The factor of 2 is necessary to make P_{joint} a true probability density function (see Note 3 at end of this appendix).

**See Note 4 at end of this appendix for an interesting example (i.e., $g(r) = 1$). The $g(r)$ data of Mikolaj and Pings[138] could be used to determine $\bar{r}$ for argon at the given states.

to $g(r)$ and thus density dependent is manifest from Equation (L9). As before the numerical comparison of $\bar{r}$ with a_o in Equation (81) would help determine the justification of assuming an fcc lattice for macroscopic purposes*.

Note 1: Derivation of Equation (L3)

Equation (L2) is:

$$P\{n;V\} = e^{-\int_0^V \rho'(r)dV} \frac{[\int_0^V \rho'(r)dV]^n}{n!}$$

Differentiating with respect to V gives:

$$P\{n;dV\} = e^{-\int_0^V \rho'(r)dV} \frac{n[\int_0^V \rho'(r)dV]^{n-1}}{n!} \rho'(r)dV$$

$$+ \frac{[\int_0^V \rho'(r)dV]^n}{n!} e^{-\int_0^V \rho'(r)dV} \cdot (-1)\rho'(r)dV$$

or:

$$P\{n;dV\} = e^{-\int_0^V \rho'(r)dV} \frac{[\int_0^V \rho'(r)dV]^n}{n!} \left(\frac{n}{\int_0^V \rho'(r)dV} - 1 \right) \rho'(r)dV$$

and noting Equation (L2):

---

*If the method developed for the determination of a_o is verified this quantity might be used as a quantitative measure of liquid structure (see Note 5 at the end of this appendix).

$$P\{n;dV\} = P\{n;V\}\left(\frac{n}{\int_0^V \rho'(r)dV} - 1\right)\rho'(r)dV \qquad (L3)$$

which is Equation (L3).

Note 2: Derivation of Equations (L4) and (L5)

From Equation (L2) with $n = 0$:

$$P\{0;V\} = e^{-\int_0^V \rho'(r)dV} \qquad (L4)$$

which is Equation (L4).

By definition:

$$\sum_{n=0}^{\infty} P\{n;V\} = 1$$

and since:

$$\sum_{n=0}^{\infty} P\{n;V\} = P\{0;V\} + \sum_{n=1}^{\infty} P\{n;V\}$$

$$\sum_{n=1}^{\infty} P\{n;V\} = 1 - P\{0;V\}$$

Differentiating with respect to V gives:

$$\sum_{n=1}^{\infty} P\{n;dV\} = - P\{0;dV\}$$

The right-hand-side may be determined by differentiating Equation (L4) with respect to V :

$$P\{0;dV\} = - e^{-\int_0^V \rho'(r)dV}\,\rho'(r)dV$$

giving:

$$\sum_{n=1}^{\infty} P\{n;dV\} = e^{-\int_0^V \rho'(r)dV} \rho'(r)dV$$

Since by definition:

$$P\{\geq 1;dV\} \equiv \sum_{n=1}^{\infty} P\{n;dV\}$$

$$P\{\geq 1;dV\} = e^{-\int_0^V \rho'(r)dV} \rho'(r)dV \qquad \text{(L5)}$$

which is Equation (L5).

Note 3: Conversion of P_{joint} to a Probability Density Function--Derivation of Equation (L7)

For a function $f(x)$ to be a probability density function (pdf) it must, by definition, have the properties[164]:

$$f(x) \geq 0$$

$$\int_{-\infty}^{+\infty} f(x)\,dx = 1$$

If P_{joint} in Equation (L6) is a pdf it must conform to these conditions. From Equation (L6):

$$P_{joint} = e^{-2\int_0^V \rho'(r)dV} \rho'(r) \qquad \text{(L6)}$$

and clearly the first condition is met since $\rho'(r) \geq 0$. The second condition may be tested by finding the integral:

$$\int_{-\infty}^{+\infty} P_{joint}\, dV = \int_{-\infty}^{+\infty} e^{-2\int_0^V \rho'(r)dV} \rho'(r)dV$$

Since V is defined from $V = 0$ to $V = \infty$, this becomes:

$$\int_{-\infty}^{+\infty} P_{joint}\, dV = \int_0^{+\infty} e^{-2u}\, du$$

where

$$u = \int_0^V \rho'(r)dV$$

Integration gives:

$$\int_{-\infty}^{+\infty} P_{joint}\, dV = \frac{e^{-2u}}{-2}\Bigg]_0^{+\infty} = -\frac{1}{2}[0 - 1] = +\frac{1}{2}$$

Clearly this does not satisfy the condition; P_{joint} is, by itself, not a pdf. However, multiplying P_{joint} by 2 normalizes the integration to 1 , satisfying the condition. Therefore $2P_{joint}$ is a pdf.

The mean value of the variable of a pdf is defined by[164]:

$$\bar{x} = \int_{-\infty}^{+\infty} xf(x)\, dx$$

Therefore the mean value of r for the pdf $2P_{joint}$ is given by:

$$\bar{r} = 2\int_{-\infty}^{+\infty} r\, P_{joint}\, dV \qquad \text{(L7)}$$

which is Equation (L7).

Note 4: Integration of Equation (L9) for $g(r) = 1$

Equation (L9) is:

$$\bar{r} = 8\pi\left(\frac{\rho_o N}{M}\right) \int_0^\infty e^{-8\pi\left(\frac{\rho_o N}{M}\right) \int_0^r g(r) r^2 dr} g(r) r^3 dr \qquad \text{(L9)}$$

For the case of no intermolecular forces, corresponding to a perfect gas, $g(r) \equiv 1$ and:

$$\bar{r} = 8\pi\left(\frac{\rho_o N}{M}\right) \int_0^\infty e^{-8\pi\left(\frac{\rho_o N}{M}\right) \int_0^r r^2 dr} r^3 dr$$

or:

$$\bar{r} = 8\pi\left(\frac{\rho_o N}{M}\right) \int_0^\infty e^{-\frac{8\pi}{3}\left(\frac{\rho_o N}{M}\right) r^3} r^3 dr$$

Let:

$$\alpha = \frac{8\pi}{3}\left(\frac{\rho_o N}{M}\right)$$

and:

$$y = \alpha r^3$$

Therefore:

$$r^3 = \frac{y}{\alpha} \quad , \quad r = \frac{y^{1/3}}{\alpha^{1/3}} \quad , \quad dr = \frac{1}{\alpha^{1/3}} \frac{1}{3} y^{-2/3} \, dy$$

and*:

---

*When $r = 0$, $y = 0$ and when $r = \infty$, $y = \infty$.

$$\bar{r} = 3\alpha \int_0^\infty e^{-y} \frac{y}{\alpha} \frac{1}{\alpha^{1/3}} \frac{1}{3} y^{-2/3} \, dy$$

$$\bar{r} = \frac{1}{\alpha^{1/3}} \int_0^\infty y^{1/3} e^{-y} \, dy$$

The integral is the gamma function[127] with $m - 1 = 1/3$ or $m = 4/3$. Therefore:

$$\int_0^\infty y^{1/3} e^{-y} \, dy = \Gamma(4/3)$$

and:

$$\bar{r} = \frac{\Gamma(\frac{4}{3})}{\alpha^{1/3}} = \frac{\Gamma(\frac{4}{3})}{[\frac{8\pi}{3}(\frac{\rho_o N}{M})]^{1/3}}$$

$$\bar{r} = \frac{1}{2}(\frac{3}{\pi})^{1/3} \Gamma(\frac{4}{3}) (\frac{M}{\rho_o N})^{1/3}$$

$$\bar{r} = 0.440 (\frac{M}{\rho_o N})^{1/3}$$

Comparison of this to Equation (81) (noting that $2^{1/6} \simeq 1.1$) shows that, as expected, the mean nearest neighbor for a perfect gas would be much less (a factor of ~ 3) than for a liquid of the same density where strong repulsion occurs at the smaller distances.

Note 5: Use of a_o as a Measure of Liquid Structure

The structure factor $a_o(\rho_o N/M)^{1/3}$ and first coordination number (i.e., number of nearest neighbors) N_1 for various specific crystal structures are shown in Table L1. These entries are exact in that they are uniquely determined by the structure type (see Figure 10). Noting that $a_o(\rho_o N/M)^{1/3}$ and N_1 generally appear correlated in Table L1, it is possible to conceive of intermediate (or mixed) structures by joining the discrete points of an $a_o(\rho_o N/M)^{1/3}$ vs. $N_1^{1/3}$ plot with a smooth curve. This is shown in Figure L4 where the curve has been extrapolated (dashed line) to small values of N_1.

Although developed with solids, Figure L4 should be applicable to liquids (and perhaps gases) at least for appropriate time averaged values of a_o and N_1. For an appropriate calculation of a_o (assuming ρ_o is known) N_1 can be found from the curve and the liquid structure sharply defined*.

Equation (L9) is:

$$\bar{r} = 8\pi(\rho_o N/M) \int_0^\infty e^{-8\pi(\rho_o N/M) \int_0^r g(r) r^2 dr} \; g(r)\, r^3 dr \qquad \text{(L9)}$$

Assuming that $\bar{r} \approx a_o$ and multiplying both sides by $(\rho_o N/M)^{1/3}$ gives:

*It may be noted that this procedure overcomes the difficulty with liquids that, knowing $g(r)$ (and ρ_o) alone, "there is no unique manner of computing the (first) coordination number(s)".[20]

Table L1

STRUCTURE FOR VARIOUS CRYSTAL LATTICES[37]

Structure Name	$a_o(\rho_o N/M)^{1/3}$	First Coordination Number = Number of Nearest Neighbors N_1
fcc hcp*	$2^{1/6} = 1.1225$	12
bcc	$3^{1/2}2^{-1/3} = 1.0911$	8
sc**	1.0000	6
diamond	$3^{1/2}\ 2^{-1} = 0.8660$	4

*hcp = hexagonal close-packed

**sc = simple cubic

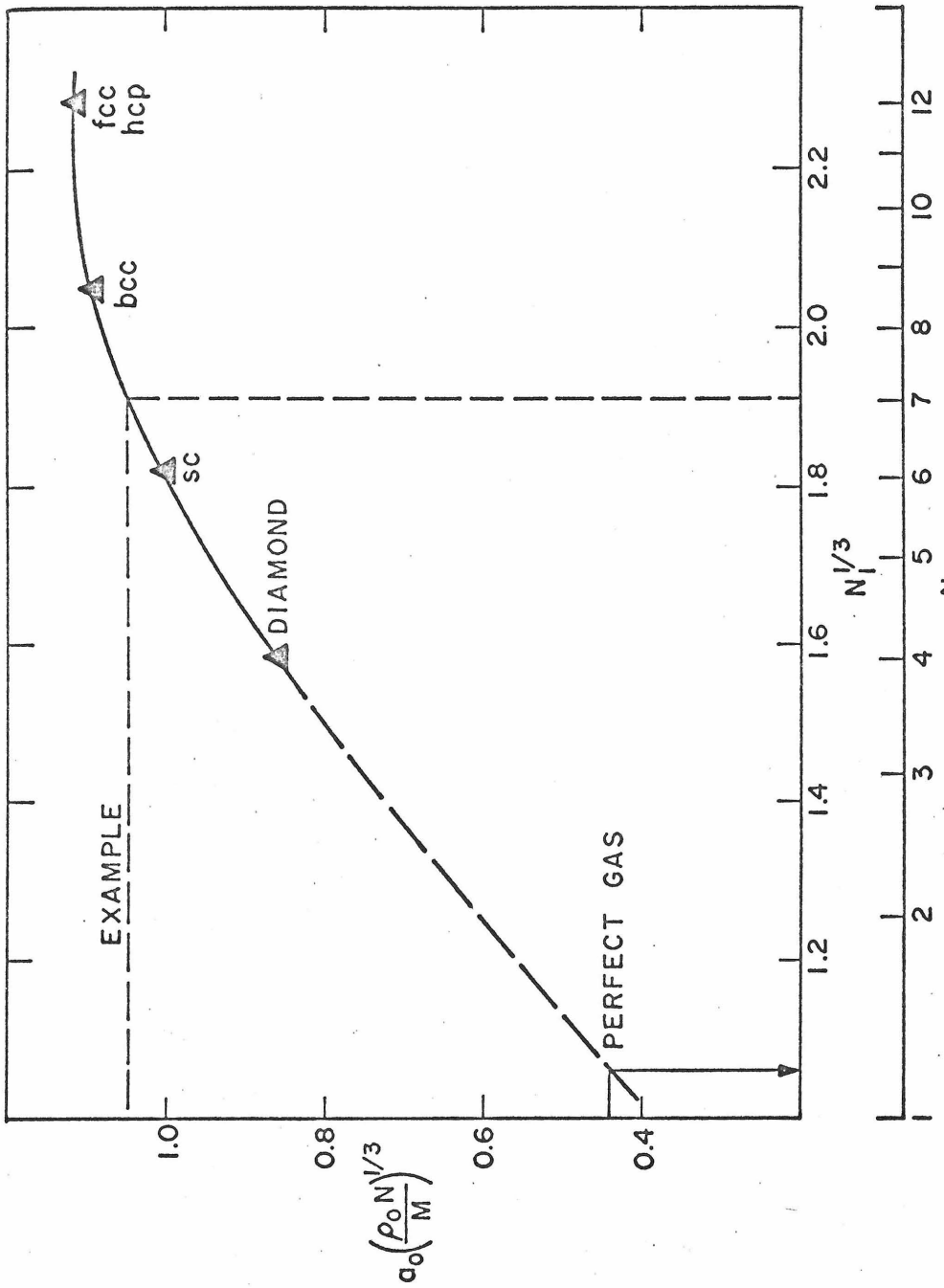

Figure L4. Intermediate Structures

$$a_o(\rho_o N/M)^{1/3} \tilde{=} 8\pi(\rho_o N/M)^{4/3} \int_0^{\infty} e^{-8\pi(\rho_o N/M) \int_0^r g(r)r^2dr} g(r)r^3dr$$

Therefore knowing $g(r)$ and ρ_o for a given liquid, a_o and $a_o(\rho_o N/M)^{1/3}$ can be numerically determined. Using the latter value in Figure L4 a unique value of N_1 can be determined; e.g., if $a_o(\rho_o N/M)^{1/3} = 1.05$, $N_1 \tilde{=} 7$ and the structure would be said to be either part-way between a sc and bcc lattice or a mixture of the two. In either case a quantitative measure of the liquid structure would result*.

---

*It is interesting to note that if $\bar{r} \tilde{=} a_o$, the calculation for a perfect gas in Note 4 leads to $a_o(\rho_o N/M)^{1/3} \tilde{=} 0.44$ which, according to the extrapolation in Figure L4, gives a first coordination number of ~ 1.02.

Appendix M

Relation of r^* to r_o

In general it has been shown that[17]:

$$g(r) = e^{-\frac{\phi(r) + w(r)}{kT}} \tag{M1}$$

where $g(r)$ is the pair distribution function $\phi(r)$ is the pair potential function and $w(r)$ accounts for the effect of all other molecules on the first of the pair*. Clearly then, $g(r)$ is a measure of the real system since it includes three-body and higher interactions. Since $\phi(r)$ accounts only for the "pair" interaction, it is clear that the minimum energy position for such a pair (i.e., r_o) is not the same as the minimum energy position of the pair in the presence of other molecules (i.e., r^*); $r_o \neq r^*$. However, in the limit as $\rho \to 0$, $w(r) \to 0$ and[18,17]:

$$g(r) = e^{-\frac{\phi(r)}{kT}} \tag{M2}$$

In this case it is easy to show that the maximum in $g(r)$ corresponds exactly to the minimum in $\phi(r)$; $r^* = r_o$. Clearly this special case implies an interaction of two otherwise isolated molecules (no three-body forces) which is exactly the assumption of $\phi(r)$.

---

*Since it is certainly possible that the introduction of a third molecule into the system might affect the potential between a given pair (e.g., consider dispersion forces), $w(r)$ may be considered as a sum of the necessary correction to $\phi(r)$ and the direct effect of the third molecule on the first.

To determine the effect of three-body forces on the relation between r^* and r_o consider the potential function in Figure M1. This shows an isolated pair with the "first molecule" at the origin and the "second molecule" at the "bottom of the potential well" (at r_o) which is the equilibrium position.

A third molecule is then brought along the r axis from $\infty \rightarrow r$ as in Figure M2.

Define:

$$\textcircled{1} = \text{the first molecule} \tag{M3}$$

$$\textcircled{2} = \text{the second molecule} \tag{M4}$$

$$\textcircled{3} = \text{the third molecule} \tag{M5}$$

as ③ approaches ① and ② there is a net attraction for both until ③ is $\leq r_o$ from ② . At this point ③ is still attracted to ① but begins to act repulsively on ② which acts repulsively on ①. When these forces balance a new equilibrium has been obtained. The repulsive force of ③ on ② requires that ② must move to the left. The final distance between ① and ② and between ② and ③ will each be $< r_o$. Therefore the actual minimum energy position r^* should be less than r_o .

Egelstaff[17] has evaluated $w(r)$ for argon and shows that when it is added to $\phi(r)$, the actual $g(r)$ can be reasonably well reproduced. Comparison of $g(r)$ from $\phi(r)$ alone and $g(r)$ from $\phi(r) + w(r)$ shows clearly that $r^* < r_o$ thus supporting the above conclusion.

In general it may be concluded that:

Figure M1. Isolated Pair of Molecules

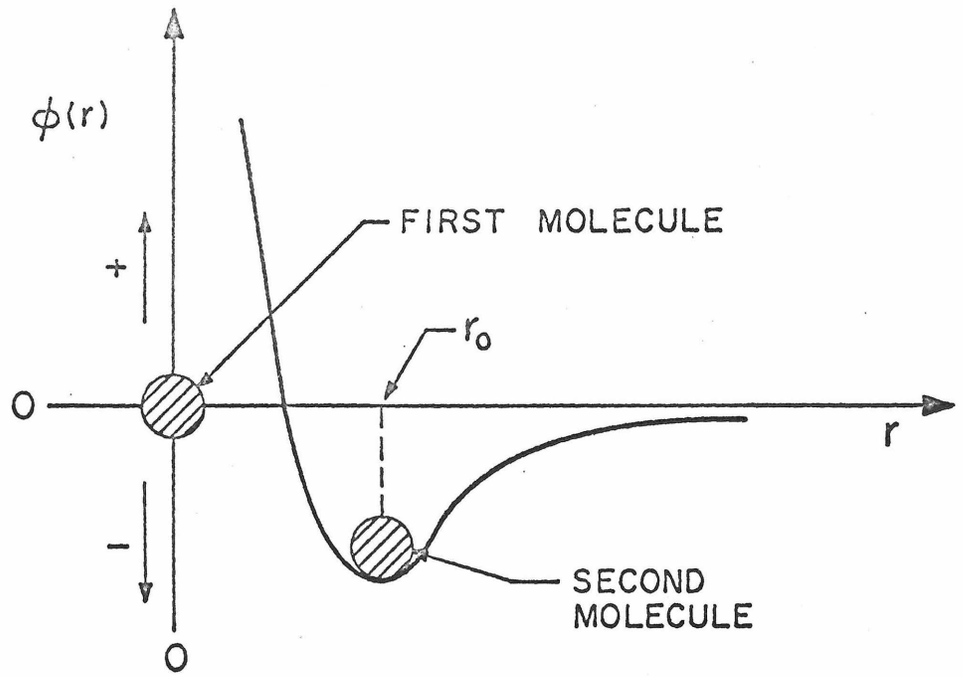

Figure M2. Effect of Third Molecule

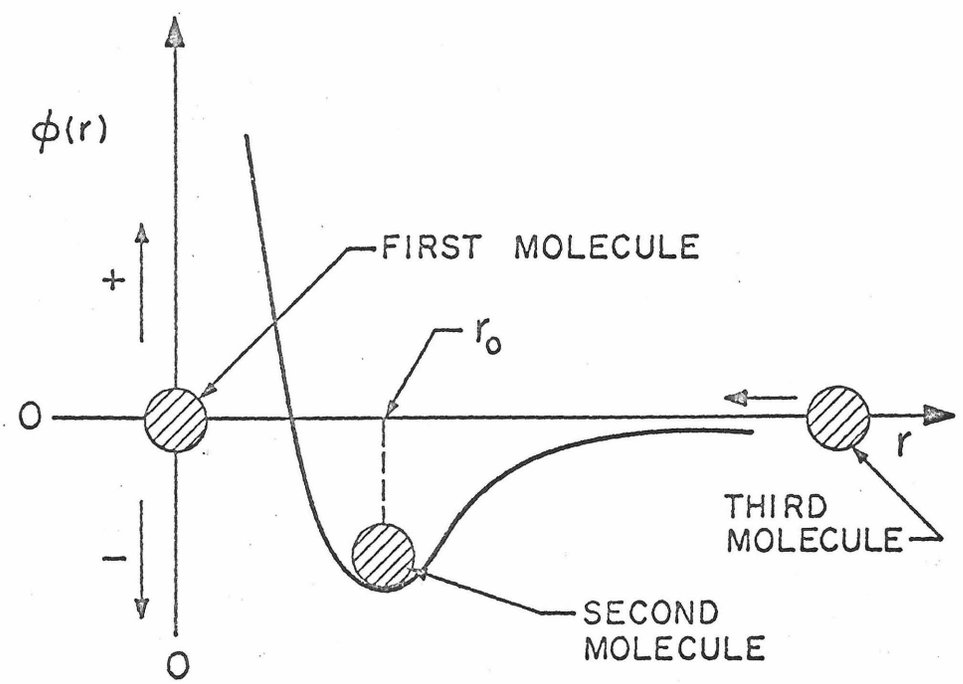

Figure M1. Three-Body Interaction

$$r^* \leq r_o \tag{M6}$$

Although this conclusion may be considered generally valid, it is expected that r^* and r_o will not differ greatly because two-body forces are expected to dominate the ① - ② interaction. This is supported by Egelstaff's result[17] where $r_o \simeq 3.8\text{Å}$ and $r^* \simeq 3.7\text{Å}$.

Appendix N

Derivation of Equation (94)

Equation (80) is:

$$\Delta E = 2\pi\epsilon\left(\frac{N}{M}\right)^2 f(n)\left[\frac{\sigma^n}{(n-2)(n-3)}\left(\frac{\rho}{z^{n-3}} - \frac{\rho_o}{z_o^{n-3}}\right) - \frac{\sigma^6}{12}\left(\frac{\rho}{z^3} - \frac{\rho_o}{z_o^3}\right)\right] \qquad (80)$$

and Equations (88) and (93) are:

$$z_o = (M/2^s\rho_o N)^{1/3} \qquad (88)$$

$$z = (M/2^2\rho_o N)^{1/3}\,\rho_o/\rho \qquad (93)$$

Dividing and multiplying Equation (80) by ρ_o and rearranging the z_o terms gives:

$$\Delta E = 2\pi\epsilon\left(\frac{N}{M}\right)^2 \rho_o f(n)\left[\frac{\sigma^n}{(n-2)(n-3)}\frac{1}{z_o^{n-3}}\left(\frac{\rho}{\rho_o}\left(\frac{z_o}{z}\right)^{n-3} - 1\right)\right.$$
$$\left. - \frac{\sigma^6}{12}\frac{1}{z_o^3}\left(\frac{\rho}{\rho_o}\left(\frac{z_o}{z}\right)^3 - 1\right)\right] \qquad (N1)$$

Now:

$$x \equiv \rho/\rho_o \qquad (N2)$$

and from Equation (92) (or Equations (88) and (93)):

$$z/z_o = \rho_o/\rho = 1/x \qquad (92)$$

Substituting Equations (88), (N2) and (92) into Equation (N1) gives:

$$\Delta E = 2\pi\varepsilon\left(\frac{N}{M}\right)^2 \rho_o f(n)\left[\frac{\sigma^n}{(n-2)(n-3)}\left(\frac{2^s\rho_o N}{M}\right)^{\frac{n-3}{3}}(x^{n-2}-1) - \frac{\sigma^6}{12}\left(\frac{2^s\rho_o N}{M}\right)(x^4-1)\right] \tag{N3}$$

Multiplying and dividing by $\left(\frac{2^s\rho_o N}{M}\right)$ gives:

$$\Delta E = \frac{2\pi\varepsilon\left(\frac{N}{M}\right)^2 \rho_o f(N)}{\left(2^s\rho_o N/M\right)}\left[\frac{\sigma^n}{(n-2)(n-3)}\left(\frac{2^s\rho_o N}{M}\right)^{n/3}(x^{n-2}-1) - \frac{\sigma^6}{12}\left(\frac{2^s\rho_o N}{M}\right)^2(x^4-1)\right] \tag{N4}$$

or:

$$\Delta E = \frac{2}{2^s}\left(\frac{N\pi\varepsilon}{M}\right) f(n)\left[\frac{\sigma^n}{(n-2)(n-3)}\left(\frac{2^s\rho_o N}{M}\right)^{n/3}(x^{n-2}-1) - \frac{\sigma^6}{12}\left(\frac{2^s\rho_o N}{M}\right)^2(x^4-1)\right] \tag{94}$$

which is Equation (94).

Appendix O

Derivation of Equation (103)

Equation (102) is:

$$U_o = \frac{1}{2} \lim_{x \to 1} \frac{[(n-2)\alpha x^{n-3} - 4\beta x^3]}{\mu} \Rightarrow \frac{0}{0} \tag{102}$$

Application of L'Hôspital's rule[15] gives:

$$U_o = \frac{1}{2} \lim_{x \to 1} \frac{(n-2)(n-3)\alpha x^{n-4} - 12\beta x^2}{d\mu/dx} \tag{01}$$

or:

$$U_o = \frac{1}{2} \frac{[(n-2)(n-3)\alpha - 12\beta]}{\lim_{x \to 1} \frac{d\mu}{dx}} \tag{02}$$

But from Equation (18):

$$\lim_{x \to 1} \frac{d\mu}{dx} = U_o \tag{18}$$

and the above becomes:

$$U_o^2 = \frac{1}{2}[(n-2)(n-3)\alpha - 12\beta] \tag{103}$$

which is Equation (103).

Note: Equation (103) can be derived more conveniently in the following way. By definition:

$$U_o \equiv \lim_{\mu \to 0} U \tag{17}$$

and therefore:

$$U_o^2 = \lim_{\mu \to 0} U^2 \tag{03}$$

From Equation (4):

$$U = \frac{\mu}{1 - \frac{1}{x}} = \frac{x\mu}{x-1} \tag{04}$$

and:

$$U^2 = \frac{x^2 \mu^2}{(x-1)^2} \tag{05}$$

Therefore:

$$U_o^2 = \lim_{\mu \to 0} \frac{x^2 \mu^2}{(x-1)^2} \tag{06}$$

Since $x \to 1$ as $\mu \to 0$ this may also be written:

$$U_o^2 = \lim_{\substack{x \to 1 \\ \mu \to 0}} \frac{x^2 \mu^2}{(x-1)^2} = \lim_{\substack{x \to 1 \\ \mu \to 0}} \frac{\mu^2}{(x-1)^2} \Rightarrow \frac{0}{0} \tag{07}$$

Applying L'Hôspital's rule gives:

$$U_o^2 = \lim_{x \to 1} \frac{\frac{d\mu^2}{dx}}{2(x-1)} \tag{08}$$

From Equation (96):

$$\frac{d\mu^2}{dx} = (n-2)\alpha x^{n-3} - 4\beta x^3 \tag{09}$$

and:

$$U_o^2 = \frac{1}{2} \lim_{x \to 1} \frac{(n-2)\alpha x^{n-3} - 4\beta x^3}{x-1} \tag{010}$$

which will yield $\frac{0}{0}$ if, and only if :

$$(n-2)\alpha - 4\beta = 0 \tag{101}$$

For this case:

$$U_o^2 = \frac{1}{2} \lim_{x \to 1} \frac{(n-2)\alpha x^{n-3} - 4\beta x^3}{x-1} \Rightarrow \frac{0}{0} \tag{011}$$

and L'Hôspital's rule gives:

$$U_o^2 = \frac{1}{2} \lim_{x \to 1} \left[\frac{(n-2)(n-3)\alpha x^{n-4} - 12\beta x^2}{1} \right] \tag{012}$$

or:

$$U_o^2 = \frac{1}{2} [(n-2)(n-3)\alpha - 12\beta] \tag{103}$$

which is Equation (103).

Appendix P

Derivation of Equation (108)

Equation (95) is:

$$\mu^2 = \frac{4}{2^s}\left(\frac{N\pi\varepsilon}{M}\right) f(n)\left[\frac{\sigma^n}{(n-2)(n-3)}\left(\frac{2^s\rho_o N}{M}\right)^{n/3}(x^{n-2}-1) - \frac{\sigma^6}{12}\left(\frac{2^s\rho_o N}{M}\right)^2(x^4-1)\right] \tag{95}$$

and Equations (106) and (107) are:

$$\sigma = \left(\frac{n-3}{3}\right)^{\frac{1}{n-6}}\left(\frac{M}{2^s N\rho_o}\right)^{1/3} \tag{106}$$

$$U_o^2 = \frac{2}{3\cdot 2^s}\left(\frac{N\pi\varepsilon}{M}\right)(n-6)\, f(n)\left(\frac{n-3}{3}\right)^{\frac{6}{n-6}} \tag{107}$$

Solving Equation (107) for ε and substituting it and Equation (106) into Equation (95) gives:

$$\mu^2 = \frac{4}{2^s}\left(\frac{N\pi}{M}\right) U_o^2 \frac{3\cdot 2^s}{2}\left(\frac{M}{N\pi}\right)\frac{1}{(n-6)f(n)}\left(\frac{3}{n-3}\right)^{\frac{6}{n-6}} f(n)$$

$$\times\left[\frac{\left(\frac{n-3}{3}\right)^{\frac{n}{n-6}}}{(n-2)(n-3)}\left(\frac{M}{2^s N\rho_o}\right)^{n/3}\left(\frac{2^s\rho_o N}{M}\right)^{n/3}(x^{n-2}-1) - \frac{\left(\frac{n-3}{3}\right)^{6/n-6}}{12}\left(\frac{M}{2^s N\rho_o}\right)^2\left(\frac{2^s\rho_o N}{M}\right)^2(x^4-1)\right] \tag{P1}$$

$$\mu^2 = \frac{6U_o^2}{(n-6)} \left(\frac{3}{n-3}\right)^{\frac{6}{n-6}} \left[\frac{\left(\frac{n-3}{3}\right)^{\frac{n}{n-6}}}{(n-2)(n-3)} (x^{n-2} - 1) - \frac{\left(\frac{n-3}{3}\right)^{\frac{6}{n-6}}}{12} (x^4 - 1) \right] \quad \text{(P2)}$$

$$\mu^2 = \frac{6U_o^2}{(n-6)} \left[\frac{\left(\frac{n-3}{3}\right)^{\frac{n}{n-6} - \frac{6}{n-6}}}{(n-2)(n-3)} (x^{n-2} - 1) - \frac{x^4 - 1}{12} \right] \quad \text{(P3)}$$

$$\mu^2 = \frac{6U_o^2}{(n-6)} \left[\frac{(n-3)}{3(n-2)(n-3)} (x^{n-2} - 1) - \frac{x^4 - 1}{12} \right] \quad \text{(P4)}$$

or:

$$\mu^2 = U_o^2 \left(\frac{2}{n-6}\right) \left[\frac{x^{n-2} - 1}{n-2} - \frac{x^4 - 1}{4} \right] \quad (108)$$

which is Equation (108).

Appendix Q

Derivation of Equation (114)

Equation (95) is:

$$\mu^2 = \frac{4}{2^s}\left(\frac{N\pi\varepsilon}{M}\right) f(n)\left[\frac{\sigma^n}{(n-2)(n-3)}\left(\frac{2^s\rho_o N}{M}\right)^{n/3}(x^{n-1}-1) - \frac{\sigma^6}{12}\left(\frac{2^s\rho_o N}{M}\right)^2(x^4-1)\right] \tag{95}$$

where:

$$f(n) = \frac{(n/6)^{n/n-6}}{(n/6-1)} \tag{71}$$

Taking the limit as $n \to 6$ gives:

$$\mu^2 = \frac{4}{2^s}\left(\frac{N\pi\varepsilon}{M}\right) \lim_{n \to 6}\left\{f(n)\left[\frac{\sigma^n}{(n-2)(n-3)}\left(\frac{2^s\rho_o N}{M}\right)^{n/3}(x^{n-2}-1) - \frac{\sigma^6}{12}\left(\frac{2^s\rho_o N}{M}\right)^2(x^4-1)\right]\right\} \tag{Q1}$$

Since the limit of a product is the product of the limits[161] this may be written, considering Equation (71), as:

$$\mu^2 = \frac{4}{2^s}\left(\frac{N\pi\varepsilon}{M}\right) \lim_{n \to 6}(n/6)^{\frac{n}{n-6}} \times \lim_{n \to 6}\frac{\left[\frac{\sigma^n}{(n-2)(n-3)}\left(\frac{2^s\rho_o N}{M}\right)^{n/3}(x^{n-2}-1) - \frac{\sigma^6}{12}\left(\frac{2^s\rho_o N}{M}\right)(x^4-1)\right]}{n/6-1} \tag{Q2}$$

From Equations (G6)-(G9):

$$\lim_{n \to 6} \left(\frac{n}{6}\right)^{\frac{n}{n-6}} = e \qquad (Q3)$$

The second factor is:

$$\lim_{n \to 6} \frac{\left[\frac{\sigma^n}{(n-2)(n-3)} \left(\frac{2^s \rho_o N}{M}\right)^{n/3} (x^{n-2} - 1) - \frac{\sigma^6}{12} \left(\frac{2^s \rho_o N}{M}\right)^2 (x^4 - 1)\right]}{n/6 - 1} \qquad (Q4)$$

which on careful examination clearly $\Rightarrow \frac{0}{0}$. Applying L'Hôspital's rule[15] gives:

$$= \lim_{n \to 6} \frac{\frac{\sigma^n}{(n-2)(n-3)}\left(\frac{2^s \rho_o N}{M}\right)^{n/3} x^{n-2} \ell n x + \frac{\sigma^n}{(n-2)(n-3)} \left(\frac{2^s \rho_o N}{M}\right)^{n/3} \ell n\, \sigma \left(\frac{2^s \rho_o N}{M}\right)^{1/3} (x^{n-2} - 1) - \sigma^n \left(\frac{2^s \rho_o N}{M}\right)^{n/3} \frac{(x^{n-2} - 1)(2n-5)}{(n-2)^2 (n-3)^2}}{1/6} \qquad (Q5)$$

$$= \lim_{n \to 6} \frac{6\sigma^n}{(n-2)(n-3)} \left(\frac{2^s \rho_o N}{M}\right)^{n/3} \left[x^{n-2} \ell n\, x + (x^{n-2} - 1) \left| \ell n\, \sigma \left(\frac{2^s \rho_o N}{M}\right)^{1/3} - \frac{2n - 5}{(n-2)(n-3)} \right| \right] \qquad (Q6)$$

$$= \frac{\sigma^6}{2} \left(\frac{2^2 \rho_o N}{M}\right)^2 \left[x^4 \ell n\, x + (x^4 - 1)\left(\ell n\, \sigma \left(\frac{2^2 \rho_o N}{M}\right)^{1/3} - \frac{7}{12}\right) \right] \qquad (Q7)$$

Substituting for the two limits (Equations (Q3) and (Q7)) in the

expression for μ^2 (Equation (Q2)) gives:

$$\mu^2 = \frac{4}{2^s}\left(\frac{N\pi\varepsilon}{M}\right) e \frac{\sigma^6}{2}\left(\frac{2^s\rho_o N}{M}\right)^2 \left[x^4 \ln x + (x^4 - 1)\left(\ln \sigma\left(\frac{2^s\rho_o N}{M}\right)^{1/3} - \frac{7}{12}\right)\right] \quad (Q8)$$

or:

$$\mu^2 = \frac{2e}{2^s}\left(\frac{N\pi\varepsilon}{M}\right) \sigma^6\left(\frac{2^s\rho_o N}{M}\right)^2 \left[x^4 \ln x + \left(\ln \sigma\left(\frac{2^s\rho_o N}{M}\right)^{1/3} - \frac{7}{12}\right)(x^4 - 1)\right] \quad (114)$$

which is Equation (114).

Appendix R

Derivation of Equations (115) - (122)

Equation (114) is:

$$\mu^2 = \frac{2e}{2^s}\left(\frac{N\pi\varepsilon}{M}\right)\sigma^6\left(\frac{2^s\rho_o N}{M}\right)^2\left[x^4\ \ell n\, x + \left(\ell n\ \sigma\left(\frac{2^s\rho_o N}{M}\right)^{1/3} - \frac{7}{12}\right)(x^4 - 1)\right] \tag{114}$$

Letting:

$$\alpha' = \frac{2e}{2^s}\left(\frac{N\pi\varepsilon}{M}\right)\sigma^6\left(\frac{2^s\rho_o N}{M}\right)^2 \tag{116}$$

$$\beta' = \frac{2e}{2^s}\left(\frac{N\pi\varepsilon}{M}\right)\sigma^6\left(\frac{2^s\rho_o N}{M}\right)^2\left(\ell n\ \sigma\left(\frac{2^s\rho_o N}{M}\right)^{1/3} - \frac{7}{12}\right) \tag{117}$$

this becomes:

$$\mu^2 = \alpha' x^4\ \ell n\, x + \beta'(x^4 - 1) \tag{115}$$

which are Equations (115) - (117). From Equation (18):

$$U_o = \lim_{x \to 1}\frac{d\mu}{dx} \tag{18}$$

and Equation (115) becomes:

$$2\mu\frac{d\mu}{dx} = \alpha' x^4 \cdot \frac{1}{x} + 4\alpha' x^3\ \ell n\, x + 4\beta' x^3 \tag{R1}$$

or:

$$\frac{d\mu}{dx} = \frac{x^3}{2}\,\frac{\alpha'(1 + 4\ell n\, x) + 4\beta'}{\mu} \tag{R2}$$

Therefore:

$$U_o = \frac{1}{2} \lim_{\substack{x \to 1 \\ \mu \to 0}} x^3 \frac{\alpha'(1 + 4\ell n\ x) + 4\beta'}{\mu} \Rightarrow \frac{1}{2} \frac{\alpha' + 4\beta'}{0} \Rightarrow \infty \qquad \text{(R3)}$$

which diverges. The limit can exist if, and only if:

$$\alpha' + 4\beta \equiv 0 \qquad \text{(R4)}$$

in which case:

$$U_o = \frac{1}{2} \lim_{\substack{x \to 1 \\ \mu \to 0}} \frac{\alpha'(1 + 4\ell n\ x) + 4\beta'}{\mu} \Rightarrow \frac{0}{0} \qquad \text{(R5)}$$

Applying L'Hôspital's rule[15] again gives:

$$U_o = \frac{1}{2} \lim_{x \to 1} \frac{4\alpha'/x}{\frac{d\mu}{dx}} = \frac{2\alpha'}{\lim\limits_{x \to 1} \frac{d\mu}{dx}} \qquad \text{(R6)}$$

and using Equation (18):

$$U_o^2 = 2\alpha' \qquad \text{(R7)}$$

or:

$$U_o^2 = \frac{4e}{2^s} \left(\frac{N\pi\varepsilon}{M}\right) \sigma^6 \left(\frac{2^s \rho_o N}{M}\right)^2 \qquad \text{(118)}$$

which is Equation (118). The "condition", Equation (R4), can be written, after substitution of α' and β' :

$$\frac{2e}{2^s}\left(\frac{N\pi\varepsilon}{M}\right) \sigma^6 \left(\frac{2^s \rho_o N}{M}\right)^2 + 4 \frac{2e}{2^s}\left(\frac{N\pi\varepsilon}{M}\right) \sigma^6 \left(\frac{2^s \rho_o N}{M}\right)^2 \left(\ell n\ \sigma \left(\frac{2^s \rho_o N}{M}\right)^{1/3} - \frac{7}{12}\right) = 0 \qquad \text{(R8)}$$

or:

$$\ln \sigma\left(\frac{2^s \rho_o N}{M}\right)^{1/3} = -\frac{1}{4} + \frac{7}{12} = \frac{4}{12} = \frac{1}{3} \tag{R9}$$

$$\sigma^3\left(\frac{2^s \rho_o N}{M}\right) = e \tag{119}$$

Solution of Equation (119) for σ gives:

$$\sigma = e^{1/3}(M/2^s \rho_o N)^{1/3} \tag{120}$$

which is Equation (120). This fixes σ and substitution into Equation (118) gives:

$$U_o^2 = \frac{4e}{2^s}\left(\frac{N\pi\varepsilon}{M}\right) e^2 \cancel{\left(\frac{M}{2^s \rho_o N}\right)^2} \cancel{\left(\frac{2^s \rho_o N}{M}\right)^2} \tag{R10}$$

$$U_o^2 = \frac{4e^3}{2^s}\left(\frac{N\pi\varepsilon}{M}\right) \tag{121}$$

which is Equation (121).

Substitution of Equations (120) and (121) (solved for ε) into Equation (114) gives:

$$\mu^2 = \cancel{\frac{2e}{2^s}}\left(\cancel{\frac{N\pi}{M}} \frac{U_o^2 \cancel{2^s M}}{4e^3 \cancel{N\pi}}\right) \cancel{e^2}\cancel{\left(\frac{M}{2^s \rho_o N}\right)^2} \cancel{\left(\frac{2^s \rho_o N}{M}\right)^2} \left[x^4 \ln x + \right.$$

$$\left. \left(\ln e^{1/3} \cancel{\left(\frac{M}{2^s \rho_o N}\right)^{1/3}} \cancel{\left(\frac{2^s \rho_o N}{M}\right)^{1/3}} - \frac{7}{12}\right)(x^4 - 1)\right] \tag{R11}$$

$$\mu^2 = \frac{1}{2} U_o^2 [x^4 \ln x - \frac{1}{4}(x^4 - 1)] \tag{122}$$

which is Equation (122).

Appendix S

Compilation of Raw and Adjusted U-μ Data

Notes:

1) Symbol, Group-Period Numbers (in Periodic Table) and Atomic Number follow each element name. For compounds the atomic formula follows the name.

2) M = molecular weight -g/g mole

m = number of data points

s = "structure" constant - s=1, fcc; s=2, bcc; s=3, diamond

m1,m2,etc. = number of data points for succeeding references

ρ_o = initial density

V_o = initial specific volume

T_o = initial temperature

P_o = initial pressure

C_o = sound speed

3) U and μ are given in units of cm/sec

4) $\overline{\mu^2}$ = mean-squared-particle velocity = $\sum_i \mu_i^2/m$

$\overline{\rho_o}$ = mean initial density = $\frac{1}{m}\sum_i \rho_{oi} m_i = \frac{1}{m}\sum_i m_i/V_{oi}$

$\overline{V_o}$ = mean initial specific volume = $\frac{1}{m}\sum_i V_{oi} m_i = \frac{1}{m}\sum_i m_i/\rho_{oi}$

$\overline{T_o}$ = mean initial temperature

$\overline{P_o}$ = mean initial pressure

$\overline{C_o}$ = mean sound speed

5) $C_B \equiv$ sound speed from P. N. Bridgman data as quoted; used when C_o is not available.

6) $$\sigma_{\overline{\rho_o}} = \left(\frac{1}{n}\sum_i (\rho_{oi} - \overline{\rho_o})^2\right)^{1/2}$$

$$\sigma_{\overline{V_o}} = \left(\frac{1}{n}\sum_i (V_{oi} - \overline{V_o})^2\right)^{1/2}$$

In both cases these are the standard deviation of the data from reference-to-reference and do not represent the accuracy of the data itself. The result is presented as:

$$\overline{\rho_o} = \overline{\rho_o} \pm \sigma_{\overline{\rho_o}}$$

$$\overline{V_o} = \overline{V_o} \pm \sigma_{\overline{V_o}}$$

7) $s=1;\ a_o = 1.12246(M/\rho_o N)^{1/3}$ - fcc

$s=2;\ a_o = 1.09112(M/\rho_o N)^{1/3}$ - bcc

$s=3;\ a_o = 0.86603(M/\rho_o N)^{1/3}$ - diamond

where

a_o = nearest neighbor distance

ARGON

A

0-3 ; Z = 18

M = 39.944

m = 19

s = 1

U		μ		Reference	Initial Conditions
0.544	E 06	0.252	E 06	ml = 19	64
0.340	E 06	0.123	E 06		
0.541	E 06	0.257	E 06		
0.526	E 06	0.254	E 06		
0.518	E 06	0.258	E 06		
0.715	E 06	0.365	E 06		
0.636	E 06	0.320	E 06		
0.676	E 06	0.340	E 06		
0.270	E 06	0.088	E 06		
0.498	E 06	0.232	E 06		
0.152	E 06	0.0301	E 06		
0.219	E 06	0.0674	E 06		
0.644	E 06	0.330	E 06		
0.540	E 06	0.258	E 06		
0.334	E 06	0.134	E 06		
0.345	E 06	0.135	E 06		
0.338	E 06	0.133	E 06		
0.334	E 06	0.132	E 06		
0.334	E 06	0.133	E 06		

$\overline{\rho_o} = 1.405 \pm 0.002$ g/cc

$T_o = 86^oK$

$P_o = 2$ bar

$C_o = 0.0848 \times 10^6$ cm/sec*

$\overline{\mu^2} = 0.504 \times 10^{11}$ cm^2/sec^2**

$\overline{\rho_o} = 1.405 \pm 0.002$ g/cc

$\overline{V_o} = 0.7117 \pm 0.0011$*** cc/g

$\overline{T_o} = 86^oK$

$\overline{P_o} = 1.97$ atm

$\overline{C_o} = 0.0848 \quad 10^{6*}$ cm/sec

$a_o = 4.057\text{Å}$

---

*Reference 96

**Hand Calc. (Monroe): $\overline{\mu^2} = 0.05044477 \times 10^{12}$; computer output: $\overline{\mu^2} = 0.05044476 \times 10^{12}$

***Found from $\frac{1}{\overline{\rho_o} + 0.002}$ and $\frac{1}{\overline{\rho_o} - 0.002}$

ARGON
A - II

0-3 ; Z = 18

M = 39.944

m = 19

s = 1

U		μ			Reference	Initial Conditions
0.3700	E 06	0.1923	E 06	ml = 6	64	$\rho_o = 0.919 \pm 0.0$g/cc
0.5424	E 06	0.3188	E 06			
0.6497	E 06	0.404	E 06			$T_o = 148.2^oK$
0.3183	E 06	0.1592	E 06			
0.4934	E 06	0.2876	E 06			$P_o = 70$ bar
0.654	E 06	0.4005	E 06			$C_o = 0.035 \times 10^6$cm/sec*

$\overline{\mu^2} = 0.950 \times 10^{11}\text{cm}^2/\text{sec}^2$

$\overline{\rho_o} = 0.919 \pm 0.0\text{g/cc}$

$\overline{V_o} = 1.088 \pm 0.0\text{g/cc}$

$\overline{T_o} = 148.2^oK$

$\overline{P_o} = 69.2$ atm

$\overline{C_o} = 0.035 \times 10^6\text{cm/sec}$*

$a_o = 4.673\text{Å}$

*Reference 96

ARGON
A-III

0-3 ; Z = 18

M = 39.944

m = 19

s = 1

U	μ		Ref.	Initial Conditions ρ_o-g/cc	T_o-°K	P_o-K bar	$C_o \times 10^{-6}$ cm/sec
0.287 E 06	0.142 E 06	ml = 5	96	0.971	302.2	1.034	0.075
0.385 E 06	0.186 E 06			0.994	299.0	1.074	0.077
0.472 E 06	0.253 E 06			0.972	303.0	1.040	0.0775
0.484 E 06	0.266 E 06			0.988	302.7	1.081	0.0772
0.6873 E 06	0.410 E 06			0.986	307.7	1.110	0.0775

$\overline{\mu^2} = 0.715 \times 10^{11} \text{cm}^2/\text{sec}^2$

$\overline{\rho_o} = 0.982 \pm 0.009$ g/cc

$\overline{V_o} = 1.018 \pm 0.010$ cc/g

$\overline{T_o} = 302.9^{\circ}\text{K}$

$\overline{P_o} = 1054.0$ atm

$\overline{C_o} = 0.077 \times 10^{6} \text{cm/sec}$

$a_o = 4.571\text{Å}$

ARGON
A - IV

0-3 ; Z = 18

M = 39.944

m = 2

s = 1

U		μ			Ref.	Initial Conditions ρ_o-g/cc	T_o-°K	P_o-K bar	$C_o \times 10^{-6}$- cm/sec
0.4968	E 06	0.252	E 06	m1 = 2	96	1.138	305.4	1.662	0.091
0.6779	E 06	0.397	E 06			1.135	298.3	1.586	0.091

$\overline{\mu^2} = 0.111 \times 10^{12} cm^2/sec^2$

$\overline{\rho_o} = 1.137 \pm 0.002$ g/cc

$\overline{V_o} = 0.8799 \pm 0.0012$ cc/g

$\overline{T_o} = 301.9°K$

$\overline{P_o} = 1602.7$ atm

$\overline{C_o} = 0.091 \times 10^6 cm/sec$

$a_o = 4.353 Å$

MERCURY
Hg

II-6 ; Z=80

M = 200.61

m = 3

s = 1

U		μ			Ref.	Initial Conditions V_o-cc/g	T_o-°C	
0.2752	E 06	0.0608	E 06	ml = 3	90	0.0739	25	$C_o = 0.145 \times 10^6$ cm/sec*
0.3101	E 06	0.0772	E 06			0.0739	17	
0.3504	E 06	0.0978	E 06			0.0739	24	

$\overline{\mu^2} = 0.641 \times 10^{10} \text{cm}^2/\text{sec}^2$

$\overline{\rho_o} = 13.53 \pm 0.0$ g/cc

$\overline{V_o} = 0.0739 \pm 0.0$ cc/g

$\overline{T_o} = 22^\circ\text{C}$

$\overline{C_o} = 0.1451 \times 10^6$ cm/sec

$a_o = 3.265\text{Å}$

*Reference 96

NITROGEN* N_2

V-2 ; Z = 7

M = 28.016

m = 14

s = 1

U		μ			Reference	Initial Conditions
0.314	E 06	0.117	E 06	m1 = 5	42	$\rho_o = 0.808$ g/cc
0.374	E 06	0.157	E 06			
0.500	E 06	0.250	E 06			$T_o = 77.4^oK$
0.745	E 06	0.427	E 06			$C_o = 0.0849 \times 10^6$cm/sec**
0.905	E 06	0.552	E 06			
0.379	E 06	0.172	E 06	m2 = 9	96	
0.381	E 06	0.144	E 06			$\rho_o = 0.808$ g/cc
0.297	E 06	0.110	E 06			
0.411	E 06	0.174	E 06			$V_o = 1.238$ cc/g
0.492	E 06	0.232	E 06			
0.220	E 06	0.064	E 06			$T_o = 77^oK$
0.568	E 06	0.274	E 06			
0.566	E 06	0.270	E 06			$C_o = 0.0857 \times 10^6$cm/sec
0.647	E 06	0.326	E 06			

$\overline{\mu^2} = 0.0709 \times 10^{12} cm^2/sec^2$

$\overline{\rho_o} = 0.808 \pm 0.0$ g/cc

$\overline{V_o} = 1.238 \pm 0.0$ cc/g

$\overline{T_o} = 77.2^oK$

$\overline{C_o} = 0.0853 \times 10^6$cm/sec

$a_o = 4.334\mathring{A}$

---

*These raw data were adjusted (see following page) in the selection process (see text).

**Reference 96

NITROGEN*

N_2

V-2 ; Z = 7

M = 28.016

m = 9

s = 1

U	μ		Reference	Initial Conditions
0.314 E 06	0.117 E 06	m1 = 3	42	$\rho_o = 0.808$ g/cc
0.374 E 06	0.157 E 06			$T_o = 77.4^oK$
0.500 E 06	0.250 E 06			$C_o = 0.0849 \times 10^6$ cm/sec**
0.379 E 06	0.172 E 06	m2 = 6	96	$\rho_o = 0.808$ g/cc
0.381 E 06	0.144 E 06			$V_o = 1.238$ cc/g
0.297 E 06	0.110 E 06			$T_o = 77^oK$
0.411 E 06	0.174 E 06			$C_o = 0.0857 \times 10^6$ cm/sec
0.492 E 06	0.232 E 06			
0.220 E 06	0.064 E 06			

$\overline{\mu^2} = 0.279 \times 10^{11} cm^2/sec^2$

$\overline{\rho_o} = 0.808 \pm 0.0$ g/cc

$\overline{V_o} = 1.238 \pm 0.0$ cc/g

$\overline{T_o} = 77.1^oK$

$\overline{C_o} = 0.0854 \times 10^6$ cm/sec

$a_o = 4.334\text{Å}$

---

*Adjusted data

**Reference 96

HYDROGEN
H_2

I-1 ; Z = 1

M = 2.0160

m = 1

s = 1

				Initial Conditions				
U	μ		Ref.	V_o-cc/g	T_o-°K	P_o-bar	$C_o \times 10^{-6}$-cm/sec*
0.940 E 06	0.592 E 06	ml = 1	60	14.1	20.45	1.8	0.11193

$\overline{\mu^2} = 0.350 \times 10^{12} cm^2/sec^2$

$\overline{\rho_o} = 0.0709 \pm 0.0$ g/cc

$\overline{V_o} = 14.1 \pm 0.0$ cc/g

$\overline{T_o} = 20.45°K$

$\overline{P_o} = 1.78$ atm

$\overline{C_o} = 0.11193 \times 10^6$ cm/sec

$a_o = 4.057 Å$

*Reference 99

CARBON DISULPHIDE*

CS_2

M = 76.143

m = 6

s = 1

U		μ			Reference	Initial Conditions T_o °C	$C_o \times 10^{-6}$ cm/sec	
0.432	E 06	0.2412	E 06	m1 = 2	90	33	0.112	P_o = 1 atm
0.337	E 06	0.1415	E 06			17	0.117	
0.270	E 06	0.063	E 06	m2 = 4	100			
0.191	E 06	0.030	E 06					
0.190	E 06	0.028	E 06					
0.165	E 06	0.019	E 06					

$\overline{\mu^2} = 0.140 \times 10^{11} cm^2/sec^2$

$\overline{\rho_o} = 1.255 \pm 0.0$ g/cc**

$\overline{V_o} = 0.7968 \pm 0.0$ cc/g***

$\overline{T_o} = 25.0^{\circ}C$

$\overline{P_o}$ = 1 atm

$\overline{C_o} = 0.115 \times 10^6$ cm/sec

$a_o = 5.223\text{Å}$

---

*These raw data were adjusted (see following page) in the selection process (see text).

**Estimated from Reference 101:

ρ_o-g/cc	T-°C	Page
1.2628	20	911
1.293	0	2139

$\therefore \rho_o$ @ 25°C is given by: $\frac{\rho_o - 1.293}{-0.0302} = \frac{25-0}{20}$; $\rho_o = 1.293 - (\frac{5}{4})(0.0302)$

$= 1.255$ g/cc

*** $\overline{V_o} = 1/\overline{\rho_o}$

CARBON DISULPHIDE*

CS_2

M = 76.143

m = 4

s = 1

U	μ	Reference	Initial Conditions
0.270 E 06	0.063 E 06	ml = 4	100
0.191 E 06	0.030 E 06		
0.190 E 06	0.028 E 06		
0.165 E 06	0.019 E 06		

$\overline{\mu^2} = 0.150 \times 10^{10} cm^2/sec^2$

$\overline{\rho_o} = 1.255 \pm 0.0$ g/cc**

$\overline{V_o} = 0.7968 \pm 0.0$ cc/g**

$\overline{T_o} = 25.0^oC$**

$\overline{P_o} = 1$ atm**

$\overline{C_o} = 0.115 \times 10^6$ cm/sec**

$a_o = 5.223\text{Å}$

---

*Adjusted data

**Estimated to be the same as Reference 90 since no data given in Reference 100. See previous page.

CARBON TETRACHLORIDE

CCl_4

M = 153.839

m = 14

s = 1

U	μ		Reference	ρ_o g/cc	Initial Conditions V_o cc/g	T_o °C	$C_o \times 10^{-6}$ cm/sec	
0.485 E 06	0.2235 E 06	m1 = 2	90		0.634	25	0.0930	
0.351 E 06	0.1325 E 06				0.629	22	0.0940	P_o = 1 atm
0.420 E 06	0.193 E 06	m2 = 5	100					
0.329 E 06	0.136 E 06							
0.285 E 06	0.110 E 06							
0.218 E 06	0.0605 E 06							
0.193 E 06	0.0390 E 06							
0.251 E 06	0.071 E 06	m3 = 7	96	1.576		29		
0.460 E 06	0.207 E 06			1.584		25		
0.337 E 06	0.118 E 06			1.594		20		$C_o = 0.0943 \times 10^6$
0.332 E 06	0.119 E 06			1.603		16		cm/sec @ 20°C
0.397 E 06	0.158 E 06			1.604		15		
0.345 E 06	0.121 E 06			1.607		13		
0.492 E 06	0.232 E 06			1.582		26		

$\overline{\mu^2} = 0.221 \times 10^{11} cm^2/sec^2$

$\overline{\rho_o} = 1.591 \pm 0.011$ g/cc

$\overline{V_o} = 0.629 \pm 0.005$ cc/g

$\overline{T_o} = 21.2°C$

$\overline{P_o} = 1$ atm

$\overline{C_o} = 0.0941 \times 10^6$ cm/sec

$a_o = 6.100 Å$

METHANOL

CH_3OH

M = 32.0430

m = 5

s = 1

U		μ			Reference	Initial Conditions V_o-cc/g	T_o-°C	
0.551	E 06	0.2525	E 06	m1 = 2	90	1.271	24	P_o = 1 atm
0.395	E 06	0.1483	E 06			1.255	15	C_o = 0.1125 $\times 10^6$@20°C*
0.550	E 06	0.246	E 06	m2 = 3	100			
0.530	E 06	0.230	E 06					
0.534	E 06	0.242	E 06					

$\overline{\mu^2} = 0.515 \times 10^{11}$

$\overline{\rho_o} = 0.7918 \pm 0.0050$ g/cc

$\overline{V_o} = 1.263 \pm 0.008$ cc/g

$\overline{T_o} = 19.5°C$

$\overline{P_o} = 1$ atm

$\overline{C_o} = 0.1125 \times 10^6$ cm/sec

$a_o = 4.563\text{Å}$

---

* From Reference 98

ETHANOL

C_2H_5OH

M = 46.0700

m = 5

s = 1

Initial Conditions

U	μ		Reference	ρ_o-g/cc	V_o-cc/g	T_o-°C	$C_o \times 10^{-6}$- cm/sec	
0.563 E 06	0.2500 E 06	m1= 2	90		1.275	26	0.1162**	
0.403 E 06	0.1487 E 06				1.267	21	0.1141**	P_o= 1 atm
0.374 E 06	0.132 E 06	m2= 3	94	0.78097*		30		
0.413 E 06	0.1485 E 06			0.78267*		28		P_o= 1 atm
0.604 E 06	0.284 E 06			0.78522*		25		

$\overline{\mu^2} = 0.409 \times 10^{11} cm^2/sec^2$

$\overline{\rho_o} = 0.7845 \pm 0.0028$ g/cc

$\overline{V_o} = 1.275 \pm 0.005$ cc/g

$\overline{T_o} = 26.0^oC$

$\overline{P_o} = 1$ atm

$\overline{C_o} = 0.1152 \times 10^6$ cm/sec

$a_o = 5.166\text{Å}$

*From Reference 101

**From Reference 98

ETHYL ETHER

$(C_2H_5)_2O$

M = 74.1240

m = 11

s = 1

U	μ		Reference	V_o-cc/g	T_o-°C	Initial Conditions
0.540 E 06	0.2550 E 06	m1 = 2	90	1.433	32	P_o = 1 atm
0.388 E 06	0.1517 E 06			1.407	21	C_o = 0.1155×10^6 cm/sec @ 20°C*
0.671 E 06	0.350 E 06	m2 = 9	98			
0.686 E 06	0.355 E 06					
0.711 E 06	0.359 E 06					ρ_o = 0.71 g/cc
0.812 E 06	0.458 E 06					V_o = 1.41 cc/g
0.792 E 06	0.472 E 06					
0.836 E 06	0.467 E 06					
0.815 E 06	0.474 E 06					
1.346 E 06	0.847 E 06					
1.421 E 06	0.852 E 06					

$\overline{\mu^2} = 0.253 \times 10^{12}\ cm^2/sec^2$

$\overline{\rho_o} = 0.709 \pm 0.004$ g/cc

$\overline{V_o} = 1.41 \pm 0.01$ cc/g

$\overline{T_o} = 26.5°C$

$\overline{P_o}$ = 1 atm

$\overline{C_o} = 0.1155 \times 10^6$ cm/sec

$a_o = 6.261 Å$

*From Reference 98

HEXANE

C_6H_{14}

M = 86.1780

m = 4

s = 1

Initial Conditions

U	μ		Reference	V_o-cc/g	T_o-°C	
0.554 E 06	0.2590 E 06	m1 = 2	90	1.499	32	P_o = 1 atm
0.402 E 06	0.1517 E 06			1.471	19	C_o = 0.1083×10^6 cm/sec @ 20°C*
0.417 E 06	0.152 E 06	m2 = 2	94	1.484**	25	
0.392 E 06	0.156 E 06			1.486**	26	P_o = 1 atm

$\overline{\mu^2}$ = 0.344×10^{11} cm^2/sec^2 $\quad \overline{T_o}$ = 25.5 °C $\quad a_o$ = 6.698 Å

$\overline{\rho_o}$ = 0.6734 ± 0.0045 g/cc $\quad \overline{P_o}$ = 1 atm.

$\overline{V_o}$ = 1.485 ± 0.010 cc/g $\quad \overline{C_o}$ = 0.1083×10^6 cm/sec

---

*From Reference 98

**For Hexane from data in Reference 90:

V_o-cc/g	T_o-°C
1.471	19
1.499	32

$\therefore V_o$ @ 25°C is given by: $\frac{V_o - 1.471}{0.028} = \frac{25-19}{32-19}$; V_o = 1.484 cc/g

V_o @ 26°C is given by: $\frac{V_o - 1.471}{0.028} = \frac{26-19}{32-19}$; V_o = 1.486 cc/g

BENZENE

C_6H_6

M = 78.1140

m = 19

s = 1

U		μ			Reference	ρ_o-g/cc	Initial Conditions V_o-cc/g	T_o-°C	$C_o \times 10^6$ cm/sec	
0.566	E 06	0.2470	E 06	m1 = 2	90		1.155	32	0.128	P_o = 1 atm
0.410	E 06	0.1448	E 06				1.133	16	0.135	
0.459	E 06	0.192	E 06	m2 = 6	100					
0.459	E 06	0.188	E 06							
0.316	E 06	0.0980	E 06							
0.277	E 06	0.0670	E 06							
0.247	E 06	0.0560	E 06							
0.197	E 06	0.0280	E 06							
0.542	E 06	0.232	E 06	m3 = 11	98	0.877		22		
0.537	E 06	0.228	E 06			0.877		22		
0.335	E 06	0.093	E 06			0.874		23		C_o = 0.129
0.531	E 06	0.229	E 06			0.879		20		$\times 10^6$ cm/sec
0.599	E 06	0.262	E 06			0.884		15		
0.590	E 06	0.253	E 06			0.881		18		
0.465	E 06	0.174	E 06			0.884		15		
0.588	E 06	0.251	E 06			0.895		5		
0.574	E 06	0.253	E 06			0.877		22		
0.405	E 06	0.132	E 06			0.887		13		
0.580	E 06	0.255	E 06			0.872		26		

$\overline{\mu^2} = 0.374 \times 10^{11} cm^2/sec^2$; $\overline{\rho_o} = 0.880 \pm 0.007$ g/cc; $\overline{V_o} = 1.137 \pm 0.009$ cc/g; $\overline{T_o} = 19°C$; P_o = 1 atm;

$\overline{C_o} = 0.129 \times 10^6$ cm/sec; $a_o = 5.929$ Å

TOLUENE

$C_6H_5CH_3$

M = 92.1410

m = 2

s = 1

U		μ			Reference	V_o-cc/g	Initial Conditions T_o-°C	
0.573	E 06	0.2412	E 06	ml= 2	90	1.138	4	P_o = 1 atm
0.412	E 06	0.1443	E 06			1.141	15	C_o = 0.1328×10^6 cm/sec* @ 20°C

$\overline{\mu^2} = 0.395 \times 10^{11} cm^2/sec^2$

$\overline{\rho_o} = 0.8776 \pm 0.0012$ g/cc

$\overline{V_o} = 1.140 \pm 0.0016$ cc/g

$\overline{T_o} = 9.5°C$

$\overline{P_o} = 1$ atm

$\overline{C_o} = 0.1328 \times 10^6$ cm/sec

$a_o = 6.270Å$

*Reference 98

WATER*
H_2O

M = 18.0160
m = 52
s = 1,3

U		μ			Reference	Initial Conditions
0.3354	E 06	0.0952	E 06	m1 = 16	90	
0.4093	E 06	0.1392	E 06			
0.4126	E 06	0.1411	E 06			V_o = 1.0018 cc/g
0.4536	E 06	0.1655	E 06			T_o = 20°C
0.4813	E 06	0.1829	E 06			P_o = 1 atm
0.4777	E 06	0.1806	E 06			C_o = 0.14829
0.4757	E 06	0.1798	E 06			$\times 10^6$ cm/sec**
0.5626	E 06	0.2385	E 06			
0.5626	E 06	0.2370	E 06			
0.5601	E 06	0.2335	E 06			
0.807	E 06	0.413	E 06			
0.807	E 06	0.424	E 06			
0.845	E 06	0.460	E 06			
0.849	E 06	0.472	E 06			
0.859	E 06	0.472	E 06			
0.874	E 06	0.481	E 06			
0.706	E 06	0.332	E 06	m2 = 7	96	
0.705	E 06	0.339	E 06			ρ_o = 1.00 g/cc
0.689	E 06	0.344	E 06			V_o = 1.002 cc/g
0.826	E 06	0.453	E 06			C_o = 0.15 $\times 10^6$ cm/sec
1.285	E 06	0.809	E 06			
1.269	E 06	0.843	E 06			
1.309	E 06	0.871	E 06			
0.442	E 06	0.152	E 06	m3 = 1	102	ρ_o = 1.00 g/cc
0.5835	E 06	0.2365	E 06	m4 = 26	96	
0.5900	E 06	0.2270	E 06			
0.5725	E 06	0.2140	E 06			
0.5625	E 06	0.2115	E 06			
0.5555	E 06	0.2125	E 06			ρ_o = 1.00 g/cc
0.5545	E 06	0.2110	E 06			$\overline{V_o}$ = 1.00 cc/g
0.5460	E 06	0.2180	E 06			
0.5395	E 06	0.2120	E 06			
0.5260	E 06	0.2185	E 06			
0.5235	E 06	0.2140	E 06			
0.5160	E 06	0.2005	E 06			
0.5225	E 06	0.1980	E 06			
0.5185	E 06	0.1975	E 06			
0.4830	E 06	0.1915	E 06			
0.4730	E 06	0.1840	E 06			

WATER*

U		μ		Reference Initial Conditions		
0.4570	E 06	0.1675	E 06			
0.4165	E 06	0.1465	E 06			
0.4280	E 06	0.1390	E 06			
0.4075	E 06	0.1340	E 06			
0.3885	E 06	0.1300	E 06			
0.3635	E 06	0.1100	E 06			
0.3465	E 06	0.1110	E 06			
0.3625	E 06	0.1060	E 06			
0.3480	E 06	0.1080	E 06			
0.3240	E 06	0.0970	E 06			
0.3205	E 06	0.0970	E 06			
0.387	E 06	0.1245	E 06	m5 = 2	94	ρ_o = 0.99626 g/cc***
0.409	E 06	0.140	E 06			V_o = 1.00375 cc/g***
						T_o = 28°C

$\overline{\mu^2} = 0.989 \times 10^{11}\ cm^2/sec^2$

$\overline{\rho_o} = 0.999 \pm 0.001$ g/cc

$\overline{V_o} = 1.001 \pm 0.0005$ cc/g

$\overline{T_o} = 21°C$

$\overline{P_o} = 1$ atm

$\overline{C_o} = 0.15 \times 10^6$ cm/sec

$a_o = 3.485\text{Å}$ (s=1)

$a_o = 2.689\text{Å}$ (s=3)

---

*These raw data were adjusted (see following page) in the selection process (see text).

**From Reference 96

***From Reference 101, p. 2143 @ T = 28°C

WATER*

H_2O

M = 18.0160

m = 23

s = 1,3

U		μ		Reference	Initial Conditions
0.3354	E 06	0.0952	E 06	m1 = 7	90	V_o = 1.0018 cc/g
0.4093	E 06	0.1392	E 06			T_o = 20°C
0.4126	E 06	0.1411	E 06			P_o = 1 atm
0.4536	E 06	0.1655	E 06			C_o = 0.14829×10^6 cm/sec*
0.4813	E 06	0.1829	E 06			
0.4777	E 06	0.1806	E 06			
0.4757	E 06	0.1798	E 06			
0.442	E 06	0.152	E 06	m2 = 1	102	ρ_o = 1.00 g/cc
0.4830	E 06	0.1915	E 06	m3 = 13	96	
0.4730	E 06	0.1840	E 06			
0.4570	E 06	0.1675	E 06			ρ_o = 1.00 g/cc
0.4165	E 06	0.1465	E 06			$\overline{V_o}$ = 1.00 cc/g
0.4280	E 06	0.1390	E 06			
0.4075	E 06	0.1340	E 06			
0.3885	E 06	0.1300	E 06			
0.3635	E 06	0.1100	E 06			
0.3465	E 06	0.1110	E 06			
0.3625	E 06	0.1060	E 06			
0.3480	E 06	0.1080	E 06			
0.3240	E 06	0.0970	E 06			
0.3205	E 06	0.0970	E 06			
0.387	E 06	0.1245	E 06	m4 = 2	94	ρ_o = 0.99626 g/cc**
0.409	E 06	0.140	E 06			V_o = 1.00375 cc/g**
						T_o = 28°C

$\overline{\mu^2}$ = 0.206×10^{11} cm²/sec²

$\overline{\rho_o}$ = 0.999 ± 0.001 g/cc

$\overline{V_o}$ = 1.001 ± 0.001 cc/g

$\overline{T_o}$ = 22°C

$\overline{P_o}$ = 1 atm

$\overline{C_o}$ = 0.14829×10^6 cm/sec

a_o = 3.485Å (s=1)

a_o = 2.689Å (s=3)

---

*Adjusted data

**Reference 96

***From Reference 101, p.2143 @ T = 28°C

COPPER
Cu

I-4 ; Z=29

M = 63.54

m = 98

s = 1

U		μ			Reference	Initial Conditions
0.4744	E 06	0.0511	E 06	m1 = 5	85	
0.4768	E 06	0.0570	E 06			ρ_o = 8.90 g/cc
0.5070	E 06	0.0711	E 06			$C_o = 0.392 \times 10^6$ cm/sec*
0.5015	E 06	0.0731	E 06			
0.5508	E 06	0.1032	E 06			
0.536	E 06	0.094	E 06	m2 = 3	92	ρ_o = 8.93 g/cc
0.713	E 06	0.229	E 06			$C_o = 0.395 \times 10^6$ cm/sec
1.016	E 06	0.419	E 06			
0.664	E 06	0.182	E 06	m3 = 4	103	
0.806	E 06	0.271	E 06			
1.012	E 06	0.414	E 06			
1.058	E 06	0.443	E 06			
1.420	E 06	0.715	E 06	m4 = 1	104	ρ_o = 8.93 g/cc
0.668	E 06	0.210	E 06	m5 = 9	96	
0.619	E 06	0.176	E 06			ρ_o = 8.97 g/cc
0.649	E 06	0.175	E 06			V_o = 0.111 cc/g
0.618	E 06	0.175	E 06			
0.683	E 06	0.208	E 06			
0.616	E 06	0.135	E 06			
0.622	E 06	0.168	E 06			
0.590	E 06	0.136	E 06			
0.623	E 06	0.169	E 06			
0.524	E 06	0.087	E 06	m6 = 10	102	
0.669	E 06	0.182	E 06			
0.592	E 06	0.131	E 06			ρ_o = 8.93 g/cc**
0.554	E 06	0.106	E 06			V_o = 0.112 cc/g**
0.811	E 06	0.277	E 06			
0.767	E 06	0.247	E 06			
0.714	E 06	0.212	E 06			
0.662	E 06	0.177	E 06			
1.02	E 06	0.418	E 06			
0.943	E 06	0.370	E 06			
0.633	E 06	0.157	E 06	m7 = 6	13	
0.623	E 06	0.158	E 06			ρ_o = 8.90 g/cc
0.626	E 06	0.157	E 06			$C_B = 0.398 \times 10^6$ cm/sec
0.726	E 06	0.220	E 06			
0.729	E 06	0.221	E 06			
0.732	E 06	0.222	E 06			

COPPER

U		μ			Reference	Initial Conditions
0.7150	E 06	0.2290	E 06	m8 = 45	96	
0.7120	E 06	0.223	E 06			
0.7540	E 06	0.243	E 06			
0.6925	E 06	0.212	E 06			ρ_o = 8.93 g/cc
0.7235	E 06	0.232	E 06			V_o = 0.112 cc/g
0.6790	E 06	0.2035	E 06			
0.7240	E 06	0.2215	E 06			
0.7090	E 06	0.2210	E 06			
0.7225	E 06	0.2310	E 06			
0.6830	E 06	0.1960	E 06			
0.6640	E 06	0.1780	E 06			
0.6490	E 06	0.1730	E 06			
0.7160	E 06	0.2195	E 06			
0.6910	E 06	0.2020	E 06			
0.6700	E 06	0.1910	E 06			
0.644	E 06	0.1790	E 06			
0.688	E 06	0.1930	E 06			
0.679	E 06	0.200	E 06			
0.666	E 06	0.173	E 06			
0.662	E 06	0.1795	E 06			
0.6845	E 06	0.205	E 06			
0.7230	E 06	0.233	E 06			
0.7260	E 06	0.231	E 06			
0.7050	E 06	0.218	E 06			
0.6890	E 06	0.213	E 06			
0.685	E 06	0.202	E 06			
0.686	E 06	0.199	E 06			
0.691	E 06	0.208	E 06			
0.6775	E 06	0.182	E 06			
0.675	E 06	0.1835	E 06			
0.668	E 06	0.185	E 06			
0.654	E 06	0.190	E 06			
0.6555	E 06	0.173	E 06			
0.650	E 06	0.171	E 06			
0.652	E 06	0.174	E 06			
0.626	E 06	0.170	E 06			
0.620	E 06	0.146	E 06			
0.627	E 06	0.153	E 06			
0.650	E 06	0.1815	E 06			
0.655	E 06	0.1820	E 06			
0.639	E 06	0.1720	E 06			
0.6445	E 06	0.1646	E 06			
0.640	E 06	0.178	E 06			
0.588	E 06	0.142	E 06			
0.584	E 06	0.144	E 06			

COPPER

U	μ		Reference	Initial Conditions
0.4556 E 06	0.0460 E 06	m9 = 12	105	
0.4525 E 06	0.04595 E 06			
0.4768 E 06	0.0547 E 06			
0.4769 E 06	0.05495 E 06			
0.494 E 06	0.06715 E 06			ρ_o = 8.903 g/cc
0.4913 E 06	0.06835 E 06			
0.5258 E 06	0.08225 E 06			
0.5128 E 06	0.0780 E 06			
0.5240 E 06	0.0835 E 06			
0.5285 E 06	0.0855 E 06			
0.5391 E 06	0.09635 E 06			
0.5397 E 06	0.09685 E 06			
0.4086 E 06	0.01181 E 06	m10 = 3	95	ρ_o = 8.939 g/cc
0.4191 E 06	0.01475 E 06			C_o = 0.3894 × 10^6 cm/sec
0.4426 E 06	0.02921 E 06			

$\overline{\mu^2} = 0.420 \times 10^{11} \text{cm}^2/\text{sec}^2$

$\overline{\rho_o} = 8.93 \pm 0.02$ g/cc

$\overline{V_o} = 0.112 \pm 0.0003$ cc/g

$\overline{C_o} = 0.394 \times 10^6$ cm/sec

$a_o = 2.556 \text{Å}$

---

*Reference 96

**From Reference 96

SILVER
Ag

I-5 ; Z=47

M = 107.880

m = 14

s = 1

U		μ			Reference	Initial Conditions
0.4065	E 06	0.0504	E 06	m1 = 5	85	
0.4113	E 06	0.0527	E 06			ρ_o = 10.49 g/cc
0.4378	E 06	0.0717	E 06			C_o = 0.309×10^6 cm/sec*
0.4846	E 06	0.0985	E 06			
0.4848	E 06	0.1010	E 06			
0.598	E 06	0.177	E 06	m2 = 6	13	
0.596	E 06	0.178	E 06			
0.673	E 06	0.214	E 06			ρ_o = 10.49 g/cc
0.663	E 06	0.217	E 06			C_B = 0.319×10^6 cm/sec
0.668	E 06	0.216	E 06			
0.672	E 06	0.217	E 06			
0.469	E 06	0.093	E 06	m3 = 3	92	ρ_o = 10.49 g/cc
0.676	E 06	0.219	E 06			C_o = 0.308×10^6 cm/sec
0.945	E 06	0.405	E 06			

$\overline{\mu^2} = 0.357 \times 10^{11} \text{cm}^2/\text{sec}^2$

$\overline{\rho_o} = 10.49 \pm 0.0$ g/cc

$\overline{V_o} = 0.09533 \pm 0.0$ cc/g

$\overline{C_o} = 0.313 \times 10^6$ cm/sec

$a_o = 2.890\text{Å}$

---

*Reference 96

GOLD
Au

I-6 ; Z=79

M = 197.0

m = 12

s = 1

U		μ			References	Initial Conditions
0.3679	E 06	0.0380	E 06	m1 = 3	85	ρ_o = 19.24 g/cc
0.3864	E 06	0.0505	E 06			$C_o = 0.284 \times 10^6$ cm/sec*
0.4130	E 06	0.0666	E 06			
0.525	E 06	0.137	E 06	m2 = 6	13	
0.521	E 06	0.141	E 06			ρ_o = 19.24 g/cc
0.580	E 06	0.173	E 06			$C_B = 0.305 \times 10^6$ cm/sec
0.578	E 06	0.174	E 06			
0.578	E 06	0.174	E 06			
0.579	E 06	0.174	E 06			
0.427	E 06	0.071	E 06	m3= 3	92	ρ_o = 19.30 g/cc
0.570	E 06	0.178	E 06			$C_o = 0.298 \times 10^6$ cm/sec
0.806	E 06	0.330	E 06			

$\overline{\mu^2} = 0.261 \times 10^{11} \text{cm}^2/\text{sec}^2$

$\overline{\rho_o} = 19.26 \pm 0.03$ g/cc

$\overline{V_o} = 0.05193 \pm 0.00007$ cc/g

$\overline{C_o} = 0.298 \times 10^6$ cm/sec

$a_o = 2.885\text{Å}$

*Reference 96

COBALT
Co
VIII-4; Z=27

M = 58.94

m = 16

s = 1

U		μ		References	Initial Conditions
0.5445	E 06	0.0502	E 06	m1 = 5	85
0.5696	E 06	0.0683	E 06		
0.5632	E 06	0.0653	E 06		ρ_o = 8.82 g/cc
0.6019	E 06	0.0901	E 06		
0.6052	E 06	0.0955	E 06		
0.715	E 06	0.179	E 06	m2 = 11	13
0.715	E 06	0.180	E 06		
0.712	E 06	0.183	E 06		
0.750	E 06	0.206	E 06		ρ_o = 8.82 g/cc
0.745	E 06	0.207	E 06		C_B = 0.463×10^6 cm/sec
0.743	E 06	0.207	E 06		
0.781	E 06	0.230	E 06		
0.779	E 06	0.230	E 06		
0.777	E 06	0.230	E 06		
0.788	E 06	0.231	E 06		
0.783	E 06	0.232	E 06		

$\overline{\mu^2} = 0.325 \times 10^{11} \text{cm}^2\text{sec}^2$

$\overline{\rho_o} = 8.82 \pm 0.0$ g/cc

$\overline{V_o} = 0.113 \pm 0.0$ cc/g

$\overline{C_o} = 0.463 \times 10^6$ cm/sec

$a_o = 2.503\text{Å}$

NICKEL*

Ni

VIII-4; Z=28

M = 58.69

m = 63

s = 1

U		μ			Reference	Initial Conditions
0.5417	E 06	0.0490	E 06	m1 = 6	85	
0.5653	E 06	0.0678	E 06			
0.5620	E 06	0.0687	E 06			ρ_o = 8.86 g/cc
0.6031	E 06	0.0957	E 06			$C_o = 0.447 \times 10^6$ cm/sec**
0.5969	E 06	0.0982	E 06			
0.5952	E 06	0.0887	E 06			
0.695	E 06	0.164	E 06	m2 = 6	13	
0.699	E 06	0.164	E 06			
0.711	E 06	0.162	E 06			ρ_o = 8.86 g/cc
0.778	E 06	0.215	E 06			$C_B = 0.463 \times 10^6$ cm/sec
0.776	E 06	0.217	E 06			
0.780	E 06	0.216	E 06			
0.728	E 06	0.172	E 06	m3 = 4	104	ρ_o = 8.87 g/cc
0.872	E 06	0.263	E 06			
1.120	E 06	0.435	E 06			$C_o = 0.4573 \times 10^6$ cm/sec***
1.460	E 06	0.709	E 06			
0.5682	E 06	0.0935	E 06	m4 = 47	96	
0.5834	E 06	0.0910	E 06			
0.5675	E 06	0.0898	E 06			
0.5643	E 06	0.0910	E 06			ρ_o = 8.905 g/cc
0.5598	E 06	0.0835	E 06			V_o = 0.1123 cc/g
0.5549	E 06	0.0815	E 06			
0.5586	E 06	0.0845	E 06			
0.5624	E 06	0.0840	E 06			
0.5668	E 06	0.0823	E 06			
0.5668	E 06	0.0810	E 06			
0.5624	E 06	0.0815	E 06			
0.5518	E 06	0.0805	E 06			
0.5488	E 06	0.0733	E 06			
0.5488	E 06	0.0733	E 06			
0.5296	E 06	0.0780	E 06			
0.5230	E 06	0.0785	E 06			
0.5411	E 06	0.0715	E 06			
0.5506	E 06	0.0715	E 06			
0.5524	E 06	0.0725	E 06			
0.5393	E 06	0.0725	E 06			
0.5387	E 06	0.0657	E 06			
0.5422	E 06	0.0642	E 06			

NICKEL*

U		μ		Reference	Initial Conditions
0.5549	E 06	0.0635	E 06		
0.5512	E 06	0.0635	E 06		
0.5593	E 06	0.0610	E 06		
0.5330	E 06	0.0620	E 06		
0.5175	E 06	0.0635	E 06		
0.5202	E 06	0.0635	E 06		
0.5000	E 06	0.0529	E 06		
0.4970	E 06	0.0534	E 06		
0.5170	E 06	0.0520	E 06		
0.5112	E 06	0.0525	E 06		
0.4931	E 06	0.0405	E 06		
0.5097	E 06	0.0401	E 06		
0.5092	E 06	0.0406	E 06		
0.4496	E 06	0.0370	E 06		
0.4634	E 06	0.0363	E 06		
0.4617	E 06	0.0360	E 06		
0.4570	E 06	0.0365	E 06		
0.4604	E 06	0.0413	E 06		
0.4673	E 06	0.0409	E 06		
0.4960	E 06	0.0403	E 06		
0.4936	E 06	0.0402	E 06		
0.4840	E 06	0.0375	E 06		
0.4892	E 06	0.0370	E 06		
0.4713	E 06	0.0349	E 06		
0.4638	E 06	0.0354	E 06		

$\overline{\mu^2} = 0.198 \times 10^{11} \text{cm}^2/\text{sec}^2$

$\overline{\rho_o} = 8.89 \pm 0.02$ g/cc

$\overline{V_o} = 0.112 \pm 0.0006$ cc/g

$\overline{C_o} = 0.456 \times 10^6 \text{cm/sec}$

$a_o = 2.493 \text{Å}$

---

*These raw data were adjusted (see following page) in the selection process (see text).

**Reference 96

***Reference 96

NICKEL*

Ni

VIII-4; Z=28

M = 58.69

m = 16

s = 1

U		μ			Reference	Initial Conditions
0.5417	E 06	0.0490	E 06	m1 = 6	85	
0.5653	E 06	0.0678	E 06			
0.5620	E 06	0.0687	E 06			ρ_o = 8.86 g/cc
0.6031	E 06	0.0957	E 06			C_o = 0.447×10^6 cm/sec**
0.5969	E 06	0.0982	E 06			
0.5952	E 06	0.0887	E 06			
0.695	E 06	0.164	E 06	m2 = 6	13	
0.699	E 06	0.164	E 06			
0.711	E 06	0.162	E 06			ρ_o = 8.86 g/cc
0.778	E 06	0.215	E 06			C_B = 0.463×10^6 cm/sec
0.776	E 06	0.217	E 06			
0.780	E 06	0.216	E 06			
0.728	E 06	0.172	E 06	m3 = 4	104	ρ_o = 8.87 g/cc
0.872	E 06	0.263	E 06			
1.120	E 06	0.435	E 06			C_o = 0.4573×10^6 cm/sec***
1.460	E 06	0.709	E 06			

$\overline{\mu^2} = 0.656 \times 10^{11} \text{cm}^2/\text{sec}^2$

$\overline{\rho_o} = 8.86 \pm 0.005$ g/cc

$\overline{V_o} = 0.113 \pm 0.0007$ cc/g

$\overline{C_o} = 0.456 \times 10^6$ cm/sec

$a_o = 2.496 \text{Å}$

** Adjusted data

*** Reference 96

PALLADIUM
Pd

VIII-5; Z =46

M = 106.7

m = 17

s = 1

U		μ			Ref.	ρ_o g/cc	Initial Conditions
0.4673	E 06	0.04728	E 06	m1 = 3	85		ρ_o = 11.95 g/cc
0.5004	E 06	0.06200	E 06				
0.5374	E 06	0.08219	E 06				
0.4737	E 06	0.0467	E 06	m2 = 11	96	12.00	
0.4992	E 06	0.0619	E 06			12.00	V_o = 0.0833 cc/g
0.5396	E 06	0.0856	E 06			12.00	C_o = 0.390×10^6 cm/sec
0.5522	E 06	0.0927	E 06			12.01	
0.6271	E 06	0.1435	E 06			12.00	
0.6305	E 06	0.1435	E 06			12.00	
0.6304	E 06	0.1440	E 06			12.00	
0.6981	E 06	0.1885	E 06			12.00	
0.7294	E 06	0.2108	E 06			12.00	
0.7398	E 06	0.2196	E 06			12.00	
0.7691	E 06	0.2361	E 06			12.00	
0.608	E 06	0.144	E 06	m3 = 3	96		ρ_o = 12.02 g/cc
0.622	E 06	0.143	E 06				V_o = 0.0832 cc/g
0.671	E 06	0.181	E 06				

$\overline{\mu^2} = 0.209 \times 10^{11} \text{cm}^2/\text{sec}^2$

$\overline{\rho_o} = 12.00 \pm 0.02$ g/cc

$\overline{V_o} = 0.0833 \pm 0.0002$ cc/g

$\overline{C_o} = 0.390 \times 10^6$ cm/sec

$a_o = 2.754$ Å

PLATINUM
Pt

VIII-6; Z=78

M = 195.23

m = 15

s = 1

U		μ			Reference	Initial Conditions
0.4199	E 06	0.0329	E 06	m1= 3	85	ρ_o= 21.37 g/cc
0.4306	E 06	0.04450	E 06			
0.4495	E 06	0.06102	E 06			
0.4179	E 06	0.0360	E 06	m2 = 12	96	
0.4365	E 06	0.0483	E 06			
0.4402	E 06	0.0488	E 06			ρ_o= 21.43 g/cc
0.4682	E 06	0.0675	E 06			V_o= 0.0469 cc/g
0.4778	E 06	0.0738	E 06			C_o= 0.351 × 10^6cm/sec
0.5420	E 06	0.1150	E 06			
0.5465	E 06	0.1152	E 06			
0.5442	E 06	0.1180	E 06			
0.6014	E 06	0.1526	E 06			
0.6316	E 06	0.1700	E 06			
0.6367	E 06	0.1787	E 06			
0.6548	E 06	0.1937	E 06			

$\overline{\mu^2}$ = 0.123 × 10^{11} cm^2/sec^2

$\overline{\rho_o}$ = 21.42 ± 0.02 g/cc

$\overline{V_o}$ = 0.0469 ± 0.00005 cc/g

$\overline{C_o}$ = 0.351 × 10^6cm/sec

a_o = 2.776Å

ALUMINUM*

Al

III-3; Z=13

M = 26.98

m = 40

s = 1

U		μ		Reference	Initial Conditions
0.874	E 06	0.270	E 06	m1 = 11 96	
0.920	E 06	0.258	E 06		
0.948	E 06	0.260	E 06		
1.014	E 06	0.353	E 06		ρ_o = 2.70 g/cc
1.004	E 06	0.358	E 06		V_o = 0.370 cc/g
1.024	E 06	0.345	E 06		
1.067	E 06	0.356	E 06		
1.195	E 06	0.513	E 06		
1.309	E 06	0.638	E 06		
1.326	E 06	0.673	E 06		
1.367	E 06	0.702	E 06		
1.913	E 06	0.280	E 06	m2 = 3 103	
1.039	E 06	0.370	E 06		ρ_o = 2.71 g/cc
1.294	E 06	0.562	E 06		
0.913	E 06	0.280	E 06	m3 = 7 102	
0.852	E 06	0.236	E 06		ρ_o = 2.71 g/cc**
0.792	E 06	0.192	E 06		V_o = 0.369 cc/g**
1.05	E 06	0.377	E 06		
1.02	E 06	0.354	E 06		
1.29	E 06	0.559	E 06		
1.20	E 06	0.493	E 06		
0.731	E 06	0.145	E 06	m4 = 8 96	
0.775	E 06	0.180	E 06		ρ_o = 2.70 g/cc
0.877	E 06	0.246	E 06		V_o = 0.370 cc/g
0.906	E 06	0.258	E 06		T_o = 17°C
0.913	E 06	0.271	E 06		
0.876	E 06	0.277	E 06		
0.877	E 06	0.270	E 06		
0.814	E 06	0.221	E 06		
0.5216	E 06	0.0003756	E 06	m5 = 11 95	
0.5249	E 06	0.001527	E 06		
0.5235	E 06	0.001722	E 06		ρ_o = 2.706 g/cc
0.5259	E 06	0.003050	E 06		$C_o = 0.5240 \times 10^6$ cm/sec
0.5285	E 06	0.004439	E 06		
0.5379	E 06	0.007853	E 06		
0.5464	E 06	0.01055	E 06		
0.5535	E 06	0.01472	E 06		

ALUMINUM*

U	μ	Reference	Initial Conditions
0.5598 E 06	0.01959 E 06		
0.5662 E 06	0.02355 E 06		
0.5652 E 06	0.02549 E 06		

$\overline{\mu^2} = 0.108 \times 10^{12} \text{cm}^2/\text{sec}^2$

$\overline{\rho_o} = 2.70 \pm 0.006$ g/cc

$\overline{V_o} = 0.370 \pm 0.0006$ cc/g

$\overline{T_o} = 17^{\circ}\text{C}$

$\overline{C_o} = 0.5240 \times 10^{6}$ cm/sec

$a_o = 2.863\text{Å}$

*These raw data were adjusted (see following page) in the selection process (see text).

**Reference 96

ALUMINUM*

Al

III-3; Z=13

M = 26.98

m = 29

s = 1

U		μ			Reference	Initial Conditions
0.913	E 06	0.280	E 06	m1= 3	103	ρ_o= 2.71 g/cc
1.039	E 06	0.370	E 06			
1.294	E 06	0.562	E 06			
0.913	E 06	0.280	E 06	m2 = 7	102	
0.852	E 06	0.236	E 06			ρ_o= 2.71 g/cc
0.792	E 06	0.192	E 06			V_o= 0.369 cc/g**
1.05	E 06	0.377	E 06			
1.02	E 06	0.354	E 06			
1.29	E 06	0.559	E 06			
1.20	E 06	0.493	E 06			
0.731	E 06	0.145	E 06	m3 = 8	96	
0.775	E 06	0.180	E 06			ρ_o= 2.70 g/cc
0.877	E 06	0.246	E 06			V_o= 0.370 cc/g
0.906	E 06	0.258	E 06			T_o= 17°C
0.913	E 06	0.271	E 06			
0.876	E 06	0.277	E 06			
0.882	E 06	0.270	E 06			
0.814	E 06	0.221	E 06			
0.5216	E 06	0.0003756	E 06	m4 = 11	95	
0.5249	E 06	0.001527	E 06			ρ_o= 2.706 g/cc
0.5235	E 06	0.001722	E 06			C_o= 0.5240 × 10^6 cm/sec
0.5259	E 06	0.003050	E 06			
0.5285	E 06	0.004439	E 06			
0.5379	E 06	0.007853	E 06			
0.5464	E 06	0.01055	E 06			
0.5535	E 06	0.01472	E 06			
0.5598	E 06	0.01959	E 06			
0.5662	E 06	0.02355	E 06			
0.5652	E 06	0.02549	E 06			

$\overline{\mu^2}$ = 0.683 × 10^{11} cm^2/sec^2

$\overline{\rho_o}$ = 2.71 ± 0.006 g/cc

$\overline{V_o}$ = 0.369 ± 0.006 cc/g

$\overline{T_o}$ = 17°C

$\overline{C_o}$ = 0.5240 × 10^6 cm/sec

a_o = 2.859Å

---

*Adjusted data

**Reference 96

CALCIUM
Ca

II-4 ; Z=20

M = 40.08

m = 10

s = 1

U	μ		Reference	ρ_o g/cc	Initial Conditions
0.561 E 06	0.215 E 06	m1 = 5	96	1.523	V_o = 0.656 cc/g
0.547 E 06	0.216 E 06			1.523	
0.464 E 06	0.115 E 06			1.527	
0.673 E 06	0.344 E 06			1.526	
0.709 E 06	0.345 E 06			1.524	
0.45 E 06	0.095 E 06	m2 = 5	106		ρ_o = 1.52 g/cc
0.55 E 06	0.205 E 06				$C_o = 0.335 \times 10^6$ cm/sec
0.58 E 06	0.245 E 06				
0.63 E 06	0.285 E 06				
0.70 E 06	0.375 E 06				

$\overline{\mu^2} = 0.676 \times 10^{11}\ cm^2/sec^2$

$\overline{\rho_o} = 1.52 \pm 0.003$ g/cc

$\overline{V_o} = 0.657 \pm 0.001$ cc/g

$\overline{C_o} = 0.335 \times 10^6$ cm/sec

$a_o = 3.956\text{Å}$

LEAD
Pb

IV-6; Z=82

M = 207.21

m = 37

s = 1

U		μ			Reference	ρ_o g/cc	Initial Conditions
0.2914	E 06	0.0590	E 06	m1 = 4	85		ρ_o = 11.34 g/cc
0.3268	E 06	0.0819	E 06				
0.3250	E 06	0.0802	E 06				$C_o = 0.200 \times 10^6$ cm/sec*
0.3724	E 06	0.1118	E 06				
0.452	E 06	0.164	E 06	m2 = 4	13		ρ_o = 11.34 g/cc
0.452	E 06	0.164	E 06				
0.544	E 06	0.225	E 06				$C_B = 0.202 \times 10^6$ cm/sec
0.542	E 06	0.225	E 06				
0.352	E 06	0.097	E 06	m3 = 3	92		ρ_o = 11.34 g/cc
0.533	E 06	0.234	E 06				
0.765	E 06	0.426	E 06				$C_o = 0.191 \times 10^6$ cm/sec
0.492	E 06	0.188	E 06	m4 = 4	103		
0.607	E 06	0.276	E 06				
0.774	E 06	0.418	E 06				ρ_o = 11.34 g/cc
0.826	E 06	0.445	E 06				
1.136	E 06	0.700	E 06	m5 = 1	104		ρ_o = 11.35 g/cc
0.491	E 06	0.189	E 06	m6 = 9	102		
0.416	E 06	0.120	E 06				
0.372	E 06	0.110	E 06				ρ_o = 11.34 g/cc**
0.617	E 06	0.282	E 06				
0.553	E 06	0.234	E 06				V_o = 0.08826 cc/g**
0.483	E 06	0.184	E 06				
0.441	E 06	0.156	E 06				
0.792	E 06	0.428	E 06				
0.701	E 06	0.351	E 06				
0.466	E 06	0.174	E 06	m7 = 5	96	11.35	
0.291	E 06	0.059	E 06			11.35	
0.370	E 06	0.109	E 06			11.35	V_o = 0.08811 cc/g
0.263	E 06	0.040	E 06			11.35	
0.245	E 06	0.030	E 06			11.34	

LEAD

U		μ			Reference	Initial Conditions
0.1921	E 06	0.001902	E 06	m8 = 7	95	
0.1930	E 06	0.002837	E 06			
0.1980	E 06	0.005227	E 06			ρ_o = 11.355 g/cc
0.2143	E 06	0.01144	E 06			$C_o = 0.1972 \times 10^6$ cm/sec
0.2265	E 06	0.01832	E 06			
0.2369	E 06	0.02544	E 06			
0.2435	E 06	0.02820	E 06			

$\overline{\mu^2} = 0.545 \times 10^{11} \text{cm}^2/\text{sec}^2$

$\overline{\rho_o} = 11.34 \pm 0.007$ g/cc

$\overline{V_o} = 0.08817 \pm 0.00007$ cc/g

$\overline{C_o} = 0.198 \times 10^6$ cm/sec

$a_o = 3.501 \text{Å}$

---

*From Reference 96

**From Reference 96

LITHIUM*

Li

I-2 ; Z=3

M = 6.940

m = 29

s = 2

U		μ			Reference	ρ_o g/cc	Initial Conditions
0.6329	E 06	0.1425	E 06	m1 = 10	93		ρ_o = 0.530 g/cc
0.6382	E 06	0.1457	E 06				T_o = 20°C
0.6734	E 06	0.1941	E 06				P_o = 1 atm
0.7433	E 06	0.2554	E 06				C_o = 0.469 × 10^6 cm/sec**
0.7449	E 06	0.2553	E 06				
0.8251	E 06	0.3231	E 06				
0.8893	E 06	0.3679	E 06				
0.8929	E 06	0.3727	E 06				
1.0192	E 06	0.4908	E 06				
1.0335	E 06	0.4887	E 06				
0.586	E 06	0.114	E 06	m2 = 11	107		
0.643	E 06	0.187	E 06				
0.725	E 06	0.259	E 06				
0.932	E 06	0.445	E 06				ρ_o = 0.53 g/cc
1.075	E 06	0.554	E 06				T_o = 300°K
1.164	E 06	0.642	E 06				
1.210	E 06	0.681	E 06				
1.243	E 06	0.715	E 06				
1.240	E 06	0.723	E 06				
1.314	E 06	0.797	E 06				
1.439	E 06	0.915	E 06				
0.971	E 06	0.477	E 06	m3 = 8	96	0.537	
0.704	E 06	0.214	E 06			0.533	
0.625	E 06	0.129	E 06			0.531	
1.126	E 06	0.568	E 06			0.534	V_o = 1.87 cc/g
0.845	E 06	0.348	E 06			0.533	
0.866	E 06	0.372	E 06			0.533	
0.997	E 06	0.487	E 06			0.533	
0.931	E 06	0.433	E 06			0.533	

$\overline{\mu^2}$ = 0.220 × 10^{12} cm^2/sec^2

$\overline{\rho_o}$ = 0.531 ± 0.002 g/cc

$\overline{V_o}$ = 1.88 ± 0.01 cc/g

$\overline{T_o}$ = 24°C

$\overline{P_o}$ = 1 atm

$\overline{C_o}$ = 0.469 × 10^6 cm/sec

a_o = 3.043Å

*These raw data were adjusted (see following page) in the selection process (see text).

**Reference 96

LITHIUM*

Li

I-2 ; Z=3

M = 6.940

m = 17

s = 2

U		μ			Reference	ρ_o g/cc	Initial Conditions
0.6329	E 06	0.1425	E 06	m1 = 8	93		ρ_o = 0.530 g/cc
0.6382	E 06	0.1457	E 06				T_o = 20°C
0.6734	E 06	0.1941	E 06				P_o = 1 atm
0.7433	E 06	0.2554	E 06				C_o = 0.469 × 10^6 cm/sec**
0.7449	E 06	0.2553	E 06				
0.8251	E 06	0.3231	E 06				
0.8893	E 06	0.3679	E 06				
0.8929	E 06	0.3727	E 06				
0.586	E 06	0.114	E 06	m2 = 4	107		ρ_o = 0.53 g/cc
0.643	E 06	0.187	E 06				T_o = 300°K
0.725	E 06	0.259	E 06				
0.932	E 06	0.445	E 06				
0.704	E 06	0.214	E 06	m3 = 5	96	0.533	
0.625	E 06	0.129	E 06			0.531	V_o = 1.87 cc/g
0.845	E 06	0.348	E 06			0.533	
0.866	E 06	0.372	E 06			0.533	
0.931	E 06	0.433	E 06			0.533	

$\overline{\mu^2}$ = 0.830 × 10^{11} cm^2/sec^2

$\overline{\rho_o}$ = 0.531 ± 0.001 g/cc

$\overline{V_o}$ = 1.88 ± 0.01 cc/g

$\overline{T_o}$ = 22°C

$\overline{P_o}$ = 1 atm

$\overline{C_o}$ = 0.469 × 10^6 cm/sec

a_o = 3.043Å

---

*Adjusted data

**Reference 96

SODIUM*

Na

I-3; Z=11

M = 22.991

m = 25

s = 2

U		μ			Reference	Initial Conditions
0.4336	E 06	0.1417	E 06	m1 = 18	93	
0.4229	E 06	0.1335	E 06			
0.4238	E 06	0.1347	E 06			
0.4913	E 06	0.1842	E 06			ρ_o = 0.968 g/cc
0.4883	E 06	0.1869	E 06			T_o = 20°C
0.4914	E 06	0.1849	E 06			P_o = 1 atm
0.5521	E 06	0.2407	E 06			$C_o = 0.233 \times 10^6$ cm/sec**
0.5529	E 06	0.2404	E 06			
0.5540	E 06	0.2419	E 06			
0.5505	E 06	0.2375	E 06			
0.5561	E 06	0.2423	E 06			
0.6245	E 06	0.2998	E 06			
0.6225	E 06	0.2996	E 06			
0.6925	E 06	0.3518	E 06			
0.6911	E 06	0.3547	E 06			
0.7942	E 06	0.4300	E 06			
0.8036	E 06	0.4392	E 06			
0.8076	E 06	0.4392	E 06			
0.391	E 06	0.110	E 06	m2 = 7	107	
0.472	E 06	0.177	E 06			ρ_o = 0.97 g/cc
0.553	E 06	0.243	E 06			T_o = 300°K
0.770	E 06	0.409	E 06			
0.926	E 06	0.525	E 06			
1.057	E 06	0.632	E 06			
1.252	E 06	0.796	E 06			

$\overline{\mu^2} = 0.121 \times 10^{12}$ cm^2/sec^2

$\overline{P_o}$ = 1 atm

$\overline{\rho_o}$ = 0.97 ± 0.002 g/cc

$\overline{C_o} = 0.233 \times 10^6$ cm/sec

$\overline{V_o}$ = 1.03 ± 0.003 cc/g

a_o = 3.711Å

$\overline{T_o}$ = 22°C

---

*These data were adjusted (see following page) in the selection process (see text).

**Reference 96

SODIUM*

Na

I-3; Z=11

M = 22.991

m = 18

s = 2

U		μ			Reference	Initial Conditions
0.4336	E 06	0.1417	E 06	m1 = 15	93	
0.4229	E 06	0.1335	E 06			
0.4238	E 06	0.1347	E 06			ρ_o = 0.968 g/cc
0.4918	E 06	0.1842	E 06			T_o = 20°C
0.4883	E 06	0.1869	E 06			P_o = 1 atm
0.4914	E 06	0.1849	E 06			$C_o = 0.233 \times 10^6$ cm/sec*
0.5521	E 06	0.2407	E 06			
0.5529	E 06	0.2404	E 06			
0.5540	E 06	0.2419	E 06			
0.5505	E 06	0.2375	E 06			
0.5561	E 06	0.2423	E 06			
0.6245	E 06	0.2998	E 06			
0.6225	E 06	0.2996	E 06			
0.6925	E 06	0.3518	E 06			
0.6911	E 06	0.3547	E 06			
0.391	E 06	0.110	E 06	m2 = 3	107	ρ_o = 0.97 g/cc
0.472	E 06	0.177	E 06			T_o = 300°K
0.553	E 06	0.243	E 06			

$\overline{\mu^2} = 0.545 \times 10^{11} cm^2/sec^2$

$\overline{\rho_o} = 0.97 \pm 0.002$ g/cc

$\overline{V_o} = 1.03 \pm 0.003$ cc/g

$\overline{T_o} = 21°C$

$\overline{P_o} = 1$ atm

$\overline{C_o} = 0.233 \times 10^6 cm/sec$

$a_o = 3.711 Å$

---

*Adjusted data

**Reference 96

POTASSIUM*

K

I-4 ; Z = 19

M = 39.110

m = 23

s = 2

U		μ		Reference	Initial Conditions
0.3641	E 06	0.1391	E 06	ml = 18 93	
0.3633	E 06	0.1402	E 06		
0.4198	E 06	0.1882	E 06		ρ_o = 0.860 g/cc
0.4187	E 06	0.1928	E 06		T_o = 20°C
0.4258	E 06	0.1917	E 06		P_o = 1 atm
0.4864	E 06	0.2513	E 06		C_o = 0.206 × 10^6 cm/sec**
0.4874	E 06	0.2532	E 06		
0.4921	E 06	0.2522	E 06		
0.4943	E 06	0.2561	E 06		
0.4949	E 06	0.2561	E 06		
0.5489	E 06	0.2993	E 06		
0.5641	E 06	0.3149	E 06		
0.5683	E 06	0.3174	E 06		
0.5747	E 06	0.3183	E 06		
0.5845	E 06	0.3318	E 06		
0.7108	E 06	0.4324	E 06		
0.7258	E 06	0.4468	E 06		
0.7392	E 06	0.4573	E 06		
0.337	E 06	0.115	E 06	m2 = 5 107	ρ_o = 0.86 g/cc
0.486	E 06	0.238	E 06		T_o = 300°K
0.699	E 06	0.429	E 06		
0.939	E 06	0.632	E 06		
1.187	E 06	0.841	E 06		

$\overline{\mu^2}$ = 0.127 × 10^{12} cm^2/sec^2

$\overline{\rho_o}$ = 0.86 ± 0.0 g/cc

$\overline{V_o}$ = 1.16 ± 0.0 cc/g

$\overline{T_o}$ = 22°C

$\overline{P_o}$ = 1 atm

$\overline{C_o}$ = 0.206 × 10^6 cm/sec

a_o = 4.612Å

---

*These data were adjusted (see following page) in the selection process (see text).

**Reference 96

POTASSIUM*

K

I-4 ; Z =19

M = 39.110

m = 17

s = 2

U		μ			Reference	Initial Conditions
0.3641	E 06	0.1391	E 06	m1 = 15	93	
0.3633	E 06	0.1402	E 06			
0.4198	E 06	0.1882	E 06			
0.4187	E 06	0.1928	E 06			ρ_o = 0.860 g/cc
0.4258	E 06	0.1917	E 06			T_o = 20°C
0.4864	E 06	0.2513	E 06			P_o = 1 atm
0.4874	E 06	0.2532	E 06			C_o = 0.206 × 10^6 cm/sec**
0.4921	E 06	0.2522	E 06			
0.4943	E 06	0.2561	E 06			
0.4949	E 06	0.2561	E 06			
0.5489	E 06	0.2993	E 06			
0.5641	E 06	0.3149	E 06			
0.5683	E 06	0.3174	E 06			
0.5747	E 06	0.3183	E 06			
0.5845	E 06	0.3318	E 06			
0.337	E 06	0.115	E 06	m2 = 2	107	ρ_o = 0.86 g/cc
0.486	E 06	0.238	E 06			T_o = 300°K

$\overline{\mu^2} = 0.612 \times 10^{11} cm^2/sec^2$

$\overline{\rho_o} = 0.86 \pm 0.0$ g/cc

$\overline{V_o} = 1.16 \pm 0.0$ cc/g

$\overline{T_o} = 22°C$

$\overline{P_o} = 1$ atm

$\overline{C_o} = 0.206 \times 10^6 cm/sec$

$a_o = 4.612 Å$

---

*Adjusted data

**Reference 96

RUBIDIUM*

Rb

I-5;Z=37

M = 85.48

m = 10

s = 2

U		μ			Reference	Initial Conditions
0.2786	E 06	0.1289	E 06	ml = 10	93	
0.2820	E 06	0.1312	E 06			ρ_o = 1.530 g/cc
0.3412	E 06	0.1814	E 06			T_o = 20°C
0.4032	E 06	0.2320	E 06			P_o = 1 atm
0.4050	E 06	0.2373	E 06			$C_o = 0.113 \times 10^6$ cm/sec**
0.4988	E 06	0.3085	E 06			
0.5187	E 06	0.3220	E 06			
0.5574	E 06	0.3563	E 06			
0.6256	E 06	0.4001	E 06			
0.6349	E 06	0.4043	E 06			

$\overline{\mu^2} = 0.826 \times 10^{11} cm^2/sec^2$

$\overline{\rho_o} = 1.530 \pm 0.0$ g/cc

$\overline{V_o} = 0.6536 \pm 0.0$ cc/g

$\overline{T_o} = 20°C$

$\overline{P_o} = 1$ atm

$\overline{C_o} = 0.113 \times 10^6 cm/sec$

$a_o = 4.939 Å$

---

*These data were adjusted (see following page) in the selection process (see text).

**Reference 96

RUBIDIUM*

Rb

I-5; Z=37

M = 85.48

m = 5

s = 2

U		μ		Reference	Initial Conditions
0.2786	E 06	0.1289	E 06	ml = 5	93	ρ_o = 1.530 g/cc
0.2820	E 06	0.1312	E 06			T_o = 20°C
0.3412	E 06	0.1814	E 06			P_o = 1 atm
0.4032	E 06	0.2320	E 06			C_o = 0.113 × 10^6 cm/sec**
0.4050	E 06	0.2373	E 06		

$\overline{\mu^2}$ = 0.354 × 10^{11} cm^2/sec^2

$\overline{\rho_o}$ = 1.530 ± 0.0 g/cc

$\overline{V_o}$ = 0.6536 ± 0.0 cc/g

$\overline{T_o}$ = 20°C

$\overline{P_o}$ = 1 atm

$\overline{C_o}$ = 0.113 × 10^6 cm/sec

a_o = 4.939Å

---

*Adjusted data

**Reference 96

CESIUM
Cs
I-6;Z=55

M = 132.91

m = 9

s = 2

U		μ			Reference	Initial Conditions
0.2489	E 06	0.1402	E 06	ml = 9	93	
0.2493	E 06	0.1395	E 06			ρ_o = 1.826 g/cc
0.2994	E 06	0.1758	E 06			T_o = 20°C
0.2998	E 06	0.1770	E 06			P_o = 1 atm
0.3695	E 06	012239	E 06			C_o = 0.087 × 10^6cm/sec*
0.3719	E 06	0.2268	E 06			
0.4953	E 06	0.3202	E 06			
0.5822	E 06	0.3894	E 06			
0.5847	E 06	0.3919	E 06			

$\overline{\mu^2}$ = 0.679 × 10^{11}cm^2/sec^2

$\overline{\rho_o}$ = 1.826 ± 0.0 g/cc

$\overline{V_o}$ = 0.5476 ± 0.0 cc/g

$\overline{T_o}$ = 20°C

$\overline{P_o}$ = 1 atm

$\overline{C_o}$ = 0.087 × 10^6cm/sec

a_o = 5.395Å

---

*Reference 96

VANADIUM
V

V-4; Z=23

M = 50.95

m = 14

s = 2

U		μ			Reference	Initial Conditions
0.578	E 06	0.058	E 06	m1 = 14	13	
0.573	E 06	0.058	E 06			
0.616	E 06	0.080	E 06			
0.607	E 06	0.081	E 06			ρ_o = 6.1 g/cc
0.608	E 06	0.081	E 06			C_B = 0.518 × 10^6 cm/sec
0.605	E 06	0.082	E 06			
0.608	E 06	0.081	E 06			
0.649	E 06	0.112	E 06			
0.650	E 06	0.111	E 06			
0.646	E 06	0.112	E 06			
0.729	E 06	0.186	E 06			
0.728	E 06	0.186	E 06			
0.732	E 06	0.185	E 06			
0.734	E 06	0.185	E 06			
0.820	E 06	0.259	E 06			
0.817	E 06	0.249	E 06			

$\overline{\mu^2}$ = 0.215 × 10^{11} cm^2/sec^2

$\overline{\rho_o}$ = 6.1 ± 0.0 g/cc

$\overline{V_o}$ = 0.16 ± 0.0 cc/g

$\overline{C_o}$ = 0.518 × 10^6 cm/sec

a_o = 2.621Å

NIOBIUM

Nb

V-5 ; Z=41

M = 92.91

m = 14

s = 2

U		μ		Reference	Initial Conditions
0.5177	E 06	0.05489	E 06	m1 = 3	85	ρ_o = 8.604 g/cc
0.5311	E 06	0.07434	E 06		
0.5642	E 06	0.09929	E 06		
0.5195	E 06	0.0527	E 06	m2 = 11	96	ρ_o = 8.583 g/cc
0.5335	E 06	0.0706	E 06			V_o = 0.1165 cc/g
0.5687	E 06	0.0978	E 06			C_o = 0.439 × 10^6 cm/sec
0.5793	E 06	0.1061	E 06		
0.6449	E 06	0.1643	E 06		
0.6432	E 06	0.1650	E 06		
0.6471	E 06	0.1651	E 06		
0.7114	E 06	0.2158	E 06		
0.7417	E 06	0.2450	E 06		
0.7518	E 06	0.2508	E 06		
0.7734	E 06	0.2705	E 06		

$\overline{\mu^2}$ = 0.265 × 10^{11} cm^2/sec^2

$\overline{\rho_o}$ = 8.588 ± 0.009 g/cc

$\overline{V_o}$ = 0.1164 ± 0.0003 cc/g

$\overline{C_o}$ = 0.439 × 10^6 cm/sec

a_o = 2.858Å

TANTALUM*

Ta

V-6; Z=73

M = 180.95

m = 16

s = 2

U	μ		Reference	Initial Conditions
0.3811 E 06	0.04327 E 06	m1 = 3	85	ρ_o = 16.46 g/cc
0.4010 E 06	0.05800 E 06			
0.4323 E 06	0.07685 E 06			
0.3981 E 06	0.0429 E 06	m2 = 10	96	ρ_o = 16.66 g/cc
0.4134 E 06	0.0576 E 06			V_o = 0.0600 cc/g
0.4395 E 06	0.0804 E 06			C_o = 0.339 × 10^6 cm/sec
0.4495 E 06	0.0872 E 06			
0.5092 E 06	0.1358 E 06			
0.5061 E 06	0.1359 E 06			
0.5621 E 06	0.1790 E 06			
0.5889 E 06	0.2003 E 06			
0.5967 E 06	0.2087 E 06			
0.6103 E 06	0.2262 E 06			
0.524 E 06	0.145 E 06	m3 = 3	108	
0.645 E 06	0.228 E 06			ρ_o = 16.6 g/cc
0.836 E 06	0.374 E 06			

$\overline{\mu^2}$ = 0.279 × 10^{11} cm^2/sec^2

$\overline{\rho_o}$ = 16.6 ± 0.08 g/cc

$\overline{V_o}$ = 0.0602 ± 0.0003 cc/g

$\overline{C_o}$ = 0.339 × 10^6 cm/sec

a_o = 2.865Å

---

*These data were adjusted (see following page) in the selection process (see text).

TANTALUM*

Ta

V-6;Z=73

M = 180.95

m = 14

s = 2

U		μ			Reference	Initial Conditions
0.3811	E 06	0.04327	E 06	m1 = 3	85	ρ_o = 16.46 g/cc
0.4010	E 06	0.05800	E 06			
0.4323	E 06	0.07685	E 06			
0.3981	E 06	0.0429	E 06	m2 = 10	96	
0.4134	E 06	0.0576	E 06			ρ_o = 16.66 g/cc
0.4395	E 06	0.0804	E 06			V_o = 0.0600 cc/g
0.4495	E 06	0.0872	E 06			C_o = 0.339 × 10^6 cm/sec
0.5092	E 06	0.1358	E 06			
0.5061	E 06	0.1359	E 06			
0.5621	E 06	0.1790	E 06			
0.5889	E 06	0.2003	E 06			
0.5967	E 06	0.2087	E 06			
0.6103	E 06	0.2262	E 06			
0.524	E 06	0.145	E 06	m3 = 1	108	ρ_o = 16.6 g/cc

$\overline{\mu^2} = 0.182 \times 10^{11} \text{cm}^2/\text{sec}^2$

$\overline{\rho_o} = 16.6 \pm 0.08$ g/cc

$\overline{V_o} = 0.0602 \pm 0.0003$ cc/g

$\overline{C_o} = 0.339 \times 10^6$ cm/sec

$a_o = 2.865 \text{Å}$

---

*Adjusted data

CHROMIUM

Cr

VI-4 ; Z=24

M = 52.01

m = 13

s = 2

U		μ			Reference	Initial Conditions
0.6043	E 06	0.05448	E 06	m1 = 8	13	
0.5923	E 06	0.05395	E 06			ρ_o = 7.10 g/cc
0.6381	E 06	0.07436	E 06			$C_B = 0.515 \times 10^6$ cm/sec
0.6370	E 06	0.07449	E 06			
0.6355	E 06	0.07407	E 06			
0.6357	E 06	0.07403	E 06			
0.6660	E 06	0.1007	E 06			
0.6674	E 06	0.1008	E 06			
0.763	E 06	0.171	E 06	m2 = 5	85	
0.759	E 06	0.171	E 06			ρ_o = 7.13 g/cc
0.844	E 06	0.225	E 06			$C_o = 0.515 \times 10^6$ cm/sec*
0.857	E 06	0.227	E 06			
0.863	E 06	0.225	E 06			

$\overline{\mu^2} = 0.200 \times 10^{11} \text{cm}^2/\text{sec}^2$

$\overline{\rho_o} = 7.11 \pm 0.01$ g/cc

$\overline{V_o} = 0.141 \pm 0.0006$ cc/g

$\overline{C_o} = 0.515 \times 10^6$ cm/sec

$a_o = 2.508\text{Å}$

*Reference 96

MOLYBDENUM

Mo

VI-5 ; Z=42

M = 95.95

m = 18

s = 2

U		μ			Reference	Initial Conditions
0.5699	E 06	0.0437	E 06	m1 = 6	85	
0.5647	E 06	0.0444	E 06			ρ_o = 10.20 g/cc
0.5955	E 06	0.0591	E 06			
0.5861	E 06	0.0606	E 06			
0.6210	E 06	0.0850	E 06			
0.6124	E 06	0.0792	E 06			
0.729	E 06	0.169	E 06	m2 = 6	13	ρ_o = 10.20 g/cc
0.720	E 06	0.170	E 06			$C_B = 0.519 \times 10^6$ cm/sec
0.729	E 06	0.168	E 06			
0.765	E 06	0.206	E 06			
0.771	E 06	0.206	E 06			
0.775	E 06	0.207	E 06			
0.721	E 06	0.160	E 06	m3 = 4	108	
0.839	E 06	0.252	E 06			ρ_o = 10.2 g/cc
1.016	E 06	0.392	E 06			
1.035	E 06	0.424	E 06			
0.585	E 06	0.079	E 06	m4 = 2	96	ρ_o = 10.13 g/cc
0.538	E 06	0.050	E 06			V_o = 0.0987 cc/g

$\overline{\mu^2} = 0.372 \times 10^{11} \text{cm}^2/\text{sec}^2$

$\overline{\rho_o} = 10.2 \pm 0.02$ g/cc

$\overline{V_o} = 0.0981 \pm 0.0002$ cc/g

$\overline{C_o} = 0.519 \times 10^6$ cm/sec

$a_o = 2.727 \text{Å}$

TUNGSTEN
W

VI-6; Z=74

M = 183.92

m = 9

s = 2

U	μ		Reference	Initial Conditions
0.456 E 06	0.045 E 06	ml = 9	13	
0.455 E 06	0.045 E 06			
0.478 E 06	0.064 E 06			ρ_o = 19.17 g/cc
0.482 E 06	0.064 E 06			V_o = 0.05216 cc/g
0.547 E 06	0.117 E 06			C_B = 0.405 × 10^6 cm/sec
0.549 E 06	0.117 E 06			
0.621 E 06	0.173 E 06			
0.619 E 06	0.173 E 06			
0.624 E 06	0.173 E 06			

$\overline{\mu^2}$ = 0.144 × 10^{11} cm^2/sec^2

$\overline{\rho_o}$ = 19.17 ± 0.0 g/cc

$\overline{V_o}$ = 0.05216 ± 0.0 cc/g

$\overline{C_o}$ = 0.405 × 10^6 cm/sec

a_o = 2.745Å

ZIRCONIUM*

Zr

IV-5 ; Z=40

M = 91.22

m = 14

s = 2

Initial Conditions

U		μ		Reference		ρ_o g/cc	
0.4494	E 06	0.07117	E 06	m1= 3	85		ρ_o = 6.49 g/cc
0.4674	E 06	0.09563	E 06				
0.4920	E 06	0.1275	E 06				
0.4440	E 06	0.0634	E 06	m2 = 11	96	6.506	V_o = 0.1537 cc/g
0.4609	E 06	0.0841	E 06			6.506	
0.4661	E 06	0.0850	E 06			6.509	C_o = 0.388 × 10^6 cm/sec
0.4804	E 06	0.1168	E 06			6.503	
0.4938	E 06	0.1267	E 06			6.505	
0.5720	E 06	0.1911	E 06			6.505	
0.5758	E 06	0.1917	E 06			6.512	
0.5753	E 06	0.1956	E 06			6.505	
0.6467	E 06	0.2476	E 06			6.506	
0.6867	E 06	0.2732	E 06			6.506	
0.7211	E 06	0.3065	E 06			6.505	

$\overline{\mu^2}$ = 0.300 × 10^{11} cm^2/sec^2

$\overline{\rho_o}$ = 6.50 ± 0.007 g/cc

$\overline{V_o}$ = 0.154 ± 0.0003 cc/g

$\overline{C_o}$ = 0.388 × 10^6 cm/sec

a_o = 3.116Å

*These data were adjusted (see following page) in the selection process (see text).

ZIRCONIUM*

Zr

IV-5 ; Z=40

M = 91.22

m = 5

s = 2

Initial Conditions

U		μ			Reference	ρ_o g/cc	
0.4494	E 06	0.07117	E 06	m1 = 2	85		ρ_o = 6.49 g/cc
0.4674	E 06	0.09563	E 06				
0.4440	E 06	0.0634	E 06	m2 = 3	96	6.506	
0.4609	E 06	0.0841	E 06			6.506	V_o = 0.1537 cc/g
0.4661	E 06	0.0850	E 06			6.509	C_o = 0.388×10^6 cm/sec

$\overline{\mu^2} = 0.651 \times 10^{10} cm^2/sec^2$

$\overline{\rho_o} = 6.50 \pm 0.008$ g/cc

$\overline{V_o} = 0.154 \pm 0.0005$ cc/g

$\overline{C_o} = 0.388 \times 10^6$ cm/sec

$a_o = 3.116 Å$

---

*Adjusted data

BARIUM
Ba

II-6; Z=56

M = 137.36

m = 4

s = 2

U		μ			Reference	Initial Conditions
0.230	E 06	0.091	E 06	ml = 4	106	ρ_o = 3.63 g/cc
0.355	E 06	0.179	E 06			$C_o = 0.161 \times 10^6$ cm/sec
0.535	E 06	0.312	E 06			
0.940	E 06	0.600	E 06			

$\overline{\mu^2} = 0.124 \times 10^{12} \text{cm}^2/\text{sec}^2$

$\overline{\rho_o} = 3.63 \pm 0.0$ g/cc

$\overline{V_o} = 0.275 \pm 0.0$ cc/g

$\overline{C_o} = 0.161 \times 10^6$ cm/sec

$a_o = 4.338 \text{Å}$

Appendix T

Phase Transitions and the Shock Model

Huang[165] has shown from statistical mechanical considerations that a reasonable* description of phase transitions can be made in terms of the pressure-fugacity behavior of the material of concern**. When converted to the $P - (1/\rho)$ plane his examples of first-order (FO) and second-order (SO) transitions may be pictured[165] as in Figure T1.

The particular example chosen for the FO transition is an isotherm passing through the coexistence region between two phases. Under shock loading, isothermal conditions will not prevail and the $P - (1/\rho)$ behavior should look more like the dashed line in Figure T1***. On the other hand the SO transition would look much the same as that shown.

---

*Reasonable in the sense that it cannot be (easily) shown that the scheme is unique; there may be other descriptions of transitions that work equally well[165].

**If, for a given value of fugacity $f = f_o$, $P(f)$ is continuous but $\partial P/\partial f$ is discontinuous, this corresponds to a first-order transition. If both $P(f)$ and $\partial P/\partial f$ are continuous but $\partial^2 P/\partial f^2$ is discontinuous, this corresponds to a second-order transition.

***From Equations (4) and (5), eliminating μ : $P - P_o = (\rho_o U)^2 \left(\frac{1}{\rho_o} - \frac{1}{\rho}\right)$ and the slope becomes:

$$\frac{\partial P}{\partial (1/\rho)} = - (\rho_o U)^2$$

Clearly, the slope < 0 in all cases. Since $\rho_o > 0$ and $U > 0$ it is clear that for shock loading, even the case $\partial P/\partial(1/\rho) = 0$ cannot occur.

This justifies the dashed line in Figure T1.

Phases Connected by a First-Order Transition

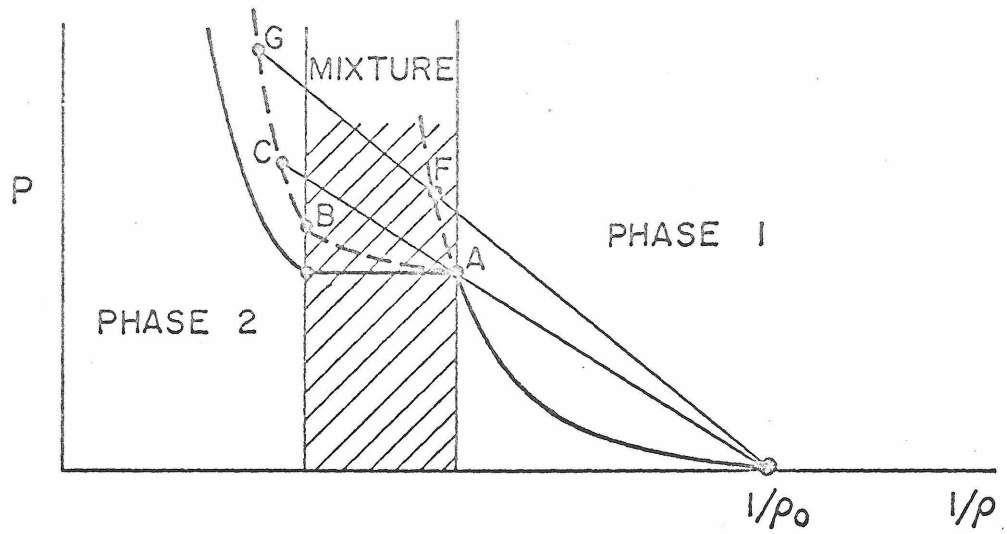

Phases Connected by a Second-Order Transition

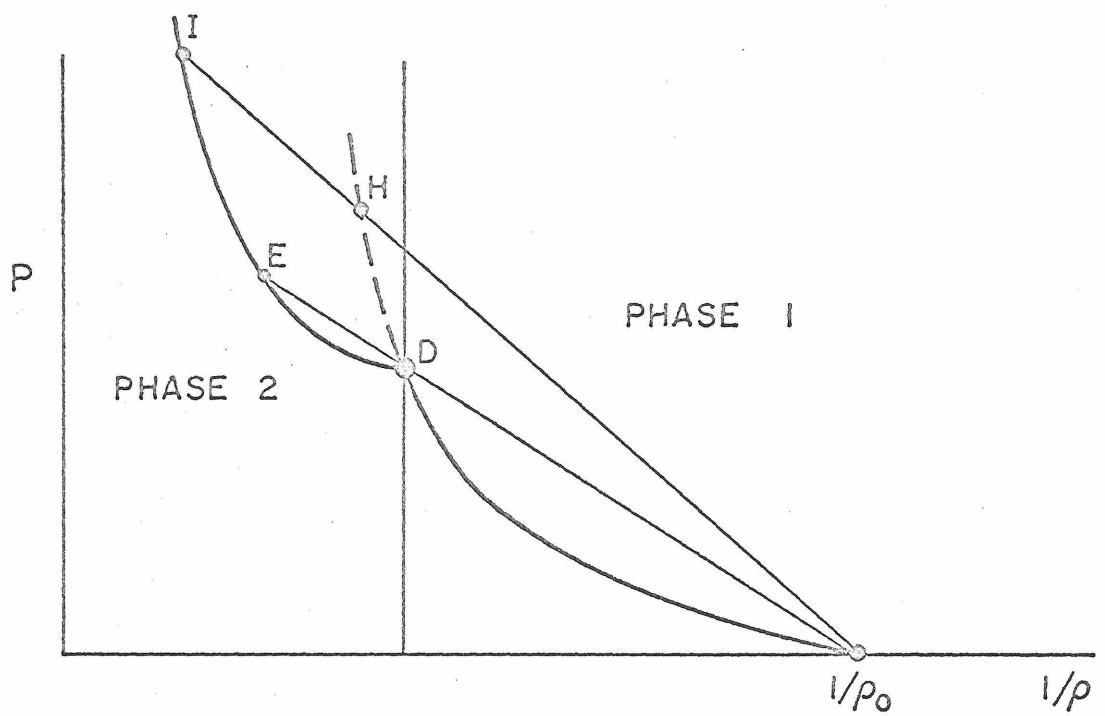

Figure T1. First- and Second-Order Phase Transitions [From Huang(165, p.319)]

For the FO transition, compression is "normal" for phase 1 up to point A, and the ordinary U-μ behavior for phase 1 obtains. This is shown in Figure T2. For compressions between points A and C (found by connecting $1/\rho_o$ and A with a straight line) "the shock wave is split into two independent waves moving at different"velocities [12]. The velocity of the leading wave is given by the shock in phase 1 at point A and is constant for compressions through point C. This is shown as the horizontal dashed line in Figure T2. The trailing wave starts at some low velocity at point A* which gradually increases through the two-phase region to point B where the last of phase 1 disappears. For increased compression between points B and C the trailing wave speed increases along the characteristic phase 2 U-μ curve. These are shown as the dotted lines in Figure T2. At point C the trailing wave catches up to the leading wave and coalesces with it. Further compression takes place in a "normal" fashion along the phase 2 U-μ curve. From the FO transition diagram in Figure T2 it is clear that the trailing wave never overtakes the leading wave (until point C is reached), since the velocity of the latter is always higher.

From this it is clear that, for FO transitions, observation of the first wave arrival will yield a U-μ curve similar to the upper part of the FO transition curve in Figure T2; the dotted curves representing the trailing wave will not be seen.

For the SO transition in Figure T1, similar behavior occurs except that there is no coexistence region. "Normal" compression in

---

*The sound velocity of the material behind the shock at point A .

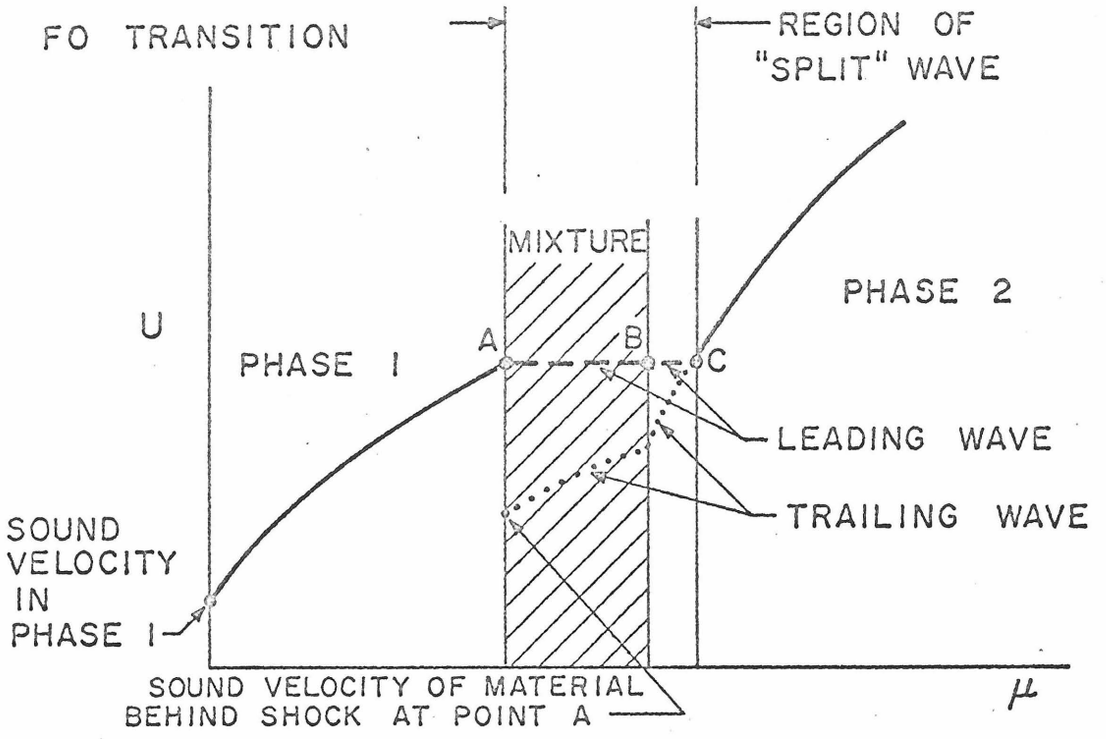

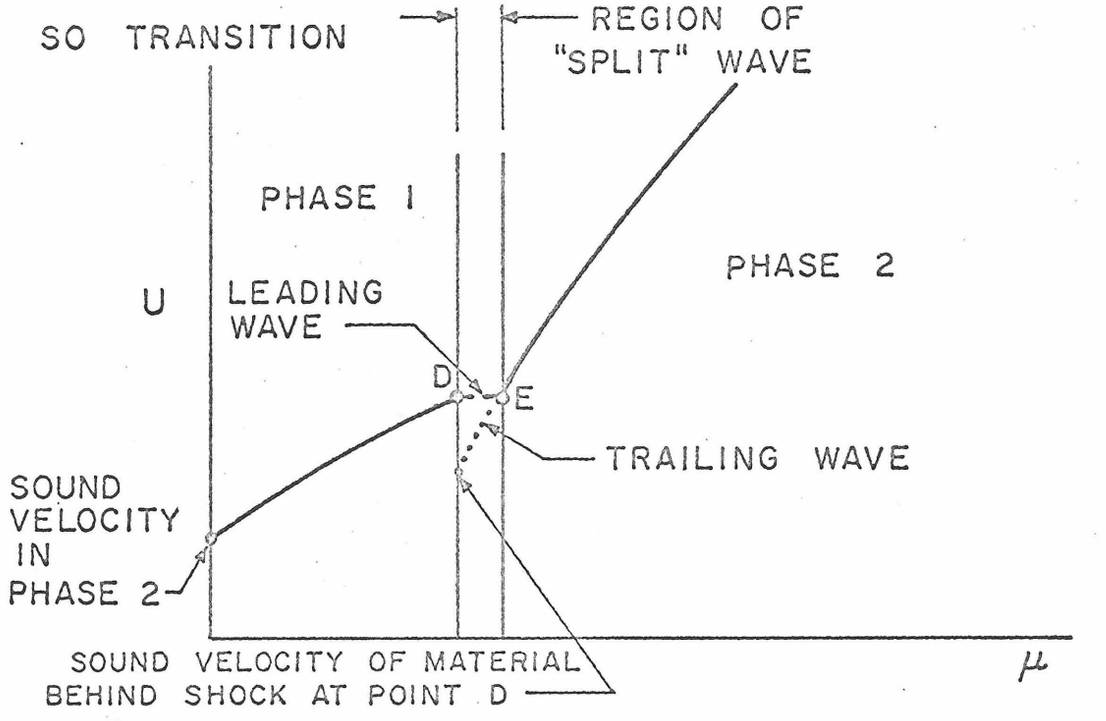

Figure T2. U-μ Behavior Corresponding to FO and SO Transitions

phase 1 takes place from $1/\rho_o$ to point D where the transition takes place (suddenly) and the new phase is formed. Again the shock wave splits for compressions between states D and E in which the leading wave propagates at constant velocity. This and the trailing wave are shown as the dashed and dotted lines in the SO transition curve of Figure T2. Continued compression takes place along the normal U-μ curve for phase 2.

If points D and E for SO transitions are close together (Figure T2), the split wave region would be very small and the U-μ curve would appear (essentially) simply as the intersection of the U-μ curves for phases 1 and 2 respectively with no (apparent) horizontal region.

If, correspondingly, points B and C for FO transitions are close together, the horizontal region indicated in Figure T2 is shortened proportionately but remains nevertheless because of the coexistence region.

For either FO or SO transitions the region of phase 1 compression corresponds to the case of "normal" propagation of a shock wave through the material. The shock structure is "normal" and the shock model developed in this study applies as such.

When the shock wave splits for FO (point A) or SO (point D) transitions, the pressure distribution in the two waves can be pictured as in Figure T3 which is taken from Zel'dovich and Raizer[12]. The initial pressure rise is sharp fronted and characteristic of "ordinary" shock waves; the transition region is "small". The phase transition itself takes place in the second wave*; i.e., conditions behind the

*For FO transitions the second wave could end in the 2-phase region (between A and B) or in the phase 2 region (between B and C).

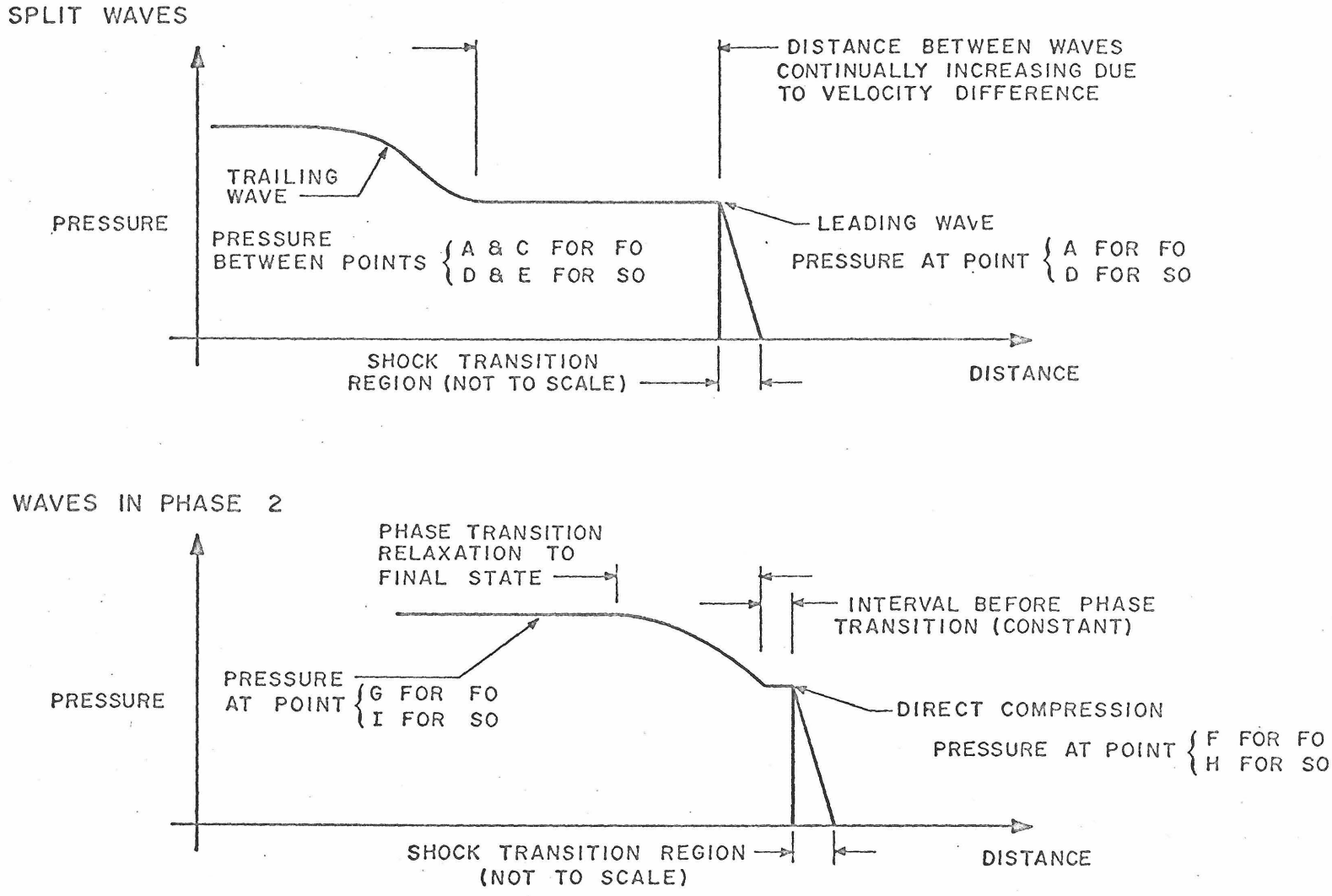

Figure T3. Pressure Distributions in Split Waves and in Phase 2 Region[12]

first wave are at point A (or D) which is in phase 1. Because the waves are separated it is assumed that the full equilibrium state is reached behind the first wave and thus that the model can be applied without alteration. Considering conditions behind this wave as a new set of "initial" conditions* the theory could again be applied to the second wave to predict the Hugoniot from point A (or D) to point C (or E). However, since it appears that FO transitions take much longer than that required to reach equilibrium[105,12] the second wave will not be sharp fronted (see Figure T3) and one of the fundamental assumptions of the theory (i.e., the transition zone is "thin") is violated. In this case Equation (27) cannot be justified and Equation (31) is incorrect**. Therefore the model does not apply and cannot be used to predict the Hugoniot in the "split wave" region. For SO transitions it is not known if the trailing wave rise time is sufficiently rapid to satisfy Equation (27) and thus to justify application of the shock model. An investigation of this point would be worthwhile.

When the compression is such that the phase 2 region is reached directly (past point C for FO transitions and point E for SO transitions) a single wave is formed. The initial shock state is along an extension of the phase 1 Hugoniot (point F for FO and point H for SO transitions; see Figure T3). After this the transition begins, relaxing to the final state at points G and I for FO and SO transitions,

---

*Clearly, in this case, P_o would not be negligible (i.e., P_o = pressure at point A (or D)) and Equations (1)-(3) would have to be rederived considering that the second wave moves into a moving (not stationary) medium moving at the particle velocity associated with P_o.

**Thermal effects cannot be neglected.

respectively*. Since the former case has a relaxation time known to be large compared to equilibrium times, the pressure rise for the transition will not be steep. As before the speed for SO transitions is unknown and the steepness of the second pressure rise is, consequently, unknown.

If the initial compression is found along the extension of the phase 1 Hugoniot, there must be a finite time interval between this event and the start of relaxation in the phase transition. If thermal equilibrium is established in this interval, all the assumptions of the model hold and it may be applied to predict the "extended" Hugoniot for phase 1 material. Using the conditions behind this wave the model may again be applied to the second pressure rise if the assumptions of the model (i.e., Equation (27)) are satisfied. As before, for FO transitions they are not, while for SO transitions the question is moot.

From this discussion it may be concluded that for both FO and SO transitions the model should not be applied past the phase 1 region. Therefore whenever the U-μ behavior in Figure T2 is manifest** the data outside of the phase 1 region should not be considered. The one exception would be a FO transition in which the coexistence region is very small and the transition is so slow that all measurements correspond to the extension of the phase 1 Hugoniot. In that instance, of

---

*In this case, of course, the second pressure rise is propagating at the same shock velocity as the initial rise and therefore does not detach from it.

**A determination of the type of transition occurring (FO or SO) might be made by comparing the U-μ data with the two curves in Figure T2.

course, no transition would be evident from the data and its existence (say in the ensuing expansion to P_o) could be ignored.

Structural transitions* are FO phase transitions[12] and are known to occur in a number of substances[91,86,13,11,10,12,109]. The two-wave structure predicted in Figure T3 is, in fact, observed. Some transitions may not appear because they are too slow[105].

Melting transitions are FO phase transitions and have been inferred from calculations for many substances[85,13,103,104,111,93,60,64,96,12,..,..](see Table 6). However, no direct experimental evidence of melting has been presented. Apparently there is doubt that the melting will appear in the experimental region[13,105] and consequently most authors have ignored melting in their calculations[85,93]. In an interesting study of melting under shock compression, Urlin and Ivanov[111]** computed the pressure required for melting of four metals although "the published experimental results ...does not permit us to speak with certainty concerning the absence of discontinuities in the slope of the shock adiabatics."

---

*Called polymorphic transitions[12].

**It is also interesting that they found that the slope of the $(P - (1/\rho))$ Hugoniot in the mixed phase region was generally greater than that in phase 1 (see Figure T1), and that therefore the melting process cannot result in split waves; i.e., no trailing wave appears. This follows from an examination of Figure T1 for the condition specified.

Fusion transitions are FO phase transitions and have been reported (see Table 6) based on an examination of the U-μ data[110, 109] and on opacity measurements[90,110]. However, the fusion process might be too slow to be recorded in shock experiments[90] and the effect on the U-μ function is questionable.

Electronic transitions[107,106,68], amongst other effects[10], might be examples of SO phase transitions, although this is not altogether clear*. In general the transition seems to involve demotion of an s-level electron to the next lowest d-level. As previously mentioned the nature and speed of these transitions is unknown, but it is notable that the U-μ behavior for SO transitions postulated in Figure T2 is matched by data presented in Reference (106).

---

*In Reference (107) the transitions are referred to as FO, since a sudden volume change is assumed (see Figure T1).

Appendix U

Fit of Theory Using σ and C_{ab}

The pair potential in terms of σ and C_{ab} is given by Equation (133):

$$\phi(r) = \frac{C_{ab}}{\sigma^6}\left[\left(\frac{\sigma}{r}\right)^n - \left(\frac{\sigma}{r}\right)^6\right] \tag{133}$$

which can be derived from Equation (72) noting that:

$$C_{ab} = \varepsilon f(n)\, \sigma^6 \tag{132}$$

The Hugoniot is given (generally) by Equation (95):

$$\mu^2 = \frac{4}{2^s}\left(\frac{N\pi\varepsilon}{M}\right) f(n)\left[\frac{\sigma^n}{(n-2)(n-3)}\left(\frac{2^s\rho_o N}{M}\right)^{n/3}(x^{n-2}-1) - \frac{\sigma^6}{12}\left(\frac{2^s\rho_o N}{M}\right)^2(x^4-1)\right] \tag{95}$$

Multiplying numerator and denominator by σ^6 and using Equation (132) this becomes (with rearrangement):

$$\mu^2 = \frac{4}{2^s}\left(\frac{N\pi}{M}\right)\left(\frac{C_{ab}}{6}\right)\left\{\sigma^n\left[\left(\frac{2^s\rho_o N}{M}\right)^{1/3}\right]^n \frac{(x^{n-2}-1)}{(n-2)(n-3)} - \frac{\sigma^6}{12}\left(\frac{2^s\rho_o N}{M}\right)^2(x^4-1)\right\} \tag{U1}$$

which is the Hugoniot in terms of the desired parameters. Letting:

$$C_1 = \frac{4}{2^s}\left(\frac{N\pi}{M}\right) \tag{U2}$$

$$C_2 = \left(\frac{2^s\rho_o N}{M}\right)^{1/3} \tag{U3}$$

$$C_3 = \frac{1}{12}\left(\frac{2^s\rho_o N}{M}\right)^2 \tag{U4}$$

Equation (U1) can be written:

$$\mu^2 = C_1 C_{ab} \left[\sigma^{n-6} \, C_2^n \, \frac{(x^{n-2} - 1)}{(n-2)(n-3)} - C_3 (x^4 - 1) \right] \tag{U5}$$

Following Equations (138) - (141), the residuals R_i become:

$$R_i = \mu_i^2 - C_1 C_{ab} \left[\sigma^{n-6} \, C_2^n \, \frac{(x_i^{n-2} - 1)}{(n-2)(n-3)} - C_3 (x_i^4 - 1) \right] \tag{U6}$$

and the equations of interest are:

$$\frac{\partial \sum_i R_i^2}{\partial n} = 0 \tag{U7}$$

$$\frac{\partial \sum_i R_i^2}{\partial \sigma} = 0 \tag{U8}$$

$$\frac{\partial \sum_i R_i^2}{\partial C_{ab}} = 0 \tag{U9}$$

which fix the values of σ, C_{ab} and n which minimize the sum of the squares of the residuals R_i.

Some or all of Equations (U7) - (U9) are used depending on which of σ, C_{ab} and n are considered fixed (i.e., known). This leads to the general scheme shown in Table U1. For a one-parameter fit (1PF) σ and C_{ab} are fixed and only Equation (U7) is considered. Substituting Equation (U6) into Equation (U7) gives:

$$\frac{\partial \sum_i R_i^2}{\partial n} = \sum_i 2 \left\{ \mu_i^2 - C_1 C_{ab} \left[\sigma^{n-6} \, C_2^n \, \frac{(x_i^{n-2} - 1)}{(n-2)(n-3)} - C_3 (x_i^4 - 1) \right] \right\}$$

$$\times \left\{ \cancel{(-C_1 C_{ab})} \left[\frac{\cancel{\sigma^{n-6}} \, \cancel{C_2^n}}{\cancel{(n-2)(n-3)}} \, x_i^{n-2} \, \ln x_i + \frac{\cancel{\sigma^{n-6}} (x_i^{n-2} - 1)}{\cancel{(n-2)(n-3)}} \, \cancel{C_2^n} \ln C_2 \right. \right. +$$

Table U1

FITTING OF DATA USING σ AND C_{ab}--LIQUIDS

Parameter Fit	Fix	Seeking
1	σ, C_{ab}	n
2	C_{ab}	σ,n
2	σ	C_{ab},n
3	---	σ, C_{ab},n

$$+ \frac{C_2^n(x_i^{n-2} - 1)}{(n-2)(n-3)} \sigma^{n-6} \ln \sigma - \frac{\sigma^{n-6} C_2^n (x_i^{n-2} - 1)}{(n-2)^2(n-3)^2} (2n - 5) \Bigg] \Bigg\} = 0 \quad \text{(U10)}$$

or :

$$\sum_i \left\{ \mu_i^2 - C_1 C_{ab} \left[\sigma^{n-6} \frac{C_2^n (x_i^{n-2} - 1)}{(n-2)(n-3)} - C_3 (x_i^4 - 1) \right] \right\}$$

$$\times \left\{ x_i^{n-2} \ln x_i + (x_i^{n-2} - 1)(\ln C_2 \sigma - \frac{2n - 5}{(n-2)(n-3)}) \right\} = 0 \quad \text{(U11)}$$

Equation (U11) is an implicit relation for the desired value of n. However, because Equation (U11) is complex it might have many roots and the one of interest might be difficult to locate. Therefore, instead, n was indexed (by 0.1) throughout the entire range of values of interest and the sum-of-the-squares of the residuals computed from*:

$$L = \sum_i R_i^2 = \sum_i \left\{ \mu_i^2 - C_1 C_{ab} \left[\sigma^{n-6} \frac{C_2^n (x_i^{n-2} - 1)}{(n-2)(n-3)} - C_3 (x_i^4 - 1) \right] \right\} \quad \text{(U12)}$$

at each step. The desired (best fit) value of n was that which gave a minimum in L.

Computations were performed on an IBM 360/75 digital computer using a program called FIFI**. The resultant values of n for argon and nitrogen were 10.4 and 9.2 respectively. The $(\mu_i - x_i)$ data and ρ_o, M and s (and thus C_1, C_2 and C_3 from Equations (U2) - (U4)) were taken from Appendix S, while σ and C_{ab} were chosen from Table 7.

---

*This follows the discussion leading to Equation (142).

**Available from the author on request.

Appendix V

Effect of Added Attraction

Equation (59) is:

$$\phi_{attraction} = br^{-6} + cr^{-8} + dr^{-10} + \cdots \tag{59}$$

Considering only two additional terms (compared to Equation (65)) and substituting along with Equation (57) into Equation (55) gives:

$$\phi(r) = ar^{-n} - (br^{-6} + cr^{-8} + dr^{-10}) \tag{61}$$

which is Equation (61). This can be written:

$$\phi(r) = ar^{-n} - br^{-6} - cr^{-8} - dr^{-10} \tag{V1}$$

Noting the discussion following Equation (131) it is clear that:

$$C_{ab} \equiv b \tag{V2}$$

and for convenience we may define:

$$C'_{ab} = c \tag{V3}$$

$$C''_{ab} = d \tag{V4}$$

Substituting Equations (V2) - (V4) into Equation (V1) gives:

$$\phi(r) = ar^{-n} - C_{ab}r^{-6} - C'_{ab}r^{-8} - C''_{ab}r^{-10} \tag{V5}$$

Equations (66) - (68) are:

$$\phi(\sigma) = 0 \tag{66}$$

$$\phi(r_o) = -\varepsilon \tag{67}$$

$$\left[\frac{d\phi(r)}{dr}\right]_{r=r_o} = 0 \tag{68}$$

Use of Equation (66) in Equation (V5) gives:

$$\phi(\sigma) = 0 = a\sigma^{-n} - C_{ab}\sigma^{-6} - C'_{ab}\sigma^{-8} - C''_{ab}\sigma^{-10} \tag{V6}$$

and from Equation (67):

$$\phi(r_o) = -\varepsilon = ar_o^{-n} - C_{ab}r_o^{-6} - C'_{ab}r_o^{-8} - C''_{ab}r_o^{-10} \tag{V7}$$

Differentiating Equation (V5) gives:

$$\frac{d\phi(r)}{dr} = -nar^{-n-1} + 6C_{ab}r^{-7} + 8C'_{ab}r^{-9} + 10C''_{ab}r^{-11} \tag{V8}$$

and using Equation (68):

$$0 = -nar_o^{-n-1} + 6C_{ab}r_o^{-7} + 8C'_{ab}r_o^{-9} + 10C''_{ab}r_o^{-11} \tag{V9}$$

Multiplying by r_o gives:

$$0 = -nar_o^{-n} + 6C_{ab}r_o^{-6} + 8C'_{ab}r_o^{-8} + 10C''_{ab}r_o^{-10} \tag{V10}$$

From Equation (V6):

$$a = \sigma^n(C_{ab}\sigma^{-6} + C'_{ab}\sigma^{-8} + C''_{ab}\sigma^{-10}) \tag{V11}$$

or:

$$a = \sigma^{n-6}(C_{ab} + C'_{ab}\sigma^{-2} + C''_{ab}\sigma^{-4}) \tag{V12}$$

From Equation (V7):

$$ar_o^{-n} = -\varepsilon + R_o^{-6}(C_{ab} + C'_{ab}r_o^{-2} + C''_{ab}r_o^{-4}) \tag{V13}$$

and from Equation (V10):

$$nar_o^{-n} = 2r_o^{-6}(3C_{ab} + 4C'_{ab}r_o^{-2} + 5C''_{ab}r_o^{-4}) \tag{V14}$$

or:

$$(\tfrac{n}{6})ar_o^{-n} = r_o^{-6}(C_{ab} + \tfrac{4}{3}C'_{ab}r_o^{-2} + \tfrac{5}{3}C''_{ab}r_o^{-4}) \tag{V15}$$

Letting:

$$C(\sigma) = C_{ab} + C'_{ab}\sigma^{-2} + C''_{ab}\sigma^{-4} \tag{V16}$$

$$C(r_o) = C_{ab} + C'_{ab}r_o^{-2} + C''_{ab}r_o^{-4} \tag{V17}$$

$$C_1(r_o) = C_{ab} + \tfrac{4}{3}C'_{ab}r_o^{-2} + \tfrac{5}{3}C''_{ab}r_o^{-4} \tag{V18}$$

Equations (V11), (V13) and (V15) become:

$$a = \sigma^{n-6}C(\sigma) \tag{V19}$$

$$ar_o^{-n} = - + r_o^{-6}C(r_o) \tag{V20}$$

$$(\tfrac{n}{6})ar_o^{-n} = r_o^{-6}C_1(r_o) \tag{V21}$$

Substituting Equation (V19) into Equations (V20) and (V21) gives:

$$\sigma^{n-6}r_o^{-n}C(\sigma) = -\varepsilon + r_o^{-6}C(r_o) \tag{V22}$$

$$(\tfrac{n}{6})\sigma^{n-6}r_o^{-n}C(\sigma) = r_o^{-6}C_1(r_o) \tag{V23}$$

Taking a ratio gives:

$$\frac{\cancel{\sigma^{n-6}r_o^{-n}C(\sigma)}}{(\tfrac{n}{6})\cancel{\sigma^{n-6}r_o^{-n}C(\sigma)}} = \frac{-\varepsilon + r_o^{-6}C(r_o)}{r_o^{-6}C_1(r_o)} \tag{V24}$$

$$n = 6\left[\frac{r_o^{-6}\, C_1(r_o)}{r_o^{-6}\, C(r_o) - \varepsilon}\right] \tag{V25}$$

or :

$$n = 6\left[\frac{C_1(r_o)}{C(r_o) - \varepsilon r_o^6}\right] \tag{V26}$$

Substituting into Equation (V22), after rearrangement, gives:

$$\left(\frac{\sigma}{r_o}\right)^{6\left[\frac{C_1(r_o)}{C(r_o)-\varepsilon r_o^6}-1\right]} = -\frac{\varepsilon r_o^6 + C(r_o)}{C(\sigma)} \tag{V27}$$

or:

$$6\left[\frac{C_1(r_o)}{C(r_o)-\varepsilon r_o^6} - 1\right] \ln\left(\frac{\sigma}{r_o}\right) = \ln\left[\frac{C(r_o) - r_o^6}{C(\sigma)}\right] \tag{V28}$$

which may be written:

$$\underbrace{6\left[\frac{C_1(r_o)}{C(r_o)-\varepsilon r_o^6} - 1\right] \ln\left(\frac{\sigma}{r_o}\right)}_{A} + \underbrace{\ln\left[\frac{C_1(r_o)}{C(r_o)-\varepsilon r_o^6} \cdot \frac{C(\sigma)}{C_1(r_o)}\right]}_{B} = 0 \tag{V29}$$

Knowing σ and ε, r_o may be found by trial and error from Equation (V29) noting Equations (V16) - (V18) if C_{ab}, C'_{ab} and C''_{ab} are known. This value may be used in Equation (V26) to determine n.

From Table 8, for argon:

$$\sigma = 3.28\text{Å} \tag{V30}$$

$$\varepsilon/k = 138.2^{\circ}\text{K} \tag{V31}$$

and:

$$C_{ab} = 65.9 \times 10^{-60} \text{erg-cm}^6 \tag{V32}$$

Values of C'_{ab} and C''_{ab} are given by Fontana[118] but they are believed to be in error, since his corresponding value of C_{ab} (55.9×10^{-60}erg-cm^6) is low compared to the more recent value[122] in Equation (V32). Assuming the error in C_{ab} propagates linearly to C'_{ab} and C''_{ab}, a correction factor of 1.179 (i.e., 65.9/55.9) can be applied to Fontana's values to give:

$$C'_{ab} = (121 \times 10^{-76})(1.179) = 143 \times 10^{-76} \text{erg-cm}^8 \tag{V33}$$

$$C''_{ab} = (320 \times 10^{-92})(1.179) = 377 \times 10^{-92} \text{erg-cm}^{10} \tag{V34}$$

Therefore from Equation (V16):

$$C(\sigma) = 65.9 \times 10^{-60} + 143 \times 10^{-76}(3.28 \times 10^{-8})^{-2} + 377 \times 10^{-92}(3.28 \times 10^{-8})^{-4} \tag{V35}$$

or:

$$C(\sigma) = 82.5 \times 10^{-60} \text{erg-cm}^6 \tag{V36}$$

Trial and error solution using Equations (V29) and (V26):

r_o	$C(r_o)$	$C_1(r_o)$	εr_o^6	n	σ/r_o	$C(\sigma)/C_1(r_o)$	A	B	A+B
4.0	76.31	80.27	78.14	<0	-	-	-	-	-
3.7	78.36	83.18	48.95	16.97	0.886	0.992	-1.328	+1.033	-0.295
3.4	81.09	87.09	29.47	10.12	0.965	0.947	-0.147	+0.470	+0.323
3.5	80.08	85.64	35.07	11.42	0.937	0.963	-0.353	+0.604	+0.251
3.6	79.17	84.34	41.53	13.44	0.911	0.978	-0.693	+0.784	+0.091
3.65	78.75	83.74	45.11	14.94	0.899	0.985	-0.951	+0.896	-0.055
3.63	78.92	83.99	43.65	14.29	0.904	0.982	-0.837	+0.850	+0.013

which is close enough. Interpolation gives:

$$n \tilde{=} 14.4 \tag{V37}$$

which is not substantially less than the value of n given in Table 8 (i.e., $n = 16.7$).

The form of the potential with the two attractive terms added may be compared to Equation (133) to see why the reduction in n is small. Substitution of Equation (V12) into Equation (V5) gives:

$$\phi(r) = \sigma^{n-6}\, r^{-n}(C_{ab} + C'_{ab}\sigma^{-2} + C''_{ab}\sigma^{-4}) - r^{-6}(C_{ab} + C'_{ab}r^{-2} + C''_{ab}r^{-4}) \quad \text{(V38)}$$

or:

$$\phi(r) = \frac{C_{ab}}{\sigma^6}\left[\left(\frac{\sigma}{r}\right)^n \left(1 + \frac{C'_{ab}}{C_{ab}}\sigma^{-2} + \frac{C''_{ab}}{C_{ab}}\sigma^{-4}\right) - \left(\frac{\sigma}{r}\right)^6 \left(1 + \frac{C'_{ab}}{C_{ab}}r^{-2} + \frac{C''_{ab}}{C_{ab}}r^{-4}\right)\right] \quad \text{(V39)}$$

which is the form of the potential desired. Note that when $C'_{ab} = C''_{ab} = 0$, Equation (V39) reduces to Equation (133). Note also that the use of the extra terms affects both the repulsive $((\sigma/r)^n)$ and attractive $((\sigma/r)^6)$ terms in Equation (133). It is because the coefficients of the two terms in Equation (V39) are similar (and that $\sigma \simeq r_o$ (3.28Å vs. 3.63Å)) that only a small reduction in n occurs.

Appendix W

ε/k vs. T_M - Linear Least Squares

From the bracketed values in Table 7 and Reference [101]:

Substance	ε/k-^oK	T_M-^oK
Argon	138.2	83.9
Nitrogen	91.5	63.2
Carbon Tetrachloride	378.	250.1

Letting:

$$y = \varepsilon/k\ ^oK \tag{W1}$$

$$x = T_M\ ^oK \tag{W2}$$

the assumed form of the correlation is:

$$y = a + bx \tag{W3}$$

where a and b are constants. The residuals are given by:

$$R_i = y_i - a - bx_i \quad \text{or} \quad R_i^2 = (y_i - a - bx_i)^2 \tag{W4}$$

The least-squares - best-fit values of a and b are given from[15]:

$$\frac{\partial \sum_i R_i^2}{\partial a} = 0 = \frac{\partial \sum_i R_i^2}{\partial b} \tag{W5}$$

Substituting Equation (W4) into Equations (W5) gives:

$$\frac{\partial \sum_i R_i^2}{\partial a}: \qquad \sum_i 2(y_i - a - bx_i)(-1) = 0 \tag{W6}$$

$$\frac{\partial \sum_i R_i^2}{\partial b} : \quad \sum_i 2(y_i - a - bx_i)(-x_i) = 0 \qquad \text{(W7)}$$

or:

$$\sum_i y_i = an_o + b \sum_i x_i \qquad \text{(W8)}$$

$$\sum_i y_i x_i = a \sum_i x_i + b \sum_i x_i^2 \qquad \text{(W9)}$$

where $n_o = \sum_i$ = number of points. The determinant of the coefficient is given by:

$$D = \begin{vmatrix} n_o & \sum_i x_i \\ \sum_i x_i & \sum_i x_i^2 \end{vmatrix} = n_o \sum_i x_i^2 - \left(\sum_i x_i\right)^2 \qquad \text{(W10)}$$

and:

$$aD = \begin{vmatrix} \sum_i y_i & \sum_i x_i \\ \sum_i x_i y_i & \sum_i x_i^2 \end{vmatrix} = \sum_i y_i \sum_i x_i^2 - \sum_i x_i \sum_i x_i y_i \qquad \text{(W11)}$$

$$bD = \begin{vmatrix} n_o & \sum_i y_i \\ \sum_i x_i & \sum_i x_i y_i \end{vmatrix} = n_o \sum_i x_i y_i - \sum_i x_i \sum_i y_i \qquad \text{(W12)}$$

From the above data:

$$n_o = 3 , \quad \sum_i x_i = 397.2 , \quad \sum_i y_i = 607.7 , \quad \sum_i x_i^2 = 73583.46 \qquad \text{(W13)}$$

$$\sum_i x_i y_i = 111915.58 , \quad \left(\sum_i x_i\right)^2 = 157767.84 \qquad \text{(W14)}$$

From Equation (W10):

$$D = 62982.54 \tag{W15}$$

and from Equations (W11) and (W12):

$$a = 4.188 \quad , \quad b = 1.498 \tag{W16}$$

As a reasonable approximation:

$$a \cong 4\,^{o}K \quad , \quad b \cong 1.5 \tag{W17}$$

and Equation (W3) becomes (noting Equations (W1) and (W2)):

$$\varepsilon/k = 1.5\ T_M + 4\ \ ^{o}K \tag{134}$$

which is Equation (134).

Appendix X

Derivation of 1, 2 and 3 Parameter Fit Equations

The residuals R_i are given by Equation (138):

$$R_i = \mu_i^2 - C_1 \varepsilon \sigma^6 \frac{(n/6)^{\frac{n}{n-6}}}{(\frac{n}{6} - 1)} \left[\frac{\sigma^{n-6} C_2^n}{(n-2)(n-3)} (x_i^{n-2} - 1) - C_3 (x_i^4 - 1) \right] \quad (138)$$

where C_1, C_2 and C_3 are given by Equations (136). Of interest are the equations:

$$\frac{\partial \sum_i R_i^2}{\partial n} = 0 \quad (139)$$

$$\frac{\partial \sum_i R_i^2}{\partial \sigma} = 0 \quad (140)$$

$$\frac{\partial \sum_i R_i^2}{\partial \varepsilon} = 0 \quad (141)$$

Substituting Equation (138) into Equations (139) - (141) gives:

$$\frac{\partial \sum_i R_i^2}{\partial n} = 0 = \sum_i 2[R_i] \left\{ \cancel{C_1 \varepsilon \sigma^6} \frac{(n/6)^{\frac{n}{n-6}}}{(\frac{n}{6} - 1)} \left[\frac{\sigma^{n-6} C_2^n}{(n-2)(n-3)} x_i^{n-2} \ln x_i \right. \right.$$

$$+ \frac{\sigma^{n-6} (x_i^{n-2} - 1)}{(n-2)(n-3)} C_2^n \ln C_2 + \frac{C_2^n (x_i^{n-2} - 1)}{(n-2)(n-3)} \sigma^{n-6} \ln \sigma$$

$$\left. - \frac{\sigma^{n-6} C_2^n (x_i^{n-2} - 1)(2n-5)}{(n-2)^2 (n-3)^2} \right] \cancel{- C_1 \varepsilon \sigma^6} \left[\frac{\sigma^{n-6} C_2^n}{(n-2)(n-3)} (x_i^{n-2} - 1) \right.$$

$$\left. - C_3 (x_i^4 - 1) \right] \quad \times$$

$$\times \left[\frac{(\frac{n}{6}-1)\left(\frac{n}{n-6}(\frac{n}{6})^{\frac{n}{n-6}-1}\cdot\frac{1}{6}+(\frac{n}{6})^{\frac{n}{n-6}}\ln(\frac{n}{6})\right)\frac{(\frac{n}{6}-1)\frac{1}{6}-(\frac{n}{6})\frac{1}{6}}{(\frac{n}{6}-1)^2}-(\frac{n}{6})^{\frac{n}{n-6}}\cdot\frac{1}{6}}{(\frac{n}{6}-1)^2}\right] \Bigg\} \quad \text{(X1)}$$

$$\frac{\partial \sum_i R_i^2}{\partial \sigma} = 0 = \sum_i 2[R_i] \left\{ C_1\varepsilon \frac{(\frac{n}{6})^{\frac{n}{n-6}}}{(\frac{n}{6}-1)} \left[\frac{n\sigma^{n-1}C_2^n(x_i^{n-2}-1)}{(n-2)(n-3)} - 6\sigma^5 C_3(x_i^4-1) \right] \right\} \quad \text{(X2)}$$

$$\frac{\partial \sum_i R_i^2}{\partial \varepsilon} = 0 = \sum_i 2[R_i] \left\{ C_1\sigma^6 \frac{(\frac{n}{6})^{\frac{n}{n-6}}}{(\frac{n}{6}-1)} \left[\frac{\sigma^{n-6}C_2^n}{(n-2)(n-3)}(x_i^{n-2}-1) - C_3(x_i^4-1) \right] \right\} \quad \text{(X3)}$$

Noting Equation (71), these may be written:

$$\sum_i R_i \left\{ \frac{f(n)\sigma^{n-6}C_2^n}{(n-2)(n-3)} \left[x_i^{n-2}\ln x_i + (\ln C_2\sigma - \frac{2n-5}{(n-2)(n-3)})(x_i^{n-2}-1) \right] \right.$$

$$\left. + f(n)\left[\frac{\sigma^{n-6}C_2^n}{(n-2)(n-3)}(x_i^{n-2}-1) - C_3(x_i^4-1) \right] \left[\frac{(\frac{n}{6}-1)(\frac{1}{n-6} - \frac{1/6}{(n/6-1)^2}\ln(\frac{n}{6})) - \frac{1}{6}}{(\frac{n}{6}-1)} \right] \right\} \quad \text{(X4)}$$

$$\sum_i R_i \left\{ (\frac{n}{6}) \frac{\sigma^{n-6}C_2^n}{(n-2)(n-3)}(x_i^{n-2}-1) - C_3(x_i^4-1) \right\} = 0 \quad \text{(X5)}$$

$$\sum_i R_i \left\{ \frac{\sigma^{n-6}C_2^n}{(n-2)(n-3)}(x_i^{n-2}-1) - C_3(x_i^4-1) \right\} = 0 \quad \text{(X6)}$$

or:

$$\sum_i \left\{ \mu_i^2 - C_1 \varepsilon \sigma^6 \, f(n) \left[\frac{\sigma^{n-6} \, C_2^n}{(n-2)(n-3)} \, (x_i^{n-2} - 1) - C_3 (x_i^4 - 1) \right] \right\}$$

$$\times \left\{ \frac{\sigma^{n-6} \, C_2^n}{(n-2)(n-3)} \left[x_i^{n-2} \, \ell n \, x_i + (\ell n \, C_2 \sigma - \frac{2n-5}{(n-2)(n-3)}) (x_i^{n-2} - 1) \right] \right.$$

$$\left. - \frac{1}{6} \frac{\ell n (\frac{n}{6})}{(\frac{n}{6} - 1)^2} \left[\frac{\sigma^{n-6} \, C_2^n}{(n-2)(n-3)} \, (x_i^{n-2} - 1) - C_3 (x_i^4 - 1) \right] \right\} = 0 \qquad \text{(X7)}$$

$$\sum_i \left\{ \mu_i^2 - C_1 \varepsilon \sigma^6 \, f(n) \left[\frac{\sigma^{n-6} \, C_2^n}{(n-2)(n-3)} \, (x_i^{n-2} - 1) - C_3 (x_i^4 - 1) \right] \right\}$$

$$\times \left\{ (\frac{n}{6}) \, \frac{\sigma^{n-6} \, C_2^n}{(n-2)(n-3)} \, (x_i^{n-2} - 1) - C_3 (x_i^4 - 1) \right\} = 0 \qquad \text{(X8)}$$

$$\sum_i \left\{ \mu_i^2 - C_1 \varepsilon \sigma^6 \, f(n) \left[\frac{\sigma^{n-6} \, C_2^n}{(n-2)(n-3)} \, (x_i^{n-2} - 1) - C_3 (x_i^4 - 1) \right] \right\}$$

$$\times \left\{ \frac{\sigma^{n-6} \, C_2^n}{(n-2)(n-3)} \, (x_i^{n-2} - 1) - C_3 (x_i^4 - 1) \right\} = 0 \qquad \text{(X9)}$$

For the fitting scheme outlined in Table 10, Equation (X7) defines the best fit value of n for the 1PF. Equations (X7) and (X8) jointly define the best fit values of n and ε when σ is fixed for the 2PF, while Equations (X7) and (X9) define n and ε when σ is fixed for the other 2PF. For the 3PF Equations (X7) - (X9) jointly define n, σ and ε.

Expansion of Equation (X8) (for which σ is the parameter of interest) gives:

$$\left(\frac{n}{6}\right) \frac{\sigma^{n-6}\, C_2^n}{(n-2)(n-3)} \sum_i \mu_i^2 (x_i^{n-2} - 1) - C_3 \sum_i \mu_i^2 (x_i^4 - 1)$$

$$- C_1 \varepsilon \sigma^6 \, f(n) \left(\frac{n}{6}\right) \left(\frac{\sigma^{n-6}\, C_2^n}{(n-2)(n-3)} \right)^2 \sum_i (x_i^{n-2} - 1)^2$$

$$+ C_1 \varepsilon \sigma^6 \, f(n) \frac{\sigma^{n-6}\, C_2^n}{(n-2)(n-3)} C_3 \sum_i (x_i^{n-2} - 1)(x_i^4 - 1)$$

$$+ C_1 \varepsilon \sigma^6 \, f(n) \left(\frac{n}{6}\right) \frac{\sigma^{n-6}\, C_2^n}{(n-2)(n-3)} C_3 \sum_i (x_i^4 - 1)(x_i^{n-2} - 1)$$

$$- C_1 \varepsilon \sigma^6 \, f(n) \, C_3^2 \sum_i (x_i^4 - 1)^2 = 0 \qquad \text{(X10)}$$

Letting:

$$S_1 = \sum_i \mu_i^2 (x_i^{n-2} - 1) \qquad \text{(X11)}$$

$$S_2 = \sum_i \mu_i^2 (x_i^4 - 1) \qquad \text{(X12)}$$

$$S_3 = \sum_i (x_i^{n-2} - 1)^2 \qquad \text{(X13)}$$

$$S_4 = \sum_i (x_i^4 - 1)^2 \qquad \text{(X14)}$$

$$S_5 = \sum_i (x_i^4 - 1)(x_i^{n-2} - 1) \qquad \text{(X15)}$$

Equation (X10) becomes, after rearrangement:

$$\sigma^{n-6}\left[\left(\frac{n}{6}\right)\frac{C_2^n S_1}{(n-2)(n-3)}\right] - C_3S_2 - \sigma^{2n-6}\left[\left(\frac{n}{6}\right)\frac{C_1\varepsilon\, f(n)\, C_2^{2n} S_3}{(n-2)^2\,(n-3)^2}\right]$$

$$+ \sigma^n\left[\left(\frac{n}{6}+1\right)\frac{C_1\varepsilon\, f(n)\, C_2^n\, C_3S_5}{(n-2)(n-3)}\right] - \sigma^6\left[C_1\varepsilon\, f(n)\, C_3^2\, S_4\right] = 0 \qquad \text{(X16)}$$

Solving for σ^{2n-6} and finding the root gives:

$$\sigma = \left\{ \frac{\sigma^{n-6}\left[\left(\frac{n}{6}\right)\frac{C_2^n S_1}{(n-2)(n-3)}\right] + \sigma^n\left[\left(\frac{n}{6}+1\right)\frac{C_1\varepsilon\, f(n) C_2^n\, C_3S_5}{(n-2)(n-3)}\right] - \sigma^6\left[C_1\varepsilon\, f(n) C_3^2\, S_4\right] - C_3S_2}{\left(\frac{n}{6}\right)\frac{C_1\varepsilon\, f(n)\, C_2^{2n} S_3}{(n-2)^2\,(n-3)^2}} \right\}^{\frac{1}{2n-6}} \qquad \text{(X17)}$$

from which an iterative solution for σ can be found.

Expansion of Equation (X9) (for which ε is the parameter of interest) gives:

$$\frac{\sigma^{n-6}\, C_2^n}{(n-2)(n-3)} \sum_i \mu_i^2(x_i^{n-2}-1) - C_3 \sum_i \mu_i^2(x_i^4-1) - C_1\varepsilon\sigma^6\, f(n)\left(\frac{\sigma^{n-6}C_2^n}{(n-2)(n-3)}\right)^2$$

$$\times \sum_i (x_i^{n-2}-1)^2 + C_1\varepsilon\sigma^6 f(n)\,\frac{\sigma^{n-6}\, C_2^n}{(n-2)(n-3)}\, C_3 \sum_i (x_i^{n-2}-1)(x_i^4-1)$$

$$+ C_1\varepsilon\sigma^6 f(n) C_3\,\frac{\sigma^{n-6}\, C_2^n}{(n-2)(n-3)} \sum_i (x_i^4-1)(x_i^{n-2}-1)$$

$$- C_1\varepsilon\sigma^6 f(n) C_3^2 \sum_i (x_i^4-1)^2 = 0 \qquad \text{(X18)}$$

Using Equations (X11) - (X15) this becomes:

$$-\frac{\sigma^{n-6}\,C_2^n\,S_1}{(n-2)(n-3)} + C_3S_2 = \varepsilon C_1\sigma^6 f(n)\left[-S_3\left(\frac{\sigma^{n-6}\,C_2^n}{(n-2)(n-3)}\right)^2 + \frac{2\sigma^{n-6}\,C_2^n\,C_3}{(n-2)(n-3)}\,S_5 - C_3^2\,S_4\right] \qquad \text{(X19)}$$

or:

$$\varepsilon = \frac{1}{C_1\sigma^6 f(n)}\left[\frac{\frac{\sigma^{n-6}\,C_2^n}{(n-2)(n-3)}\,S_1 - C_3S_2}{\left(\frac{\sigma^{n-6}\,C_2^n}{(n-2)(n-3)}\right)^2 S_3 - 2\,\frac{\sigma^{n-6}\,C_2^n\,C_3}{(n-2)(n-3)}\,S_5 + C_3^2\,S_4}\right] \qquad \text{(X20)}$$

which determines ε directly.

When σ and ε are both parameters of interest, Equations (X16) and (X19) may be considered jointly. They are, with some rearrangement:

$$\left(\frac{n}{6}\right)\frac{\sigma^{n-6}\,C_2^n}{(n-2)(n-3)}\,S_1 - C_3S_2 - \left(\frac{n}{6}\right)C_1\varepsilon\,f(n)\sigma^6\left(\frac{\sigma^{n-6}\,C_2^n}{(n-2)(n-3)}\right)^2 S_3$$

$$+\left(\frac{n}{6}+1\right)\frac{C_1\varepsilon\,f(n)\sigma^n\,C_2^n}{(n-2)(n-3)}\,S_5 - C_1\varepsilon\,f(n)\sigma^6\,C_3^2\,S_4 = 0 \qquad \text{(X21)}$$

$$\frac{\sigma^{n-6}\,C_2^n}{(n-2)(n-3)}\,S_1 - C_3S_2 - C_1\varepsilon\,f(n)\sigma^6\left(\frac{\sigma^{n-6}\,C_2^n}{(n-2)(n-3)}\right)^2 S_3$$

$$+2\,\frac{C_1\varepsilon\,f(n)\sigma^n C_2^n\,C_3}{(n-2)(n-3)}\,S_5 - C_1\varepsilon\,f(n)\sigma^6\,C_3^2\,S_4 = 0 \qquad \text{(X22)}$$

or:

$$\left(\frac{n}{6}\right)\frac{\sigma^{n-6}\,C_2^n}{(n-2)(n-3)}\,S_1 - C_3S_2 = C_1\varepsilon\, f(n)\sigma^6\left[\left(\frac{n}{6}\right)\left(\frac{\sigma^{n-6}\,C_2^n}{(n-2)(n-3)}\right)^2 S_3 - \left(\frac{n}{6}+1\right)\frac{\sigma^{n-6}\,C_2^n\,C_3}{(n-2)(n-3)}\,S_5 + C_3^2\,S_4\right] \tag{X23}$$

$$\frac{\sigma^{n-6}\,C_2^n}{(n-2)(n-3)}\,S_1 - C_3S_2 = C_1\varepsilon\, f(n)\sigma^6\left[\left(\frac{\sigma^{n-6}\,C_2^n}{(n-2)(n-3)}\right)^2 S_3 - 2\,\frac{\sigma^{n-6}\,C_2^n\,C_3}{(n-2)(n-3)}\,S_5 + C_3^2\,S_4\right] \tag{X24}$$

Letting:

$$\delta = \frac{\sigma^{n-6}\,C_2^n}{(n-2)(n-3)} \tag{X25}$$

these become:

$$\left(\frac{n}{6}\right)\delta S_1 - C_3S_2 = C_1\varepsilon\, f(n)\sigma^6\left[\left(\frac{n}{6}\right)\delta^2 S_3 - \left(\frac{n}{6}+1\right)\delta C_3S_5 + C_2^2\,S_4\right] \tag{X26}$$

$$\delta S_1 - C_3S_2 = C_1\varepsilon\, f(n)\sigma^6\left[\delta^2 S_3 - 2\delta C_3S_5 + C_3^2\,S_4\right] \tag{X27}$$

Taking the ratio of Equations (X26) and (X27) gives:

$$\frac{\left(\frac{n}{6}\right)\delta S_1 - C_3S_2}{\delta S_1 - C_3S_2} = \frac{\left(\frac{n}{6}\right)\delta^2 S_3 - \left(\frac{n}{6}+1\right)\delta C_3S_5 + C_3^2\,S_4}{\delta^2 S_3 - 2\delta C_3S_5 + C_3^2\,S_4} \tag{X28}$$

Cross-multiplication gives:

$$\cancel{(\tfrac{n}{6})\delta^3 S_1 S_3} - 2(\tfrac{n}{6})\delta^2 S_1 C_3 S_5 + (\tfrac{n}{6})\delta S_1 C_3^2 S_4 - \cancel{C_3 S_2 \delta^2 S_3} + 2\delta C_3^2 S_2 S_5$$

$$- \cancel{C_3^3 S_2 S_4} = \cancel{(\tfrac{n}{6})\delta^3 S_1 S_3} - (\tfrac{n}{6}+1)\delta^2 S_1 C_3 S_5 + \delta S_1 C_3^2 S_4 - (\tfrac{n}{6})\delta^2 S_3 C_3 S_2$$

$$+ (\tfrac{n}{6}+1)\delta C_3^2 S_2 S_5 - \cancel{C_3^3 S_2 S_4} \qquad \text{(X29)}$$

or:

$$- 2(\tfrac{n}{6})\delta S_1 S_5 + (\tfrac{n}{6}) S_1 C_3 S_4 - S_2 \delta S_3 + 2 C_3 S_2 S_5$$

$$= -(\tfrac{n}{6}+1)\delta S_1 S_5 + S_1 C_3 S_4 - (\tfrac{n}{6})\delta S_3 S_2 + (\tfrac{n}{6}+1) C_3 S_2 S_5 \qquad \text{(X30)}$$

$$\delta[S_1 S_5(-2(\tfrac{n}{6}) + \tfrac{n}{6} + 1) + S_2 S_3(-1 + \tfrac{n}{6})] = S_1 C_3 S_4(1 - \tfrac{n}{6}) + C_3 S_2 S_5(\tfrac{n}{6} + 1 - 2) \qquad \text{(X31)}$$

$$\delta = \frac{C_3 \cancel{(\frac{n}{6} - 1)} (S_2 S_5 - S_1 S_4)}{\cancel{(\frac{n}{6} - 1)}(S_2 S_3 - S_1 S_5)} \qquad \text{(X32)}$$

and from Equation (X25):

$$\frac{\sigma^{n-6} C_2^n}{(n-2)(n-3)} = C_3 \frac{(S_2 S_5 - S_1 S_4)}{(S_2 S_3 - S_1 S_5)} \qquad \text{(X33)}$$

or

$$\sigma = \left[\frac{(n-2)(n-3) C_3}{C_2^n} \left(\frac{S_2 S_5 - S_1 S_4}{S_2 S_3 - S_1 S_5} \right) \right]^{\frac{1}{n-6}} \qquad \text{(X34)}$$

which determines σ. Substituting Equation (X33) into Equation (X20) gives:

$$\varepsilon = \frac{1}{C_1\sigma^6 f(n)}\left[\frac{\left(\frac{S_2S_5 - S_1S_4}{S_2S_3 - S_1S_5}\right) C_3S_1 - C_3S_2}{\left(\frac{S_2S_5 - S_1S_4}{S_2S_3 - S_1S_5}\right)^2 C_3^2 S_3 - 2\left(\frac{S_2S_5 - S_1S_4}{S_2S_3 - S_1S_5}\right)C_3^2 S_5 - C_3^2 S_4}\right] \qquad (X35)$$

$$\varepsilon = \frac{1}{C_1C_3\sigma^6 f(n)}\left[\frac{\left(\frac{S_2S_5 - S_1S_4}{S_2S_3 - S_1S_5}\right)S_1 - S_2}{\left(\frac{S_2S_5 - S_1S_4}{S_2S_3 - S_1S_5}\right) S_3 - 2\left(\frac{S_2S_5 - S_1S_4}{S_2S_3 - S_1S_5}\right)S_5 - S_4}\right] \qquad (X36)$$

which determines ε .

Summarizing*:

One Parameter Fit (1PF)-- σ and ε fixed

$$\sum_i \left\{\mu_i^2 - C_1\varepsilon\sigma^6 f(n)\left[\frac{\sigma^{n-6}\, C_2^n}{(n-2)(n-3)}\,(x_i^{n-2} - 1) - C_3(x_i^4 - 1)\right]\right\}\left\{\frac{\sigma^{n-6}\, C_2^n}{(n-2)(n-3)}\left[x_i^{n-2}\ln x_i + \right.\right.$$

$$\left.(\ln C_2\sigma - \frac{2n-5}{(n-2)(n-3)})(x_i^{n-2} - 1)\right] - \frac{1}{6}\,\frac{\ln(\frac{n}{6})}{(\frac{n}{6} - 1)^2}\left[\frac{\sigma^{n-6}\, C_2^n}{(n-2)(n-3)}\,(x_i^{n-2} - 1)\right.$$

$$\left.\left. - C_3(x_1^4 - 1)\right]\right\} = 0 \qquad (X7)$$

which fixes n .

Two Parameter Fit (2PF)-- ε fixed

---

*C_1, C_2 and C_3 are given by Equations (136), S_1, S_2, S_3, S_4 and S_5 are given by Equations (X11) - (X15), and $f(n)$ is given by Equation (71).

$$\sigma = \left\{ \frac{\sigma^{n-6}\left[\left(\frac{n}{6}\right)\frac{C_2^n S_1}{(n-2)(n-3)}\right] + \sigma^n\left[\left(\frac{n}{6}+1\right)\frac{C_1\varepsilon\, f(n) C_2^n C_3 S_5}{(n-2)(n-3)}\right] - \sigma^6[C_1\varepsilon\, f(n) C_3^2 S_4] - C_3 S_2}{\left(\frac{n}{6}\right)\frac{C_1\varepsilon\, f(n)\, C_2^{2n} S_3}{(n-2)^2\,(n-3)^2}} \right\}^{\frac{1}{2n-6}} \qquad \text{(X17)}$$

which iteratively fixes σ for given values of n. Equation (X17), along with Equation (X7) fix σ and n.

Two Parameter Fit (2PF)-- σ fixed

$$\varepsilon = \frac{1}{C_1\sigma^6 f(n)}\left[\frac{\frac{\sigma^{n-6}C_2^n}{(n-2)(n-3)} S_1 - C_3 S_2}{\left(\frac{\sigma^{n-6}C_2^n}{(n-2)(n-3)}\right)^2 S_3 - 2\frac{\sigma^{n-6}C_2^n C_3}{(n-2)(n-3)} S_5 + C_3^2 S_4}\right] \qquad \text{(X20)}$$

which fixes ε. This value and Equation (X7) fix n.

Three Parameter Fit (3PF)--no parameters fixed

$$\sigma = \left[\frac{(n-2)(n-3)C_3}{C_2^n}\left(\frac{S_2S_5 - S_1S_4}{S_2S_3 - S_1S_5}\right)\right]^{\frac{1}{n-6}} \qquad \text{(X34)}$$

$$\varepsilon = \frac{1}{C_1C_3\sigma^6 f(n)}\left[\frac{\left(\frac{S_2S_5 - S_1S_4}{S_2S_3 - S_1S_5}\right) S_1 - S_2}{\left(\frac{S_2S_5 - S_1S_4}{S_2S_3 - S_1S_5}\right)^2 S_3 - 2\left(\frac{S_2S_5 - S_1S_4}{S_2S_3 - S_1S_5}\right) S_5 - S_4}\right] \qquad \text{(X36)}$$

which fix σ and ε. These values and Equation (X7) fix n.

Appendix Y

Demonstration of Additional Root of Equation (135)

Equation (135) is:

$$\mu^2 = \frac{4}{2^s}\left(\frac{N\pi\varepsilon}{m}\right)\frac{\left(\frac{n}{6}\right)^{\frac{n}{n-6}}}{\left(\frac{n}{6}-1\right)}\left[\frac{\sigma^n}{(n-2)(n-3)}\left(\frac{2^s\rho_o N}{M}\right)^{n/3}(x^{n-2}-1)\right] - \frac{\sigma^6}{12}\left(\frac{2^s\rho_o N}{M}\right)^2(x^4-1) \qquad (135)$$

Expansion gives (noting Equation (71)):

$$\mu^2 = \left[\frac{4}{2^s}\left(\frac{N\pi\varepsilon}{M}\right) f(n) \frac{\sigma^n}{(n-2)(n-3)}\left(\frac{2^s\rho_o N}{M}\right)^{n/3}\right](x^{n-2}-1) - \left[\frac{4}{2^s}\left(\frac{N\pi\varepsilon}{M}\right) f(n) \frac{\sigma^6}{12}\left(\frac{2^s\rho_o N}{M}\right)^2\right](x^4-1) \qquad (Y1)$$

Clearly, if the second term is ever greater than the first, for some value of x (sufficiently small but > 1), $\mu^2 < 0$ and there will be two roots to Equation (135); the other root occurs at $x = 1$. This is seen in Figure 28. The additional root occurs at $x = X_R$.

An evaluation of the relative magnitude of the two terms in Equation (135) can be made by considering their ratio. This may be written:

$$R = \frac{\cancel{\frac{4}{2^s}\left(\frac{N\pi\varepsilon}{M}\right) f(n)} \frac{\sigma^6}{12}\left(\frac{2^s\rho_o N}{M}\right)^2(x^4-1)}{\cancel{\frac{4}{2^s}\left(\frac{N\pi\varepsilon}{M}\right) f(n)} \frac{\sigma^n}{(n-2)(n-3)}\left(\frac{2^s\rho_o N}{M}\right)^{n/3}(x^{n-2}-1)} \qquad (Y2)$$

or:

$$R = \frac{(n-2)(n-3)}{2} \frac{\left[\sigma\left(\frac{2^s \rho_o N}{M}\right)^{1/3}\right]^6 (x^4 - 1)}{\left[\sigma\left(\frac{2^s \rho_o N}{M}\right)^{1/3}\right]^n (x^{n-2} - 1)} \tag{Y3}$$

$$R = \frac{(n-2)(n-3)}{12} \frac{1}{\left[\sigma\left(\frac{2^s \rho_o N}{M}\right)^{1/3}\right]^{n-6} \left[\frac{x^{n-2} - 1}{x^4 - 1}\right]} \tag{Y4}$$

Letting

$$\delta = \sigma\left(\frac{2^s \rho_o N}{M}\right)^{1/3} \tag{Y5}$$

this may be written:

$$R = \left[\frac{(n-2)(n-3)}{12}\right] \Big/ \left[\delta^{n-6}\right] \left[\frac{x^{n-2} - 1}{x^4 - 1}\right] \tag{Y6}$$

Clearly when $R > 1$ the second root at X_R occurs.

Although the second factor in the denominator of Equation (Y6) increases with x (for any $n > 6$) and will eventually assure that $R < 1$, it is necessary to determine if $R > 1$ for <u>any</u> value of x. Therefore, consider the value of x giving the smallest value of the factor and thus the largest value of R. Let:

$$f(x) = \frac{x^{n-2} - 1}{x^4 - 1} \tag{Y7}$$

Since $1 \leq x \leq \infty$:

$$\lim_{x \to 1} f(x) = \lim_{x \to 1} \frac{x^{n-2} - 1}{x^4 - 1} \Rightarrow \frac{0}{0} \tag{Y8}$$

Using L'Hôspital's rule:

$$\lim_{x \to 1} f(x) = \lim_{x \to 1} \frac{(n-2)x^{n-3}}{4x^3} = \left(\frac{n-2}{4}\right) \tag{Y9}$$

Also:

$$\lim_{x \to \infty} f(x) = \lim_{x \to \infty} \frac{x^{n-2} - 1}{x^4 - 1} = \infty \tag{Y10}$$

If $f(x)$ increases monotonically with an increase in x :

$$\frac{df(x)}{dx} > 0 \tag{Y11}$$

From Equation (Y7):

$$\frac{df(x)}{dx} = \frac{(x^4 - 1)(n-2)\, x^{n-3} - (x^{n-2} - 1)\, 4x^3}{(x^4 - 1)^2} \tag{Y12}$$

Equation (Y11) is satisfied if:

$$(x^4 - 1)(n-2)x^{n-3} > (x^{n-2} - 1)4x^4 \tag{Y13}$$

Multiplying both sides by x and rearranging gives:

$$\frac{1}{4} \frac{x^4 - 1}{x^4} > \frac{1}{n-2} \frac{x^{n-2} - 1}{x^{n-2}} \tag{Y14}$$

Since $n > 6$, $n-2 > 4$ and Equation (Y14) will be satisfied if:

$$\frac{d\left[\frac{1}{n-2}\,\frac{x^{n-2}-1}{x^{n-2}}\right]}{dn} < 0 \qquad \text{(Y15)}$$

This becomes:

$$\frac{(n-2)x^{n-2}\,x^{n-2}\,\ell n\,x - (x^{n-2}-1)[(n-2)x^{n-2}\,\ell n\,x + x^{n-2}]}{(n-2)^2\,x^{2(n-2)}} < 0 \qquad \text{(Y16)}$$

or:

$$x^{n-2}\,\ell n\,x^{n-2} - (x^{n-2}-1)(\ell n\,x^{n-2}+1) < 0 \qquad \text{(Y17)}$$

$$x^{n-2}\,\ell n\,x^{n-2} - x^{n-2}\,\ell n\,x^{n-2} - x^{n-2} + \ell n\,x^{n-2} + 1 < 0 \qquad \text{(Y18)}$$

$$x^{n-2} - 1 > \ell n\,x^{n-2} \qquad \text{(Y19)}$$

or:

$$e^{x^{n-2}} - 1 > x^{n-2} \qquad \text{(Y20)}$$

Expanding the left-hand side in a Taylor series[127] gives:

$$1 + (x^{n-2} - 1) + \text{Rem} > x^{n-2} \qquad \text{(Y21)}$$

$$x^{n-2} + \text{Rem} > x^{n-2} \qquad \text{(Y22)}$$

which satisfies the condition. Therefore Equation (Y15) is satisfied and thus Equations (Y14) and (Y11) are satisfied. Clearly $f(x)$ increases monotonically with x ; the minimum value is given by Equation (Y9) (where $x \to 1$):

$$[f(x)]_{min} = \frac{n-2}{4} \qquad \text{(Y23)}$$

Using Equation (Y23) in Equation (Y6) gives:

$$R = \left[\frac{(n-2)(n-3)}{12}\right] \Big/ \left[\delta^{n-6}\right]\left[\frac{n-2}{4}\right] \tag{Y24}$$

or:

$$R = \left[\frac{n-3}{3}\right] \Big/ \left[\delta^{n-6}\right] \tag{Y25}$$

The numerator of Equation (Y25) increases monotonically with n for all $n > 6$. The smallest value is given by:

$$\lim_{n \to 6} \frac{(n-3)}{3} = 1 \tag{Y26}$$

The denominator of Equation (Y25) increases (decreases) monotonically with n for all $n > 6$ if $\delta > 1$ ($\delta < 1$) . The smallest (largest) value is given by:

$$\lim_{n \to 6} \delta^{n-6} = 1 \tag{Y27}$$

independent of δ .

Therefore from Equations (Y26) and (Y27) the starting value for R in Equation (Y25) is unity and when $\delta \leq 1$ the numerator increases with n while the denominator decreases or remains constant. Clearly, $R > 1$ for all $n > 6$ in this instance and the second root exists.

When $\delta > 1$ the starting value of R is still unity but both numerator and denominator increase with n . The relative magnitude of each is determined directly from Equation (Y25) assuming δ is known.

Initially the greater of the numerator or denominator will be determined by their rates of change with n at $n = 6$. These are

determined from:

$$\frac{d[\text{numerator}]}{dn} = \frac{d[\frac{n-3}{3}]}{dn} = \frac{1}{3} \tag{Y28}$$

$$\frac{d[\text{denominator}]}{dn} = \frac{d[\delta^{n-6}]}{dn} = \delta^{n-6} \ln \delta \tag{Y29}$$

and :

$$\left[\frac{d[\text{numerator}]}{dn}\right]_{n=6} = \frac{1}{3} \tag{Y30}$$

$$\left[\frac{d[\text{denominator}]}{dn}\right]_{n=6} = \ln \delta \tag{Y31}$$

The numerator will therefore exceed the denominator (in the neighborhood of $n = 6$) when:

$$\ln \delta < \frac{1}{3} \tag{Y32}$$

$$\delta < e^{1/3} \tag{Y33}$$

$$\delta < 1.40 \tag{Y34}$$

This condition is satisfied for all the liquids considered in this study* and $R > 1$ initially.

In the limit of large n the behavior of Equation (Y25) may be determined from:

$$\lim_{n \to \infty} R = \lim_{n \to \infty} [\frac{n-3}{3}] \Big/ [\delta^{n-6}] \Rightarrow \frac{\infty}{\infty} \tag{Y35}$$

---

*See Table Y1. For A-II and H_2 $\delta \leq 1$ and the second root must exist.

assuming $\delta > 1$. Using L'Hôspital's rule:

$$\lim_{n \to \infty} R = \lim_{n \to \infty} \left[\frac{1}{3}\right] \Big/ \left[\delta^{n-6} \ln\delta\right] \tag{Y36}$$

or:

$$\lim_{n \to \infty} R = 0 \tag{Y37}$$

Clearly, in all cases $R < 1$ eventually.

The value of n (denoted n_1) at which R crosses from < 1 to > 1 can be found from Equation (Y25) by setting $R = 1$. This gives:

$$1 = \left[\frac{n_1 - 3}{3}\right] \Big/ \left[\delta^{n_1-6}\right] \tag{Y38}$$

Since the numerator is larger initially, it will stay larger longer (i.e., for higher values of n) for smaller values of $\delta(> 1)$. That is, the denominator will increase least rapidly with n for the smallest value of $\delta(>1)$ and will therefore catch up to the numerator at the highest values of n . Conversely the largest value of δ will cause the denominator to increase most rapidly with n and will equal the denominator at the lowest value of n . Values of δ for all the liquids considered in this study are shown in Table Y1. The corresponding values of n_1 from a solution of (a rearrangement of) Equation (Y38) are also shown. Clearly, $R > 1$ (i.e., there is a second root) for:

$$6 < n < n_1 \tag{Y39}$$

Table Y1

DETERMINATION OF $\sigma(2^s\rho_o N/M)^{1/3}$ FOR LIQUIDS

Substance	$(2^s\rho_o N/M) \times 10^{24}$-cm^{-3}	$\sim(2^s\rho_o N/M)^{1/3}$-Å^{-1}	σ^*-Å	$\delta = \sigma(2^s\rho_o N/M)^{1/3}$	n_1^{**}
A	0.04237	0.349	3.28	1.14	> 12.0
A-II	0.02771	0.303	3.28	0.994	> 12.0
A-III	0.02961	0.309	3.28	1.01	> 12.0
A-IV	0.03429	0.325	3.28	1.07	> 12.0
Hg	0.08124	0.433	2.86(2.88)	1.24(1.25)	9.8(9.4)
N_2	0.03474	0.326	3.73	1.22	10.8
H_2	0.04236	0.349	2.87	1.00	> 12.0
CS_2	0.01985	0.271	4.438	1.20	12.0
CCl_4	0.01246	0.232	5.77	1.34	6.85
CH_3OH	0.02977	0.310	3.666	1.14	> 12.0
C_2H_5OH	0.02051	0.274	4.370	1.20	12.0
$(C_2H_5)_2O$	0.01152	0.226	5.539	1.25	9.4
C_6H_{14}	0.00941	0.211	5.916	1.25	9.4
C_6H_6	0.01357	0.239	5.270	1.26	9.0
$C_6H_5CH_3$	0.01147	0.226	5.932	1.34	6.85
H_2O	0.06680	0.406	2.725	1.11	> 12.0

*From Table 14: two values of σ are given for Hg.

**Approximate solution to: $((n_1-3)/3)^{1/(n_1-6)} = \delta$.

The resultant values of n determined for all the liquids are shown in Table 14. Since in all but three instances the C results for $C_6H_5CH_3$ and the C and L results for Hg*, $n < n_1$, Equation (Y39) is satisfied and the second root at X_R must occur.

The demonstration of the additional root of Equation (135) was carried out assuming $n > 6$ which was the case for all the liquids considered in Table 14. A similar analysis for $n = 6$, $3 < n < 6$, $n = 3$, $2 < n < 3$, $n = 2$ and $0 \leq n < 2$ was performed and it was shown that for $n = 6$ and $3 < n < 6$, $R > 1$ for all n if $\delta < e^{1/3}$ (see Equation (Y33)) and therefore that the second root must exist. Since Equation (135) has a singularity at $n = 3$ the existence of a second root in this instance is academic. For $2 < n < 3$, $n = 2$ and $0 \leq n < 2$ it was shown that the second root cannot exist.

Note 1: Additional Roots of Equations (108) and (122)

Equation (108) is:

$$\mu^2 = U_o^2 \left(\frac{2}{n-6}\right)\left[\frac{x^{n-2} - 1}{n-2} - \frac{x^4 - 1}{4}\right] \tag{108}$$

To determine if the first term exceeds the second, consider the function:

$$f(m) = \frac{x^m - 1}{m} \tag{Y40}$$

If $f(m)$ is monotonically increasing with an increase in m, then:

$$\frac{df(m)}{dm} > 0 \tag{Y41}$$

---

*Indeed in these cases the computed value of $X_R = 1.000$ (see Table 14).

For Equation (40):

$$\frac{df(m)}{dm} = \frac{mx^m \ln x - (x^m - 1)}{m^2} = \frac{x^m \ln x^m - (x^m - 1)}{m^2} \qquad (Y42)$$

and Equation (Y41) will be satisfied if:

$$x^m \ln x^m > (x^m - 1) \qquad (Y43)$$

$$\ln x^m > \frac{x^m - 1}{x^m} \qquad (Y44)$$

From Equation (I18) it is clear that:

$$\ln x^m = \frac{x^m - 1}{x^m} + \text{Remainder} \qquad (Y45)$$

and therefore that Equation (Y44) is valid for all $x > 1$. Clearly, f(m) (Equation (Y40)) increases (decreases) with an increase (decrease) of m.

When $n > 6$, $n - 2 > 4$ and:

$$\frac{x^{n-2} - 1}{n - 2} > \frac{x^4 - 1}{4} \qquad (Y46)$$

for all $x > 1$. Therefore $\mu^2 > 0$ and no second root exists.

When $2 < n < 6$, Equation (108) should more properly be written:

$$\mu^2 = U_o^2 \left(\frac{2}{6 - n}\right) \left[\frac{x^4 - 1}{4} - \frac{x^{n-2} - 1}{n - 2} \right] \qquad (Y47)$$

Since in this case $4 > n - 2$, it is clear from Equations (Y40) - (Y45) that:

$$\frac{x^4 - 1}{4} > \frac{x^{n-2} - 1}{n - 2} \qquad (Y48)$$

for all $x > 1$. Therefore $\mu^2 > 0$ and no second root exists.

When $n = 2$ Equation (108) becomes:

$$\mu^2 = U_o^2 \lim_{n \to 2} \left(\frac{2}{n-6}\right)\left[\frac{x^{n-2} - 1}{n-2} - \frac{x^4 - 1}{4}\right] \tag{Y49}$$

or:

$$\mu^2 = U_o^2\left(\frac{1}{2}\right)\left[\frac{x^4 - 1}{4} - \lim_{n \to 2} \frac{x^{n-2} - 1}{n-2}\right] \tag{Y50}$$

Since:

$$\lim_{n \to 2} \frac{x^{n-2} - 1}{n-2} \Rightarrow \frac{0}{0} \tag{Y51}$$

L'Hôspital's rule may be used to give:

$$\lim_{n \to 2} \frac{x^{n-2} - 1}{n-2} = \lim_{n \to 2} \frac{x^{n-2} \ln x}{1} = \ln x \tag{Y52}$$

and Equation (Y50) becomes:

$$\mu^2 = \frac{1}{2} U_o^2\left[\frac{x^4 - 1}{4} - \ln x\right] \tag{Y53}$$

which may be written:

$$\mu^2 = \frac{1}{8} U_o^2 \left[(x^4 - 1) - \ln x^4\right] \tag{Y54}$$

In this case $\mu^2 > 0$ if:

$$x^4 - 1 > \ln x^4 \tag{Y55}$$

or:

$$e^{x^4 - 1} > e^{\ln x^4} = x^4 \tag{Y56}$$

Expanding the left-hand side in a Taylor series[127] gives:

$$x + (x^4 - 1) + \text{Rem.} > x^4 \tag{Y57}$$

$$x^4 + \text{Rem} > x^4 \tag{Y58}$$

Since Equation (Y55) is satisfied, $\mu^2 > 0$ for all $x > 1$ and no second root exists.

When $0 \leq n < 2$, Equation (108) should be written:

$$\mu^2 = U_o^2 \left(\frac{2}{6-n}\right)\left[\frac{x^4 - 1}{4} - \frac{1 - \frac{1}{x^{2-n}}}{2-n}\right] \tag{Y59}$$

or:

$$\mu^2 = U_o^2 \left(\frac{2}{6-n}\right)\left[\frac{x^4 - 1}{4} - \frac{1}{(2-n)}\left(\frac{x^{2-n} - 1}{x^{2-n}}\right)\right] \tag{Y60}$$

The condition for which $\mu^2 > 0$ is:

$$\frac{x^4 - 1}{4} > \frac{1}{(2-n)}\left(\frac{x^{2-n} - 1}{x^{2-n}}\right) \tag{Y61}$$

Since $x > 1$, $x^{2-n} > 1$ (since $2 - n > 0$) and Equation (Y61) is satisfied if:

$$\frac{x^4 - 1}{4} > \frac{x^{2-n} - 1}{2-n} \tag{Y62}$$

Since $4 > 2-n$ this is clearly valid from Equations (Y40) - (Y45). Therefore $\mu^2 > 0$ and no second root exists.

Therefore, for all $x > 1$, for any $n \geq 0$ (except $n = 6$), $\mu^2 > 0$ and Equation (108) has no additional roots.

Equation (122) is:

$$\mu^2 = \frac{1}{2} U_o^2 \left[x^4 \ln x - \frac{1}{4}(x^4 - 1)\right] \tag{122}$$

Clearly, $\mu^2 > 0$ if:

$$x^4 \ln x > \frac{1}{4}(x^4 - 1) \tag{Y63}$$

or:

$$\ln x^4 > \frac{x^4 - 1}{x^4} \tag{Y64}$$

Since this is generally valid (Equation (I18)), $\mu^2 > 0$ for all $x > 1$ and Equation (122) has no second root.

Appendix Z

Derivation of Equation (147)

Equation (95) or its equivalent, Equation (135), may be written in functional form as in Equation (96):

$$\mu^2 = \alpha(x^{n-2} - 1) - \beta(x^4 - 1) \tag{96}$$

where α and β are given by Equations (97) and (98). One root of Equation (96) occurs at $x = 1$, another at $x = X_R$. In the latter case the above becomes ($\mu^2 = 0$):

$$0 = \alpha(X_R^{n-2} - 1) - \beta(X_R^4 - 1) \tag{Z1}$$

Rearranging gives:

$$X_R^{n-2} - \alpha - \beta X_R^4 + \beta = 0 \tag{Z2}$$

$$X_R^{n-2} - \frac{\beta}{\alpha} X_R^4 + (\frac{\beta}{\alpha} - 1) = 0 \tag{Z3}$$

which is a transcendental equation in X_R (if n is non-integer), which must be solved by an iterative technique. For the Newton-Raphson method, the recursion relation is given by[166]:

$$X_{R_{i+1}} = X_{R_i} - \frac{f(X_{R_i})}{f'(X_{R_i})} \tag{Z4}$$

where $f(X_{R_i})$ is found from Equation (Z3):

$$f(X_{R_i}) = X_{R_i}^{n-2} - \frac{\beta}{\alpha} X_{R_i}^4 + (\frac{\beta}{\alpha} - 1) \tag{Z5}$$

and:

$$f'(X_{R_i}) = \frac{df(X_{R_i})}{dX_{R_i}} \tag{Z6}$$

From Equation (Z5):

$$f'(X_{R_i}) = (n-2)\, X_{R_i}^{n-3} - 4\,\frac{\beta}{\alpha}\, X_{R_i}^{3} \tag{Z7}$$

Substituting Equations (Z5) and (Z7) into Equation (Z4) gives:

$$X_{R_{i+1}} = X_{R_i} - \frac{X_{R_i}^{n-2} - \frac{\beta}{\alpha} X_{R_i}^{4} + (\frac{\beta}{\alpha} - 1)}{(n-2)X_{R_i}^{n-3} - 4\,\frac{\beta}{\alpha}\, X_{R_i}^{3}} \tag{147}$$

which is Equation (147).

Note 1: X_R when $n = 6$

When $n = 6$, Equation (95) becomes Equation (114). This may be written as in Equation (115):

$$\mu^2 = \alpha' x^4 \ln x + \beta'(x^4 - 1) \tag{115}$$

where α' and β' are given by Equations (116) and (117). Again, one root of Equation (115) occurs at $x = 1$, another at $x = X_R$. In the latter case the above becomes ($\mu^2 = 0$):

$$0 = \alpha' X_R^4 \ln X_R + \beta'(X_R^4 - 1) \tag{Z8}$$

Rearrangement gives:

$$X_R^4 \ln X_R + \frac{\beta'}{\alpha'} (X_R^4 - 1) = 0 \qquad (Z9)$$

which is a transcendental equation in X_R. Using the Newton-Raphson method (Equation (Z4)):

$$f(X_{R_i}) = X_{R_i}^4 \ln X_{R_i} + \frac{\beta'}{\alpha'} (X_{R_i}^4 - 1) \qquad (Z10)$$

and:

$$f'(X_{R_i}) = X_{R_i}^4 \cdot \frac{1}{X_{R_i}} + 4X_{R_i}^3 \ln x_{R_i} + 4 \frac{\beta'}{\alpha'} X_{R_i}^3 \qquad (Z11)$$

or:

$$f'(X_{R_i}) = X_{R_i}^3 (1 + 4 \ln X_{R_i} + \frac{\beta'}{\alpha'}) \qquad (Z12)$$

Substituting Equations (Z10) and (Z12) into Equation (Z4) gives:

$$X_{R_{i+1}} = X_{R_i} - \frac{X_{R_i}^4 \ln X_{R_i} + \frac{\beta'}{\alpha'} (X_{R_i}^4 - 1)}{X_{R_i}^3 (1 + 4 \ln X_{R_i} + \frac{\beta'}{\alpha'})} \qquad (Z13)$$

which is the recursion relation for X_R when $n = 6$. From Equations (116) and (117):

$$\frac{\beta'}{\alpha'} = \ln \sigma(\frac{2^s \rho_o N}{M})^{1/3} - \frac{7}{12} \qquad (Z14)$$

Appendix AA

Removal of Singularities

Equation (149) is:

$$U^2 = U_o^2 \left(\frac{2}{n-6}\right) \left(\frac{x}{x-1}\right)^2 \left[\frac{x^{n-2} - 1}{n-2} - \frac{x^4 - 1}{4}\right] \tag{149}$$

Letting:

$$f(x) = \frac{x^{n-2} - 1}{n-2} - \frac{x^4 - 1}{4} \tag{AA1}$$

the Taylor series expansion (with remainder) around $x = 1$ is given by[127]:

$$f(x) = f(1) + \frac{(x-1)}{1!} f'(1) + \frac{(x-1)^2}{2!} f''(1) + \cdots + \frac{(x-1)^m}{m!} f^m(1) + R_{m+1} \tag{AA2}$$

where:

$$R_{m+1} = \frac{f^{m+1}[1 + \theta(x-1)]}{(m+1)!} (x-1)^{m+1}, \quad 0 < \theta < 1 \tag{AA3}$$

From Equation (AA1):

$$f(x) = \frac{x^{n-2} - 1}{n-2} - \frac{x^4 - 1}{4} \quad , \quad f(1) = 0 \tag{AA4}$$

$$f'(x) = x^{n-3} - x^3 \quad , \quad f'(1) = 0 \tag{AA5}$$

$$f''(x) = (n-3)x^{n-4} - 3x^2 \quad , \quad f''(1) = (n-3) - 3 = n - 6 \tag{AA6}$$

$$f'''(x) = (n-3)(n-4)x^{n-5} - 6x \quad , \quad f'''(1) = (n-3)(n-4) - 6 = n^2 - 7x + 6 = (n-6)(n-1) \tag{AA7}$$

$$f^{iv}(x) = (n-3)(n-4)(n-5)x^{n-6} - 6 \quad , \quad f^{iv}(1) = (n-3)(n-4)(n-5) - 6$$
$$= (n-6)(n^2 - 6n + 11) \qquad \text{(AA8)}$$

$$f^{v}(x) = (n-3)(n-4)(n-5)(n-6)x^{n-7} \quad , \quad f^{v}(1) = (n-3)(n-4)(n-5)(n-6) \qquad \text{(AA9)}$$

$$f^{vi}(x) = (n-3)(n-4)(n-5)(n-6)(n-7)x^{n-8}, \quad f^{vi}(1) = (n-3)(n-4)(n-5)(n-6)(n-7) \qquad \text{(AA10)}$$

$$\vdots \qquad\qquad \vdots$$

$$f^{n}(x) = \underbrace{(n-3)(n-4)\cdots(n-m-1)}_{m-1 \text{ terms}} x^{n-m-2} \quad , \quad f^{m}(1) = \underbrace{(n-3)(n-4)\cdots(n-m-1)}_{m-1 \text{ terms}} \qquad \text{(AA11)}$$

$$\vdots$$

$$f^{m+1}(x) = \underbrace{(n-3)(n-4)\cdots(n-m-1)(n-m-2)}_{m \text{ terms}} x^{n-m-3} \qquad \text{(AA12)}$$

Substituting Equations (AA4) - (AA11) into Equation (AA2) gives:

$$f(x) = 0 + 0 + \frac{(x-1)^2}{1}\frac{(n-6)}{2} + \frac{(x-1)^3}{1}\frac{(n-6)}{2}\frac{(n-1)}{3}$$
$$+ \frac{(x-1)^4}{1}\frac{(n-6)}{2}\frac{(n^2-6n+11)}{12} + \frac{(x-1)^5}{1}\frac{(n-6)}{2}\frac{(n-5)}{3}\frac{(n-4)}{4}\frac{(n-3)}{5}$$
$$+ \frac{(x-1)^6}{1}\frac{(n-6)}{2}\frac{(n-5)}{3}\frac{(n-4)}{4}\frac{(n-3)}{5}\frac{(n-7)}{6}$$
$$+ \frac{(x-1)^7}{1}\frac{(n-6)}{2}\frac{(n-5)}{3}\frac{(n-4)}{4}\frac{(n-3)}{5}\frac{(n-7)}{6}\frac{(n-8)}{7}$$
$$+ \frac{(x-1)^8}{1}\frac{(n-6)}{2}\frac{(n-5)}{3}\frac{(n-4)}{4}\frac{(n-3)}{5}\frac{(n-7)}{6}\frac{(n-8)}{7}\frac{(n-9)}{8}$$
$$+ \cdots + \frac{(x-1)^m}{1}\frac{(n-6)}{2}\frac{(n-5)}{3}\frac{(n-4)}{4}\frac{(n-3)}{5}\frac{(n-7)}{6}\frac{(n-8)}{7}\cdots\frac{(n-m-1)}{m} + R_{m+1} \qquad \text{(AA13)}$$

which may be written:

$$f(x) = \frac{(n-6)}{2}(x-1)^2\left[1+(x-1)\frac{(n-1)}{3}+(x-1)^2\frac{(n^2-6n+11)}{12}\right.$$

$$+(x-1)^3\frac{(n-5)}{3}\frac{(n-4)}{4}\frac{(n-3)}{5}+(x-1)^4\frac{(n-5)}{3}\frac{(n-4)}{4}\frac{(n-3)}{5}\frac{(n-7)}{6}$$

$$+(x-1)^5\frac{(n-5)}{3}\frac{(n-4)}{4}\frac{(n-3)}{5}\frac{(n-7)}{6}\frac{(n-8)}{7}$$

$$+(x-1)^6\frac{(n-5)}{3}\frac{(n-4)}{4}\frac{(n-3)}{5}\frac{(n-7)}{6}\frac{(n-8)}{7}\frac{(n-9)}{8}+\cdots$$

$$+(x-1)^{m-2}\frac{(n-5)}{3}\frac{(n-4)}{4}\frac{(n-3)}{5}\frac{(n-7)}{6}\frac{(n-8)}{7}\frac{(n-9)}{8}\cdots\frac{(n-m-1)}{m}$$

$$\left.+R_{m+1}\frac{2}{(n-6)}\frac{1}{(x-1)^2}\right] \qquad \text{(AA14)}$$

or:

$$f(x) = \left(\frac{n-6}{2}\right)(x-1)^2\left[1+(x-1)\left(\frac{n-1}{3}\right)+(x-1)^2\left(\frac{n^2-6n+11}{12}\right)\right.$$

$$+\left(\frac{n-3}{3}\right)\left(\frac{n-4}{4}\right)\left(\frac{n-5}{5}\right)(x-1)^3\left\{1+\left(\frac{n-7}{6}\right)(x-1)+\left(\frac{n-7}{6}\right)\left(\frac{n-8}{7}\right)(x-1)^2\right.$$

$$\left.\left.+\left(\frac{n-7}{6}\right)\left(\frac{n-8}{7}\right)\left(\frac{n-9}{8}\right)(x-1)^3+\cdots+\left(\frac{n-7}{6}\right)\left(\frac{n-8}{7}\right)\left(\frac{n-9}{8}\right)\cdots\left(\frac{n-m-1}{m}\right)(x-1)^{m-5}\right\}\right.$$

$$\left.+\left(\frac{2}{n-6}\right)\frac{1}{(x-1)^2}R_{m+1}\right] \qquad \text{(AA15)}$$

The remainder term can be written, noting Equations (AA3) and (AA12):

$$\text{Rem.} = \left(\frac{2}{n-6}\right)\frac{1}{(x-1)^2}\frac{\overbrace{(n-3)(n-4)\cdots(n-m-1)(n-m-2)}^{m \text{ terms}}}{(m+1)!}(1+\theta(x-1))^{n-m-3}(x-1)^{m+1} \qquad \text{(AA16)}$$

where $0 < \theta < 1$. This can be written:

$$\text{Rem} = \left[\frac{(n-3)}{1}\frac{(n-4)}{2}\frac{(n-5)}{3}\frac{(n-6)}{4}\right]\left[\frac{(n-7)}{5}\frac{(n-8)}{6}\cdots\frac{(n-2-(m-1)}{m-1}\frac{(n-2-m)}{m}\right]$$

$$\times \frac{[1+\theta(x-1)]^{n-4-(m-1)}}{(m+1)}(x-1)^{m-1}\frac{2}{n-6} \qquad \text{(AA17)}$$

or:

$$\text{Rem} = \left[\frac{(n-2)-1}{1}\right]\left[\frac{(n-2)-2}{2}\right]\left[\frac{(n-2)-3}{3}\right]\cdot\left[\frac{(n-2)-5}{5}\right]\left[\frac{(n-2)-6}{6}\right]\cdots$$

$$\left[\frac{(n-2)-(m-1)}{(m-1)}\right]\left[\frac{(n-2)-m}{m}\right]\frac{[1+\theta(x-1)]^{n-4}}{2(m+1)}\left[\frac{x-1}{1+\theta(x-1)}\right]^{m-1} \qquad \text{(AA18)}$$

If $n > 2$, $n-2 > 0$ and letting

$$k = n-2 \qquad \text{(AA19)}$$

Equation (AA18) may be written:

$$\text{Rem} = \left[\left(\frac{k-1}{1}\right)\left(\frac{k-2}{2}\right)\left(\frac{k-3}{3}\right)\right]\left[\left(\frac{k-5}{5}\right)\left(\frac{k-6}{6}\right)\cdots\left(\frac{k-m-1}{m-1}\right)\left(\frac{k-m}{m}\right)\right]\left[\frac{[1+\theta(x-1)]^{k-2}}{2(m+1)}\right]$$

$$\times \left[\frac{1}{\frac{1}{x-1}+\theta}\right]^{m-1} \qquad \text{(AA20)}$$

When $m > k$ the coefficient terms will become negative for all further values of m; Rem will alternate sign for each additional term. For any given m the sign will be determined by the number of terms past the one where $m > k$. Equation (AA20) may be written:

$$\text{Rem} = \pm\left[\left(\frac{1-k}{1}\right)\left(\frac{2-k}{2}\right)\left(\frac{3-k}{3}\right)\right]\left[\left(\frac{5-k}{5}\right)\left(\frac{6-k}{6}\right)\cdots\left(\frac{m-1-k}{m-1}\right)\left(\frac{m-k}{m}\right)\right]\left[\frac{[1+\theta(x-1)]^{k-2}}{2(m+1)}\right]$$

$$\times \left[\frac{1}{\frac{1}{x-1}+\theta}\right]^{m-1} \qquad \text{(AA21)}$$

For the series (Equation (AA15)) to converge:

$$\lim_{m \to \infty} \text{Rem} = 0 \tag{AA22}$$

This will be satisfied if at least one of the (four) factors $\to 0$ as $m \to \infty$ and none of the rest increase without limit.

For a given value of $k(> 0)$ the first factor will be constant. The second factor will also approach a constant since:

$$\lim_{m \to \infty} \left(\frac{m-k}{m}\right) = \lim_{m \to \infty} \left(\frac{1 - \frac{k}{m}}{1}\right) = 1 \tag{AA23}$$

Since, for a given value of x and k, the third factor has a constant numerator, it $\to 0$ as $m \to \infty$. The fourth factor will not increase without limit (in fact it will $\to 0$) if:

$$\frac{1}{x - 1} + \theta > 1 \tag{AA24}$$

This may be written:

$$\frac{1}{x - 1} > 1 - \theta \tag{AA25}$$

which is the condition for convergence. If $\frac{1}{x - 1} > 1$ then, clearly, $\frac{1}{x - 1} > 1 - \theta$ and Equation (AA25) may (conservatively) be written ($\theta = 0$):

$$\frac{1}{x - 1} > 1 \tag{AA26}$$

or:

$$1 > x - 1 \tag{AA27}$$

$$x < 2 \tag{AA28}$$

Since, by definition:

$$x \geq 1 \tag{AA29}$$

the range of convergence of Equation (AA15) is:

$$1 \leq x < 2 \tag{AA30}$$

Noting the conservative value of θ (i.e., $\theta = 0$), Equation (AA21) becomes:

$$\text{Rem} = \pm \left[\left(\frac{1-k}{1}\right)\left(\frac{2-k}{2}\right)\left(\frac{3-k}{3}\right)\right]\left[\left(\frac{5-k}{5}\right)\left(\frac{6-k}{6}\right)\cdots\left(\frac{m-1-k}{m-1}\right)\left(\frac{m-k}{m}\right)\right]\frac{[x-1]^{m-1}}{2(m+1)} \tag{AA31}$$

To determine the value of m that gives an arbitrarily small value of Rem, consider the (reasonable) values of k and x that will maximize Rem. Letting $n_{max} = 15.5$, ($k_{max} = 13.5$) and $x_{max} = 1.95$ ($x_{max}-1 = 0.95$), Equation (AA31) becomes (ignoring the negative signs in the first two factors):

$$\text{Rem} = \pm \left[\left(\frac{12.5}{1}\right)\left(\frac{11.5}{2}\right)\left(\frac{10.5}{3}\right)\right]\left[\left(\frac{8.5}{5}\right)\left(\frac{7.5}{6}\right)\left(\frac{6.5}{7}\right)\cdots\left(\frac{1.5}{12}\right)\left(\frac{0.5}{13}\right)\left(\frac{0.5}{14}\right)\left(\frac{1.5}{15}\right)\right.$$
$$\left.\cdots\left(\frac{m-13.5}{m}\right)\right]\frac{(0.95)^{m-1}}{2(m+1)} \tag{AA32}$$

For various values of m :

m	± Rem
12	0.0371
13	0.00126
14	0.00004
15	0.000002
16	0.0000003

To get accuracy to 5 decimal places (in $f(x)$; see Equation (AA1)), choose $m = 15$. Therefore Equation (AA15), neglecting the remainder

term becomes:

$$f(x) = \left(\frac{n-6}{2}\right)(x-1)^2\left[1 + (x-1)\left(\frac{n-1}{3}\right) + (x-1)^2\left(\frac{n^2-6n+11}{12}\right)\right.$$
$$+ \left(\frac{n-3}{3}\right)\left(\frac{n-4}{4}\right)\left(\frac{n-5}{5}\right)(x-1)^3\left\{1 + \left(\frac{n-7}{6}\right)(x-1) + \left(\frac{n-7}{6}\right)\left(\frac{n-8}{7}\right)(x-1)^2 + \cdots\right.$$
$$\left.\left. + \left(\frac{n-7}{6}\right)\left(\frac{n-8}{7}\right)\cdots\left(\frac{n-16}{15}\right)(x-1)^{10}\right\}\right] , \qquad 1 \le x < 2 \qquad \text{(AA33)}$$

which by repeated factoring may be written:

$$f(x) = \left(\frac{n-6}{2}\right)(x-1)^2\left[1 + (x-1)\left(\frac{n-1}{3}\right) + (x-1)^2\left(\frac{n^2-6n+11}{12}\right)\right.$$
$$+ \left(\frac{n-3}{3}\right)\left(\frac{n-4}{4}\right)\left(\frac{n-5}{5}\right)(x-1)^3$$
$$\left.\times\left\{1 + \left(\frac{n-7}{6}\right)(x-1)\left(1 + \left(\frac{n-8}{7}\right)(x-1)\cdots\left(1 + \left(\frac{n-16}{15}\right)(x-1)\right)\right)\right\}\right] ,$$
$$1 \le x < 2 \qquad \text{(AA34)}$$

Substitution into Equation (149), noting Equation (AA1) gives:

$$U^2 = U_o^2 x^2\left[1 + (x-1)\left(\frac{n-1}{3}\right) + (x-1)^2\left(\frac{n^2-6n+11}{12}\right) + \left(\frac{n-3}{3}\right)\left(\frac{n-4}{4}\right)\left(\frac{n-5}{5}\right)(x-1)^3\right.$$
$$\left.\times\left\{1 + \left(\frac{n-7}{6}\right)(x-1)\left(1 + \left(\frac{n-8}{7}\right)(x-1)\cdots\left(1 + \left(\frac{n-16}{15}\right)(x-1)\right)\right)\right\}\right] ,$$
$$1 \le x < 2 \qquad \text{(AA35)}$$

It should be noted that both singularities at $x = 1$ (see Equation (149)) have been removed* (which was desired) and the computation of U can be made using a (convergent) series expansion. Defining:

$$U^2 = U_o^2\, f(x,n) \quad , \qquad 1 \le x < 2 \qquad (151)$$

---

*As has the one at $n = 6$.

$f(x,n)$ can be written, using Equation (AA35), as:

$$f(x,n) = x^2\left[1+\left(\frac{n-1}{3}\right)(x-1)+\left(\frac{n^2-6n+11}{12}\right)(x-1)^2+\left(\frac{n-3}{3}\right)\left(\frac{n-4}{4}\right)\left(\frac{n-5}{5}\right)(x-1)^3\right.$$

$$\left.\times\left\{1+\left(\frac{n-7}{6}\right)(x-1)\left(1+\left(\frac{n-8}{7}\right)(x-1)\cdots\left(1+\left(\frac{n-16}{15}\right)(x-1)\right)\right)\right\}\right] \quad (152)$$

which is Equation (152). For $x \geq 2$, Equation (149) is used.

As indicated prior to Equation (AA19) the evaluation of Rem assumes that $n > 2$ $(k > 0)$. When $0 \leq n < 2$ $(-2 \leq k \leq 0)$, Rem can be evaluated as follows. From Equation (AA21):

$$\text{Rem} = \pm\left[\left(\frac{1-k}{1}\right)\left(\frac{2-k}{2}\right)\left(\frac{3-k}{3}\right)\right]\left[\left(\frac{5-k}{5}\right)\left(\frac{6-k}{6}\right)\cdots\left(\frac{m-1-k}{m-1}\right)\left(\frac{m-k}{m}\right)\right]$$

$$\times\left[\frac{[1+\theta(x-1)^{k-2}]}{2(m+1)}\right]\left[\frac{1}{\frac{1}{x-1}+\theta}\right]^{m-1} \quad (AA21)$$

When $k < 0$ the numerator of each factor will be $> k$ (in the prior case when $k > 0$, the numerator was always $< k$) and a larger value of m is required for an equal value of Rem for the interval $1 \leq x < 2$. Another approach is to consider the same values of m and Rem and restrict the range of x over which the expansion is made.

As before, the most conservative estimate of Rem in Equation (AA21) occurs when $\theta = 0$. This gives:

$$\text{Rem} = \pm\left[\left(\frac{1-k}{1}\right)\left(\frac{2-k}{2}\right)\left(\frac{3-k}{3}\right)\right]\left[\left(\frac{5-k}{5}\right)\left(\frac{6-k}{6}\right)\cdots\left(\frac{m-1-k}{m-1}\right)\left(\frac{m-k}{m}\right)\right]\frac{(x-1)^{m-1}}{2(m+1)} \quad (AA36)$$

Assuming Rem $\leq \pm 0.000002$, $m = 15$ (as before) this may be written:

$$\pm\ 0.000002 \geq \pm\left[\left(\frac{1-k}{1}\right)\left(\frac{2-k}{2}\right)\left(\frac{3-k}{3}\right)\right]\left[\left(\frac{5-k}{5}\right)\left(\frac{6-k}{6}\right)\cdots\left(\frac{14-k}{14}\right)\left(\frac{15-k}{15}\right)\right]\frac{(x-1)^{14}}{32} \quad \text{(AA37)}$$

Consider the extreme values of k for the interval of interest $(-2 \leq k \leq 0)$. When $k = 0$:

$$0.000002 \geq [(1)(1)(1)][(1)(1)\cdots(1)(1)]\ \frac{(x-1)^4}{32} \quad \text{(AA38)}$$

$$(x-1)^4 \leq 32(0.000002) \quad \text{(AA39)}$$

or:

$$x \leq 1.50 \quad \text{(AA40)}$$

When $k = -2$:

$$0.000002 \geq \left[\left(\frac{3}{1}\right)\left(\frac{4}{2}\right)\left(\frac{5}{3}\right)\right]\left[\left(\frac{7}{5}\right)\left(\frac{8}{6}\right)\left(\frac{9}{7}\right)\left(\frac{10}{8}\right)\left(\frac{11}{9}\right)\left(\frac{12}{10}\right)\left(\frac{13}{11}\right)\left(\frac{14}{12}\right)\left(\frac{15}{13}\right)\left(\frac{16}{14}\right)\left(\frac{17}{15}\right)\right] \times \frac{(x-1)^4}{32} \quad \text{(AA41)}$$

$$(x-1)^4 \leq \frac{6}{17}\ (0.000002) \quad \text{(AA42)}$$

or:

$$x \leq 1.36 \quad \text{(AA43)}$$

Since Rem is monotonically decreasing with a decrease in k, it is clear that the latter case (i.e., $k = -2$, $n = 0$) is most conservative. That is, five decimal place accuracy can be obtained with Equation (AA33) if the interval is restricted to $1 \leq x \leq 1.36$. Therefore, Equations (151) and (152) apply with equal accuracy when $0 \leq n \leq 2$ if $1 \leq x \leq 1.36$. For $x > 1.36$, Equation (149) is used.

Equation (150) is:

$$U^2 = U_o^2 \frac{1}{2} \left(\frac{x}{x-1}\right)^2 \left[x^4 \ln x - \frac{x^4 - 1}{4}\right] \tag{150}$$

Letting:

$$f(x) = x^4 \ln x - \frac{x^4 - 1}{4} \tag{AA44}$$

the Taylor series expansion (with remainder) around $x = 1$ is given by Equation (AA2). The remainder term is given by Equation (AA3). From Equation (AA44):

$$f(x) = x^4 \ln x - \frac{x^4 - 1}{4} \quad , f(1) = 0 \tag{AA45}$$

$$f'(x) = x^4 \frac{1}{x} + 4x^3 \ln x - x^3 = 4x^3 \ln x \quad , f'(1) = 0 \tag{AA46}$$

$$f''(x) = 4x^3 \frac{1}{x} + 12x^2 \ln x = 4x^2 + 12x^2 \ln x \quad , f''(1) = 4 \tag{AA47}$$

$$f'''(x) = 8x + 12x^2 \frac{1}{x} + 24x \ln x$$

$$= 20x + 24x \ln x \quad , f'''(1) = 20 \tag{AA48}$$

$$f^{iv}(x) = 20 + 24x \frac{1}{x} + 24 \ln x = 44 + 24 \ln x \quad , f^{iv}(1) = 44 \tag{AA49}$$

$$f^{v}(x) = 24 \frac{1}{x} = 24x^{-1} \quad , f^{v}(1) = 24 \tag{AA50}$$

$$f^{vi}(x) = (24)(-1)x^{-2} \quad , f^{vi}(1) = -24 \tag{AA51}$$

$$f^{vii}(x) = (24)(-1)(-2)x^{-3} \quad , f^{vii}(1) = (24)(2) \tag{AA52}$$

$$\vdots \qquad\qquad \vdots$$

$$f^{m}(x) = (24)(-1)^{m+1}(m-5)!x^{-(m-4)} \quad , f^{m}(x) = (24)(-1)^{m+1}(m-5)! \tag{AA53}$$

$$f^{m+1}(x) = (24)(-1)^{m+2}(m-4)!x^{-(m-3)} \tag{AA54}$$

Substituting Equations (AA45) - (AA53) into Equation (AA2) gives:

$$f(x) = 0+0+\frac{(x-1)^2}{2!}(4)+\frac{(x-1)^3}{3!}(20)+\frac{(x-1)^4}{4!}(44)+\frac{(x-1)^5}{5!}(24)-\frac{(x-1)^6}{6!}(24)$$

$$+\frac{(x-1)^7}{7!}(24)(2)+\cdots+\frac{(x-1)^m}{m!}(24)(-1)^{m+1}\ (m-5)!+R_{m+1} \qquad \text{(AA55)}$$

or:

$$f(x) = 2(x-1)^2\ [1+\frac{5}{3}(x-1)+\frac{11}{12}(x-1)^2+12(x-1)^3\{\frac{0!}{5!}-\frac{1!}{6!}(x-1)$$

$$+\frac{2!}{7!}(x-1)^2-\frac{3!}{8!}(x-1)^3+\cdots+(-1)^{m+1}\frac{(m-5)!}{m!}(x-1)^{m-5}\}+\frac{1}{2(x-1)^2}R_{m+1}] \qquad \text{(AA56)}$$

which may be written:

$$f(x) = 2(x-1)^2[1+\frac{5}{3}(x-1)+\frac{11}{12}(x-1)^2+\frac{12(x-1)^3}{5!}\{\frac{0!5!}{5!}-\frac{1!5!}{6}(x-1)$$

$$+\frac{2!5!}{7!}(x-1)^2-\frac{3!5!}{8!}(x-1)^3+\cdots+(-1)^{m+1}\frac{(m-5)!5!}{m!}(x-1)^{m-5}$$

$$+\frac{5!}{24(x-1)^5}R_{m+1}\}] \qquad \text{(AA57)}$$

The remainder term can be written, noting Equation (AA3) and (AA54):

$$\text{Rem} = \frac{5!}{\cancel{24}(x-1)^5}\ \cancel{(24)}(-1)^{m+2}\ (m-4)!\ \frac{[1+\theta(x-1)]^{-(m-3)}}{(m+1)!}(x-1)^{m+1} \qquad \text{(AA58)}$$

where $0 < \theta < 1$. This can be written:

$$\text{Rem} = 120(-1)^{m+2}\frac{(m-4)!}{(m+1)!}\frac{(x-1)^{m-4}}{[1+\theta(x-1)]^{m-3}} = [\frac{120(-1)^{m+2}}{(x-1)}][\frac{(m-4)!}{(m+1)!}]$$

$$\times\ [\frac{1}{\frac{1}{x-1}+\theta}]^{m-3} \qquad \text{(AA59)}$$

Noting that $(-1)^{m+2}$ alternates the sign of Rem and:

$$(m+1)! = (m+1)(m)(m-1)(m-2)(m-3)(m-4)! \tag{AA60}$$

this becomes:

$$\text{Rem} = \pm \left[\frac{120}{(x-1)}\right] \left[\frac{1}{(m+1)(m)(m-1)(m-2)(m-3)}\right]\left[\frac{1}{\frac{1}{x-1}+\theta}\right]^{m-3} \tag{AA61}$$

For the series to converge, Equation (AA22) must be satisfied; at least one of the factors must $\to 0$ as $m \to \infty$ while none of the rest increase without limit.

For a given value of $x(> 1)$ the first factor is constant. The second factor will clearly $\to 0$ as $m \to \infty$. The third factor will not increase without limit if:

$$\frac{1}{x-1} + \theta > 1 \tag{AA62}$$

which is the same as Equation (AA24). This leads to (following Equations (AA25) - (AA29)) the range of convergence* of Equation (AA57):

$$1 \leq x < 2 \tag{AA63}$$

Noting the conservative value of θ (i.e., $\theta = 0$), Equation (AA61) becomes:

---

*The apparent singularity in Equation (AA61) at $x = 1$ is removed when Rem is substituted into Equation (AA57) and multiplied by the coefficient of the inner bracketed term,

$$\frac{12(x-1)^3}{5!}$$

$$\text{Rem} = \pm \left[\frac{120}{(m+1)(m)(m-1)(m-2)(m-3)}\right][x-1]^{m-4} \qquad \text{(AA64)}$$

To determine the value of m that gives an arbitrarily small value of Rem, consider $x_{max} = 1.95$ ($x_{max} - 1 = 0.95$). The above becomes:

$$\text{Rem} = \pm \left[\frac{120}{(m+1)(m)(m-1)(m-2)(m-3)}\right](0.95)^{m-4} \qquad \text{(AA65)}$$

For various values of m :

m	± Rem
10	0.00167
12	0.00052
16	0.000087
20	0.000022
24	0.0000067
25	0.0000052
26	0.0000040

To get 5 decimal place accuracy choose $m = 26$. Therefore, Equation (AA57), neglecting the remainder term, becomes:

$$f(x) = 2(x-1)^2\left[1 + \frac{5}{3}(x-1) + \frac{11}{12}(x-1)^2 + \frac{1}{10}(x-1)^3 \left\{\frac{0!5!}{6!} - \frac{1!5!}{6!}(x-1) + \frac{2!5!}{7!}(x-1)^2 - \frac{3!5!}{8!}(x-1)^3 + \cdots + (-1)^{27}\frac{21!5!}{26!}(x-1)^{21}\right\}\right], \quad 1 \le x < 2 \qquad \text{(AA66)}$$

Substitution into Equation (150), noting Equation (AA44) gives:

$$U^2 = U_o^2\, x^2 \left[1 + \frac{5}{3}(x-1) + \frac{11}{12}(x-1)^2 + \frac{1}{10}(x-1)^3 \left\{\frac{0!5!}{5!} - \frac{1!5!}{6!}(x-1)\right.\right.$$

$$\left.\left. + \frac{2!5!}{7!}(x-1)^3 + \cdots + (-1)^{27}\, \frac{21!5!}{26!}(x-1)^2 \right\}\right], \quad 0 \le x < 2 \qquad \text{(AA67)}$$

Both singularities at $x = 1$ (see Equation (150)) have been removed (which was desired) and the computation of U can be made using a (convergent) series expansion. Defining:

$$U^2 = U_o^2\, g(x) \quad , \qquad 1 \le x < 2 \qquad (154)$$

$g(x)$ can be written, using Equation (AA66) as:

$$g(x) = x^2 \left[1 + \frac{5}{3}(x-1) + \frac{11}{12}(x-1)^2 + \frac{1}{10}(x-1)^3 \left\{1 - \frac{1}{6}(x-1) + \frac{1}{21}(x-1)^2\right.\right.$$

$$- \frac{1}{56}(x-1)^3 + \frac{1}{126}(x-1)^4 - \frac{1}{252}(x-1)^5 + \frac{1}{462}(x-1)^6 - \frac{1}{792}(x-1)^7$$

$$+ \frac{1}{1287}(x-1)^8 - \frac{1}{2002}(x-1)^9 + \frac{1}{3003}(x-1)^{10} - \frac{1}{4368}(x-1)^{11} + \frac{1}{6188}(x-1)^{12}$$

$$- \frac{1}{8568}(x-1)^{13} + \frac{1}{11628}(x-1)^{14} + \frac{1}{15504}(x-1)^{15} + \frac{1}{20349}(x-1)^{16}$$

$$- \frac{1}{26334}(x-1)^{17} + \frac{1}{33649}(x-1)^{18} - \frac{1}{42504}(x-1)^{19} + \frac{1}{53130}(x-1)^{20}$$

$$\left.\left. - \frac{1}{65780}(x-1)^{21} \right\}\right]$$

or:

$$g(x) = x^2 \left[1 + \frac{5}{3}(x-1) + \frac{11}{12}(x-1)^2 + \frac{1}{10}(x-1)^3 \left\{1 + (x-1)\left(-\frac{1}{6} + (x-1)\left(\frac{1}{21}\right.\right.\right.\right.$$

$$+ (x-1)\left(-\frac{1}{56} + (x-1)\left(\frac{1}{126} + (x-1)\left(-\frac{1}{252} + (x-1)\left(\frac{1}{462} + (x-1)\left(-\frac{1}{792}\right.\right.\right.\right.\right.\right.$$

$$+ (x-1)\left(\frac{1}{1287} + (x-1)\left(-\frac{1}{2002} + (x-1)\left(\frac{1}{3003} + (x-1)\left(-\frac{1}{4368} + (x-1)\left(\frac{1}{6188}\right.\right.\right.\right.\right.\right.$$

$$+ (x-1)(-\frac{1}{8568}+(x-1)(\frac{1}{11628}+(x-1)(-\frac{1}{15504}+(x-1)(\frac{1}{20349}$$

$$+ (x-1)(-\frac{1}{26334}+(x-1)(\frac{1}{33649}+(x-1)(-\frac{1}{42504}+(x-1)(\frac{1}{53130}$$

$$+ (x-1)(-\frac{1}{65780}))))))))))))))))))))\} \;] \qquad (155)$$

which is Equation (155). For $x \geq 2$ Equation (150) is used.

PROPOSITION 1

OPTIMIZATION OF CHEMICAL REACTIONS

*****

The initial reactant composition and time of reaction that will maximize the yield of a given reaction in a multiple reaction system not at equilibrium, can be determined from a generalized rate expression using mathematical methods.

*****

INTRODUCTION

DeDonder and Van Lerberghe[1], Prigogine and Defay[2], Pings[3-7] and Lu[8] have considered the problem of finding the initial reactant mixture that will maximize the yield (or other desired result) of single or multiple reaction systems at equilibrium. Results have been obtained for a variety of situations and are usually expressed as the classic solution of stoichiometric ratios[1,2] plus other terms. This proposition is concerned with essentially the same problem for the non-equilibrium (i.e., kinetic) situation where the additional parameter, "time of reaction" is to be considered.

GENERALIZED RATE EXPRESSION

Consider the set of r chemical reactions:

$$\sum_{i=1}^{m_\rho} \nu_{i,\rho} A_{i,\rho} = 0 \quad , \qquad \rho = 1, 2, \cdots, r \qquad (1)$$

where $A_{i,\rho}$ is the chemical symbol for species i in reaction ρ, $\nu_{i,\rho}$ is the stoichiometric coefficient of component i in reaction ρ (taken as negative for reactants, positive for products and zero for non-participants) and m_ρ is the number of components in the ρth reaction. In general, the extent of reaction ξ_ρ is defined by[2]:

$$d\xi_\rho = \frac{d_\rho n_1}{\nu_{1,\rho}} = \frac{d_\rho n_2}{\nu_{2,\rho}} = \cdots = \frac{d_\rho n_i}{\nu_{i,\rho}} = \cdots = \frac{d_\rho n_{m_\rho}}{\nu_{m_\rho,\rho}} \quad , \quad \rho = 1, 2, \cdots, r \qquad (2)$$

where n_i is the symbol for the number of moles of component i at time t and the symbol $d_\rho n_i$ represents the change in the number of moles n_i of component i in the time dt, due to the ρth reaction. Adding the n_i for all reactions and integrating there is found from Equation (2):

$$n_i = n_i^o + \sum_{\rho=1}^{r} \nu_{i,\rho} \xi_\rho \qquad (3)$$

where n_i^o denotes the total initial moles of component i.

It is assumed that the reaction rate of each of the r reactions is expressible as the difference of two terms (exceptions are possible[9]) containing products of concentrations and rate constants. In this case, the most general form of the rate expression may, using Equations (2) and (3), be written:

$$\nu_{i,\rho} \frac{d\xi_\rho}{dt} = \frac{(n_i^o + \sum_{\rho=1}^{r} \nu_{i,\rho}\xi_\rho)}{V} \frac{dV}{dt} + \frac{k_{f\rho}}{V^{\alpha_\rho (m_\rho)-1}} \prod_{i=1}^{m_\rho} \left(n_i^o + \sum_{\rho=1}^{r} \nu_{i,\rho}\xi_\rho \right)^{\alpha_{i,\rho}} -$$

$$- \frac{k_{b\rho}}{V^{\alpha_\rho' (m_\rho)-1}} \prod_{i=1}^{m_\rho} \left(n_i^o + \sum_{\rho=1}^{r} \nu_{i,\rho}\xi_\rho \right)^{\alpha'_{i,\rho}} \quad , \quad \rho = 1, 2, \cdots, r \qquad (4)$$

where $k_{f\rho}$ and $k_{b\rho}$ are the forward and backward rate constants (both > 0) of the ρth reaction, $\alpha_{i,\rho}$ and $\alpha'_{i,\rho}$ are constants of the ρth reaction, V is the system volume and:

$$\alpha_\rho^{(m_\rho)} = \sum_{i=1}^{m_\rho} \alpha_{i,\rho} \quad \text{and} \quad \alpha_\rho'^{(m_\rho)} = \sum_{i=1}^{m_\rho} \alpha'_{i,\rho} \tag{5}$$

THERMODYNAMIC RESTRICTIONS ON THE GENERALIZED RATE EXPRESSION

Any set of chemical reactions will approach equilibrium given sufficient time (i.e., as $t \to \infty$). At equilibrium, by definition, $\frac{d\xi_\rho}{dt} = 0 = \frac{dV}{dt}$ and the ratio $k_{f\rho}/k_{b\rho}$ is related to the equilibrium constant K_ρ. These conditions, when substituted into Equation (4), lead to [10]:

$$V_e^{\alpha_\rho^{(m_\rho)} - \alpha_\rho'^{(m_\rho)}} \prod_{i=1}^{m_\rho} \left(n_i^o + \sum_{\rho=1}^{r} \nu_{i,\rho}\xi_{\rho e}\right)^{\alpha'_{i,\rho} - \alpha_{i,\rho}} = \phi_\rho \left[\prod_{i=1}^{m_\rho} f_{ie}^{\nu_{i,\rho}}\right], \quad \rho = 1, 2, \cdots, r \tag{6}$$

where the subscript e refers to equilibrium conditions, f_{ie} is the equilibrium fugacity of component i (a standard state of unit fugacity and pure material has been chosen) and ϕ_ρ is an unspecified function[10]. Equations (6) are r equations for each of the r reactions which, because of the thermodynamic nature of equilibrium, must be obeyed. These relations serve to restrict the unspecified parameters of the system $\alpha_{i,\rho}$ and $\alpha'_{i,\rho}$. As the nature of the ϕ_ρ are unknown the nature of the restrictions on these parameters cannot be generalized. However, in particular cases the ϕ_ρ can be reasonably assumed and more definitive relations for the $\alpha_{i,\rho}$ and $\alpha'_{i,\rho}$ determined.

Because the ϕ_ρ in Equations (6) are generally unspecified it should be noted that "the restrictions on the permissible form of

the kinetic equations are rather less stringent than it is often supposed"[9].

MAXIMIZATION PROCEDURE

The specific objective of this proposition is to determine the initial composition of reactants n_i^o and time of reaction (and any other necessary conditions) that will maximize a desired result with the restraints that the initial quantity of material remains constant and the rate expressions are obeyed. In this case the restraint relations are $\sum_{i=1}^{m} n_i^o = n^o$ (where m is the number of unique components) and the r (differential) rate equations; Equations (4). Any function:

$$g = g(n_i^o, \xi_\rho, V \text{ (or } P), T, t) \qquad (7)$$

can be the "desired result" to be maximized. Here T is added since $k_{f\rho}$ and $k_{b\rho}$ are functions of T. V and P are alternates since together with T, ξ_ρ and n_i^o one or the other is fixed through the equation of state of the system.

The problem of maximizing g with the restraints indicated is a classic problem that can be treated rigorously using Lagrange multipliers[11]. There are obtained $m + 2r + 4$ equations in $m + 2r + 4$ unknowns that can be solved simultaneously for the m n_i^o's, r ξ_ρ's, V (or P), T, t and the $(r + 1)$ multipliers. Substitution of these into Equation (7) yields the maximum (or minimum) of g[10].

Since this general solution gives r ξ_ρ's, V (or P) and T besides the primary desired quantities (i.e., the m n_i^o's and t), it is clear that these specific values are the "other necessary conditions" for a maximum, referred to earlier. When certain simplifications of the system are made, some or all of these conditions may be eliminated.

We consider the simple case:

$$g = \xi_x \tag{8}$$

where ξ_x is one of the reaction extents in Equation (7). This results in a substantial simplification of the maximization equations when the rate equations are considered as defining equations for the ξ_ρ instead of as restraint relations. This is equivalent to setting r Lagrangian multipliers equal to zero and eliminating all derivatives with respect to the ξ_ρ $(\rho \neq x)$ [10]. This yields the maximization equations:

$$\left.\begin{aligned} &\frac{\partial \xi_x}{\partial n_i^o} + \lambda_o = 0 \ , \ i = 1, 2, \cdots, m_x \\ &\frac{\partial \xi_x}{\partial V} \left(\text{or } \frac{\partial \xi_x}{\partial P} \right) = \frac{\partial \xi_x}{\partial T} = \frac{\partial \xi_x}{\partial t} = 0 \end{aligned}\right\} \tag{9}$$

where λ_o is a single Lagrangian multiplier. The initial moles restraint relation and Equations (9) represent m + 3 equations in m + 3 unknowns which may be simultaneously solved for the m n_i^o's, V (or P), T, t and λ_o. Substitution of these into the rate equation defining ξ_x gives an implicit relation for the maximum (or minimum) of ξ_x when the ξ_ρ $(\rho \neq x)$ are eliminated through simultaneous solution of the other rate equations (which gives the ξ_ρ $(\rho \neq x)$ in terms of ξ_x).

The "other necessary conditions" for a maximum in this case are the specific values of V (or P) and T found from the solutions of the initial moles restraint relation and Equations (9).

The following sample solutions illustrate the use of the maximization procedure for reactions proceeding for a fixed time under idealized conditions.* For a single reaction it is shown that the "classic solution" obtains[1,2], independent of reaction time. For two competitive reactions the solution contains the "classic solution" plus other terms that are dependent on reaction time. In both cases the solutions are shown to be compatible with the independently determined equilibrium solutions.

---

*To additionally determine the time of reaction that will maximize yield requires use of the last of Equations (9)[10].

SAMPLE SOLUTIONS

For the following examples we assume that the system is closed, there is no flow, a single phase is present, and the initial moles of all products is zero. Further, in each case, the conditions to be determined are the n_i^o to give a maximum in ξ_1, when the process involved is carried out with perfect gases under isothermal, isochoric conditions, for a fixed time.

Solution 1

Consider a single reaction (r = 1) occurring for a fixed time (t = constant) when the rate equations obey the "simplified standard form"(10).*

Thermodynamic Restrictions

For a perfect gas mixture:

$$f_i = p_i = x_i P = x_i nRT/V = (n_i/V)RT \tag{10}$$

where p_i is the partial pressure of the ith component, x_i is the mole fraction of the ith component and n is the total number of moles. Noting Equation (3), Equations (6) become (for r = 1 and equilibrium conditions):

$$V_e^{\alpha_1^{(m_1)} - \alpha_1'^{(m_1)}} \prod_{i=1}^{m_1} (n_i^o + \nu_i \xi_{1e})^{\alpha_i' - \alpha_i} = \phi_1 \left[RTV_e^{-\sum_{i=1}^{m_1} \nu_i} \prod_{i=1}^{m_1} (n_i^o + \nu_i \xi_{1e})^{\nu_i} \right] \tag{11}$$

*Defined as the case when the $\alpha_{i,\rho}$ for all products are zero in the forward reaction and the $\alpha'_{i,\rho}$ for all reactants are zero in the backward reaction; see Equations (4).

This equality will be satisfied for all possible values of $(n_i^o + \nu_i \xi_{1e})$ if:

$$\phi_1 = \left[V_e^{-\sum_{i=1}^{m_1} \nu_i} \prod_{i=1}^{m_1} (n_i^o + \nu_i \xi_{1e})^{\nu_i} \right]^s \tag{12}$$

where $s > 0$ [9] and if:

$$\alpha_i' - \alpha_i = s\nu_i, \; i = 1, 2, \cdots, m_1 \tag{13}$$

If the index i is so ordered that the species 1 through h_1 represent reactants and the species $(h_1 + 1)$ through m_1 represent products, the choice of the simplified standard form of the rate equations implies that:

$$\alpha_i' = 0, \; i = 1, 2, \cdots, h_1 \text{ and } \alpha_i = 0, \; i = h_1 + 1, h_1 + 2, \cdots, m_1 \tag{14}$$

and from Equation (13) that:

$$\alpha_i = -s\nu_i, \; i = 1, 2, \cdots, h_1 \text{ and } \alpha_i' = s\nu_i, \; i = h_1 + 1, h_1 + 2, \cdots, m_1 \tag{15}$$

Therefore from Equations (5), (14) and (15):

$$\alpha^{(m_1)} = -s\nu^{(h_1)}, \; \alpha'^{(m_1)} = s\left[\nu^{(m_1)} - \nu^{(h_1)}\right] \tag{16}$$

where:

$$\nu^{(m_1)} = \sum_{i=1}^{m_1} \nu_i, \; \nu^{(h_1)} = \sum_{i=1}^{h_1} \nu_i \tag{17}$$

Form of the Generalized Rate Expression

Considering a single reaction (r = 1), isochoric conditions (dV = 0), Equations (15) and (16), and the fact that $n_i^o = 0$ for products, Equations (4) become:

$$\nu_i \frac{d\xi_1}{dt} = \frac{k_{f1}}{V^{-s\nu^{(h_1)}-1}} \prod_{i=1}^{h_1} (n_i^o + \nu_i \xi_1)^{-s\nu_i}$$

$$- \frac{k_{b1}}{V^{s[\nu^{(m_1)}-\nu^{(h_1)}]-1}} \prod_{i=h_1+1}^{m_1} (\nu_i \xi_1)^{s\nu_i} \qquad (18)$$

The restraint relation is:

$$\sum_{i=1}^{h_1} n_i^o = n^o \qquad (19)$$

Optimization Equations

Considering that the function to be maximized is ξ_1, Equation (8) applies and $g = \xi_x = \xi_1$. Equations (9) then become (for isothermal, isochoric, fixed time conditions, noting Equation (19)):

$$\frac{\partial \xi_1}{\partial n_i^o} + \lambda_o = 0, \; i = 1, 2, \cdots, h_1 \qquad (20)$$

Solution

Equations (18) - (20) define the complete solution. Consider the reaction:

$$\nu_1 A_1 + \nu_2 A_2 \underset{k_{b1}}{\overset{k_{f1}}{\rightleftharpoons}} \nu_3 A_3 \qquad (21)$$

where A_3 is clearly the "desired" product. In this case $m_1 = 3$, $h_1 = 2$ and Equations (18) - (20) become:

$$\nu_3 \frac{d\xi_1}{dt} = \frac{k_{f1}}{V^{-s(\nu_1+\nu_2)-1}} (n_i^o + \nu_1\xi_1)^{-s\nu_1} (n_2^o + \nu_2\xi_1)^{-s\nu_2} - \frac{k_{b1}}{V^{s\nu_3-1}} (\nu_3\xi_1)^{s\nu_3} \tag{22}$$

$$n_1^o + n_2^o = n^o \tag{23}$$

$$\frac{\partial \xi_1}{\partial n_1^o} + \lambda_o = 0 \text{ and } \frac{\partial \xi_1}{\partial n_2^o} + \lambda_o = 0 \tag{24}$$

By taking the difference, in Equations (24) (to eliminate λ_o) and implicitly differentiating Equation (22) with respect to n_1^o and n_2^o, there is obtained upon combining these results:

$$\nu_1 n_2^o - \nu_2 n_1^o = 0 \tag{25}$$

Simultaneous solution with Equation (23) gives:

$$n_1^o = \frac{\nu_1}{\nu_1 + \nu_2} n^o \text{ and } n_2^o = \frac{\nu_2}{\nu_1 + \nu_2} n^o \tag{26}$$

which are the desired solutions. It is noteworthy that Equations (25) are independent of time t, extent of reaction ξ_1, s and the rate constants k_{f1} and k_{b1}. The maximum value of ξ_1 may be found by integrating Equation (22) and substituting the values of n_1^o and n_2^o from Equations (26).

Check on Solution

Since Equations (25) are independent of time t, they represent the solution for all time and thus also for the equilibrium case. This is the classic problem considered by DeDonder and Van Lerberghe[1] and Prigogine and Defay[2]. They showed that, for any number of reactants and products the maximum yield is obtained when:

$$n_i^o = \frac{|\nu_i|}{\sum_{i=1}^{h_1} |\nu_i|} n^o \qquad (27)$$

Equations (26) are certainly consistent with this result for the limited number of reactants and products considered and it is expected that Equations (27) would be obtained if Equations (20) were applied to Equation (18) and the result solved simultaneously with Equation (19).

Solution 2

Consider two competitive reactions (r = 2) occurring for a fixed time (t = constant) when the rate equations obey the "simplified standard form"[10].

Thermodynamic Restrictions

Since conditions for both reactions are identical to those in Solution 1, the same results (Equations (15) - (17)) are obtained for each reaction. That is:

$$\left.\begin{aligned} \alpha_{i,1} &= -s_1 \nu_{i1},\ i = 1, 2, \cdots, h_1 \qquad \text{and} \\ \alpha_{i,2} &= -s_2 \nu_{i2},\ i = 1, 2, \cdots, h_2 \\ \alpha'_{i,1} &= s_1 \nu_{i1},\ i = h_1 + 1, h_1 + 2, \cdots, m_1 \qquad \text{and} \\ \alpha'_{i,2} &= s_2 \nu_{i2},\ i = h_2 + 1, h_2 + 2, \cdots, m_2 \end{aligned}\right\} \quad (28)$$

where $s_1 > 0$, $s_2 > 0$.*

Therefore from these and Equation (5):

$$\left.\begin{aligned} \alpha_1^{(m_1)} &= -s_1 \nu_1^{(h_1)} \quad \text{and} \quad \alpha_2^{(m_2)} = -s_2 \nu_2^{(h_2)} \\ \alpha_1'^{(m_1)} &= s_1 \left[\nu_1^{(m_1)} - \nu_1^{(h_1)} \right] \quad \text{and} \quad \alpha_2'^{(m_2)} = s_2 \left[\nu_2^{(m_2)} - \nu_2^{(h_2)} \right] \end{aligned}\right\} \quad (29)$$

where:

$$\left.\begin{aligned} \nu_1^{(m_1)} &= \sum_{i=1}^{m_1} \nu_{i1},\ \nu_1^{(h_1)} = \sum_{i=1}^{h_1} \nu_{i1} \\ \nu_2^{(m_2)} &= \sum_{i=1}^{m_2} \nu_{i2},\ \nu_2^{(h_2)} = \sum_{i=1}^{h_2} \nu_{i2} \end{aligned}\right\} \quad (30)$$

and h_1 and h_2 and m_1 and m_2 are the number of reactants and products in reactions 1 and 2 respectively.

Form of the General Rate Expressions

Considering two reactions (r = 2), isochoric conditions (dV = 0), Equations (28) and (29), and the fact that $n_i^o = 0$ for products, Equations (4) become:

---

*A different s (such as defined in Equation (12)) might obtain for each reaction.

$$\nu_{i1}\frac{\partial \xi_1}{dt} = \frac{k_{f1}}{V^{-s\nu_1}} \prod_{i=1}^{h_1} (n_i^o + \nu_{i1}\xi_1 + \nu_{i2}\xi_2)^{-s_1\nu_{i1}}$$

$$- \frac{k_{b1}}{V^{s[\nu_1^{(m_1)} - \nu_1^{(h_1)}]-1}} \cdot \prod_{i=h_1+1}^{m_1} (\nu_{i1}\xi_1 + \nu_{i2}\xi_2)^{s_1\nu_{i1}} \qquad (31)$$

and:

$$\nu_{i2}\frac{\partial \xi_2}{dt} = \frac{k_{f2}}{V^{-s\nu_2-1}} \prod_{i=1}^{h_2} (n_i^o + \nu_{i1}\xi_1 + \nu_{i2}\xi_2)^{-s_2\nu_{i2}}$$

$$- \frac{k_{b2}}{V^{s[\nu_2^{(m_2)} - \nu_2^{(h_2)}]-1}} \cdot \prod_{i=h_2+1}^{m_2} (\nu_{i1}\xi_1 + \nu_{i2}\xi_2)^{s_2\nu_{i2}} \qquad (32)$$

where h_1 and h_2 have been so ordered that common reactants are considered first. The restraint relation becomes:

$$\sum_{i=1}^{h} n_i^o = n^o \qquad (33)$$

where h is either h_1 or h_2, whichever is the larger.

Optimization Equations

As conditions are again identical to those in Solution 1 (i.e., $g = \xi_x = \xi_1$), Equations (20) again apply.

Solution

Equations (20), (31) - (33) define the complete solution to the problem. Consider the competing reactions:

$$\nu_{11}A_1 + \nu_{21}A_2 \underset{k_{b1}}{\overset{k_{f1}}{\rightleftharpoons}} \nu_{31}A_3, \quad (\rho = 1) \tag{34}$$

$$\nu_{12}A_1 + \nu_{22}A_2 \underset{k_{b2}}{\overset{k_{f2}}{\rightleftharpoons}} \nu_{42}A_4, \quad (\rho = 2) \tag{35}$$

Since ξ_1 is to be maximized it is clear that compound A_3 is the "desired" product while A_4 is "undesirable." Now* $m_1 = 4$, $h_1 = 2$, $m_2 = 4$, $h_2 = 2$ and $h = h_1 = h_2 = 2$ and Equations (31) - (33) and (20) become:

$$\nu_{31}\frac{d\xi_1}{dt} = \frac{k_{f1}}{V^{-s_1[\nu_{11}+\nu_{21}]-1}}(n_1^o+\nu_{11}\xi_1+\nu_{12}\xi_2)^{-s_1\nu_{11}}(n_2^o+\nu_{21}\xi_1+\nu_{22}\xi_2)^{-s_1\nu_{21}}$$

$$- \frac{k_{b1}}{V^{s_1\nu_{31}-1}}(\nu_{31}\xi_1)^{s_1\nu_{31}} \tag{36}$$

*To allow consistent (sequential) and general use of the index i in Equations (31) and (32), A_3 and A_4 are considered products of reactions 1 and 2 respectively although, in this example, the associated coefficients $\nu_{32} = \nu_{41} = 0$. Thus, formally, $m_1 = m_2 = 4$ (not 3).

$$\nu_{42}\frac{d\xi_2}{dt}=\frac{k_{f2}}{V^{-s_2\left[\nu_{12}+\nu_{22}\right]-1}}\left(n_1^o+\nu_{11}\xi_1+\nu_{12}\xi_2\right)^{-s_2\nu_{12}}\left(n_2^o+\nu_{21}\xi_1+\nu_{22}\xi_2\right)^{s_2\nu_{22}}$$

$$-\frac{k_{b2}}{V^{s_2\nu_{42}-1}}\left(\nu_{42}\xi_2\right)^{s_2\nu_{42}} \tag{37}$$

and:

$$n_1^o + n_2^o = n^o \tag{38}$$

$$\frac{\partial\xi_1}{\partial n_1^o}+\lambda_o = 0 \text{ and } \frac{\partial\xi_1}{\partial n_2^o}+\lambda_o = 0 \tag{39}$$

By taking the difference of Equations (39) (to eliminate λ_o) and implicitly differentiating Equation (36) with respect to n_1^o and n_2^o there is obtained upon combining these results:

$$-\nu_{11}n_2^o+\nu_{21}n_1^o=\left(-\nu_{21}\nu_{12}+\nu_{11}\nu_{22}\right)\xi_2-\left[-\nu_{11}\nu_{12}\left(n_2^o+\nu_{21}\xi_1+\nu_{22}\xi_2\right)\right.$$

$$\left.-\nu_{21}\nu_{22}\left(n_1^o+\nu_{11}\xi_1+\nu_{12}\xi_2\right)\right]Q \tag{40}$$

where:

$$Q=\frac{\partial\xi_2}{\partial n_1^o}-\frac{\partial\xi_2}{\partial n_2^o} \tag{41}$$

Simultaneous solution of (40) with (38) gives:

$$n_1^o=\frac{\nu_{11}}{\nu_{11}+\nu_{21}}n^o-\left(\frac{\nu_{21}\nu_{12}-\nu_{11}\nu_{22}}{\nu_{11}+\nu_{21}}\right)\xi_2+\left[\frac{\nu_{11}\nu_{12}\left(n_2^o+\nu_{21}\xi_1+\nu_{22}\xi_2\right)}{\nu_{11}+\nu_{21}}\right.$$

$$\left.\frac{+\nu_{21}\nu_{22}\left(n_1^o+\nu_{11}\xi_1+\nu_{12}\xi_2\right)}{\nu_{11}+\nu_{21}}\right]Q \tag{42}$$

The solution is, as yet, incomplete since Q has not yet been evaluated. However, the other rate equation (i.e., Equation (37)) may be considered as the defining equation for ξ_2 and therefore used to find this quantity. Implicit differentiation of Equation (37) with respect to n_1^o and n_2^o and finding the difference in the results gives:

$$\frac{dQ}{dt} = \frac{s_2\, k_{f2}}{V^{-s_2\left[\nu_{12}+\nu_{22}\right]-1}} \frac{(n_1^o + \nu_{11}\xi_1 + \nu_{12}\xi_2)^{-s\nu_{12}-1}\,(n_2^o + \nu_{21}\xi_1 + \nu_{22}\xi_2)^{-s\nu_{12}-1}}{\nu_{42}}$$

$$\cdot\left[-\nu_{12}n_2^o + \nu_{22}n_1^o + (-\nu_{12}\nu_{21} + \nu_{22}\nu_{11})\,\xi_1 + \left\{-\nu_{12}^2(n_2^o + \nu_{21}\xi_1 + \nu_{22}\xi_2)\right.\right.$$

$$\left.\left. -\nu_{22}^2(n_1^o + \nu_{11}\xi_1 + \nu_{12}\xi_2)\right\} Q\right] - \frac{s_2\, k_{b2}}{V^{s_2\nu_{42}-1}}\,\nu_{42}\,(\nu_{42}\xi_2)^{s\nu_{42}-1}\,Q \qquad (43)$$

an ordinary differential equation in Q the solution of which gives this quantity for substitution into Equation (42). The constant of integration of Equation (43) can be evaluated by noting that when $t = 0$, $\xi_1 = \xi_2 = 0$ and from Equation (40):

$$Q_o = \frac{\nu_{21}n_1^o - \nu_{11}n_2^o}{\nu_{21}\nu_{22}n_1^o + \nu_{11}\nu_{12}n_2^o} \qquad (44)$$

Equation (42) is the desired solution with Q defined by Equations (43) and (44). It is noteworthy that the solution again gives the classic solution (for the first reaction) plus another term which depends on both reactions (i.e., on ξ_1 and ξ_2 (and therefore on the fixed time t), s, k_{f1} and k_{b1}, k_{f2} and k_{b2}). Further, since the correction terms

depend on n_1^o and n_2^o as well as ξ_1, ξ_2 and Q (which are functions of n_1^o and n_2^o through Equations (36), (37), and (43) respectively) the solutions obtained are clearly implicit. The numerical values of n_1^o and n_2^o must be determined by an iterative process (as must Q in Equation (43) since this is an implicit ordinary differential equation in Q) in which the maximum in ξ_1 is also found.

Check on Solution

The equilibrium solution to this problem has been determined independently[8] and may be compared to the present case in the following manner.

As $t \to \infty$, $d\xi_1/dt \to 0$, $d\xi_2/dt \to 0$ and Equations (36) and (37) yield the familiar equilibrium forms which define ξ_{1e} and ξ_{2e} in terms of n_1^o and n_2^o. From the definition of Q it is clear that $(dQ/dt)_e = 0$. Substitution of this into Equation (43) and simultaneous solution of the result with the equilibrium forms yields, after rearrangement:

$$Q_e = \frac{-\nu_{12}n_2^o+\nu_{22}n_1^o + (-\nu_{12}\nu_{21}+\nu_{22}\nu_{11})\xi_{1e}}{\nu_{42}^2(n_1^o+\nu_{11}\xi_{1e}+\nu_{12}\xi_{2e})(n_2^o+\nu_{21}\xi_{1e}+\nu_{22}\xi_{2e})(\nu_{42}\xi_{2e})^{-1}}$$

$$\frac{}{+\nu_{12}^2\ (n_2^o+\nu_{21}\xi_{1e}+\nu_{22}\xi_{2e})\ +\nu_{22}^2\ (n_1^o+\nu_{11}\xi_{1e}+\nu_{12}\xi_{2e})} \qquad (45)$$

which can be substituted into Equation (42) to give the equilibrium solution.

By careful comparison of this result with that of Lu[8], for the more general case, it can be shown[12] that they are identical.*

Another check on the general solution (Equation (42)) can be made by simply letting $\xi_2 = 0$ for all time (i.e., Solution 1). In this case $Q = 0$ and Equation (42) reduces directly to Equation (26). The solution is consistent with the less general, previously determined, case.

*It is noteworthy that, in this case, the general equilibrium solution does not yield the classic solution.

NOMENCLATURE

$A_{i,\rho}$ - chemical species i in reaction ρ

f_i - fugacity of component i

g - objective function

h_ρ - number of reactants in reaction ρ

K_ρ - equilibrium constant of reaction ρ

$k_{b\rho}$ - backward rate constant of reaction ρ

$k_{f\rho}$ - forward rate constant of reaction ρ

m - number of unique components

m_ρ - number of components in reaction ρ

n - total number of moles

n_i - number of moles of component i

p - pressure

p_i - partial pressure of component i

Q - Equation (41)

R - universal gas constant

r - number of chemical reactions

s - constant > 0 for reaction ρ

T - temperature

t - time

V - volume

x_i - mole fraction of component i

Greek

$\alpha_{i,\rho}$ - constant of reaction ρ

$\alpha'_{i,\rho}$ - constant of reaction ρ

$\alpha_{\rho}^{(m_\rho)}$ - Equation (5)

$\alpha'^{(m_\rho)}_{\rho}$ - Equation (5)

λ_o - Lagrangian multiplier

ϕ_ρ - unspecified function for reaction ρ

$\nu_{i,\rho}$ - stoichiometric coefficient of component i in reaction ρ

$\nu^{(m_\rho)}$ - Equation (17)

$\nu^{(h_\rho)}$ - Equation (17)

$\nu_{\rho}^{(m_\rho)}$ - Equation (30)

$\nu_{\rho}^{(h_\rho)}$ - Equation (30)

ξ_p - extent of reaction ρ

Subscripts

b - backward

e - equilibrium

f - forward

i - index for components

x - any value of ρ

ρ - index for reactions

Superscripts

o	-	initial state

Operators

d	-	differential
$\frac{d}{dt}$	-	time derivative
$\frac{\partial}{\partial}$	-	partial derivative
Π	-	product
Σ	-	summation

REFERENCES

1. Th. DeDonder and G. Van Lerbehge, Bull. Acad. Roy. Belg. (Cl. Sc.) 12, 151 (1926).

2. E. Prigogine, R. Defay and D. H. Everett, Chemical Thermodynamics (Longmans, Green and Co., London, 1954), p. 14.

3. C. J. Pings, Ind. Eng. Chem. Fundamentals 2, 244 (1963).

4. C. J. Pings, Ind. Eng. Chem. Fundamentals 2, 321 (1963).

5. C. J. Pings, Chem. Eng. Prog. 59, 90 (1963).

6. C. J. Pings, AIChE J. 10, 934 (1964).

7. C. J. Pings, Ind. Eng. Chem. Fundamentals 4, 260 (1965).

8. C. S. Lu, Doctoral Thesis, California Institute of Technology, Pasadena, California, 1967.

9. K. Denbigh, The Principles of Chemical Equilibrium (Cambridge at the University Press, London, 1963).

10. P. K. Salzman, Optimization of Chemical Reactions, Research Report, Chemical Engineering Laboratory, California Institute of Technology, Pasadena, California, December 1965.

11. P. Franklin, A Treatise on Advanced Calculus (John Wiley and Sons, Inc., New York, 1940), p. 353.

12. P. K. Salzman, Research Notebook 5055, Chemical Engineering Laboratory, California Institute of Technology, Pasadena, California, 1967, pp. 81-106.

PROPOSITION 2

DETERMINATION OF THE MAXIMUM TRANSMITTED SHOCK AT THE INTERFACE BETWEEN TWO CONDENSED MEDIA

*****

The maximum transmitted shock at the interface between two condensed media is incorrectly given by the "impedance-mismatch" approximation but may be estimated from the Hugoniot "reflection" method.

*****

Determination of the Maximum Transmitted Shock at the Interface between Two Condensed Media

P. K. SALZMAN*
Aerojet-General Corporation, Downey, Calif.

WHEN a shock wave is normally incident upon the interface between two media, two shock waves are formed. One is transmitted to the second medium while the other is reflected back into the original medium. The ratio of the transmitted shock pressure (P_t) to the incident shock pressure (P_i) is often computed[1-3] from the "impedance-mismatch" approximation

$$\frac{P_t}{P_i} \cong \frac{2\rho_t U_t}{\rho_t U_t + \rho_i U_i} \tag{1}$$

which is strictly valid only for acoustic waves. In Eq. (1) $\rho_t U_t$ and $\rho_i U_i$ are the shock impedances (density times shock velocity) of the transmitted and incident media, respectively. From Eq. (1), for $\rho_t U_t \gg \rho_i U_i$, it has been assumed that the maximum value of P_t/P_i is two. However, examination of the true "impedance-mismatch" relation

$$\frac{P_t}{P_i} = \frac{1 + (\rho_r U_r/\rho_i U_i)}{1 + (\rho_r U_r/\rho_t U_t)} \tag{2}$$

shows that if $\rho_t U_t \gg \rho_r U_r \gg \rho_i U_i$, (P_t/P_i) may be greater than two. Unfortunately, the maximum value of (P_t/P_i) cannot be deduced from Eq. (2).

Using the graphical Hugoniot "reflection" method[4-6] an estimate of $(P_t/P_i)_{max}$ may be made. In this method, the incident medium Hugoniot is plotted on the pressure-particle velocity (P-u) plane and reflected 180° around a vertical line drawn through the point of intersection of the incident pressure (P_i) and the incident medium Hugoniot. The transmitted pressure (P_t) is then determined by the intersection of this "reflected" Hugoniot with the Hugoniot of the acceptor material. Ideally, the maximum value of P_t for the given value of P_i will occur when the acceptor material has as its Hugoniot a vertical line at the origin (i.e., $\rho_t \to \infty$). This is visualized in Fig. 1. From symmetry, the "reflected" Hugoniot is seen to intersect the abscissa at $2u_i$.

In many cases, the incident medium Hugoniot may be written in quadratic form[2, 6, 8]:

$$P = au^2 + bu \tag{3}$$

where a and b are constants. Since the "reflected" Hugoniot is simply a reflection of Eq. (3), it may also be written in quadratic form. However, since the "reflected" Hugoniot does not pass through the origin it must be written more generally as

$$P_{reflected} = cu^2 + du + e \tag{4}$$

where c, d, and e are constants. The boundary conditions pertaining to Eqs. (3) and (4) can be used to relate c, d, and e to a and b. These conditions may be deduced from Fig. 1 and are: 1) when $u = 0$, $P_{reflected} = P$ at $(u = 2u_i)$; 2) when $u = u_i$, $P_{reflected} = P_i$; and 3) when $u = 2u_i$, $P_{reflected} = 0$. Applying these conditions gives

$$e = a(2u_i)^2 + b(2u_i) \tag{5}$$

$$c(u_i^2) + d(u_i) + e = a(u_i^2) + b(u_i) \tag{6}$$

$$c(2u_i)^2 + d(2u_i) + e = 0 \tag{7}$$

which are simultaneous equations in c, d, and e.

The solutions are

$$c = a \tag{8}$$

$$d = -4au_i - b \tag{9}$$

$$e = 4au_i^2 + 2bu_i \tag{10}$$

Substituting these into Eq. (4) and rearranging gives

$$P_{reflected} = a(2u_i - u)^2 + b(2u_i - u) \tag{11}$$

From the diagram it is clear that $P_{t\,max}$ is given by $P_{reflected}$ when $u = 0$. Thus

$$P_{t\,max} = 4au_i^2 + 2bu_i \tag{12}$$

Also, P_i is found from Eq. (3) when $u = u_i$, and thus

$$P_i = au_i^2 + bu_i \tag{13}$$

Forming the ratio of Eqs. (12) and (13) gives

$$\frac{P_{t\,max}}{P_i} = \frac{4au_i^2 + 2bu_i}{au_i^2 + bu_i} = \frac{4au_i + 2b}{au_i + b} \tag{14}$$

This represents the maximum value of P_t/P_i for a given value of u_i. However, it is desired to compute the maximum of P_t/P_i for *any* value of u_i. Since u_i can have any value on the abscissa, it may be replaced by u. Eq. (14) becomes

$$P_t/P_i = (4au + 2b)/(au + b) \tag{15}$$

The maximum value of this function is found by determining the derivative with respect to u and setting the resulting expression equal to zero; therefore,

$$\frac{d(P_t/P_i)}{du} = \frac{2ab}{(au + b)^2} = 0 \tag{16}$$

from which it may be deduced that as $u \to \infty$, $(P_t/P_i) \to$ maximum (the second derivative is negative). Therefore,

$$\left(\frac{P_t}{P_i}\right)_{max} = \lim_{u\to\infty}\left(\frac{4au + b}{au + b}\right) = \lim_{u\to\infty}\left(\frac{4a + (b/u)}{a + (b/u)}\right) = \frac{4a}{a} \tag{17}$$

or

$$(P_t/P_i)_{max} = 4 \tag{18}$$

It should be noted that this result depends directly on the fact that the Hugoniot of the incident medium (in this case Plexiglas) can be expressed as a quadratic in u. This in turn depends on the assumption (empirically supported)[2, 6, 8] that the U-u curve of the medium is linear. Because it is not known if this relation stays linear as u becomes very large, the result in Eq. (18) may be considered semiempirical in nature. However, if the "true" Hugoniot can be expressed in a polynomial of any degree, $(P_t/P_i)_{max}$ can always be found in a manner similar to that shown herein. For materials with a Hugoniot expressible as a cubic equation,[6] the fore-

Received July 22, 1963.

* Senior Research Engineer, Ordnance Division.

Reprinted from AIAA JOURNAL

Copyright, 1964, by the American Institute of Aeronautics and Astronautics, and reprinted by permission of the copyright owner

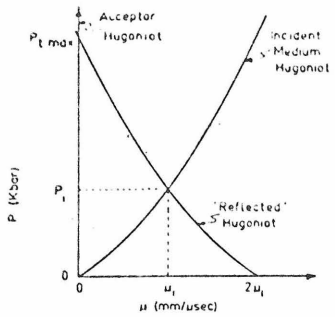

Fig. 1 Hugoniot "reflection" method.

mentioned approach gives $(P_t/P_i)_{max} = 8$. It should also be pointed out that the result also depends on the inherent accuracy of the Hugoniot "reflection" method itself.

In order to illustrate some of the foregoing remarks, (P_t/P_i) was computed for shock transmission from Plexiglas[9] to iron[10] and Plexiglas to platinum[10] using both the "impedance-mismatch" approximation [Eq.(1)] and the Hugoniot "reflection" method. The results are shown in columns 1–5 of Table 1. It is seen that Eq. (1) gives quite low values in this region and that the ratio can, as indicated, be greater than two at finite pressures in real materials. Columns 6 and 7 in Table 1 show the values of $(P_{t\,max}/P_i)$ as computed from Eq. (14) compared to the maximum value from Eq. (1). Clearly, increases in P_i give increases in $(P_{t\,max}/P_i)$, approaching the limiting value of 4 computed in Eq. (18).

Table 1 Comparison of values of (P_t/P_i) for shock transmission from Plexiglas to iron and platinum computed by the "impedance-mismatch" approximation and the Hugoniot "reflection" method

Plexiglas $\rho_t = 1.18$ g/cm³	Iron $\rho_t = 7.84$ g/cm³		Platinum $\rho_t = 21.37$ g/cm³		Ordinate $\rho_t \to \infty$	
P_i, kbar	$\left(\frac{P_t}{P_i}\right)^a$	$\left(\frac{P_t}{P_i}\right)^b$	$\left(\frac{P_t}{P_i}\right)^a$	$\left(\frac{P_t}{P_i}\right)^b$	$\left(\frac{P_t}{P_i}\right)^a$	$\left(\frac{P_{t\max}}{P_i}\right)^c$
102.7	1.70	2.14	1.86	2.61	2.00	3.13
162.4	1.66	2.12	1.83	2.56	2.00	3.25
235.0	1.65	2.11	1.83	2.60	2.00	3.35

[a] Computed from "impedance-mismatch" approximation, Eq. (1).
[b] Computed by Hugoniot "reflection" method.
[c] Computed from Eq. (14).

References

[1] Cook, M. A. and Udy, L. L., "Calibrations of the card-gap test," ARS J. 31, 52–57 (1961).

[2] Jaffe, I., Beauregard, R., and Amster, A., "Determination of the shock pressure required to initiate detonation of an acceptor in the shock sensitivity test," ARS J. 32, 22–25 (1962).

[3] Deal, W. E., "Measurement of Chapman-Jouget pressure for explosives," J. Chem. Phys. 27, 796–800 (1957).

[4] Price, D. and Jaffe, I., "Large scale gap-tests: interpretation of results for propellants," ARS J. 31, 595 (1961).

[5] Walsh, J. M. and Rice, M. H., "Dynamic compression of liquids from measurements on strong shock waves," J. Chem. Phys. 26, 815 (1957).

[6] Rice, M. H., McQueen, R. G., and Walsh, J. M., "Compression of solids by strong shock waves," *Solid State Physics*, edited by F. Seitz and D. Turnball (Academic Press Inc., New York, 1958), Vol. 6, pp. 1–63.

[7] Rice, M. H. and Walsh, J. M., "Equation of state of water to 250 kilobars," J. Chem. Phys. 26, 824 (1957).

[8] Al'tshuler, L. V., Kropnikov, K. K., and Brazhnik, M. I., "Dynamic compressibilities of metals under pressures from 400,000 to 4,000,000 atmospheres," Soviet Phys.—JETP 34(7), 614 (1958).

[9] Salzman, P. K., "Analysis of shock attenuation for 0.5 and 2.0 in. diameter card-gap sensitivity tests," ARS Preprint 2344-A-62 (January 1962).

[10] Walsh, J. M., Rice, M. H., McQueen, R. G., and Yarger, F. L., "Shock-wave compressions of twenty-seven metals. Equations of state of metals," Phys. Rev. 108, 196–216 (1957).

PROPOSITION 3

THE THEORY OF CRITICAL GEOMETRY

*****

The critical dimensions for steady detonation of a long uniform charge of any constant cross-sectional shape (i.e., the "critical geometry") may be determined from the critical diameter of the same material using geometric reasoning.

*****

The purpose of this proposition is to develop a geometric theory (called the "theory of critical geometry") that will predict the dimensions of a long, uniform non-cylindrical charge that will allow sustainment of detonation, as a function of the critical diameter of a cylindrical charge of the same material.

Consider a long uniform acceptor charge of any constant, cross-sectional shape.* It is assumed that regardless of shape, there are certain charge geometries that will support a unique steady-state detonation to infinite length. Further, for those geometries capable of supporting detonation, there is, at some distance from the point of initiation, a point at which the detonation characteristics will be independent of the mode of initiation (although this initiation must be strong enough to start detonation in the first place). For such geometries, the ability to support detonation becomes purely a property of the acceptor material without regard to the donor, and for a given acceptor material, becomes purely a property of acceptor.

---

*The following definitions are used when discussing the acceptor: shape = form of the cross-section (e.g., square, rectangle, circle, etc.). geometry = the size or magnitude of a given shape.

geometry. Therefore, sustainment of detonation can be analyzed as a function of acceptor geometry only.

The critical diameter of a particular material is known to depend on the relative energy gains and loses in the region of the detonation reaction zone[1,2,3,4]. The gains depend upon reaction zone length, which is a function of both the kinetics of the detonation reaction and the velocity of the detonation wave, while the losses depend solely on the rarefaction waves moving in from the lateral portions of the charge.

Therefore, in the case of a right-solid cylinder, the two factors affecting the distribution of energy gains and losses are: (a) detonation reaction zone length (i.e., kinetics and wave velocity) and (b) charge <u>diameter</u> (i.e., rarefaction waves).

In the general case, the critical dimensions of a given shape will also be dependent on the relative energy gains and losses in the region of the reaction zone. Again the gains will depend on the reaction zone length, and thus on the kinetics and wave velocity. Energy losses will be dependent solely on the lateral rarefaction waves, and thus on charge <u>shape</u>.

That is, in the general case, the two factors that affect the distribution of energy gains and losses are (a) detonation reaction zone length, and (b) charge <u>shape</u>.

Since the kinetics in the reaction zone are dependent only on the material properties and wave velocity, they will be the same for any shape at the same velocity. Thus energy gains will be affected by charge shape only insofar as the detonation velocity is affected.

If it is assumed that the detonation velocity is approximately the same for any shape at the critical dimensions of the shape, reaction zone length will be the same for every shape of the same material, energy gains will be the same, and the only factor affecting the energy balance (and thus the critical dimensions) will be charge geometry.

The "theory of critical geometry," when based on an extension of the critical diameter concept, may then be formulated on a purely geometrical basis, since the particular kinetics and wave velocity of the system are already accounted for in the critical diameter evaluation. Also, since charge composition, particle size, density, and temperature affect the reaction zone length (but not the rarefaction waves) the effect of changes in these quantities on critical geometry will be accounted for by their effect on critical diameter.

The theory is developed for a given material (i.e., unconfined, fixed composition, density, particle size, etc.) by finding a function, based on the parameters that describe the charge geometry, that can be made the critical criterion.

It is assumed that: (a) there is one critical criterion for any given shape, and (b) this same criterion holds for all shapes. Therefore, for criticality in any case, the parameters used must combine in such a way as to give the critical diameter d_c, for a solid cylinder, since criticality for the cylindrical case is specified in terms of only one parameter, namely the charge diameter.

In terms of energy gains and losses, the important features of charge geometry for any shape would be:

(a) Reactive volume (proportional to total energy output, and thus to energy gains).

(b) Surface area of reactive volume (proportional to losses by rarefaction waves).

For long, uniform charges of constant cross-section:

$$\text{Reactive volume} \propto (\text{cross-sectional area})(\text{reaction zone length}) \tag{1}$$

and:

$$\text{Surface area} \propto (\text{cross-sectional perimeter})(\text{reaction zone length}) \tag{2}$$

However, since it has been assumed that the reaction zone length is approximately constant for any shape, the pertinent parameters of charge shape are clearly cross-sectional area and cross-sectional perimeter. If these are the important features in determining the critical condition for detonation of any shape, they must also be applicable to cylinders. As noted above, since it is known that for cylinders only one shape parameter (i.e., charge diameter) is necessary to do this, these features must, in the cylindrical case, combine to give charge diameter d. For a cylinder, the cross-sectional area A is given by:

$$A = \pi d^2/4 \tag{3}$$

and the cross-sectional perimeter P by:

$$P = \pi d \tag{4}$$

The proper combination must be (4A/P), since:

$$[4A/P] = \frac{4(\pi d^2/4)}{\pi d} = d \tag{5}$$

Therefore, the critical condition for the cylinder becomes:

$$[4A/P]_c = d_c \tag{6}$$

as expected. Because the proper combination of parameters has been found in the particular case, Equation (6) may be generalized using the first assumption on page 518 to define the critical criterion in the general case as:

$$[4A/P]_c = \sigma \tag{7}$$

where:

$$\sigma = \text{the "critical geometry"} \tag{8}$$

Based on the second assumption this may be further generalized by observing that, if d_c is the critical geometry for the cylindrical case (Equation (6)), it must be the critical geometry for all shapes. Thus, it is clear that:

$$\sigma = d_c \tag{9}$$

and Equation (6) can be assumed applicable to all shapes.

To use Equation (6) for determining the critical values of the parameters that describe a given shape, the area and perimeter of that shape are written in terms of these parameters, and (4A/P) is found. Criticality results when this becomes equal to d_c. Solving the resultant equation for the parameters, gives their critical values

in terms of d_c. This has been done for a variety of non-perforated and perforated shapes and the results are shown in Table 1. Although the perimeter used for the perforated shapes is the sum of the outside and inside perimeters, it should be noted that the lateral expansion waves in the perforated sections may affect one another (i.e., interact) in such a way as to delay the rarefaction waves and thus reduce the loss of energy. Accordingly, the results for perforated shapes shown in Table 1 may be considered conservative in that the critical dimensions may be smaller than those indicated.

Table 1

CRITICAL DIMENSIONS FOR VARIOUS SHAPES

Shape and Characterizing Dimensions	Critical Value of Characterizing Dimensions
Circle 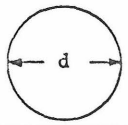	$d_c = d_c$
Square 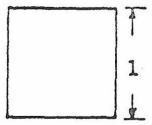	$l_c = d_c$
Equilateral Triangle 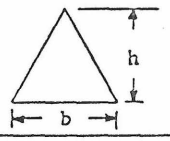	$b_c = \sqrt{3}d_c$ or $h_c = (3/2)d_c$
Ellipse 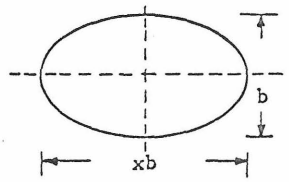 where $x > 1$	$b_c = \left[\int_0^{\pi/2} \sqrt{1 - \frac{x^2-1}{x^2}\sin^2\phi}\, d\phi\right](d_c/\pi)$ $b_{c\infty} = \lim_{x\to\infty} b_c = d_c/\pi$
Rectangle 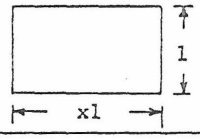 where $x > 1$	$l_c = ((x+1)/2x)d_c$ $l_{c\infty} = \lim_{x\to\infty} l_c = d_c/2$
Isosceles Triangle 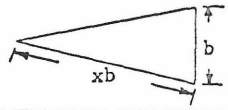 where $x > 1$	$b_c = \sqrt{(2x+1)/(2x-1)}\, d_c$ $b_{c\infty} = \lim_{x\to\infty} b_c = d_c$
Circular Core Cylinder 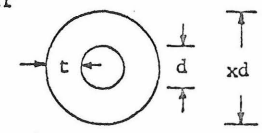 where $x > 1$	$d_c = (1/(x-1))d_c$ or $t_c = d_c/2$
Square Core Cylinder 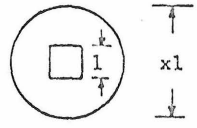 where $x > 1$	$l_c = ((\pi x+4)/(\pi x^2-4))d_c$
Equilateral Triangle Core Cylinder 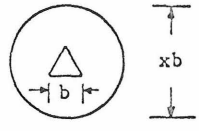 where $x > 1$	$b_c = ((\pi x+3)/(\pi x^2 - \sqrt{3}))d_c$
Cross Core Cylinder 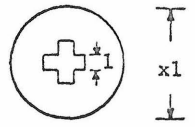 where $x > 1$	$l_c = ((\pi x+12)/(\pi x^2-20))d_c$

REFERENCES

1. H. Jones, Proc. Roy. Soc. (London) A189, 415 (1947).

2. H. Eyring, R. E. Powell, G. H. Duffey, and R. B. Parlin, Chem. Rev. 45, 69 (1949).

3. W. W. Wood, and J. G. Kirkwood, J. Chem. Phys. 24, 60 (1954).

4. M. A. Cook, The Science of High Explosives (American Chemical Society Monograph Series, Reinhold Publishing Corp., New York, 1958).